Synthesis and Characterisation of Novel Ferrocenyl Compounds

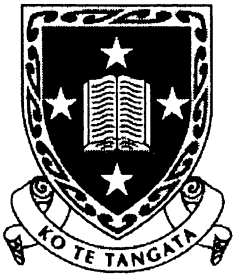

The University of Waikato

Te Whare Wānanga o Waikato

A thesis

submitted in partial fulfilment

of the requirements for the degree of

Doctor of Philosophy in Chemistry

At the University of Waikato

By

Steven R. Alley

University of Waikato 2001

τουτο μοι παν εν τηι Ελληνικηι

"Thesis Plus Antithesis Equals Synthesis"

-G. W. F. Hegel

"Thesis Plus Antithesis Equals Hysteresis"

-Terry Pratchett

Abstract

The ferrocenyl phosphonate mono-ester $FcCH_2P(O)(OPh)OH$ **1** (Fc = ferrocenyl) was prepared from $FcCH_2P(O)(OPh)_2$. The related mono-ester $FcCH_2P(O)(OEt)OH$ **2** was prepared by the reaction of $FcCH_2NMe_3I$ with diethyl phosphite. The ferrocenyl phosphonic acids $FcP(O)(OH)_2$ **3**, $FcCH_2P(O)(OH)_2$ **4**, $FcCH_2CH_2P(O)(OH)_2$ **5**, 1,1'-Fc' $[P(O)(OH)_2]_2$ **6** and 1,1'-Fc'$[CH_2P(O)(OH)_2]_2$ **7** were synthesised by hydrolysis of the corresponding phosphonate esters. X-ray crystal structure determinations were carried out for compounds **4** and **7**. The ferrocenyl phenylphosphonate esters $FcP(O)(OPh)_2$ **8** and 1,1'-Fc'$[P(O)(OPh)_2]_2$ **9** were also synthesised and characterised. The ferrocenyl arsonic acid $FcCH_2CH_2AsP(O)(OH)_2$ **10** was prepared by the reaction of $FcCH_2CH_2Br$ with Na_3AsO_3. The behaviour of **10** and the arsenic acids $PhAs(O)(OH)_2$, $2\text{-}NH_2\text{-}(C_6H_4)As(O)(OH)_2$ and $Me_2As(O)(OH)$ in negative ion ESMS was investigated in some depth. The carbon-arsenic bond in these compounds was found to cleave at moderate cone voltages.

The bis(triphenylphosphine)platinum complexes $(Ph_3P)_2PtO_3PR$ (R = Fc **11**, CH_2Fc **12**, CH_2CH_2Fc **13**) and 1,1'-Fc'$[PO_3Pt(PPh_3)_2]_2$ **14** were prepared and characterised. Single crystal structural determination of these compounds showed the expected chelation of the ferrocenyl phosphonate ligand to the platinum centre.

The reduction of various ferrocenyl ethylphosphonate esters gave the known primary ferrocenyl phosphines $FcCH_2PH_2$ **15**, $FcPH_2$ **16**, and 1,1'-Fc'$[PH_2]_2$ **17** in high yield. In addition the novel ferrocenyl phosphines $FcCH_2CH_2PH_2$ **18**, 1,1'-Fc'$[CH_2PH_2]_2$ **19**, 1,2'-Fc'$[CH_2PH_2]_2$ **20** and the ferrocenyl arsine $FcCH_2CH_2AsH_2$ **25** were prepared and characterised. The X-ray crystal structure determination was carried out for **25**. This is one of the few structures known for primary arsine compounds. The crystal structure of **18** was found to be isomorphous with that of **25**. The stability of phosphines **15-20** toward air oxidation was investigated using ^{31}P nmr. The phosphines **18**, **19** and **20** were found to be remarkably stable in air. The stability of **25** toward oxidation in air was investigated using elemental analysis. The arsine showed appreciable stability in air despite the sterically unencumbered nature of the arsine group.

Reaction of **19** and **20** with (Pip)$Mo(CO)_4$ (Pip = Piperidine) and (thf)$Mo(CO)_5$ resulted in the complexes, 1,2'-Fc'$[CH_2PH_2]_2Mo(CO)_4$ **21**, 1,1'-Fc'$[CH_2PH_2]_2Mo(CO)_4$ **22**, 1,1'-Fc'$[CH_2PH_2Mo(CO)_5]_2$ **23**, and 1,2'-Fc'$[CH_2PH_2Mo(CO)_5]_2$ **24** which were routinely characterised. A by-product of the synthesis of **22** was the larger oligomer [1,1'-Fc'$[CH_2PH_2]_2Mo(CO)_4]_2$ **22a** which was identified by ESMS.

The chemical oxidation of **15** was undertaken using H_2O_2 and monitored by ^{31}P nmr. Oxidation of the phosphine to phosphine oxide and phosphinic acid products was observed. Excess oxidant led to the oxidation of the ferrocene group and decomposition of the sample. The compounds $FcCH_2P(O)H_2$ **26** and $FcCH_2P(O)(OH)H$ **27** were prepared and characterised by nmr and ESMS.

The ferrocenyl hydroxymethyl phosphines $FcP(CH_2OH)_2$ **28** and 1,1'-Fc'$[P(CH_2OH)_2]_2$ **29** were prepared by the reaction of **16** and **17** with formaldehyde. The crystal structure of **28** was determined and compared with that of the known compound ferrocenyl hydroxymethyl phosphine $FcCH_2P(CH_2OH)_2$.

The hydroxymethyl phosphine chalcogenides $FcP(O)(CH_2OH)_2$ **30**, $FcP(S)(CH_2OH)_2$ **31** and $FcP(Se)(CH_2OH)_2$ **32** were prepared and fully characterised. The crystal structures of **30** and **31** were determined from single crystal X-ray data. The structure of **32** was found to be isomorphous with that of **31**. Hydrogen bonding networks in the structures of **30** and **31** were compared to each other and to other analogous compounds. The hydroxymethyl phosphine chalcogenides 1,1'-Fc'$[P(O)(CH_2OH)_2]_2$ **33**, 1,1'-Fc'$[P(S)(CH_2OH)_2]_2$ **34** and 1,1'-Fc'$[P(Se)(CH_2OH)_2]_2$ **35** were also prepared and characterised.

The platinum complex $[FcP(CH_2OH)_2]_2PtCl_2$ **36** was synthesised by the reaction of **28** and (COD)$PtCl_2$. Reaction of **29** with (COD)MCl_2 (M = Pt and Pd) gave the analogous metal complexes, 1,1'-Fc'$[P(CH_2OH)_2]_2MCl_2$ which were unable to be fully characterised. The platinum and palladium complexes of ferrocenyl hydroxymethylphosphines were found to form $[M+Cl^-]^-$ ions under ESMS conditions.

Acknowledgments.

First and foremost I would like to thank Associate Professor Bill Henderson for being a supervisor above and beyond the call of duty. Without his unceasing enthusiasm, ideas and suggestions, none of this would have ever reached completion. Thank you very much Bill.

I have knocked on the doors of many other members of staff in the course of this work. Without exception they have answered my queries with patience and good humour. Especial thanks go to Professor Brian Nicholson for assistance in all matters crystallographic, Professor Alistair Wilkins for aid in interpretation of GC-MS and nmr data and Dr Ralph Thomson for much assistance with all things resonating in a nuclear magnetic way.

I have also darkened the doors of many of the technical staff in my academic travels. Again without exception, my requests and casual thievery of miscellaneous glassware have been met with more tolerance than I could have hoped. Thank you, Wendy, Jannine, Pat, Annie, Amu, Natalie and John for your time and cornucopia of equipment.

Further afield, Professor Ward Robinson at the University of Canterbury and Associate Professor Cliff Rickard at the University of Auckland collected crystallographic data (including that of S_8 and $CODPdCl_2$) for which I am very grateful. I would also like to thank Marianne Dick of the University of Otago microanalytical lab for undertaking elemental analyses on my behalf.

The labrats of C3.08, with whom I shared many moments amid the hum of the extractor fans and the sound of three radios set to three different stations: Dr Lea Bonnington (diamonds and pearls), Dr Maarten Dinger and Dr Nick

Goodwin (comparative theology), Dr Allen Oliver (computers and their wily ways), Dr Scott McIndoe (cryptic crosswords), Paul Oswald (lab cricket), Dr Trevor Matheison (diving and fishing), Jane Woodcock (chocolate), Gwion Harfoot (explosions and fires), Corry Decker (German Oaths) and the coffee twins Wade Mace and Cameron Evans, all made going to the lab a lot more fun and a little more dangerous. For this I thank them deeply.

Jeremy Yeo and Audi Fong of the National University of Singapore introduced me to the general theory of ley-line mediated crystal growth and helped develop the 'Skinner box' approach to organometallic synthesis. Their good humour and work ethic proved infectious, for which I am eternally thankful.

Dr Karen Murphy and Cameron Evans kindly 'volunteered' to proofread many parts of this thesis, a task I would wish on few people, but one that I am most grateful for. Any mistakes that remain are mine alone.

A chance purchase of Histories by Herodotus led me to Associate Professor James F. Johnson of Austin College Texas, who kindly provided much needed aid with translation.

The University of Waikato deserves praise for supplying a doctoral scholarship that kept me alive and a rugby team that kept me fit.

And last but not least I wish to thank my family. Mum and Dad, Sandra, Marie, Dave and Brett. There are few words able to convey how much my family means to me. Their support is unquestioning and their love unconditional. Was ever anyone so blessed with kith and kin as I?

Contents

List of Figures

List of Schemes

List of Tables

List of Abbreviations and Symbols

Å	Angstrom	acac	acetylacetonate
bipy	2,2'-bipyridine	Binol	1,1'-bis-2-naphthol
b.p.	boiling point	BPPFA	N,N-dimethyl-1-[-2,2'-bis(diphenylphosphino)ferrocenyl]-ethylamine
br.	broad (NMR, IR)	Bu	butyl
^{n}Bu	butyl	^{t}Bu	tertiary butyl
Bz	benzyl	°C	degrees Celcius
CCDC	Cambridge Crystallographic Data Centre	$CDCl_3$	deuterated chloroform
Cisplatin	*cis*-$Pt(NH_3)_2Cl_2$	COD	1,5-cyclo-octadiene
Cp	cyclopentadienyl	Cp^*	pentamethylcyclopentadienyl
CV	cyclic voltammogram	c.v.	cone voltage
d	doublet (NMR)	δ	chemical shift
DACH	1,2-diaminohexane	dba	*trans*, *trans*-dibenzylidene acetone
dec.	decomposed.	dmpf	1,1'-bis(dimethylphosphino) ferrocene
DMSO	dimethylsulfoxide	d^6-DMSO	hexadeutero dimethylsulfoxide
DNA	deoxyribose nucleic acid	D_2O	deuterium oxide
DPPE	1,2-bis(diphenylphosphino) ethane	dppf	1,1'-bis(diphenylphosphino) ferrocene
dpmf	1,1'-bis(diphenylphosphinomethyl) ferrocene	Et_2O	diethyl ether
Et	ethyl	EtOH	ethanol
EtOAc	ethyl acetate	ES	electrospray
ESMS	electrospray mass spectrometry	Fc	ferrocenyl
Fc'	di-substituted ferrocenyl	Fc"	tri-substituted ferrocenyl
Fc"'	tetra-substituted ferrocenyl	Ferriphos	2,2'-bis(α-(dimethylamino)(GRP)methyl-1,1'-bis(diphenylphosphino)ferrocene GRP =alkyl, aryl
g	gram	GC	gas chromatography

GC-MS	gas chromatography-mass spectrometry	HMBC	heteronuclear multiple bond correlation
HSQC	heteronuclear single quantum coherence	*i*	iso
IC_{50}	concentration required to kill 50% of a population	IR	infra red
Josiphos	2-[-1-(diphenylphosphino)-ethyl]-1-(diphenylphosphino)-ferrocene	L	litre
m	multiplet (NMR)	*m*	meta
m	medium (IR)	MAS-NMR	magic angle spinning – nuclear magnetic resonance
Mes*	2,4,6-tri-*t*-butylphenyl	MDP	methylenediphosphonic acid
Me	methyl	MeCN	acetonitrile
MeOH	methanol	min	minute
Mol/mol	mole	m.p.	melting point
m/z	mass to charge ratio	*n*	straight chain
NMR/nmr	nuclear magnetic resonance	NTMP	nitrilotris(methylenephosphonic acid)
o	ortho	OAc	acetyl
OTf or Tf	$CF_3SO_3^-$	*p*	para
PES	photon emission spectroscopy	pet. spirits	petroleum spirits
PFA	phosphonoacetic acid	Ph	phenyl
Pip	Piperidine	PPFA	(R, S_p)-N,N-dimethyl-1-[(2-diphenyl phosphino)ferrocene]ethylamine
ppm	parts per million	^{i}Pr	*iso*-propyl
p.s.i	pounds per square inch	R	*rectus*
R_f	retention factor	R_t	retention time (GCMS)
R. T.	room temperature	*s*	singlet (NMR)
S	*sinister*	s	strong (IR)
solv	coordinated solvent	*t*	Tertiary
t	triplet (NMR)	TEP	triethylphosphite
thf	tetrahydrofuran	TFA	trifluoroacetic acid

TMEDA	N, N, N', N'-tetramethyl ethylenediamine	TPP	triphenyl phosphine
TRAPS	2,2''-bis[diGRPphosphino)-ethyl]-1,1''-biferrocene (GRP = alkyl, aryl)	Triphosgene	bis-(trichloromethyl) carbonate
UV	ultraviolet light	V	Volts
w	weak (IR)	XRD	X-ray diffraction

Chapter 1: A Review of Ferrocenyl Phosphorus Chemistry

1.1: Introduction

Despite its antiquity (in organometallic chemistry terms), interest in the chemistry of ferrocene [$(\eta^5\text{-}C_5H_5)_2Fe$] and its derivatives remains intense. This review is not concerned with the great majority of ferrocenyl compounds, focussing instead on those ferrocenyl compounds that also contain phosphorus. At a stroke, the vast ocean of ferrocene research becomes merely a large sea, one a reviewer might hope to cross in the course of a thesis.

This review is divided into two sections. The first section deals with the chemistry of ferrocenyl phosphines, with special consideration given to the chemistry of 1,1'-bis(diphenylphosphino)ferrocene and of chiral ferrocenyl phosphines. The second section explores ferrocenyl phosphorus compounds, which contain non-phosphine phosphorus groups.

1.2: Ferrocenyl Phosphines

The study of ferrocenyl phosphines constitutes one of the largest and most active areas of research in organometallic chemistry. A comprehensive review would occupy the remainder of this thesis. What follows is a brief look at the fundamental aspects of ferrocenyl phosphine chemistry, illustrated with examples from the contemporary literature. For a more detailed examination of the trends in this field of chemistry several excellent reviews are available[1].

1.2.1: 1,1'-Bis(diphenylphosphino)ferrocene

In the late 1970s Kumada *et al.*[2] discovered that (dppf)$PdCl_2$ (dppf = 1,1'-bis(diphenylphosphino)ferrocene **1**$^{\Omega}$) was an outstanding catalyst for the cross

---

[1] (a) Ferrocenes, A. Togni and T. Hayashi Eds., VCH Verlagsgesellschaft, Weinheim, Germany, 1995. (b) G. Bandoli and A. Dolmella, *Coord. Chem. Rev.*, 2000, **209**, 161.

[2] (a) T. Hayashi, M. Konishi and M. Kumada, *Tetrahedron Lett.*, 1979, **174**, 321. (b) T. Hayashi, M. Konishi and M. Kumada, *J. Organomet. Chem.*, 1980, **186**, C1.

coupling of Grignard reagents with alkylhalides and alcohols. This result provided the impetus for two decades of intense research into the chemistry of dppf, its metal complexes and their utility as homogeneous catalysts. From this research a vast array of dppf-metal complexes have been prepared and characterised.

Dppf is most commonly found as a chelating ligand, forming two bonds to a metal centre. In this bonding mode, dppf is able to stabilise a range of coordination numbers at the metal centre due to the flexibility of the substituted cyclopentadienyl (Cp) rings, which can rotate and/or tilt to relieve any strain imposed by complex formation. The trigonal planar silver complexes exemplified by (dppf)Ag(PPh_3)[3] **2**, represent the lowest coordination number that chelating dppf can stabilise. Two-coordinate linear complexes where dppf is the sole ligand are not known, presumably for steric reasons (linear two-coordinate complexes containing bridging dppf are common and will be addressed shortly).

Four-coordinate complexes of dppf are very common. Square planar complexes of group 10 metals remain at the forefront of dppf chemistry. Recent examples include (dppf)Pt(biphenyl)[4] **3**, (dppf)Pt$(Me)_2$[5] and the fullerene complex (dppf)Pd(η^2-C_{60})[6] **4**. More complex structural types include sulfur bridged complexes

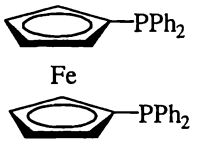

1

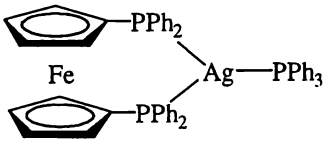

2

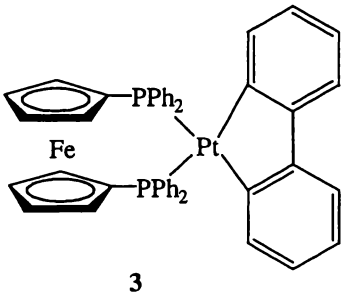

3

[Ω] Numbering applies to compounds whose illustration accompanies the text in this review chapter. Numbering starts anew in chapter two denoting compounds synthesised in the course of this research.

[3] M. C. Gimeno, P. G. Jones, A. Laguna, C. Sarroca, *J. Chem. Soc., Dalton. Trans.*, 1995, 1473.

[4] G. Y. Zheng, D. P. Rillema and J. H. Reibenspies, *Inorg. Chem.*, 1999, **38**, 794.

[5] D. C. Smith, C. M. Haar, E. D. Stephens, S. P. Nolan, W. J. Marshall and K. J. Moloy, *Organometallics*, 2000, **19**, 1427.

[6] V. V. Bashilov, T. V. Magdesieva, D. N. Kravchuk, P. V. Petrovskii, A. G. Ginzburg, K. P. Butin and V. I. Sokolov, *J. Organomet. Chem.*, 2000, **599**, 37.

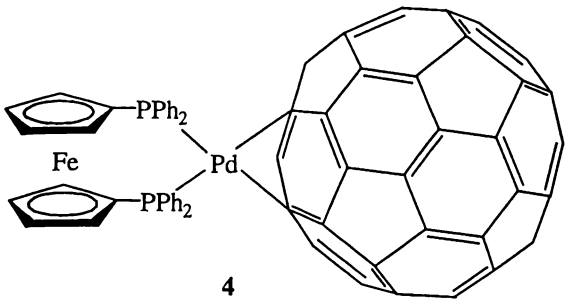

4

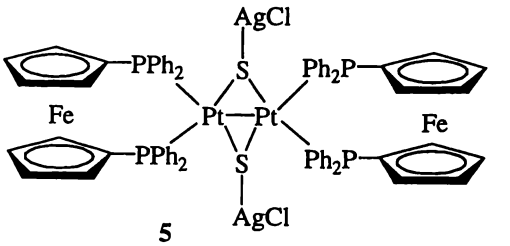

5

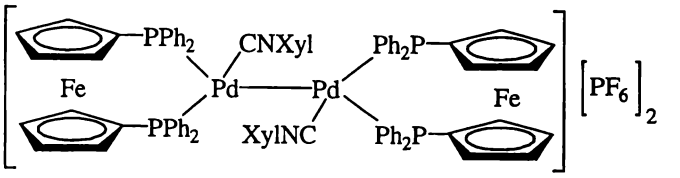

Xyl = Xylyl

6

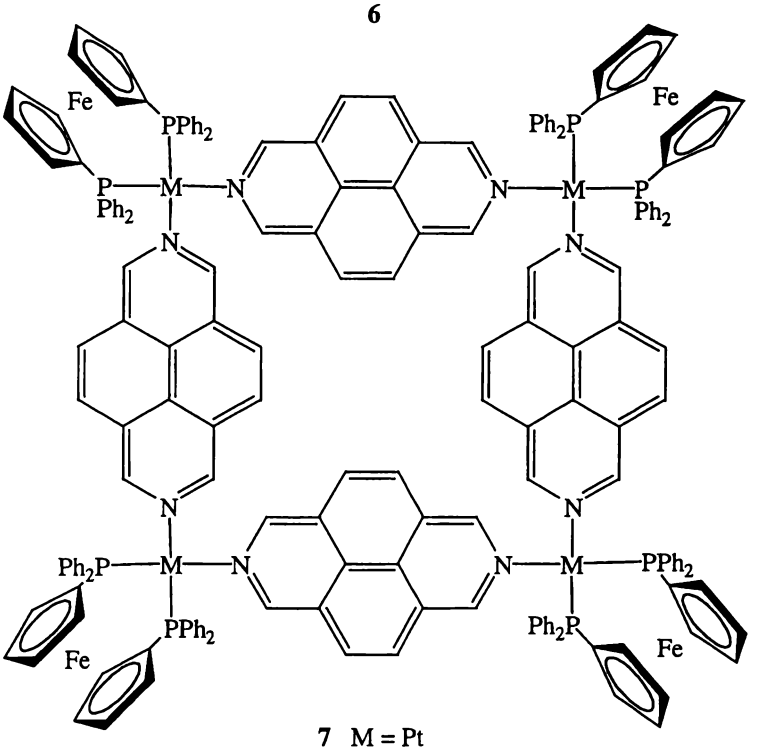

7 M = Pt
8 M = Pd

such as $Pt_2Ag_2Cl_2(dppf)_2(\mu^3\text{-}S)_2$[7] **5**, and complexes with formal M-M bonds such as $[Pd_2(dppf)_2(RNC)_2](PF_6)_2$ (R = 2,6-xylyl **6**, 2,4,6-mesityl)[8]. Larger macrocyclic compounds such as **7**, and **8** have been prepared by reaction of $[(dppf)M(H_2O)_2][OTf]_2$ (M = Pt, Pd, OTf = $CF_3SO_3^-$) with suitable polycyclic organic

[7] G. Li, S. Li, A. L. Tan, W. -H. Yip, T. C. W. Mak and T. S. A. Hor, *J. Chem. Soc., Dalton Trans.*, 1996, 4315.

[8] T. Tanase, J. Matsuo, T. Onaka, R. A. Begum, M. Hamaguchi, S. Yano and Y. Yamamoto, *J. Organomet. Chem.*, 1999, **592**, 103.

ligands[9]. Tetrahedral dppf complexes are well known for nickel[10], silver[3], copper[11], mercury[12], iron[13] and cobalt[14]. Piano stool complexes such as $[Cp^*RuCl(dppf)][PF_6]$[15] (Cp^* = pentamethylcyclopentadienyl) **9**, also have four-coordinate geometry. The Ir(0) complex $Ir(dppf)_2$ has been recently characterised[16] and has a four-coordinate geometry intermediate between square planar and tetrahedral.

The five-coordinate iron carbonyl complex $(dppf)Fe(CO)_3$[13,17] is well known, as are five-coordinate derivatives of the piano stool complexes such as $[Cp^*Ru(dppf)HX]$[18] (X = H, Cl, Br **10** and I).

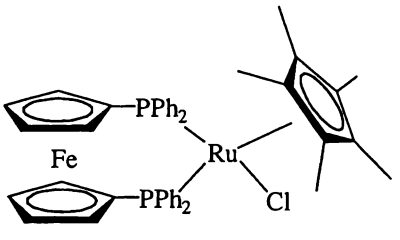

9

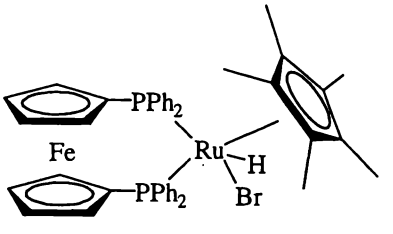

10

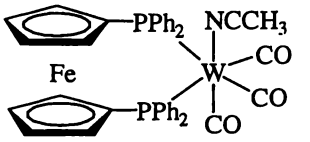

13

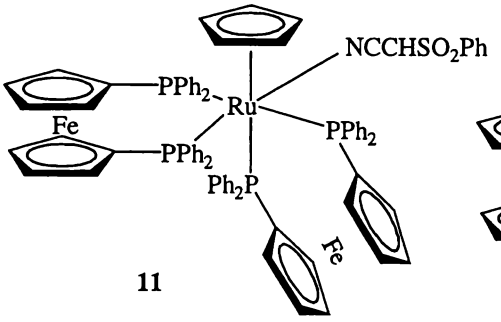

11

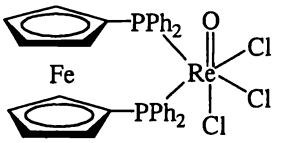

12

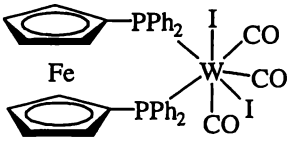

14

Octahedral complexes of dppf are very common; recent examples include the ruthenium complexes $[(dppf)_2RuCp(NCCHSO_2Ph)]$[19] **11** and

---

[9] P. J. Stang, B. Olenyuk, J. Fan and A. M. Arif, *Organometallics*, 1996, **15**, 904.
[10] U. Casellato, D. Ajo, G. Valle, B. Corain, B. Longato and R. Graziani, *J. Cryst. Spectr. Res.*, 1988, **18**, 583.
[11] S. P. Neo, Z. –Y. Zhou, T. C. W. Mac and T. S. A. Hor, *J. Chem. Soc., Dalton Trans.*, 1994, 3451.
[12] J. McGinley, V. McKee and C. J. McKenzie, *Acta. Cryst.*, 1998, C54, 345.
[13] A. E. Gerbase, E. J. S. Vichi, E. Stein, L. Amaral, A. Vasquez, M. Horner and C. Maichle-Mossmer, *Inorg. Chem. Acta.*, 1997, **266**, 19.
[14] T. –J. Park, S. Huh, Y. Kim and M. –J. Jun, *Acta. Cryst.*, 1999, C55, **6**, 848.
[15] J. –F. Ma and Y. Yamamoto, *J. Organomet. Chem.*, 1999, **574**, 148.
[16] B. Longato, L. Riello, G. Bandoli and G. Pilloni, *Inorg. Chem.*, 1999, **38**, 12.
[17] T. –J. Kim, K. –H. Kwon, S. –C. Kwon, J. -O. Baeg, S. –C. Shim and D. –H. Lee, *J. Organomet. Chem.*, 1990, **389**, 205.
[18] (a) R. T. Hembre and J. S. McQueen, *Angew. Chem. Int. Ed. Eng.*, 1997, **36**, 65. (b) R. T. Hembre and J. S. McQueen, *J. Am. Chem. Soc.*, 1996, **118**, 798.
[19] T. Naota, A. Tanna and S. –I. Murahashi, *J. Am. Chem. Soc.*, 2000, **122**, 2960.

$[Ru(bipy)_2(dppf)][PF_6]_2$[20] and the rhenium complexes $(dppf)ReCl_3(NC_6H_5)$[21] and $ReO(dppf)Cl_3$[22] **12**. The reaction of $W(CO)_3(NCCH_3)_3$ with dppf gave the octahedral complex $W(CO)_3(NCCH_3)(\eta^2\text{-dppf})$ **13** which was further oxidised by I_2 to give seven coordinate $W(CO)_3I_2(\eta^2\text{-dppf})$[23] **14**. This represents the largest coordination sphere stabilised by dppf.

As well as simple chelate complexes, a wide range of compounds are known in which dppf acts as a bridging ligand. The types of bridging modes that have been observed are shown in Figure 1.1.

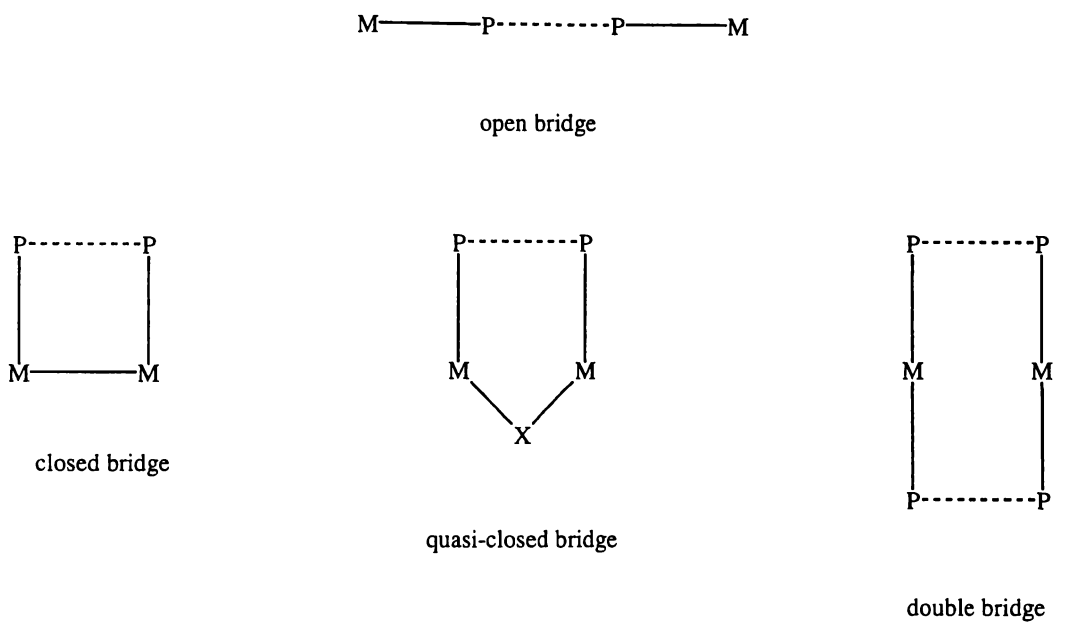

Figure 1.1: Common Bridging Modes of Dppf (P-----P = dppf, M = metal).

Open bridged complexes are typified by the simple linear gold(I) compounds $Au_2X_2(\mu\text{-dppf})$ (X = Me, C_6H_5, $C_{10}H_7$, $C_{14}H_7$, $C_{16}H_9$, C≡CPh, C≡C^{t}Bu[24], Cl, C_6F_5[25], Br, I, pyridinethiolate, diethyldithiocarbamate[26], CF_3CO_2[27], $Co(CO)_4$[28] and SC_6F_5[29]

---

[20] V. W. –W. Yam, V. W. –M. Lee and K. K. Cheung, *J. Chem. Soc., Dalton Trans.*, 1997, 2335.
[21] S. W. Lee and N. –S. Choi, *Acta. Cryst.*, 1999, C55, **12**, 2018.
[22] O. Knoesen, H. Gorls and S. Lotz, *J. Organomet. Chem.*, 2000, **598**, 108.
[23] S. C. Hsu, W. –Y. Yeh and M. Y. Chang, *J. Organomet. Chem.*, 1995, **492**, 121.
[24] V. W. -W. Yam, S. W. -K. Choi and K. -K. Cheung, *J. Chem. Soc., Dalton Trans.*, 1996, 3411.
[25] M. C. Gimeo, A. Laguna and C. Sarroca, *Inorg. Chem.*, 1993, **32**, 5926.
[26] F. Canales, M. C. Gimeno, P. G. Jones, A. Laguna and C. Sarroca, *Inorg. Chem.*, 1997, **36**, 5206.
[27] P. M. N. Low, Z. -Y. Zhang, T. C. W. Mak and T. S. A. Hor, *J. Organomet. Chem.*, 1997, **539**, 45.
[28] S. Onaka, Y. Katsukawa and M. Yamashita, *J. Organomet. Chem.*, 1998, **564**, 249.
[29] O. Crespo, F. Canales, M. C. Gimeno, P. G. Jones and A. Laguna, *Organometallics*, 1999, **18**, 3142.

15). Gold complexes containing both bridging and chelating dppf are known[30], while the complex $[Au_6Cu_2(\mu^3\text{-}SC_6F_5)_6(\mu\text{-dppf})_3][PF_6]$[29] contains both open bridged and quasi-closed bridging dppf ligands. Dppf has also been used as a bridging ligand for boranes, thiaboranes and carboranes, giving a range of products including $dppf(BH_3)_2$ and *arachno*-9-dppf-6-SB_9H_{11}[31] **16**.

Closed bridges are most common in cluster chemistry. Recent additions to this class of compound include $Ru_5C(CO)_{10}(dppf)(C_{60})$[32],

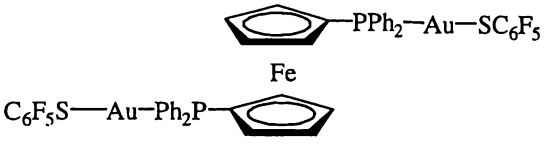

15

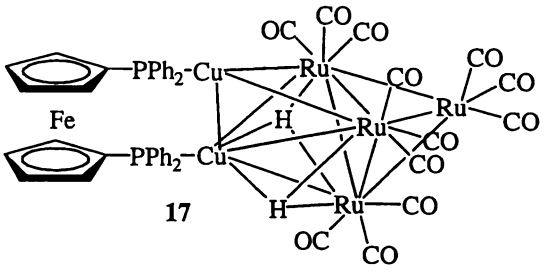

17

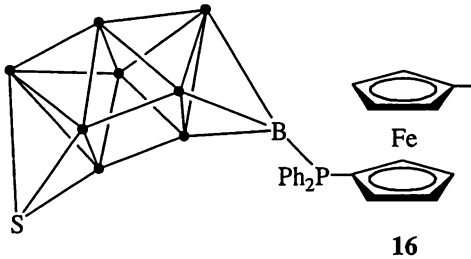

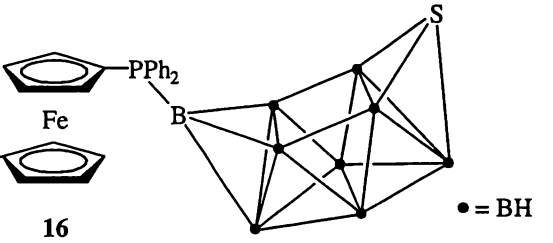

16

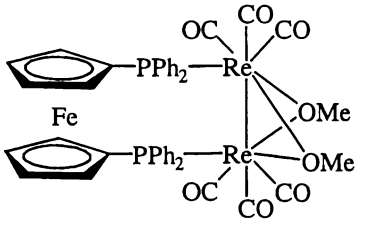

18

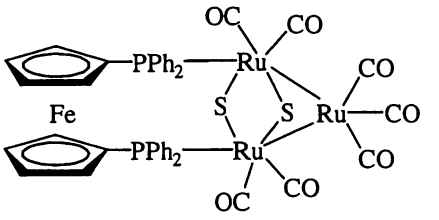

19

$[Os_7(CO)_{17}(\mu^4\text{-}\eta^2\text{-CO})(MeCN)(\mu\text{-dppf})]$[33] and the heteronuclear clusters $[M_2Ru_4H_2(\mu\text{-dppf})(CO)_{12}]$ (M = Cu **17**, Ag or Au)[34]. The structure of $[Re_2(\mu\text{-OMe})_2(\mu\text{-dppf})(CO)_6]$

---

[30] (a) A. Houlton, D. M. P. Mingos, D. M. Murphy and D. J. Williams, *Acta. Cryst.*, 1995, C51, 30. (b) L. -T. Phang, T. S. A. Hor, Z. -Y. Zhou and T. C. W. Mak, *J. Organomet. Chem.*, 1994, **469**, 253.

[31] K. J. Donaghy, P. J. Carroll and L. G. Sneddon, *Inorg. Chem.*, 1997, **36**, 547.

[32] K. Lee and J. R. Shapley, *Organometallics*, 1998, **17**, 3020.

[33] K. S. –Y. Leung, *Inorg. Chem. Commun.*, 1999, **2**, 498.

[34] I. D. Salter, S. A. Williams and T. Adatia, *Polyhedron*, 1995, **14**, 2803.

18 has recently been reported[35] though the compound has been known for some time[36]. Addition of dppf to $Ru_6C(CO)_{17}$ resulted in the series $Ru_6C(CO)_{16}(\eta^1$-dppf), $Ru_6C(CO)_{15}(\mu$-dppf) and $Ru_5C(CO)_{13}(\mu$-dppf), containing unidentate, quasi-bridged and closed bridged dppf respectively[37].

Recent examples of quasi-bridged dppf can be found in the copper complex $[Cu_2(\mu\text{-}\eta^1\text{-}C{\equiv}CC_6H_4CH_3)_2(\mu\text{-dppf})_2]$[38], the iron complex $[Fe_3(\mu^3\text{-Se})_2(CO)_7(dppf)]$[39] and the ruthenium complex $[Ru_3(CO)_7(\mu\text{-dppf})(\mu^3\text{-S})_2]$[40] **19**.

1.2.2: Catalysis by Dppf-Metal Complexes

The search for efficient catalysts remains the driving force behind the majority of dppf chemistry. Since the seminal work of Kumada *vide supra*, dppf-palladium complexes have been used as catalysts in a wide range of organic coupling reactions. The catalytic cycle for simple cross-coupling reactions is typified by that shown in Scheme 1.1 for reaction of Grignard reagents with alkylhalides. The active species is the Pd(0) complex $(dppf)Pd(solv)_2$ (solv = solvent).

---

[35] Y. –K. Yan, W. Koh, C. Jiang, W. K. Leong and T. S. A. Hor, *Polyhedron*, 2000, **19**, 641.
[36] Y. –K. Yan, H. S. O. Chan, T. S. A. Hor, K. L. Tan, L. K. Liu and Y. S. Wen, *J. Chem. Soc., Dalton. Trans.*, 1992, 423.
[37] D. S. Shephard, B. F. G. Johnson, A. Harrison, S. Parsons, S. P. Smidt, L. J. Yellowlees and D. Reed, *J. Organomet. Chem.*, 1998, **563**, 113.
[38] J. Diez, M. P. Gamasa, J. Gimeno, A. Aguirre, S. Garcia-Granda, J. Holubova and L. R. Falvello, *Organometallics*, 1999, **18**, 662.
[39] D. Cauzzi, C. Graiff, M. Lanfranchi, G. Predieri and A. Tiripicchio, *J. Organomet. Chem.*, 1997, **536-537**, 497.
[40] S. -W. A. Fong, J. J. Vittal and T. S. A. Hor, *Organometallics*, 2000, **19**, 918.

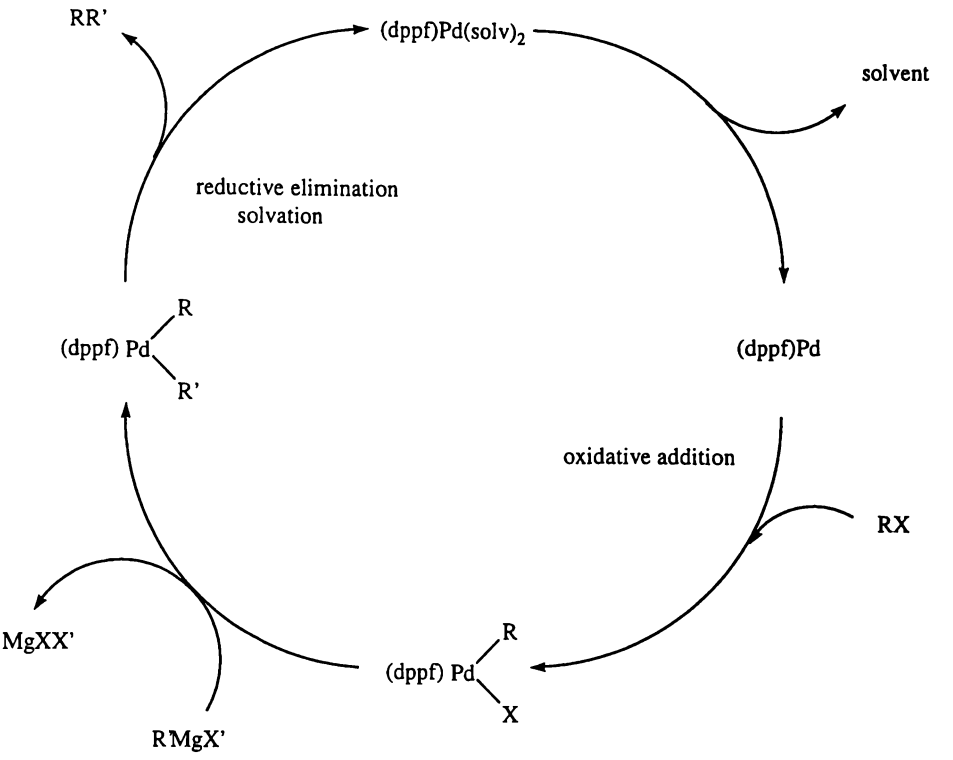

Scheme 1.1: Catalytic Cycle Observed in Grignard Cross-Coupling Reactions Catalysed by (dppf)$PdCl_2$.

The full catalytic potential of palladium-dppf systems is yet to be realised and research is ongoing. Some examples of recent applications for these catalysts are given below (Scheme 1.2).

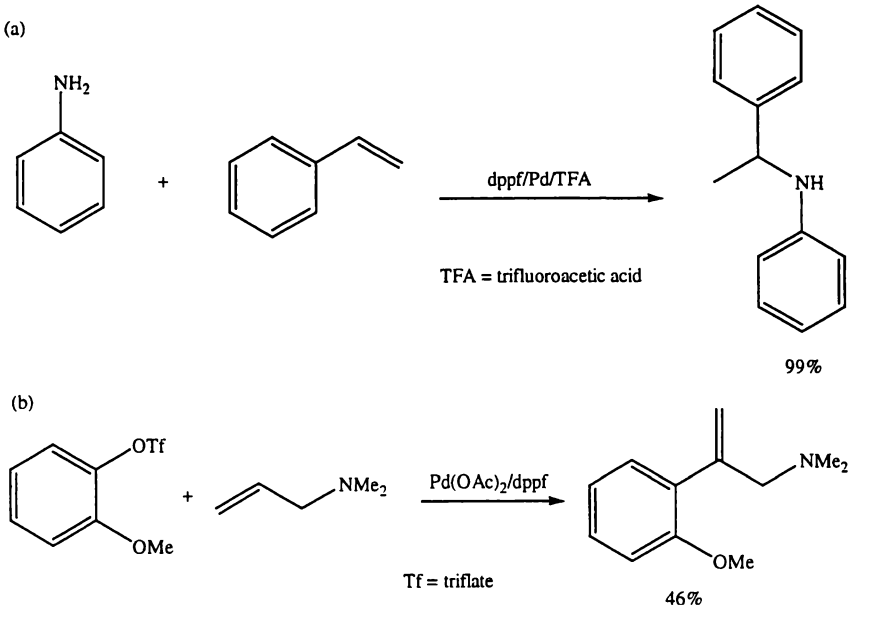

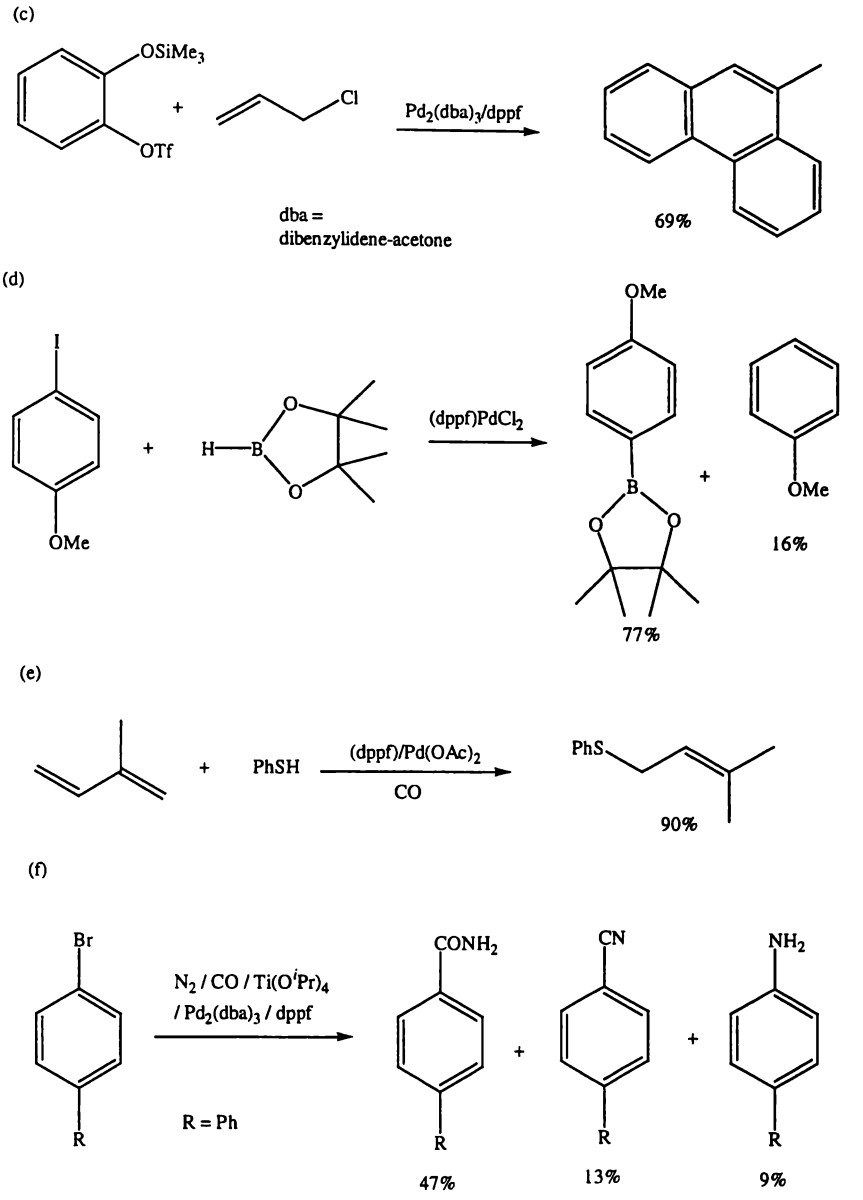

Scheme 1.2: Recent Examples of Reactions Subject to Dppf-Palladium Catalysis. References: (a) hydroamination[41], (b) benzyne/benzyne/alkene insertion[42], (c) borylation[43], (d) phosphorylation[44], (e) thiocarbonylation[45] and (f) carbonylation and nitrogenation[46].

[41] M. Kawatsura and J. F. Hartwig, *J. Am. Chem. Soc.*, 2000, **122**, 9546.
[42] E. Yoshikawa, K. V. Radhakrishnan and Y. Yamamoto, *J. Am. Chem. Soc.*, 2000, **122**, 7280.
[43] M. Murata, T. Oyama, S. Watanabe and Y. Masuda, *J. Org. Chem.*, 2000, **65**, 164.
[44] C. –Q. Zhao, L. –B. Han and M. Tanaka, *Organometallics*, 2000, **19**, 4196.
[45] W. –J. Xiao, G. Vasapollo and H. Alper, *J. Org. Chem.*, 2000, **65**, 4138.
[46] K. Ueda, Y. Sato and M. Mori, *J. Am. Chem. Soc.*, 2000, **122**, 10722.

While square planar palladium-dppf complexes have seized the lions share of attention, dppf catalysts based on metals such as rhodium[47] and nickel[48] are also known.

1.2.3: Chiral Ferrocenyl Phosphines

Control of the stereochemical outcome of chemical reactions is of vital importance in many areas of organic chemistry. The most efficient way to achieve this control is to use a chiral catalyst and the easiest way to prepare a chiral catalyst is to use a chiral ligand. The development of chiral ferrocenyl phosphine ligands has been the focus of a substantial amount of research over the past two decades.

The first chiral ferrocenyl phosphine, (R, S_p)-N,N-dimethyl-1-[(2-diphenylphosphino)ferrocene]ethylamine (PPFA) **20** was prepared by Hayashi and Kumada in 1974[49], (Scheme 1.3).

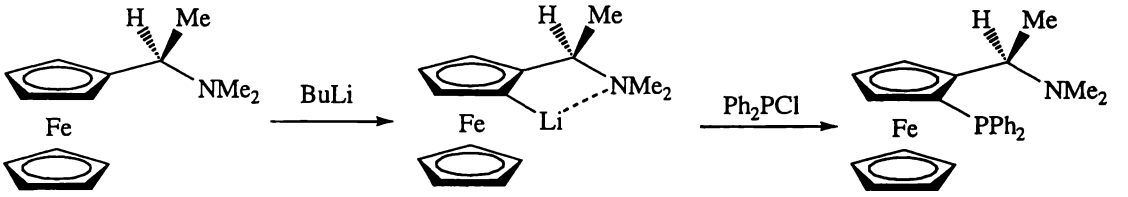

20 PPFA

Scheme 1.3: Synthesis of PPFA **20**.

The synthesis of PPFA relies on the initial substitution of the Cp ring by a side chain containing a chiral centre. This side chain directs the site of ortho-lithiation and in turn, the site of the phosphine group. The ability to direct the site of ortho-substitution results in PPFA possessing two types of chirality. The first is atom centred, the α-carbon of the side chain. The second is planar chirality, which arises whenever a ferrocenyl Cp ring is bound to two different substituents. Planar chirality is described as (R_p) or (S_p) to distinguish it from atom centred chirality. To assign a ferrocenyl compound as (R_p) or (S_p), the molecule must be viewed from above. The substituents are then ranked using Cahn-Ingold-Prelog rules. If the shortest path

[47] (a) M. Ueda and N. Miyaura, *J. Org. Chem.*, 2000, **65**, 4450. (b) R. Kuwano, K. Sato and Y. Ito, *Chem. Lett.*, 2000, **4**, 428.
[48] C. A. Busacca, M. C. Eriksson and R. Fiaschisi, *Tetrahedron Lett.*, 1999, **40**, 3101.
[49] T. Hayashi, K. Yamamoto and M. Kumada, *Tetrahedron Lett.*, 1974, **49-50**, 4405.

around the ring, from the highest ranked substituent to the next highest ranked substituent, is in the clockwise direction then the compound is designated (R_p), otherwise it is (S_p), (Figure 1.2).

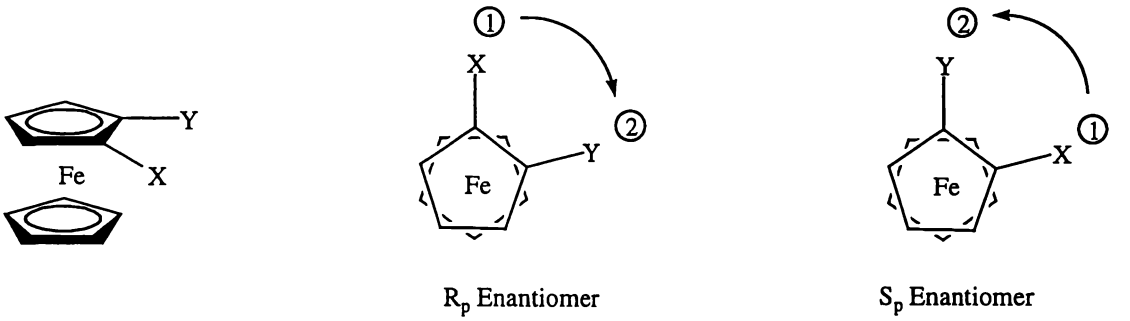

Figure 1.2: Assignment of Planar Chiral Descriptors.

Modification and extension of the synthesis outlined in Scheme 1.3 has given rise to several types of chiral ferrocenyl bis-phosphine ligands, some of which are illustrated in Figure 1.3

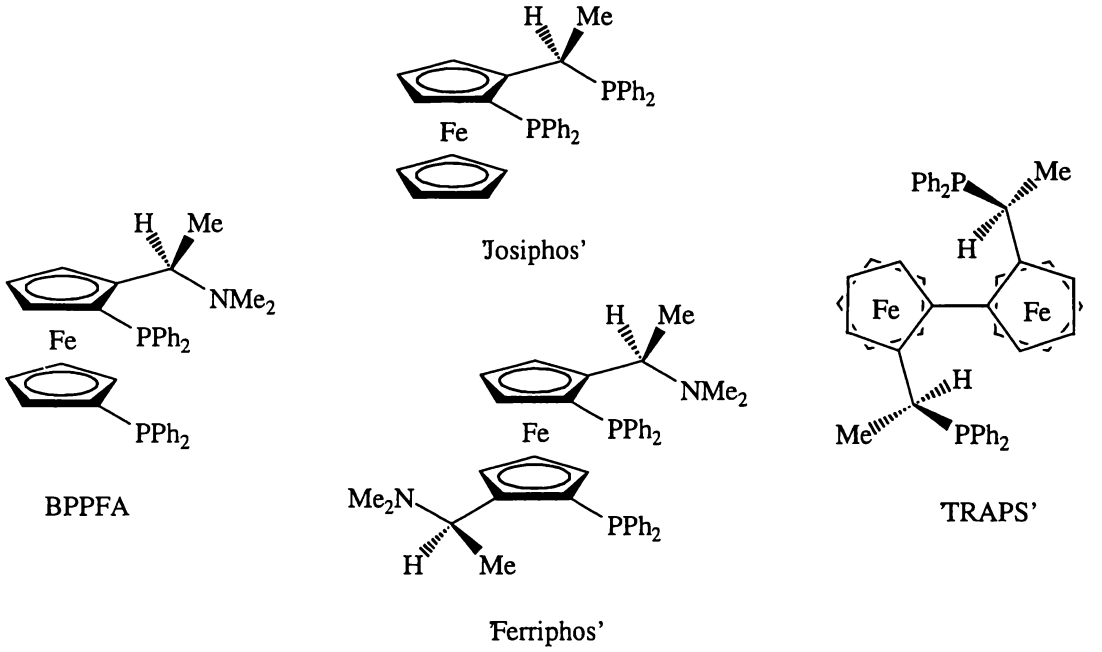

Figure 1.3: Chiral Ferrocenyl Bis-Phosphines. References: BPPFA[50], Josiphos[50,51], Ferriphos[52] and TRAPS[53].

[50] T. Hayashi, T. Mise, M. Fukushima, M. Kagotani, N. Nagashima, Y. Hamada, A. Matsumoto, S. Kawakami, M. Konishi, K. Yamamoto and M. Kumada, *Bull. Chem. Soc. Jap.*, 1980, **53**, 1138.

The use of chiral auxiliaries other than N,N-dimethyl ethylamine has also been pursued by a number of research groups. Chiral sulfoxide[54] and more extensively, chiral acetal[55] and oxazoline[56] auxiliaries have been particularly useful in inducing diastereoselective ortho-lithiation. Subsequent addition of phosphine group(s) gives chiral ferrocenyl phosphines such as **21**[54b], **22**[55a] and **23**[56c] derived from sulfoxide, acetal and oxazoline substituted ferrocene respectively.

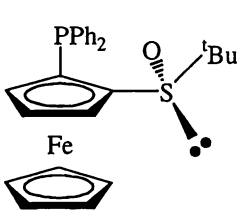

21

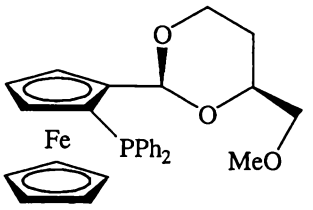

22

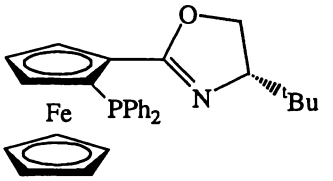

23

Figure 1.4: Chiral Ferrocenyl Phosphines Derived from Sulfoxide, Acetal and Oxazoline Substituted Ferrocene.

A major advantage of chiral ferrocenyl phosphines over more traditional chiral ligands is their synthetic flexibility. Both the chiral auxiliary and the phosphine group can be modified extensively. This enables links between structure and function to be investigated and the properties of chiral ferrocenyl phosphines can be fine tuned to specific catalytic tasks. An idea of the diversity of chiral ferrocenyl phosphines available is given in Figure 1.5.

---

[51] A. Togni, C. Breutel, A. Schnyder, F. Spindler, H. Landert and A. Tijani, *J. Am. Chem. Soc.*, 1994, **116**, 4062.

[52] (a) T. Hayashi, A. Yamamoto and Y. Ito, *J. Chem. Soc., Chem. Commun.*, 1989, 495. (b) T. Hayashi, A. Yamamoto, M. Hojo, K. Kishi, Y. Ito, E. Nishioka, H. Miura and K. Yanagai, *J. Organomet. Chem.*, 1989, **370**, 129.

[53] M. Sawamura, H. Hamashima and Y. Ito, *Tetrahedron: Asymmetry*, 1991, **2**(7), 593.

[54] (a) F. Rebiere, O. Riant, L. Ricard and H. B. Kagan, *Angew. Chem., Int. Ed. Eng.*, 1993, **32**, 568. (b) D. H. Hua, N. M. Lagneau, Y. Chen, P. M. Robben, G. Clapham and P. D. Robinson, *J. Org. Chem.*, 1996, **61**, 4508. (c) O. Riant, G. Argouarch, D. Guillaneux, O. Samuel and H. B. Kagan, *J. Org. Chem.*, 1998, **63**, 3511. (d) N. M. Lagneau, Y. Chen, P. M. Robben, H. –S. Sin, K. Takasu, J. –S. Chan, P. D. Robinson and D. H. Hua, *Tetrahedron*, 1998, **54**, 7301.

[55] (a) O. Riant, O. Samuel and H. B. Kagan, *J. Am. Chem. Soc.*, 1993, **115**, 5835. (b) O. Riant, O. Samuel, T. Flessner, S. Taudien and H. B. Hagan, *J. Org. Chem.*, 1997, **62**, 6733.

[56] (a) C. J. Richards, T. Damalidis, D. E. Hibbs and M. B. Hursthouse, *Synlett.*, 1995, **74**. (b) T. Sammakia, H. A. Latham and D. R. Schaad, *J. Org. Chem.*, 1995, **60**, 10. (c) Y. Nishibayashi and S. Uemura, *Synlett.*, 1995, 79. (d) T. Sammakia and H. A. Latham, *J. Org. Chem.*, 1995, **60**, 6002.

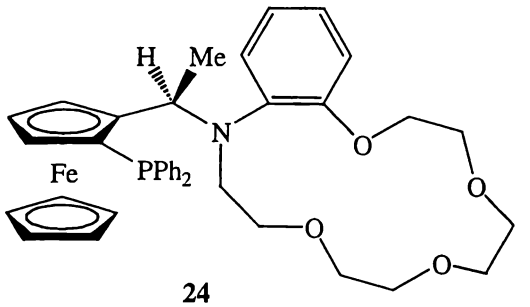

24

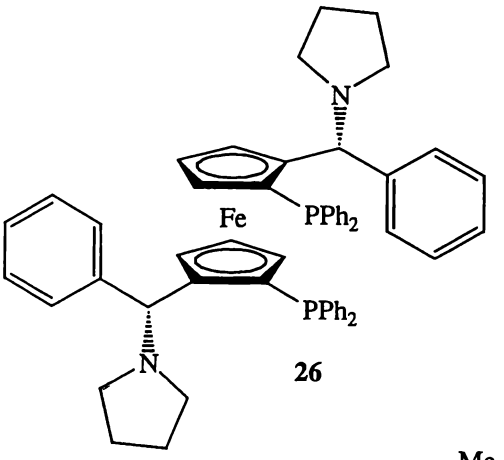

26

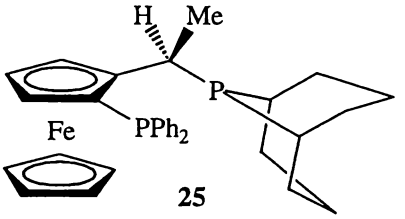

25

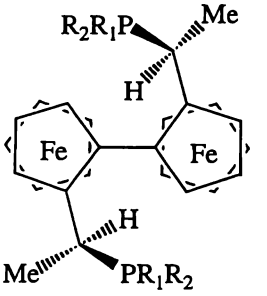

28 $R_1 = R_2 = Me$
29 $R_1 = R_2 = Et$
30 $R_1 = R_2 = Pr$
31 $R_1 = R_2 = {}^{i}Pr$
32 $R_1 = R_2 = Bu$
33 $R_1 = R_2 = Ph$
34 $R_1 = R_2 = p\text{-}C_6H_5OMe$
35 $R_1 = R_2 = p\text{-}C_6H_5Cl$
36 $R_1 = R_2 = p\text{-}C_6H_5Me$
37 $R_1 = R_2 = 2\text{-furyl}$
38 $R_1 = R_2 = p\text{-}C_6H_5F$
39 $R_1 = R_2 = p\text{-}C_6H_5CF_3$
40 $R_1 = R_2 = 3,5\text{-}(CF_3)_2C_6H_3$
41 $R_1 = Ph$ $R_2 = p\text{-}C_6H_5Me$

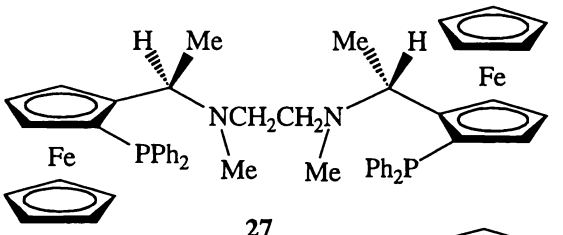

27

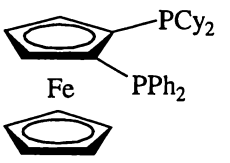

43

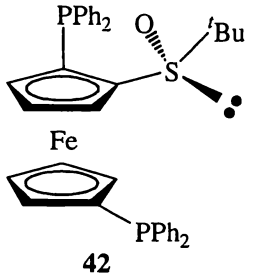

42

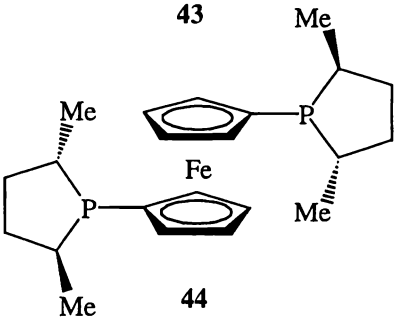

44

Figure 1.5: Chiral Ferrocenyl Phosphines. References: **24**[57], **25**[58], **26**[59], **27**[60], **28**[61], **29** and **32**[62], **30** and **31**[63], **33**[64], **34-37**[65], **38-40**[66], **41**[65], **42**[54a], **43**[54c] and **44**[67].

---

[57] C. R. Landis, R. A. Sawyer and E. Somsook, *Organometallics*, 2000, **19**, 994.
[58] H. C. L. Abbenhuis, U. Burckhardt, V. Gramlich, C. Kollner, P. S. Pregosin, R. Salzmann and R. Togni, *Organometallics*, 1995, **14**, 759.
[59] J. J. A. Perea, M. Lotz and P. Knochel, *Tetrahedron: Asymmetry*, 1999, **10**, 375.
[60] J. -H. Song, D. -J. Cho, S. -J. Jeon, Y. -H. Kim, T. -J. Kim and J. H. Jeong, *Inorg. Chem.*, 1999, **38**, 893.
[61] R. Kuwano and Y. Ito, *J. Org. Chem.*, 1999, **64**, 1232.
[62] M. Sawamura, R. Kuwano and Y. Ito, *J. Am. Chem. Soc.*, 1995, **117**, 9602.

The chiral ferrocenyl phosphine **44**[67] (Figure 1.5) was prepared by the reaction of diphosphino ferrocene (1,1'-Fc'$[PH_2]_2$[ж]) with chiral cyclic sulfates, a rare case of the chiral auxiliary being introduced after the phosphine group(s), (the chemistry of diphosphino ferrocene will be explored more fully in chapters 4 and 6).

A more recent development in this field has been the preparation of P-chiral ferrocenyl phosphines. The synthesis of P-chiral phosphines can be achieved using the method developed by Juge *et al.*[68] based on the pioneering work of Imamoto[69]. This method is characterised by the attachment of an optically active ephedrine to a borane protected phosphine centre. Stepwise removal of the ephedrine via nucleophilic substitution results in optically pure phosphines (Scheme 1.4).

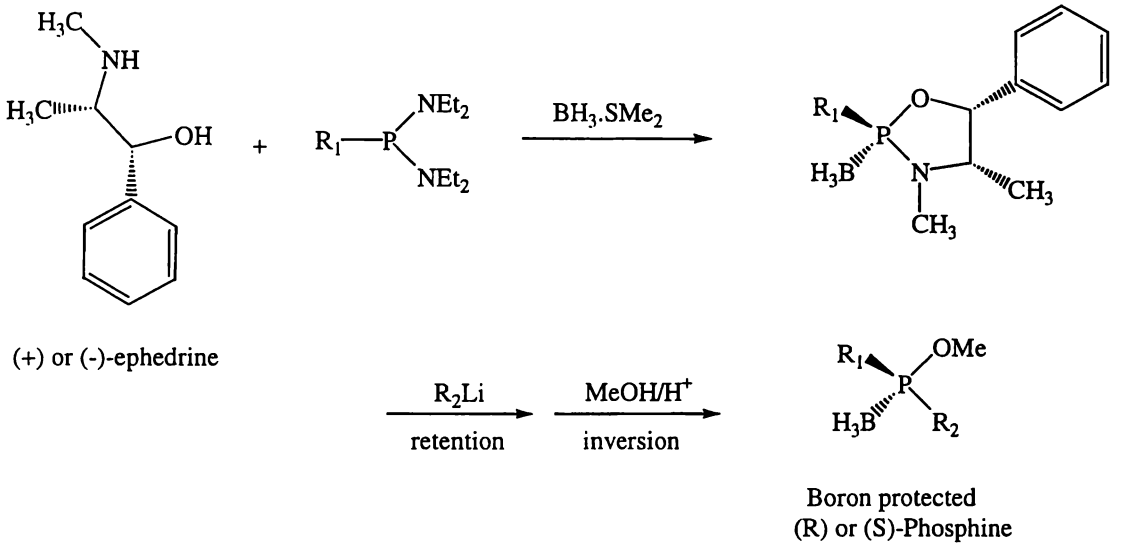

Scheme 1.4: Synthesis of Optically Active Phosphines.

The reaction of such chiral phosphines with 1,1'-Fc'Li_2 results in P-chiral ferrocenyl phosphines as illustrated in Scheme 1.5.

---

[63] R. Kuwano, H. Miyazaki and Y. Ito, *Chem. Commun.*, 1998, 71.
[64] M. Sawamura, H. Hamashima and Y. Ito, *Tetrahedron: Asymmetry*, 1991, **2**, 593.
[65] M. Sawamura, H. Hamashima, M. Sugawara, R. Kuwano and Y. Ito, *Organometallics*, 1995, **14**, 4549.
[66] A. Goeke, M. Sawamura, R. Kuwano and Y. Ito, *Angew. Chem., Int. Ed. Eng.*, 1996, **35**, 662.
[67] M. J. Burk and M. F. Gross, *Tetrahedron Lett.*, 1994, **35**, 9363.
[ж] Throughout this thesis: Fc = mono-substituted ferrocene, Fc' = di-substituted ferrocene F" = tri-substituted ferrocene etc.
[68] (a) S. Juge, M. Stephan, J. A. Lafitte and J. P. Jenet, *Tetrahedron*, 1990, **31**, 6357. (b) S. Juge, R. Merdes, M. Stephan and J. P. Genet, *Phosphorus Sulfur And Silicon*, 1993, **77**, 199. (c) S. Juge, M. Stephan, R. Merdes, J. P. Genet and D. Halut-Desportes, *J. Chem. Soc., Chem. Commun.*, 1993, 531.

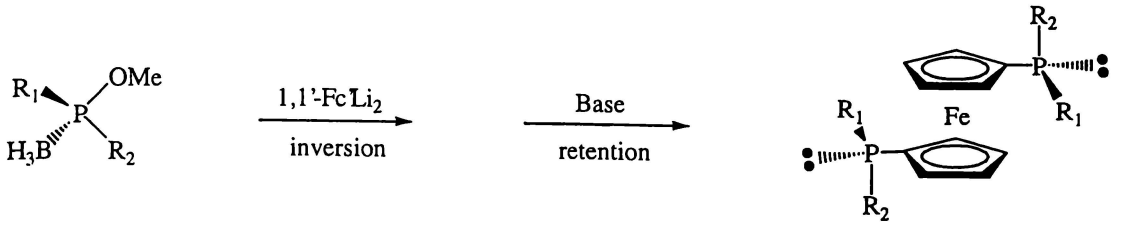

45 R_1 = Ph R_2 = 1-Naphthyl
46 R_1 = Ph R_2 = 2-Naphthyl
47 R_1 = Ph R_2 = 2-Anisyl
48 R_1 = Ph R_2 = 2-Biphenyl
49 R_1 = Ph R_2 = 9-Phenanthryl
50 R_1 = 1-Naphthyl R_2 = 4-Anisyl
51 R_1 = 1-Naphthyl R_2 = *p*-$C_6H_4CF_3$

Scheme 1.5: P-Chiral Ferrocenyl Phosphines. References: **45** and **46**[70], **47-49**[71], **50** and **51**[72].

The P-chiral phosphine (S,S)-(+)-1,1'-bis(methylphenylphosphino)ferrocene **52** has also been synthesised using the method outlined in Scheme 1.6[73].

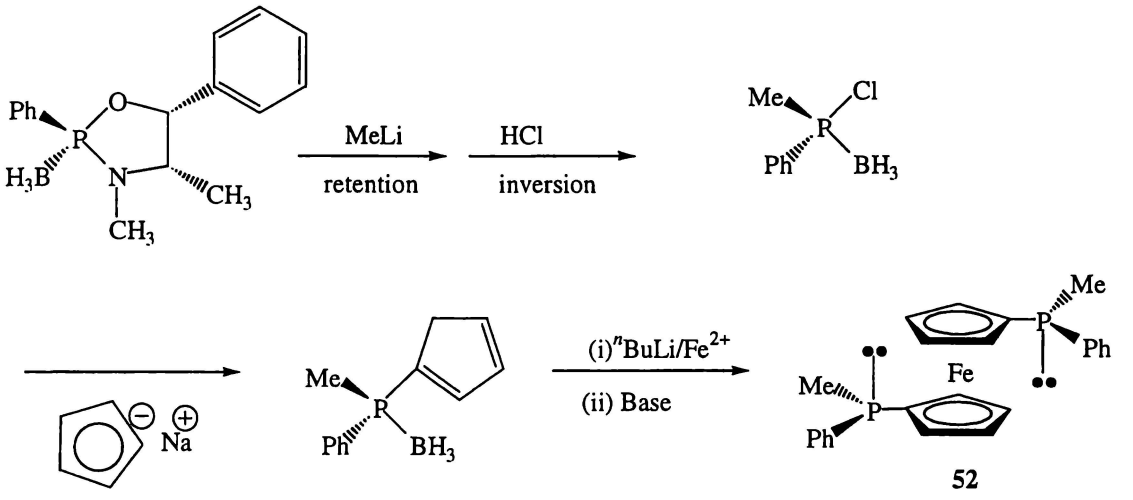

52

Scheme 1.6: Synthesis of (S,S)-(+)-1,1'-bis(methylphenylphosphino)ferrocene **52**.

---

[69] T. Imamoto, T. Oshiki, T. Onozawa, T. Kusumoto and S. Kazuhiko, *J. Am. Chem. Soc.*, 1990, **112**, 5244.
[70] U. Nettekoven, M. Widhalm, P. C. J. Kamer and P. W. N. M. van Leeuwen, *Tetrahedron: Asymmetry*, 1997, **8**, 3185.
[71] U. Nettekoven, P. C. J. Kamer, P. W. N. M. van Leeuwen, M. Widhalm, A. L. Spek and M. Lutz., *J. Org. Chem.*, 1999, **64**, 3996.
[72] U. Nettekoven, P. C. J. Kamer, M Widhalm and P. W. N. M. van Leeuwen, *Organometallics*, 2000, **19**, 4596.
[73] E. B. Kaloun, R. Merdes, J. -P. Genet, J. Uziel and S. Juge, *J. Organomet. Chem.*, 1997, **529**, 455.

Catalysis is the driving force behind all chiral ferrocenyl phosphine research. The chiral ferrocenyl phosphines discussed in this section have all been investigated to a greater or lesser degree as ligands in homogeneous catalysis. Successful examples of such catalysis are given in Scheme 1.7.

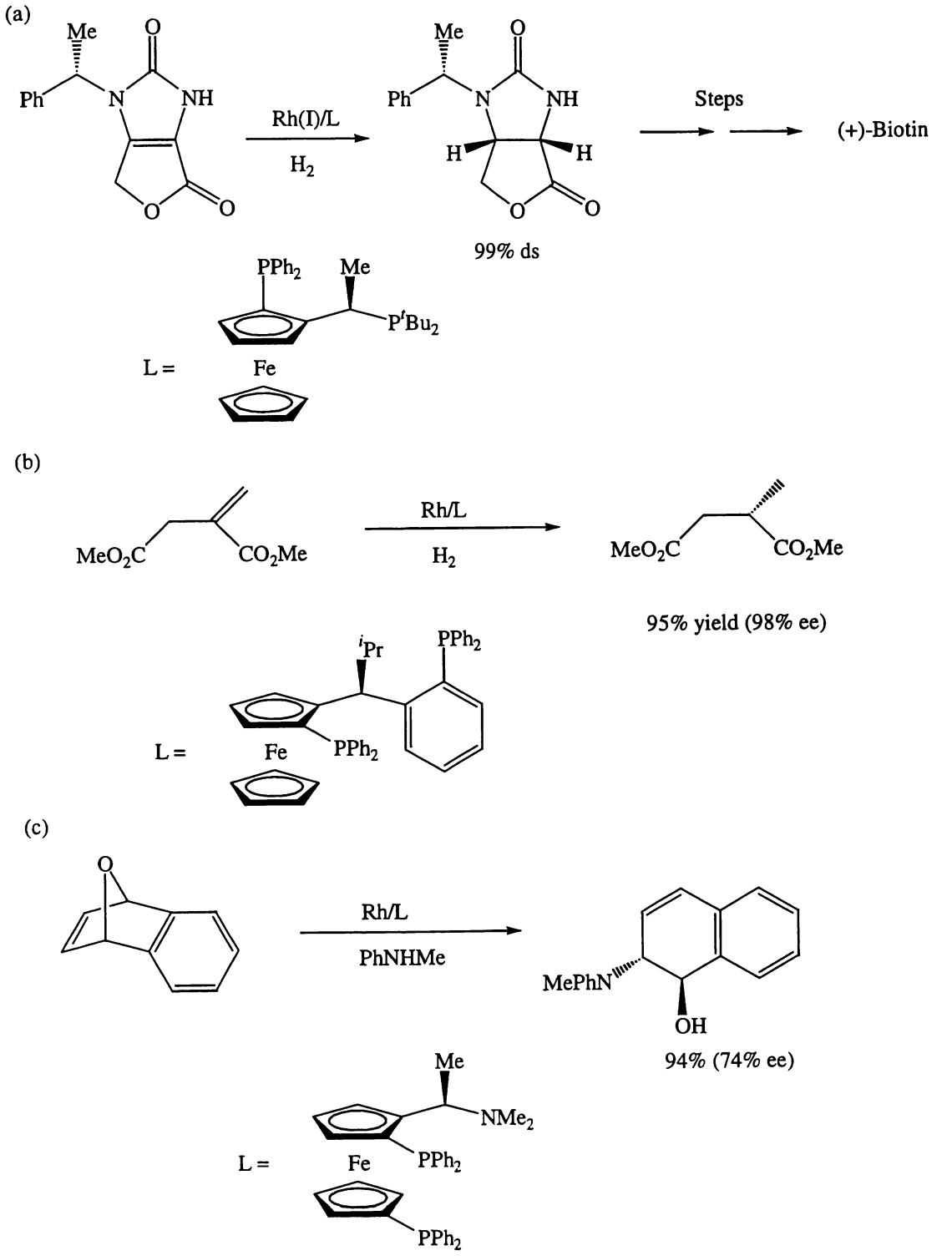

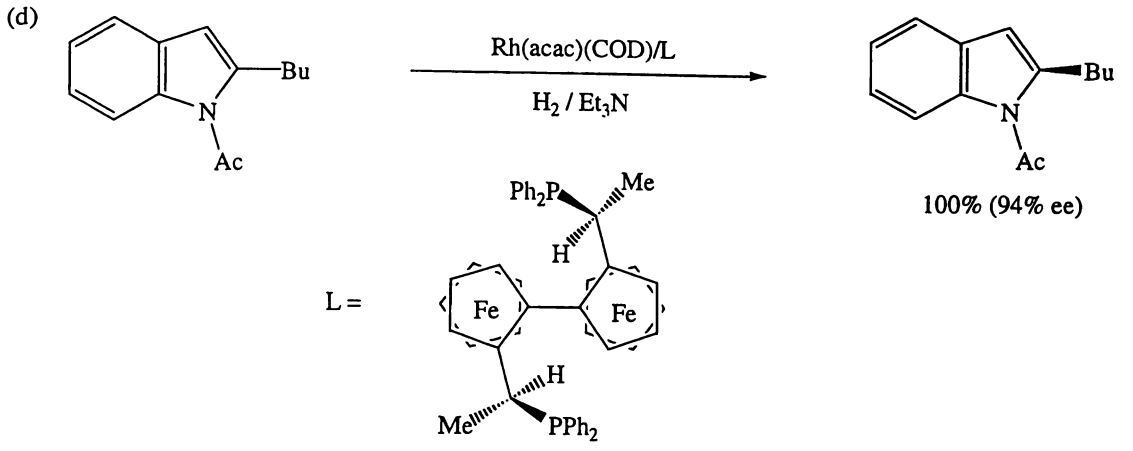

Scheme 1.7: Homogenous Catalysis Involving Chiral Ferrocenyl Phosphine Ligands. (a) synthesis of (+)-Biotin[74]. (b) asymmetric hydrogenation[75]. (c) asymmetric aminolysis[76]. (d) asymmetric hydrogenation[77].

1.2.4: Other Ferrocenyl Phosphines

Ferrocenyl phosphines related to dppf are well known. These include the analogous alkyl phosphines 1,1'-Fc'[PR_2]$_2$ (R = Me[78] **53**, Et[79] **54**, ^{i}Pr[80] **55** and ^{t}Bu[81] **56**). Yamamoto *et al.*[82] have reported the synthesis of 1,1'-bis[(diphenylphosphino)methyl] ferrocene, (dpmf, 1,1'-Fc'[CH_2PPh_2]$_2$ **57**). Reaction of **57** with $(MeCN)_2PdCl_2$ gave the dimeric complex [$PdCl_2(\mu^2$-dpmf)]$_2$ **58**[82]. The bridging nature of dpmf in this complex is in stark contrast to the chelating nature of dppf in Pd(II) complexes. Dpmf was also found to be a bridging ligand in a series of ruthenium(II) and rhodium(III) complexes[83].

---

[74] J. McGarrity, F. Spindler, R. Fuchs and M. Eyer, *Chem. Abstr.*, 1995, **122**, P81369q.
[75] T. Ireland, G. Grossheimann, C. Wieser-Jeunesse and P. Knochel, *Angew. Chem., Int. Ed. Eng.*, 1999, **38**, 3212.
[76] M. Lautens, K. Fagnou and T. Rovis, *J. Am. Chem. Soc.*, 2000, **122**, 5650.
[77] R. Kuwano, K. Sato, T. Kurokawa, D. Karube and Y. Ito, *J. Am. Chem. Soc.*, 2000, **122**, 7614.
[78] J. J. Bishop, A. Davison, M. L. Katcher, D. W. Lichtenberg, R. E. Merrill and J. C. Smart, *J. Organomet. Chem.*, 1971, **27**, 241.
[79] V. Rautenstrauch, K. P. M. Vanhessche, J. Genet and J. Lenoir, Patent Application 1997, WO 9718894.
[80] I. R. Butler, W. R. Cullen and T. J. Kim, *Synth. React. Inorg. Met-Org. Chem.*, 1985, **15**, 109.
[81] W. R. Cullen, T. J. Kim, F. W. B. Einstein and T. Jones, *Organometallics*, 1983, **2**, 714.
[82] Y. Yamamoto, T. Tanase, I. Mori and Y. Nakamura, *J. Chem. Soc., Dalton Trans.*, 1994, 3191.
[83] (a) J. –F. Mai and Y. Yamamoto, *J. Organomet. Chem.*, 1997, **545**, 577. (b) J. –F. Mai and Y. Yamamoto, *J. Organomet. Chem.*, 1998, **560**, 223. (c) J. –F. Mai and Y. Yamamoto, *J. Organomet. Chem.*, 1999, **574**, 148.

Butler *et al.* have prepared a range of diphenylphosphine substituted ferrocenes such as 1,3-Fc'$(PPh_2)_2$ **59**[84], 1,2,1'-Fc"$[PPh_2]_3$[84,85] **60** 1,2,3,1'-Fc"'$[PPh_2]_4$[84] **61** and 1,1',2,2'-Fc"'$[PPh_2]_4$[84] **62**. More distantly related to dppf are the mono-substituted ferrocenyl phosphines $FcPR_2$ (R = Me[86], Et[87], ^{i}Pr[88], ^{t}Bu[89], and Ph[90] **63**). Not surprisingly, given the utility of dppf, the co-ordination chemistry of **63** has been extensively studied[91].

The diferrocenylphosphines Fc_2PR (R = Me[92] **64**, Et[92] **65** and Ph[90] **66**) are known, with the ligating chemistry of **66** being investigated in a number of recent studies[91,93]. Triferrocenylphosphine Fc_3P **67**, has also been prepared and investigated as a ligand[94].

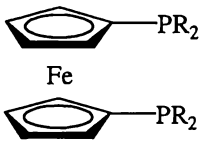

53 R = Me
54 R = Et
55 R = ^{i}Pr
56 R = ^{t}Bu

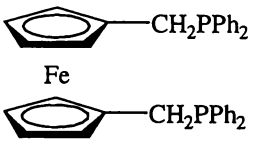

57

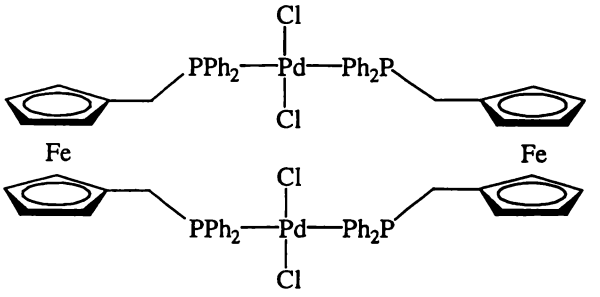

58

[84] I. R. Butler, M. G. B. Drew, C. H. Greenwell, E. Lewis, M. Plath, S. Mussig and J. Szewczyk, *Inorg. Chem. Commun.*, 1999, **2**, 576.
[85] I. R. Butler and W. R. Cullen, *Organometallics*, 1986, **5**, 2537.
[86] Y. Kiso, M. Kumada, K. Tamao and M. Umeno, *J. Organomet. Chem.*, 1973, **50**, 297.
[87] W. R. Cullen, S. J. Rettig and T. C. Zheng, *Can. J. Chem.*, 1993, **71**, 399.
[88] W. R. Cullen, S. J. Rettig and T. C. Zheng, *Organometallics*, 1992, **11**, 3434.
[89] G. Mann, C. Incarvito, A. L. Rheingold and J. F. Hartwig, *J. Am. Chem. Soc.*, 1999, **121**, 3224.
[90] C. E. Sullivan and W. E. McEwen, *Org. Prep. Proced.*, 1970, **2**, 157.
[91] (a) P. K. Baker and D. J. T. Sharp, *J. Coord. Chem.*, 1988, **16**, 389. (b) M. Onishi, K. Hiraki, H. Itoh, H. Eguchi, S. Abe and T. Kawato, *Inorg. Chim. Acta*, 1988, **145**, 105. (c) S. T. Chacon, W. R. Cullen, M. I. Bruce, O. B. Shawkataly, F. W. B. Einstein, R. H. Jones and A. C. Willis, *Can. J. Chem.*, 1990, **68**, 2001. (d) W. R. Cullen, S. J. Rettig and T. C. Zheng, *Can. J. Chem.*, 1992, **70**, 2215. (e) S. Otto, A. Roodt and J. Smith, *Inorg. Chim. Acta.*, 2000, **303**, 295.
[92] V. S. Tulkunova, A. S. Peregudov, Y. Y. Gorelikova, A. I. Krylova, E. N. Tsvetkov, V. D. Vilchevskaya and D. N. Kravstov, *Metalloorg. Khim.*, 1991, **4**, 446.
[93] (a) P. Stepnicka, R. Gyepes, O. Lavastre, P. H. Dixneuf, *Organometallics*, 1997, **16**, 5089. (b) P. Stepnicka and I. Cisarova, *J. Chem. Soc., Dalton Trans.*, 1998, 2807.
[94] (a) C. U. Pittman and G. O. Evans, *J. Organomet. Chem.*, 1972, **43**, 361. (b) J. C. Kotz and C. L. Nivert, *J. Organomet. Chem.*, 1973, **52**, 387.

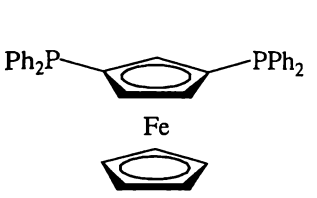

59

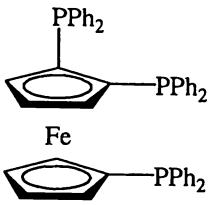

60

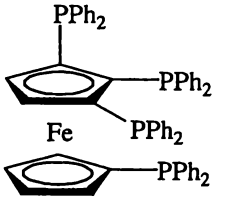

61

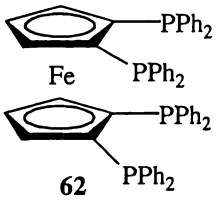

62

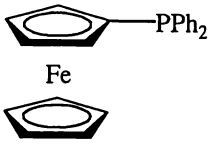

63

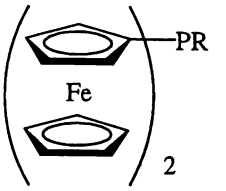

64 R = Me
65 R = Et
66 R = Ph

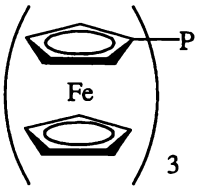

67

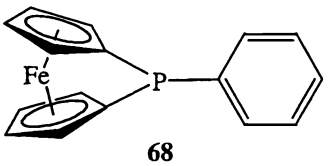

68

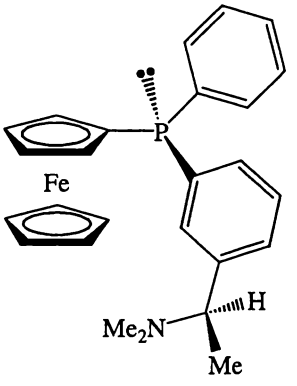

69

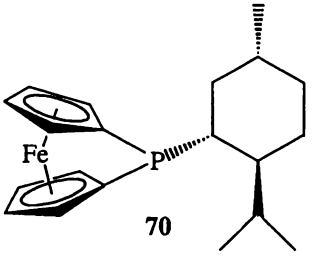

70

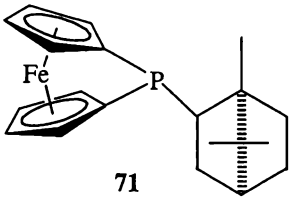

71

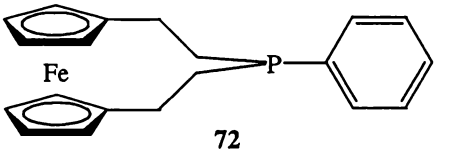

72

Phosphorus bridged ferrocenyl compounds are given the unwieldy title of [1]phosphaferrocenophanes. The archetypal [1]phosphaferrocenophane is (1,1'-ferrocenediyl)phenyl phosphine **68**, which was first synthesised in 1980 by the reaction of 1,1'-$Fc'Li_2$ with $PhPCl_2$[95]. The structure of **68**[96] revealed a significant tilt of the Cp rings to accommodate the phosphorus bridge. This strained situation endows [1]phosphaferrocenophanes with some unique chemical properties. Chief amongst these is the ring opening polymerisation reaction (Scheme 1.8), which may

[95] D. Seyferth and H. P. Withers, *J. Organomet. Chem.*, 1980, C1.
[96] H. Stoeckli-Evans, A. G. Osborne and R. H. Whiteley, *J. Organomet. Chem.*, 1980, **194**, 91.

be conducted under thermal[97], anionic[98] or coordination complex catalysed conditions[99].

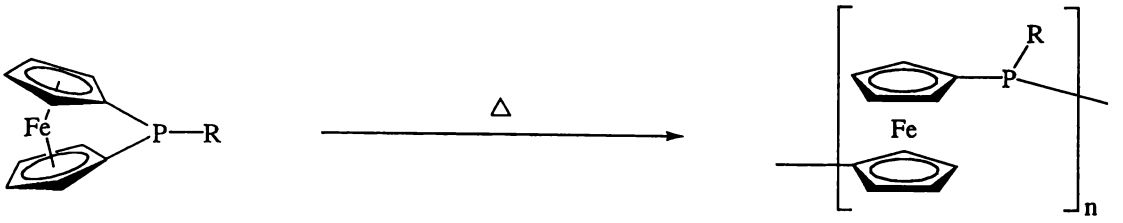

Scheme 1.8: Thermal Ring Opening Polymerisation of [1]Phosphaferrocenophanes.

The coordination chemistry of [1]phosphaferrocenophanes is akin to that of phosphines and many metal complexes of these compounds are known. More recently the chiral ferrocenyl phosphine **69** has been prepared from **68** using a chiral lithium reagent[100], while [1]phosphaferrocenophanes containing menthyl **70** and bornyl **71** chiral auxiliaries have also been characterised[101].

The [3]phosphaferrocenophane (1,1'-ferrocenedienylethyl)phenyl phosphine[102] **72** and selected platinum, palladium and molybdenum complexes thereof[103] have also been synthesised.

1.3 Other Ferrocenyl Phosphorus Compounds

The marriage of ferrocene and phosphorus is not limited to phosphines alone, many other phosphorus groups have been joined to ferrocene. The most common are the phosphine chalcogenides and most common of these are the phosphine oxides. The oxidation of ferrocenyl phosphines by chalcogenides is a simple and high yielding

---

[97] (a) D. A. Foucher, B. -Z. Tang and I. Manners, *J. Am. Chem. Soc.*, 1992, **114**, 6266. (b) C. H. Honeyman, D. A. Foucher, F. Y. Dahmen, R. Rulkens, A. J. Lough and I. Manners, *Organometallics*, 1995, **14**, 5503.

[98] (a) H. P. Withers, D. Seyferth, J. D. Fellman, P. E. Garrou and S. Martin, *Organometallics*, 1982, **1**, 1283. (b) Y. Ni, R. Rulkens and I. Manners, *J. Am. Chem. Soc.*, 1996, **118**, 4102. (c) C. H. Honeyman, T. J. Peckham, J. A. Massey and I. Manners, *Chem. Commun.*, 1996, 2589.

[99] N. P. Reddy, H. Yamashita and M. Tanaka, *J. Chem. Soc., Chem. Commun.*, 1995, 2265.

[100] I. R. Butler, W. R. Cullen, S. J. Rettig and A. S. C. White, *J. Organomet. Chem.*, 1995, **492**, 157.

[101] H. Brunner, J. Klankermayer and M. Zabel, *J. Organomet. Chem.*, 2000, **601**, 211.

[102] O. J. Curnow, G. Huttner, S. J. Smail and M. M. Turnbull, *J. Organomet. Chem.*, 1996, **524**, 267.

[103] J. J. Adams, O. J. Curnow, G. Huttner, S. J. Smail and M. M. Turnbull, *J. Organomet. Chem.*, 1999, **577**, 44.

reaction and many such derivatives exist[104] (ferrocenyl phosphine oxides are an integral component in TRAPS (Figure 1.3) ligand synthesis[53]). Chalcogenide derivatives of dppf (**73-75**) have been used as ligands in copper[105], gold[106], rhenium[107] and silver[106a, 108] complexes. The oxide 1,1'-Fc'[P(O)Ph_2]$_2$ (dppfo) forms the palladium(II) complex (dppfo)$PdCl_2$ **76**, which is unusual in crystallising with tetrahedral geometry[109].

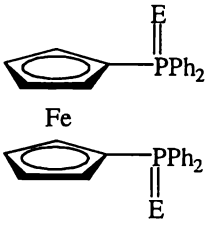

73 E = O
74 E = S
75 E = Se

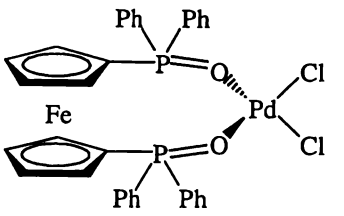

76

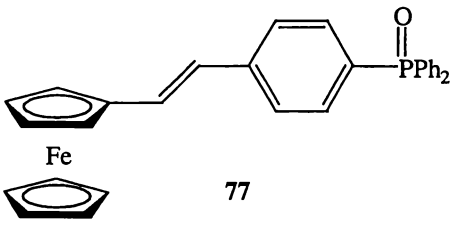

77

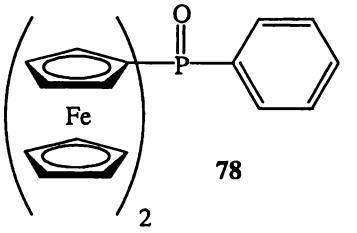

78

Further examples of ferrocenyl phosphine oxides include the conjugated compound FcCHCH(C_6H_4)P(O)Ph_2 **77**[110] and phenyldiferrocenylphosphine oxide Fc_2P(O)Ph **78**[111].

A few ferrocenyl phosphonites such as 1,1'-Fc'[P(OCH_2)$_2$$CMe_2$]$_2$[112] **79** and the chiral 1,1'-Fc'[P(O,O'-BINOL)[113] **80** (BINOL = binaphthol) are known. Rhodium

---

[104] (a) V. Munyejabo, M. Postel, J. L. Roustan and C. Bensimon, *Acta. Cryst., Sect. C.*, 1994, **C50**, 224. (b) Z. -G. Fang, T. S. A. Hor, Y. -S. Wen, L. -K. Liu and T. C. W. Mak, *Polyhedron*, 1995, **14**, 2403. (c) M. Bolte, F. Naumann and A. S. K. Hashmi, *Acta. Cryst., Sect. C.*, 1997, **C53**, 1785.

[105] (a) G. Piloni, B. Longato, G. Bandoli and B. Corain, *J. Chem. Soc., Dalton Trans.*, 1997, 819. (b) G. Piloni, B. Longato and G. Bandoli, *Inorg. Chim. Acta.*, 1998, **277**, 163.

[106] (a) M. C. Gimeno, P. G. Jones, A. Laguna and C. Sarroca, *J. Chem. Soc., Dalton Trans.*, 1995, 3563. (b) M. C. Gimeno, P. G. Jones, A. Laguna and C. Sarroca, *J. Organomet. Chem.*, 2000, **596**, 10.

[107] T. S. A. Hor, H. S. O. Chen, K. L. Tan, L. T. Phang, Y. K. Yan, L. K. Liu and Y. S. Wen, *Polyhedron*, 1991, **10**, 2437.

[108] (a) G. Piloni, B. Longato and G. Bandoli, *Inorg. Chim. Acta.*, 2000, **298**, 251. (b) M. C. Gimeno, P. G. Jones, A. Laguna and C. Sarroca, *J. Chem. Soc., Dalton Trans.*, 1998, 1277.

[109] J. S. L. Yeo, J. J. Vittal and T. S. A. Hor, *Chem. Commun.*, 1999, **16**, 1477.

[110] D. W. Allen, J. P. Mifflin and P. J. Skabara, *J. Organomet. Chem.*, 2000, **601**, 293.

[111] L. Eberhard, J. P. Lampin and F. Mathey, *J. Organomet. Chem.*, 1974, **80**, 109.

complexes of **80** were found to be excellent chiral hydrogenation catalysts[113]. The ferrocenyl phosphonite 1,1'-Fc'[P(OEt)$_2$]$_2$ is found as an intermediate in the synthesis of **44**[67].

Ferrocenolato phosphites such as [1,1'-Fc'(O)$_2$]PR (R = Cl and Ph **81**) and the more complex 1,1'-Fc'[(OP)$_2$R]$_2$ (R = 1,1'-Fc'(O)$_2$) **82** were synthesised by the reaction of ferrocenols with chlorophosphines[114]. The same report detailed the synthesis of a range of novel ferrocenolato phosphorus compounds including, (FcO)$_2$P(O)Cl **83**, (FcO)$_3$P(E) (E = O and S **84**), 1,1'-Fc'[(OP(O))$_2$R]$_2$ (R = 1,1'-Fc'(O)$_2$) **85** and the phosphonate esters RP(O)(OFc)$_2$ (R = Me, ^{n}Bu, Ph and Fc **86**)

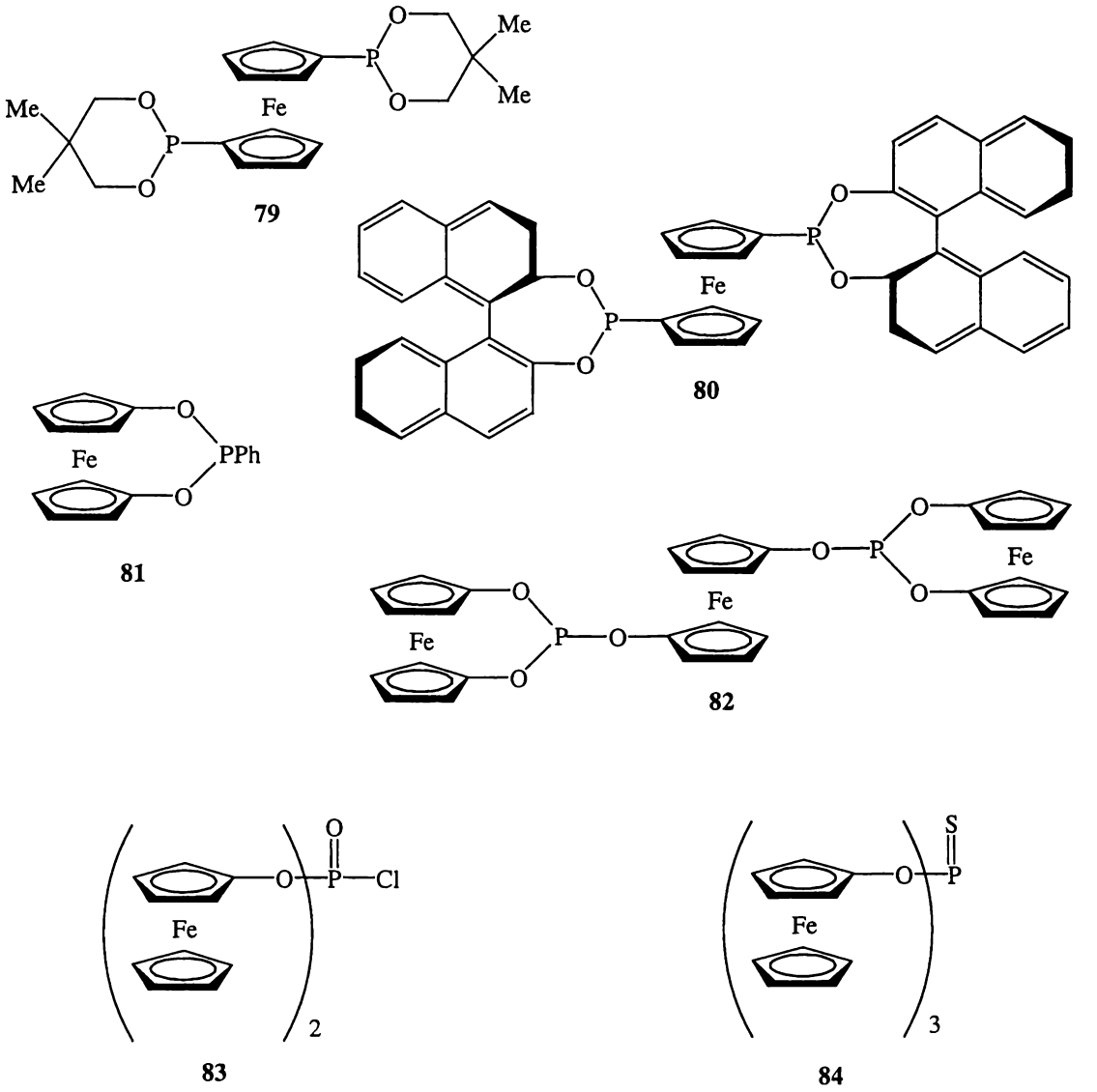

[112] I. E. Nifantev, L. F. Manzhukova, M. Y. Antipin, Y. T. Struchkov and E. E. Nifantev, *Zh. Obshch. Khim.*, 1995, **65**, 756.
[113] M. T. Reetz, A. Gosberg, R. Goddard and S. –H. Kyung, *Chem. Commun.*, 1998, **19**, 2077.
[114] M. Herberhold, A. Hofmann and W. Milius, *J. Organomet. Chem.*, 1998, **555**, 187.

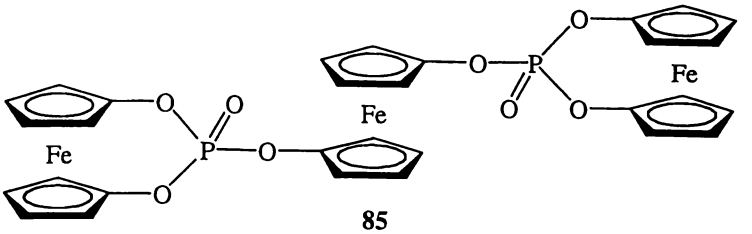

85

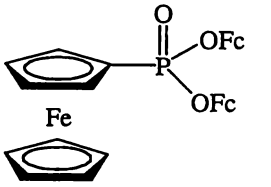

86

A series of ferrocenylmethyl phosphonates have been synthesised by Boev *et al.*[115] by the condensation of dialkyl phosphites with ferrocenylaldehyde. Typical examples of this series include $FcCH(OAc)P(O)(OEt)_2$ **87**, $FcCH(NHPh)P(O)(OEt)_2$ **88** and the thiophosphonate $FcCH(NHPh)P(S)(O^iPr)_2$ **89**. The ferrocenyl phosphonate $FcCH_2P(O)(OPh)_2$ **90** was recently synthesised from ferrocenyl methanol by the action of triphenyl phosphite[116]. The ferrocenyl phosphate salt $FcCH_2CH_2OPO_3Na_2$ **91** was recently reported as a useful substrate for electrochemical analysis of alkaline phosphatase activity[117].

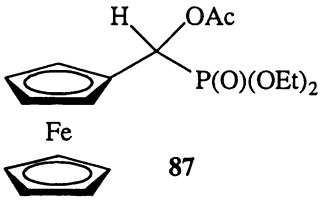

87

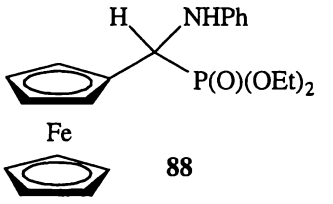

88

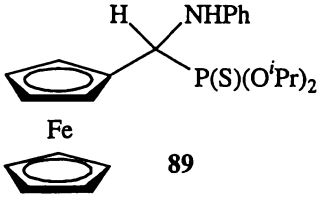

89

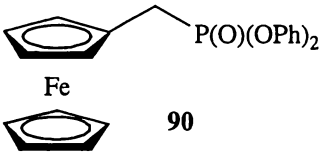

90

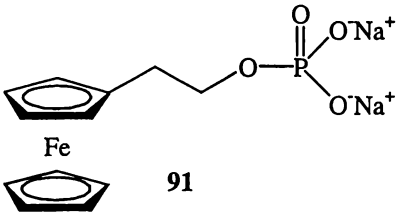

91

Ferrocenyl phosphorus compounds that contain P-N bonds were first prepared by Sollot and Peterson[118] who reacted ferrocene and amidophosphochloridates under Friedel-Crafts conditions to give a range of products including $(Fc)_2PNR_2$ and $(Fc)_2P(O)NR_2$ (R = Me and Ph).

---

[115] (a) V. I. Boev and A. V. Dombrovskii, *Zh. Obshch. Khim.*, 1977, **47**, 2215. (b) V. I. Boev, *Zh. Obshch. Khim.*, 1977, **47**, 2527. (c) V. I. Boev and Y. L. Volyanskii, *Khim. Farm. Zh.*, 1977, **11**, 39. (d) V. I. Boev and A. V. Dombrovskii, *Zh. Obshch. Khim.*, 1979, **49**, 1246. (e) V. I. Boev and Y. L. Volyanskii, *Khim. Farm. Zh.*, 1979, **13**, 68. (f) V. I. Boev and B. S. Fedorov, *Khim. Khim. Tekhnol.*, 1982, **25**, 41.

[116] W. Henderson, A. G. Oliver and A. J. Downard, *Polyhedron*, 1996, **15**, 1165.

[117] B. Limoges and C. Degrand, *Anal. Chem.*, 1996, **68**, 4141.

[118] G. P. Sollot and W. R. Peterson, *J. Organomet. Chem.*, 1969, **19**, 143.

A more specific and high yielding synthesis of ferrocenyl phosphoramides is the reaction of lithiated ferrocene with diamidophosphochloridates, Scheme 1.9.

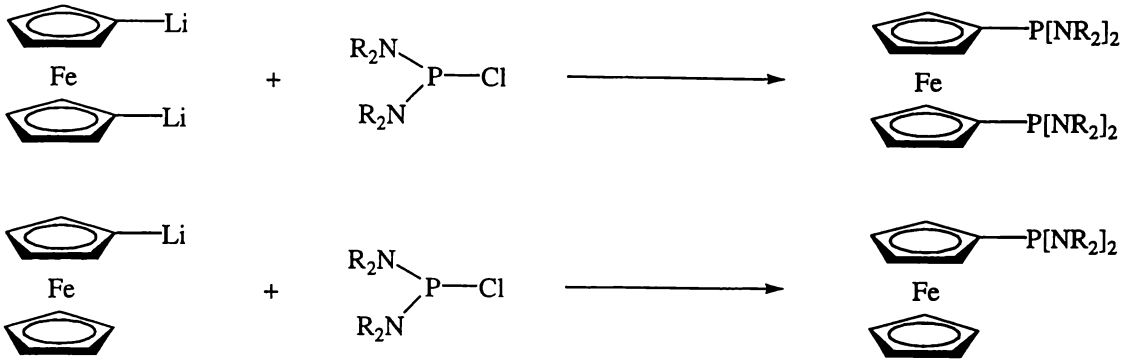

Scheme 1.9: Synthesis of Ferrocenyl Phosphoramides from Lithiated Ferrocene.

Using this method compounds such as $FcP[N(Me)CH_2CH_2N(Me)]$[119] **92**, 1,1-$Fc[P(NEt_2)_2]_2$[113] **93** and the [1]phosphaferrocenophane 1,1'-$FcPN(^iPr)_2$ **94**[120] have been prepared in high yield.

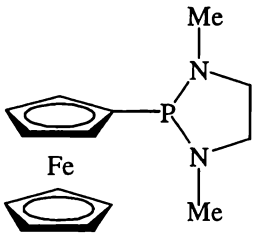

92

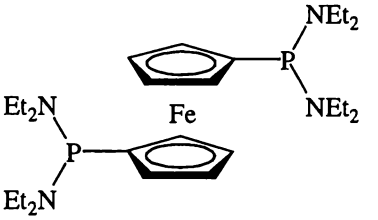

93

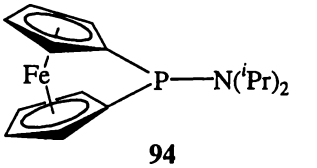

94

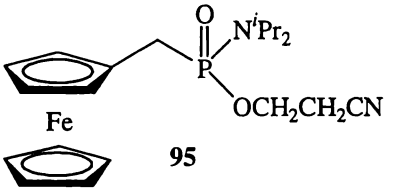

95

More recently the Michealis-Arbuzov reaction between $FcCH_2OH$ and *β*-cyano-N,N-diisopropylchlorophosphoramidite resulted in the synthesis of the ferrocenylmethyl phosphoramidate, $FcCH_2P(O)(N^iPr_2)(OCH_2CH_2CN)$ **95**[121]. A related ferrocenyl phosphoramidate $Fc(CH_2)_6OP\{N(^iPr)_2\}(OCH_2CH_2CN)$ **96** was

[119] I. E. Nifantev, A. A. Borisenko, L. F. Manzhukova and E. E. Nifantev, *Phos. Sulfur Silicon Relat. Elem.*, 1992, **68**, 99.
[120] M. Herberhold, F. Hertel, W. Milius and B. Wrackmeyer, *J. Organomet. Chem.*, 1999, **582**, 352.
[121] C. J. Isaac, M. R. J. Elsegood, W. Clegg, N. H. Rees, B. R. Horrocks and A. Houlton, *Polyhedron*, 1998, **17**, 3817.

reacted with oligonucleotides to give ferrocenyl phosphate substituted DNA fragments as shown in Figure 1.6[122]. The self-assembly chemistry of DNA was utilised to grow stable monolayers of these redox active compounds on suitably prepared gold surfaces.

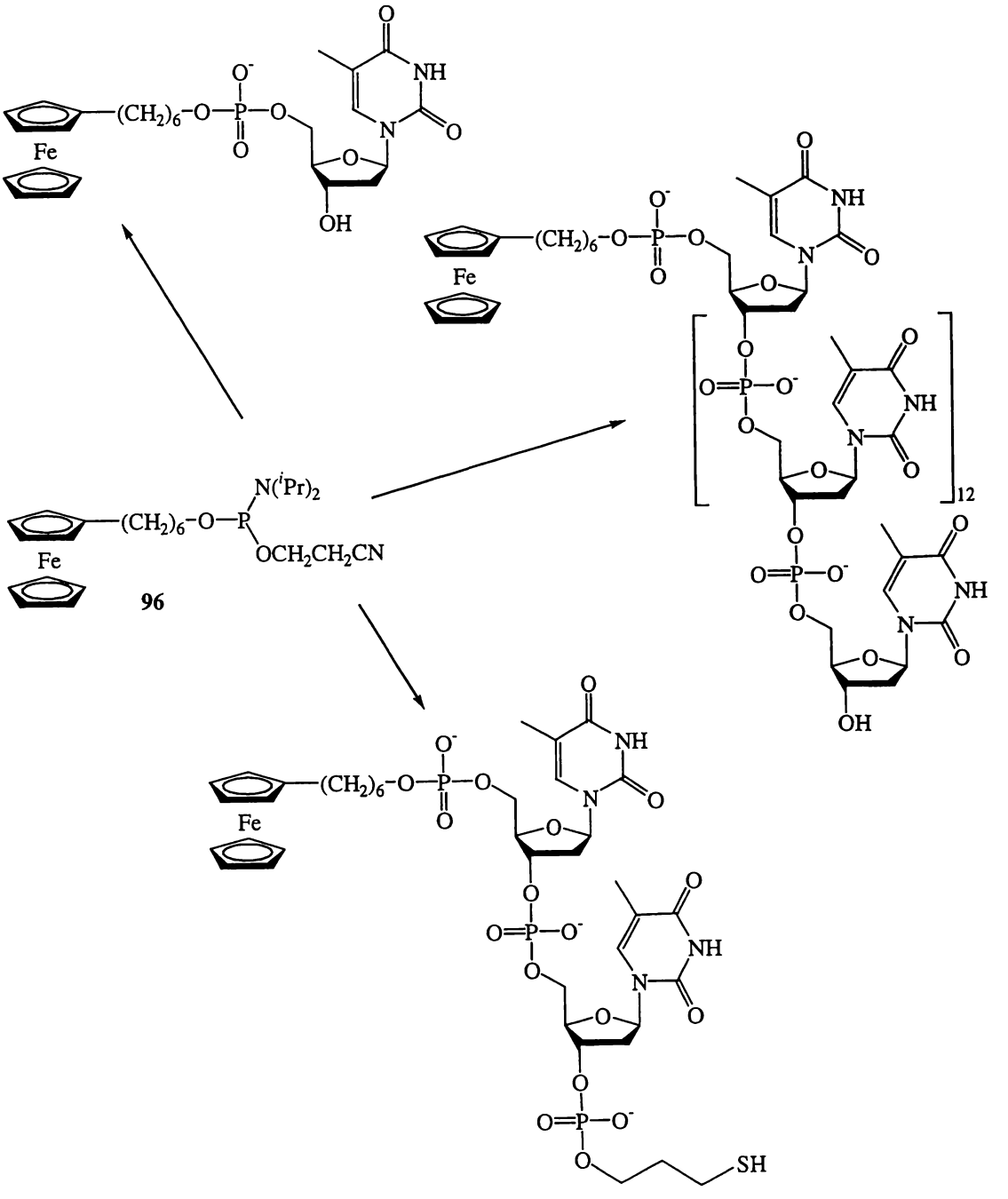

Figure 1.6: Redox Active DNA Fragments Derived from $Fc(CH_2)_6OP\{N(^iPr)_2\}(OCH_2CH_2CN)$ **96**.

[122] R. C. Mucic, M. K. Herrlein, C. A. Mirkin and R. L. Letsinger, *Chem. Commun.*, 1996, 555.

The first ferrocenyl derivatives of cylclophosphazenes, $N_3P_3F_5(Fc)$ **97** and $N_4P_4F_7(Fc)$ **98**, were synthesised in 1982[123]. A large number of related compounds have subsequently been prepared, some of which are shown in Figure 1.7.

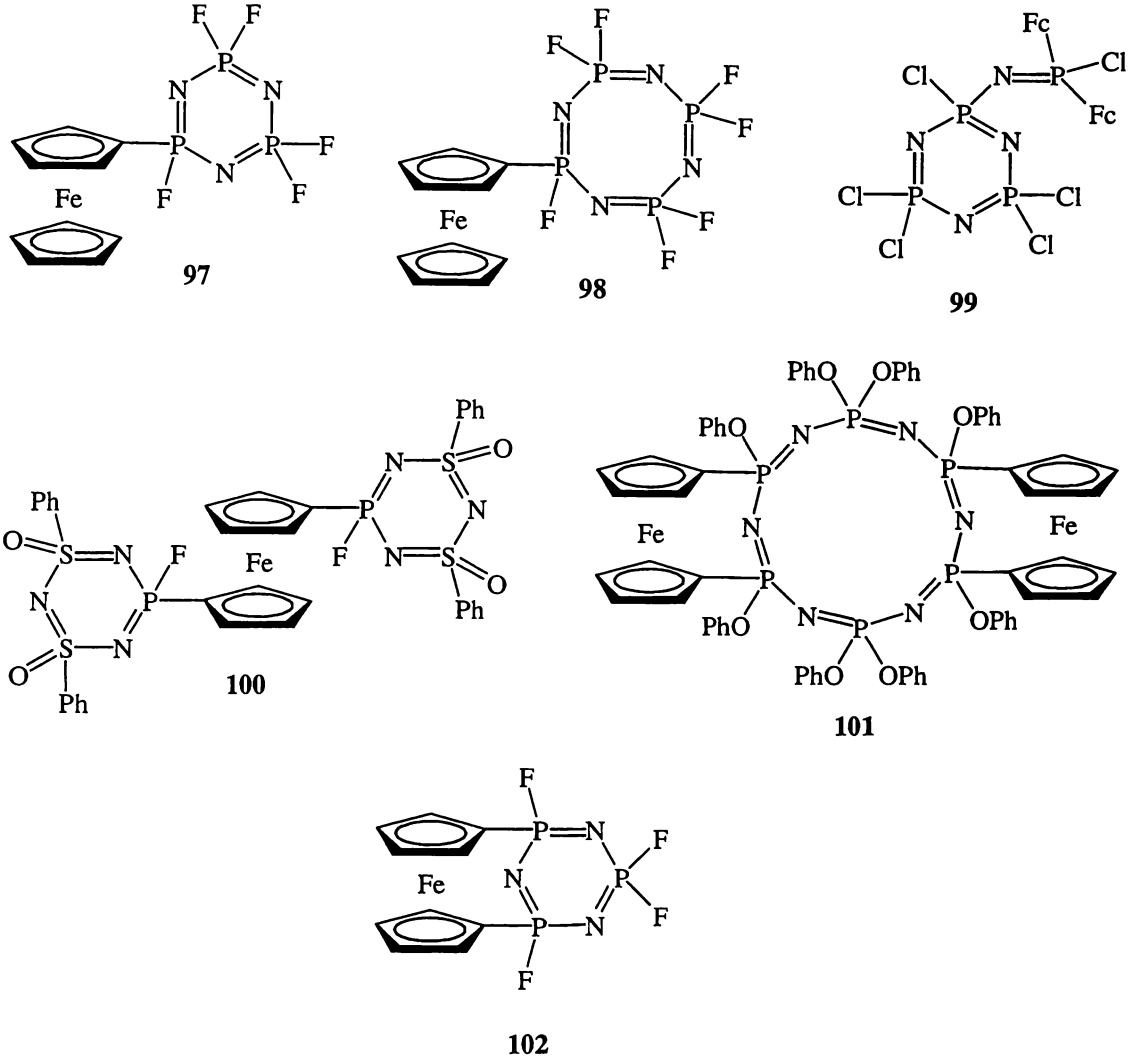

Figure 1.7: Examples of Ferrocenyl Cyclophosphazenes and Related Compounds. References: **99**[124], **100**[125], **101**[126], **102**[127].

[123] P. R. Suszko, R. R. Whittle and H. R. Allcock, *J. Chem. Soc., Chem. Commun.*, 1982, 960.
[124] H. R. Allcock, K. D. Lavin, G. H. Riding and R. R. Whittle, *Organometallics*, 1984, **3**, 663.
[125] A. Meetsma, H. F. M. Schoo, J. C. van de Grampel and W. P. Bosman, *Acta. Cryst.*, 1987, **C43**, 2314.
[126] I. Manners, G. H. Riding, J. A. Dodge and H. R. Allcock, *J. Am. Chem. Soc.*, 1989, **111**, 3067.
[127] I. Manners, W. D. Coggio, M. N. Mang, M. Parvez and H. R. Allcock, *J. Am. Chem. Soc.*, 1989, **111**, 3481.

Interest in these and related compounds, is due to their ring opening polymerisation chemistry which has been widely studied[125,128]. A typical example of ring opening polymerisation is given in Scheme 1.10.

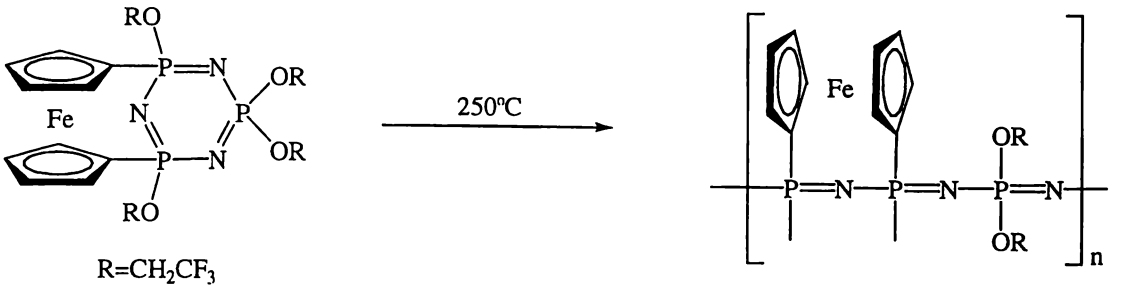

Scheme 1.10: An Example of Ring Opening Polymerisation of Ferrocenyl Cyclophosphazenes.

A significant number of ferrocenyl phosphorus compounds containing at least one P-S bond are known. The starting point for much of this chemistry has been diferrocenyldithiadiphosphetane disulphide $Fc_2P_2S_4$ **103**, which was synthesised by Woollins *et al.* in 1996 from the reaction of ferrocene with P_4S_{10} (Scheme 1.11)[129].

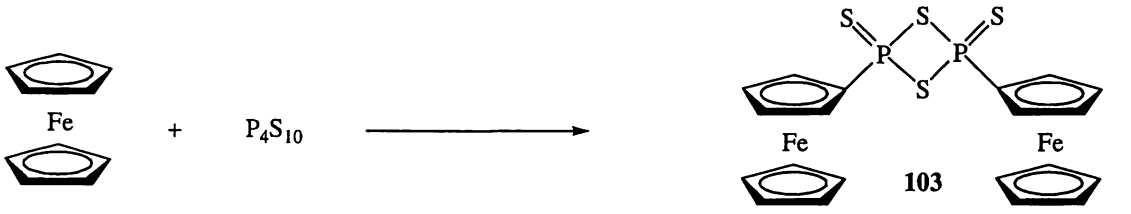

Scheme 1.11: Synthesis of $Fc_2P_2S_4$ **103**.

The most notable feature of **103** is its ability to act as a source of $FcPS_2$. The reaction of **103** with unsaturated compounds such as dialkyl cyanamides[130], imines[130],

---

[128] (a) H. R. Allcock, K. D. Lavin and G. H. Riding, *Macromolecules*, 1985, **18**, 1340. (b) H. R. Allcock, K. D. Lavin, G. H. Riding, R. R. Whittle and M. Parvez, *Organometallics*, 1986, **5**, 1626. (c) R. A. Saraceno, G. H. Riding, H. R. Allcock and A. G. Ewing, *J. Am. Chem. Soc.*, 1988, **110**, 7254. (d) H. R. Allcock, J. A. Dodge, I. Manners and G. H. Riding, *J. Am. Chem. Soc.*, 1991, **113**, 9596.

[129] M. R. St. J. Foreman, A. M. Z. Slawin and J. D. Woollins, *J. Chem. Soc., Dalton Trans.*, 1996, 3653.

[130] (a) M. R. St. J. Foreman, A. M. Z. Slawin and J. D. Woollins, *Chem. Commun.*, 1997, 1269. (b) M. R. St. J. Foreman, R. J. Mortimer, A. M. Z. Slawin and J. D. Woollins, *J. Chem. Soc., Dalton Trans.*, 1999, 3419.

olefins[131], aldehydes[131], alcohols[129,132] and metal complexes[129,132] has led to the synthesis of a wide range of FcPS compounds some of which are shown in Figure 1.8.

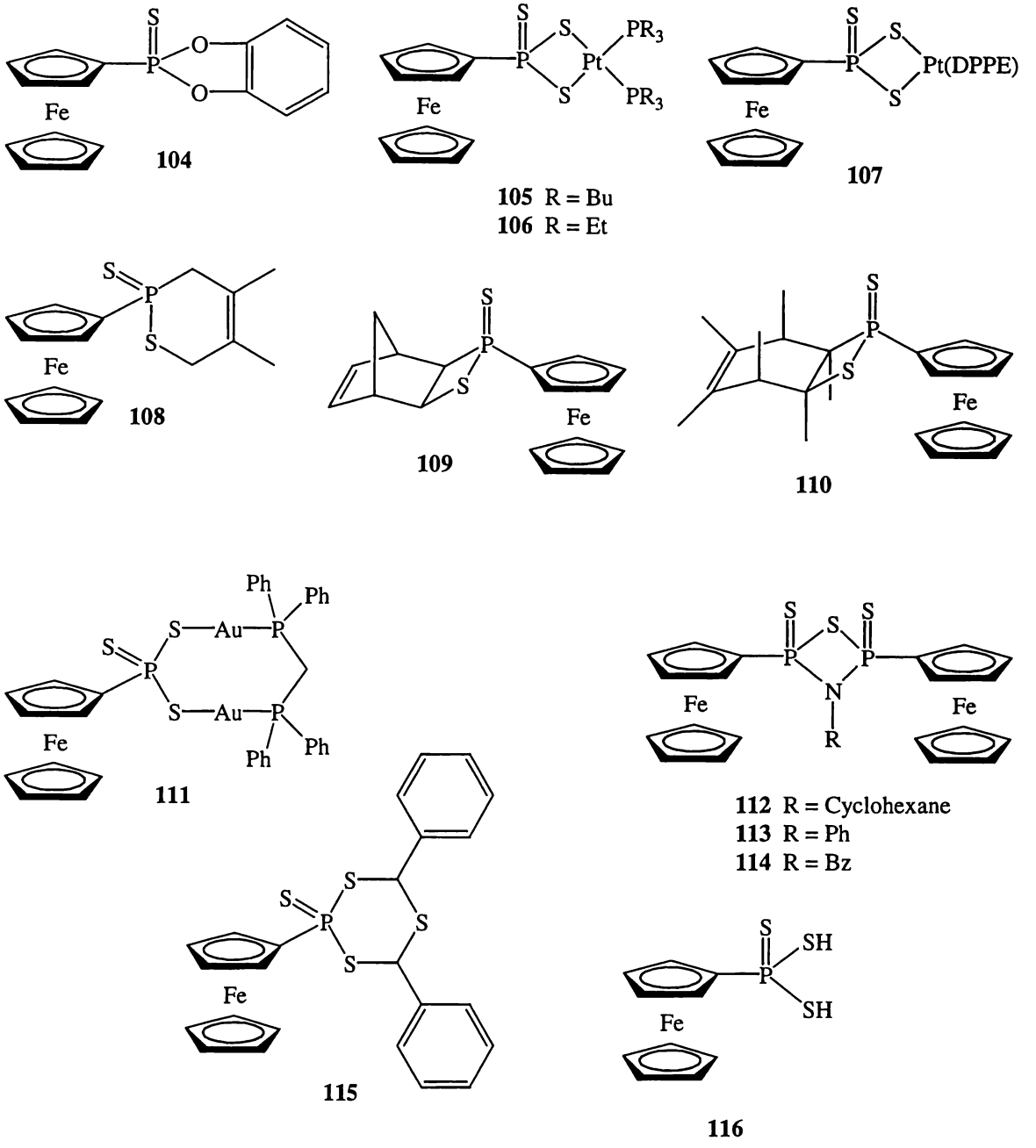

Figure 1.8: Derivatives of $Fc_2P_2S_4$ **103**. References: **104-107**[129], **108-110**[131], **111 116**[132] and **112-115**[130]

[131] (a) M. R. St. J. Foreman, A. M. Z. Slawin and J. D. Woollins, *Chem. Commun.*, 1997, 855. (b) M. R. St. J. Foreman, A. M. Z. Slawin and J. D. Woollins, *J. Chem. Soc., Dalton Trans.*, 1999, 1175.
[132] W. E. v Zyl, R. J. Staples and J. P. Fackler, *Inorg. Chem. Commun.*, 1998, **1**, 51.

Thus far, all of the ferrocenyl phosphorus compounds surveyed have been neutral species. The reaction of phosphines with acidic compounds leads to the formation of phosphonium salts that contain a quaternised phosphorus atom bearing a positive charge. Ferrocenyl phosphines are no exception and a number of ferrocenyl phosphonium compounds have precedence in the literature. Typical examples include triferrocenyliodophosphonium triiodide $Fc_3P(I)^+I_3^-$ **117**[133] and benzyldiphenylferrocenylphosphonium chloride $FcPh_2BzP^+Cl^-$ **118**[134]. The phosphonium salts $[FcPh_2P(CH_2C_6H_4X)]^+BF_4^-$ (X = H, OMe, F and CN **119**) were used to investigate the electronic relationship between the ferrocenyl group and the phosphonium phosphorus atom[135]. The ferrocenyl group was found to be weakly electron donating, presumably due to contribution from the $Cp^+=PR_3$ ylidic resonance structure. More recently the chiral, but racemic phosphonium salt $FcCH(COPh)PPh_3^+I^-$ **120**[136] and the conjugated salt $FcCHCHC_6H_4PPh_3^+Br^-$ **121**[110] have been prepared and characterised.

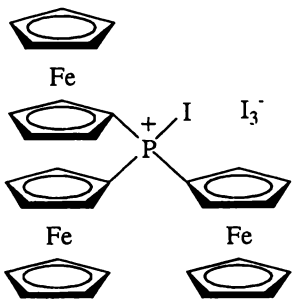

117

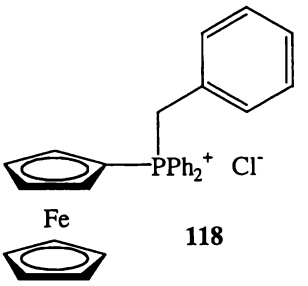

118

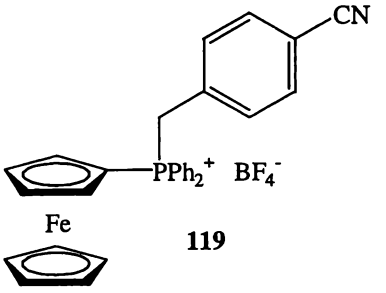

119

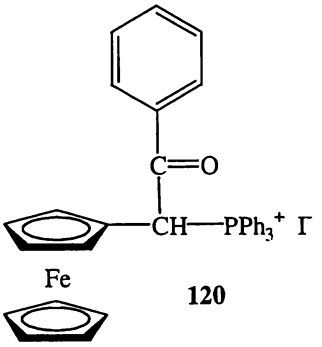

120

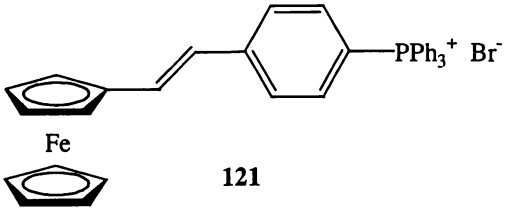

121

[133] G. V. Gridunova, V. E. Shklover, Y. T. Struchkov, V. D. Vilchevskaya, N. L. Podobedova and A. I. Krylova, *J. Organomet. Chem.*, 1982, **238**, 297.
[134] W. E. McEwen, C. E. Sullivan and R. O. Day, *Organometallics*, 1983, **2**, 420.
[135] C. Imrie, T. A. Modro and P. H. v. Rooyen, *Polyhedron*, 1994, **13**, 1677.
[136] S. Z. Ahmed, C. Glidewell and G. Ferguson, *Acta. Cryst.*, 1996, **C52**, 1634.

1.4: Concluding Remarks

The success of dppf and chiral ferrocenyl phosphines as ligands in catalytic systems dominates the study of ferrocenyl phosphorus compounds. Current research continues to focus on the development of new and improved ferrocenyl phosphine ligands and the application of existing ferrocenyl phosphine catalysts to new organic reactions. As understanding of the relationship between ligand structure and catalyst function has increased, a general trend toward the development of ever more complex ferrocenyl phosphine ligands can be observed. Ligand design is becoming more and more a considered science rather than a hopeful shot in the dark.

The foundation for this chemistry is ultimately the unique structural features of ferrocene. The ability of ferrocenyl cyclopentadienyl rings to flex and rotate about the central iron atom to relieve steric stress plays no small part in the usefulness of ferrocenyl phosphine compounds as ligands in catalytic systems. Understandably therefore, a significant body of research exists concerning phosphine derivatives of other metallocenes such as ruthenocene[137] and in a similar vein, the study of ferrocenyl arsines[138] has also been encouraged by the success of ferrocenyl phosphines. Each of these topics lies outside the scope of this review and for more information the reader is referred to the references cited.

The preparation of redox active materials accounts for most ferrocenyl phosphorus research not concerned with catalysis. For these applications the electrochemistry of the ferrocene is paramount and the phosphorus group serves solely as an atomic 'glue' for binding the ferrocene to a suitable substrate.

Despite all of the research outlined in this review there are many interesting aspects of ferrocenyl phosphorus chemistry yet to be studied. The chemistry discussed in this thesis contains elements related to both ferrocenyl phosphine

---

[137] (a) K. Kirchner, K. Mereiter, K. Mauthner and R. Schmid, *Inorg. Chim. Acta.*, 1994, **217**, 203. (b) B. Wei, S. Li, H. K. Lee, T. S. A. Hor, *J. Organomet. Chem.*, 1997, **527**, 133. (c) U. Burckhardt, M. Baumann, G. Trabesinger, V. Gramlich and A. Togni, *Organometallics*, 1997, **16**, 5252. (d) B. Wei, S. Li, H. K. Lee and T. S. A. Hor, *J. Mol. Catal. A: Chem.*, 1997, **126**, L83. (e) S. P. Yeo, W. Henderson, T. C. W. Mak and T. S. A. Hor, *J. Organomet. Chem.*, 1999, **575**, 171.

[138] (a) A. Davison and J. J. Bishop, *Inorg. Chem.*, 1971, **10**, 826. (b) A. Davison and J. J. Bishop, *Inorg. Chem.*, 1971, **10**, 832. (c) C. G. Pierpont and R. Eisenberg, *Inorg. Chem.*, 1972, **11**, 828. (d) J. T. Mague and M. O. Nutt, *Inorg. Chem.*, 1977, **16**, 1259. (e) D. Seyferth and H. P. Withers, *J. Organomet. Chem.*, 1980, **185**, C1. (f) M. G. Fitzpatrick, L. R. Hanton and J. Simpson, *Inorg. Chim. Acta.*, 1996, **244**, 131.

chemistry and the development of ferrocenyl compounds suitable for incorporation into redox active materials.

Chapters four, five and six describe the chemistry of novel ferrocenyl phosphines, particularly those possessing unusual stability in air and those possessing solubility in water. To begin with however, there are two chapters describing the chemistry of novel ferrocenyl phosphorus compounds possessing oxidatively inert phosphorus groups. These compounds are eminently suitable for incorporation into redox active materials and that is where the tale begins.

Chapter 2: Synthesis and Characterisation of Ferrocenyl Phosphonic and Arsonic Esters and Acids

2.1: Introduction

Phosphonic acids are diprotic acids with the general formula $RP(O)(OH)_2$, (R = aryl or alkyl). Typically crystalline compounds with high melting points, these acids form insoluble salts, called metal phosphonates, with most metal ions. Metal phosphonates have excited considerable interest in recent times because the chemical and physical properties of these materials can be engineered to a high degree of precision by using appropriately functionalised phosphonic acids[1]. Phosphonic acids containing macro-cyclic[2], photo-active[3], acidic[4], basic[5], chiral[6] and organometallic[7] functional groups have been incorporated into metal phosphonates. The use of appropriate phosphonic acids has resulted in metal phosphonates with ion exchange[8], molecular recognition[9], catalytic[3a,10] and light harvesting[11] properties.

The primary goal of this project was to synthesise phosphonic acids containing the ferrocene moiety and incorporate these into metal phosphonate salts. The chemistry of ferrocene and its derivatives has been intensely studied since its synthesis in 1965, but most of the interest has focused on ferrocenyl-phosphine compounds as ligands in coordination chemistry. Reports of phosphonic acid derivatives of ferrocene are rare.

---

[1] (a) G. Cao, H. –G. Hong and T. E. Mallouk, *Acc. Chem. Res.*, 1992, **25**, 420. (b) M. E. Thompson, *Chem. Mater.*, 1994, **6**, 1168. (c) A. Clearfield, *Chem. Mater.*, 1998, **10**, 2801. (d) A. Clearfield, *Prog. Inorg. Chem.*, 1998, **47**, 371.

[2] C. V. K. Sharma and A. Clearfield, *J. Am. Chem. Soc.*, 2000, **122**, 1558.

[3] L. A. Vermeulen and M. E. Thompson, *Chem. Mater.*, 1994, **6**, 77.

[4] (a) P. M. DiGiacomo and M. B. Dines, *Polyhedron*, 1982, **1**, 61. (b) D. A. Burwell and M. E. Thompson, *Chem. Mater.*, 1991, **3**, 14.

[5] (a) C. Y. Ortiz-Avila, C. Bhardwaj and A. Clearfield, *Inorg. Chem.*, 1994, **33**, 2499. (b) M. Casciola, U. Constantino, A. Peraio and T. Rega, *Solid State Ionics*, 1995, **77**, 229.

[6] F. Fredoueil, M. Evain, M. Bujoli-Doeuff and B. Bujoli, *Eur. J. Inorg. Chem.*, 1999, 1077.

[7] C. F. Lee and T. E. Mallouk, *Inorg. Chem.*, 1991, **30**, 4.

[8] M. B. Dines and P. M. DiGiacomo, *Inorg. Chem.*, 1981, **20**, 92.

[9] (a) G. Cao, M. E. Garcia, M. Alcala, L. F. Burgess and T. E. Mallouk, *J. Am. Chem. Soc.*, 1992, **114**, 7574. (b) T. Kijima, S. Watanabe, K. Ohe and M. Machida, *J. Chem. Soc., Chem. Commum.*, 1995, 75.

[10] K. P. Reis, V. K. Joshi and M. E. Thompson, *J. Catal.*, 1996, **161**, 62.

[11] (a) L. A. Vermeulen and M. E. Thompson, *Nature*, 1992, **358**, 656. (b) L. A. Vermeulen and M. E. Thompson, *Chem. Mater.*, 1994, **6**, 77.

The ferrocenyl phosphonic acid $FcP(O)(OH)_2$ has been reported in patent literature[12] as an ingredient in explosive complexes of ferrocene and inorganic nitrates, while the ferrocenyl phosphonic acid $Fc(CH_2)_6P(O)(OH)_2$ has been investigated as a surface selective electrode coating[13]. Of most interest to the current work was the synthesis of the ferrocenyl phosphonic acid $FcC(O)N(H)C_6H_4CH_2PO(OH)_2$[14]. This acid was incorporated into zirconium phosphonate multilayer films supported on gold electrodes and the electrochemistry of the ferrocene group investigated, (such supported metal phosphonate multilayers are solid state Langmuir-Blodgett analogues and the subject of a considerable body of literature[15]). This author is aware of no other published literature concerning ferrocenyl phosphonic acids.

Arsonic acids $R\text{-}As(O)(OH)_2$ are also diprotic but tend to be weaker acids than the analogous phosphonic acids. They also form salts with metals[16] but these metal arsonate materials have generated much less interest than the metal phosphonates. Synthesis of ferrocenyl arsonic acids was attempted to provide a comparison with the ferrocenyl phosphonic acids.

2.2: Synthesis and Characterisation of Ferrocenyl Phosphonic Acids

Synthetic methods for the preparation of phosphonic acids are well developed and have been the subject of several comprehensive reviews[17]. Direct syntheses of phosphonic acids from separate phosphorus and carbon-containing precursors are rare[18]. Most of the common methods require the preparation of a compound

---

12 G. P. Sollot, W. R. Peterson Jr., (United States Dept. of the Army), Patent application U.S. 69-827161 19690523, CAN. 77:128636, AN. 1972:528636

13 T. J. Gardner, C. D. Frisbie and M. S. Wrighton, *J. Am. Chem. Soc.*, 1995, **117**, 6927.

14 H. –G. Hong and T. E. Mallouk, *Langmuir*, 1991, **7**, 2362.

15 (a) H. E. Katz, *Chem. Mater*, 1994, **6**, 2227. (b) C. M. Nixon, K. Le Claire, F. Odobel, B. Bujoli and D. R. Talham, *Chem. Mater.*, 1999, **11**, 965. (c) M. A. Petruska and D. R. Talham, *Chem. Mater.*, 1998, **10**, 3672. And references therein.

16 (a) D. Cunningham, P. J. D. Hennelly and T. Deeney, Inorg. *Chem. Acta.*, 1979, **37**, 95. (b) S. S. Sandhu, G. K. Sandhu and S. K. Pushkarna, *Synth. React. Inorg. Met.-Org. Chem.*, 1981, **11**, 197. (c) R. D. W. Kemmitt, S. Mason, J. Fawcett and D. R. Russell, *J. Chem. Soc. Dalton Trans.*, 1992, 851.

17 (a) G. M. Kosolapoff, *Organophosphorus Compounds*, Wiley. N. Y. 1950. (b) L. D. Freedman and G. O. Doak, *Chem. Rev.*, 1957, **57**, 479. (c) K. H. Worms and M. Schmidt-Dunker, *Organic Phosphorus Compounds*, G. M. Kosolapoff and L. Maier (Eds.), 1973, John Wiley & Sons, Vol. 7, Chap. 18.

18 K. Moedritzer and R. R. Irani, *J. Org. Chem.*, 1966, **31**, 1603.

containing one carbon-phosphorus bond. The phosphorus group is then manipulated to produce the $-P(O)(OH)_2$ moiety.

There are very many ferrocenyl-phosphorus compounds that are candidates for such manipulation. The recently synthesised primary phosphine $FcCH_2PH_2$, was initially selected as a starting material due to its availability and unique stability[19]. Though unusually stable in air, $FcCH_2PH_2$ had been shown to undergo reactions typical of a primary phosphine. Complete oxidation of primary phosphines should yield phosphonic acids as shown in Scheme 2.1.

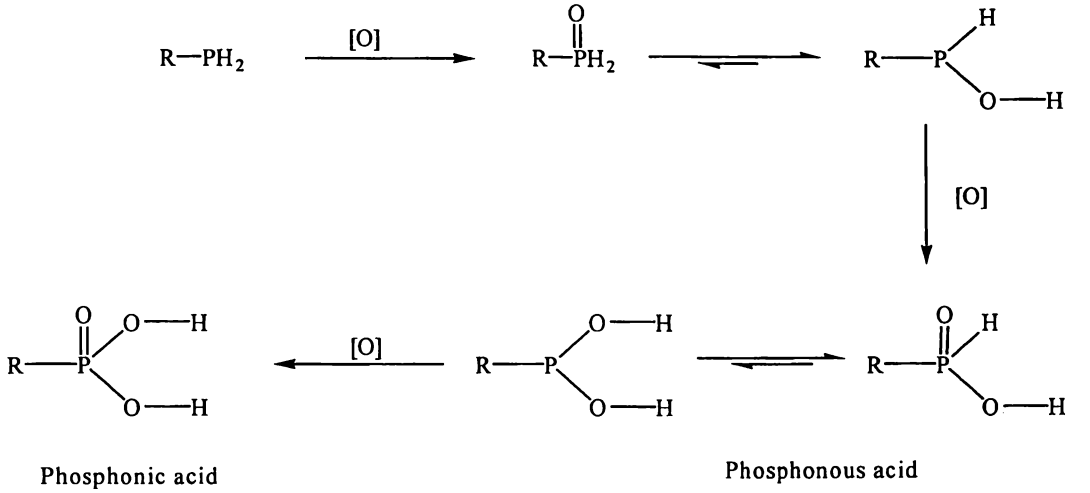

Scheme 2.1: Oxidation Path of Primary Phosphines.

Exposure of the primary phosphine, $FcCH_2PH_2$ to an excess of hydrogen peroxide in methanol did not lead to the expected phosphonic acid product. As will be further explained in chapter five, the oxidation of ferrocenyl primary phosphines is complicated by the concomitant oxidation of the ferrocene group to the ferrocenium ion.

Thus thwarted, attention turned to ferrocenyl phosphonate esters as possible starting materials for acid synthesis. Phosphonate ester synthesis is dominated by the Arbuzov-Michaelis reaction[20], (Scheme 2.2). Triaryl and trialkylphosphites react with

---

19 N. J. Goodwin, W. Henderson, B. K. Nicholson, J. Fawcett and D. R. Russell, *J. Chem. Soc., Dalton Trans.*, 1999, 1785.

20 A. Michaelis-Becker and R. Kaehne, *Chem. Ber.*, 1898, **31**, 1048.

alkyl halides to give phosphonate esters in high yield. Activated alcohols and pseudo-halides such as tosylates also react with tertiary phosphites to give phosphonate esters.

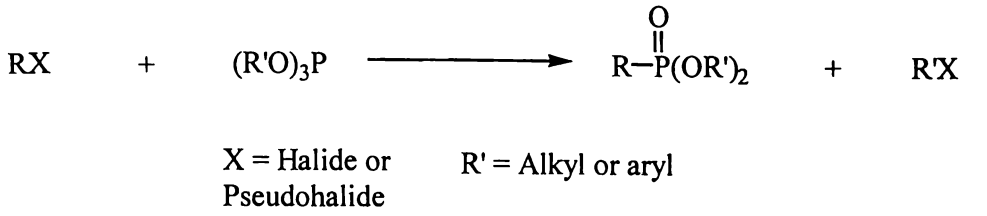

Scheme 2.2: Michaelis-Arbuzov Synthesis of Phosphonate Diesters.

A related synthesis, the Michaelis-Becker reaction[21], involves reaction of alkyl halides with the sodium salts of diaryl and dialkylphosphites, (Scheme 2.3). The Michaelis-Becker reaction is generally lower-yielding than the Michaelis-Arzubov reaction but avoids the complication of having an alkyl halide as a by-product.

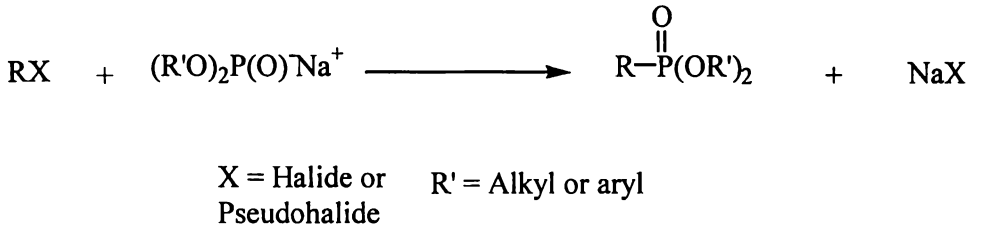

Scheme 2.3: Michaelis-Becker Synthesis of Phosphonate Diesters.

Hydrolysis of alkylphosphonate esters by reflux in concentrated acid gives the phosphonic acid in high yield[22] while phosphonic acids are prepared from arylphosphonates by the action of dihydrogen in the presence of platinum or palladium catalysts[23].

The ferrocenylphosphonate, $FcCH_2P(O)(OPh)_2$ has recently been synthesised by the Michaelis-Arbuzov reaction of $FcCH_2OH$ and triphenylphosphite $(PhO)_3P$[24]. Hydrogenation of $FcCH_2P(O)(OPh)_2$ under a dihydrogen atmosphere with Adam's

[21] A. Michaelis-Becker and T. Becker, *Chem. Ber.*, 1897, **30**, 1003.
[22] G. M. Kosolapoff, *J. Am. Chem. Soc.*, 1945, **67**, 1180.
[23] R. W. Balsiger, D. G. Jones and J. A. Montgomery, *J. Org. Chem.*, 1959, **24**, 434.
[24] W. Henderson, A. G. Oliver and A. J. Downard, *Polyhedron*, 1996, **15**, 1165.

catalyst (PtO_2), led to the isolation of the monoester $FcCH_2P(O)(OPh)OH$ **1**, rather than the desired acid, (Scheme 2.4).

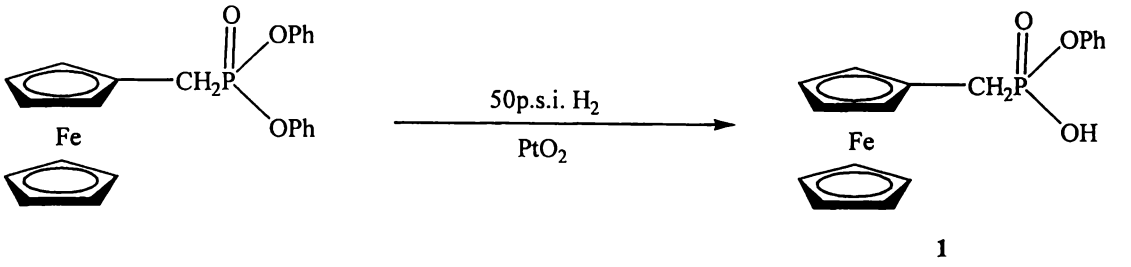

1

Scheme 2.4: Synthesis of $FcCH_2P(O)(OPh)OH$, **1**.

Attention was then turned to alkyl phosphonate esters. Hydrolysis of dialkylphosphonate esters is a well travelled route in phosphonic acid synthesis. The diethyl ester, $FcCH_2P(O)(OEt)_2$ had been prepared by V. I. Boev in 1993 by reaction of $FcCH_2OH$ with $(EtO)_2P(O)Na$, in a two phase benzene/water system in the presence of HX (X = BF_4, ClO_4)[25]. The current work found that the same product is produced in moderate yield when $FcCH_2OH$ reacts with $(EtO)_2P(O)Na$ in refluxing toluene. This synthesis required chromatography to purify the diethyl ester. Under the same reaction conditions, but using an excess of the $(EtO)_2P(O)Na$ salt, the monoester $FcCH_2P(O)(OEt)OH$, **2**, was the principal product (Scheme 2.5).

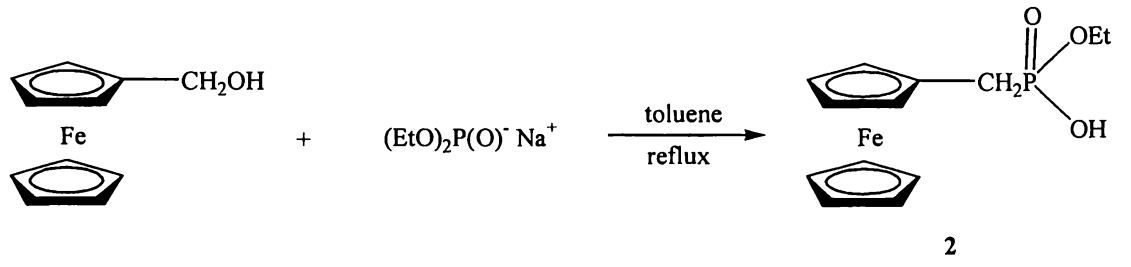

2

Scheme 2.5: Synthesis of $FcCH_2P(O)(OEt)OH$, **2**.

The preparation of such monoesters by base hydrolysis is well known[26]. In this example it seems likely the excess $NaP(O)(OEt)_2$ is effecting hydrolysis (though OH^-

25 V. I. Boev, L. V. Snegur, V. N. Babin and Y. S. Nekrasov, *Russ. Chem. Rev.*, 1997, 613.
26 (a) P. Nylen, *Chem. Ber.*, 1924, **57**, 1023. (b) P. Nylen, *Chem. Ber.*, 1926, **59**, 1119.

displaced from the alcohol is also present) as the monoester is not observed when the reactants are present in a 1:1 mole ratio. The monoester is easily purified by extracting into aqueous base and washing with organic solvent. Acidification of the basic solution leads to the precipitation of the monoester. This stable compound was conveniently prepared in good yield (50-65%) and provided a useful starting material for several ferrocenyl-phosphorus compounds.

The ferrocene moiety is prone to acid-catalysed oxidation to the ferrocenium ion. To avoid this, the usual hydrolysis of alkylphosphonate esters (refluxing in concentrated acid) was not undertaken with **2**. Rather the monoester **2** was silylated using Me_3SiBr, with NEt_3 present to ensure removal of any HBr formed. The resulting silyl ester was hydrolysed with 10% sodium bicarbonate solution. Such silyl-ester mediated hydrolysis of phosphonate esters is a common technique for the preparation of acid sensitive phosphonic acids[27]. Acidification of the sodium bicarbonate solution resulted in the precipitation of the ferrocenyl phosphonic acid $FcCH_2P(O)(OH)_2$, **3** in high yield (91%), Scheme 2.6.

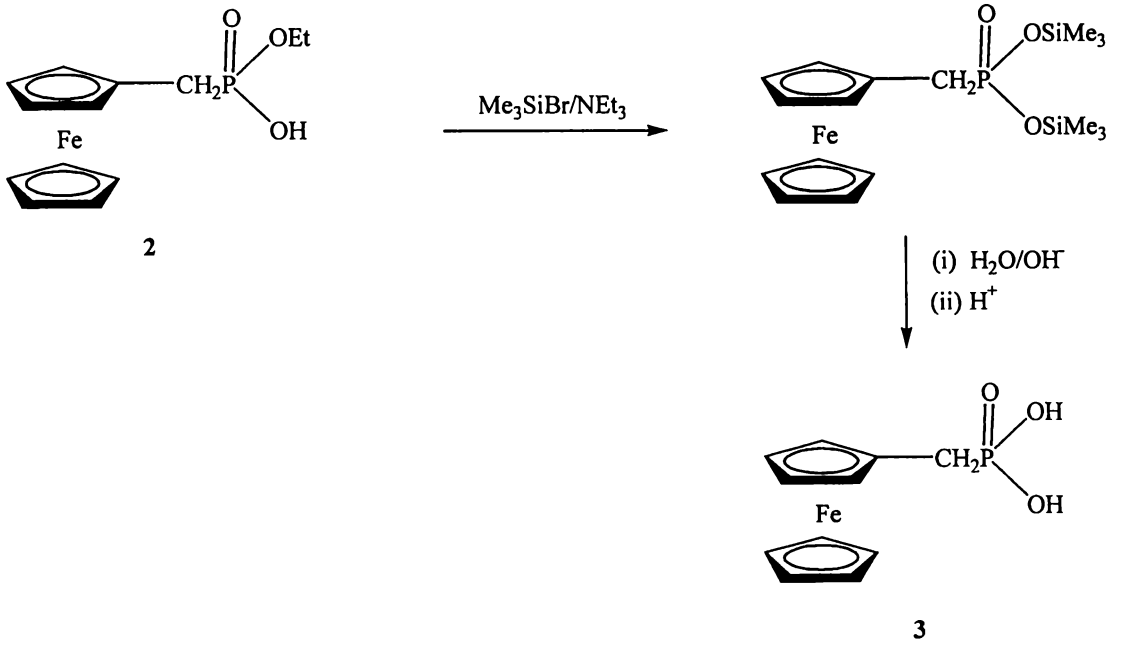

Scheme 2.6: Synthesis of Ferrocenylmethylphosphonic Acid **3**.

27 (a) R. Rabinowitz, *J. Org. Chem.*, 1963, **28**, 2975. (b) C. E. McKenna, M. T. Higa, N. H. Cheung and M. -C. McKenna, *Tetrahedron Lett.*, 1977, **2**, 155.

This compound is a yellow crystalline material, sparingly soluble in water and most organic solvents, though appreciably soluble in alcohols, (MeOH and EtOH) and DMSO. The yellow colour slowly fades to pale green upon long exposure (several months) to air at room temperature. The green colour is characteristic of the ferrocenium ion and is a result of the acid catalysing its own oxidation.

A similar synthetic method was applied to the preparation of ferrocenylethylphosphonic acid, $FcCH_2CH_2P(O)(OH)_2$, **4**, (Scheme 2.7). The starting material $FcCH_2CH_2OH$ (prepared following literature methods[28]) did not react with either triphenylphosphite or the sodium salt of diethylphosphite ($(EtO)_2P(O)Na$). However the alcohol was easily brominated using PBr_3 under an inert atmosphere. The bromide, $FcCH_2CH_2Br$ is a stable orange crystalline material, in stark contrast to the reactive nature of ferrocenylmethyl halides $FcCH_2X$, (X = halide).

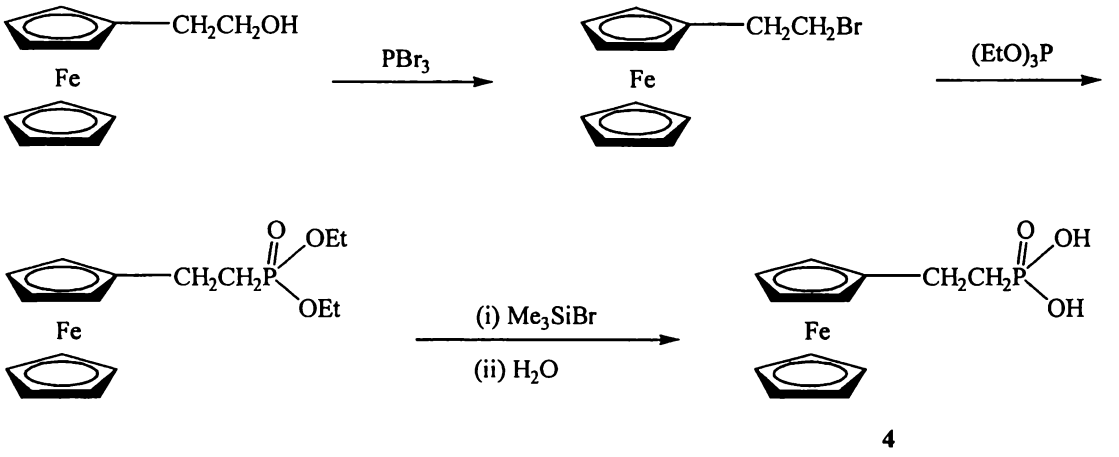

4

Scheme 2.7: Synthesis of Ferrocenylethylphosphonic Acid **4**.

The classical Michaelis-Arbuzov reaction of $FcCH_2CH_2Br$ in refluxing triethylphosphite (TEP) produced the desired diethylphosphonate $FcCH_2CH_2P(O)(OEt)_2$ in high yield, with the excess TEP being removed by distillation under vacuum. Silyl ester mediated hydrolysis of $FcCH_2CH_2P(O)(OEt)_2$ proceeded smoothly to give the acid $FcCH_2CH_2P(O)(OH)_2$ **4** as a yellow powder in high yield. The acid **4** is air stable (does not oxidise to ferrocinium), and is soluble in polar solvents such as alcohols and DMSO.

---

28 D. Lednicer, J. K. Lindsay and C. R. Hauser, *J. Org. Chem.*, 1958, **23**, 653.

Three further ferrocenyl phosphonic acids have been prepared. These are the previously reported $FcP(O)(OH)_2$ **5**, and the novel 1,1'-ferrocenylbisphosphonic acids, 1,1'-$Fc'[P(O)(OH)_2]_2$ **6**, and 1,1'-$Fc'[CH_2P(O)(OH)_2]_2$ **7**. The acids **5** and **6** are synthetically related, both being derived from the reaction of lithiated ferrocene (FcLi, or 1,1'-$Fc'Li_2$ for **5** and **6** respectively) with diethylphosphochloridate, $(EtO)_2P(O)Cl$), (Scheme 2.8).

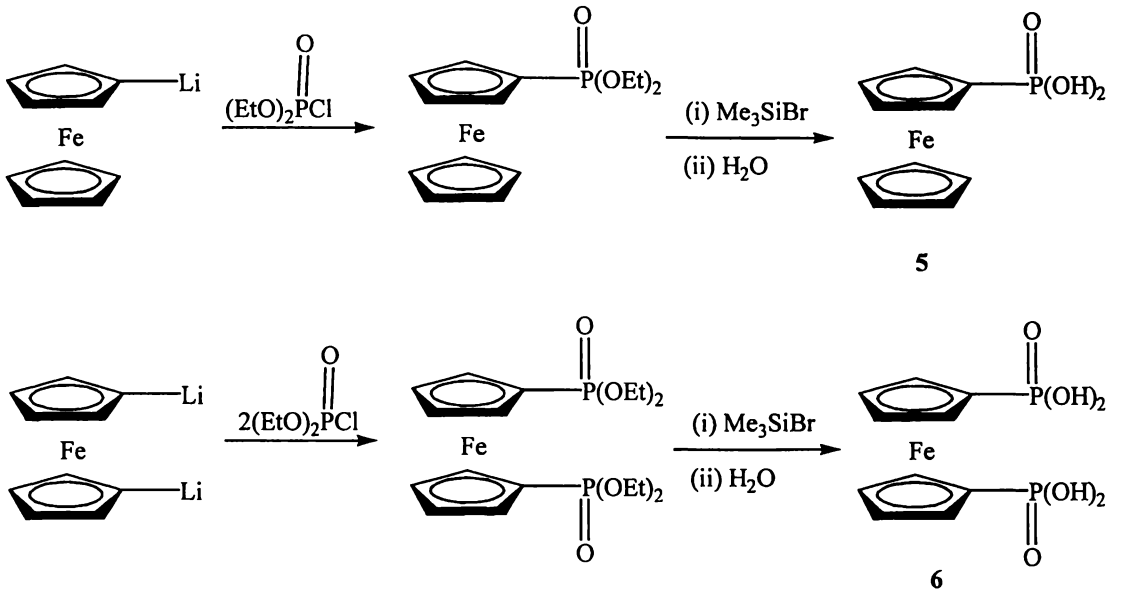

Scheme 2.8: Syntheses of Ferrocenylphosphonic Acid **5** and 1,1'-Ferrocenylbisphosphonic acid **6**.

Lithiated ferrocene is a common starting point in many ferrocenyl syntheses. Mono-lithiation is best achieved by the reaction of ferrocene with ^tBuLi[29]. The resulting FcLi reacts with electrophilic groups in high yield (70% based on ferrocene). Di-lithio ferrocene is prepared by the reaction of ferrocene with two equivalents of ^nBuLi in the presence of N,N,N',N'-tetramethylethylenediamine (TMEDA)[30]. The amine stabilises the highly reactive 1,1'-$Fc'Li_2$ and the reaction is essentially quantitative, although a small amount of mono-lithiated by-product is almost

29 F. Rebiere, O. Samuel and H. B. Kagan, *Tetrahedron Lett.*, 1990, **31**, 3121.
30 M. D. Rausch and D. J. Ciappenelli, *J. Organomet. Chem.*, 1967, **10**, 127.

inevitable. Reaction of lithiated ferrocenes with P-Cl bonds is a well established method for the synthesis of ferrocenyl-phosphorus compounds[31].

In this case the products are the ethyl ferrocenylphosphonates $FcP(O)(OEt)_2$ and $1,1'\text{-}Fc'[P(O)(OEt)_2]_2$. These compounds were purified from the crude reaction mix using alumina flash column chromatography with an EtOAc to MeOH solvent gradient and used without full characterisation.

The silyl-ester mediated hydrolysis of $FcP(O)(OEt)_2$ and $1,1'\text{-}Fc'[P(O)(OEt)_2]_2$ was complicated by the solubility of the resulting acids in water. Hydrolysis was effected by a small excess of water in CH_2Cl_2 rather than by a solution of sodium bicarbonate. $FcP(O)(OH)_2$ **5**, is a crystalline yellow compound which does not appear to react with air over time. The acid, $1,1'\text{-}Fc'[P(O)(OH)_2]_2$ **6**, is also a yellow compound, though the yellow colour fades with time. Both **5** and **6** are soluble in water and polar organic solvents.

The synthesis of **7** required a combination of the lithiation and Michaelis-Arbuzov methods, (Scheme 2.9). Lithiated ferrocenes are known to react with paraformaldehyde to give hydroxymethyl ferrocenes[32]. Reaction of dilithio ferrocene with paraformaldehyde gave the known bisalcohol, $1,1'\text{-}Fc'[CH_2OH]_2$[33].

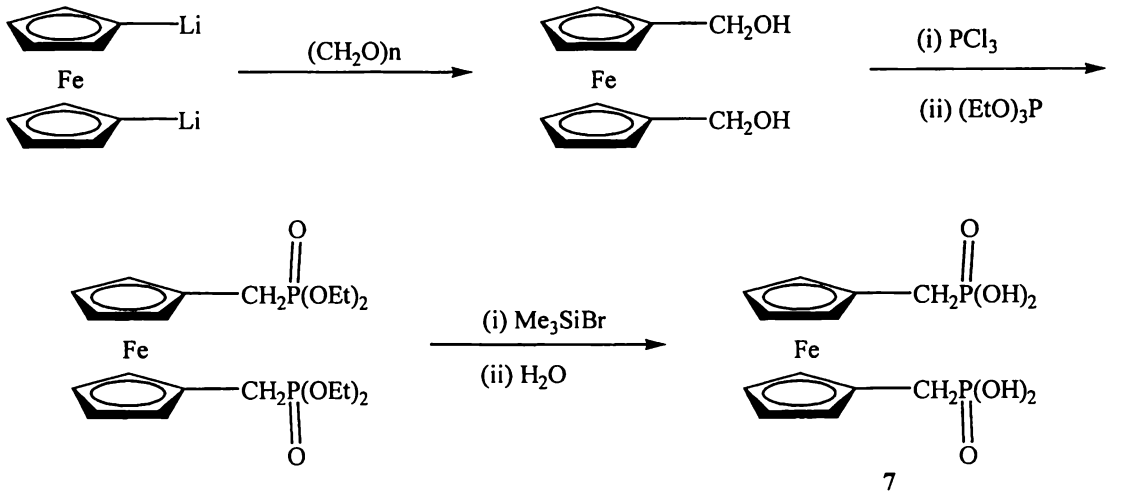

7

Scheme 2.9: Synthesis of 1,1'-Ferrocenylbis(methylphosphonic) Acid **7**.

31 (a) A. W. Rudie, D. W. Lichtenberg, M. L. Katchner and A. Davison, *Inorg. Chem.*, 1978, **17**, 2859. (b) M. J. Burk and M. F. Gross, *Tetrahedron Lett.*, 1994, **35**, 9363. (c) M. Herberhold, A. Hofmann and W. Milius, *J. Organomet. Chem.*, 1998, **555**, 187.

32 S. I. Goldberg and W. D. Bailey, *J. Am. Chem. Soc.*, 1974, **96**, 6381.

Chlorination of such alcohols with PCl_3 is a known procedure[34] and gave a high yield of the reactive dichloride 1,1'-Fc'$[CH_2Cl]_2$ as a bright yellow crystalline material that darkens on exposure to light. The dichloride was reacted, without purification, with excess refluxing triethylphosphite to give the phosphonate 1,1'-Fc'$[CH_2P(O)(OEt)_2]_2$. Silyl-ester mediated hydrolysis gave **7** as a bright yellow powder that turns green over a period of weeks on exposure to air, and is soluble in water and polar organic solvents.

2.2.1: Synthesis of Ferrocenyldiphenylesters

In addition to the acids described above, the phenylphosphonate esters $FcP(O)(OPh)_2$, **8** and 1,1'-Fc'$[P(O)(OPh)_2]_2$ **9**, were also prepared and characterised. The reaction of $(PhO)_2P(O)Cl$ with mono- and di-lithio ferrocene gave **8** and **9** respectively in high yield (Scheme 2.10).

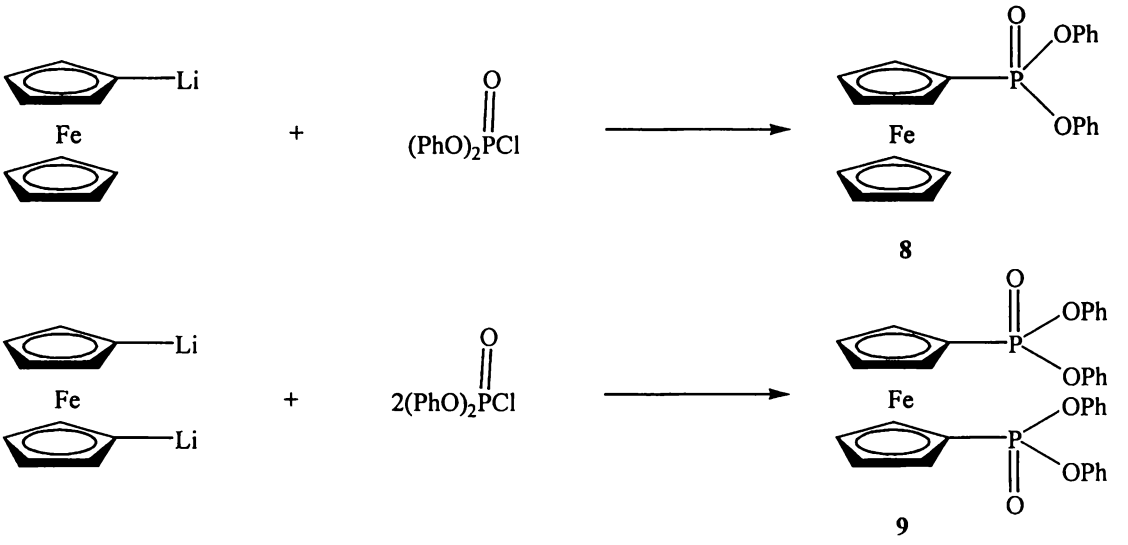

Scheme 2.10: Syntheses of $FcP(O)(OPh)_2$ **8**, and 1,1'-Fc'$[P(O)(OPh)_2]_2$ **9**.

[33] (a) V. K. Aggarwal, D. Jones, M. L. Turner and H. Adams, *J. Organomet. Chem.*, 1996, **524**, 263. (b) Aldrich Chemical Company, 2000, Product No. 37,261-5

[34] H. Plenio, D. Burth and R. Vogler, *Chem. Ber.*, 1997, **130**, 1404.

The crude products of the reactions in Scheme 2.10 are brown oils which are easily purified by silica column chromatography, using EtOAc as the eluting solvent. The pure phenylphosphonates **8** and **9** are orange crystalline solids, unlike the analogous ethylphosphonates, which are brown oils. The phenylesters **8** and **9** are soluble in organic solvents and are appreciably more stable than the analogous ethylesters, which decompose slowly at room temperature.

It was found during the synthesis of **8** that the order of addition of the FcLi and $(PhO)_2P(O)Cl$ had some bearing on the outcome of the reaction, (Scheme 2.11). If a solution of FcLi was added to a solution of $(PhO)_2P(O)Cl$ the reaction proceeded as

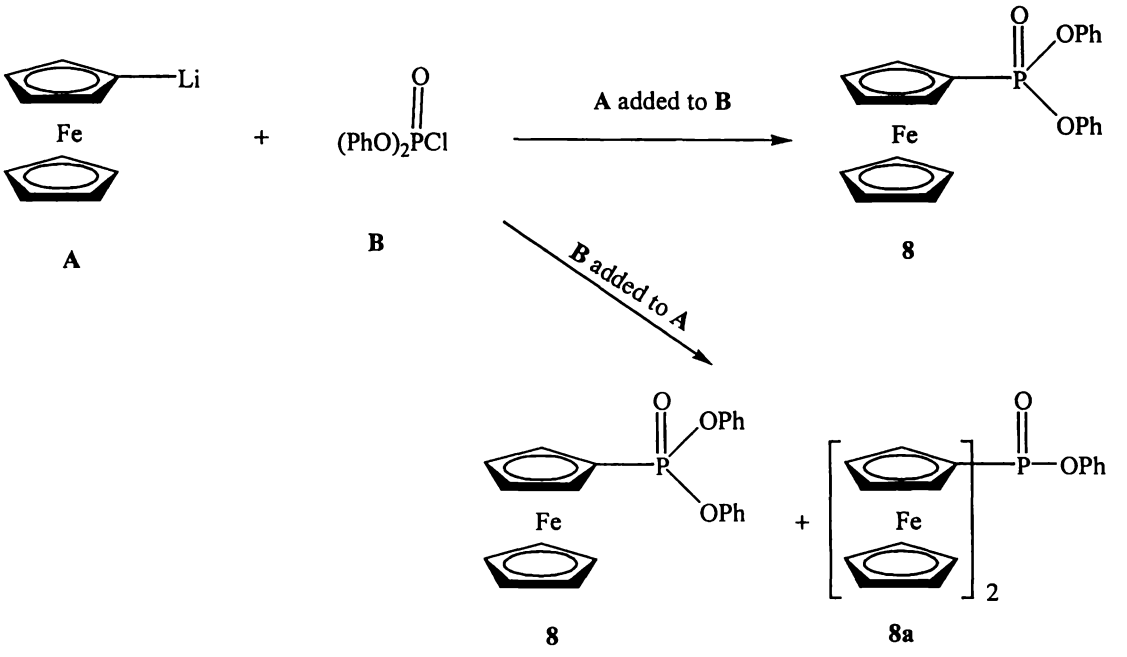

Scheme 2.11: Possible Outcomes of the Reaction of FcLi with $(PhO)_2PCl$.

expected. However addition of a solution of $(PhO)_2P(O)Cl$ to a solution of FcLi led to two products which were isolated by chromatography. These were the expected phenylester $FcP(O)(OPh)_2$ and a second product that was tentatively characterised by ^{31}P NMR and ESMS as $Fc_2P(O)(OPh)$ **8a**. Presumably the high initial concentration of FcLi (a strong base) cleaves a P-OPh bond, resulting in the substitution of an –OPh group with –Fc.

2.2.2: Electrospray Mass Spectrometry (ESMS) Analysis of Ferrocenyl Acids and Esters

Investigation of the ESMS properties of ferrocenyl compounds has only recently been undertaken. Initial research[35] showed that ferrocene and its derivatives can be oxidised to the ferrocenium ion under electrospray conditions. Subsequent work[17] has shown that some ferrocene containing compounds can exhibit protonation during ESMS provided there are basic sites, such as N or O available.

Phosphonic acids deprotonate readily under ESMS conditions[36]. As expected the negative ion ES mass spectra of the ferrocenylphosphonic acids **3**, **4**, and **5**, were dominated at low cone voltages by the respective $[M\text{-}H^+]^-$ ions. The acids were introduced to the ES mass spectrometer as solutions in methanol with pyridine added to aid deprotonation. The fragmentation behaviour of these acids was investigated by obtaining spectra over a range of cone voltages, (In the following discussion of ESMS and throughout this thesis, the terms negative ion and positive ion denote the mode in which the ion detector is operating. Cone voltage refers to the potential difference applied across the skimmer cones and these values possess magnitude but no sign).

The negative ion ES mass spectra of $FcP(O)(OH)_2$ **5** (Figure2.1) were dominated by the $[M\text{-}H^+]^-$ (*m/z* 265) ion at low cone voltages. Raising the cone voltage gave a second peak

35 (a) X. Xu, S. P. Nolan, R. B. Cole, *Anal. Chem.*, 1994, **66**, 119. (b) G. J. Van Berkel and F. Zhou, *Anal. Chem.*, 1995, **67**, 3958.

36 P. B. Smith, A. P. Snyder and C. S. Harden, *Sci. Conf. Chem. Biol. Def. Res.*, 1996, 569.

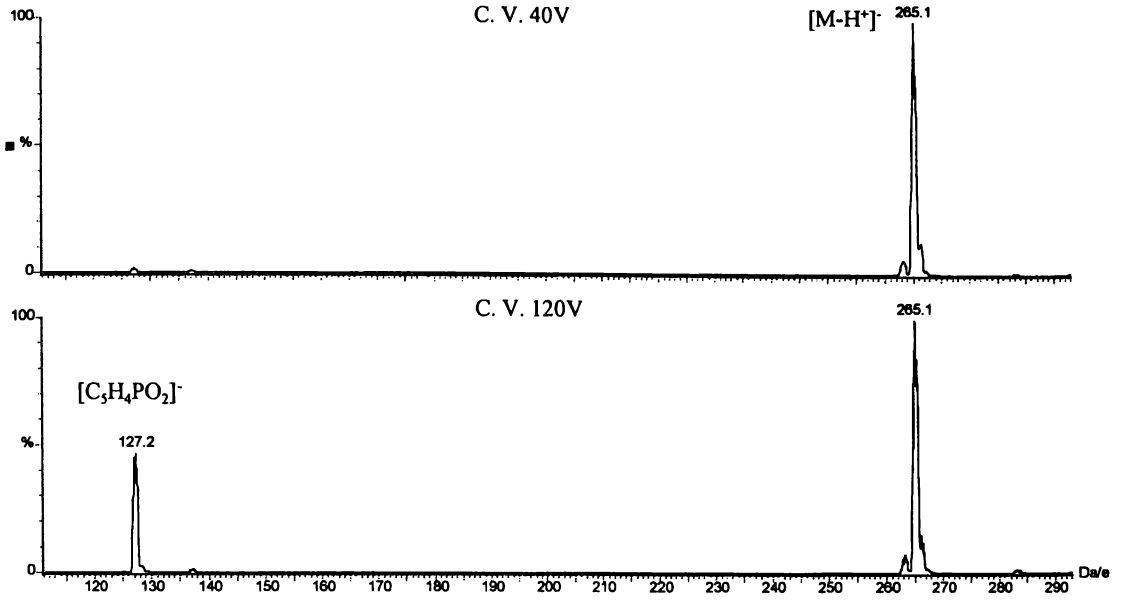

Figure 2.1: The Negative Ion ES Mass Spectra of **5** in Methanol at Cone Voltages of 40V and 120V.

at *m/z* 127 assigned to $C_5H_4PO_2^-$ formed by loss of $CpFe^+$ and H_2O from the parent molecule. The $C_5H_4PO_2^-$ (*m/z* 127) ion (Figure2.2) is an example of compounds known variously as dioxophosphoranes or metaphosphonates.

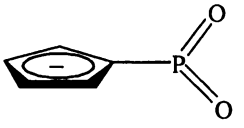

m/z 127

Figure 2.2: Proposed Structure of the Ion $C_5H_4PO_2^-$.

These highly reactive species are observed in the pyrolysis of phosphonate compounds and have a number of applications as intermediates in organophosphorus chemistry[37]. This fragment ion was also observed in the high cone voltage spectra of **6**

[37] L. D. Quin, *Coord. Chem. Rev.*, 1994, **137**, 525.

(Figure2.5), which suggests some stabilisation is conferred by the adjacent Cp^- ring. No other fragmentation of $FcP(O)(OH)_2$ was observed at cone voltages up to 180V.

In contrast the negative ion ES mass spectra for **3** and **4** gave a single fragmentation peak at *m/z* of 213 and 227 respectively at high cone voltages. This corresponds to loss of $2H^+$ and Cp^-. The resulting ion $Fe\{\eta^5\text{-}C_5H_4(CH_2)_nP(O)O_2\}^-$ (n = 1 or 2) may be stabilised by interaction between the phosphorus acid group and the exposed iron atom (Figure 2.3).

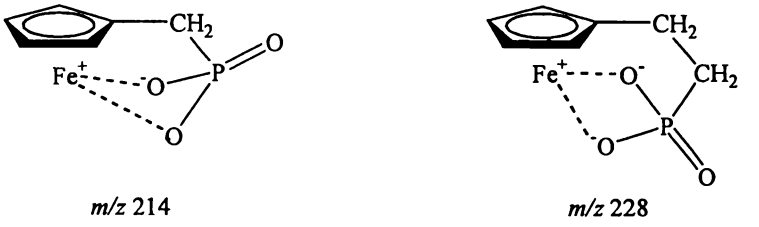

Figure 2.3: Proposed Stabilisation of $[M\text{-}2H^+\text{-}Cp^-]^-$ Ions Observed in ESMS of **3** (*m/z* 214) and **4** (*m/z* 228).

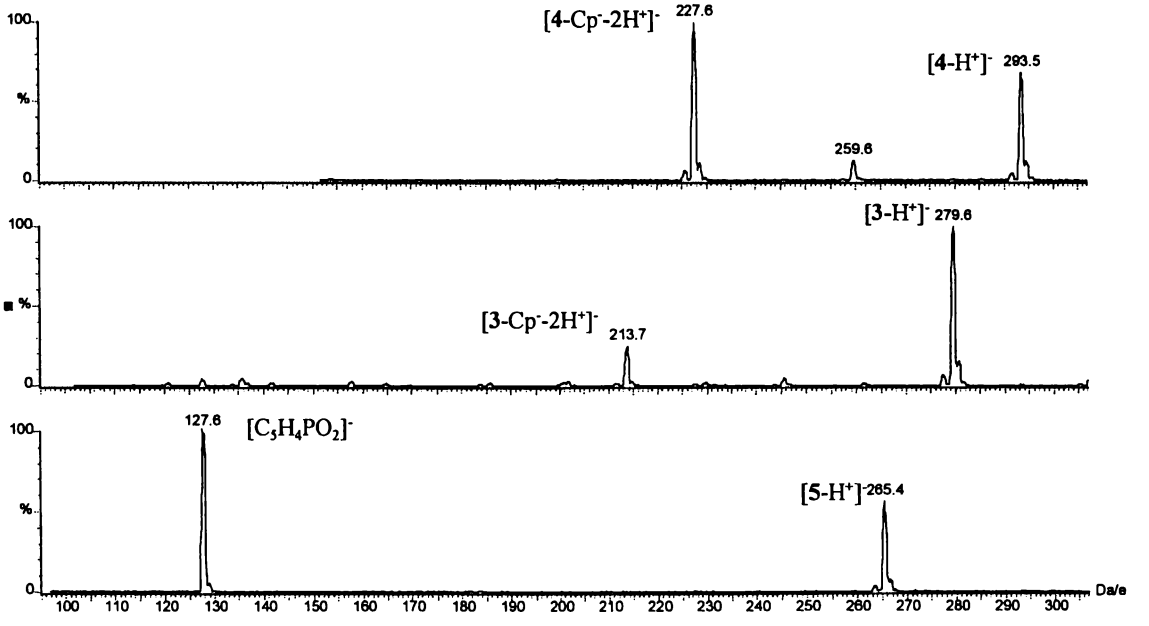

Figure 2.4: The Negative Ion ES Mass Spectra of **3**, **4**, and **5** in Methanol at a Cone Voltage of 100V.

Evidence for this comes from the far greater relative intensity of the $[M\text{-}2H^+\text{-}Cp^-]^-$ peak in the spectra of **4** when compared to the same signal in the spectra of **3** (Figure 2.4). The extra CH_2 spacer of **4** would enable the phosphorus acid to interact more easily with the bare iron atom. The analogous $[M\text{-}2H^+\text{-}Cp^-]^-$ ion is not observed in the spectra of **5**. A similar, ion $Fe\{\eta^5\text{-}C_5H_4(CH_2)P(O)(OPh)_2\}^+$ was observed in the positive ion ES mass spectra of $FcCH_2P(O)(OPh)_2$ at high cone voltages and is thought to be stabilised by interaction of the P=O group with the iron atom[17].

The negative ion ES mass spectra of 1,1'-Fc'$[P(O)(OH)_2]_2$ **6** are dominated by peaks due to the $[M\text{-}H^+]^-$ (*m/z* 345) and $[M\text{-}2H^+]^{2-}$ (*m/z* 172) ions. At higher cone voltages peaks at *m/z* 327 and *m/z* 128 are observed. The first of these corresponds to $[M\text{-}H_2O\text{-}H^+]^-$ and could indicate formation of a pyrophosphate ion in the ES mass spectrometer while the peak at *m/z* 127 is due to the $C_5H_4PO_2^-$ ion (Figure 2.5).

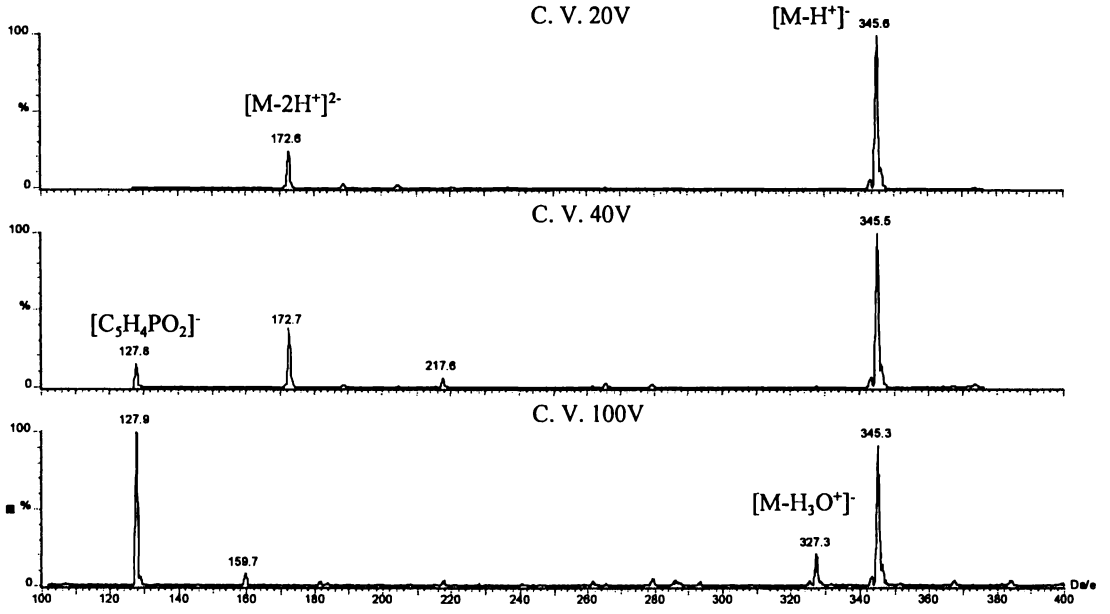

Figure 2.5: The Negative Ion ES Mass Spectra of 1,1'-Fc'$[P(O)(OH)_2]_2$ **6** in Methanol at Cone Voltages of 20V, 40V and 100V.

The negative ion spectra of 1,1'-Fc'$[CH_2P(O)(OH)_2]_2$ **7** are also dominated by the $[M\text{-}H^+]^-$ (*m/z* 373) ion at low cone voltages, however a peak due to the $[M\text{-}2H^+]^{2-}$ (*m/z* 186) ion is not observed. At higher cone voltages (≥100V) a more complex

pattern of fragmentation appears though still dominated by the $[M\text{-}H^+]^-$ ion (Figure 2.6).

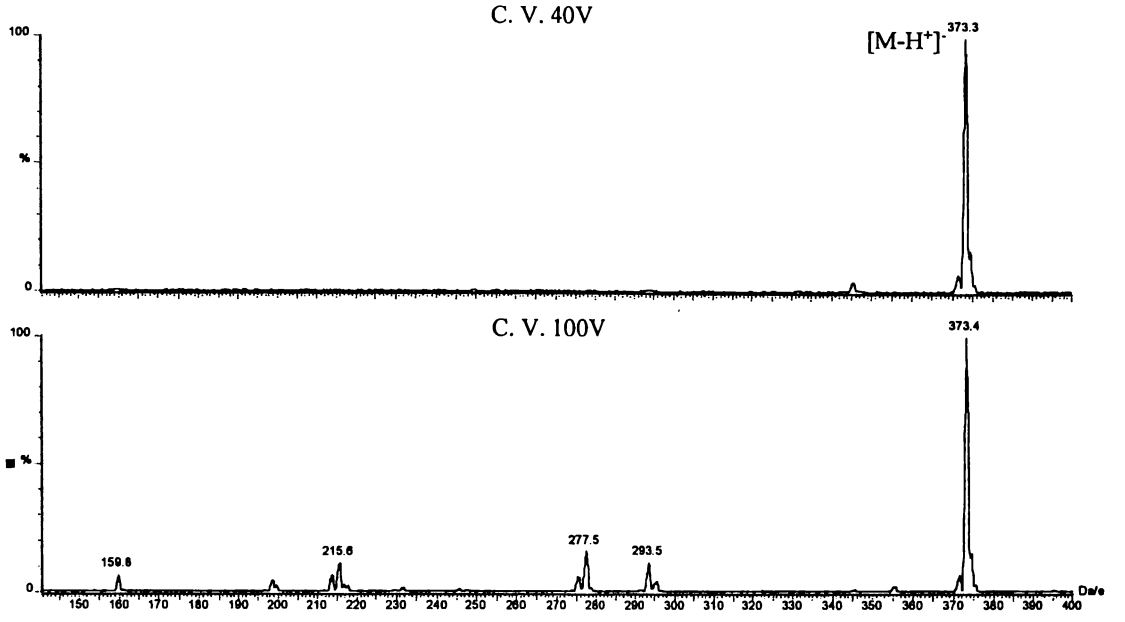

Figure 2.6: The Negative Ion ES Mass Spectra of 1,1'-Fc'$[CH_2P(O)(OH)_2]_2$ **7** in Methanol at Cone Voltages of 40V and 100V.

The monoesters **1** and **2** were introduced to the ES mass spectrometer as methanolic solutions with pyridine (Py), added to aid ionisation. As might be expected, the monoester **1** gave a strong $[M\text{-}H^+]^-$ (*m/z* 355) ion at low cone voltages with a much weaker $[2M\text{-}H^+]^-$ ion (*m/z* 711). As the cone voltage was increased (>60V) peaks corresponding to $[M\text{-}H^+\text{-}PhOH]^-$ (*m/z* 261) and $[M\text{-}H^+\text{-}PhH]^-$ (*m/z* 277) were observed. At positive cone voltages the $[M+PyH^+]^+$ (*m/z* 436) and $[M+H^+]^+$ (*m/z* 357) ions are observed. The analogous ethyl ester **2** also gave a strong $[M\text{-}H^+]^-$ peak (*m/z* 307) at low cone voltages, with a much weaker $[2M\text{-}H^+]^-$ ion also observed. At higher cone voltages (>60V) loss of the ethyl group is observed. At positive cone voltages the $[M+H^+]^+$ (*m/z* 309) and $[M+PyH^+]^+$ (*m/z* 388) ions predominate. The negative ion ES mass spectra of **1** and **2** at a cone voltage of 20 volts are given in Figure 2.7.

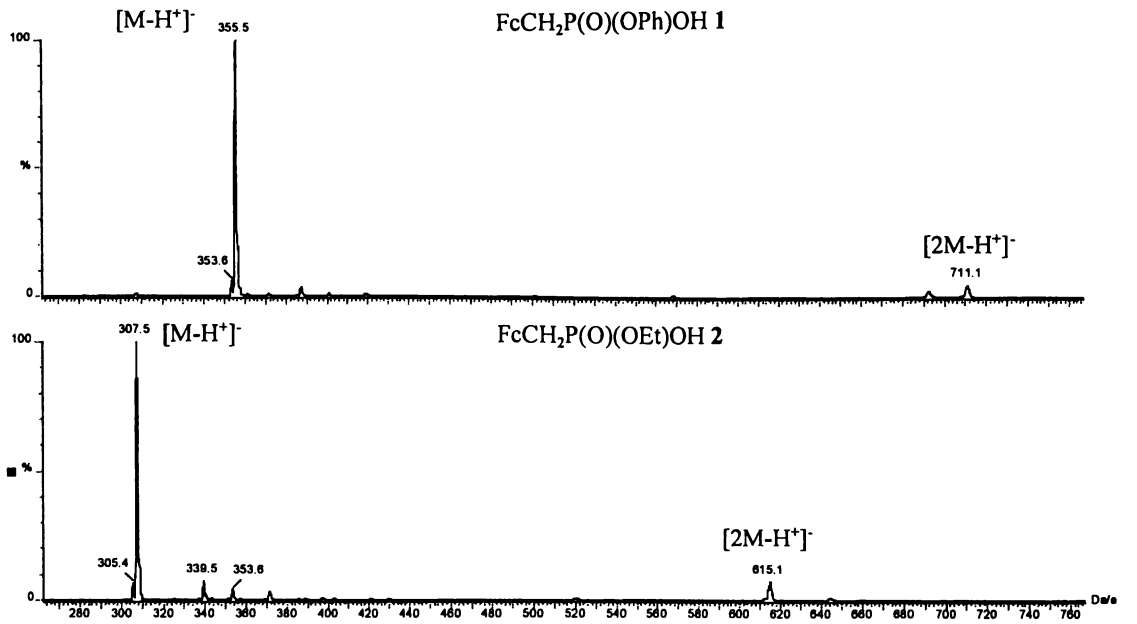

Figure 2.7: The Negative Ion ES Mass Spectra of $FcCH_2P(O)(OPh)OH$ **1** and $FcCH_2P(O)(OEt)OH$ **2** in Methanol at a Cone Voltage of 20V.

Electrospray of the ferrocenylphosphonate diester **8**, was conducted in the positive ion mode. Peaks attributable to both M^+ (ferrocenium) and $[M+H^+]^+$ (*m/z* 418 and 419 respectively) are observed, though as the cone voltage increased the relative intensity of the $[M+H^+]^+$ peak increased. At cone voltages higher than 60V a peak due to $[M-Cp^-]^+$ appears and gains in relative intensity as the cone voltage increases. This ESMS behaviour is very similar to that of $FcCH_2P(O)(OPh)_2$ which has previously been reported[11].

The positive ion ESMS properties of the $1,1'\text{-}Fc'[P(O)(OPh)_2]_2$ **9** were also studied. This ester is ideally suited for adduct formation with simple cations due to the strongly donating P=O groups. Electrospray mass spectra of **9** were dominated by the $[2M+Li^+]^+$ ion (*m/z* 1307) and the $[2M+Na^+]^+$ (*m/z* 1323) ion even when no Li^+ or Na^+ had been deliberately introduced into the sample. The $[M]^+$ (*m/z* 650), $[M+H^+]^+$ (*m/z* 651), $[M+Li^+]^+$ (*m/z* 657) and $[M+Na^+]^+$ (*m/z* 673) ions are also observed. Trace amounts of these metals are often present in the system due to other users. The bis-diester **9** proved to be very good at forming such adducts even at very low metal concentration.

Deliberate addition of a mixture of equimolar amounts of Li^+, Na^+, K^+, Rb^+ and Cs^+ gave spectra containing the complete series of $[M+Metal^+]^+$ and $[2M+Metal^+]^+$ ions, (Figure 2.8).

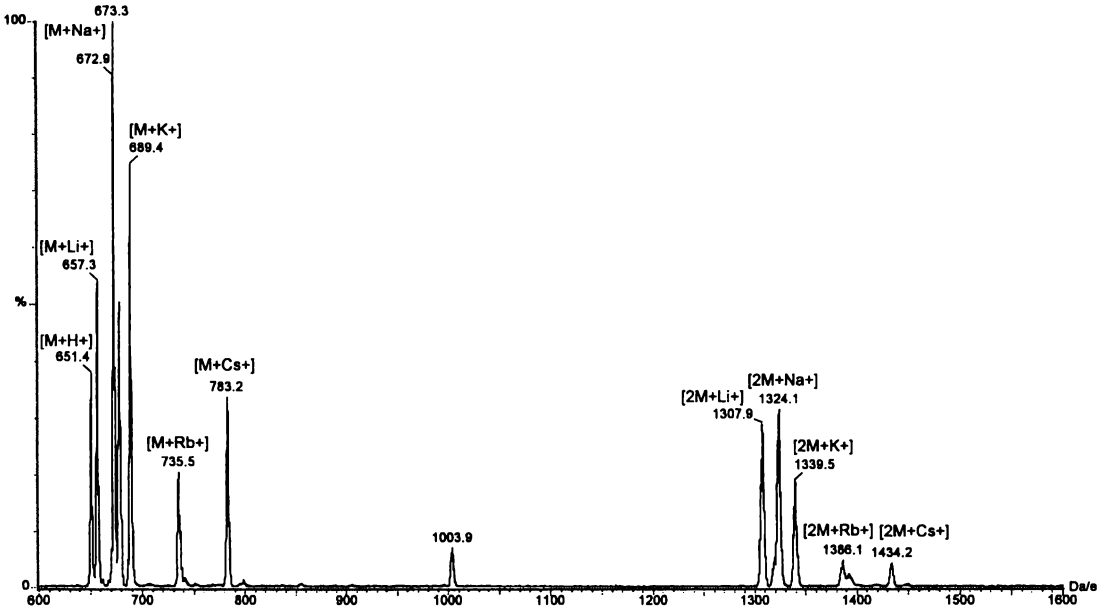

Figure 2.8: The Positive Ion ES Mass Spectrum of **9** at a Cone Voltage of 80V, with Equimolar Li^+, Na^+, K^+, Rb^+ and Cs^+ Added.

At low cone voltages the spectra are dominated by the $[2M+Metal^+]^+$ ions though the peak due to $[2M+H^+]^+$ (*m/z* 1301) is notably absent. As the cone voltage is increased the dimeric adducts are abandoned in favour of the monomeric $[M+Metal^+]^+$ species and $[M+H^+]^+$ ions. A peak at *m/z* 678 also appears and increases in intensity as the cone voltage is raised. This peak, as yet unassigned, has been shown by high resolution ESMS to be due to a 2^+ cationic species.

The binding of the bis-diester **9** to the cations seems to have a limited degree of selectivity. In all spectra the peaks due to sodium adducts (both monomeric and dimeric) are the most intense followed by those due to lithium and/or potassium. The peaks due to interaction with the larger Cs^+ and Rb^+ ions are weaker still.

The ability of the ferrocenyl group to rotate and alter the bite angle of the two P=O groups enables formation of adducts over a wide size range. Though not fully characterised, the bis-diethylesters 1,1'-Fc'$[P(O)(OEt)_2]_2$ and 1,1'-Fc'$[CH_2P(O)(OEt)_2]_2$

were isolated as pure oils and electrosprayed in the presence of metal ions. The expected adduct formation was observed. The initial spectrum of 1,1'-Fc'$[CH_2P(O)(OEt)_2]_2$ with no metal salts added was dominated by a peak at *m/z* 575. High resolution ESMS proved this peak to be to be due to an $[M+SnEt_2]^{2+}$ adduct, the diethyltin being present in trace amounts from a previous user of the equipment. The propensity of these bis-diesters to form cationic adducts is worthy of further study.

2.2.3: X-Ray Crystal Structure Determinations for Compounds $FcCH_2P(O)(OH)_2$ 3 and 1,1'-Fc'$[CH_2P(O)(OH)_2]_2$ 7

To fully characterise the acids **3** and **7** and to compare the differences in the structure of mono and bis-substituted ferrocenyl phosphonic acids the structural elucidation of these acids was undertaken. Single crystals of **3** were obtained serendipitously from a hot methanolic solution that also contained urea and zinc chloride in an attempt to prepare the zinc salt of the acid. From this solution, small yellow crystals of **3** precipitated over a period of 2-4 weeks. These crystals did not discolour in air, unlike samples of **3** obtained as powders, presumably due to the hydrogen bonding network of the crystals 'locking in' the acidic protons, though the reduction in surface area could also be a factor. Single crystals of **7** were grown from an acidic aqueous solution which contained potassium bisulfite as a reducing agent. Single crystals of **7** slowly turn green in air over a period of several months.

The structures of **3** and **7** were determined from single crystal x-ray diffraction data. All bond lengths and angles were within normal ranges. Selected bond lengths and angles are given in Tables 2.1 and 2.2. Structure diagrams of **3** and **7** are given in

Table 2.1: Selected Bond Lengths (Å) and Angles (°) for **3**.

Cp Fe-C av	2.054	P(1)-O(2)	1.566(1)
range	2.045-2.064	P(1)-O(3)	1.567(1)
Cp C-C av	1.430	O(2)-H(2)	0.78(2)
range	1.422-1.432	O(3)-H(3)	0.78(2)
C(1)-C(11)	1.514(2)	O(1)----H(2')	1.819
C(1)-P(1)	1.805(2)	O(1)----H(3')	1.829

P(1)-O(1)	1.513(1)		
C(11)-C(15) range	107.57(12)-108.54(12)	O(1)-P(1)-O(2)	113.28(6)
C(21)-C(25) range	107.6(2)-108.2(2)	O(1)-P(1)-O(3)	108.86(6)
C(15)-C(11)-C(1)	126.97(12)	O(2)-P(1)-O(3)	108.26(7)
C(12)-C(11)-C(1)	125.44(12)	P(1)-O(2)-H(2)	119.1(2)
C(11)-C(1)-P(1)	112.18(9)	P(1)-O(3)-H(3)	117.4(2)
O(1)-P(1)-C(1)	112.06(6)	O(2)-H(2)--O(1')	175.92
O(2)-P(1)-C(1)	105.95(6)	O(3)-H(3)--O(1')	166.87
O(3)-P(1)-C(1)	108.25(7)		

figures 2.9 and 2.11 respectively. Of interest in both structures are the hydrogen bonding networks between the acid hydroxyl groups and the P=O oxygen.

The structure of **3** was solved by direct methods and developed routinely with all hydrogen atom positions being found by inspection of the penultimate electron density map. The structure of **3** contained no exceptional bond angles or bond lengths. The Cp rings of the ferrocene ring are in an eclipsed formation and the C(1)-

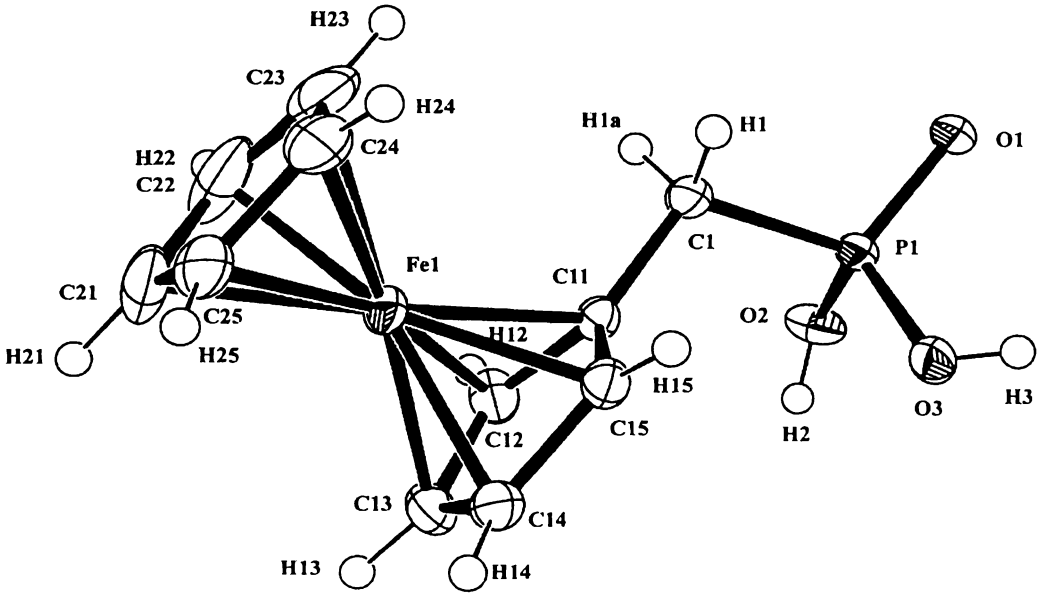

Figure 2.9: ORTEP Diagram of **3**, Non-hydrogen Atoms Shown at the 50% Probability Level.

C(11) bond lies in the plane of the Cp rings. There is no suggestion of interaction of the phosphonic acid group with the ferrocenyl iron. Indeed the phosphonic acid group is heavily involved in hydrogen bonding interactions with adjacent phosphonic acid groups. The compound crystallises with eight molecules in the unit cell and forms two dimensional ferrocenyl bi-layers in the *ab* plane. Hydrogen bonding between phosphonic acids groups on the surface of these layers, serve to hold the structure together. The individual hydrogen bonding interactions and the larger scale structure are shown in figures 2.10(a) and 2.10(b) respectively.

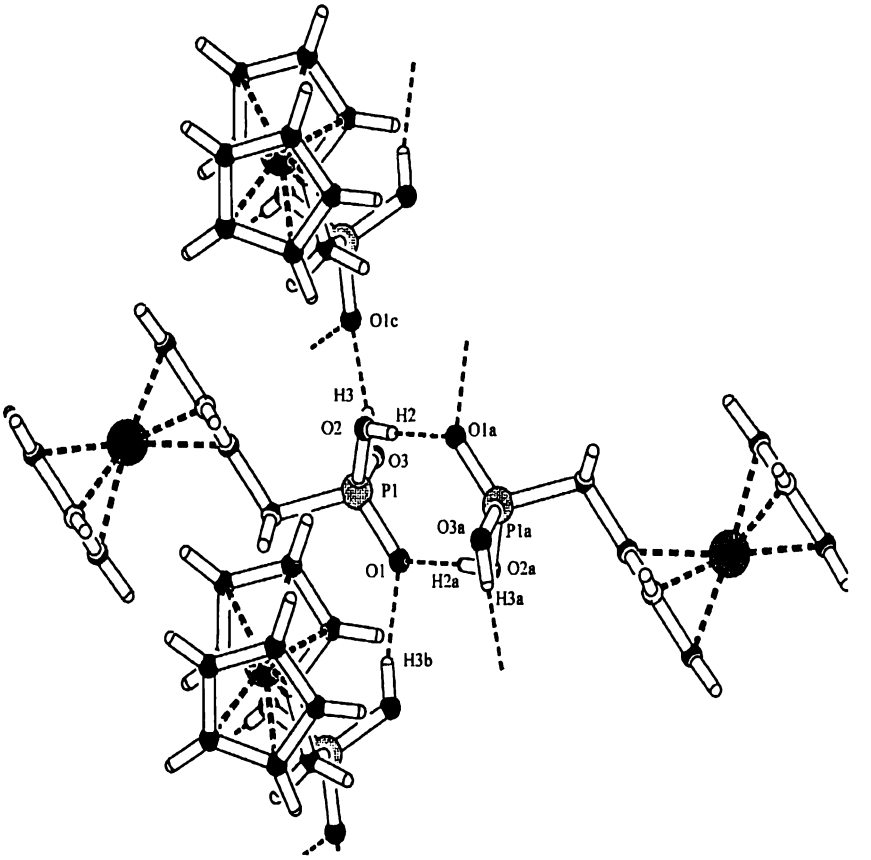

(a)

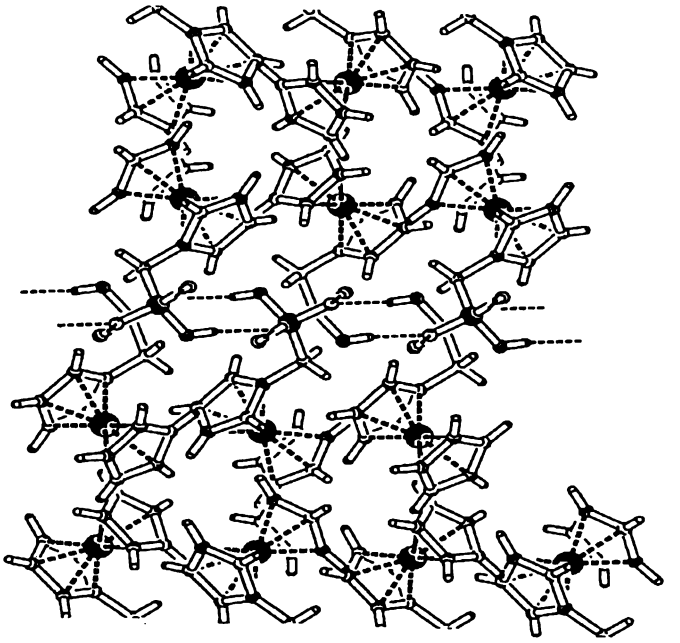

(b)

Figure 2.10: Pluton Graphics Showing the Hydrogen Bonding Network in the Structure of **3**

Each phosphonic acid group bonds to the P=O oxygen of an adjacent phosphonic acid residue in the same plane along the *b*-axis via an O(3)-H(4)---O(1') bond. The second hydroxyl group hydrogen bonds to a phosphonic acid residue in an adjacent plane with the formation of an O(2)-H(3)---O(1'') bond. This second hydrogen bond bridges the bi-layers and results in the formation of eight membered P-O-H rings (Figure 2.10(a)).

Such rings are a common feature of phosphonic acid structures. The P=O group of each ferrocenylphosphonic acid accepts two hydrogen bonds, one from a neighbour in the same plane, the second from an adjacent plane. There is little difference in the lengths of the two hydrogen bonding interactions and the P-O-H bond angles are similar for both of the hydroxyl groups.

Table 2.2: Selected Bond Lengths (Å) and Angles (°) for **7**.

Cp Fe-C av	2.039	P(1)-O(3)	1.549(2)
range	2.037-2.042	P(1)-O(2)	1.551(2)
Cp C-C av	1.420	O(2)-H(2)	0.74(3)

range	1.413-1.427	O(3)-H(3)	0.66(3)
C(1)-C(11)	1.498(2)	O(1)-----H(2')	1.832
P(1)-C(1)	1.785(2)	O(1)-----H(3')	1.923
P(1)-O(1)	1.502(2)		
C(11)-C(15)		O(2)-P(1)-O(3)	108.36(8)
range	107.43-108.37	O(2)-P(1)-O(1)	113.32(7)
C(15)-C(11)-C(1)	126.4(2)	O(3)-P(1)-O(1)	108.97(8)
C(12)-C(11)-C(1)	126.2(2)	P(1)-O(2)-(H2)	119.5(22)
C(11)-C(1)-P(1)	112.65(12)	P(1)-O(3)-(H3)	116.6(24)
C(1)-P(1)-O(2)	106.16(9)	O(2)-H(2)----O(1')	175.10
C(1)-P(1)-O(3)	108.08(9)	O(3)-H(3)----O(1')	164.52
C(1)-P(1)-O(1)	111.76(7)		

All bond angles and lengths in the structure of **7** are within the expected ranges. The two $CpCH_2P(O)(OH)_2$ units adopt an anti orientation about the iron atom. Thus the iron atom sits at a centre of symmetry and the asymmetric unit contains only half of the molecule.

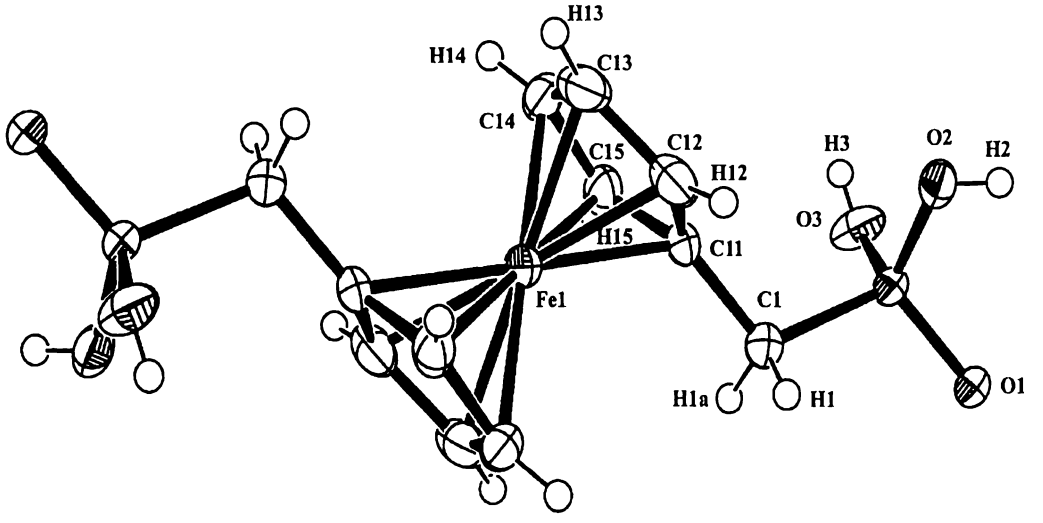

Figure 2.11: ORTEP Diagram of **7**, Non-hydrogen Atoms at 50% Probability.

As in the structure of **3** the C(1)-C(11) bond lies in the plane of the Cp rings and there is no sign of any interaction between the iron atom and the phosphonic acid groups.

The macrostructure can be described as infinite chains of hydrogen bonded $(HO)_2(O)PCH_2Fc'CH_2P(O)(OH)_2$ units. These chains run almost at right angles to each other in the structure and are cross-linked by further hydrogen bonding interactions, (Figure 2.12). A similar infinite chain motif is found in the crystal structures of the bisphosphonic acid series, $H_2O_3P(CH_2)_nPO_3H_2$ (n = 1[38], 2[39], and 3[40]). The structures that these aliphatic bisphosphonic acids adopt in the solid state are those which maximise the hydrogen bonding interactions.

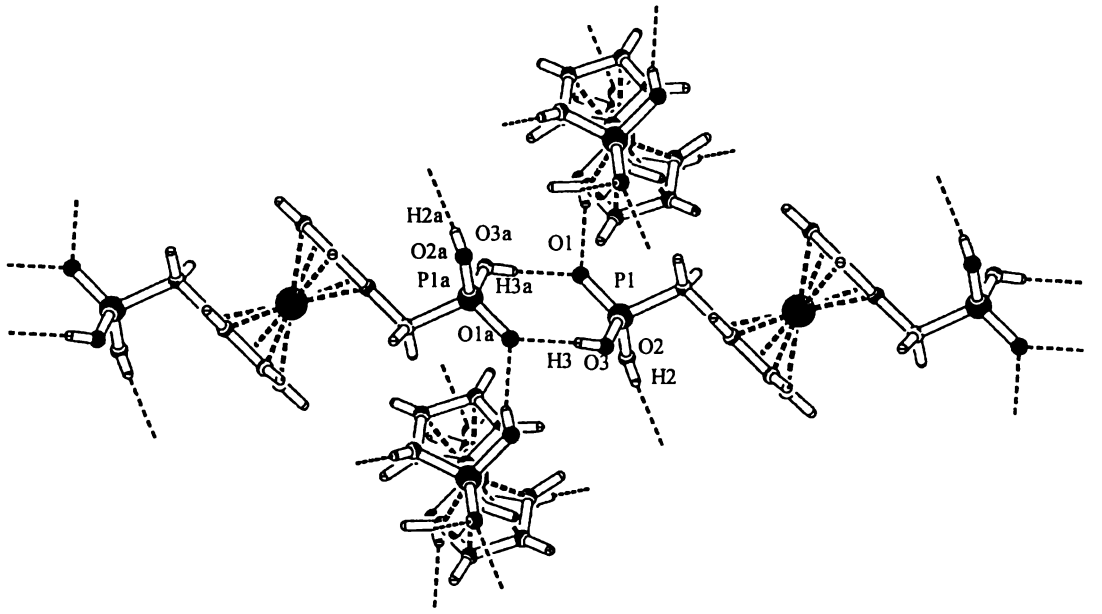

Figure 2.12: Hydrogen Bonding Network in the Structure of **7**.

Each phosphonic acid group in the crystal of **7** is involved in four hydrogen bonds, giving a total of eight hydrogen bonding interactions for each molecule. The P=O bonds accept two hydrogen bonds, one from a neighbour in the same chain, the

[38] D. DeLaMatter, J. J. McCullough and C. Calvo, *J. Phys. Chem.*, 1973, 77, 1146.
[39] S. W. Peterson, E. Gebert, A. H. Reis Jr., M. E. Druyan, G. W. Mason and D. F. Peppard, *J. Phys. Chem.*, 1977, **81**, 465.

second from a phosphonic acid residue in a neighbouring chain. Similarly each phosphonic acid group forms two donor hydrogen bonds through the two OH groups. The shorter of the two hydrogen bonds O(11)-H(4)---O(13) create the infinite chains through formation of eight membered P-O-H rings analogous to the eight membered rings found in the structure of **3**. The second and longer of the hydrogen bonds form cross links from one chain to an adjacent chain.

2.2.4: Cyclic Voltammetry of Compounds $FcCH_2P(O)(OH)_2$ 3, $FcCH_2CH_2P(O)(OH)_2$ 4 and $FcP(O)(OH)_2$ 5

Cyclic voltammetry is a technique which allows the determination of thermodynamic and quantitative properties of a system, as well as kinetic and mechanistic information regarding electron transfer processes. The experiment measures the current generated by a solution as the potential is varied linearly from a starting potential to an end potential and back again. The experiment is typically complete when the starting potential is reached again. The current generated is due to electron exchange processes (oxidation/reduction), and can offer insight into the number of electrons involved and the reversibility of the processes. By varying factors such as the temperature and rate of potential increase/decrease, information relating to mechanism of electron transfer may be acquired.

Cyclic voltammetric investigations of ferrocenyl compounds are common, as the ferrocene group is amenable to reversible oxidation/reduction processes. Most studied are the ferrocenyl phosphine species, which have complex redox behaviour due to the ability of the phosphine group(s) to become involved in redox reactions. Phosphonates and phosphonic acids contain fully oxidised phosphorus that is reduced with difficulty. Thus the cyclic voltammograms of the ferrocenyl phosphonic acids, **3**, **4** and **5** (Figure 2.13 (a), (b) and (c) respectively) were expected to be essentially that of the ferrocene oxidation-reduction couple. This expectation was not borne out for any of the acids studied. The cyclic voltammograms were more complex than expected with neither chemical or electrochemical reversibility being observed. Further study into the electrochemical behaviour of these compounds is warranted.

---

[40] E. Gebert, A. H. Reis Jr., M. E. Druyan, S. W. Peterson, G. W. Mason and D. F. Peppard, *J. Phys.*

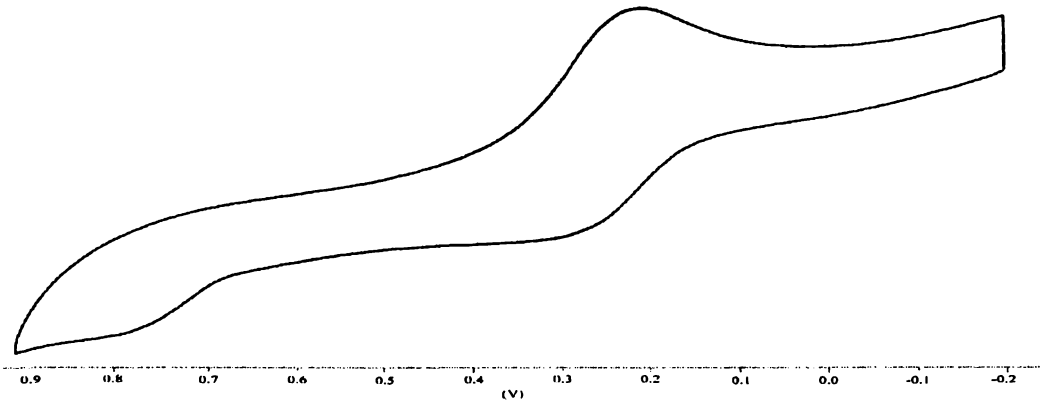

(a)

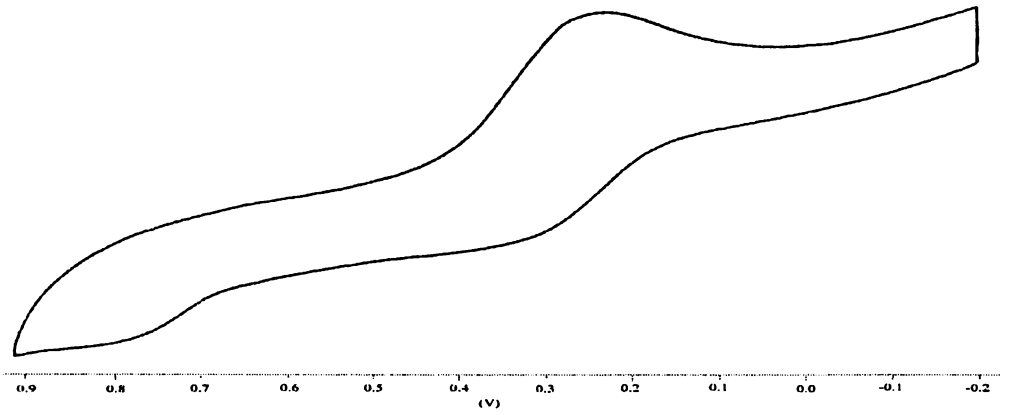

(b)

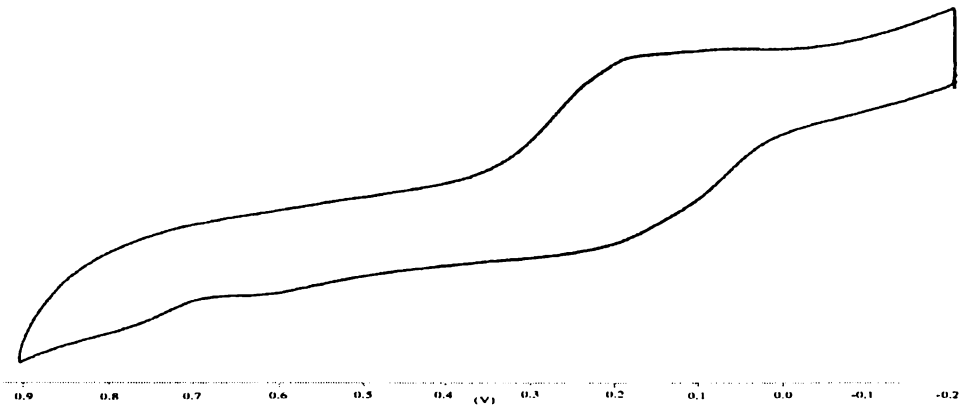

(c)

Figure 2.13: Cyclic Voltammograms for **3** (a), **4** (b) and **5** (c).

Chem., 1977, **81**, 471.

The peak voltages (aniodic and cathodic) and the $E_{1/2}$ values for these compounds are given in Table 2.3.

Table 2.3: Electrochemical Data for **3**, **4** and **5**.

	E^{ξ}_{PA}	E_{PC}	$E_{1/2}$
FcH^{ζ}	0.025	0.100	0.075
3	0.34	0.23	0.035
4	0.29	0.21	0.005
5	0.185 (E'_{PC}0.62)	0.19	0.2775

ζ: Ferrocene included as a reference. ξ: Potentials are listed with respect to Ag/Ag^{+}. Scan rate is $100mVs^{-1}$.

2.2.5: NMR Analyses of Ferrocenyl Phosphonic Acids and Esters

Phosphorus nmr is an invaluable tool for the investigation of phosphorus containing compounds. Phosphorus is mono isotopic, consisting solely of the I = ½ ^{31}P isotope. Thus ^{31}P-{^{1}H} spectra of phosphorus compounds tend to be simple and easily interpreted. The ^{31}P chemical shift of a given phosphorus compound is highly dependant on the oxidation state of the phosphorus atom as well as being sensitive to the chemical nature of any groups bound to the phosphorus atom. In addition the proton coupled (^{31}P-^{1}H) spectra of phosphorus compounds can give insight into the number of and distance to, neighbouring protons. The combination of these factors enables reactions of phosphorus compounds to be closely monitored by nmr and products to be clearly identified by ^{31}P nmr alone.

As an example of this, the silylation of the phosphonate alkylesters results in a chemical shift from ~25ppm to ~16ppm. As the reaction proceeds the peak at ~25ppm shrinks as a peak at ~16ppm grows. The reaction is judged complete when the signal at ~25ppm completely disappears and the spectrum consists of a single peak at ~16ppm.

Simple phosphonic acids ($R\text{-}CH_2\text{-}P(O)(OH)_2$) tend to give signals in the region 20-25ppm which are split into a broad triplet by the adjacent CH_2 group. (Running the sample as a sodium salt in D_2O moves the signal further up-field to 15-20ppm). The analogous esters (alkyl and aryl) give signals in the same region but with more

complex ^{31}P-^{1}H coupling. The acids and esters prepared in this chapter all gave signals of the appropriate chemical shift with the expected coupling to neighbouring protons.

The presence of a phosphorus atom in simple molecules also serves to make assignment of the ^{13}C and ^{1}H nmr spectra an easier task. The ^{31}P-^{13}C and ^{1}H-^{31}P, coupling constants within a series of organophosphorus compounds are consistent and once one member of the series has been fully assigned the rest can confidently be assigned by reference to the first. The esters **2** and **9** and the acids **3** and **4** were fully characterised by HSQC and HMBC nmr experiments. The ^{13}C and ^{1}H nmr spectra of the remaining acids and esters were subsequently assigned by inspection. The carbon and hydrogen spectra of the compounds prepared in this chapter contained no extraordinary signals or coupling behaviour.

2.2.6: Infra-Red Spectroscopy of Ferrocenyl Phosphonic Acids and Esters

The infrared spectra of phosphonic acids are dominated by a broad signal due to the phosphonic OH groups at 2400-2800cm^{-1}, while the characteristic P=O stretching bands occurs in the region 1150-1300cm^{-1}. The ferrocenyl phosphonic acids were no exception. The position of OH and P=O bond stretching bands for acids **3**, **4**, **5**, **6** and **7** are given in Table 2.4.

Table 2.4: O-H and P=O Stretching Frequencies (cm^{-1}) for the Acids **3**-**7**.

Compound	νOH	νP=O	
3	2772	1265	1226
4	2721	1230	1195
5	2797	1202	1130
6	2771	1198	-
7	2749	1265	1225

The OH band is very broad (usually 2350-3150cm^{-1}) as expected, while the P=O bands are sharp and strong. The lowest frequency P=O signals are for acids **5** and **6** which have the phosphonic acid group directly attached to the ferrocenyl Cp

ring. The ν(P=O) values for **5** and **6** are very similar to the ν(P=O) resonances observed for phenylphosphonic acid (1220 and 1140cm^{-1})[41].

Spectra of the monoesters **1** and **2** were not dominated by the νOH band, although it was present. The ν(P=O) band was observed at 1204cm^{-1} in both **1** and **2** respectively. The bands at 1189cm^{-1} and 1188cm^{-1} present in the spectra of both phenyl esters **8** and **9** are attributed to the P=O bond stretch.

2.3: Synthesis of Ferrocenyl Arsonic Acids

There are few synthetic methods available for the direct synthesis of arsonic acids R-As(O)(OH)$_2$. The preparation of aliphatic arsonic acids tends to be limited to the Meyer reaction[42] between alkyl halides and sodium arsenite (Na_3AsO_3), as shown in Scheme 2.12.

$$As_2O_3 + 6NaOH \longrightarrow 2Na_3AsO_3 + 3H_2O$$

$$Na_3AsO_3 + R\text{-}X \longrightarrow R\text{-}AsO_3Na_2 + NaX$$

X = Cl, Br or I

Scheme 2.12: Meyer Reaction for Synthesis of Arsonic Acids.

The free acid is obtained from the sodium salt by acidification. The Meyer reaction is most often carried out in water using an alkyl chloride or bromide with the desired product separating upon acidification of the reaction medium[43]. Reactions of appropriate ferrocenyl compounds with sodium arsenite might be expected to produce the ferrocenyl arsonic acids (Scheme 2.13).

---

[41] D. Dolphin and A. Wick, Chap. 7.2 in; Tabulation of Infrared Spectral Data, J. Wiley and Son, NY, 1977.

[42] G. Meyer, *Chem. Ber.*, 1883, **16**, 1439.

[43] A. J. Quick and R. Adams, *J. Am. Chem. Soc.*, 1922, **44**, 805.

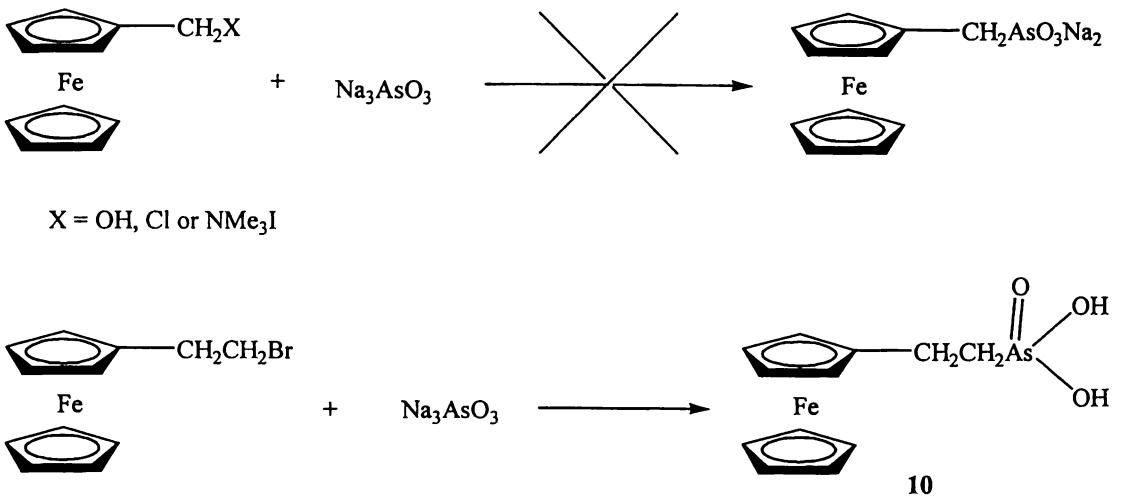

Scheme 2.13: Reaction of Ferrocenyl Compounds with Sodium Arsenite.

The reactions of $FcCH_2NMe_3I$, $FcCH_2OH$ and $FcCH_2Cl$ with sodium arsenite did not produce the arsonic acid, $FcCH_2As(O)(OH)_2$. Only starting material and ferrocenylmethyl alcohol ($FcCH_2OH$) were obtained upon work-up. The reactions of $FcCH_2OH$ and $FcCH_2NMe_3I$ with sodium arsenite were performed by reflux in a single phase aqueous solution. Work-up involved acidification of the aqueous solution with concentrated hydrochloric acid and extraction with CH_2Cl_2. The chloride $FcCH_2Cl$ was reacted with sodium arsenite in a two phase CH_2Cl_2/water system also at reflux. Separation of the layers followed by acidification of the aqueous layer and extraction with CH_2Cl_2 did not give any of the desired product.

Reaction of ferrocenylethylbromide $FcCH_2CH_2Br$ with sodium arsenite was more successful. The arsonic acid $FcCH_2CH_2As(O)(OH)_2$ **10**, was isolated in fair yield as an air-stable yellow powder. The acid did not react with air over time (though neither did the analogous phosphonic acid $FcCH_2CH_2P(O)(OH)_2$ **4**, section 2.2). Unlike the phosphonic acids, which decomposed upon melting, the arsonic acid **10** had a clearly defined melting point and did not decompose.

The difference in the reaction of $FcCH_2Cl$ and $FcCH_2CH_2Br$ with sodium arsenite is most likely related to the relative stabilities of these halides. The bromide is an air stable compound at room temperature. The chloride, as mentioned earlier, is an unstable compound, due in part to the stability of the carbocation $Fc\text{-}CH_2^+$. The

ability of ferrocene to stabilise α-carbocations is well known and much studied[44]. The chloride is therefore prone to nucleophilic attack. The sodium arsenite solution is strongly basic and it is likely that the AsO_3^{3-} ion loses out to OH^- in competition for the ferrocenylmethyl group. (The Meyer reaction is proposed to occur through reaction of the sodium arsenite species NaO_3As^{2-} that is less nucleophilic than the naked AsO_3^{3-} ion[45]).

The arsonic acid **10** gave routine ^{13}C and ^1H spectra, assigned by comparison with those of the analogous phosphonic acid **4**. The infrared spectrum of **10** is dominated by the broad ν(OH) bands at 2743cm^{-1}, 2385cm^{-1} and 2303cm^{-1}, and by the strong ν(As=O) band at 881cm^{-1}. These are within the expected regions for such groups[46].

The negative ion ES mass spectra of **10** were of some interest. The acid was introduced to the spectrometer as a solution in methanol with pyridine added to aid ionisation. Methanol was used as the carrier solvent. At a cone voltage of 20V the spectrum consists of a single peak at *m/z* 351, this is due to a $[M-2H^++Me^+]^-$ ion. This implies that the sample was methylated by the solvent.

At 60V the spectrum is more complex. The base peak is now due to the $[M-CpCH_2CH_2-2H^++Me^+]^-$ (*m/z* 259) ion, while significant peaks at *m/z* 107 and *m/z* 139 are also present. These were assigned as due to the $[M-H_2O-FcCH_2CH_2^+]^-$ (more conveniently written as $[AsO_2]^-$) and $[M-H_2O-FcCH_2CH_2^++MeOH]^-$ (more conveniently written as $[AsO_2^-+MeOH]^-$) ions respectively. At very low relative intensity peaks due to $[M-H^+]^-$ (*m/z* 337) and $[M-CpCH_2CH_2-H^+]^-$ (*m/z* 245) are also observed. The peaks at *m/z* 245 and 259 are of particular interest as they require the arsenic-carbon bond to cleave and the arsonic acid group to interact with the bare iron atom, as depicted in Figure 2.14.

---

[44] (a) W. E. Watts, *J. Organomet. Chem. Libr.*, 1979, **7**, 399. (b) E. A. Hill and R. Wiesner, *J. Am. Chem. Soc.*, 1969, **91**, 509. (c) E. A. Hill, *J. Organomet. Chem.*, 1970, **24**, 457.

[45] A. J. Quick and R. Adams, *J. Am. Chem. Soc.*, 1922, **44**, 805.

[46] J. T. Braumholtz, G. E. Hall, F. E. Mann and N. Sheppard, *J. Chem. Soc.*, 1959, 868. (b) C. F. McBrearty, K. Irgolic and R. A. Zingaro, *J. Organomet. Chem.*, 1968, **12**, 377.

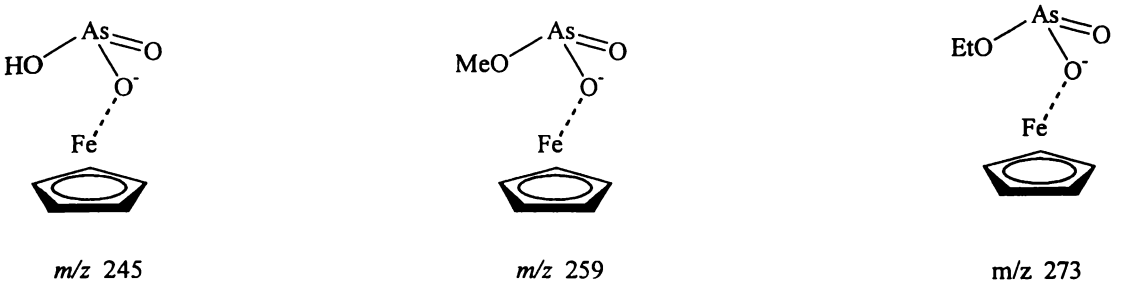

m/z 245 *m/z* 259 m/z 273

Figure 2.14: Proposed Structure of the $[M\text{-}CpCH_2CH_2\text{-}H^+]^-$ (*m/z* 245), $[M\text{-}CpCH_2CH_2\text{-}2H^+\text{+}Me^-]^-$ (*m/z* 259) and $[M\text{-}CpCH_2CH_2\text{-}2H^+\text{+}Et^-]^-$ (*m/z* 273) ions.

At a cone voltage of 100V the spectrum collapses to a single peak at *m/z* 107 due to the AsO_2^- ion. As will be shown later, this behaviour at high cone voltages is characteristic of arsonic acids. The spectra described above are displayed in Figure 2.15.

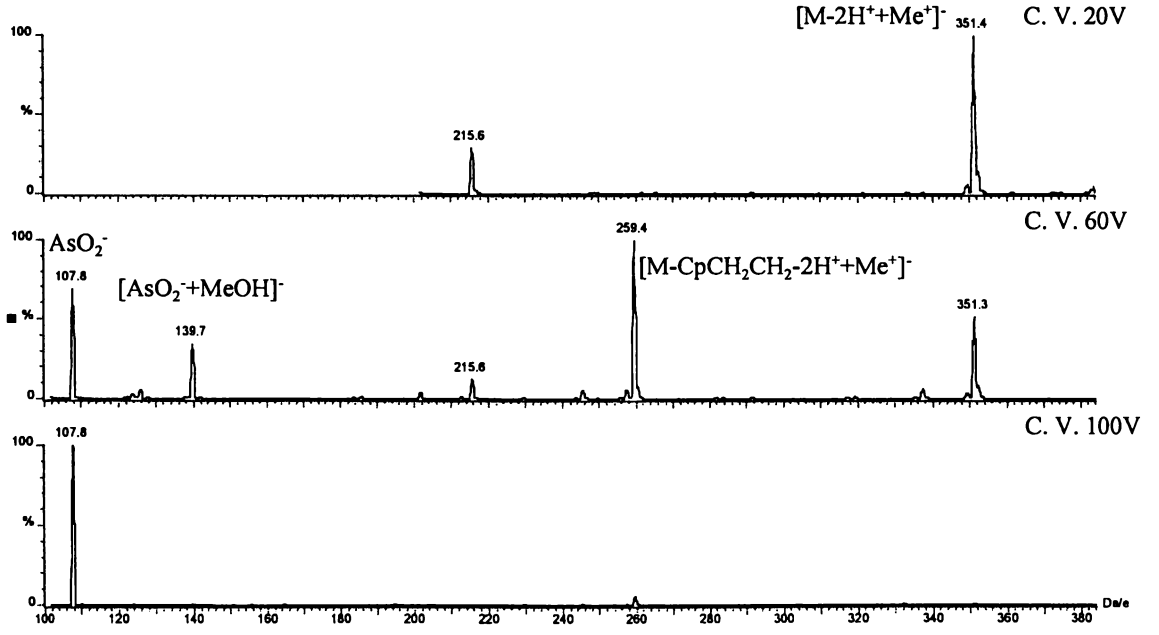

Figure 2.15: The Negative Ion ES Mass Spectra of $FcCH_2CH_2AsO_3H_2$ in Methanol at Cone Voltages of 20, 60 and 100V.

To provide proof that the solvent was methylating the arsonic acid **10**, further samples were introduced to the spectrometer as solutions in ethanol, with ethanol

being used as the carrier solvent. The spectrum at a cone voltage of 20V was dominated by peaks due to $[M\text{-}2H^+\text{+}Et^+]^-$ (*m/z* 365) and $[M\text{-}2H^+\text{+}Et^+\text{+}EtOH]^-$ (*m/z* 411). Ethylation was occurring as expected.

At 40V the ethanol adduct disappears and the spectrum contains peaks due to $[M\text{-}2H^+\text{+}Et^+]^-$ (*m/z* 365), $[M\text{-}2H^+\text{+}Me^+]^-$ (*m/z* 351) and $[M\text{-}H^+]^-$ (*m/z* 337). The methylated peak at *m/z* 351 is due to residual methanol in the system.

At 60V the peak at *m/z* 365 still dominates, but of almost equal intensity is the peak at *m/z* 273 due to $[M\text{-}CpCH_2CH_2\text{-}2H^+\text{+}Et^+]^-$. This is the ethylated version of the peak seen at *m/z* 259 in the spectrum run in methanol. At 100V the spectrum is simply a single peak at *m/z* 107 due to the AsO_2^- ion. Figure 2.16 displays the spectra of **10** in methanol and ethanol at 40V. The alkylating effect of the solvents is clearly visible.

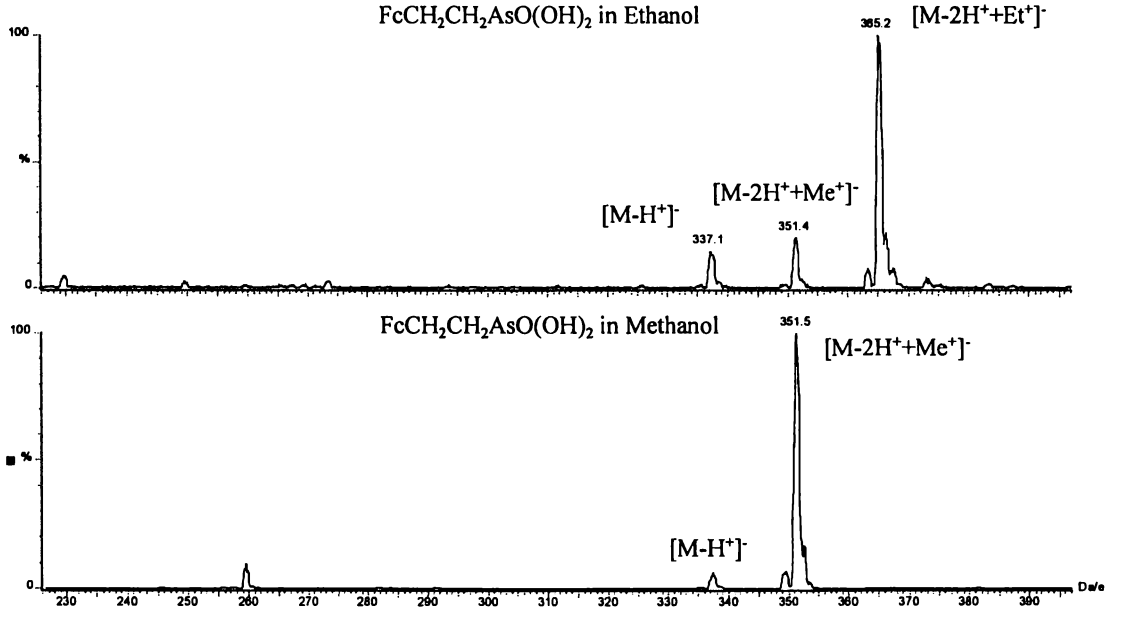

Figure 2.16: Negative Ion ES Mass Spectra of $FcCH_2CH_2AsO_3H_2$ Run in Methanol and Ethanol at a Cone Voltage of 40V.

The behaviour of the arsonic acid **10** is in stark contrast to that of the phosphonic acid **4**. No methylation of any phosphonic acid in the ES mass spectrometer was ever observed in the presence of MeOH. At high cone voltages the spectra of **4** were dominated by the $[M\text{-}2H^+\text{-}Cp^-]^-$ ion with interaction of the

phosphonic acid group and the bare iron atom assumed. The loss of the neutral $CpCH_2CH_2$ group was not seen in any ES mass spectra of **4**.

Studies of the positive ion ESMS behaviour of organoarsenic acids tend to dominate the published literature[47] which seems anomalous, given the acidic nature of these compounds and the equal ability of the ES mass spectrometer to operate in positive or negative ion modes. The acids have been found to form $[M+X^+]^+$ (X = H, Na and K) ions under ESMS conditions[47a,b] and the positive ion mode has been used in the development of analytical techniques[47c,48]. The use of methanolic solvents is commonplace in the reported studies and methanol is specifically added to increase sensitivity in one study[49].

Pergantis *et al.*[47b] looked at the positive ion behaviour of six organoarsenic acids in a methanol/water solvent system in the presence of acetic acid. In all cases the protonated molecule was the most intense ion. Interestingly however all of the spectra also contained weak peaks due to the respective $[M+H^+ + MeOH - H_2O]^+$ ions. This ion corresponds to the methylation of the acid by methanol, followed by protonation.

2.4: An ESMS Study of Organoarsenic Acids

Prompted by the lack of negative ion ESMS studies of arsonic acids, a brief study of the negative ion ESMS properties of dimethylarsinic acid (Me_2AsO_2H), *o*-amino(phenylarsonic) acid ($2\text{-}NH_2\text{-}(C_6H_4AsO_3H_2)$) and phenylarsonic acid ($PhAsO_3H_2$) was undertaken. The acids were introduced to the spectrometer as solutions in methanol and ethanol, with pyridine added to aid ionisation. The carrier solvent was methanol for methanolic samples and ethanol for ethanolic samples.

---

[47] (a) M. H. Florencio, M. F. Duarte, A. M. M. de Bettencourt, M. L. Gomes and L. F. Vilas Boas, *Rapid Commun. Mass. Spect.*, 1997, **11**, 469. (b) S. A. Pergantis, W. Winnik and D. Betowski, *J. Anal. At. Spectrom.*, 1997, **12**, 531. (c) N. Shimizu, K. Yoshida, H. Chen, K. Kuroda and G. Endo, *Appl. Organomet. Chem.*, 1999, **13**, 81.

[48] O. Schramel, B. Michalke and A. Kettrup, *J. Anal. At. Spectrom.*, 1999, **14**, 1339.

2.4.1: Samples Dissolved and Run in Methanol

Methylation of dimethylarsinic acid was not observed under the conditions of this experiment (methylation may have occurred but the resulting ester is unlikely to form negative ions). At a cone voltage of 20V the base peak was due to the $[M\text{-}H^+]^-$ ion at *m/z* 137. Smaller peaks at *m/z* 153 (unassigned) and *m/z* 169, $[M\text{-}H^+\text{+}MeOH]^-$ were also observed. As the cone voltage is increased, peaks due to AsO_2^-, *m/z* 107 and $MeAsO_2H^-$ *m/z* 123 appear. At cone voltages above 80V the spectra collapse to a single peak at *m/z* 107 (Figure 2.17).

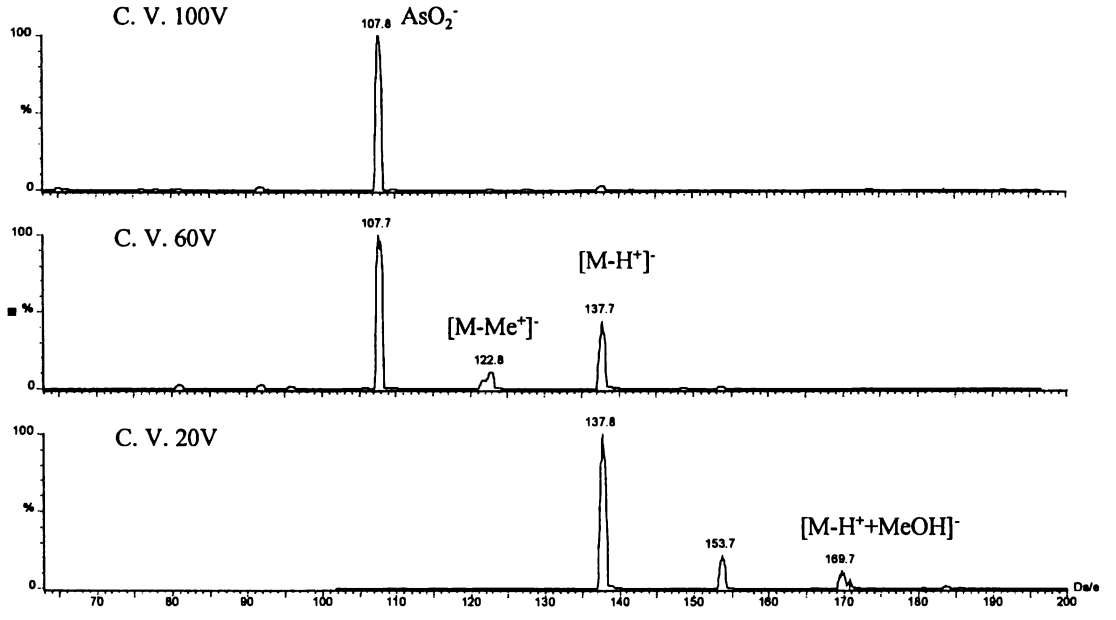

Figure 2.17: The ES Mass Spectra of Me_2AsO_2H in Methanol at Negative Cone Voltages of 20V, 60V and 100V.

In contrast phenylarsonic acid methylated to such a degree that at a cone voltage of 20V the only peak observed on the spectrum was due to $[M\text{-}2H^+\text{+}Me^+]^-$, *m/z* 215. Increasing the cone voltage gave rise to additional peaks at *m/z* 201, $[M\text{-}H^+]^-$, 139, $[AsO_2^-\text{+}MeOH]^-$ and *m/z* 107 $[AsO_2]^-$. Again, at cone voltages greater than 60V only the peak due to AsO_2^- *m/z* 107 is observed (Figure2.18).

The negative ion ESMS behaviour of the substituted acid *o*-amino(phenylarsonic) acid (shown in Figure 2.19), was more complex than that of

[49] N. Shimizu, Y. Inoue, D. Yoshinori, S. Daishima and K. Yamaguchi, *Anal. Sci.*, 1999, **15**, 685.

phenylarsonic acid. At low cone voltages the base ion was that due to methylation by the solvent, *m/z* 230 $[M\text{-}2H^{+}+Me^{+}]^{-}$, but also present are peaks at *m/z* 216, $[M\text{-}H^{+}]^{-}$, *m/z* 262 $[M\text{-}2H^{+}+Me^{-}+MeOH]^{-}$ and *m/z* 276 (unassigned).

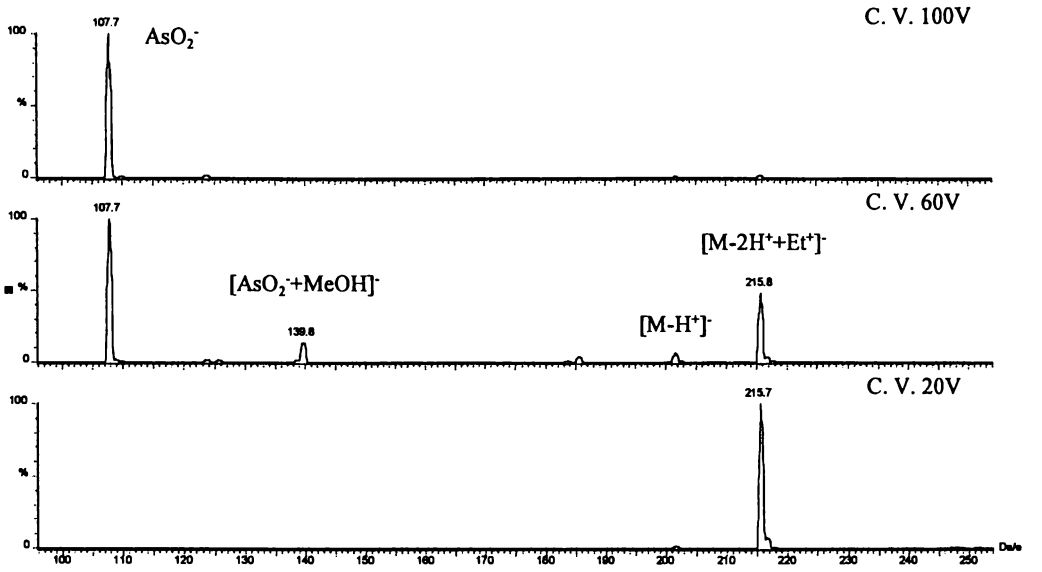

Figure 2.18: The ES Mass Spectra of $PhAsO_3H_2$ in Methanol at Negative Cone Voltages of 20V, 60V and 100V.

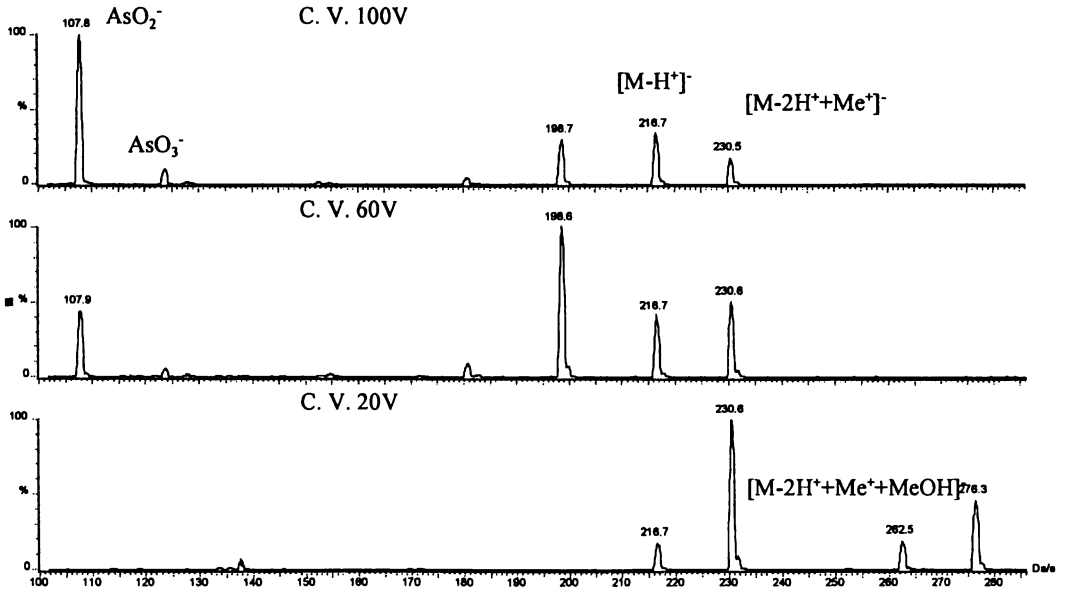

Figure 2.19: Negative Ion ES Mass Spectra of 2-NH_2-($C_6H_4AsO_3H_2$) in Methanol at Cone Voltages of 20V, 60V and 100V.

Increasing the cone voltage to 60V results in the disappearance of the methanol adducts and the appearance of peaks at *m/z* 198 (unassigned), 180 (unassigned), 123 (AsO_3^-) and 107 (AsO_2^-). The peak at *m/z* 198 dominates the spectrum at a cone voltage of 60V while at cone voltages greater than 70V the base peak is that due to AsO_2^-. Unlike the high cone voltage spectra of Me_2AsO_2H and $PhAsO_3H_2$ which collapse to a single peak (*m/z* 107), the high cone voltage spectra (70-120V) of *o*-amino(phenylarsonic) acid always contained significant peaks at *m/z* 230, 216, 198, 180 and 123.

2.4.2: Samples Dissolved and Run in Ethanol

The low cone voltage (20V) spectrum of dimethylarsinic acid, when dissolved and run in ethanol, is dominated by the $[M\text{-}H^+\text{+}EtOH]^-$ *m/z* 183 ion with a small peak due to $[M\text{-}H^+]^-$ *m/z* 137 also present. As the cone voltage is increased the ethanol adduct disappears and the spectrum at a cone voltage of 40V contains only the $[M\text{-}H^+]^-$ *m/z* 137 peak. Further increases in cone voltage mirrored the behaviour seen in the methanolic sample, with the spectra above a cone voltage of 80V containing only a peak due to the AsO_2^- *m/z* 107 ion.

The spectrum of $PhAsO_3H_2$ in ethanol at a cone voltage of 20V is dominated by the ethylated ion $[M\text{-}2H^+\text{+}Et^+]^-$ *m/z* 229 and its ethanol adduct $[M\text{-}2H^+\text{+}Et^-\text{+}EtOH]^-$ *m/z* 275. Increasing the cone voltage caused the ethanol adduct to vanish while peaks due to $[M\text{-}H^+]^-$ *m/z* 201 and $[M\text{-}2H^+\text{+}Me^+]^-$ *m/z* 215 appear. Methylation is due to residual methanol in the system. As the cone voltage is increased to 60V the *m/z* 201 peak becomes dominant, (this is in contrast to the behaviour of $PhAsO_3H_2$ in methanol where the *m/z* 201 ion is always at low relative intensity). At cone voltages above 80V the spectra are dominated by the *m/z* 107 (AsO_2^-) ion with the *m/z* 123 (AsO_3^-) ion also being observed at low relative intensity.

The low cone voltage (20V) spectra of *o*-amino(phenylarsonic acid) in ethanol is dominated as expected by the $[M\text{-}2H^+\text{+}Et^+]^-$ *m/z* 244 ion. Also observed are the $[M\text{-}H^+]^-$ *m/z* 216, $[M\text{-}H^+\text{+}EtOH]^-$ *m/z* 262 and $[M\text{-}2H^+\text{+}Et^+\text{+}EtOH]^-$ *m/z* 290 ions. As the cone voltage is increased the ethanol adducts disappear and the behaviour mimics that previously described for the methanolic *o*-amino(phenylarsonic acid) sample.

Dimethylarsinic acid cannot be easily methylated or ethylated and still produce a negative ion species in the ES mass spectrometer and none were observed. Adducts of these solvents did form at low cone voltages, though such spectra were dominated by the peak at *m/z* 137 $[M\text{-}H^+]^-$. At high cone voltages (>60V) the spectra contained only peaks due to the AsO_2^- and AsO_3^- ions at *m/z* 107 and *m/z* 123 respectively. These peaks are a result of the carbon-arsenic bonds breaking in the ES mass spectrometer. The carbon-arsenic bond is known to be much weaker than the carbon-phosphorus bond (C-As 190-225kJmol^{-1}, C-P 230-265kJmol^{-1})[50] and the equivalent C-P cleavage is not observed in the ES mass spectra of phosphonic acids.

The ESMS behaviour of arsonic acids in methanol and ethanol seems to be fairly consistent. At low cone voltages methylated and ethylated species are observed for the three arsonic acids surveyed ($PhAsO_3H_2$, 2-NH_2-($C_6H_4AsO_3H_2$) and $FcCH_2CH_2AsO_3H_2$). At moderate cone voltages (40V-80V) the fragmentation patterns are dependant on the chemical nature of the arsonic acid R group, though in all cases an $[M\text{-}H^+]^-$ ion was observed. At high cone voltages (>80V) the spectra of all of the arsonic acids contain the base peak at *m/z* 107 (AsO_2^-) and a low intensity peak at *m/z* 123 (AsO_3^-). These inorganic fragments are a result of carbon-arsenic bond cleavage.

2.5: Concluding Remarks

Ferrocenyl phosphonic acids are accessible from appropriate precursors using standard chemical techniques. The compounds are yellow crystalline solids that decompose upon heating and are soluble in methanol and ethanol. The acids containing the -$CH_2P(O)(OH)_2$ group (acids **3** and **7**) tend to oxidise in air to give the green ferrocenium derivative, from which the parent acid can be retrieved by reduction.

Characterisation by nmr, ESMS, IR and elemental analyses were routine. The cyclic voltammograms of acids **3**, **4** and **5**, were dominated by a single oxidation/reduction of the ferrocenyl group. Thus the acids have potential to act as electrochemically inert tethers for the ferrocene moiety.

---

[50] D. W. Smith, Inorganic Substances, Cambridge University Press, 1990, page 186.

The ferrocenyl arsonic acid $FcCH_2CH_2As(O)(OH)_2$ **10** was easily prepared from $FcCH_2CH_2Br$ using the Meyer reaction. The acid was an air stable yellow crystalline powder with a clearly defined melting point. The variable cone voltage ES mass spectra of this compound proved of some interest. The acid was found to be alkylated by alcoholic solvents under ESMS conditions, while at higher cone voltages cleavage of the C-As bond was observed. This behaviour was shown to be characteristic of arsonic acids.

2.6: Experimental

All solvents were LR grade or better and the solvents, thf, Et_2O, CH_2Cl_2 and petroleum spirits (b.p. 60-80°C), were distilled from drying agents (sodium/benzophenone for thf and Et_2O, calcium hydride for CH_2Cl_2 and petroleum spirits) under a dinitrogen atmosphere before being used. Reactions were carried out in air unless otherwise stated.

Platinum dioxide (BDH), H_2 (BOC Gases), Na (BDH), ^{n}BuLi, 1.6M in hexanes (Aldrich), ^{t}BuLi, 1.7M in pentane (Aldrich) and PCl_3 (Aldrich) were used as supplied. The starting materials diethylphosphite (Aldrich), triethylphosphite (BDH) and ferrocene (Strem Chemicals) were used as supplied. The ferrocenyl phosphonate $FcCH_2P(O)(OPh)_2$ was kindly supplied by Dr Bill Henderson. The starting materials $[FcCH_2NMe_3]I$[51], $FcCH_2OH$[52], $FcCH_2CH_2OH$[53], FcLi[54], 1,1'-$Fc'Li_2$[55], Me_3SiBr[56], $(PhO)_2P(O)H$[57], and $(RO)_2P(O)Cl$[58], (R = Et and Ph), were prepared by literature methods.

The known compound 1,1'-$Fc'[CH_2OH]_2$ was prepared by the reaction of 1,1'-$Fc'Li_2$ with two mol equivalents of paraformaldehyde $(CH_2O)_n$ in diethyl ether at room temperature. This was an adaption of the method outlined by Goldberg and Bailey[32] for the synthesis of 1,2-Fc' $[CH_2OH]_2$.

---

[51] D. Lednicer and C. R. Hauser, *Organic Synthesis*, **5**, 434.
[52] J. K. Lindsay and C. R. Hauser, *J. Org. Chem.*, 1957, **22**, 355.
[53] D. Lednicer, J. K. Lindsay and C. R. Hauser, *J. Org. Chem.*, 1958, **23**, 653.
[54] F. Rebiere, O. Samuel and H. B. Kagan, *Tetrahedron Lett.*, 1990, **31**, 3121.
[55] J. J. Bishop, A. Davison, M. L. Katcher, D. W. Lichtenberg, R. E. Merrill, J. C Smart, *J. Organomet. Chem.*, 1971, **27**, 241.
[56] P. A. McCusker and E. L. Reilly, *J. Am. Chem. Soc.*, 1953, **75**, 1583.
[57] E. N. Walsh, *J. Am. Chem. Soc.*, 1959, **81**, 3023.

Cyclic voltammetry measurements were undertaken by Jeremy Yeo at the National University of Singapore. Melting points were determined using a Reichert Thermopan melting point microscope and are uncorrected. Elemental analyses were performed by the Microanalytical Laboratory, Chemistry Department, University of Otago, Dunedin, New Zealand. The Fourier-transform IR spectra were obtained using a Bio-Rad FTS40 spectrometer. Samples of the phosphonic acids were run as KBr discs, while samples of the esters and arsonic acid, were run as solutions in CH_2Cl_2 Hydrogenation was undertaken in a Parr pressure reaction apparatus at an operating pressure of 50p.s.i.

Electrospray mass spectra were obtained with a VG Platform II mass spectrometer. Samples were dissolved in an appropriate solvent and introduced into the spectrometer via a 10μl sample loop using a Thermo Separation Products SpectaSystem P1000 LC pump at a flow rate of $0.01 ml min^{-1}$. Cone voltages were typically varied from 20 to 120V to maximise spectra quality. To aid ionisation, pyridine was added to acidic samples, while M^+ (M = Na, K, Li, Cs and Rb) ions were added to phosphonate ester samples as aqueous solutions of the appropriate metal chloride.

A Bruker AC300 spectrometer operating at 121.51 MHz was used to acquire all ^{31}P NMR spectra. The ^{31}P NMR chemical shift assignments were made with respect to an external reference of 85% orthophosphoric acid.

The ^{13}C and ^{1}H NMR spectra were obtained on either a Bruker AC300 or on a Bruker DRX400 spectrometer and referenced to residual solvent lines. Solvents were assigned the following chemical shift values with respect to the external $SiMe_4$ reference: $CDCl_3$, 7.26 (^{1}H), 77.06 (^{13}C); d^6-DMSO, 2.6 (^{1}H), 39.5 (^{13}C); D_2O, 3.5 (MeOH, ^{1}H), 49.3 (MeOH, ^{13}C). Acid samples were often dissolved in $NaOD/D_2O$ solution prepared by reaction of a small amount of Na (~1-3mg) with excess D_2O (~2ml).

For ^{13}C, the AC300 and DRX400 spectrometers were run at 75.47 and 100.62MHz respectively. For ^{1}H, the AC300 and DRX400 spectrometers were run at 300.13 and 400.17MHz respectively. Two-dimensional HSQC and HMBC experiments were used to unambiguously assign spectra for compounds **2**, **3**, **4**, **8** and

---

[58] G. Sosnovsky and E. H. Zaret, *J. Org. Chem.*, 1969, **34**, 968.

9. These experiments were run using standard pulse sequences supplied by Bruker. Comparison of these results with other spectra aided in full assignment of the rest of the compounds. The atom labelling scheme used for assignment of ferrocenyl NMR signals is given in figure 2.20.

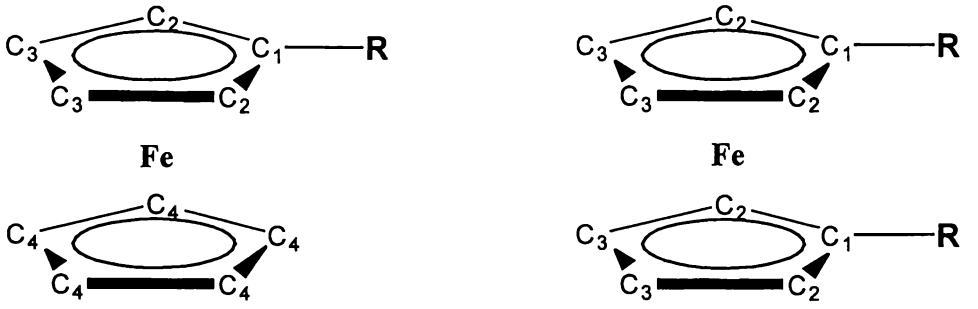

Figure 2.20: Atom Labelling Used in Assignment of Ferrocenyl NMR Signals.

2.6.1: Syntheses

2.6.1.1: Synthesis of $FcCH_2P(O)(OPh)(OH)$ **1**

To a solution of diphenyl ferrocenylmethylphosphonate (0.55g, 1.2mmol), in MeOH (25ml) was added a catalytic amount (~5mg) of PtO_2 (Adam's catalyst). This mixture was placed under a dihydrogen atmosphere (50 p.s.i.) and agitated for 4 days. The dark green solution was allowed to slowly evaporate resulting in the precipitation of dirty yellow crystals of **1**. The crystals were dissolved in CH_2Cl_2 (10ml), the solution filtered and extracted with 10% $NaHCO_3$ (2 × 10ml). The combined aqueous fractions were washed with CH_2Cl_2 (1 × 10ml), acidified with concentrated HCl then extracted with CH_2Cl_2 (2 × 10ml). The combined organic fractions were dried over $MgSO_4$ and filtered. The product was precipitated by addition of petroleum spirits, filtered and air dried to give 21.3mg (4.6%) of yellow powder.

m.p. 160^0C

Elemental Analyses: Found C, 57.39%; H, 4.86%. Calculated for $C_{17}H_{17}FeO_3P$: C, 57.30%; H, 4.81%.

^{31}P-{^{1}H} NMR ($CDCl_3$): δ 26.45

^{13}C -{^{1}H} NMR ($CDCl_3$): δ 150.18 (*d*, $^{2}J_{C-P}$ 11Hz, Ph, *i*-C), 129.62 (*s*, Ph, *m*-C), 124.86 (*s*, Ph, *p*-C), 120.76 (*s*, Ph, *o*-C), 70.10 (*s*, C2), 69.43 (*s*, C4), 68.40, (*s*, C3), 27.67 (*d*, $^{1}J_{C-P}$ 140Hz, $\underline{C}H_2P$)

^{1}H NMR ($CDCl_3$): δ 7.24-6.90 (5H, *m*, Ph), 4.24 (2H, *br. s*, H3), 4.13 (7H, *br. s*, H2,H4), 2.95 (*d*, $^{2}J_{H-P}$ 21Hz, $C\underline{H}_2P$).

ESMS: ($MeOH/H_2O$, c. v. 20V) *m/z* 355 ([M-H^+]$^-$, 100%), 325 ([M-H^++MeOH]$^-$, 10%).

IR (Solution in CH_2Cl_2) (cm^{-1}): 3053 (s, br), 2926 (w), 1204 (s), 1105, (m), 1071 (w), 1039 (w), 1025 (w), 1000 (w), 985 (w), 923 (m).

2.6.1.2: Synthesis of $FcCH_2P(O)(OEt)(OH)$ **2**

The sodium salt of diethyl phosphite was prepared by refluxing a mixture of diethyl phosphite (6.97ml, 0.054mol) and sodium metal (1.24g, 0.054mol) in dry toluene (80ml) under an inert atmosphere until no trace of the metal was observed, (1-2 hours.). To the still hot solution was added $FcCH_2OH$ (5.85g, 0.027mol) in ~1g portions and reflux continued for three hours. The reaction solution was cooled and 60ml of 10% $NaHCO_3$ solution added. The resulting two phase system was stirred for 10 minutes before the layers were separated.

The aqueous layer was washed with Et_2O (1 × 40ml), acidified with concentrated HCl and extracted with CH_2Cl_2 (3 × 30ml). The combined CH_2Cl_2 fractions were dried over $MgSO_4$ and filtered. The solution was concentrated (to ~10ml) and acetone added until no further precipitation occured. The precipitate was filtered, washed with cold water (10ml) followed by acetone (5ml), then air dried to give 5.43g (65%) of **2** as a microcrystalline yellow powder.

m.p. 183°C (dec).

Elemental Analyses: Found C, 50.32%; H, 5.59%. Calculated for $C_{13}H_{17}FeO_3P$: C, 50.67%; H, 5.56%.

^{31}P-{^{1}H} NMR ($CDCl_3$): δ 29.11.

^{13}C-{^{1}H} NMR ($CDCl_3$): δ 16.33 (*d*, $^{3}J_{C\text{-}P}$ 6.39Hz, $OCH_2\underline{C}H_3$), 28.24 (*d* $^{1}J_{C\text{-}P}$ 142Hz, $\underline{C}H_2P$), 61.56 (*d*, $^{2}J_{C\text{-}P}$ 6.93Hz, $O\underline{C}H_2CH_3$), 67.87 (*s*, C3), 68.91 (*s*, C4'), 69.47 (*d*, $^{3}J_{C\text{-}P}$ 3.10Hz, C2).

^{1}H NMR ($CDCl_3$): δ 1.24 (3H, *t*, $^{3}J_{H\text{-}H}$ 6.97Hz, $OCH_2C\underline{H}_3$), 2.85 (2H, *d*, $^{2}J_{H\text{-}P}$ 19.88Hz, $C\underline{H}_2P$), 3.93 (2H, *m*, $OC\underline{H}_2CH_3$), 4.09, (2H, *d*, $^{3}J_{H\text{-}H}$ 1.55Hz H3), 4.11 (5H, *s*, H4), 4.23 (2H, *br s*, H2), 6.7 (1H, *br s*, PO<u>H</u>).

ESMS: ($MeCN/H_2O$, c. v. 20V) *m/z* 307 ([M-H^+]$^-$, 100%), 325 ([M-H^++H_2O]$^-$, 9%).

IR (Solution in CH_2Cl_2) (cm^{-1}): 3416 (w), 1221 (m), 1204 (s), 1104 (m), 1051 (s), 1024 (s), 966 (m), 806 (m), 609 (w), 493 (m), 475 (m).

2.6.1.3: Synthesis of $FcCH_2PO_3H_2$ **3**

A solution of NEt_3 (0.82g, 8.1mmol) and **2** (2.5g, 8.11mmol) in 50ml dry CH_2Cl_2 was placed under an inert atmosphere in an oven dried flask. To this $(CH_3)_3SiBr$ (6.2g, 40mmol) was added and the mixture refluxed gently for 3 hours. The reaction was cooled to R.T., 50ml of saturated aqueous $NaHCO_3$ solution added and the two phase system stirred vigorously for a further 3 hours. The layers were separated, the aqueous phase was washed with CH_2Cl_2 (2 × 25ml) and acidified with concentr

ated HCl. The yellow precipitate was filtered and washed with H_2O (2 × 50ml) then dried in air to give 2.08g (91%) of the desired product.

m.p. 222-228°C (dec)

Elemental Analyses: Found C, 46.50%; H, 5.75%. Calculated for $C_{11}H_{13}FeO_3P$: C, 47.18%; H, 4.68%.

^{31}P-{^{1}H} NMR (DMSO):δ 23.13.

^{13}C-{^{1}H} NMR (DMSO): δ 29.68 (*d*, $^{1}J_{P\text{-}C}$ 134Hz, $\underline{C}H_2P$), 67.16 (*s*, C3), 68.66 (*s*, C4), 69.24 (*br. s*, C2), 80.26 (*br. s*, C1).

^{1}H NMR (DMSO): δ 2.65 (2H, *d*, $^{2}J_{P\text{-}H}$ 19Hz, $C\underline{H}_2P$), 4.00 (2H, *s*, H3), 4.07 (5H, *s*, H4), 4.15 (2H, *s*, H2).

ESMS: ($MeCN/H_2O$, c. v. 60V) *m/z* 279 ([M-H^+]$^-$, 100%).

IR (KBr disc) (cm^{-1}): 2753 (br, s), 1264 (m), 1225 (m), 1103 (s), 992 (s), 947 (s), 925 (m), 832 (m), 814 (m), 610 (w), 542 (w), 498 (m), 436 (m).

2.6.1.4: Synthesis of $FcCH_2CH_2P(O)(OH)_2$ **4**

$FcCH_2CH_2Br$ (0.85g, 2.9mmol) was dissolved in 5ml of triethylphosphite. The solution was placed under a dinitrogen atmosphere and brought to reflux. After 5 hours at reflux the solution was cooled and the excess triethylphosphite removed by distillation (~ 0.2mmHg R.T.). The residue was taken up into CH_2Cl_2 (10ml) and placed under a dinitrogen atmosphere. Triethylamine (1.47g, 14.5mmol) and $(CH_3)_3SiBr$, (2.22g, 14.5mmol) were added and the reaction stirred for 4 hours at R.T. 1M NaOH (20ml) was added and stirring continued for 30 minutes. The layers were separated and the aqueous layer washed with CH_2Cl_2 (2 × 20ml), then acidified with concentrated HCl. The yellow precipitate was filtered, washed liberally with cold water and air dried to give 0.58g (68%) of **4**.

m.p.: 185-190°C (dec.)

Elemental Analyses: Found C, 49.01%, H, 5.30% Calculated for $C_{12}H_{15}FeO_3P$: C 49.1%, H 5.1%.

^{31}P-{^1H} NMR (d_6-DMSO): δ 26.63

^{13}C-{^1H} NMR (d_6-DMSO): δ 22.54 (*d*, $^2J_{C\text{-}P}$ 2Hz $\underline{C}H_2CH_2P$), 28.66 (*d*, $^1J_{C\text{-}P}$ 101Hz, $\underline{C}H_2P$), 66.87 (*s*, C3), 67.33 (*s*, C2) 68.18 (*s*, C4), 89.05 (*d*, $^3J_{C\text{-}P}$ 16Hz C1).

^1H NMR (d^6-DMSO): δ 1.84 (2H, *d*, $^2J_{H\text{-}P}$ 18Hz, $C\underline{H}_2P$), 2.46 (2H, *br s*, $C\underline{H}_2CH_2P$), 4.03 (2H, br s, H3), 4.09 (9H, m, H2 and H4), 7.22 (1.2H, *br. s.*, $PO\underline{H}$).

ESMS: ($MeCN/H_2O$, c.v. 20V) *m/z* 293 ($[M\text{-}H^+]^-$ 100%), 311 ($[M\text{-}H^+ + H_2O]^-$ 10%)

IR (KBr disc) (cm^{-1}): 3414 (w), 2721 (br, m), 1230 (m), 1195 (m), 1112 (s), 1019 (s), 961 (m), 931 (s), 824 (m), 814 (m), 677 (m), 520 (m), 505 (m), 494 (m).

Note 1: Separation of the diethyl-ester intermediate $[FcCH_2CH_2P(O)(OEt)_2]$ by flash column chromatography (Al_2O_3, EtOAc to MeOH solvent gradient) prior to hydrolysis did not improve the overall yield.

Note 2: The triethylamine can be omitted if the trimethylsilylbromide is freshly distilled and glassware is dry.

2.6.1.5: Synthesis of $FcP(O)(OH)_2$ **5**

Ferrocene (0.93g, 5mmol) was dissolved in dry thf (5ml), placed under a dinitrogen atmosphere and cooled to 0°C. ^{t}BuLi (0.6ml, 1.7M, 4.16mmol) was added and the solution stirred for 15 minutes. To this diethylphosphochloridate (0.718g, 4.16mmol), was added dropwise with stirring. Once addition was complete the solution was stirred for 1 hour. The solvent was removed under reduced pressure and replaced with H_2O (20ml) and CH_2Cl_2 (20ml). The layers were separated and the organic phase washed with H_2O (2 × 20ml) before being dried over $MgSO_4$, filtered and the solvent removed under vacuum. The residue was dissolved in EtOAc (~2ml) and purified with alumina flash column chromatography, using EtOAc as the eluting solvent.

The resulting red oil [$FcP(O)(OEt)_2$, 0.45g, 1.4mmol] was taken up into CH_2Cl_2 (10ml) and placed under a dinitrogen atmosphere. Freshly distilled $(CH_3)_3SiBr$ (0.64g, 4.19mmol) was added and the solution stirred at R.T. for 4 hours. Solvent and excess silane were removed under vacuum and replaced with dry distilled CH_2Cl_2 (5ml). To this was added H_2O (0.10g, 5.56mmol). Precipitation of the acid began within 5 minutes. After 30 minutes the product was filtered and washed with CH_2Cl_2, then air dried to give 0.31g (24%) of the phosphonic acid as a micro-crystalline yellow solid.

m.p. 198-205°C (dec)

Elemental Analyses: Found C, 44.63%; H, 4.15%. Calculated for $C_{10}H_{11}FeO_3P$: C, 45.15%; H, 4.13%.

^{31}P-{^1H} NMR (Na salt in D_2O): δ 15.26.

^{13}C-{^1H} NMR (Na salt in D_2O): δ 69.76 (*s*, C4), 70.55 (*d*, $^3J_{C\text{-}P}$ 9.6Hz, C3), 71.26 (*d*, $^2J_{C\text{-}P}$ 11.3Hz, C2), 73.33 (*d*, $^1J_{C\text{-}P}$ 154Hz, C1).

^1H NMR (d^6-DMSO): δ 4.14 (2H, *br. s*, H3), 4.21 (5H, *br. s*, H4), 4.28 (2H, *br. s*, H2)

ESMS: (MeCN/H_2O, c.v.40) *m/z* 265 ([M-H^+]$^-$, 100%).

IR (KBr disc) (cm^{-1}): 2796 (br, m), 1202 (s), 1130 (s), 1106 (m), 1039 (s), 1013 (s), 944 (s), 889 (w), 816 (w), 667 (w), 585 (m), 472 (m), 452 (m).

Note 1. The intermediate diethylester $FcP(O)(OEt)_2$ was also obtained as a byproduct in the synthesis of 1,1'-Fc'$[P(O)(OEt)_2]_2$.

2.6.1.6: Synthesis of 1,1'-Fc'$[P(O)(OH)_2]_2$ **6**

Ferrocene (0.93g, 5 mmol) was dissolved in petroleum spirits (20ml) and placed under a dinitrogen atmosphere. To this, ^{n}BuLi (6.24ml, 1.6M, 10mmol) and TMEDA (0.74ml, 5mmol) were added and the reaction stirred for 12 hours. The resulting suspension was added slowly with stirring to a solution of diethylphosphochloridate (1.6ml, 10mmol) in petroleum spirits (10ml). The reaction was immediate resulting in the precipitation of a brown tar. The solvent was decanted off and replaced with water (20ml) and CH_2Cl_2 (20ml). The phases were separated and the aqueous layer further extracted with CH_2Cl_2 (2 × 20ml). The combined organic fractions were dried over $MgSO_4$ and evaporated to dryness. The residue was dissolved in EtOAc (~5ml) and purified with alumina flash column chromatography, using an EtOAc to MeOH solvent gradient. This gave 2g (88%) of 1,1'-ferrocenyl-bis(diethylphosphonate) as a brown oil.

A solution of 1,1'-ferrocenyl-bis(diethylphosphonate) (0.526g, 1.15mmol), in CH_2Cl_2 (10ml) was made up in an oven dried flask and placed under a dinitrogen atmosphere. Freshly distilled trimethylsilylbromide (0.88ml, 9.2mmol) was added dropwise and the reaction mix stirred overnight. Water (0.3ml, 0.016mol) was then added and stirring continued until precipitation was complete (~30 minutes). The microcrystalline yellow powder was filtered and washed with acetone to give 0.35g (89%) of product.

m.p. 235-238°C (dec).

Elemental Analyses: Found C, 34.52%; H, 3.31%. Calculated for $C_{10}H_{12}FeO_6P_2$: C, 34.71%; H, 3.49%.

^{31}P-{^1H} NMR (Na salt in D_2O): δ 21.68

^{13}C-{^{1}H} NMR (Na salt in D_2O): δ 72.09 (*d*, $^{1}J_{C-P}$ 149Hz, C1), 72.52 (*d*, $^{3}J_{C-P}$ 10Hz, C3), 72.71 (*d*, $^{2}J_{C-P}$ 12Hz, C2)

^{1}H NMR (Na salt in D_2O): δ 4.5-4.7 (8H, *m*, H2,H3), 8.80 (4H, *br. s*, POH).

ESMS: (MeCN, c.v. 80V) *m/z* 345 ([M-H^+]$^-$, 100%), 327 ([M-H^+-H_2O]$^-$, 17%).

IR (KBr disc) (cm^{-1}): 2771 (br, m), 1198 (s), 1058 (s), 1036 (s), 1004 (s), 956 (s), 885 (m), 839 (m), 747 (m), 638 (m), 575 (s), 501 (m), 480 (m), 461 (m), 434 (w).

2.6.1.7: Synthesis of 1,1'-Fc'[$CH_2P(O)(OH)_2$]$_2$ **7**

In a dry, nitrogen-flushed flask was placed thf (30ml), 1,1'-ferrocenylbis(methanol) (0.80g, 3.26mmol), pyridine (0.52g, 6.52mmol) and freshly distilled phosphorus trichloride (0.89g, 6.52mmol). The reaction mixture was stirred until precipitation of pyridinium hydrochloride was deemed complete, (~1 hour). The solution was filtered and the solvent removed to give a bright yellow crystalline material, crude 1,1'-Fc'(CH_2Cl)$_2$. Triethylphosphite (5ml) was added to the flask and the solution brought to reflux for 2 hours. Excess triethylphosphite was distilled off under vacuum and the resulting brown oil purified by alumina flash column chromatography using an EtOAc to MeOH solvent gradient. The 1,1'-ferrocenyl-bis-(diethylmethylphosphonate) was isolated as a viscous brown oil (1.03g, 65%).

1,1'-Ferrocenyl-bis-(diethylmethylphosphonate) (0.53g, 1.1mmol) was dissolved in dry CH_2Cl_2 (10ml) and the solution placed under a dinitrogen atmosphere. Trimethylsilylbromide (1.32g, 8.8mmol) was added and the reaction stirred at R.T. for 3 hours. Water (0.15g, 8.8mmol) was added with stirring, resulting in precipitation of a dark green powder. The solvent was removed and the residue taken up in 5ml of 1M NaOH solution. The green solution was reduced to a yellow colour by the addition of excess potassium metabisulfite, then acidified with concentrated HCl. Slow evaporation over 3 days gave dark brown crystals which were filtered and washed with water (5ml), then air-dried to give 0.173g (42%) of **7.**

m.p. darkens at 203°C (dec).

Elemental Analyses: Found C, 37.36%; H, 4.38%. Calculated for $C_{12}H_{16}FeO_6P_2$: C, 38.50%; H, 4.31%.

^{31}P-{^{1}H} NMR (Na salt in D_2O): δ 18.98

^{13}C-{^{1}H} NMR (Na salt in D_2O): δ 32.84 (*d*, $^{1}J_{C\text{-}P}$ 76Hz, $\underline{C}H_2P$), 69.64 (*s*, C2), 72.20 (*s*, C3), 86.50 (*d*, $^{2}J_{C\text{-}P}$ 2Hz C1).

^{1}H NMR (Na salt in D_2O): δ 2.49 (4H, *d*, $^{2}J_{P\text{-}H}$ 12.3Hz, $C\underline{H}_2P$), 3.98 (4H, *br s*, H3), 4.12 (4H, *br s*, H2).

ESMS: (MeCN/H_2O, c.v. 20V) *m/z* 373 ([M-H^+]$^-$, 100%), 325 ([M-2H^+]$^{2-}$, 28%).

IR (KBr) (cm^{-1}): 2749 (br, s), 1265 (m), 1225 (m), 995 (s), 946 (s), 920 (m), 829 (m), 607 (m), 483 (m), 432 (m).

2.6.1.8: Synthesis of $FcP(O)(OPh)_2$ **8** and $Fc_2P(O)(OPh)$ **8a**

Ferrocene (0.93g, 5mmol) was dissolved in 5ml dry thf, placed under a dinitrogen atmosphere and cooled to 0°C. ^{t}BuLi (2.9ml, 1.7M, 5mmol) was added and the solution stirred for 15 minutes. This solution was added dropwise to a solution of $(PhO)_2P(O)Cl$ (1.34g, 5mmol) in thf (10ml). Once addition was complete the solution was stirred for 1 hour. The solvent was removed under reduced pressure and replaced with H_2O (20ml) and CH_2Cl_2 (20ml). The layers were separated and the organic phase washed with H_2O (2 × 20ml) before being dried over $MgSO_4$. The solvent was removed and the resulting brown oil purified by silica flash column chromatography using petroleum spirits : CH_2Cl_2 : MeOH (48 : 50 : 2) as the eluting solvent. This resulted in 0.83g (40%) of a brown oil which crystallised upon standing.

m.p. 77-80°C.

Elemental Analyses: Found C, 62.36%; H, 4.61%. Calculated for $C_{22}H_{19}FeO_3P$: C, 63.15%; H, 4.55%.

^{31}P-{^{1}H} NMR ($CDCl_3$): δ 20.58.

^{13}C-{^{1}H} NMR ($CDCl_3$): δ 65.45 (*d*, $^{1}J_{C\text{-}P}$ 166Hz, C1), 70.12 (*s*, C4), 71.90 (*d/d*, $^{2}J_{C\text{-}P}$ 12Hz, $^{3}J_{C\text{-}P}$ 11Hz, C2,C3), 120.73 (*d*, $^{3}J_{C\text{-}P}$ 3Hz, *o*-C), 124.93 (*s*, *p*-C), 129.72 (*d*, $J_{C\text{-}P}$ 10Hz, *m*-C), 150.86 (*d*, $^{2}J_{C\text{-}P}$ 6Hz, *i*-C).

^{1}H NMR ($CDCl_3$): δ 4.25 (5H, *s*, H4), 4.46 (2H, *s*, H3), 4.62 (2H, *d*, $^{2}J_{H\text{-}P}$ 1.2Hz H2), 7.1-7.4 (10H, *m*, Ph).

ESMS: (MeCN/H_2O, c.v. 60V) *m/z* 419 ($[M+H^+]^+$, 100%), 436 ($[M^+ + H_2O]^+$, 31%), 460 ($[M^+ + MeCN]^+$, 11%).

IR (solution in CH_2Cl_2) (cm^{-1}): 1591 (s), 1492 (s), 1188 (m), 1107 (m), 1071 (m), 1006 (m), 944 (s), 828 (m), 619 (m), 603 (m), 496 (s).

Note 1. $FcP(O)(OPh)_2$ is also a byproduct of the synthesis of 1,1'-$Fc'[P(O)(OPh)_2]_2$.

Note 2. Addition of $(PhO)_2P(O)Cl$ to a solution of FcLi leads to two products in approximately equal amounts, the second being characterised by NMR and ESMS data as $Fc_2P(O)(OPh)$ **8a**.

^{31}P-{^1H} NMR ($CDCl_3$): δ 42.62

ESMS: (MeCN/H_2O, c.v. 20V) *m/z* 510 ($[M]^+$, 100%), 533 ($[M+Na^+]^+$, 76%).

2.6.1.9: Synthesis of 1,1'-$Fc'[P(O)(OPh)_2]_2$ **9**

Ferrocene (1g, 5.4mmol) was dissolved in 20ml of petroleum spirits and placed under a dinitrogen atmosphere. ^{n}BuLi (6.72ml, 1.6M, 10.8mmol) and freshly distilled TMEDA (0.8ml, 0.62g, 5.4mmol) were added and the reaction stirred at R.T. for 12 hours. At this time a solution of $(PhO)_2P(O)Cl$ (2.2ml, 2.9g, 10.8mmol) in Et_2O (10ml) was added slowly with stirring. The product precipitated as a brown tar along with LiCl. The solvent was removed under vacuum and the residue washed with petroleum spirits, (2 × 10ml). Water (20ml) and CH_2Cl_2 (20ml) were added and the flask agitated until dissolution was complete. The layers were separated and the organic phase washed with water (2 × 20ml), dried over $MgSO_4$ and the solvent removed. The resulting brown oil was purified by silica flash column chromatography using a CH_2Cl_2 to EtOAc to MeOH solvent gradient. The mono-substituted byproduct, $FcP(O)(OPh)_2$ eluted in EtOAc : CH_2Cl_2, 1 : 9, while the desired product eluted in EtOAc : CH_2Cl_2, 3 : 7. Removal of the solvent resulted in 2.45g (66%) of 1,1'-$Fc'[P(O)(OPh)_2]_2$ as yellow crystals.

m.p. 120-121.5°C.

Elemental Analyses: Found C, 62.66%; H, 4.46%. Calculated for $C_{34}H_{29}FeO_6P_2$: C, 62.79%; H, 4.34%.

^{31}P-{^1H} NMR ($CDCl_3$): δ 26.19.

^{13}C-{^1H} NMR ($CDCl_3$): δ 73.53 (*d*, $^2J_{C-P}$ 16Hz, C2), 74.60 (*d*, J_{C-P} 14Hz, C3), 120.63 (*d*, $^3J_{C-P}$ 4Hz, *o*-C), 125.14 (*s*, *p*-C), 128.66 (*d*, $^1J_{C-P}$ 61Hz, C1), 129.74 (*s*, *m*-C), 150.59 (*d*, $^2J_{C-P}$ 8Hz, *i*-C).

^1H NMR ($CDCl_3$): δ 4.60 (4H, *s*, H3), 4.70 (4H, *d*, $^3J_{H-P}$ 1Hz, H2), 7.1-7.4 (20H, *m*, Ph).

ESMS: (MeOH, c.v. 90V) *m/z* 651 ([M+H^+]$^+$, 100%), 673 ([M+Na]$^+$]$^-$, 19%).

IR (solution in CH_2Cl_2) (cm^{-1}): 1591 (s), 1490 (s), 1189 (m), 1163 (m), 1071 (w), 1036 (m), 1025 (m), 1007 (w), 941 (s), 837 (w), 618 (w), 602 (m), 403 (m).

2.6.1.10: Synthesis of $FcCH_2CH_2As(O)(OH)_2$ **10**

Arsenic(III) oxide (As_2O_3, 0.213g, 1.07mmol) was placed in a solution of sodium hydroxide (1.3ml, 4.98$moll^{-1}$, 6.45mmol) and stirred until dissolved. The volume was made up to 5ml with water and $FcCH_2CH_2Br$ (0.7g, 2.4mmol) was added as a solution in 5ml of CH_2Cl_2. The CH_2Cl_2 was removed under reduced pressure and 0.5ml of EtOH was added as a co-solvent. The resulting solution was brought to reflux for 7 hours. After cooling, the reaction solution was extracted with CH_2Cl_2 to remove any unreacted bromide. The aqueous layer was acidified with 1M HCl and the resulting yellow precipitate filtered off and washed with cold water to give 0.34g (41%) of **10** upon drying.

m.p. 149-152°C

Elemental Analyses: Found C, 42.73%; H, 4.67%. Calculated for $C_{12}H_{15}AsFeO_3$: C, 42.64%; H, 4.47%.

^{13}C-{^1H} NMR (Na salt in D_2O): δ 22.65 (*s*, $\underline{C}H_2CH_2As$), 31.21 (*s*, $\underline{C}H_2As$), 67.67 (*s*, C3), 68.02 (*s*, C2), 69.06 (*s*, C4), 90.08 (*s*, C1).

^1H NMR (Na salt in D_2O): δ 2.30 (2H, *m*, $C\underline{H}_2As$), 2.85 (2H, *m*, $C\underline{H}_2CH_2As$), 4.24 (2H, *br. s*, H3), 4.46 (7H, *br s*, H2, H4).

ESMS: (MeOH, c.v. 40V) *m/z* 351 ([M-2H$^+$+Me$^+$]$^-$, 30%), 337 ([M-H$^+$]$^-$, 100%), 259 ([M-2H$^+$-CpCH$_2$CH$_2$+Me$^+$]$^+$ 6%), 245 ([M-H$^+$-CpCH$_2$CH$_2$]$^-$), 10%).

IR (solution in CH_2Cl_2) (cm^{-1}): 2743 (br, s), 2385 (br, m), 2303 (br, m), 1252 (w), 1220 (w), 881 (s), 827 (m), 784 (m), 486 (m).

2.6.2: X-ray Crystal Structure Determinations for $FcCH_2P(O)(OH)_2$ 3 and 1,1'-Fc'[$CH_2P(O)(OH)_2$]$_2$ 7

Crystallographic data for **3** are given in Table 2.5. Single crystals of **3** were obtained as described in section 2.2.3. The data set was collected on a Nicolet R3 diffractometer at the University of Canterbury. The structure was solved by direct methods and developed routinely using the SHELXL-97[59] program with full least-squares refinement based on F_o^2. All non-hydrogen atoms were refined using anisotropic temperature factors. All hydrogen atoms were found from peaks of residual electron density in the penultimate electron density map and refined in a riding model with isotropic temperature factors. The largest residual electron density peaks in the final electron density map did not exceed +0.279 and -0.305 e Å^{-3}.

Crystallographic data for compound **7** are given in Table 2.5. Crystals of **7** suitable for X-ray crystallographic analysis were obtained by procedures outlined in section 2.2.3. The data set was collected on a Siemens Smart CCD diffractometer at Auckland University and corrected for absorption using SADABS[60]. The structure was solved by direct methods and developed routinely using the SHELXL-97 program with full matrix least-squares refinement based on F_o^2. All non hydrogen atoms were refined using anisotropic temperature factors. All hydrogen atoms were found from peaks of residual electron density in the penultimate electron density map and were refined with isotropic temperature factors. The largest residual electron density peaks in the final density map did not exceed +0.336 or -0.288 e Å^{-3}.

---

[59] G. M. Sheldrick, SHELXL-97, *Program for solving and refining crystals structures*, University of Gottingen, 1997.

[60] R. H. Blessing, *Acta Cryst.*, 1995, **A51**, 33.

Table 2.5: Collected Single Crystal Data and Analysis Parameters for $FcCH_2P(O)(OH)_2$ **3** and 1,1'-Fc'$[CH_2P(O)(OH)_2]_2$ **7**.

Empirical formula	$C_{11}H_{13}O_3PFe$	$C_{12}H_{16}O_6P_2Fe$
Crystal size (mm)	0.34 × 0.29 × 0.21	0.49 × 0.27 × 0.04
Formula weight	280.03	374.04
Crystal system	Orthorhombic	Monoclinic
a (Å)	9.859(3)	8.3415(2)
b (Å)	9.231(2)	9.8376(1)
c (Å)	25.017(7)	9.1540(2)
α (°)	90	90
β (°)	90	103.696(1)
γ (°)	90	90
V (Å^3)	2276.7(1)	729.82(2)
Space group	Pbca	$P2_1/c$
Z value	8	2
D_{calc}	1.634 gcm^{-3}	1.702 gcm^{-3}
F(000)	1152	384
λ(Mo Kα) (Å)	0.71	0.71
μ(Mo Kα) (mm^{-1})	3.52	1.28
Temperature (°K)	163(2)	200
2θ range for data collection	2° < θ < 27°	2° < θ < 27°
Total reflections	23529	4242
Unique reflections	2534 ($R_{int.}$ = 0.0224)	1577 ($R_{int.}$ = 0.016)
T_{min}	0.7258	0.758
T_{max}	1.0000	0.962
R_1 [I>2σ(I)]	0.0216	0.024
wR_2	0.058[ক]	0.0613[খ]
GOF	1.053	0.971

[ক] $w = [\sigma^2(F_o^2) + (0.0313P^2 + 1.2852P]^{-1}$ where $P = (F_o^2 + 2F_c^2)/3$.

[খ] $w = [\sigma^2(F_o^2) + (0.0328P^2 + 0.4962P]^{-1}$ where $P = (F_o^2 + 2F_c^2)/3$.

Chapter 3: Metal Complexes of Ferrocenyl Phosphonic Acids

3.1: Introduction

The insoluble metal phosphonates encountered in chapter two dominate the field of metal derivatives of phosphonic acids. Unfortunately these materials are difficult to characterise due to their insoluble nature. Techniques such as MAS-NMR and Rietveld refinement of powder XRD data hold much promise but are yet to become widespread.

More amenable to classical analysis are the molecular compounds containing phosphonic acid ligands known as phosphonato complexes. Phosphonato complexes of platinum and palladium are most common. This stems from the efficacy of platinum complexes such as cisplatin (*cis*-$Pt(NH_3)_2Cl_2$) as anticancer agents and the development of anticancer phosphonato analogues of cisplatin has been reviewed by Klenner *et al*[1]. Platinum phosphonato complexes such as $[Pt(NH_3)_2(NTMP)]^-$ (NTMP = nitrilotris(methylenephosphonic acid)) (Figure 3.1), were found to be effective against osteosarcoma, a specificity thought to be due to the affinity of the phosphonate group for calcified tissue[2], (it should be noted that platinum complexes containing ferrocenyl ligands are known to have a high affinity for the liver and spleen[3]).

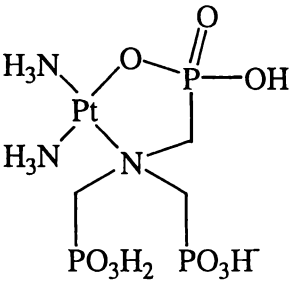

Figure 3.1: The Platinum Phosphonato Complex $[Pt(NH_3)_2(NTMP)]^-$.

---

[1] (a) T. Klenner, P. Valenzuela-Paz, F. Amelung, H. Muench, H. Zahn, B. K. Keppler and H. Blum, Metal Complexes in Cancer Chemotherapy, B. K. Keppler, Ed., VCH, Weinheim, Germany, 1993, 84-127. (b) T. Klenner, P. Valenzuela-Paz, B. K. Keppler, G. Angres, H. R. Scherf, F. Wingen, F. Amelung and D. Schmahl, *Cancer Treat. Rev.*, 1990, **17**, 253.

[2] F. Wingen and D. Schmahl, *Drug Res.*, 1985, **35**, 1565.

[3] A. Rosenfeld, J. Blum, D. Gibson and A. Ramu, *Inorg. Chim. Acta.*, 1992, **201**, 219.

The binding of aminophosphonic acid ligands to platinum and palladium centres has been widely studied[4]. Such ligands are analogues of amino acids and are of interest due to their biological and chelating properties. Solution state ^{31}P, ^{15}N and ^{195}Pt nmr spectroscopy has been used to study the reaction of *cis*-$[Pt(NH_3)_2(H_2O)_2]^{2+}$ and *cis*-$Pt(NH_3)_2(OH)_2$ with $CH_3PO_3H_2$ and $NH_2(CH_2)_nPO_3H_2$ (n = 1, 2 and 3)[5]. The binding of the phosphonic acid group to the platinum centre is pH dependent as depicted in Scheme 3.1.

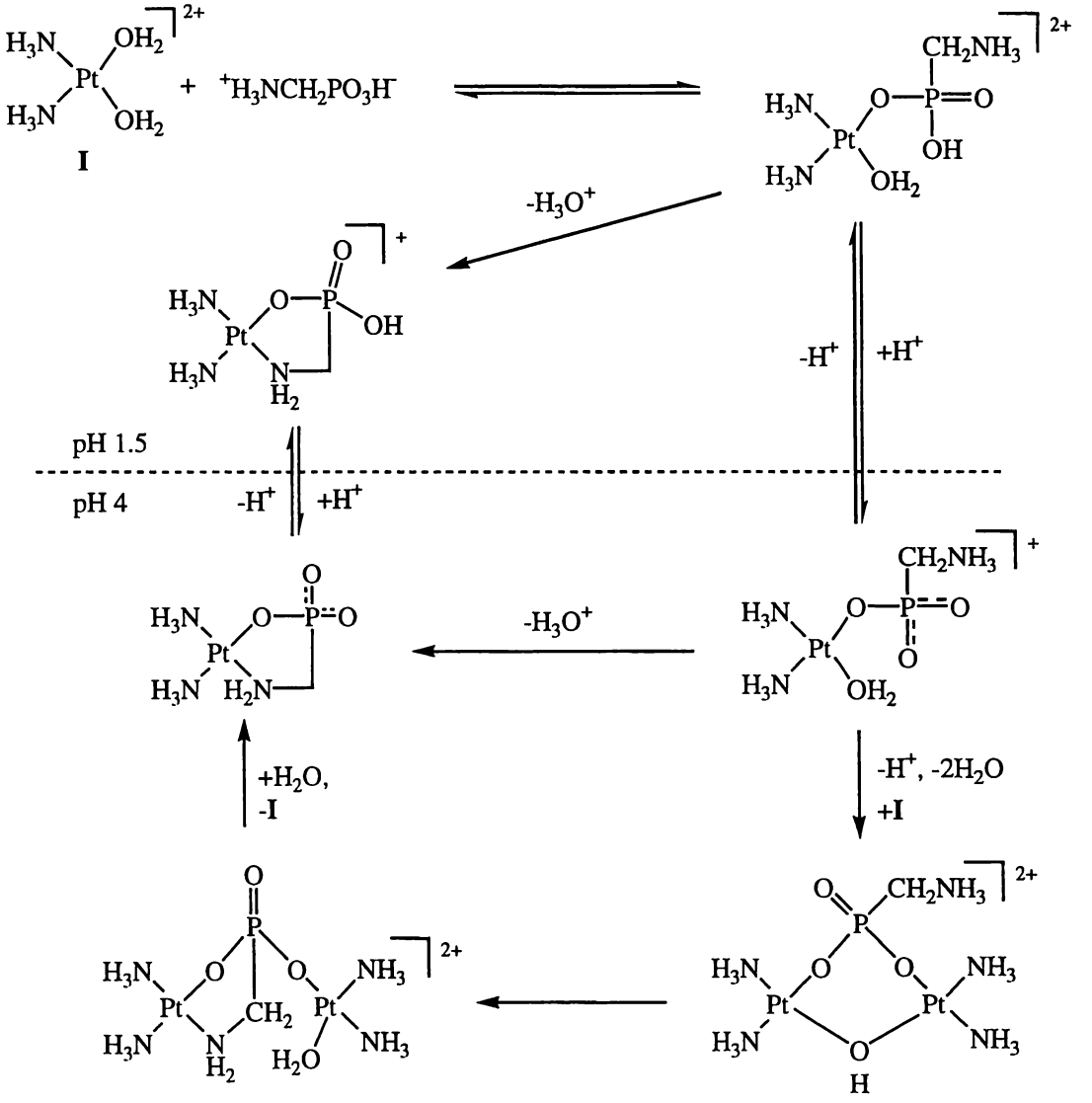

Scheme 3.1: Platinum Phosphonato Complexes of $NH_2CH_2PO_3H_2$ at pH 1.5 and pH 4.

[4] (a) E. Matczak-Jon and W. Wojciechowski, *Inorg. Chim. Acta.*, 1990, **173**, 85. (b) L. Blaha, I. Lukes, J. Rohovec and P. Hermann, *J. Chem. Soc., Dalton Trans.*, 1997, 2621. (c) I. Lukes, L. Blaha, F. Kesner, J. Rohovec and P. Hermann, *J. Chem. Soc., Dalton Trans.*, 1997, 2629.

[5] T. G. Appleton, J. R. Hall and I. J. McMahon, *Inorg. Chem.*, 1986, **25**, 720.

The results of solution state ^{31}P, ^{1}H and ^{13}C nmr studies of K_2PdCl_4 with aminophosphonic acids[4a] revealed a similar pattern of pH dependant binding of the phosphonate ligand to the metal centre.

Platinum salts of phosphonoacetic acid (PFA, H_2O_3PCOOH) and methylenediphosphonic acid (MDP, $CH_2(PO_3H_2)_2$) have also been reported in the literature[6]. PFA formed five membered (Pt-O-C-P-O) chelate rings in the complexes [*cis*-$Pt(NH_3)_2(O_3PCOO)]^-Na^+$ and [*cis*-$Pt(DACH)(O_3PCOO)]^-Na^+$ (DACH = 1,2-diaminocyclohexane) (Figure 3.2a and 3.2b respectively). Reaction of MDP with $Pt(DACH)Cl_2$ gave the phosphonate bridged dimer $[Pt_2(DACH)_2(MDP)]$ (Figure 3.2c).

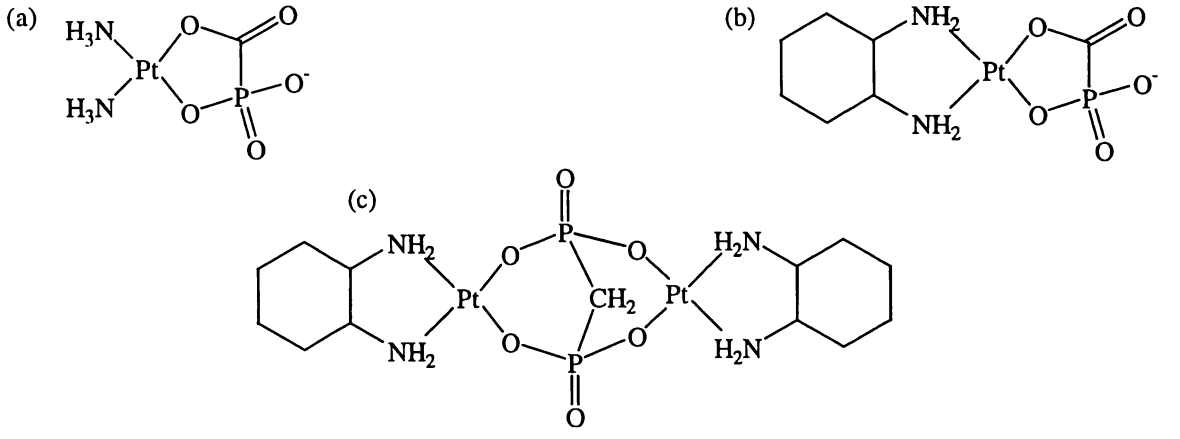

Figure 3.2: Platinum Phosphonato Complexes. (a) [*cis*-$Pt(NH_3)_2(O_3PCOO)]^-$ (b) [*cis*-$Pt(DACH)(O_3PCOO)]^-$ and (c) $[Pt_2(DACH)_2(MDP)]$.

A number of metal phosphonato complexes soluble in organic solvents are known. These include the monomeric copper complexes $Cu(PhPO_3H)_2(C_5H_5N)_4.2CH_3OH$ and $Cu(PhPO_3H)_2(C_5H_5N)_4$[7] and the dinuclear ruthenium phosphonato complex $[Ru_2(\mu\text{-}O_2CCH_3)_4(HO_3PC_6H_5)_2]H.H_2O$[8].

Walawalkar *et al.*[9] have prepared and characterised the titanium phosphonato complexes $[(Cp^*TiO_3PR)_4(\mu\text{-}O)_2]$ (Cp^* = pentamethylcyclopentadienyl, R = CH_3,

[6] R. Bau, S. K. S. Huang, J. -A. Feng and C. E. McKenna, *J. Am. Chem. Soc.*, 1988, **110**, 7546.
[7] M. McCann, E. Murphy, C. Cardin and M. Convery, *Polyhedron*, 1992, **11**, 3101.
[8] M. McCann, E. Murphy, C. Carden and M. Convery, *Polyhedron*, 1993, **12**, 1725.
[9] M. G. Walawalkar, S. Horchler, S. Dietrich, D. Chakraborty, H. W. Roesky, M. Schafer, H. Schmidt, G. M. Sheldrick and R. Murugavel, *Organometallics*, 1998, **17**, 2865.

C_6H_5) (Figure 3.3) and $[(Cp^*Ti)_3(^tBuPO_3)_2(^tBuPO_3H)(\mu\text{-}O)_2]$. These compounds contain Ti-O-P polyhedra, on the periphery of which, are the hydrophobic Cp^* and R groups.

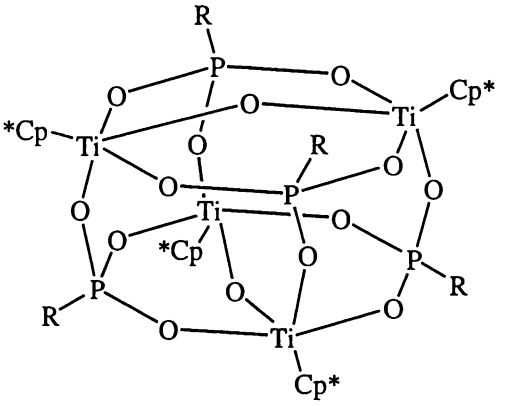

R = Me, Ph

Figure 3.3: The Structure of $[(Cp^*TiO_3PR)_4(\mu\text{-}O)_2]$.

The silver(I) oxide mediated synthesis of platinum metallacycles is well known[10] and was first applied to the synthesis of platinum phosphonato complexes by Kemmitt *et al.*[11] who prepared and characterised a range of complexes of the type $L_2Pt(O_3PR)$ (L = phosphine or arsine donor ligands, R = Me or Ph) (Scheme 3.2).

$$RPO_3H_2 + L_2PtCl_2 + Ag_2O \longrightarrow RPO_3PtL_2 + 2AgCl + H_2O$$

R = Me or Ph L = Phosphine or arsine donor ligands

Scheme 3.2: Silver Oxide Mediated Synthesis of Platinum Phosphonato Complexes.

The silver(I) oxide plays two roles in this synthetic route, firstly it acts as a halide abstracting agent (as a source of Ag^+) and secondly it acts as a strong base (as a

[10] (a) D. A. Clarke, R. D. W. Kemmitt, M. A. Mazid, P. McKenna, D. R. Russell. M. D. Schilling and L. J. S. Sherry, *J. Chem. Soc., Dalton Trans.*, 1984, 1993. (b) W. Henderson, R. D. W. Kemmitt, L. J. S. Prouse and D. R. Russell, *J. Chem. Soc., Dalton Trans.*, 1990, 1853. (c) W. Henderson, R. D. W. Kemmitt and A. L. Davis, *J. Chem. Soc., Dalton Trans.*, 1993, 2247. (d) R. D. W. Kemmitt, S. Mason, M. R. Moore and D. R. Russell, *J. Chem. Soc., Dalton Trans.*, 1992, 409.

[11] R. D. W. Kemmitt, S. Mason, J. Fawcett and D. R. Russell, *J. Chem. Soc. Dalton. Trans.*, 1992, 851.

source of O^{2-} and/or OH^-)[12]. The resulting by-product of the reaction is AgCl, which is easily removed by filtration and the use of refluxing CH_2Cl_2 as the reaction medium for such reactions is ubiquitous. The synthesis of these compounds was mild (syntheses were conducted in air with no precautions taken to exclude water) and the products were stable and crystalline. For these reasons it was decided to prepare the analogous platinum phosphonato complexes of the ferrocenyl phosphonic acids **3-7**.

3.2: Synthesis and Characterisation of Bis(triphenylphosphine)Platinum Complexes of Ferrocenyl Phosphonic Acids

The ferrocenyl phosphonic acids **3-6** (see chapter two) were reacted with *cis*-bis(triphenylphosphine)platinum dichloride and silver(I) oxide in refluxing CH_2Cl_2 to give the platinum phosphonato complexes **11-14** in high yield (Scheme 3.3).

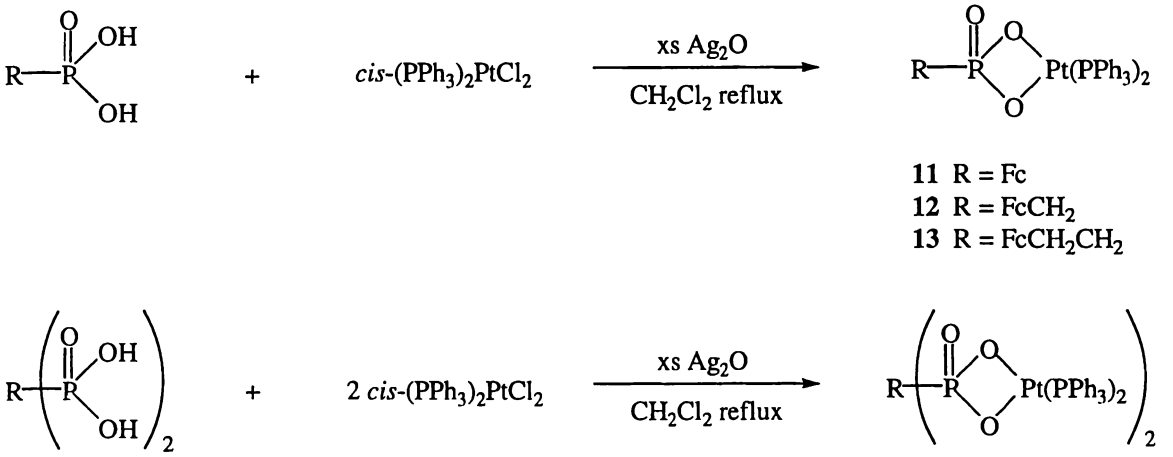

Scheme 3.3: Synthesis of the *cis*-Bis(triphenylphosphine)platinum Ferrocenyl Phosphonato Complexes.

The products were air stable, pale yellow crystalline powders, which decompose when heated. The compounds **11-13** are soluble in organic solvents such as CH_2Cl_2 and $CHCl_3$, while **14** tended to be soluble in more polar organic solvents

[12] M. A. Cairns, K. R. Dixon and M. A. R. Smith, *J. Organomet. Chem.*, 1977, **135**, C33.

such as DMSO and MeOH. Purification of these complexes by recrystallisation resulted in the incorporation of solvent molecules into the crystal lattice, which must be taken into consideration during elemental analysis.

The reaction of 1,1'-Fc'$[CH_2PO_3H_2]_2$ **7** with two equivalents of *cis*-$(Ph_3P)_2PtCl_2$ gave a mixture of products, none of which were isolated. One of the products was identified on the basis of ^{31}P-$\{^1H\}$ nmr as the desired complex 1,1'-Fc'$[CH_2PO_3Pt(PPh_3)_2]_2$.

The reaction of the arsonic acid $FcCH_2CH_2AsO_3H_2$ **10** with *cis*-$(Ph_3P)_2PtCl_2$ in the presence of silver(I) oxide did not lead to the desired platinum arsonato complex. Many products were observed using ^{31}P nmr, none of which were isolated or identified.

3.2.1: ESMS of Bis(triphenylphosphine)Platinum Complexes of Ferrocenyl Phosphonic Acids

Samples of the complexes **11-14** were introduced into the spectrometer as solutions in MeOH with methanol/water or acetonitrile/water used as the carrier solvent. The spectra of complexes **11-14** in the positive ion mode were dominated by peaks due to $[Pt(o\text{-}C_6H_4PPh_2)(PPh_3)]^+$ (*m/z* 718) and its solvated adducts, though a weak peak due to the $[M+H^+]^+$ ion was usually observed at low cone voltages. The positive ion spectrum of $FcCH_2CH_2PO_3Pt(PPh_3)_2$ **13** in methanol/water is given in Figure 3.4.

The positive ion spectra of these complexes were not particularly reproducible. The same sample run under identical conditions at different times would give spectra with different base peaks. When acetonitrile/water was used as the carrier solvent, peaks due to $[Pt(o\text{-}C_6H_4PPh_2)(PPh_3)]^+$ *m/z* 718, $[Pt(o\text{-}C_6H_4PPh_2)(PPh_3)+H_2O]^+$ *m/z* 736, $[Pt(o\text{-}C_6H_4PPh_2)(PPh_3)+MeCN]^+$ *m/z* 759 and $[Pt(o\text{-}C_6H_4PPh_2)(PPh_3)+MeOH]^+$ *m/z* 750 were all observed.

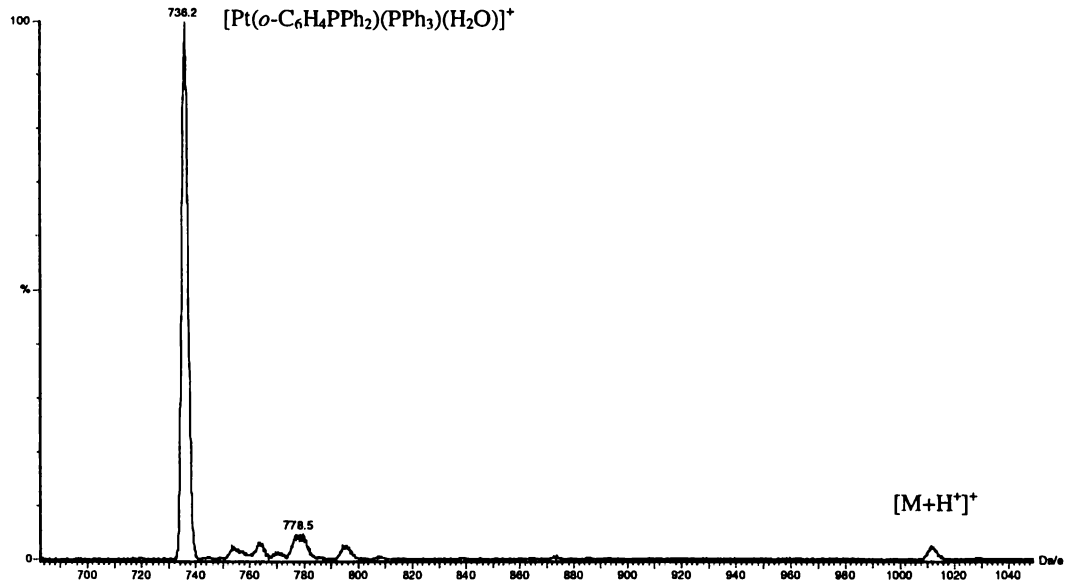

Figure 3.4: The Positive Ion ES Mass Spectrum of $FcCH_2CH_2PO_3Pt(PPh_3)_2$ **13** in Methanol/Water at a Cone Voltage of 20V.

The $[Pt(o\text{-}C_6H_4PPh_2)(PPh_3)]^+$ ion *m/z* 718 and its solvated adducts, are a result of orthometallation of one of the triphenylphosphine phenyl rings, Figure 3.5. This behaviour has been noted in the ES mass spectra of other bis(triphenylphosphine)platinum complexes[13] and the diorthometallated complex $Pt(o\text{-}C_6H_4CH_2PPh_2)_2$ is a known decomposition product of $(Ph_2PhCH_2P)_2PtO_3PPh$[11].

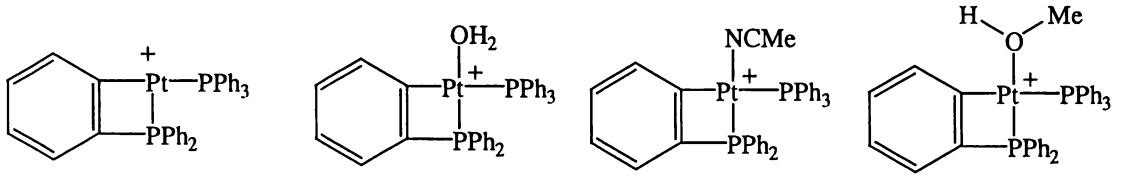

m/z 718 *m/z* 736 *m/z* 759 *m/z* 750

Figure 3.5: Commonly Observed Orthometallated Species in ES Mass Spectra of Bis(triphenylphosphine)platinum Complexes in Coordinating Solvents.

[13] (a) J. Fawcett, W. Henderson, R. D. W. Kemmit, D. R. Russell and A. Upreti, *J. Chem. Soc., Dalton Trans.*, 1996, 1897. (b) W. Henderson and B. K. Nicholson, *Polyhedron*, 1996, **15**, 4015. (c) J. M. Law, W. Henderson and B. K. Nicholson, *J. Chem. Soc., Dalton Trans.*, 1997, 4587.

The negative ion spectra of compounds **11-14** were very simple. At low cone voltages the spectra consist of a single peak due to the appropriate RPO_3H^- ion, due to the complexes dissociating in the ESMS environment, (the possibility that residual free acid was responsible for the negative ion spectra, was inconsistent with the results of ^{31}P nmr analysis). As the cone voltage was increased the fragmentation patterns previously described (chapter two) for the acids **3-6** were observed. The negative ion spectrum of $FcCH_2CH_2PO_3Pt(PPh_3)_2$ **13** is given in Figure 3.6.

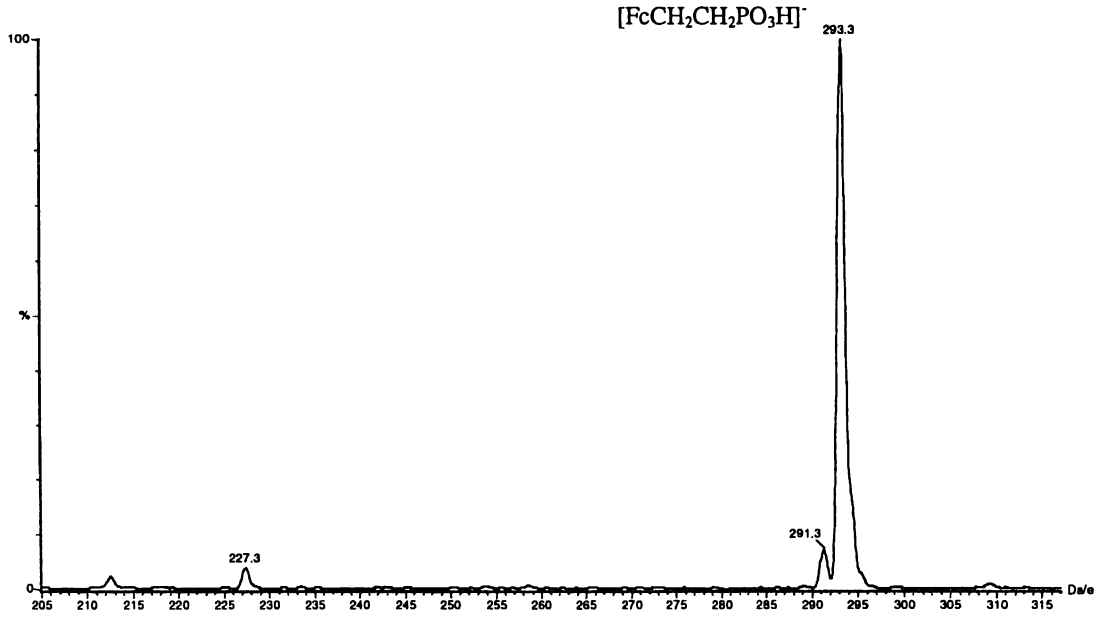

Figure 3.6: The Negative Ion ES Mass Spectrum of $FcCH_2CH_2PO_3Pt(PPh_3)_2$ **13** in Methanol/Water at a Cone Voltage of 40V.

A brief look at solvent effects on the observed spectra was also undertaken. The fragmentation of these compounds into positive and negative ions was assumed to be in part due to the protic and polar nature of the solvent(s) used. Further spectra of salts **11-13** were obtained using samples dissolved in CH_2Cl_2 and with CH_2Cl_2 as the carrier solvent. The resulting positive ion spectra were dominated by a single $[M+H^+]^+$ peak but at the cost of a tenfold reduction in intensity. Figure 3.7 shows the positive ion spectrum of $FcCH_2CH_2PO_3Pt(PPh_3)_2$ **13** obtained under these conditions.

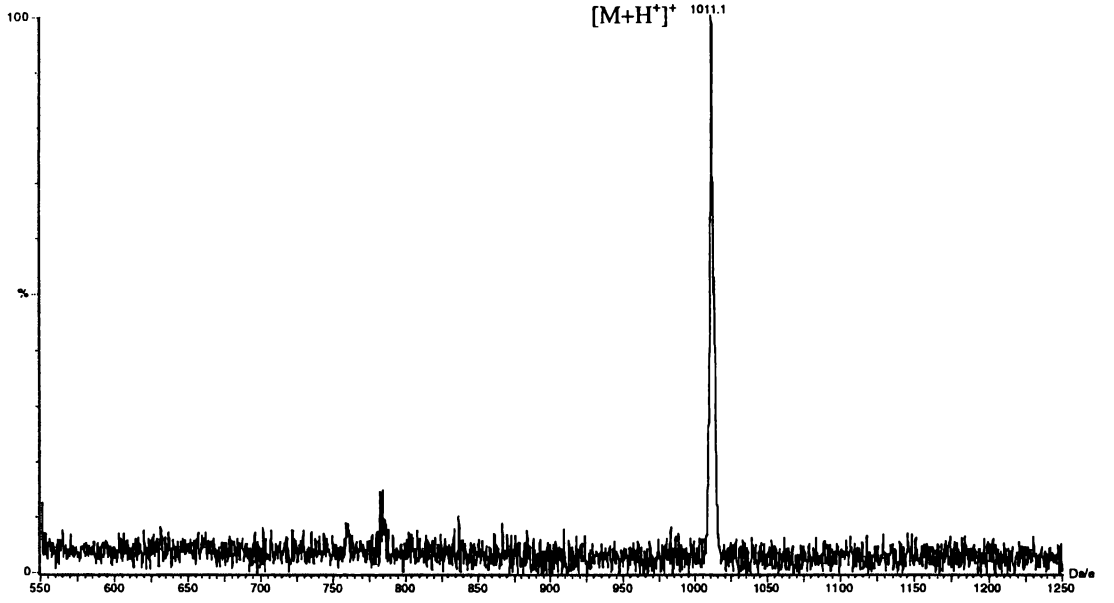

Figure 3.7: The Positive Ion ES Mass Spectrum of $FcCH_2CH_2PO_3Pt(PPh_3)_2$ **13** in CH_2Cl_2 at a Cone Voltage of 40V.

Further investigation into solvent effects and the use of weak acids as ionisation aids, might allow the full potential of ESMS as an analytical technique for these complexes to be realised.

3.2.2: X-Ray Crystal Structure Determinations for Compounds $FcCH_2PO_3Pt(PPh_3)_2$ 12, $FcCH_2CH_2PO_3Pt(PPh_3)_2$ 13, and 1,1'-$Fc[PO_3Pt(PPh_3)_2]_2$ 14

The structures of compounds **12**, **13** and **14** were determined from single crystal X-ray diffraction data. Single crystals of **12** and **13** were obtained by vapour diffusion of Et_2O into a CH_2Cl_2 solution of the appropriate complex at 4°C. Single crystals of **14** were obtained by vapour diffusion of Et_2O into a CH_2Cl_2/MeOH (9:1) solution of **14** at -20°C. The crystals of each compound contained solvent of crystallisation molecules, though only the crystals of **14** lost solvent and crystallinity when exposed to air. Selected bond lengths and angles for compounds **12** and **13** are given in Tables 3.1 and 3.2 respectively.

The structure of **12** was solved by Patterson methods for platinum and iron, with the rest of the structure being developed routinely and hydrogen atoms being

placed in calculated positions. The compound crystallised in the Pbca space group accompanied by two CH_2Cl_2 molecules of crystallisation.

Table 3.1: Selected Bond Lengths (Å) and Angles (°) for Compound **12**.

Cp Fe-C av.	2.032	O(1)-Pt	2.081(3)
Range	2.014-2.042	O(2)-Pt	2.075(3)
Cp C-C av.	1.413	Pt-P(2)	2.2253(10)
Range	1.364-1.439	Pt-P(3)	2.2378(10)
C(1)-C(11)	1.502(6)	P(2)-C av	1.818
C-P(1)	1.807(5)	range	1.809-1.829
P(1)-O(1)	1.563(3)	P(3)-C av.	1.821
P(1)-(O2)	1.566(3)	range	1.819-1.823
P(1)-O(3)	1.476(3)		
O(1)-Pt-P(3)	93.18(8)	O(1)-P(1)-C(1)	110.41(19)
O(2)-Pt-P(2)	99.01(8)	O(2)-P(1)-O(3)	116.42(17)
P(2)-Pt-P(3)	97.31(4)	O(2)-P(1)-C(1)	105.69(19)
O(1)-Pt-O(2)	71.14(11)	O(3)-P(1)-C(1)	107.41(19)
Pt-O(1)-P(1)	93.21(13)	C(11)-C(1)-P(1)	116.8(3)
Pt-O(2)-P(1)	93.34(13)	C(1)-C(11)-C(12)	127.0(4)
O(1)-P(1)-O(2)	101.17(15)	C(1)-C11)-C(15)	126.0(4)
O(1)-P(1)-O(3)	115.29(18)		

The Cp rings of the ferrocene group adopt an eclipsed formation and the C(11)-C(1) bond lies in the plane of the Cp rings. The position of the ferrocene group relative to the plane of the platinum, constrained by the angle P(1)-C(1)-C(11) of 116.8°, is shown in Figure 3.8. The platinum and ferrocene groups adopt a *cis* conformation about the P(1)-C(1) bond rather than the more sterically forgiving *trans* conformation. The square planar geometry of the platinum is slightly distorted presumably to accommodate the steric requirements of the triphenylphosphine groups.

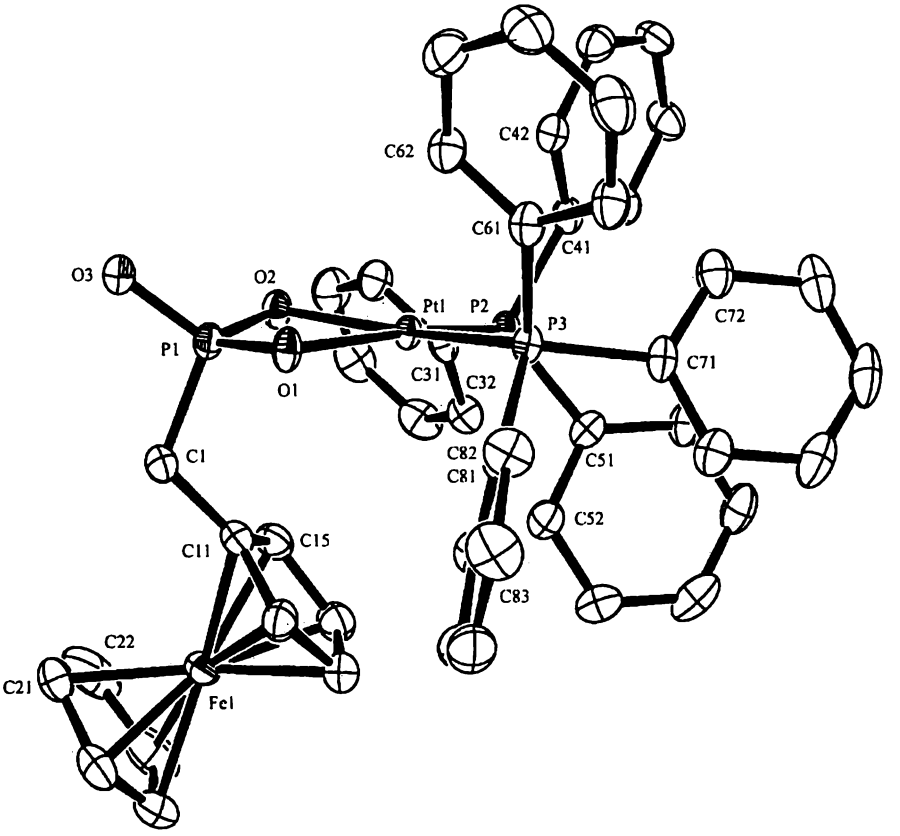

Figure 3.8: Ortep Diagram of **12**. Hydrogen Atoms and the Two CH_2Cl_2 of Crystallisation Omitted. All Atoms at the 50% Probability Level.

The structure of $FcCH_2PO_3Pt(PPh_3)_2$ **12**, when compared to that of the free acid $FcCH_2PO_3H_2$ shows only minor shifts in bond angles and lengths occur upon binding to the platinum moiety. Most notable are the reduction in the length of the P=O bond, (1.566 Å in the free acid vs. 1.476 Å in **12**), as the opportunity for hydrogen bonding is removed and the reduction in the O-P-O angle (108° vs. 101°) as the oxygen atoms bind to the platinum.

Table 3.2: Selected Bond Lengths (Å) and Angles (°) for Compound **13**.

Cp Fe-C av.	2.041	P(1)-O(3)	1.481(4)
Range	2.028-2.063	O(1)-Pt	2.077(3)
Cp C-C av.	1.415	O(2)-Pt	2.066(3)
Range	1.387-1.436	Pt-P(2)	2.2330(13)
C(1)-C(11)	1.505(8)	Pt-P(3)	2.2656(11)

C(1)-C(2)	1.512(9)	P(2)-C av	1.829
C-P(1)	1.812(5)	range	1.827-1.831
P(1)-O(1)	1.571(3)	P(3)-C av.	1.823
P(1)-(O2)	1.577(3)	range	1.812-1.832
O(1)-Pt-P(3)	96.51(9)	O(1)-P(1)-C(1)	109.4(4)
O(2)-Pt-P(2)	94.32(10)	O(2)-P(1)-O(3)	115.6(2)
P(2)-Pt-P(3)	98.45(5)	O(2)-P(1)-C(1)	105.3(2)
O(1)-Pt-O(2)	71.00(0)	O(3)-P(1)-C(1)	110.2(2)
Pt-O(1)-P(1)	93.8(2)	C(1)-C(2)-P(1)	115.3(4)
Pt-O(2)-P(1)	93.99(14)	C(11)-C(1)-C(2)	115.9(5)
O(1)-P(1)-O(2)	99.7(2)	C(1)-C(11)-C(12)	125.8(5)
O(1)-P(1)-O(3)	115.9(2)	C(1)-C11)-C(15)	126.9(6)

The complex $FcCH_2CH_2PO_3Pt(PPh_3)_2$, **13** crystallised in the space group P_1 with two CH_2Cl_2 molecules of crystallisation and two molecules in the unit cell. The structure was solved using Patterson methods for platinum and iron, with the remainder of the structure being developed routinely. The bidentate bonding of the phosphonate group to the platinum atom mirrors that observed in the structure of **12** and the internal angles of the resulting four membered metallacycles are very similar in both compounds. Similarly, the geometry of the square planar platinum is slightly distorted in **13** presumably due to steric demands of the triphenylphosphine ligands (Figure 3.9).

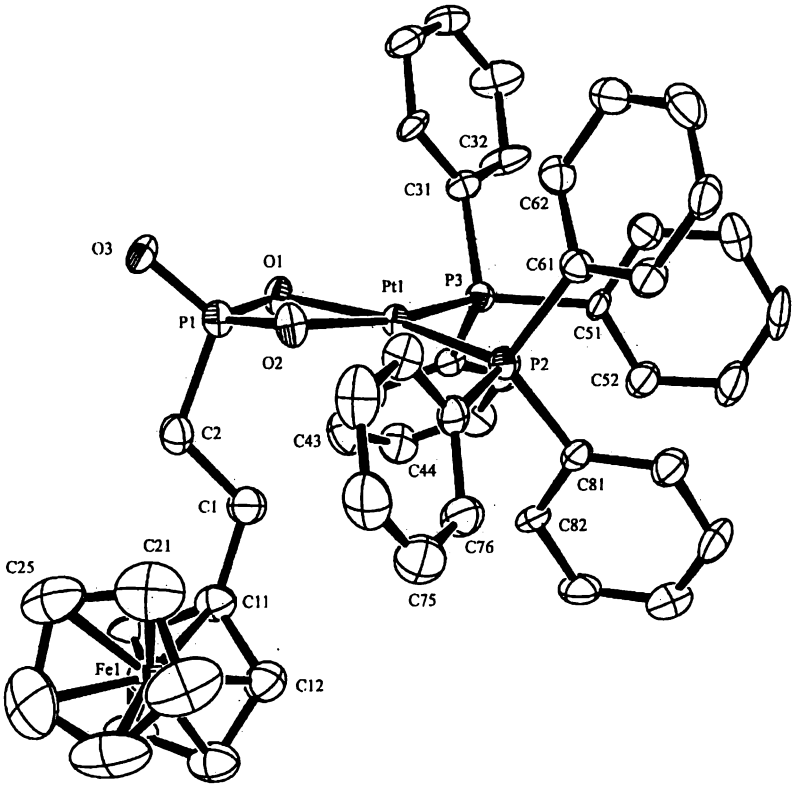

Figure 3.9: Ortep Diagram of **13**. Hydrogen Atoms and the Two CH_2Cl_2 of Crystallisation Omitted. All Atoms at the 50% Probability Level.

The chief difference between the structures of **12** and **13** lies in the orientation of the ferrocene unit with respect to the plane of the platinum atom (Figure 3.10). In **12**, the ferrocene axis through the iron atom perpendicular to the Cp rings is only 6° from parallel with the Pt----P(1) axis of the platinum plane. This minimises interaction between the ferrocene and the phenyl rings of the triphenylphosphine ligands. In contrast, the ferrocene axis through iron atom, perpendicular to the Cp rings in **13**, is at an angle of 59° to the Pt----P(1) axis of the platinum plane. The additional CH_2 spacer in **13** reduces congestion between the ferrocene and the $(PPh_3)_2Pt$ group, thus the ferrocene is free to adopt an orientation more dictated by crystal packing forces rather than internal steric demands.

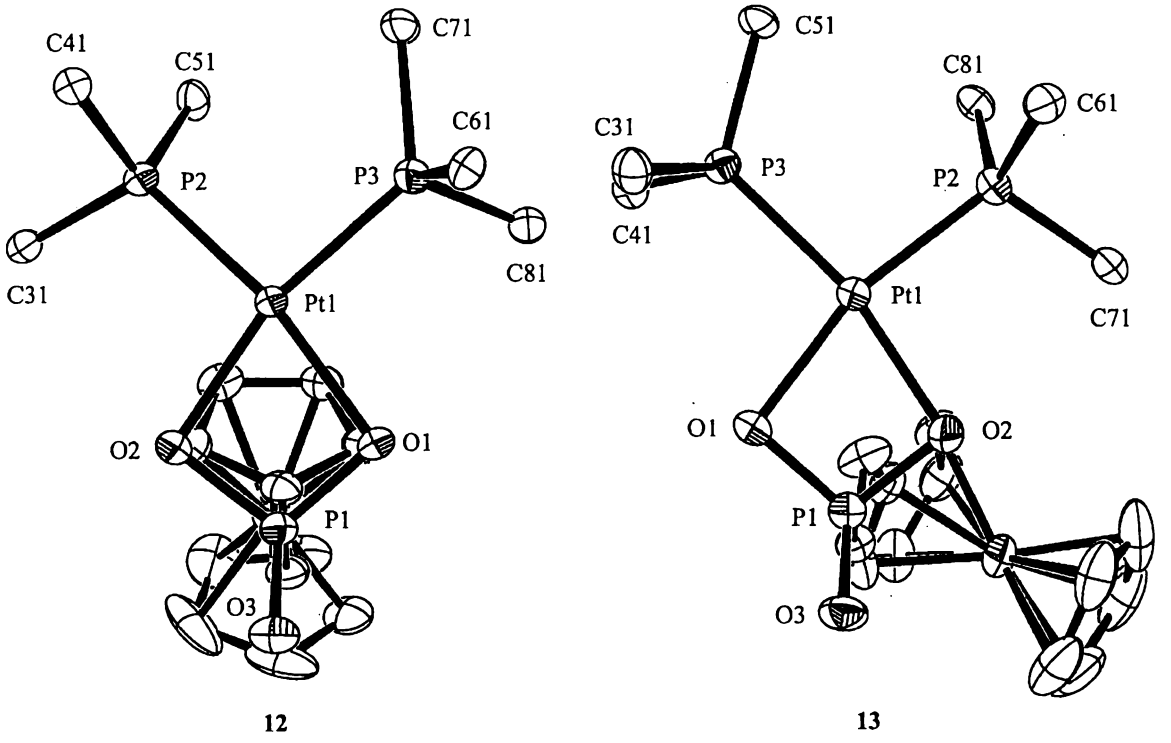

Figure 3.10: Orientation of the Ferrocenyl Group with Respect to the Platinum Square Plane for **12** and **13**. Hydrogen Atoms and Phenyl Rings Omitted. All Atoms at the 50% Probability Level.

The compound 1,1'-Fc'$[PO_3Pt(PPh_3)_2]_2$ **14**, crystallised in the space group P_1 with two molecules in the unit cell. The solution of the structure was achieved using the method outlined for **12**. Complete refinement was hampered by the presence of disordered solvent. A single methanol of crystallisation was successfully modelled but the final difference map contained several large peaks of residual electron density, some of which were able to be successfully modelled as four carbon atoms but were unable to be refined into chemically sensible solvent molecule(s). Despite this an R_1 of 0.047 was achieved and the structure of the ferrocenyl platinum complex was refined without ambiguity.

All bond lengths and angles are within normal ranges (Table 3.3 and Table 3.4 respectively) and the ferrocene Cp rings are staggered with the $-PO_3$ units in the anti configuration. This minimises the steric interactions of the triphenylphosphine ligands

and maximises the symmetry of the molecule, (the same anti configuration is seen in the structure of **7**). The Cp-P bonds lie in the plane of the Cp rings (Figure 3.11).

Table 3.3: Selected Bond Lengths (Å) for Compound **14**.

Cp Fe-C av.	2.048	O(21)-Pt(2)	2.094(4)
Range	2.040-2.059	O(22)-Pt(2)	2.086(4)
Cp C-C av.	1.425	Pt(1)-P(11)	2.258(2)
Range	1.413-1.436	Pt(1)-P(12)	2.255(2)
P(1)-C(11)	1.801(7)	Pt(2)-P(21)	2.255(2)
P(2)-C(21)	1.795(7)	Pt(2)-P(22)	2.242(2)
P(1)-O(11)	1.565(5)	P(11)-C av	1.826
P(1)-(O12)	1.576(5)	range	1.817-1.842
P(1)-O(13)	1.501(5)	P(12)-C av.	1.834
P(2)-O(21)	1.565(4)	range	1.832-1.836
P(2)-O(22)	1.567(5)	P(21)-C av.	1.831
P(2)-O(23)	1.505(5)	range	1.824-1.838
O(11)-Pt(1)	2.097(4)	P(22)-C av.	1.825
O(12)-Pt(1)	2.092(4)	range	1.818-1.834

The core of this complex (*sans* triphenylphosphine phenyl rings) is very nearly centrosymmetric about the ferrocenyl iron atom; bond lengths in particular are identical (within margin of error) across the two halves of the molecule.

Table 3.4: Selected Bond Angles (°) for Compound **14**.

P(11)-Pt(1)-P(12)	99.91(6)	O(11)-P(1)-O(13)	115.1(2)
P(21)-Pt(2)-P(22)	100.35(6)	O(21)-P(2)-O(23)	114.8(3)
P(11)-Pt(1)-O(11)	98.06(13)	O(11)-P(1)-C(11)	109.1(3)
P(21)-Pt(2)-O(21)	93.73(12)	O(21)-P(2)-C(21)	105.9(3)
O(11)-Pt(1)-O(12)	70.62(17)	O(12)-P(1)-O(13)	114.2(3)
O(21)-Pt(2)-O(22)	70.86(17)	O(22)-P(2)-O(23)	115.7(3)

O(12)-Pt(1)-P(12)	91.33(13)	O(12)-P(1)-C(11)	107.9(3)
O(22)-Pt(2)-P(22)	94.77(13)	O(22)-P(2)-C(21)	107.3(3)
Pt(1)-O(11)-P(1)	93.4(2)	O(13)-P(1)-C(11)	109.0(3)
Pt(2)-O(21)-P(2)	92.5(2)	O(23)-P(2)-C(21)	110.9(3)
Pt(1)-O(12)-P(1)	93.3(2)	P(1)-C(11)-C(12)	124.9(6)
Pt(2)-O(22)-P(2)	92.7(2)	P(2)-C(21)-C(22)	126.5(5)
O(11)-P(1)-O(12)	100.8(2)	P(1)-C(11)-C(15)	127.6(5)
O(21)-P(2)-O(22)	101.3(2)	P(2)-C(21)-C(25)	125.9(6)

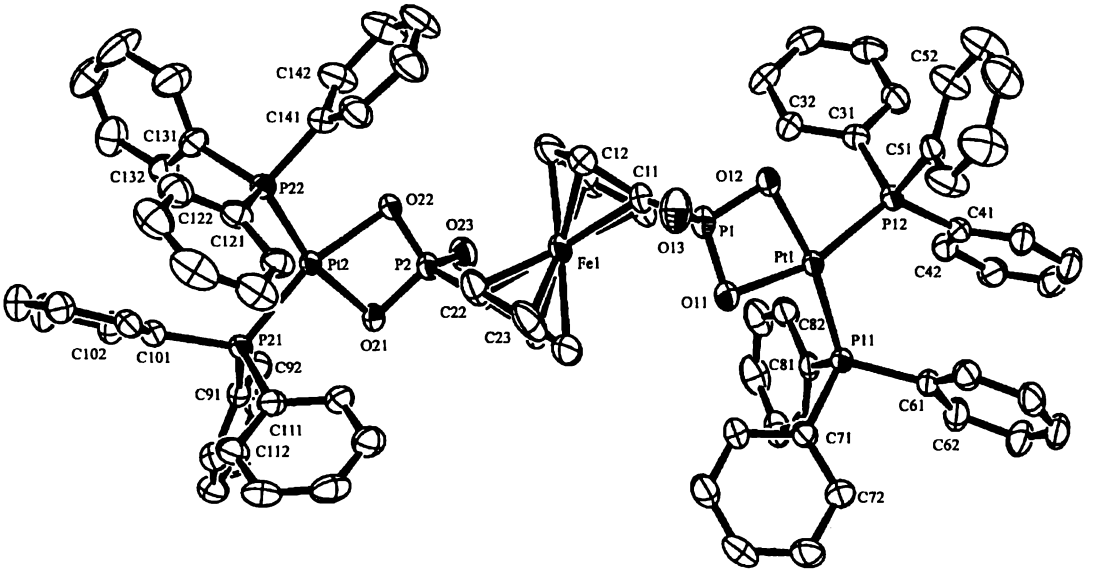

Figure 3.11: Ortep Diagram of Compound **14** with Hydrogen Atoms and Solvent of Crystallisation omitted. All Atoms at the 50% Probability Level.

As in the structures of **12** and **13**, the phosphonic acid groups in **14** act as bidentate ligands toward the platinum atoms. The geometry of the platinum atoms is again slightly distorted square planar. The plane of the platinum atoms is almost perpendicular to the plane of the ferrocenyl Cp rings and can be considered to adopt *trans* configurations with respect to each other across the ferrocene unit (Figure 3.12).

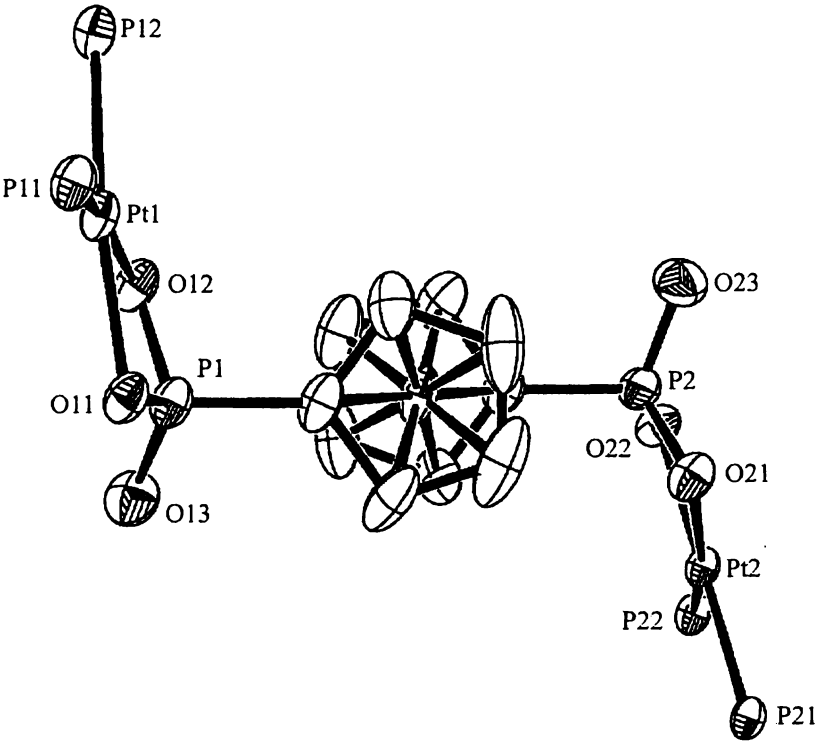

Figure 3.12: Ortep Diagram of **14** Viewed Down the Cp-Fe-Cp Axis. Hydrogen Atoms and Phenyl Rings Omitted for Clarity. All Atoms at the 50% Probability Level.

Table 3.5: Twist and Fold Angles (°) About the Platinum Centre for Complexes **12-14** and $(Ph_2MeP)_2PtO_3PPh$.

Compound		Twist Angle	Fold Angle
12		9.2	11.3
13		10.7	13.1
14	Pt(1)	3.0	14.3
	Pt(2)	5.5	17.0
$(Ph_2MeP)_2PtO_3PPh$		2.2	12.9

The structures of $FcCH_2PO_3Pt(PPh_3)_2$ **12**, $FcCH_2CH_2PO_3Pt(PPh_3)_2$ **13** and 1,1'-$Fc'[PO_3Pt(PPh_3)_2]_2$ **14** were routine. Bond angles and bond lengths were consistent with those in the published structure of $(Ph_2MeP)_2PtO_3PPh$[11]. All of the complexes

possess a distorted platinum square plane. Table 3.5 lists the twist and fold angles across the platinum square plane for the compounds **12-14** and the known compound $(Ph_2MeP)_2PtO_3PPh$. The twist angle is a measure of distortion about the platinum centre, while the fold angle is a measure of the co-planarity of the platinum and phosphonate centres (Figure 3.13).

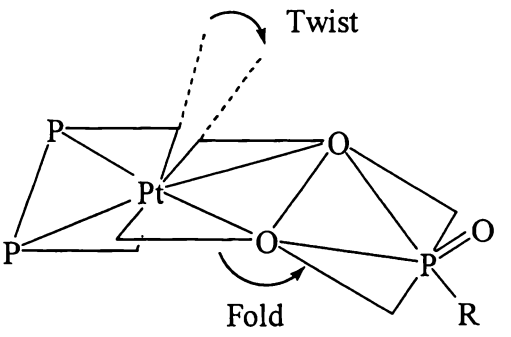

Figure 3.13: Schematic Representation of the Measured Twist and Fold Angles for Platinum Phosphonato Complexes.

The twist angle is larger in complexes **12** and **13** than in $(Ph_2MeP)_2PtO_3PPh$ presumably due to the bulk of ferrocenylphosphonate groups and the triphenylphosphine ligands when compared to the phenylphosphonate and diphenylmethylphosphine ligands of $(Ph_2MeP)_2PtO_3PPh$. The twist angles in **14** are similar to that reported for $(Ph_2MeP)_2PtO_3PPh$ but the fold angles of **14** are significantly larger than those of $(Ph_2MeP)_2PtO_3PPh$.

Another feature common to the structures of **12-14** is the presence of intermolecular phosphine-phosphine P-P distances of less than 9Å. This is characteristic of a structural phenomena known as phenyl embraces[14]. The phenyl rings of phenylphosphine ligands on adjacent molecules are able to weakly interact and influence the overall structure, such interactions are common being found in 87% of complexes that contain triphenylphosphine ligands[15].

[14] (a) I. Dance and M. L. Scudder, *J. Chem. Soc., Chem. Commun.*, 1995, 1039.
[15] (a) I. Dance and M. Scudder, *J. Chem. Soc., Dalton Trans.*, 2000, 1587. (b) I. Dance and M. Scudder, *J. Chem. Soc., Dalton Trans.*, 2000, 2909.

3.2.3: NMR Analysis of Bis(triphenylphosphine)platinum Ferrocenyl Phosphonates

While the carbon and hydrogen nmr of these compounds were routine, the ^{31}P-$\{^{1}H\}$ spectra were particularly distinctive. The phosphorus atoms of the phosphine and phosphonate groups coupled to each other and to the platinum metal centre. The result is two sets of signals, the first due to the phosphonate group at ~45ppm and the second due to the triphenylphosphine groups at ~10ppm, each set exhibiting multiplicity due to ^{31}P-^{31}P and ^{31}P-^{197}Pt coupling. A typical ^{31}P-$\{^{1}H\}$ NMR spectrum, that of $FcCH_2PO_3Pt(PPh_3)_2$ **12**, is given in Figure 3.14.

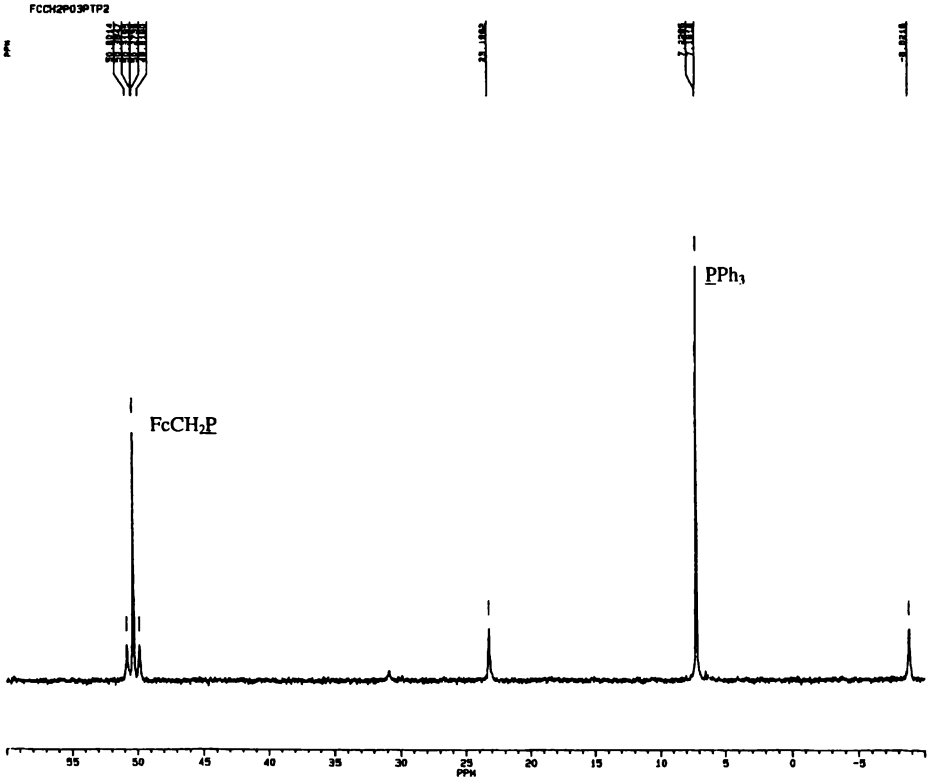

Figure 3.14: ^{31}P-$\{^{1}H\}$ NMR Spectrum of $FcCH_2PO_3Pt(PPh_3)_2$ **12**.

The triphenylphosphine $^{1}J_{P\text{-}Pt}$ coupling constants for compounds **11-14** were consistent with a phosphine ligand *trans* to oxygen[16]. These and other coupling constants are given in Table 3.6.

[16] T. G. Appleton, H. C. Clark and L. E. Manzer, *Coord. Chem. Rev.*, 1973, **10**, 335.

Table 3.6: ^{31}P NMR Data for Platinum Ferrocenylphosphonate Complexes.

Compound	Coupling Constants (Hz)		
	$^{3}J_{P\text{-}P}$	$^{2}J_{P\text{-}Pt}$ ($\underline{P}O_3Pt$)	$^{1}J_{P\text{-}Pt}$ ($Pt\underline{P}Ph_3$)
11	5.7	125	3850
12	6.0	116	3895
13	6.0	113	3845
14	5.7	122	3844
1,1'-$Fc'[CH_2PO_3Pt(PPh_3)_2]_2$*	5.9	111	3886

* This compound was characterised within a mixture by ^{31}P nmr.

3.2.4: Biological Activity of $FcCH_2PO_3Pt(PPh_3)_2$ 12 and $FcCH_2CH_2PO_3Pt(PPh_3)_2$ 13

Interest in the biological activity of platinum complexes stems from the potency of complexes such as cis-platin (*cis*-$Pt(NH_3)_2Cl_2$) as anti-cancer agents. Platinum phosphonato complexes such as $[Pt(NH_3)_2(NTMP)]^-$ have anti-cancer properties[2] as do a number of platinum complexes containing ferrocene groups[17]. For this reason the activity of ferrocenylphosphonato platinum complexes against cancer cells was considered worthy of investigation.

Samples of **12** and **13** were assayed for activity against P388 leukemia cells. Anti tumour assays of the free ferrocenyl phosphonic acids $FcCH_2PO_3H_2$ **3** and $FcCH_2CH_2PO_3H_2$ **5** were also undertaken to provide comparison. Results are tabulated (Table 3.7) as IC_{50} values, where IC_{50} is the amount required ($ngml^{-1}$) to inhibit 50% of cell growth and are standardised relative to the antibiotic mitomycin. The ferrocenyl phosphonic acids **3** and **5** with IC_{50} values of $538115ngml^{-1}$ and $>62500ngml^{-1}$ respectively can be considered inactive against cancer cells. The platinum complexes **12** and **13** show moderate activity with IC_{50} values of $5838ngml^{-1}$ and $5046ngml^{-1}$ respectively.

[17] (a) E. W. Neuse, M. G. Meirim and N. F. Blom, *Organometallics*, 1988, **7**, 2562. (b) T. A. K. Al-Allaf and L. J. Rashan, *Appl. Organomet. Chem.*, 1999, **13**, 63. (c) R. W. Mason, K. McGrouther, P. R. R. Ranatunge-Bandarage, B. H. Robinson and J. Simpson, *Appl. Organomet. Chem.*, 1999, **13**, 163.

Table 3.7: Antitumour (P388) Assay Results for Compounds **3**, **5**, **12** and **13**.

Compound	IC_{50} ($ngml^{-1}$)[a]
3	538115
5	>62500
12	5838
13	5046

[a] The concentration of sample in $ngml^{-1}$ required to reduce the cell growth of the P388 leukemia cell line by 50%.

3.3: Reaction of $FcCH_2PO_3H_2$ 3 with Palladium and Gold Complexes

Silver oxide mediated synthesis of metallacycles is not limited to platinum. Recent studies have included the preparation of palladium[18] and gold(III)[19] metallacycles. As an extension of this, the ferrocenyl phosphonic acid, $FcCH_2PO_3H_2$ **3** was reacted with (DPPE)$PdCl_2$ and [Au{C_6H_4-2-(CH_2NMe_2)Cl_2] with the intention of preparing the analogous palladium and gold ferrocenyl phosphonato complexes (Scheme 3.4).

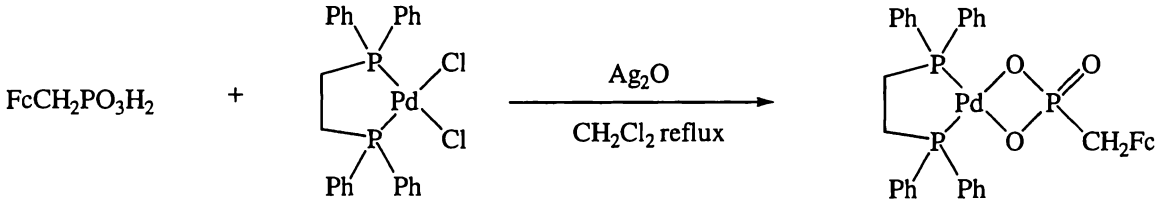

[18] (a) W. Henderson, J. Fawcett, R. D. W. Kemmitt, C. Proctor and D. R. Russell, *J. Chem. Soc., Dalton Trans.*, 1994, 3085. (b) W. Henderson, B. K. Nicholson and A. G. Oliver, *Polyhedron*, 1994, **13**, 3099.

[19] (a) M. B. Dinger and W. Henderson, *J. Organomet. Chem.*, 1997, **547**, 243. (b) M. B. Dinger and W. Henderson, *J. Organomet. Chem.*, 1998, **557**, 231. (c) M. B. Dinger, W. Henderson, B. K. Nicholson and W. T. Robinson, *J. Organomet. Chem.*, 1998, **560**, 169. (d) M. B. Dinger and W. Henderson, *J. Organomet. Chem.*, 1998, **560**, 233. (e) M. B. Dinger and W. Henderson, *J. Organomet. Chem.*, 1999, **577**, 219.

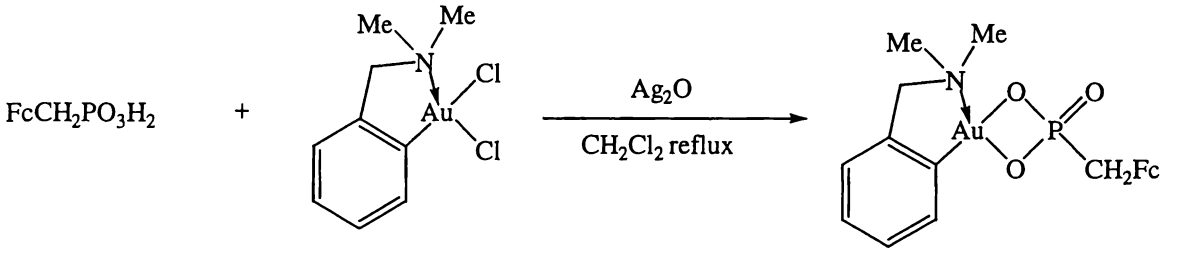

Scheme 3.4: Reaction of $FcCH_2PO_3H_2$ with $(DPPE)PdCl_2$ and $[Au\{C_6H_4\text{-}2\text{-}(CH_2NMe_2)Cl_2]$.

The reaction of **3** with $(DPPE)PdCl_2$ (DPPE = 1,2-bis-(diphenylphosphino)ethane) was monitored by ^{31}P nmr and was deemed complete after one hour. Workup of the reaction solution resulted in the isolation of a brown powder that was soluble in CH_2Cl_2. Positive ion ESMS of this product gave a single peak at *m/z* 1566 at a cone voltage of 20V. Increasing the cone voltage to 100V gave rise to a second peak at *m/z* 783 (Figure 3.15).

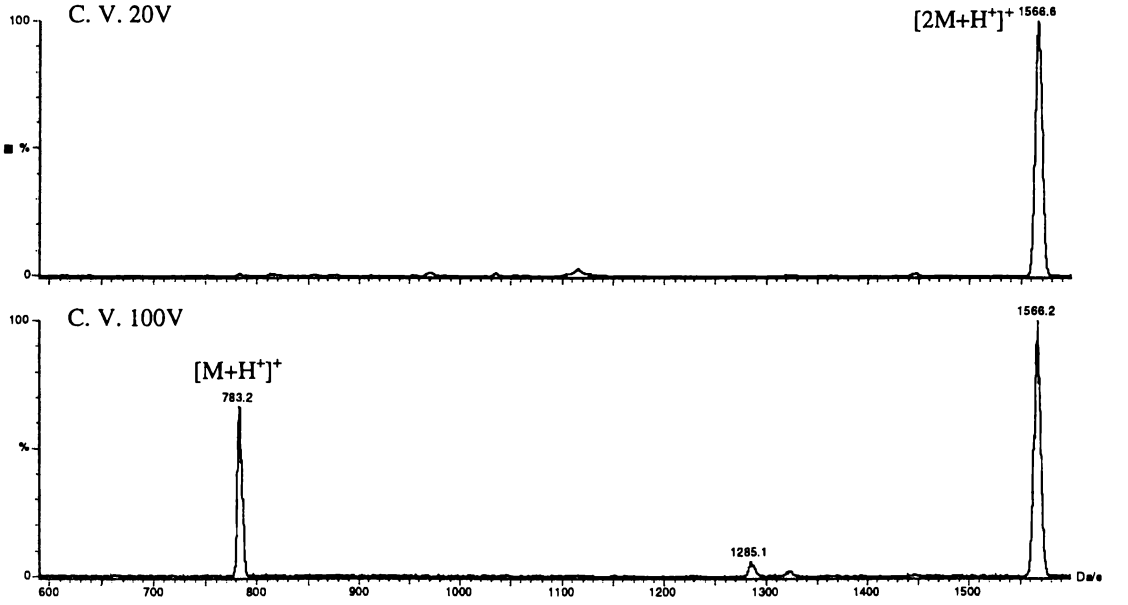

Figure 3.15: Positive Ion ES Mass Spectra of $FcCH_2PO_3H_2$ + $(DPPE)PdCl_2$ in Methanol at Cone Voltages of 20V and 100V.

These peaks were assigned from their isotope patterns as $[\{FcCH_2PO_3Pd(DPPE)\}_2+H^+]^+$ and $[FcCH_2PO_3Pd(DPPE)+H^+]^+$ respectively (Figure

3.16). The formation of dimeric adducts is a common phenomena under ESMS conditions. However peaks due to dimerisation are almost always accompanied by peaks due to the monomer in ES mass spectra, unless there is a very strong driving force for dimerisation to occur.

The absence of a peak due to $[FcCH_2PO_3Pd(DPPE)+H^+]^+$ *m/z* 783 at low cone voltages led to assumption that the main product of this reaction was a dimeric species $[FcCH_2PO_3Pd(DPPE)]_2$. The ^{31}P nmr of the crude product was less promising, revealing the presence of several products in addition to the desired complex. Attempts at crystallisation were unsuccessful.

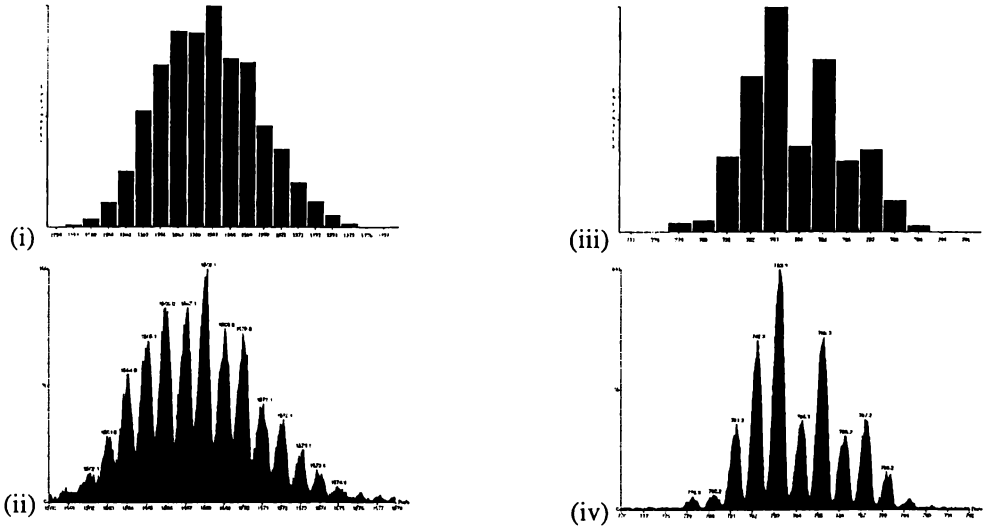

Figure 3.16: Calculated and Observed Isotope Patterns for $[\{FcCH_2PO_3Pd(DPPE)\}_2+H^+]^+$ [(i) and (ii)] and $[FcCH_2PO_3Pd(DPPE)+H^+]^+$ [(iii) and (iv)].

The reaction of **3** with $[Au\{C_6H_4\text{-}2\text{-}(CH_2NMe_2)Cl_2]$ was allowed to proceed for one hour. Workup led to the isolation of a pale yellow powder that was soluble in CH_2Cl_2 and sensitive to light. Attempts at recrystallisation led to the deposition of gold mirrors. Preliminary ESMS, ^{13}C and ^{31}P nmr evidence suggested that the desired product $FcCH_2P(O)O_2[Au\{C_6H_4\text{-}2\text{-}(CH_2NMe_2)Cl_2]$ did form in low yield though a pure sample was never obtained.

It appears that silver(I) oxide mediated synthesis of phosphonato complexes can be extended to palladium and gold, but isolation of the resulting products is more difficult than for the analogous platinum complexes.

3.4: Experimental

General experimental techniques in this chapter are in keeping with those outlined in chapter 2.2 with the following alterations/additions. All reactions are carried out in air unless otherwise stated.

Samples of the starting material *cis*-$(PPh_3)_2PtCl_2$ were kindly supplied by Allen Oliver, Maarten Dinger and Corry Decker. Samples of silver(I) oxide (DPPE)$PdCl_2$ and [Au{C_6H_4-2-$(CH_2NMe_2)Cl_2$] were supplied by Allen Oliver.

The bis(triphenylphosphine)platinum complexes were introduced to the ES mass spectrometer as methanolic solutions with 50/50 methanol/water or 50/50 acetonitrile/water as the carrier solvent. Spectra were acquired over a range of positive and negative cone voltages. Samples were also introduced to the ES mass spectrometer dissolved in CH_2Cl_2 when CH_2Cl_2 was used as the carrier solvent. Infrared spectra of complexes **11-14** were obtained as KBr discs.

Anti-tumour assays were undertaken at the University of Canterbury chemistry department.

3.4.1: Syntheses

The synthetic method used was that described by Kemmitt et al[10]. The ferrocenyl phosphonic acid was placed in dry CH_2Cl_2 and a molar equivalent of *cis*-$(Ph_3P)_2PtCl_2$ was added, along with an excess of Ag_2O. The mixture was refluxed with stirring for two hours, or until ^{31}P nmr showed no trace of *cis*-$(Ph_3P)_2PtCl_2$. At this time the solution was filtered to remove Ag_2O and other insoluble silver salts. The resulting yellow solution was concentrated (to ~2ml) and petroleum spirits added to precipitate the product as a pale yellow powder.

3.4.1.1: Synthesis of $FcPO_3Pt(PPh_3)_2$ **11**

Prepared as described above, $FcP(O)(OH)_2$ (0.017g, 0.063mmol), *cis*-$(Ph_3P)_2PtCl_2$ (0.05g, 0.063mmol) and Ag_2O (0.03g, excess) were refluxed in CH_2Cl_2 (5ml) for 1.5 hours. Work-up gave 0.042g (68%) of **11** as a yellow powder.

m.p. 138-142°C (dec).

Elemental Analyses: Found C, 53.93%; H, 4.20%. Calculated for $C_{46}H_{39}FeO_3P_3Pt$: C, 56.17%; H, 3.99%. Calculated for **11**.CH_2Cl_2: C, 52.83%; H, 3.87%.

^{31}P-{^1H} NMR ($CDCl_3$): δ 8.23 (*d*, $^3J_{P\text{-}P}$ 5.75Hz, (*d*, $^1J_{P\text{-}Pt}$ 3850Hz), $\underline{P}Ph_3$), 43.37 (*t*, $^2J_{P\text{-}Pt}$ 125Hz, $\underline{P}O_3Pt$).

^{13}C-{^1H} NMR ($CDCl_3$): δ 69.47 (*s*, C4), 69.62 (*d* $^3J_{C\text{-}P}$ 12Hz, C3), 71.95 (*d*, $^2J_{C\text{-}P}$ 14Hz, C2), 128.32 (*d*,(*d*, $^2J_{C\text{-}P}$ 5.45Hz), *o*-C PPh_3), 131.17 (*s*, *p*-C PPh_3), 134.51 (*d*, (*d*, $^3J_{C\text{-}P}$ 5.43Hz), *m*-C, PPh_3).

^1H NMR ($CDCl_3$): δ 4.06 (5H, *s*, H4), 4.23 (2H, *d*, $^3J_{H\text{-}P}$ 0.4Hz, H2), 4.54 (2H, *s*, H3), 7.18 (12H, *br t*, *o*-C$\underline{H}$, PPh_3), 7.33 (6H, *br t*, *p*-C$\underline{H}$, PPh_3), 7.45 (12H, *m*, *m*-C$\underline{H}$, PPh_3).

ESMS: (MeOH, c.v. 20V) *m/z* 736 ([Pt(*o*-$C_6H_4PPh_2$)(PPh_3)+H_2O]$^+$, 100%) (MeCN/H_2O, c.v. -20V) *m/z* 265 [$FcPO_3^{2-}$+H^+]$^-$, 100%).

IR (cm^{-1}): 1482 (w), 1211(w), 1174(w), 1098(m), 1027(w), 999(w), 927(m), 879(w), 610(m), 555(s), 529(s).

3.4.1.2: Synthesis of $FcCH_2PO_3Pt(PPh_3)_2$.**12**

Prepared as described above. $FcCH_2P(O)(OH_2)$, (0.019g, 0.07mmol), *cis*-$(PPh_3)_2PtCl_2$, (0.053g, 0.07mmol) and Ag_2O (0.03g, excess) were placed in CH_2Cl_2 (10ml) and the mixture refluxed for 1 hour. Work up gave 0.057g (86%) of **12** as a pale yellow powder.

m.p. 165-168°C (dec).

Elemental Analyses: Found C, 54.50%; H, 4.06%. Calculated for $C_{47}H_{39}FeO_3P_3Pt$: C, 56.60%; H, 4.11%. Calculated for **12**.CH_2Cl_2: C, 53.20%, H, 3.97%. Calculated for **12**.$2CH_2Cl_2$: C, 50.4%, H, 3.85%.

^{31}P-{^{1}H} NMR ($CDCl_3$): δ 7.20 (*d*, $^{2}J_{P\text{-}P}$ 6Hz, (*d*, $^{1}J_{P\text{-}Pt}$ 3895Hz), $\underline{P}Ph_3$), 50.48 (*t*, $^{3}J_{P\text{-}P}$ 6Hz, (*d*, $^{2}J_{P,Pt}$ 116Hz), $CH_2\underline{P}$).

^{13}C-{^{1}H} NMR ($CDCl_3$): δ 32.53 (*d*, $^{1}J_{C\text{-}P}$ 117Hz, $\underline{C}H_2P$), 66.74 (*s*, C3), 68.82 (*s*, C4), 70.28 (*s*, C2), 127.75 (*d*, $^{1}J_{C\text{-}P}$ 31Hz, *i*-C, PPh_3), 128.19 (*d*, (*d*, $^{3}J_{C\text{-}P}$ 5Hz), *m*-C, PPh_3), 131.06 (*s*, *p*-C, PPh_3), 134.55 (*d*, (*d* $^{2}J_{C\text{-}P}$ 5Hz), *o*-C, PPh_3).

^{1}H NMR ($CDCl_3$): δ 2.72 (2H, *d*, $^{1}J_{H\text{-}P}$ 18.74Hz, $C\underline{H}_2P$), 4.02 (5H, *s*, H4), 4.04 (2H, *s*, H3), 4.10, (2H, *s*, H2), 7.13-7.31 (30H, *m*, $C\underline{H}$, PPh_3).

ESMS: ($MeCN/H_2O$, c.v. 60V) *m/z* 998 ($[M+H^+]^+$ 17%), 759 ($[Pt(o\text{-}C_6H_4PPh_2)(PPh_3)+MeCN]^+$, 99%), 718 ($[Pt(o\text{-}C_6H_4PPh_2)(PPh_3)]^+$, 100%). ($MeCN/H_2O$, c.v. -40V) *m/z* 279 $[FcCH_2PO_3^{2-}+H^+]^-$, 100%).

IR (cm^{-1}): 1217(w), 1182(m), 1098(m), 999(w), 924(m), 612(w), 584(w), 554(s), 530(s).

3.4.1.3: Synthesis of $FcCH_2CH_2PO_3Pt(PPh_3)_2$.**13**

$FcCH_2CH_2P(O)(OH)_2$ (0.04g, 0.13mmol), *cis*-$(PPh_3)_2PtCl_2$ (0.107g, 0.13mmol) and Ag_2O (0.05g, excess) were placed in 10ml of CH_2Cl_2 and the mixture refluxed for 1 hour, at which time ^{31}P nmr indicated the reaction was complete. Work up gave **13** (0.13g, 94%) as a pale yellow powder.

m.p. 209-212°C (melt-dec).

Elemental Analyses: Found C, 50.73%; H, 4.11%. Calculated for $C_{50}H_{47}Cl_4FeO_3P_3Pt$: C, 50.85%, H 4.01%.

^{31}P-{^{1}H} NMR (d^6-DMSO): 7.90 (*d*, $^{3}J_{P\text{-}P}$ 6Hz, (*d*, $^{1}J_{P\text{-}Pt}$ 3845Hz), $\underline{P}Ph_3$, 49.76 (*t*, $^{3}J_{P\text{-}P}$ 6Hz, (*d*, $^{2}J_{P\text{-}Pt}$ 113Hz), $CH_2\underline{P}$).

^{13}C-{^{1}H} NMR (d^6-DMSO): δ 25.09 (*s*, $\underline{C}H_2CH_2P$), 32.70 (*d* $^{1}J_{C\text{-}P}$ 120Hz, $CH_2\underline{C}H_2P$), 67.49 (*s*, C3), 68.07 (*s*, C2), 68.75 (*s*, C4), 127.7 (*d*, $^{1}J_{C\text{-}P}$ 63Hz, *i*-C, PPh_3), 128.95 (*d*, (*d*, $^{3}J_{C\text{-}P}$ 5Hz), *m*-C, PPh_3), 132.02 (*s*, *p*-C, PPh_3), 134.52 (*d*, (*d*, $^{2}J_{P\text{-}C}$ 4Hz), *o*-C, PPh_3).

^{1}H NMR (d^6-DMSO): δ 1.93 (2H, *m*, $C\underline{H}_2PO_3$), 2.68 (2H, *m*, $C\underline{H}_2CH_2PO_3$), 4.05 (2H, *s*, H3), 4.09 (5H, *s*, H4), 4.13 (2H, *s*, H2), 7.2-7.5 (30H, PPh_3).

ESMS: ($MeCN/H_2O$, c.v. +60V) *m/z* 1011 ($[M+H^+]^+$, 27%), 736 ($[Pt(o\text{-}C_6H_4PPh_2)(PPh_3)+H_2O]^+$, 100%). ($MeCN/H_2O$, c.v. -40V) *m/z* 293 ($[FcCH_2CH_2PO_3^{2-}+H^+]^-$, 100%).

IR (cm^{-1}): 1482 (w), 1437 (w), 1196 (m), 1098 (m), 999 (w), 918 (m), 595 (m), 555 (s), 529 (s), 512 (m).

3.4.1.4: Synthesis of 1,1'-Fc'[$PO_3Pt(PPh_3)_2]_2$.**14**

1,1'-Fc'[$P(O)(OH)_2]_2$ (0.023g, 0.067mmol), *cis*-$(PPh_3)_2PtCl_2$ (0.106g, 0.134mmol) and Ag_2O (0.1g, excess) were placed in CH_2Cl_2 (5ml) and the reaction mixture refluxed for two hours. Standard work-up gave 0.088g (74%) of **14** as a pale yellow powder. Vapour diffusion of Et_2O into a CH_2Cl_2:methanol solution of the crude product gave crystals upon which X-ray crystallography and elemental analysis were performed.

m.p. 218-226°C (melt-dec).

Elemental Analyses: Found C, 58.79%; H, 5.38%. Calculated for $C_{82}H_{68}FeO_6P_6Pt_2$ C, 55.29%; H, 3.84%. Calculated for **14**.CH_3OH: C, 54.98%, H, 4.00%.

^{31}P-{^1H} NMR (DCM with D_2O lock stick): δ 8.05 (*d*, $^3J_{P\text{-}P}$ 5.7Hz, (*d*, $^1J_{P\text{-}Pt}$ 3844Hz), $\underline{P}Ph_3$), 41.92 (*t*, $^3J_{P\text{-}P}$ 5.8Hz, (*d*, $^2J_{P\text{-}Pt}$ 122Hz), $\underline{P}O_3Pt$).

^{13}C-{^1H} NMR (d^6-DMSO): δ 68.52 (*s*, C3), 69.35 (*s*, C2), 128.32 (*d*,(*d*, $^2J_{C\text{-}P}$ 5.45Hz), *o*-C PPh_3), 132.17 (*s*, *p*-C PPh_3), 134.51 (*d*, (*d*, $^3J_{C\text{-}P}$ 5.43Hz), *m*-C, PPh_3).

^1H NMR (d^6-DMSO): δ 4.08 (4H, *s*, H3), 4.31 (2H, *s*, H2), 7.25-7.65 (60H, *m*, Ph)

ESMS: (MeCN/H_2O, c.v. +60V) *m/z* 1780 ([M+H^+]$^+$, 10%), 1471 ([2{$(Ph_3P)_2Pt$}-2H^++2H_2O]$^+$, 37%), 776 ([$(Ph_3P)_2$Pt-H^++MeCN+H_2O]$^+$ 18%), 759 ([$(Ph_3P)_2$Pt-H^++MeCN]$^+$, 54%), 736 ([$(Ph_3P)_2$Pt-H^++H_2O]$^+$, 98%), 718 ([$(Ph_3P)_2$Pt-H^+]$^+$, 100%).

3.4.1.5: Reaction of (DPPE)$PdCl_2$ with $FcCH_2PO_3H_2$ **3**

To a slurry of **3** (0.028g, 0.01mmol) and Ag_2O (0.42g, excess) in CH_2Cl_2 (10ml) was added (DPPE)$PdCl_2$ (0.052g, 0.09mmol) and the solution brought to reflux for 2.5 hours. The reaction solution was cooled to room temperature and filtered to remove silver salts. The solvent was removed to give 0.35g of pale brown powder. Initial analysis by ESMS seemed to indicate a single product, but ^{31}P nmr revealed the presence of significant impurities. All attempts at purification by recrystallisation were unsuccessful.

3.4.1.6: Reaction of [Au{C_6H_4-2-(CH_2NMe_2)Cl_2] with $FcCH_2PO_3H_2$ **3**

Silver(I) oxide (0.1g, excess) was added to a solution of [Au{C_6H_4-2-(CH_2NMe_2)Cl_2] (0.069g, 0.17mmol) and **3** (0.048g, 0.17mmol) in CH_2Cl_2 (10ml). The solution was placed under a dinitrogen atmosphere and brought to reflux in the dark. Reflux was discontinued after 1 hour. The solution was allowed to cool before being filtered. Activated carbon was added and the solution filtered a second time to give a pale yellow solution. The solvent was removed to give 0.02g of a pale yellow powder. The initial ^{31}P and ^{13}C nmr analysis of the crude product indicated one major product and several minor products. Attempts at recrystallisation from a variety of solvents invariably led to the deposition of gold mirrors.

3.4.2: X-ray Crystal Structure Determination for Compounds 12, 13 and 14

Single crystals of these complexes were obtained by methods described in the preceding text. The data sets for **12** were collected on a Nicolet R3 diffractometer at Canterbury University and corrected for absorption using SADABS. The data sets for **13** and **14** were collected on a Siemens CCD SMART diffractometer at the University of Auckland and corrected for absorption using SADABS. The structures were solved by direct methods for platinum and developed routinely using the SHELXL-97 program with full matrix least squares refinement based on F_o^2. The structures of **12** and **13** each include two independent CH_2Cl_2 molecules (solvent of crystallisation), while poorly refined solvent molecules are present in the structure of **14**. All non-hydrogen atoms were refined using anisotropic temperature factors, while hydrogen atoms were placed in calculated positions. Crystallographic data and analysis parameters for compounds **12**, **13** and **14** are given in Table 3.8.

Table 3.8: Collected Single Crystal Data and Analysis Parameters for **12**, **13** and **14**.

Compound	**12**	**13**	**14**
Empirical Formula	$C_{47}H_{41}FeO_3P_3Pt.$ $2CH_2Cl_2$	$C_{48}H_{43}FeO_3P_3Pt.$ $2CH_2Cl_2$	$C_{82}H_{68}FeO_6P_6Pt_2.$ CH_3OH
Crystal Size (mm)	0.65×0.55×0.32	0.45×0.13×0.06	0.37×0.33×0.23

Formula Weight	1167.5	1181.53	1863.12
Crystal System	Orthorhombic	Triclinic	Triclinic
a(Å)	20.4241(9)	13.3696(2)	12.5981(1)
b(Å)	18.4116(9)	14.3472(3)	16.3884(2)
c(Å)	25.0622(13)	14.6522(2)	23.0691(2)
α(°)	90	74.144(1)	93.815(1)
β(°)	90	83.00(0)	104.156(1)
γ(°)	90	62.248(1)	111.58
V(Å^3)	9424.40	2392.56(7)	4229.22(7)
Space Group	Pbca	P-1	P-1
Z Value	8	2	2
D (calc.)(gcm^{-3})	1.646	1.64	1.463
F(000)	4640	1176	1944
λ(Mo-Kα)(Å)	0.71	0.71	0.71
μ (Mo-Kα)(mm^{-1})	3.64	3.36	3.63
Temp. (K)	158(2)	200(2)	200(2)
2θ range for Data Collection	6°<2θ<53°	3°<2θ<55°	2°<2θ<54°
Total Reflections	24352	8329	17728
Unique Reflections	8654 ($R_{int.}$ = 0.0256)	7064 ($R_{int.}$ = 0.0157)	15684 ($R_{int.}$ = 0.0196)
T_{min}	0.658444	0.638619	0.450436
T_{max}	1.00000	0.860819	0.549434
Residual e$^-$ density:			
max (e Å^{-3})	1.227	0.741	3.462
min (e Å^{-3})	-1.205	-0.853	-0.775
R_1 [I>2σ(I)]	0.0318	0.0283	0.0473
wR_2	0.0797[ϑ]	0.808[℘]	0.1379[ℵ]
GOF	1.037	1.058	1.138

[ϑ] $w = [\sigma^2(F_o^2) + (0.0262P)^2 + 37.6334P]^{-1}$ where $P = (F_o^2 + 2F_c^2)/3$. [℘] $w = [\sigma^2(F_o^2) + (0.0406P)^2 + 2.5846P]^{-1}$ where $P = (F_o^2 + 2F_c^2)/3$. [ℵ] $w = [\sigma^2(F_o^2) + (0.0673P)^2 + 24.25P]^{-1}$ where $P = (F_o^2 + 2F_c^2)/3$.

Chapter 4: Synthesis and Characterisation of Ferrocenyl Primary Phosphines

4.1: Introduction

Primary phosphines are compounds of the general formula R-PH_2. They possess a rich chemistry largely due to the weakness of the P-H bond, which is reactive towards unsaturated compounds, acid halides, halogens and metal centres. Primary phosphines are especially renowned for their sensitivity toward oxidation in air and some are pyrophoric. This sensitivity to air has been a serious impediment in the development of primary phosphine chemistry. However there are a few examples of air-stable primary phosphines, most of which are based on the sterically crowded 2,4,6,-tri-*t*-butylphenylphosphine ('supermesityl phosphine' or Mes*PH_2)[1], (Figure 4.1).

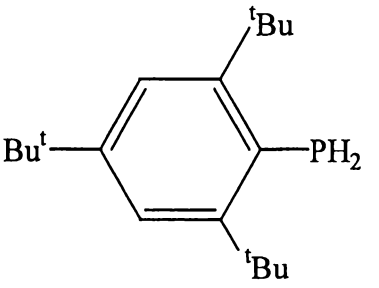

Figure 4.1: Supermesityl Phosphine.

This primary phosphine and closely related derivatives are quite stable in air and have been used in a number of published studies[2]. The steric congestion of the

[1] K. Issleib, H. Schmidt and C. Wirkner, *Z. Anorg. Allg. Chem.*, 1982, **488**, 75.

[2] (a) D. K. Wicht, I. V. Kourkine, B. M. Lew, J. M. Nthenge and D. S. Glueck, *J. Am. Chem. Soc.*, 1997, **119**, 5039. (b) A. H. Cowley, J. E. Kilduff, T. H. Newman and M. Pakulski, *J. Am. Chem. Soc.*, 1982, **104**, 5820. (c) N. Yoshifuji, K. Shibayama, K. Toyota and N. Inamoto, *Tetrahedron Lett.*, 1983, **24**, 4227. (d) H. Schmidbaur, G. Weidenhiller, O. Steigelman and G. Muller, *Chem. Ber.*, 1990, **123**, 285. (e) D. J. Brauer, F. Bitterer, F. Dorrenbach, G. Hessler, O. Stelzer, C. Kruger and F. Lutz, *Z. Naturforsch.*, 1996, **51b**, 1183. (f) R. Felsberg, S. Blaurock, S. Jelonek, T. Gelbrich, R. Kirmse, A. Voight and E. Hey-Hawkins, *Chem. Ber./Recueil*, 1997, **130**, 807. (g) G. W. Rabe, I. A. Guzei and A. L. Rheingold, *Inorg. Chem.*, 1997, **36**, 4914. (h) M. -A. David, D. K. Wicht, D. S. Glueck, G. P. A. Yap, L. M. Liable-Sands and A. L. Rheingold, *Organometallics*, 1997, **16**, 4768. (i) D. K. Wicht, S.

phosphine group in supermesitylphosphine would seem to adequately explain its immunity to air oxidation.

More recently details of the synthesis and structure of the air stable primary phosphine, dibenzobarrellenephosphine (Figure 4.2), have been published[3].

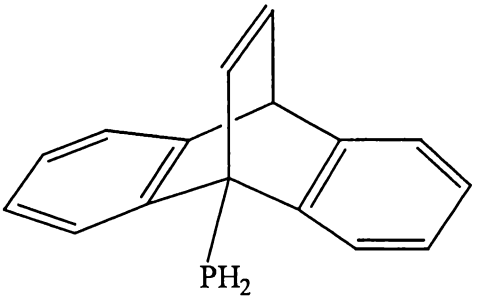

Figure 4.2: Dibenzobarellenephosphine.

The oxidative stability of this phosphine was attributed to the proximity of the double bond *trans* to the -PH_2 group, though further explanation was not given. It seems unlikely that steric crowding is a significant factor in the resistance of dibenzobarellenephosphine to air oxidation, for although the dibenzobarellene group is bulky, it shields one side only of the phosphine moiety. In the solid state the C-P bonds lies along a mirror plane and the phosphine group is oriented such that there is an all-trans geometry from the double bond of the ethylene bridge to the lone pair of the phosphine group. There is no free rotation of the PH_2 group at 180K.

The synthesis of a range of air stable amide, carboxylate and thiol functionalised phosphines derived from $H_2N(CH_2)_3PH_2$ has also recently been published[4], (Scheme 4.1). The reason(s) for the air stability of these compounds was not discussed and as characterisation was by nmr and MS only, interaction of the phosphine groups with the other functional groups present was not investigated. While not pyrophoric, the aminopropyl phosphine used as the starting material in these reactions is not stable toward air oxidation and required manipulation under a

---

N. Paisner, B. M. Lew, D. S. Glueck, G. P. A. Yap, L. M. Liable-Sands, A. L. Rheingold, C. M. Haar and S. P. Nolan, *Organometallics*, 1998, **17**, 652.

[3] M. Brynda, M. Geoffroy and G. Bernardinelli, *Chem. Commun.*, 1999, 961.

[4] K. R. Prabhu, N. Pillarsetty, H. Gali and K. V. Katti, *J. Am. Chem. Soc.*, 2000, **122**, 1554.

dinitrogen atmosphere. The common feature of the air stable derivatives is an amide link four bonds removed from the PH_2 group(s).

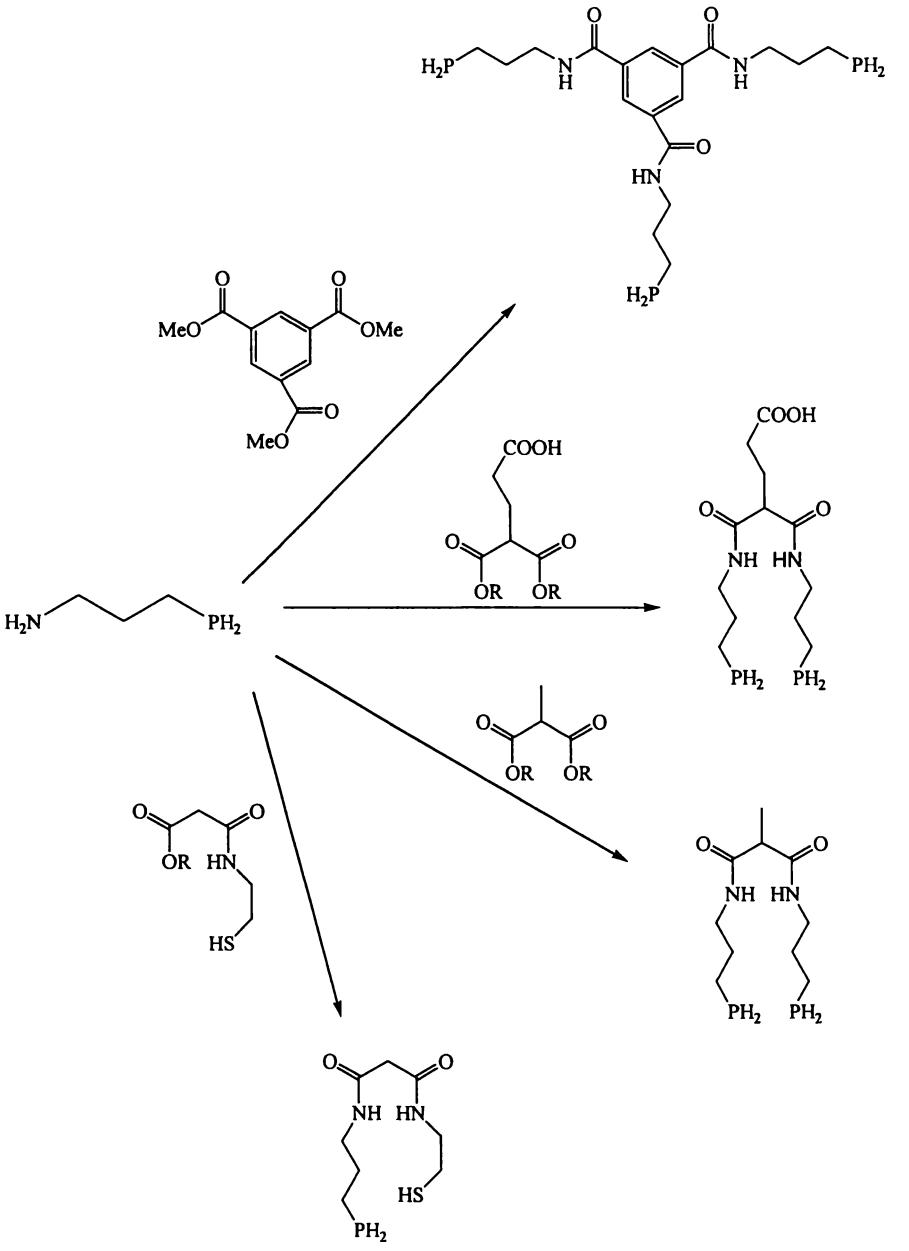

Scheme 4.1: Air Stable Derivatives of Aminopropyl Phosphine.

There is also a series of cationic primary phosphines of the type $[R'R''_2N(CH_2)_nPH_2]I$[5] which are air stable, presumably due to their positively charged nature, which may prevent attack by electrophilic oxygen, (Table 4.1).

[5] D. J. Brauer, J. Fischer, S. Kuken, K. P. Langhans, O. Stelzer and N. Weferling, *Z. Naturforsch.*, 1994, **49b**, 1511.

Table 4.1: The Air Stable Cations of the General Formula $[R'R''_2N(CH_2)_nPH_2]^+$.

	R'	R''	n
1	Me	Me	2
2	Me	Me	3
3	C_5H_{10}	Me	2
4	C_4H_8O	Me	2
5	Me	C_6H_{13}	2
6	Me	C_7H_{15}	2
7	Me	C_8H_{17}	2
8	Me	$C_{12}H_{25}$	2
9	Me	$C_{16}H_{33}$	2
10	Me	$C_{18}H_{37}$	2
11	$R'R''N(CH_2)_n$ = 2-(1-methyl-2-pyrrolidinyl)ethyl		

Of most interest to this work was the synthesis in 1997 of the air stable ferrocenylphosphine, $FcCH_2PH_2$ **15**[6], (Figure 4.3).

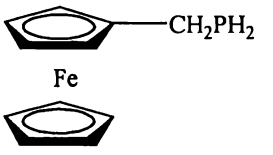

15

Figure 4.3: Ferrocenylmethyl Phosphine $FcCH_2PH_2$ **15**.

This compound is an orange crystalline material that can be easily purified by sublimation. It has a strong phosphine odour, is soluble in all organic solvents and does not react with oxygen in air in either the solid or solution state. The crystal structure of this unique phosphine revealed that the $-CH_2PH_2$ group extends away from the ferrocene moiety, precluding steric effects or physical interaction with the Fe atom as a source of the phosphine's remarkable stability. The phosphine $FcCH_2PH_2$ **15**

[6] N. J. Goodwin, W. Henderson and B. K. Nicholson, *Chem. Commun.*, 1997, 31.

displayed reactivity typical of primary phosphines[7]. At this time the reason for its indifference to oxygen is not known.

Two other primary ferrocenyl phosphines $FcPH_2$ **16** and 1,1'-$Fc'[PH_2]_2$ **17** have precedence in the published literature[8,9], (Figure 4.4). Both compounds have been recently used as intermediates in ferrocenyl phosphorus chemistry though no mention was made of their stability or otherwise in air.

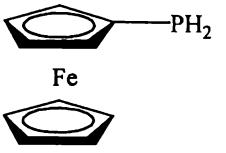

16

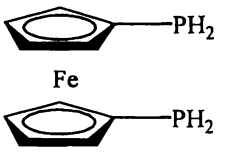

17

Figure 4.4: $FcPH_2$ **16** and 1,1'-$Fc'[PH_2]_2$ **17**.

The goals of the research presented in this chapter were to investigate new routes for the synthesis of the primary ferrocenyl phosphine $FcCH_2PH_2$ **15**, to prepare and characterise related primary ferrocenyl phosphines and to determine structural features that influence stability in air.

4.2: Synthesis and Characterisation of Primary Ferrocenyl Phosphines

The primary phosphine **15** was originally prepared from the methiodide salt, $FcCH_2NMe_3^+I^-$ in a two step process. The first step involved reaction of the methiodide salt with tris-hydroxymethyl phosphine. Formaldehyde was then removed from the resulting hydroxymethyl phosphine $FcCH_2P(CH_2OH)_2$, using sodium

[7] N. J. Goodwin, W. Henderson, B. K. Nicholson, J. Fawcett and D. R. Russell, *J. Chem. Soc., Dalton Trans.*, 1999, 1785.

[8] For $FcPH_2$: (a) C. Spang, F. T. Edelmann, M. Noltemeyer and H. W. Roesky, *Chem. Ber.*, 1989, **122**, 1247. (b) R. Pietschnig, M. Nieger, E. Niecke and K. Airola, *J. Organomet. Chem.*, 1997, **541**, 237. (c) R. Pietschnig, E. Niecke, M. Nieger and K. Airola, *J. Organomet. Chem.*, 1997, **529**, 127.

[9] For 1,1'-$Fc'[PH_2]_2$: (a) K. Fujiwara, M. Kudo and K. Yabutani, Patent Application JP 89-94423 19890414, CAN. 114:246929, AN. 1991:246929. (b) M. J. Burk and M. F. Gross, *Tetrahedron Lett.*, 1994, **35**, 9363. (c) H. Brunner and A. Reimer, *Chem. Ber.*, 1997, **130**, 1495. (d) A. Marinetti, F. Labrue and J-P. Genet, *Synlett.*, 1999, **12**, 1975. (e) U. Berens, M. J. Burk, A. Gerlach and W. Hems, *Angew. Chemie, Int. Ed.*, 2000, **39**, 1981.

metabisulfite to give the primary phosphine as depicted in Scheme 4.2. The overall yield of the primary phosphine was 35% with respect to the methiodide starting material.

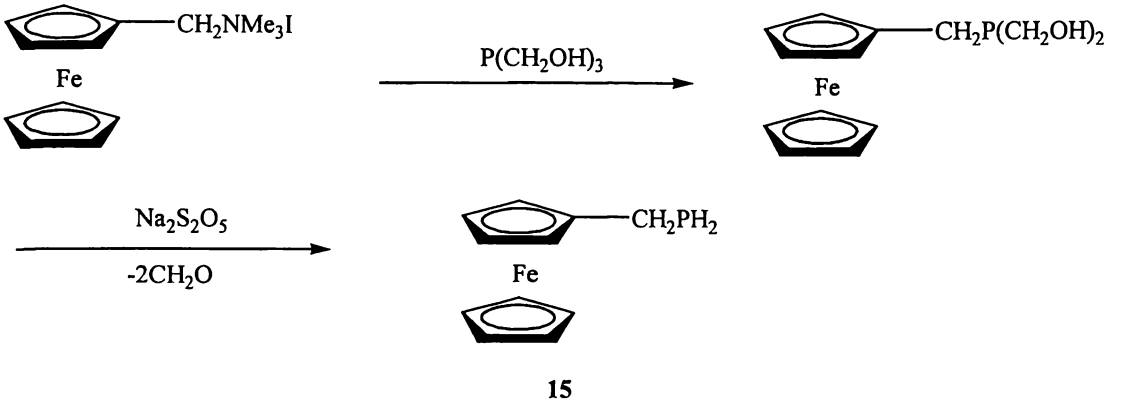

15

Scheme 4.2: Published[6] Synthesis of $FcCH_2PH_2$.

This method was somewhat unorthodox when compared to the usual synthetic routes to primary phosphines. Primary phosphines are most commonly prepared by the reduction of phosphonate esters. The reducing agent of choice is a mixture of lithium aluminium hydride ($LiAlH_4$) and trimethylsilyl chloride (Me_3SiCl)[10].

It was recognised that the phosphonate monoester $FcCH_2P(O)(OH)(OEt)$ **2**, (section 2.2), was a prime candidate for reduction to **15**. Reduction of **2** with $LiAlH_4/Me_3SiCl$ led to a very low yield (<10%) of the primary phosphine. The low yield is presumably due to the formation of insoluble lithium salts of the type $FcCH_2P(O)(OEt)O^-Li^+$. Methylation of **2** with excess diazomethane (CH_2N_2) gave a quantitative yield of the mixed ester $FcCH_2P(O)(OEt)(OMe)$ which was then reduced in high yield (>90%) to the desired primary phosphine, (Scheme 4.3).

The known ferrocenyl primary phosphines $FcPH_2$ **16** and 1,1'-$Fc'(PH_2)_2$ **17** were prepared by $LiAlH_4/Me_3SiCl$ reduction of $FcP(O)(OEt)_2$ and 1,1'-$Fc'(P(O)(OEt)_2)_2$ respectively (the synthesis of these phosphonate esters is detailed in chapter 2.2). These primary phosphines were characterised by reference to published nmr data[8a,9b]. In addition, the novel primary phosphines, $FcCH_2CH_2PH_2$ **18**, 1,1'-$Fc'[CH_2PH_2]_2$ **19** and 1,2-$Fc'[CH_2PH_2]_2$ **20**, were also prepared.

[10] E. P. Kyba, S. -T. Liu and R. L. Harris, *Organometallics*, 1983, **2**, 1877.

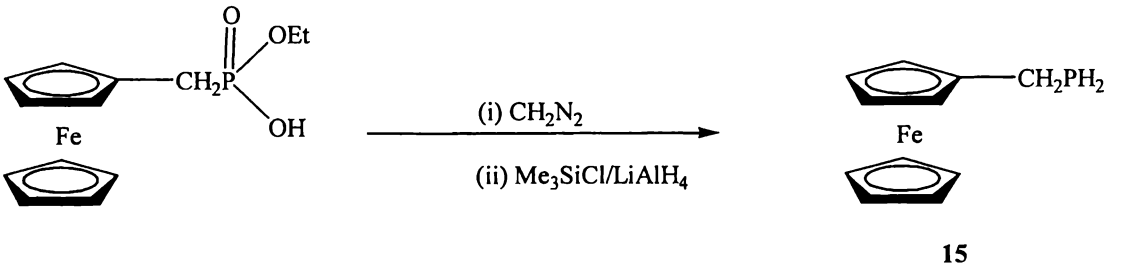

15

Scheme 4.3: Synthesis of $FcCH_2PH_2$ **15**, from $FcCH_2P(O)(OEt)OH$ **2**.

$FcCH_2CH_2PH_2$ **18**, was prepared by methylation of the acid $FcCH_2CH_2PO_3H_2$ **4**, using CH_2N_2, followed by reduction (Scheme 4.4). Initially isolated as an oil, **18** sublimed under vacuum at 40°C to give a dark orange crystalline solid.

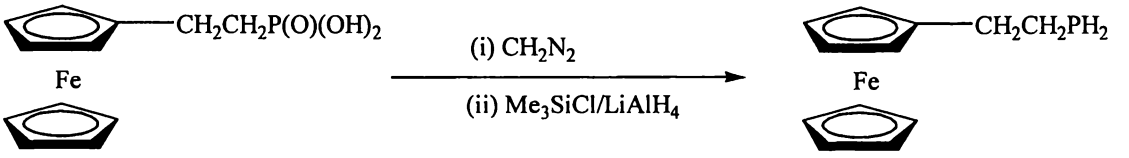

4 18

Scheme 4.4: Synthesis of $FcCH_2CH_2PH_2$ **18**.

This phosphine possessed a strong odour and was soluble in all organic solvents. Remarkably, it was also perfectly stable in air for periods of at least two years, with neither decomposition nor oxidation observed.

The bisphosphine 1,1'-Fc'$[CH_2PH_2]_2$ **19**, was prepared in high yield from the bis-diester 1,1'-Fc'$[CH_2P(O)(OEt)_2]_2$ by reduction with $LiAlH_4/Me_3SiCl$ (Scheme 4.5). The resulting bisphosphine, soluble in organic solvents, sublimed as a dark orange oil.

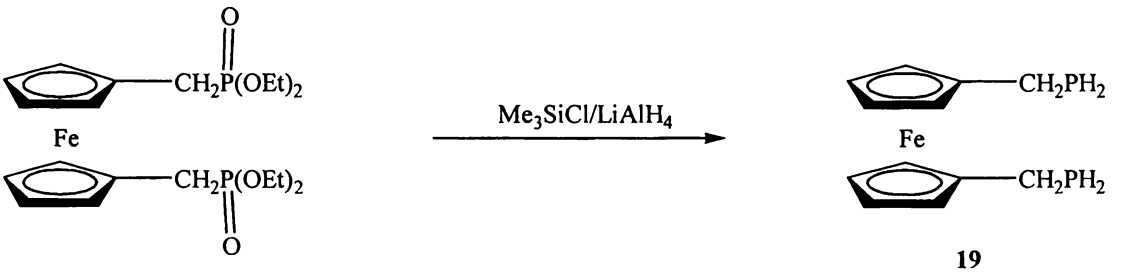

19

Scheme 4.5: Synthesis of 1,1'-Fc'$[CH_2PH_2]_2$ **19**.

The bis-phosphine **19** was stable in air for periods of up to two weeks as an oil, with only some darkening occurring. Longer exposure in air led to decomposition/oxidation, though residual phosphine was amenable to re-purification by silica gel flash column chromatography using petroleum spirits as the eluting solvent. The synthesis of the analogous phenyl phosphine 1,1'-Fc'$[CH_2PPh_2]_2$ has been recently published[11], and though no mention was made of the air stability or otherwise of this compound, all reported reactions were carried out under an inert atmosphere.

The synthesis of 1,2-Fc'$(CH_2PH_2)_2$ **20** required a slightly different approach. The known compound 1,2-Fc'$(CH_2OH)_2$ was prepared following the method of Goldberg and Bailey[12]. This was reacted with PCl_3 to give the bischloride 1,2,-Fc'$(CH_2Cl)_2$[13]. The reaction of the bischloride with triethyl phosphite gave the novel ferrocenyl-bis-(diethyl)phosphonate 1,2-Fc'$[CH_2P(O)(OEt)_2]_2$. This phosphonate ester, (purified using alumina flash column chromatography with an EtOAc to MeOH solvent gradient) was not characterised before being reduced using $LiAlH_4/Me_3SiCl$, to give a high yield of the desired bisphosphine **20** (Scheme 4.6).

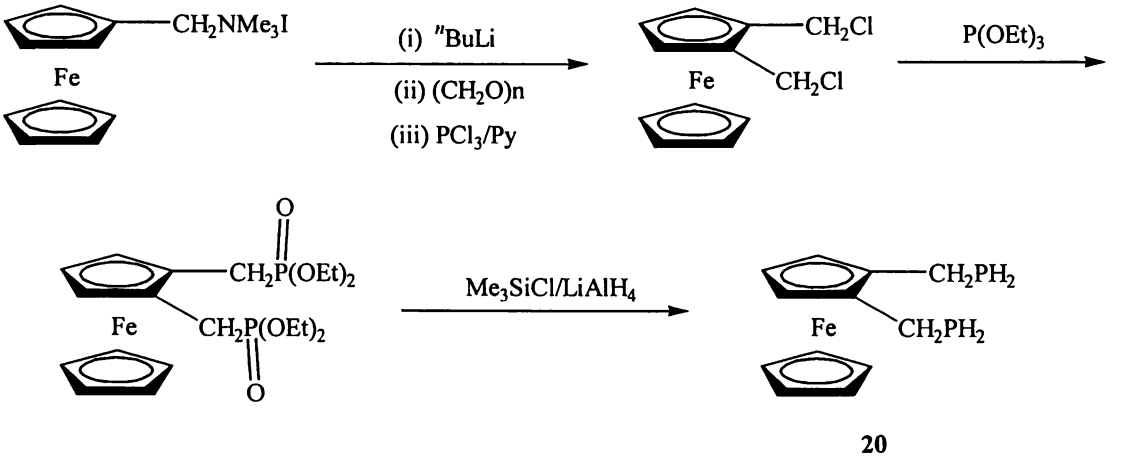

20

Scheme 4.6: The Synthesis of 1,2-Fc'$[CH_2PH_2]_2$ **20**.

---

[11] (a) Y. Yamamoto, T. Tanase, I. Mori and Y. Nakamura, *J. Chem. Soc. Dalton Trans.*, 1994, 3191. (b) J. -F. Ma and Y. Yamamoto, *J. Organomet. Chem.*, 1997, **545**, 577. (c) J. -F. Ma and Y. Yamamoto, *J. Organomet. Chem.*, 1998, **560**, 223. (d) J. -F. Ma and Y. Yamamoto, *J. Organomet. Chem.*, 1999, **574**, 148.

[12] S. I. Goldberg and W. D. Bailey, *J. Am. Chem. Soc.*, 1974, **96**, 6381.

[13] H. Plenio, D. Burth and R. Vogler, *Chem. Ber.*, 1997, **130**, 1405.

The bis-phosphine **20**, was isolated as a dark orange oil that was soluble in all organic solvents, though sparingly in methanol. In addition, the bis-phosphine **20** possessed a strong odour and was found to be stable in air for periods of at least two months.

4.2.1: NMR Analysis of Primary Ferrocenyl Phosphines

Primary phosphines give distinctive ^{31}P nmr spectra. The reduced phosphorus results in a high field signal, typically in the range -100 to -160ppm. Furthermore the ^{31}P spectra consist of a triplet with $^{1}J_{P\text{-}H}$ coupling constants of 190 to 195Hz. A typical $^{31}P\text{-}\{^{1}H\}$ spectrum, that of $FcCH_2CH_2PH_2$ **18**, is given in Figure 4.5. Inset is the non-decoupled ^{31}P spectrum of the same compound, illustrating the characteristic 1:2:1 triplet due to P-H coupling of 195Hz.

The ^{13}C and ^{1}H spectra of the novel ferrocenyl primary phosphines were routine and assigned by inspection. The ^{13}C and ^{1}H nmr spectra of $FcCH_2PH_2$, $FcPH_2$ and 1,1'-$Fc'[PH_2]_2$ were in agreement with published data.

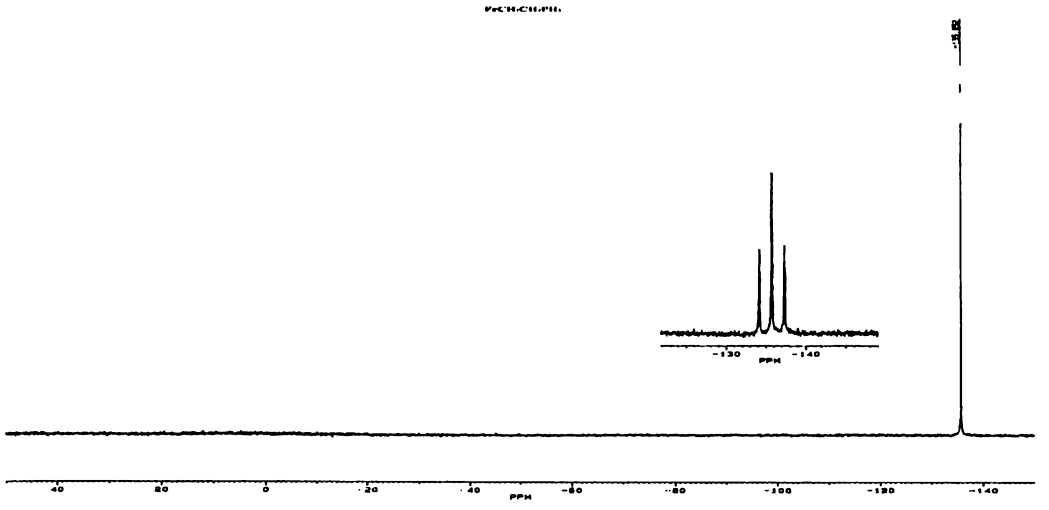

Figure 4.5: The $^{31}P\text{-}\{^{1}H\}$ NMR Spectrum of $FcCH_2CH_2PH_2$ **18**. Inset: $^{31}P\text{-}^{1}H$ Coupled Spectrum of **18**.

4.2.2: ESMS of Primary Ferrocenyl Phosphines

The positive ion ES mass spectra of these compounds are dominated by peaks due to the respective $[M]^+$ ion, though peaks due to $[M+H^+]^+$ may also be observed. To avoid confusion, silver ions (Ag^+) were added in the form of aqueous $AgNO_3$. The resulting spectra collapse to a single pair of peaks due to the $[M+Ag^+]^+$ adduct (samples left for any length of time also contained a significant peak due to M^+, a result of oxidation by silver). Such adducts have a distinctive isotope pattern due to silver, which has two naturally occurring isotopes, ^{107}Ag (51.82%) and ^{109}Ag (48.18%). The ES mass spectrum of 1,2-Fc'$[CH_2PH_2]_2$ in the presence of excess silver ions is given in Figure 4.6.

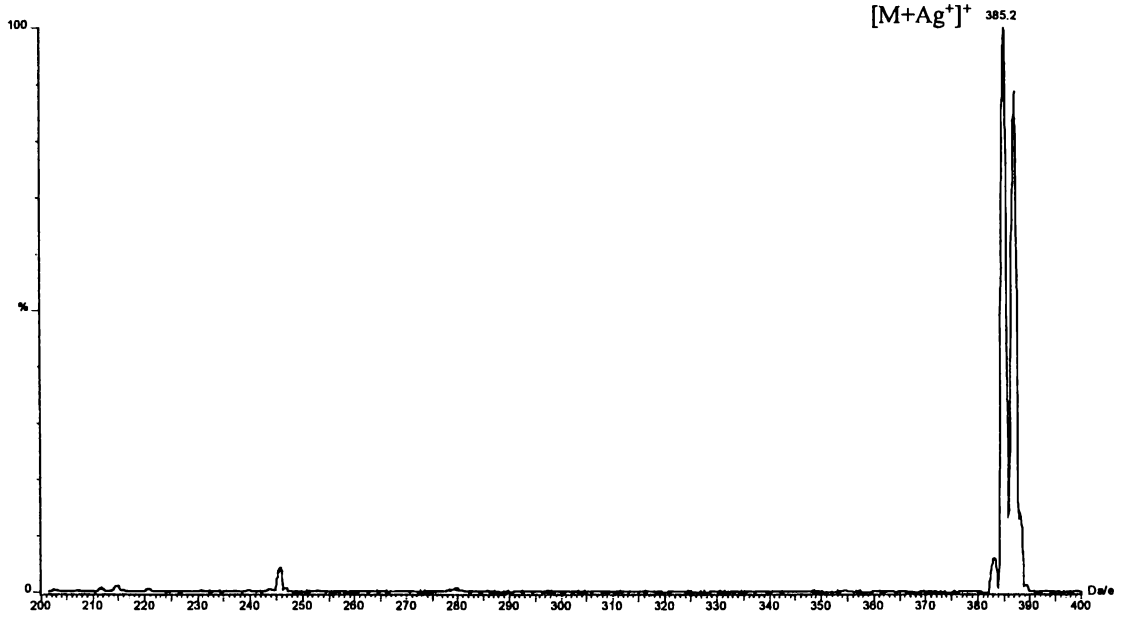

Figure 4.6: The Positive Ion ES Mass Spectrum of 1,2-Fc'$[CH_2PH_2]_2$ in Methanol at a Cone Voltage of 20V with Silver Ions Added.

4.2.3: Infrared Spectroscopy of Primary Ferrocenyl Phosphines

The infra-red spectra of **18**, **19** and **20** contained bands characteristic of ν(P-H)[14] at 2294cm^{-1}, 2290cm^{-1} and 2256cm^{-1} respectively. The remaining bands are due to the organic framework of the molecules.

4.2.4: GCMS of Primary Ferrocenyl Phosphines

Compounds **18**, **19** and **20** were further characterised using GCMS. The mass spectra of all three compounds contained strong peaks due to the respective $[M]^{+\bullet}$ ions, but the overall fragmentation pattern was dependent on the structure of each compound[b].

The fragmentation pattern of $FcCH_2CH_2PH_2$ **18** (Figure 4.7) is dominated by $[M]^{+\bullet}$ (m/z 246) and ions due to Fe^+ (*m/z* 56) and $[FeCp]^+$ (*m/z* 121).

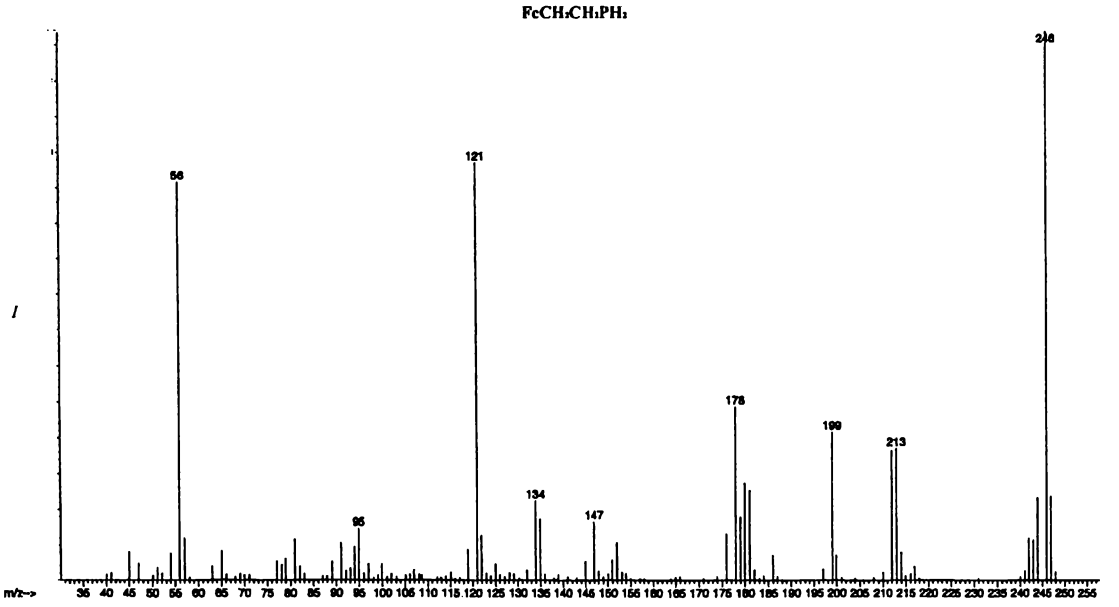

Figure 4.7: The GC Mass Spectrum of $FcCH_2CH_2PH_2$ **18**.

[14] E. Lee and C. K. Wu, *Trans. Faraday Soc.*, 1939, **35**, 1366.

[b] For gas chromatograms see Appendix B.

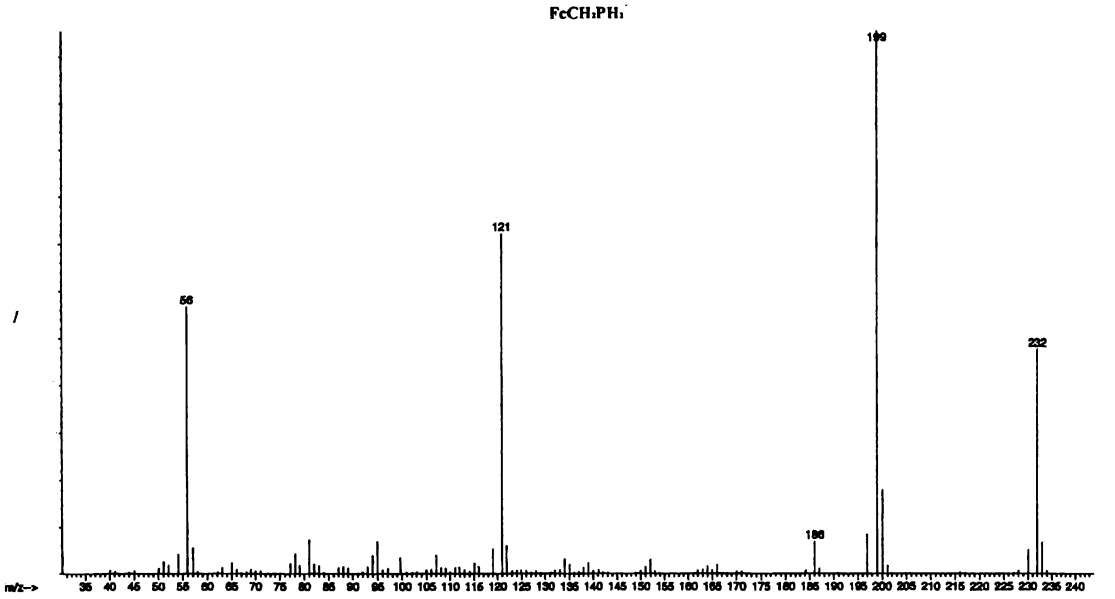

Figure 4.8: The GC Mass Spectrum of $FcCH_2PH_2$ **15**.

Also present at lower intensity are ions at *m/z* 213 and *m/z* 199, formed by loss of PH_2 and CH_2PH_2 respectively from the ethylphosphine side chain. The peak at *m/z* 178 remains unassigned. The fragmentation pattern of **18** is similar to that observed for $FcCH_2PH_2$ **15** (Figure 4.8). The spectrum of **15** is dominated by the *m/z* 199 ion formed by loss of $-PH_2$ from the methylphosphine chain. The *m/z* 199 ion, an α-carbocation $FcCH_2^+$, is stabilised by the ferrocenyl group[15].

The GC mass spectra of the bis-substituted phosphines 1,1'-Fc'$[CH_2PH_2]_2$ **19** and 1,2-Fc'$[CH_2PH_2]_2$ **20** provided an interesting comparison of structural influences on mass spectra. Against expectation, the spectra of **19** and **20** contained more similarities than differences, as shown in Figure 4.9.

In both spectra the molecular ion $[M]^{+\bullet}$ (*m/z* 278), is strong, as are peaks due to Fe^+ (*m/z* 56) and $[M\text{-}PH_2]^+$ (*m/z* 245). However the base peak in both spectra occurs at *m/z* 200. Taking into account relative intensities, it seemed likely that a similar fragmentation pathway afforded the ion at *m/z* 200 for both compounds. A proposed pathway based on the loss of a $CpCH_2$ radical from $M^{+\bullet}$ does give rise to an ion of *m/z* 200 for **19** (Scheme 4.7). However this pathway cannot produce the same fragment from **20**.

[15] E. A. Hill and R. Wiesner, *J. Am. Chem. Soc.*, 1969, **91**, 509.

(a)

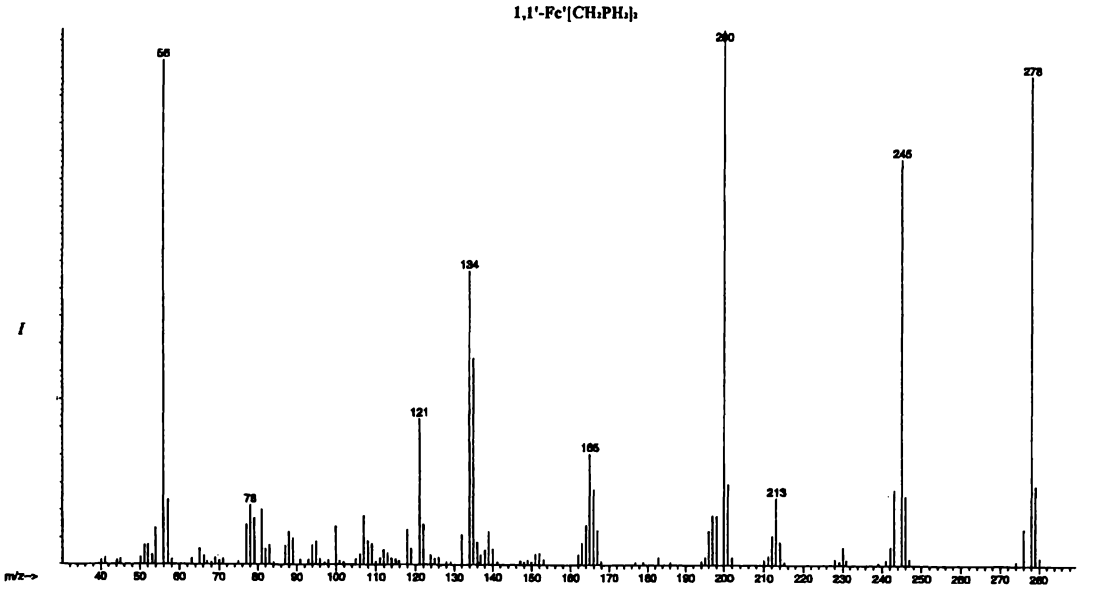

(b)

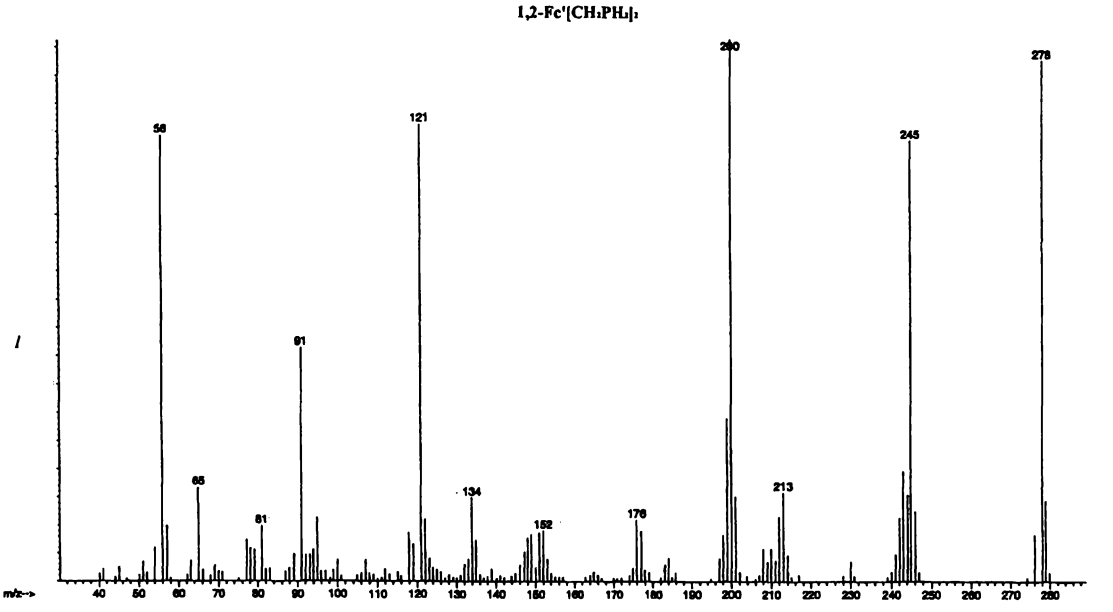

Figure 4.9: The GC Mass Spectra for (a): 1,1'-Fc'$[CH_2PH_2]_2$ **19** and (b): 1,2-Fc'$[CH_2PH_2]_2$ **20**.

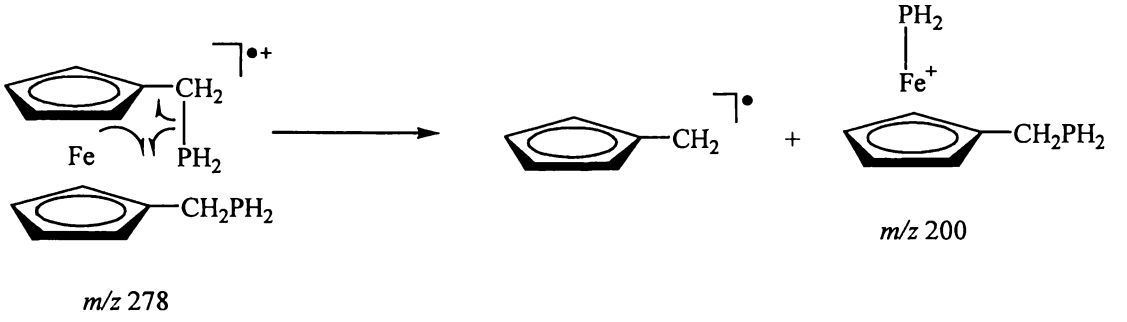

Scheme 4.7: Proposed Pathway for $CpCH_2$ Loss from 1,1'-Fc'$[CH_2PH_2]_2$ **19**.

A more complex pathway must be invoked for 1,2-Fc'$[CH_2PH_2]_2$ **20**. The *m/z* 200 peak in the spectrum of **20** could be due to $CpFe(PH_2)(CH{=}PH_2)]^+$. The formation of this fragment ion would require the elimination of a C_6H_6 radical and the attachment of PH_2 and CH_2PH_2 (via α,β cleavages) to the iron atom (Scheme 4.8).

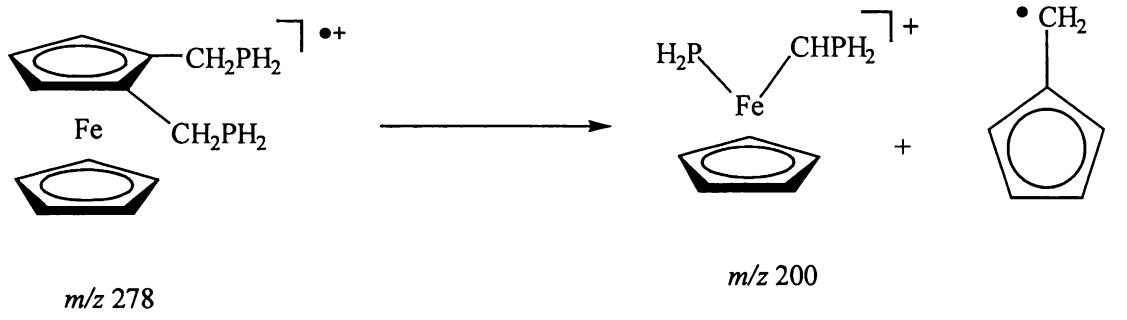

Scheme 4.8: Proposed Primary Fragmentation for 1,2-Fc'$[CH_2PH_2]_2$ **20**.

The peak at *m/z* 91 in the spectrum of 1,2-Fc'$[CH_2PH_2]_2$ (Figure 4.9(b)) is attributed to a $[C_6H_6]^+$ ion. The fragmentation pathway outlined in Scheme 4.8 would produce such an ion if the final positions of the radical electron and the ionic charge were reversed.

The relative intensities of the *m/z* 121 and *m/z* 134 ions in the spectra of **19** and **20** can be explained with reference to the structural differences between these compounds. The peak at *m/z* 121 is assigned to the $[FeCp]^+$ ion. For this ion to form there must be a non-substituted Cp ring in the molecule. Compound **19** (1,1'-Fc'$[CH_2PH_2]_2$) does not have a non-substituted Cp ring and therefore is unable to form the *m/z* 121 ion easily.

The peak at *m/z* 134 is assigned to the $[FeC_5H_4CH_2]^+$ ion. For this ion to form there must be a singly substituted Cp ring in the molecule. Compound **20** (1,2-Fc'$[CH_2PH_2]_2$) does not contain any singly substituted Cp rings, therefore there is no simple mechanism by which the $[FeC_5H_4CH_2]^+$ ion can form.

The peak at *m/z* 65, in the spectrum of **20** was assigned as $[Cp]^+$. For this ion to form, a non-substituted Cp ring must be present in the molecule, thus a similar peak was unlikely to be observed in the spectrum of **19**.

The proposed primary fragmentation pathway of 1,1'-Fc'$[CH_2PH_2]_2$ **19** (Scheme 4.7), is analogous to that previously proposed as the major fragmentation pathway for 1,1'-Fc'$[CH_2OH]_2$[16] (Scheme 4.9). Interestingly the expelled *m/z* 78 fragment, assigned as the benzene ion $C_6H_6^+$, carries the major portion of the ion current in the spectrum of 1,1'-Fc'$[CH_2OH]_2$. This is in contrast to the proposed fragmentation pathway for **19** (Scheme 4.7), where the iron containing moiety is the ionic fragment.

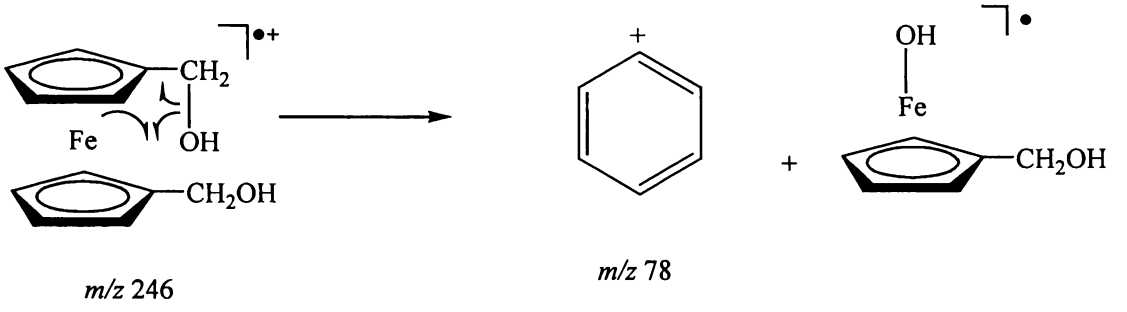

Scheme 4.9: Proposed Primary Fragmentation Pathway for 1,1'-Fc'$[CH_2OH]_2$.

Out of interest, the GC mass spectrum of 1,2-Fc'$[CH_2OH]_2$ was obtained (Figure 4.10 (a)) and compared to that of 1,1'-Fc'$[CH_2OH]_2$ (Figure 4.10 (b)) and 1,2-Fc'$[CH_2PH_2]_2$ **20** (Figure 4.9(b)).

The base peak in the spectrum of 1,2-Fc'$[CH_2OH]_2$ occurs at *m/z* 91, corresponding to a $[M-155]^+$ fragment ion. The most likely source of the *m/z* 155 fragment is $CpFe(OH)_2$, indicating simultaneous β,β fragmentation processes are occurring (Scheme 4.10).

[16] H. Budzikiewicz, C. Djerassi and D. H. Williams, Mass Spectrometry of Organic Compounds, Holden-Day 1967, chap. 27, p 658.

(a)

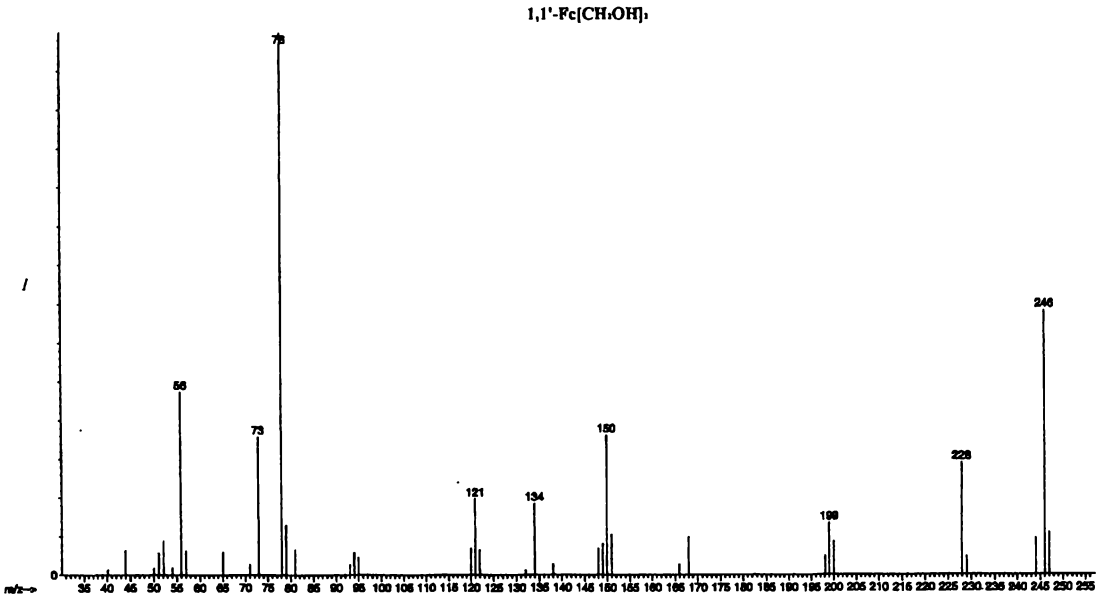

(b)

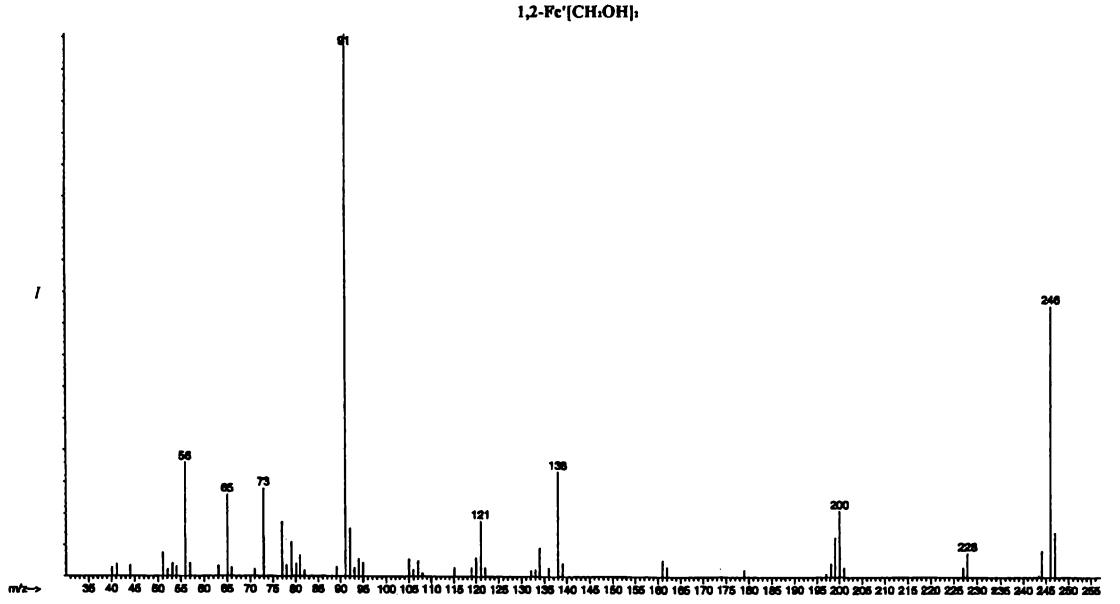

Figure 4.10: The GC Mass Spectra of (a): 1,2-Fc'$[CH_2OH]_2$ and (b): 1,1'-Fc'$[CH_2OH]_2$.

This is similar to the pathway invoked for the fragmentation of 1,2-Fc'$[CH_2PH_2]_2$ **20** (Scheme 4.8), though as in the case of the 1,1'-substituted

compounds, the species carrying the major portion of the ion current differs between the analogous 1,2-diol and 1,2-bis-phosphine.

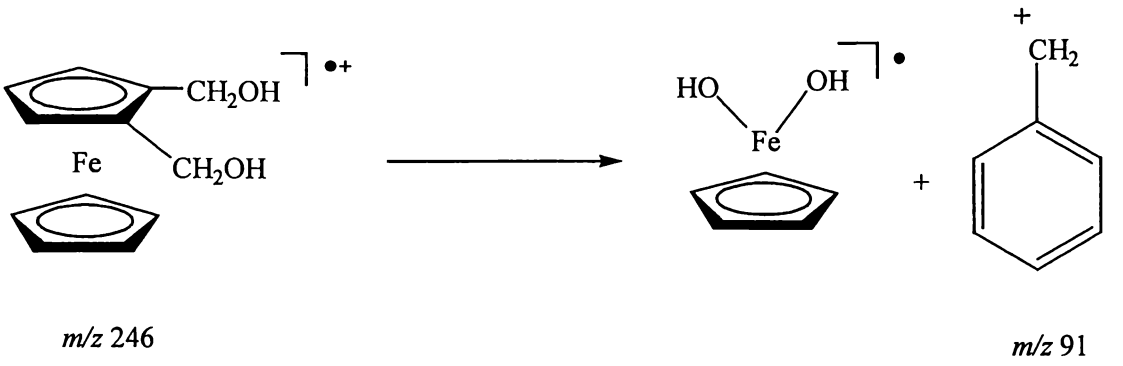

m/z 246 *m/z* 91

Scheme 4.10: Proposed Primary Fragmentation Pathway for 1,2-Fc'[CH_2OH]$_2$.

A detailed analysis of the fragmentation pathways of bis-substituted ferrocenes is beyond the scope of this thesis. Interestingly all of the bis-substituted ferrocenes studied appear to have eliminated a C_6H_6 fragment during the major fragmentation process. Observed differences between analogous diol and bis-phosphine MS spectra involve the location of charge rather than gross mechanistic disparities.

4.2.5: Air Stability of Ferrocenyl Primary Phosphines

The ferrocenyl primary phosphine $FcCH_2PH_2$ was found to be immune to oxidation by oxygen in air in both the solid and solution states. It was of interest therefore to determine the reactivity of the analogous phosphines **16-20** toward air. To this end, samples (~10mg of solid or oil) of the ferrocenyl primary phosphines were left exposed to air and their composition monitored by ^{31}P nmr spectroscopy at regular intervals.

Of the phosphines prepared in this chapter, 1,1'-Fc'[PH_2]$_2$ **17** was found to be most rapidly oxidised in air. A sample left for three days in air contained no trace of the original phosphine. ^{31}P nmr revealed the sample contained a mixture of the primary phosphine oxide -$P(O)H_2$, and two compounds containing a single P-H bond (characteristic of phosphinic acid -P(O)(OH)H groups). Integrals of the peaks were not obtained as the sample did not dissolve without residue in methanol. In addition,

exposure to air of solutions of **17** in organic solvents resulted in an immediate yellow precipitate, presumably of the primary phosphine oxide.

While not as reactive as **17**, the primary phosphine $FcPH_2$ **16** was also oxidised by air over a period of several days. The sample, after five days exposure to air, proved to be a mixture of the primary phosphine oxide and phosphinic acid with very little residual phosphine present.

1,1'-Fc'$[CH_2PH_2]_2$ **19** was found to be considerably more stable in air than **16** or **17**. This phosphine proved to be stable in air for up to fourteen days without significant oxidation being observed. After fourteen days, oxidation occurred at a genteel pace, with ^{31}P nmr revealing the presence of phosphorus centres in oxidation states ranging from primary phosphine to phosphinic acid(s). The ^{31}P nmr spectrum after forty-two days exposure to air is given in Figure 4.11.

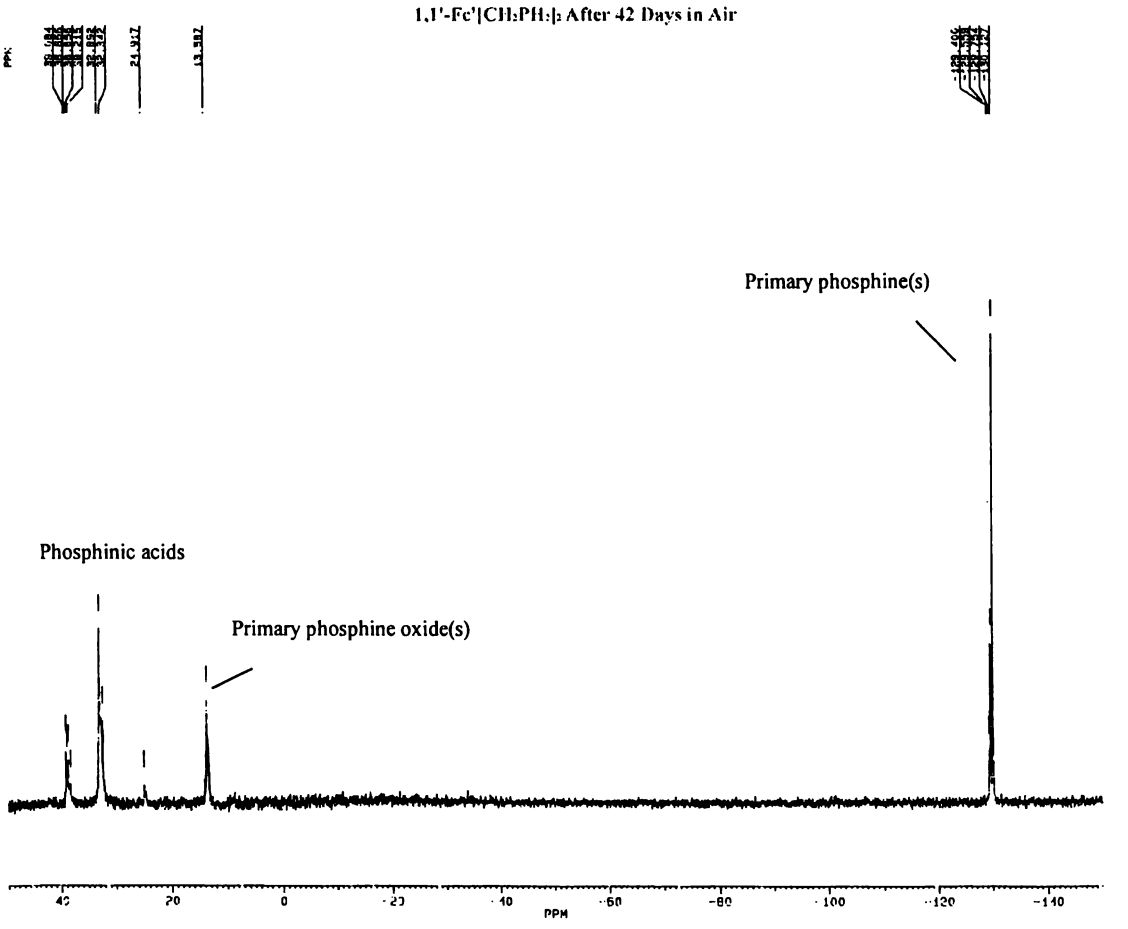

Figure 4.11: The ^{31}P-{^1H} NMR Spectrum of 1,1'-Fc'$[CH_2PH_2]_2$ **19** After Forty Two Days Exposed to Air.

This reveals the presence of a number of compounds, some of which must contain two phosphorus atoms in different oxidation states, one being the fully reduced primary phosphine and the other an oxidised derivative.

Remarkably, the two remaining ferrocenyl primary phosphines were found to be stable in air. A sample of $FcCH_2CH_2PH_2$ **18**, exposed to air for two years was found to be pure by ^{31}P nmr and GCMS. Similarly a sample of 1,2-Fc'$[CH_2PH_2]_2$ **20** was essentially pure primary phosphine after two months exposure to air.

The results of these simple air stability experiments provide more questions than answers. As expected, the presence of a CH_2 spacer between the ferrocenyl group and the phosphine moiety increased resistance toward air oxidation when compared to those compounds where the PH_2 group was attached directly to the ferrocene group. The 1,1'-bis-substituted primary phosphines were more prone to air oxidation than the mono-substituted analogues.

Of most note was the stability of the primary phosphines $FcCH_2CH_2PH_2$ **18** and 1,2-Fc'$[CH_2PH_2]_2$ **20**. When $FcCH_2PH_2$ **15** was found to be air stable it was speculated that physical interaction of the phosphine group with the ferrocenyl iron atom might be the cause. Subsequent solution of the crystal structure showed no such interaction. If electronic effects were the cause of the air-stability of **15**, it was thought that they might manifest themselves for $-CH_2PH_2$ groups only, due to the known ability of the ferrocene group to interact electronically with the α-carbon. The oxidative stability in air of the ferrocenyl primary phosphines **16** and **17**, when compared to the stability of phosphines **15**, **19** and **20**, seemed to bear this out. However the indefinite stability of **18** does not fit this hypothesis. Thus the reasons for the stability of **15**, **18**, **19** and **20** toward air oxidation are unknown. Synthesis of analogous compounds with longer alkyl side chains or based on other metallocenes may provide some insight.

4.2.6: Molybdenum Carbonyl Derivatives of 1,1'-Fc'[CH_2PH_2]$_2$ 19, and 1,2-Fc'[CH_2PH_2]$_2$ 20

Molybdenum carbonyl complexes of the air stable phosphines **19** and **20**, were prepared in the hope of obtaining crystalline derivatives. Phosphines readily react with octahedral $L_2M(CO)_4$ (M = Cr, Mo, W, L_2 = norbornadiene, L = piperidine) complexes, to give compounds of the type $(RPH_2)_2M(CO)_4$[17] (Scheme 4.11).

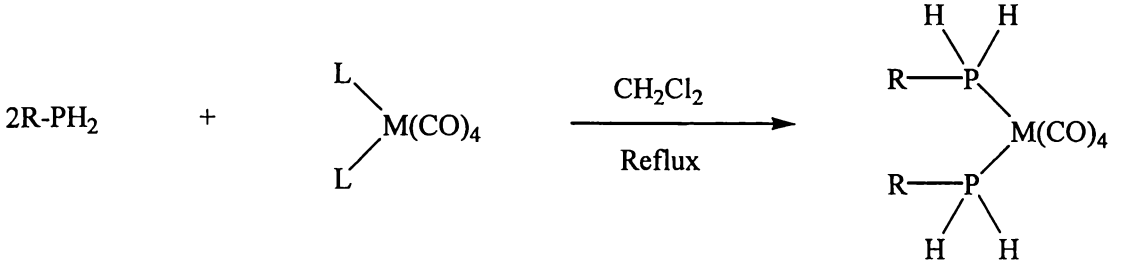

Scheme 4.11: Reaction of Primary Phosphines with $(L_2)M(CO)_4$.

Ferrocenyl phosphine derivatives of $Mo(CO)_5$[7] and $M(CO)_4$ (M = Cr, Mo and W)[7,18] have been previously reported. The derivatives of the type $P_2M(CO)_4$ adopt *cis*-geometry where M = Mo, and *trans*- geometry where M = Cr or W. The combination of bis-phosphine ligands such as dppf with mixtures of $M(CO)_4/M(CO)_5$ (M = Mo, Cr and/or W) resulted in the formation of oligomers of the type $(CO)_5M(\mu^2$-dppf$)M(CO)_4(\mu^2$-dppf$)M(CO)_5$[17].

The reaction of 1,2-Fc'[CH_2PH_2]$_2$ **20** with $(Pip)_2Mo(CO)_4$ (Pip = piperidine) in refluxing CH_2Cl_2 gave the expected molybdenum phosphino complex 1,2-Fc'[CH_2PH_2]$_2$Mo$(CO)_4$ **21** as the sole product (Scheme 4.12). The progress of the reaction was monitored by ^{31}P nmr. Complexation of the metal by the phosphine ligand resulted in an up-field shift of the phosphorus signal from ~-130ppm to ~-80ppm.

[17] G. Hasselkuss, S. Hietkamp and O. Stelzer, *Z. Anorg. Allg. Chem.*, 1986, **534**, 50.
[18] L. T. Phang, K. S. Gan, H. K. Lee and T. S. A. Hor, *J. Chem. Soc., Dalton Trans.*, 1993, 2697.

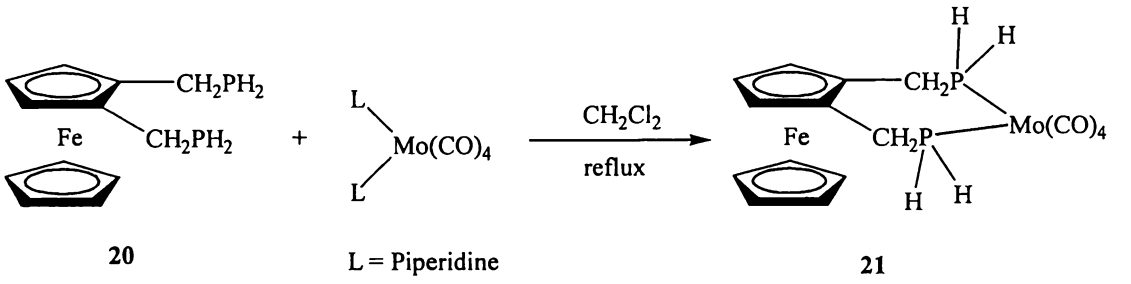

20 L = Piperidine **21**

Scheme 4.12: Synthesis of 1,2-Fc'$[CH_2PH_2]_2Mo(CO)_4$ **21**.

A yellow crystalline solid, **21** was fully characterised by nmr, ESMS, IR, and elemental analysis. Negative ion ESMS proved to be a versatile analytical technique in the characterisation of these types of compounds. The ES mass spectra of carbonyl complexes are typically obtained by the addition of NaOMe to the sample[19]. The methoxide ion (OMe^-) can bind to carbonyl complexes to give the $[M+OMe^-]^-$ ion, or the methoxide ion can remove acidic hydrogens to give the $[M-H^+]^-$ ion. Previous work had shown that OMe^- ionises primary phosphine carbonyl complexes under ESMS conditions by removal of a phosphine hydrogen[7]. Addition of NaOMe to a sample of **21** gave a very strong $[M-H^+]^-$ ion (*m/z* 487) as the base peak of the spectrum, (Figure 4.12).

Comparison of the observed and calculated isotope patterns is a useful technique to ensure the correct assignment of peaks observed in ESMS. The observed and calculated[20] isotope patterns for $[\mathbf{21}\text{-}H^+]^-$ are given in Figure 4.13.

[19] W. Henderson, J. Scott McIndoe, B. K. Nicholson and P. J. Dyson, *J. Chem. Soc., Dalton Trans.*, 1998, 519.

[20] L. J. Arnold, *J. Chem. Ed.*, 1992, **69**, 811.

Figure 4.12: The Negative Ion ES Mass Spectrum of 1,2-Fc'$[CH_2PH_2]_2Mo(CO)_4$ **21** at a Cone Voltage of 5V with NaOMe Added.

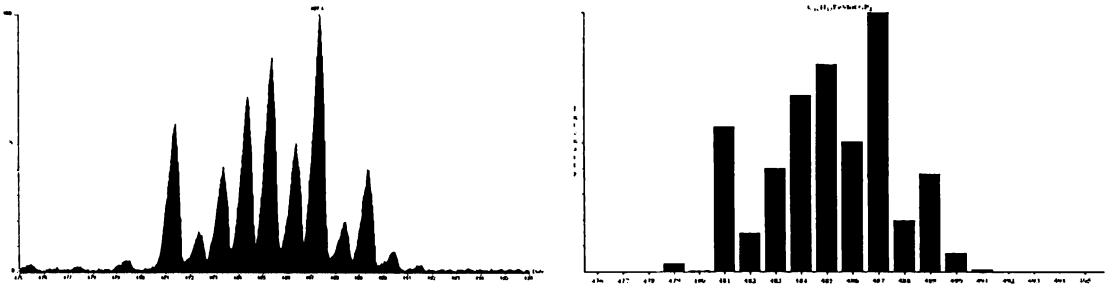

Figure 4.13 Observed (left) and Calculated (right) Isotope Patterns for [**21**-H^+]$^-$.

Crystals of **21** deemed suitable for single crystal X-ray structural determination were grown from CH_2Cl_2/petroleum spirits at -20°C. The crystal chosen for analysis proved to be weakly diffracting and the resulting data set was of poor quality. This, allied with ambiguities in the assignment of the space group, prevented an adequate structural solution from being obtained. Refinement to $R_1 = 0.21$ was achieved in the tetragonal space group I4(1)/a. This allowed the overall form of the structure to be observed (Figure 4.14) but was not of sufficient quality for a meaningful discussion of bond length and bond angle parameters to be entered into. The non-linearity of the CO ligands is testament to the poor refinement of the data. Figure 4.14 is a

representation of the structure with hydrogen atoms absent and non hydrogen atoms represented as spheres rather than as ellipsoids based on thermal parameters (Pluton graphics).

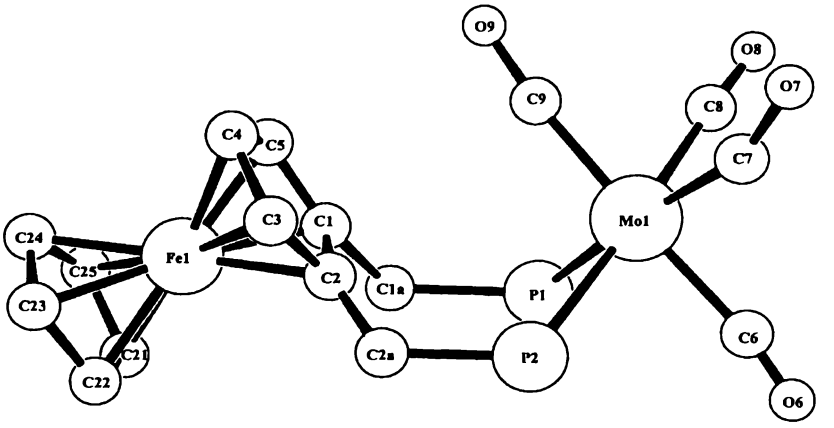

Figure 4.14: Pluton Drawing of the Structure of 1,2-Fc'$[CH_2PH_2]_2Mo(CO)_4$ **21**, from X-Ray Crystal Data.

The structure shows the expected chelating diphosphine-$Mo(CO)_4$ complex; the resulting seven-membered system has adopted a 'boat' configuration.

The reaction of 1,1'-Fc'$[CH_2PH_2]_2$ **19**, with $(Pip)_2Mo(CO)_4$ in refluxing CH_2Cl_2 gave rise to two compounds, (Scheme 4.13).

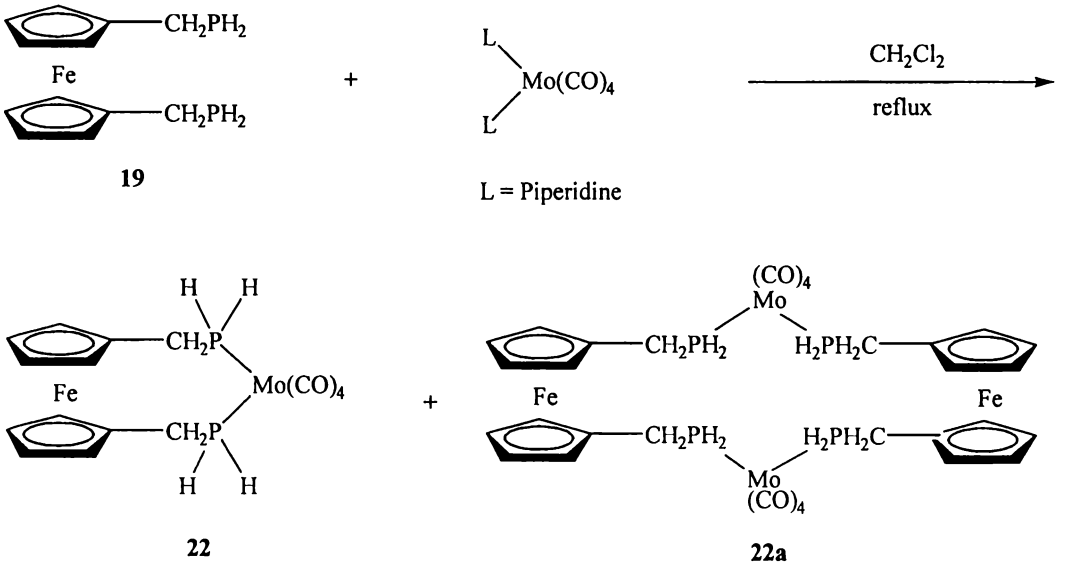

Scheme 4.13: Reaction of 1,1'-Fc'$[CH_2PH_2]_2$ with $(Pip)_2Mo(CO)_4$.

The major product was the expected chelate complex 1,1'-Fc'$[CH_2PH_2]_2Mo(CO)_4$ **22**. This compound, a yellow crystalline solid, was isolated using silica thin layer chromatography and fully characterised. The variable cone voltage ES mass spectra of **22** are given in Figure 4.15. In this figure, the sequential loss of four CO ligands is clearly shown

The minor product was isolated by thin layer chromatography and characterised using ES mass spectroscopy as [1,1'-Fc'$[CH_2PH_2]_2Mo(CO)_4]_2$ **22a** (Figure 4.16). The production of this cyclic complex was insensitive to the order of addition of the reactants, but could be minimised (though not eliminated) by conducting the reaction in dilute solution. The ES mass spectrum of the crude reaction liquor revealed no evidence of larger oligomers.

The calculated and observed isotope patterns for [**22**-H^+]$^-$ (*m/z* 487) and [**22a**-H^+]$^-$ (*m/z* 971) are shown in Figure 4.17.

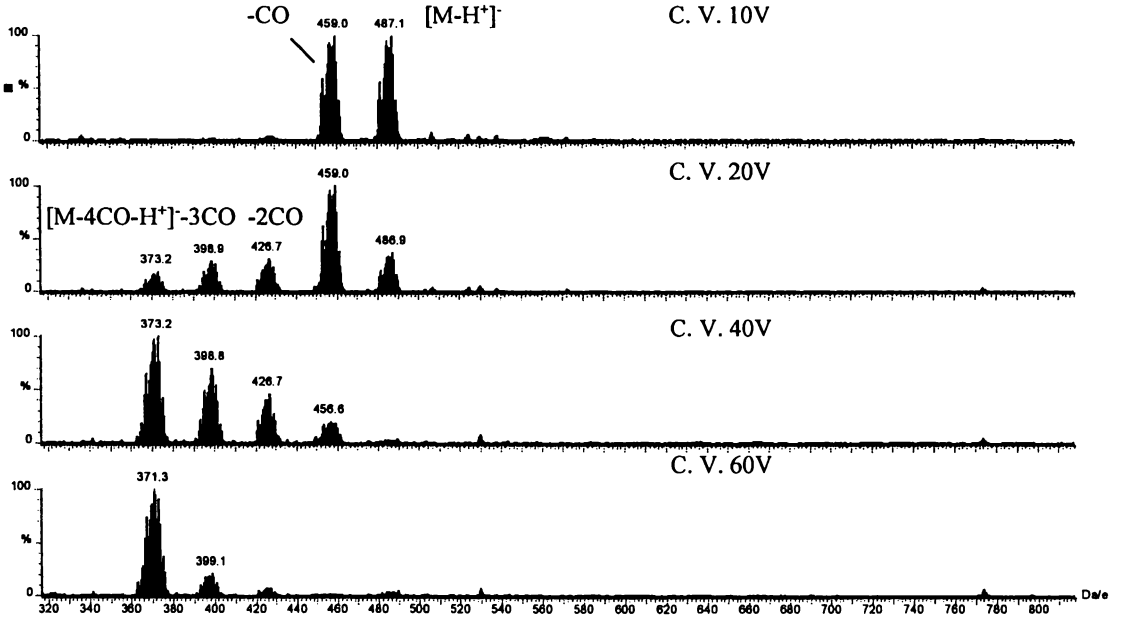

Figure 4.15: Variable Cone Voltage, Positive Ion ES Mass Spectra of **22** in Methanol with NaOMe Added.

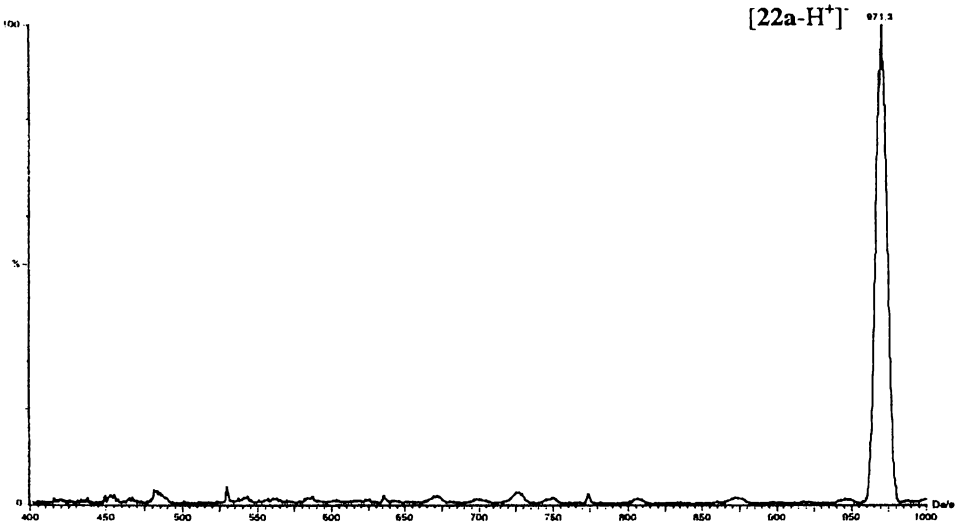

Figure 4.16: The Negative Ion ES Mass Spectrum of $[1,1'\text{-Fc}'[CH_2PH_2]_2Mo(CO)_4]_2$ **22a** with NaOMe Added at a Cone Voltage of 5V.

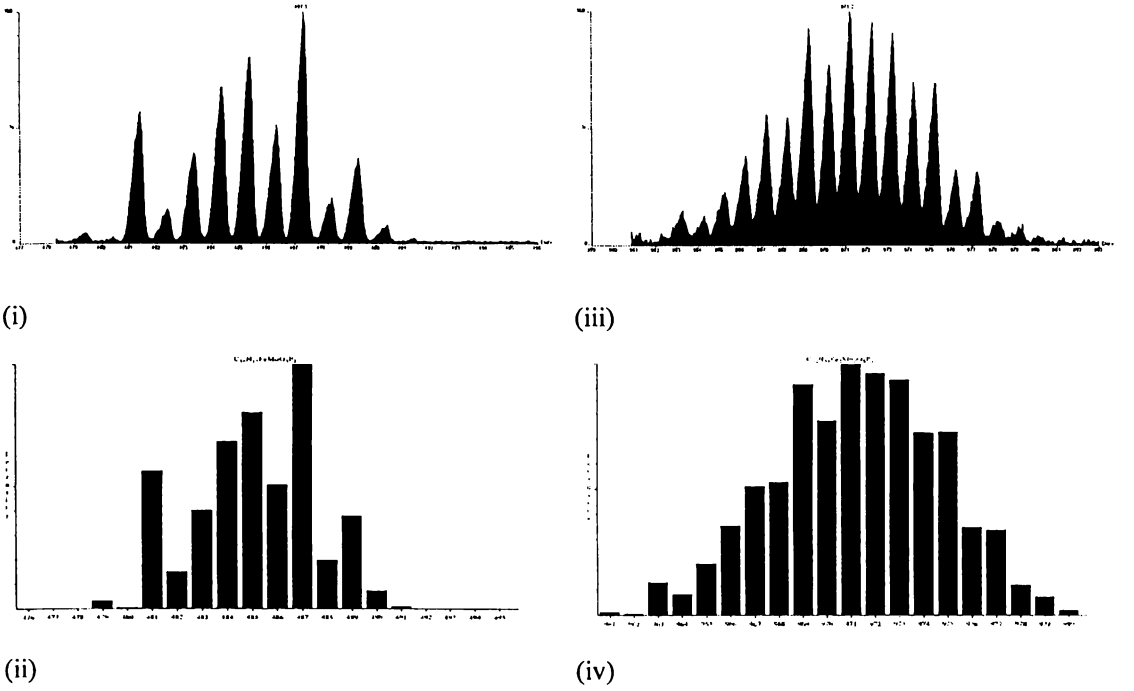

Figure 4.17: Observed and Calculated Isotope Patterns for $[\mathbf{22}\text{-}H^+]^-$ ((i) and (ii)) and $[\mathbf{22a}\text{-}H^+]^-$ ((iii) and (iv)).

Further molybdenum carbonyl derivatives of **19** and **20** were prepared from molybdenum hexacarbonyl, $Mo(CO)_6$. Molybdenum hexacarbonyl can be reacted with thf using UV light, to give the complex $(thf)Mo(CO)_5$[21]. The labile thf ligand is easily replaced by phosphine ligands. The reaction of 1,1'-Fc'$[CH_2PH_2]_2$ **19** with a large excess of $(thf)Mo(CO)_5$ gave the complex 1,1'-Fc'$[CH_2PH_2Mo(CO)_5]_2$ **23** as the sole product, Scheme 4.14.

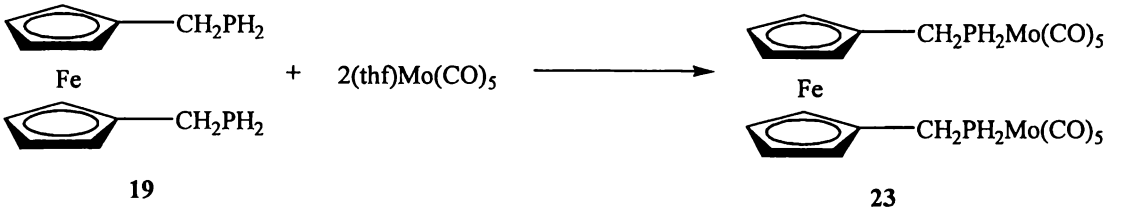

19 **23**

Scheme 4.14: Reaction of $(thf)Mo(CO)_6$ with the Primary Ferrocenyl Phosphine 1,1'-Fc'$[CH_2PH_2]_2$ **19**.

Again the progress of reaction was followed using ^{31}P nmr, with a shift from ~-130ppm to ~-60ppm being observed. This complex was easily purified by silica thin layer chromatography and was isolated as a yellow crystalline solid. Characterisation by positive ion ESMS, nmr, IR, and elemental analysis was routine. The variable cone voltage ES mass spectra of **23** (Figure 4.18) clearly shows the loss of ten CO ligands leaving a single peak at *m/z* 469 at a cone voltage of 130V.

[21] (a) E. Lindner and W. P. Meier, *J. Organomet. Chem.*, 1974, **67**, 277. (b) S. A. R. Knox, J. W. Koepke, M. A. Andrews and H. D. Kaesz, *J. Am. Chem. Soc.*, 1975, **97**, 3942.

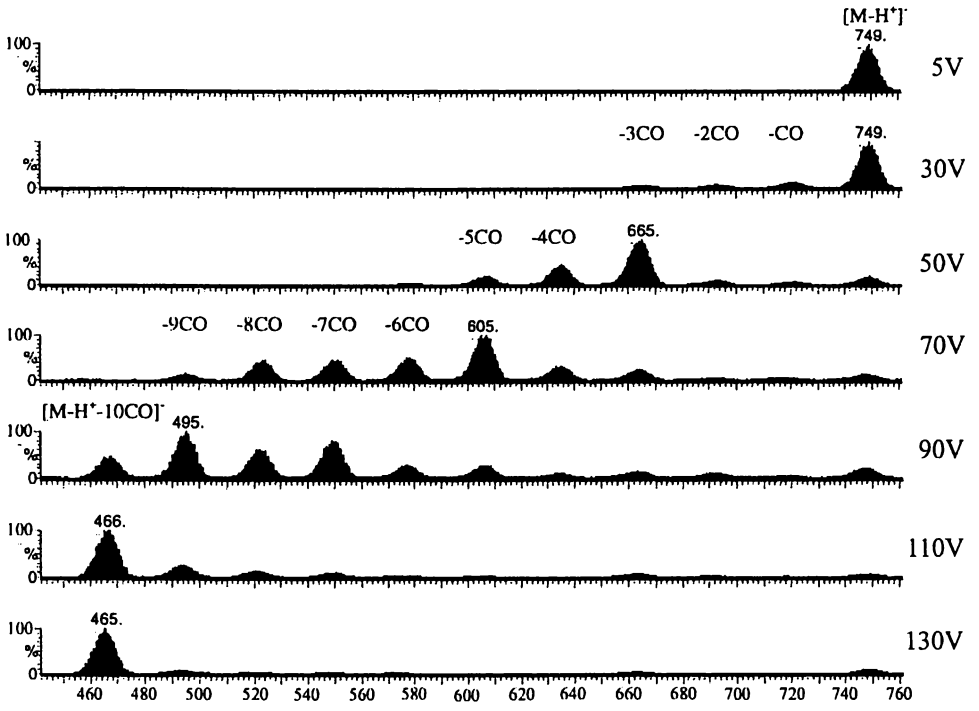

Figure 4.18: Variable Cone Voltage, Positive Ion ES Mass Spectra for 1,1'-Fc'$[CH_2PH_2Mo(CO)_5]_2$ **23**, Run in Methanol with NaOMe Added to Aid Ionisation.

The reaction of 1,2-Fc'$[CH_2PH_2]_2$ **20** with (thf)$Mo(CO)_5$ gave the analogous complex 1,2-Fc'$[CH_2PH_2Mo(CO)_5]_2$ **24** as the principal product, (Scheme 4.15). As with all of the molybdenum carbonyl derivatives, the complex **24** was a yellow crystalline solid stable in air for long periods at ambient temperatures.

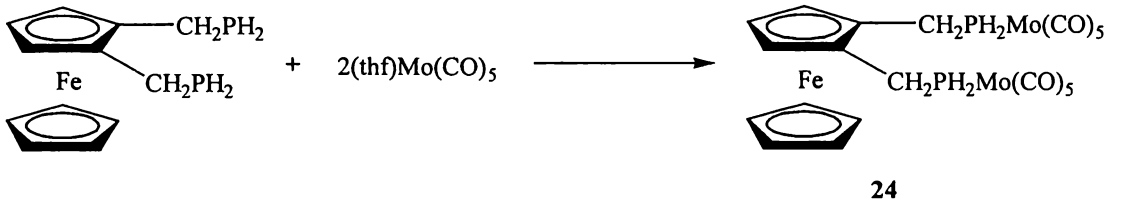

24

Scheme 4.15: Synthesis of 1,2-Fc'$[CH_2PH_2Mo(CO)_5]_2$ **24**.

The molybdenum carbonyl derivatives of the primary ferrocenyl phosphines **19** and **20** proved to be easily prepared and handled. This allowed full characterisation including elemental analyses to be achieved, something which was difficult for the parent primary phosphines. The molybdenum carbonyl derivatives are yellow crystalline powders that turn green upon long exposure to air (several months). The green appearance, characteristic of the ferrocinium ion, was not seen when the parent phosphines were exposed to air. The chelate complexes **21** and **22** decomposed upon heating whereas the bridging complexes **23** and **24** had clearly defined melting points. The molybdenum carbonyl complexes were amenable to purification using thin layer chromatography though the recovery from the plates was poor.

4.2.7: Synthesis and Characterisation of Ferrocenylethyl Arsine

Primary arsines R-AsH_2, are the arsenic analogues of primary phosphines. Like phosphines, arsines are reactive compounds due to the weakness of the As-H bond and are prone to oxidation in air.

There are several synthetic routes to primary arsines, though they are most commonly prepared by the reduction of arsonic acids using zinc and hydrochloric acid[22] (Scheme 4.16).

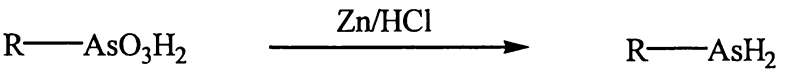

Scheme 4.16: Synthesis of Arsines from Arsonic Acids.

A number of ferrocenyl arsines Fc(AsR_2) (R = aryl, alkyl) have been prepared by the reaction As-Cl bonds with lithiated species. This reaction is exemplified in the synthesis of 1,1'-bis(dimethylarsino)ferrocene and 1,1'-bis(diphenylarsino)ferrocene[23] (arsenic analogues of DPPF and DMPF), as well as the [1]arsenaferrocenophane, (1,1'-ferrocenediyl)phenyl arsine[24], (Scheme 4.17).

---

[22] I. Millar, H. Heaney, D. Heinekey and W. Fernelius, *Inorg. Synth.*, 1962, **6**, 113.
[23] (a) A. Davison and J. J. Bishop, *Inorg. Chem.*, 1971, **10**, 826. (b) A. Davison and J. J. Bishop, *Inorg. Chem.*, 1971, **10**, 832.
[24] D. Seyferth and H. P. Withers, *J. Organomet. Chem.*, 1980, **185**, C1-C5.

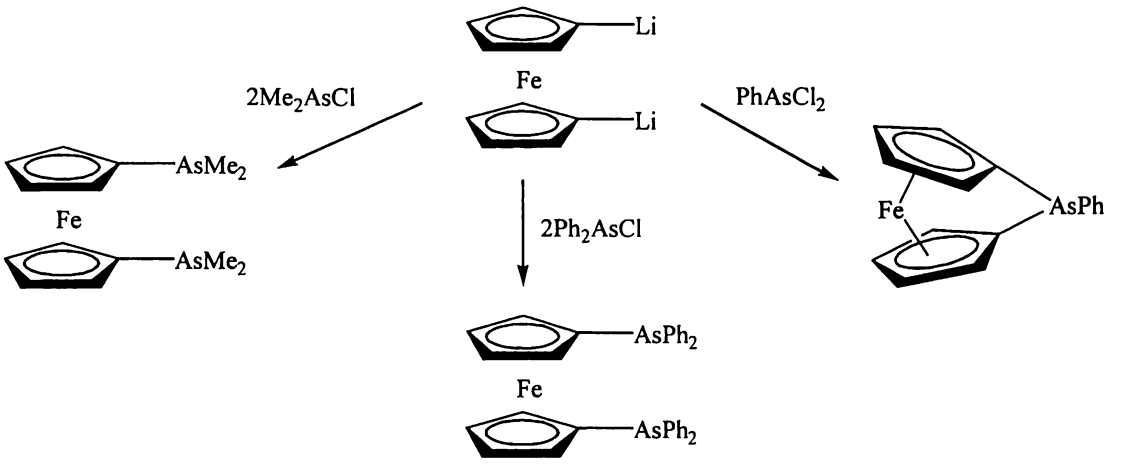

Scheme 4.17: Synthesis of Ferrocenyl Arsines from Di-lithio Ferrocene.

The chloroarsine, $FcAsCl_2$, was similarly prepared by the reaction of lithio ferrocene with $AsCl_3$[8b]. To the best of this author's knowledge, no examples of primary ferrocenyl arsines exist in the published literature.

Ferrocenylethyl arsonic acid $FcCH_2CH_2AsO_3H_2$, the synthesis of which was detailed in chapter two, was reduced using zinc and hydrochloric acid to give ferrocenylethyl arsine $FcCH_2CH_2AsH_2$ **25** in good yield (Scheme 4.18).

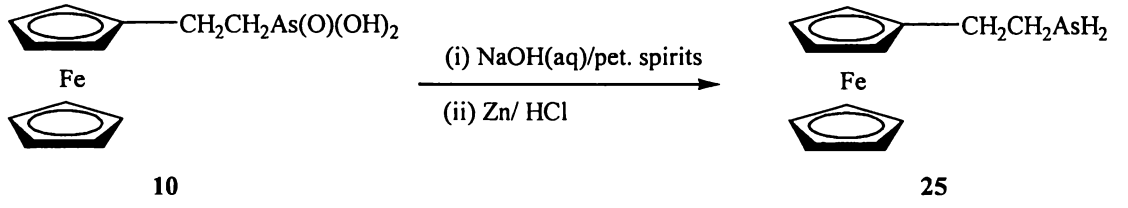

10 **25**

Scheme 4.18: Synthesis of $FcCH_2CH_2AsH_2$ **25**.

The ferrocenylarsonic acid **10** was dissolved in the aqueous layer of a two phase petroleum spirits/sodium hydroxide system that also contained powdered zinc. Concentrated hydrochloric acid was slowly added and the primary arsine migrated into the organic phase as it formed. Separation and removal of solvent gave the primary arsine as a yellow oil that crystallised upon standing. The arsine, which had an unpleasant odour, was further purified by sublimation onto a cold finger under

vacuum (~1mmHg) at 30°C. Soluble in organic solvents except alcohols and DMSO, the arsine was characterised by nmr (^{1}H and ^{13}C), GCMS and elemental analysis. The GC mass spectrum of **25** is given in Figure 4.19.

The observed fragmentation pattern was similar to that of $FcCH_2CH_2PH_2$ **18** (Figure 4.7), dominated by the molecular ion $M^{+\bullet}$ (*m/z* 290), and peaks due to $[FeCp]^+$ (*m/z* 121) and $[Fe]^+$ (*m/z* 56). The peaks at *m/z* 212 and 213 are due to loss of $AsH_2^\bullet$ and $AsH_3^\bullet$ respectively from the molecular ion.

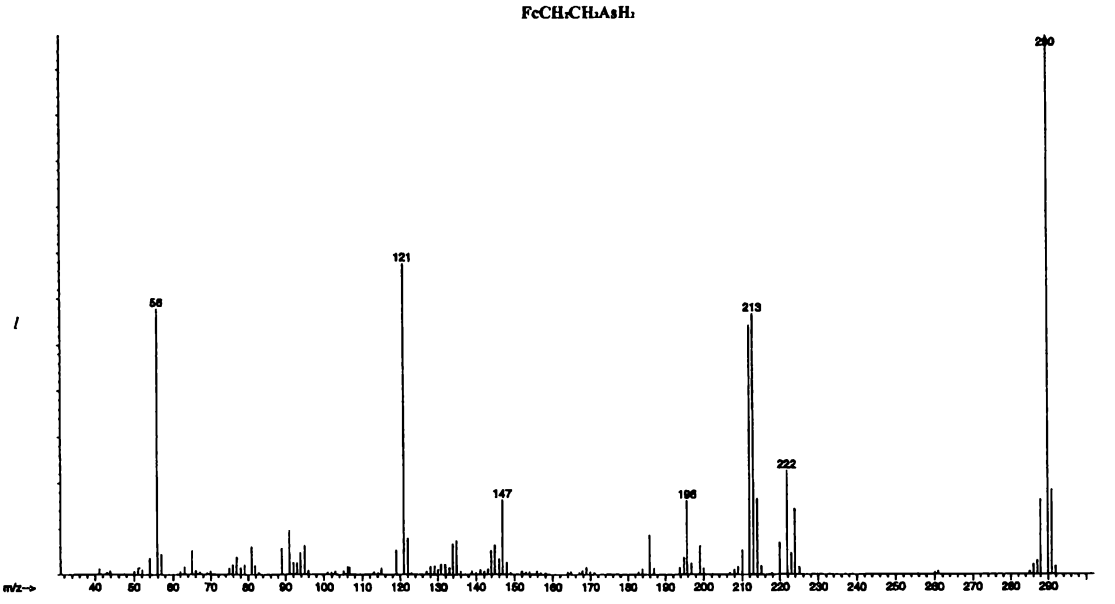

Figure 4.19: The GC Mass Spectrum of $FcCH_2CH_2AsH_2$ **25**.

The infra-red spectrum of **25** was dominated by a strong peak at 2072cm^{-1} which was assigned as νAs-H. This is similar to the value reported for νAs-H in gaseous AsH_3 (2122cm^{-1})[14].

4.2.8: X-Ray Crystal Structure Determination for Compounds $FcCH_2CH_2AsH_2$ 25 and $FcCH_2CH_2PH_2$ 18

Structures of primary arsines are very rare in the published literature. A search of the Cambridge Crystallographic Data Centre archives[25] revealed that the structure of the chromium carbonyl complex $PhAsH_2Cr(CO)_5$[26] is known, as is that of the silyl arsine (^{t}butyl)(2,4,6-^{i}PrC_6H_2)Si$(AsH_2)_2$[27]. More recently the primary pnictane series $ArEH_2$ (Ar = -C_6H_3-2,6-Trip, (Trip = 2,4,6-tri-isopropylphenyl), E = N, P, As and Sb) have been structurally characterised[28] (Figure 4.20). As far as this author is aware, the arsine member of this series represents the only reported structure of a free primary arsine.

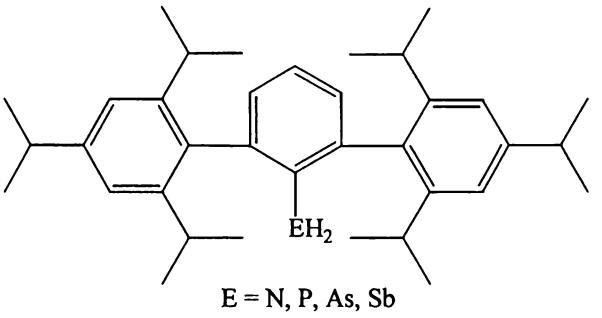

Figure 4.20: Series of Primary Pnictanes that have been Structurally Characterised.

From a sample of sublimed $FcCH_2CH_2AsH_2$ **25**, a crystal suitable for single crystal X-ray structure determination was chosen. Crystals of $FcCH_2CH_2PH_2$ **18** suitable for single crystal X-ray structure determination were also obtained by sublimation.

The arsine **25** crystallised in the P2(1)/c space group. Preliminary investigation of the structure of $FcCH_2CH_2PH_2$ **18** revealed that these two compounds were iso-structural, thus the full structural determination of **18** was not undertaken. The cell parameters of the arsine **25** and phosphine **18** are given in Table 4.2.

---

[25] CCDC, Conquest Version 1.1, 15/01/01.
[26] J. v. Seyerl, A. Frank and G. Huttner, *Cryst. Struct. Commun.*, 1981, **10**, 97.
[27] M. Driess and H. Pritzkow, *Chem. Ber.*, 1994, **127**, 477.
[28] B. Twamley, C. –S. Hwang, N. J. Hardman and P. P. Power, *J. Organomet. Chem.*, 2000, **609**, 152.

Table 4.2: Cell Parameters for $FcCH_2CH_2AsH_2$ **25** and $FcCH_2CH_2PH_2$ **18**.

Compound	$FcCH_2CH_2AsH_2$ **25**	$FcCH_2CH_2PH_2$ **18**
a(Å)	14.3996(1)	14.247(4)
b(Å)	7.5871(1)	7.550(2)
c(Å)	10.4835(1)	10.382(3)
α(°)	90.00	90.00
β(°)	97.496(1)	96.870(4)
γ(°)	90.00	90.00

Selected bond lengths and angles for $FcCH_2CH_2AsH_2$ **25** are given in Table 4.3. All bond lengths and angles are within usual ranges. The structure diagram of $FcCH_2CH_2AsH_2$ **25** is shown in Figure 4.21.

Table 4.3: Selected bond lengths (Å) and Angles (°) for $FcCH_2CH_2AsH_2$ **25**.

Cp Fe-C av.	2.039(4)	C(11)-C1)	1.518(7)
range	2.032(4)-2.045(4)	C(1)-C(2)	1.517(9)
Cp C-C av.	1.404(7)	C(2)-As(1)	1.966(6)
range	1.379(7)-1.428(6)		
C(11)-C(15) range	107.2(4)-108.8(4)	C(12)-C(11)-C(1)	131.4(4)
C(21)-C(25) range	107.3(4)-108.7(4)	C(11)-C(1)-C(2)	112.2(5)
C(15)-C(11)-C(1)	121.2(4)	C(1)-C(2)-As(1)	111.9(4)

The Cp rings adopt a slightly staggered orientation and the ethyl arsine side chain, which extends away from the ferrocene group, is slightly disordered. The hydrogen atoms in the arsine group were unable to be found in the penultimate electron density map.

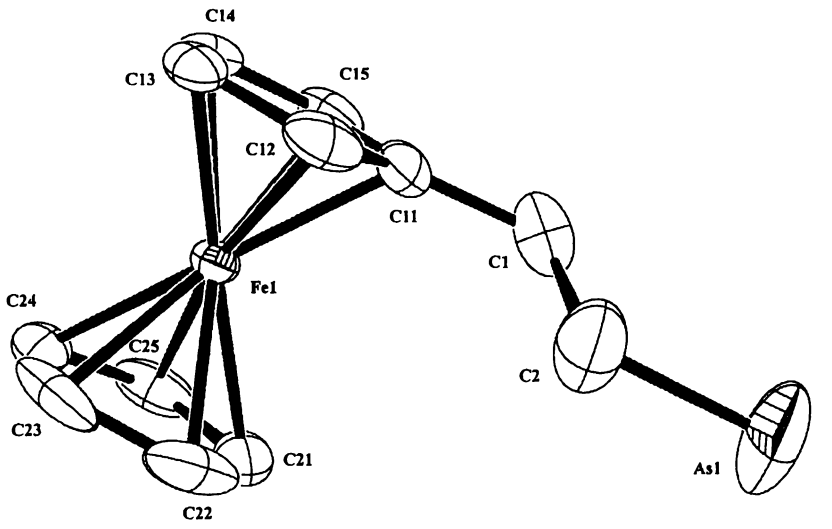

Figure 4.21: Ortep Diagram of $FcCH_2CH_2AsH_2$ **25** at the 50% Probability Level.

The arsine $FcCH_2CH_2AsH_2$ **25** was stable in air and no special precautions were made to exclude air from the compound after the initial synthesis. The crystal sent for X-ray analysis and those sent for elemental analysis were in air for up to three days prior to analysis and showed no appreciable decomposition. A sample of sublimed **25** was left exposed to air for three months at which time elemental analysis indicated no oxidation or decomposition of the sample. As in the case of primary phosphines, it seems the proximity to a ferrocene group endows remarkable stability onto primary arsines. It would be of interest to prepare further ferrocenyl primary arsines and investigate their chemistry.

4.3: Experimental

General experimental techniques in this chapter are in keeping with those outlined in chapter 2.2 with the following alterations/additions. All reactions are carried out under a dinitrogen atmosphere unless otherwise stated. The starting materials $Mo(CO)_6$ (Pressure Chemical), triethyl phosphite (BDH), $LiAlH_4$ (Aldrich), zinc powder (Prolabo) and Me_3SiCl (Aldrich) were used as supplied. Diazomethane

was prepared from N-methyl-N-nitrosourea using the method described by Arndt[29]. The starting material $(Pip)_2Mo(CO)_4$ was kindly supplied by Miss Corry Decker. The diol 1,1'-Fc'$[CH_2OH]_2$ was prepared as described in chapter two. The diol 1,2-Fc'$[CH_2OH]_2$ was prepared as described in the preceding text. The starting material $Mo(CO)_5$(thf) was prepared by irradiating a solution of $Mo(CO)_6$ in thf using a Lighting Technology MBF 400W lamp, placed ~10cm from the reaction vessel (a pyrex Schlenk flask).

The primary phosphines were introduced to the ES mass spectrometer as methanolic solutions with methanol as the carrier solvent. Silver ions in the form of aqueous $AgNO_3$ ($0.1moll^{-1}$, ~1mmol per ml of sample solution) were added to aid ionisation. The ferrocenylphosphine molybdenum carbonyl complexes were introduced to the ES mass spectrometer as solutions in CH_2Cl_2 with methanol as the carrier solvent. Methoxide ions were added to aid ionisation. Solutions of methoxide were prepared by dissolving ~2mg of sodium metal in 5ml of methanol.

Infrared spectra of ferrocenyl primary phosphines and their molybdenum carbonyl derivatives were acquired as solutions in CH_2Cl_2.

The atom labelling Scheme used in the assignment of ferrocenyl nmr signals of mono- and 1,1-bis-substituted ferrocenes is the same as used in chapter 2. The atom labelling Scheme used in the assignment of ferrocenyl nmr signals of 1,2-disubstituted ferrocenes is given in Figure 4.22.

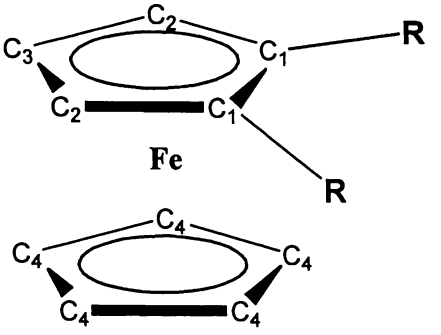

Figure 4.22: Atom Labelling Scheme for NMR Assignment of 1,2-Bis-substituted Ferrocenyl Signals.

[29] F. Arndt, *Org. Synth., Coll. Vol.*, 1943, **2**, 165

GCMS data were acquired for ferrocenyl diols and bis-phosphines using a Hewlett Packard 5890 series 1 gas chromatograph allied with a Hewlett Packard 5970 series mass selective detector operating at 70eV. The samples were introduced into the GC as solutions in CH_2Cl_2 and were eluted using a 50°C to 280°C temperature ramp, at 10°Cmin^{-1} with a three minute solvent delay. The column used was an HP1 column containing cross-linked methylsilicone gum 24m × 0.2mm × 0.33μm film thickness.

4.3.1: Syntheses

4.3.1.1: Synthesis of $FcCH_2PH_2$ **15**

Excess ethereal diazomethane was added to a slurry of $FcCH_2P(O)(OEt)OH$ (0.99g, 3.2mmol) in methanol (5ml) until the solid was completely dissolved (10 minutes). Dinitrogen gas was bubbled through the resulting solution to remove excess CH_2N_2, then the solvent was removed under vacuum. The residual brown oil was taken up into thf (5ml) and added dropwise to a slurry of $LiAlH_4$ (0.7g, 19.2mmol) and Me_3SiCl (2.4ml, 19.2mmol) in thf (10ml). The reaction solution was stirred for 12 hours before methanol (5ml) was added to destroy excess $LiAlH_4$. The solvent was then removed and the residue extracted with petroleum spirits (5 × 10ml). The combined petroleum spirits fractions were filtered through celite and the solvent removed to give 0.69g (92%) of **15** as a crystalline yellow powder. Spectroscopic properties of this powder were identical with those of an authentic sample of $FcCH_2PH_2$ prepared by the literature method[6].

^{31}P NMR ($CDCl_3$): δ -129.09 (*t*, $^1J_{P-H}$ 193Hz)

^{13}C-{^1H} NMR ($CDCl_3$): δ 14.49 (*d*, $^1J_{C-P}$ 8.7Hz, $\underline{C}H_2PH_2$), 67.38 (*s*, C3), 67.88 (*d*, $^3J_{P-C}$ 2.8Hz, C2), 68.71 (*s*, C4), 89.17 (*d*, $^2J_{P-C}$ 2Hz, C1).

^1H NMR ($CDCl_3$): δ 2.61 (2H, *s*, $C\underline{H}_2PH_2$), 2.94 (2H, *d/t*, $^1J_{P-H}$ 191Hz, $^3J_{H-H}$ 7.1Hz, $CH_2P\underline{H}_2$), 4.07-4.13 (9H, *m*, H2,H3,H4)

GCMS (R_t = 13.45min): *m/z* 232 $[M]^+$, 199 $[FcCH_2]^+$, 121 $[CpFe]^+$, 56 $[Fe]^+$.

4.3.1.2: Synthesis of $FcPH_2$ **16**

To a slurry of $LiAlH_4$ (0.32g, 8.5mmol) and Me_3SiCl (1ml, 8.5mmol) in thf (10ml) was added a solution of $FcP(O)(OEt)_2$ (0.91g, 2.8mmol) in thf (10ml). The reaction mixture was stirred for 12 hours. Methanol was added (5ml) and the solvent removed under reduced pressure. The residue was extracted with petroleum spirits (5 × 10ml) and the combined organic fractions were filtered through celite. The solvent was removed to give 0.5g (87%) of $FcPH_2$ as a brown oil that crystallised upon standing.

^{31}P NMR ($CDCl_3$): δ -143.34 (*t*, $^1J_{P-H}$ 203Hz).

$^{13}C-\{^1H\}$ NMR ($CDCl_3$): δ 69.20 (*s*, C4), 70.64 (*d*, $^3J_{P-C}$ 3.8Hz C3), 75.61 (*d*, $^2J_{P-C}$ 14Hz, C2).

^1H NMR ($CDCl_3$): δ 3.84 (2H, *d*, $^1J_{P-H}$ 203Hz, $P\underline{H}_2$), 4.19 (5H, *s*, H4), 4.28 (2H, *s*, H3), 4.30 (2H, *s*, H3)

Lit[8b]: ^{31}P NMR ($CDCl_3$): δ -145.5. ^1H NMR ($CDCl_3$): δ 3.8 (2H, *d*, $^1J_{P-H}$ 206Hz), 4.2 (5H, *s*, $C_5\underline{H}_5$), 4.3 (4H, *s*, $C_5\underline{H}_4$). ^{13}C NMR ($CDCl_3$): δ 69.4 (*s*, C_5H_5), 70.2 (*d*, $^1J_{P-C}$ 25.7Hz), 71.6 (*d*, $^3J_{P-C}$ 7.9Hz), 73.7 (*d*, $^2J_{P-C}$ 12.7Hz).

4.3.1.3: Synthesis of 1,1'-$Fc'[PH_2]_2$ **17**

A suspension of $LiAlH_4$ (0.27g, 7mmol) and Me_3SiCl (0.9ml, 7mmol) in Et_2O was prepared under a dinitrogen atmosphere. To this was added a solution of 1,1'-$Fc'[P(O)(OEt)_2]_2$ (0.54g, 1.2mmol) in thf (5ml). The reaction was stirred at room temperature for 12 hours before methanol (5ml) was added. The solvent was then removed under reduced pressure and the residue extracted with petroleum spirits (5 × 10ml). The combined organic fractions were filtered through celite and the solvent removed to give 0.24g (82%) of **17** as a brown oil that crystallised upon standing.

^{31}P NMR ($CDCl_3$): δ -143.75 (*d/t*, $^1J_{P-H}$ 205Hz $^3J_{P-H}$ 3.5Hz).

$^{13}C-\{^1H\}$ NMR ($CDCl_3$): δ 71.98 (*br. s*, C2/C3), 77.37 (*d*, $^1J_{P-C}$ 40Hz C1).

^{1}H NMR ($CDCl_3$): δ 3.80 (4H, *d/t*, $^1J_{P-H}$ 203Hz, $^4J_{H-H}$ 3Hz, P$\underline{H}_2$), 4.20 (4H, *d/d*, $^3J_{H-H}$ 1.6Hz, $^4J_{P-H}$ 3.5Hz, H2), 4.27 (4H, *d/d*, $^3J_{H-H}$ 1.7Hz, H3).

Lit[9b]: ^{31}P NMR (C_6D_6): δ -145.5 (*t*, $^1J_{P-H}$ 202Hz). ^{1}H NMR (C_6D_6): δ 3.69 (4H, *d/d*, $^1J_{P-H}$ 202Hz, $^4J_{H-H}$ 3Hz, P$\underline{H}_2$), 3.92 (4H, *d*, $^3J_{H-H}$ 1.7Hz, Cp-H), 3.96 (4H, *d*, $^3J_{H-H}$ 1.5Hz, Cp-H).

4.3.1.4: Synthesis of $FcCH_2CH_2PH_2$ **18**

Excess ethereal diazomethane (CH_2N_2) was added slowly to a slurry of ferrocenylethylphosphonic acid **4**[30], (0.39g, 1.34mmol) in CH_2Cl_2 (5ml) until the solid had completely dissolved. Dinitrogen gas was bubbled through the resulting solution to remove excess CH_2N_2 then the solvent was removed under vacuum.

The residue was taken up into thf (5ml) and added dropwise to a solution of $LiAlH_4$ (0.25g, 6.7mmol) and Me_3SiCl (0.72g, 6.7mmol) in thf (10ml) under a dinitrogen atmosphere. The resulting solution was stirred for 12 hours at room temperature. Methanol (5ml) was then added and stirring continued for 30 minutes before the solvent was removed under vacuum and replaced with petroleum spirits (20ml). The resulting yellow solution was filtered through celite and the solvent removed to give 0.27g (82%) of **18** as a yellow powder.

m.p. 53-55°C

Elemental Analysis: Found: C, 58.65%; H, 5.97%. Calculated for $C_{12}H_{15}FeP$: C, 58.57%; H, 6.14%.

^{31}P NMR ($CDCl_3$): δ -135.79 (*t*, $^1J_{P-H}$ 195Hz).

^{13}C-{^{1}H} NMR ($CDCl_3$): δ 15.50 (*d*, $^1J_{C-P}$ 8.4Hz, $\underline{C}H_2P$), 33.25 (*d*, $^2J_{C-P}$ 3Hz, $\underline{C}H_2CH_2P$), 67.33 (*s*, C3), 68.05 (*s*, C2), 68.57 (*s*, C4), 89.04 (*d*, $^3J_{C-P}$ 6Hz, C1).

^{1}H NMR ($CDCl_3$): δ 2.57 (2H, *d/t* $^2J_{P-H}$ 2.5Hz, $^3J_{H-H}$ 7Hz, C$\underline{H}_2$P), 2.74 (2H, *d/t*, $^1J_{H-P}$ 194Hz, $^3J_{H-H}$ 7Hz, P$\underline{H}_2$), 4.08-4.12 (11H, *m*, C$\underline{H}_2CH_2PH_2$/H2/H3/H4).

ESMS: (MeOH, c.v. 40V, Ag^+ added) *m/z* 246 (M^+, 8%), 353/355 ($[M+Ag^+]^+$, 100%).

[30] For synthesis of **4** see chapter two, section 2.2.

IR (cm^{-1}): 3096 (w), 2921 (w), 2294 (m, νPH) 1412 (w), 1319 (w), 1081 (m), 1040 (w), 1001 (m), 822 (m), 501 (m), 484 (m).

GCMS (R_t = 15.1min): *m/z* 246 $[M]^+$, 213 $[M\text{-}PH_2]^-$, 199 $[FcCH_2]^+$, 121 $[FeCp]^+$, 56 $[Fe]^+$.

4.3.1.5: Synthesis of 1,1'-Fc'$(CH_2PH_2)_2$ **19**

In a dry, nitrogen flushed flask was placed thf (30ml), 1,1'-ferrocenylbis(methanol)[31] (0.23g, 0.93mmol), pyridine (0.15g, 1.9mmol) and freshly distilled phosphorus trichloride (0.26g, 1.9mmol). The reaction mixture was stirred until precipitation of pyridinium hydrochloride was deemed complete (~1 hour). The solution was filtered and the solvent removed to give a bright yellow crystalline material, crude 1,1'-Fc'$(CH_2Cl)_2$. Triethylphosphite (TEP, 5ml) was added to the flask and the solution bought to reflux for 2 hours. Excess TEP was distilled off under vacuum and the resulting brown oil purified by alumina flash column chromatography using an EtOAc to MeOH solvent gradient. The 1,1'-ferrocenyl-bis-(diethyl methylphosphonate) was isolated as a viscous brown oil (0.45g, 96%).

A slurry of $LiAlH_4$ (0.18g 4.7mmol) and Me_3SiCl (0.53g 4.7mmol) in thf (10ml) was placed under a dinitrogen atmosphere. To this was added a solution of 1,1'-ferrocenyl-bis-(diethyl methylphosphonate) (0.45g, 0.9mmol) in dry thf (5ml) and the resulting slurry stirred at room temperature for 6 hours. At this time 5ml of methanol was added and stirring continued for 30 minutes. The solvent was then removed, and the residue taken up into 20ml of petroleum spirits. The resulting solution was filtered through celite and the solvent removed to give **19** as a yellow oil (0.16g, 62%).

^{31}P NMR ($CDCl_3$): δ -132.01 (*t*, $^1J_{P\text{-}H}$ 196Hz).

$^{13}C\text{-}\{^1H\}$ NMR ($CDCl_3$): δ 14.30 (*d*, $^1J_{C\text{-}P}$ 8.7Hz, $\underline{C}H_2P$), 68.29 (*s*, C3), 68.57 (*d*, $^3J_{C\text{-}P}$ 2.7Hz, C2), 89.30 (*d*, $^2J_{C\text{-}P}$ 3Hz C1).

^1H NMR ($CDCl_3$): δ 1.54 (4H, *br. s*, $C\underline{H}_2P$), 2.93 (4H, *d/t*, $^1J_{H\text{-}P}$ 192Hz, $^3J_{H\text{-}H}$ 7Hz $P\underline{H}_2$), 4.04 (8H, *s*, H2/H3).

ESMS: (MeOH, c.v. 40V, Ag^+ added) *m/z* 278 (M^+, 100%), 385/387 ($[M+Ag^+]^+$, 45%).

IR (cm^{-1}): 3082 (m), 2922 (m), 2290 (s, $\underline{PH_2}$), 1083 (m), 1039 (m), 1019 (w), 927 (m), 859 (w), 852 (w), 823 (w), 485 (m).

GCMS (R_t = 16.94min): *m/z* 278 $[M]^+$, 245 $[M\text{-}PH_2]^+$ 200, 165 $[FeC_5H_4CH_2P]^+$, 134 $[FeC_5H_4CH_2]^+$, 121 $[FeCp]^+$, 56 $[Fe]^+$.

4.3.1.6: Synthesis of 1,2-Fc'$(CH_2PH_2)_2$ **20**

In a dry, nitrogen flushed flask was placed thf (10ml), 1,2-ferrocenylbis(methanol)[12] (0.23g, 0.93mmol), pyridine (0.15g, 1.86mmol) and freshly distilled phosphorus trichloride (0.25g, 1.86mmol). The reaction mixture was stirred until precipitation of pyridinium hydrochloride was deemed complete, (~1 hour). The solution was filtered and the solvent removed to give a bright yellow crystalline material, crude 1,2-Fc'$(CH_2Cl)_2$. Triethylphosphite (3ml) was added to the flask and the solution brought to reflux for 4 hours. Excess TEP was distilled off under vacuum and the resulting brown oil purified by alumina flash column chromatography using an EtOAc to MeOH solvent gradient. The 1,2-ferrocenyl-bis-(diethyl methylphosphonate) was isolated as a viscous brown oil (0.39g, 85%).

A slurry of $LiAlH_4$ (0.30g 8mmol) and Me_3SiCl (0.87g 8mmol) in thf (10ml) was placed under a dinitrogen atmosphere. To this was added a solution of 1,1'-ferrocenyl-bis-(diethyl methylphosphonate) (0.39g, 0.8mmol) in dry thf (5ml) and the resulting slurry stirred at room temperature for 9 hours. At this time 5ml of methanol was added and stirring continued for 30 minutes. The solvent was then removed, and the residue taken up into 20ml of petroleum spirits. The resulting solution was filtered through celite and the solvent removed to give **20** as a yellow crystalline solid, (0.18g 80%) which melted as it warmed to room temperature.

^{31}P NMR ($CDCl_3$): δ -127.57 (*t*, $^1J_{P\text{-}H}$ 198Hz)

$^{13}C\text{-}\{^1H\}$ NMR ($CDCl_3$): δ 12.86 (*d*, $^1J_{C\text{-}P}$ 10Hz, $\underline{C}H_2P$), 65.64 (*s*, C1), 67.39 (*s*, C2), 69.43 (*s*, C4), 86.94 (*s*, C3).

[31] For synthesis of 1,1'-ferrocenylbis(methanol) see chapter two section 2.1.

^{1}H NMR ($CDCl_3$): δ 2.62 (4H, *m*, C$\underline{H}_2$P), 2.94 (4H, *d/t*, $^1J_{H\text{-}P}$ 196Hz, $^3J_{H\text{-}H}$ 7Hz, P$\underline{H}_2$), 4.00 (1H, *t*, $^3J_{H\text{-}H}$ 2.5Hz, H1), 4.05 (5H, *s*, H4), 4.01 (2H, *d*, $^3J_{H\text{-}H}$ 2.5Hz, H2).

ESMS: (MeOH, c.v. 20V, Ag^+ added) *m/z* 385/387 ([M+Ag^+]$^+$ 100%).

IR (cm^{-1}): 3097 (w), 2916 (m), 2285 (s, P$\underline{H}_2$), 1105 (s), 1080 (m), 1034 (m), 997 (m), 929 (w), 819 (m), 485 (m).

GCMS (R_t = 17.46min): *m/z* 278 [M]$^+$, 245 [M-PH_2]$^+$ 200, 121 [FeCp]$^+$, 56 [Fe]$^+$.

4.3.1.7: Synthesis of 1,2-Fc'[CH_2PH_2]$_2$Mo(CO)$_4$, **21**

The bis-phosphine **20** (0.06g, 0.23mmol) was dissolved in CH_2Cl_2 (5ml) and placed under a dinitrogen atmosphere. To this was added a solution of (Pip)$_2$Mo(CO)$_4$ (0.08g, 0.23mmol) in CH_2Cl_2 (5ml). The reaction was brought to reflux and monitored by ^{31}P nmr until reaction was deemed complete (2 hours). The reaction solution was concentrated and purified by silica flash column chromatography using 1:1 CH_2Cl_2:petroleum spirits as the eluting solvent. The solvent was removed to give 0.092g (83%) of **21** as a bright yellow powder.

m.p. dec. 133-135°C.

Elemental Analyses: Found: C, 39.66%; H, 3.49%. Calculated for $C_{16}H_{16}FeMoO_4P_2$: C, 39.54%; H, 3.34%.

^{31}P NMR ($CDCl_3$): δ -78.52 (*t/d/t*, $^1J_{P\text{-}H}$ 312Hz, $^2J_{P\text{-}H}$ 17Hz, $^2J_{P\text{-}H}$ 13Hz).

^{13}C-{^{1}H} NMR ($CDCl_3$): δ 19.87 (*d/d*, $^1J_{C\text{-}P}$ 11Hz, $^3J_{C\text{-}P}$ 11Hz, C$\underline{H}_2$), 67.15 (*s*, C3), 68.84 (*s*, C2), 69.57 (*s*, C4), 82.569 (*d/d*, $^2J_{P\text{-}C}$ 5Hz $^3J_{P\text{-}C}$ 5Hz, C1) 206.85 and 209.47 (*s*, C$\underline{O}$ × 2).

^{1}H NMR ($CDCl_3$): δ 2.67 (4H, *d/t*, $^3J_{H\text{-}H}$ 13Hz, $^2J_{P\text{-}H}$ 1.5Hz, C$\underline{H}_2$P), 4.05 (5H, *s*, H4), 4.08 (2H, *d*, $^2J_{H\text{-}H}$ 2.4Hz, H2), 4.12 (1H, *d/d*, $^2J_{H\text{-}H}$ 2.5Hz, H3).

ESMS: (MeOH, c.v. 5V, NaOMe added) *m/z* 487 ([M-H^+]$^-$ 100%).

IR (cm^{-1}): 2960 (w), 2917 (w), 2028 (vs), 1926 (vs), 1105 (w), 1075 (w), 1010 (w), 931 (m), 606 (w), 583 (w).

4.3.1.8: Synthesis of 1,1'-Fc'$[CH_2PH_2]_2Mo(CO)_4$ **22** and [1,1'-Fc'$[CH_2PH_2]_2Mo(CO)_4]_2$ **22a**

A solution of 1,1'-Fc'$[CH_2PH_2]_2$ **19** (0.056g, 0.2mmol) in CH_2Cl_2 (5ml) was added to a solution of $(Pip)_2Mo(CO)_4$ (0.076g, 0.2mmol) and the resulting solution was brought to reflux for 2 hours. The solvent was then removed and the products **22** (r.f. 0.65, 15mg, 15%) and **22a** (r.f. 0.48, 0.5mg) were isolated from the residue using silica thin layer chromatography with 4:6 CH_2Cl_2:petroleum spirits as the developing solvent.

22

m.p. dec. 146-148°C.

Elemental Analyses: Found: C, 39.78%; H, 3.13%. Calculated for $C_{16}H_{16}FeMoO_4P_2$: C, 39.54%; H, 3.34%.

^{31}P NMR ($CDCl_3$): δ -79.75 (*t/m*, $^1J_{P-H}$ 308Hz).

$^{13}C-\{^1H\}$ NMR ($CDCl_3$): δ 17.57 (*d/d*, $^1J_{P-C}$ 13Hz, $^3J_{P-C}$ 13Hz $\underline{C}H_2PH_2$), 67.59 (*s*, C3), 69.32 (*d*, $^3J_{P-C}$ 3Hz, C2), 81.58 (*s*, C1), 208.45 and 212.67 (*s*, 2 × CO).

^1H NMR ($CDCl_3$): δ 2.89 (4H, *m*, $C\underline{H}_2P$), 4.18 (4H, *t*, $^3J_{H-H}$ 1.7Hz, H3), 4.23 (4H, *t*, $^3J_{H-H}$ 1.7Hz, H2) 4.76 (4H, *d/m*, $^1J_{P-H}$ 311Hz, $P\underline{H}_2$).

ESMS: (MeOH, c.v. 5V, NaOMe added) *m/z* 487 ($[M-H^+]^-$, 100%), 459 ($[M-H^+-CO]^-$, 98%).

IR (cm^{-1}): 2984 (w), 2027 (s), 1909 (s), 1041 (w), 937 (w), 609 (w), 579 (w).

22a

ESMS: (MeOH, c.v. 5V, NaOMe added) *m/z* 971 ($[M-H^+]^-$, 100%).

4.3.1.9: Synthesis of 1,1'-Fc'$[CH_2PH_2Mo(CO)_5]_2$, **23**

Molybdenum hexacarbonyl (1.62g, 6mmol) was dissolved in thf (15ml) and placed under a dinitrogen atmosphere. To this, a solution of 1,1'-Fc'$[CH_2PH_2]_2$ (0.057g, 0.2mmol) in thf (5ml) was added. The reaction solution was then exposed to

UV light for three hours. The solvent was removed under vacuum and the excess molybdenum carbonyl was removed by sublimation under vacuum at 45°C over a period of two days. The residue was taken up into CH_2Cl_2 (2ml) and purified by silica thin layer chromatography using 4:6 CH_2Cl_2:petroleum spirits as the eluting solvent. The solvent was removed to give 0.052g (36%) of **23** as a yellow crystalline powder.

m.p. 138-142°C

Elemental Analyses: Found: C, 35.27%; H, 2.14%. Calculated for $C_{22}H_{16}FeMo_2O_{10}P_2$: C, 35.23%; H, 2.15%.

^{31}P-{^1H} NMR ($CDCl_3$): δ -62.46 (*t*, $^1J_{P\text{-}H}$ 320Hz).

^{13}C-{^1H} NMR ($CDCl_3$): δ 22.84 (*d*, $^1J_{C\text{-}P}$ 16Hz, $\underline{C}H_2$), 69.00 (*s*, C3), 69.50 (*s*, C2), 85.41 (*d*, $^2J_{C\text{-}P}$ 3.2Hz, C1), 201.07, 204.70 and 204.82, (*s*, $\underline{C}O \times 3$).

^1H NMR ($CDCl_3$): δ 2.89 (4H, *m*, $C\underline{H}_2P$), 4.14 (8H, *br. s*, H2/H3), 4.36 (4H, *d/t*, $^1J_{P\text{-}H}$ 319Hz, $^3J_{H\text{-}H}$ 7Hz, $P\underline{H}_2$).

ESMS: (MeOH, c.v. 5V, NaOMe added) *m/z* 749 ($[M\text{-}H^+]^-$ 100%).

IR (cm^{-1}): 3053 (w), 2990 (w), 2076 (s), 1941 (s), 928 (w), 876 (w), 606 (m), 582 (m).

4.3.1.10: Synthesis of 1,2-Fc'$[CH_2PH_2Mo(CO)_5]_2$ **24**

Molybdenum hexacarbonyl (0.361g, 1.3mmol) was dissolved in thf (15ml) and placed under a dinitrogen atmosphere. A solution of 1,2-Fc'$[CH_2PH_2]_2$ (0.038g, 0.13mmol) in thf (5ml) was added. The reaction solution was then exposed to UV light for three hours. The solvent was removed under vacuum and the excess molybdenum carbonyl was removed by sublimation under vacuum at 45°C over a period of two days. The residue was taken up into CH_2Cl_2 (5ml) to which activated charcoal had been added. The activated charcoal was removed by filtration and the resulting yellow solution was purified by thin layer chromatography using 4:6 Et_2O:petroleum spirits as the developing solvent. Removal of solvent gave 0.025g (24%) of **25** as a yellow powder.

m.p. 119-121°C

Elemental Analyses: Found: C, 35.48%; H, 2.30%. Calculated for $C_{22}H_{16}FeMo_2O_{10}P_2$: C, 35.23%; H, 2.15%.

^{31}P NMR ($CDCl_3$): δ -61.44 (*t*, $^1J_{P-H}$ 318Hz)

^{13}C-{^1H} NMR ($CDCl_3$): δ 21.90 (*d*, $^1J_{C-P}$ 22Hz, $\underline{C}H_2$), 67.51 (*s*, C3), 68.33 (*s*, C2), 70.04 (*s*, C4), 83.64 (*d*, $^2J_{C-P}$ 5Hz, C1), 204.6 (*d*, $^2J_{C-P}$ 9Hz, $\underline{C}O$), 208.4 (*d*, $^2J_{C-P}$ 24Hz, $\underline{C}O$).

^1H NMR ($CDCl_3$): δ 2.93 (4H, *m*, $C\underline{H}_2PH_2$), 4.13 (5H, *s*, H4), 4.20 (1H, *d/d*, $^3J_{H-H}$ 2.5Hz, H3), 4.24 (2H, *d*, $^3J_{H-H}$ 2.5Hz, H2), 4.40 (4H, *d/t*, $^1J_{P-H}$ 319Hz, $^3J_{H-H}$ 6.7Hz, $P\underline{H}_2$).

ESMS: (MeOH, c.v. -10V, NaOMe added), *m/z* 749 ([M-H^+]$^-$, 100%), 781 ([M+OMe^-]$^-$, 28%).

IR (cm^{-1}): 2955 (w), 2925 (w), 2871 (w), 2349 (w), 2076 (s), 1948 (s), 1937 (s), 1919 (s), 1916 (s), 1106 (w), 1090 (w),1038 (w), 999 (w), 927 (w), 882 (w), 606 (m), 582 (m).

4.3.1.11: Synthesis of $FcCH_2CH_2AsH_2$ **25**

$FcCH_2CH_2AsO_3H_2$ (0.11g, 0.33mmol) was dissolved in 10ml of 0.13$moll^{-1}$ aqueous sodium hydroxide. To this was added zinc powder (0.21g, 3.3mmol) and petroleum spirits (15ml). The entire system was placed under a dinitrogen atmosphere and concentrated HCl (10ml) was added drop-wise over ten minutes. At this time the layers were separated and the aqueous phase extracted with petroleum spirits (1 × 10ml). The combined organic fractions were dried over $MgSO_4$ and the solvent removed to give 0.055g (57%) of **25** as a yellow oil that crystallised upon standing.

m.p. 44-46°C.

Elemental Analyses: Found C, 50.32%; H, 5.59% Found after three months exposure to air: C, 50.59%; H, 5.42%. Calculated for $C_{12}H_{15}AsFe$ C, 49.69%; H, 5.21%.

^{13}C-{^1H} NMR ($CDCl_3$): δ 14.02 (*s*, $\underline{C}H_2As$), 33.55 (*s*, $\underline{C}H_2CH_2As$), 67.57 (*s*, C2), 68.26 (*s*, C3), 68.84 (*s*, C4), 90.16 (*s*, C1).

^1H NMR ($CDCl_3$): δ 1.84 (2H, *m*, $C\underline{H}_2As$), 2.24 (2H, *t*, $^3J_{H-H}$ 6Hz, $As\underline{H}_2$), 2.65 (2H, *t*, $C\underline{H}_2CH_2As$), 4.09 (2H, *d*, $^3J_{H-H}$ 1.5Hz H2), 4.09 (2H, *d*, $^3J_{H-H}$ 1.5Hz H3), 4.14 (5H, *s*, H4).

GCMS (R_t = 16.85min): *m/z* 290 $[M]^{+\bullet}$, 213 $[FcCH_2CH_2]^+$, 212 $[M^{+\bullet}\text{-}AsH_3^{\bullet}]^+$, 121 $[CpFe]^+$, 56 $[Fe]^+$.

IR (cm^{-1}): 3081 (w), 2920 (w), 2881 (w), 2836 (w), 2072 (s, νAs-H), 1103 (s), 1045 (m), 1020 (m), 999 (m), 961 (m), 920 (w), 869 (w), 817 (s), 482 (s).

4.3.2: X-ray Crystal Structure Determinations for $FcCH_2CH_2PH_2$ 18, 1,2-$Fc'[CH_2PH_2]_2Mo(CO)_4$ 21 and $FcCH_2CH_2AsH_2$ 25

Crystals of the ferrocenyl primary phosphine **18** and arsine **25** suitable for X-ray crystal structural analysis were grown by sublimation onto a cold finger at 30°C under vacuum (~1mmHg). Single crystal X-ray diffraction data for **25** were acquired at the University of Auckland using a Siemens Smart CCD diffractometer and corrected for absorption using SADABS. The single crystal X-ray diffraction data for **18** was collected on a Nicolet R3 diffractometer at the University of Canterbury and was assigned the space group C2 prior to data being merged. The structure was solved using direct methods but a satisfactory refinement in this space group was unable to be achieved and in light of the iso-structural nature of the arsine **25**, complete structural analysis of the phosphine **18** was discontinued.

The structure of **25** was solved for iron and arsenic using the Patterson methods option of SHELX-97. The remainder of the structure was developed routinely using direct methods with full-matrix least squares refinement based on F_o^2. In this structure the carbon atoms C(1) and C(2) were each disordered over two positions. Refinement as C(1)/C(111) and C(2)/C(112) resulted in occupancies of 0.95/0.05 respectively for each disordered pair. All hydrogen atoms were placed in calculated positions except those bound to arsenic. Attempts to locate arsine hydrogens from the penultimate electron density map were unsuccessful. The largest residual electron density peaks in the final density map did not exceed 0.614 and –1.108 $eÅ^{-3}$.

Suitable crystals of the molybdenum carbonyl complex **21** were grown from a CH_2Cl_2/petroleum spirits solution at -20°C. The crystal proved to be weakly diffracting and the resulting data set (collected at Auckland University) was of poor quality. The structure was solved using Patterson methods for iron and molybdenum.

Attempts to refine the structure in the tetragonal space group I4(1)/a were partially successful but adequate refinement could not be achieved.

Table 4.4: Collected Single Crystal Data and Analysis Parameters for $FcCH_2CH_2PH_2$ **18**, 1,2-Fc'$[CH_2PH_2]_2Mo(CO)_4$ **21** and $FcCH_2CH_2AsH_2$ **25**.

Compound	**18**	**21**	**25**
Empirical formula	$C_{12}H_{15}FeP$	$C_{16}H_{16}FeO_4P_2Mo$	$C_{12}H_{15}AsFe$
Formula weight	245.1	486	290.01
Crystal system	Monoclinic	Tetragonal	Monoclinic
a (Å)	10.382(3)	35.0413(1)	14.3996(1)
b (Å)	7.550(2)	35.0413(1)	7.5871(1)
c (Å)	14.247(4)	6.2610(1)	10.4835(1)
α (°)	90.00	90.00	90.00
β (°)	96.870(4)	90.00	97.496(1)
γ (°)	90.00	90.00	90.00
V (Å^3)	1108.82(8)	7687.84(1)	1135.55(2)
Space group		I4(1)/a	P2(1)/c
Z value			4
D_{calc}			1.696 gcm^{-3}
F(000)			584
λ(Mo Kα) (Å)			0.71
μ(Mo Kα) (mm^{-1})			4.18
Temperature (K)			150(2)
2θ range for data collection			1.4° < θ < 26.6°
Total reflections			10760
Unique reflections			2324 ($R_{int.}$ = 0.0346)
T_{min}			0.613076
T_{max}			0.805393
R_1 [I>2σ(I)]			0.043

wR_2	0.1051
GOF	1.035

ζ $w = [\sigma^2(F_o^2) + (0.0514P^2 + 2.88P]^{-1}$ where $P = (F_o^2 + 2F_c^2)/3$.

Chapter 5: Oxidation of $FcCH_2PH_2$ as a Route to Ferrocenyl Phosphorus Acids

5.1: Introduction

The ferrocenyl primary phosphine $FcCH_2PH_2$ **15** was originally synthesised by deformylation of the ferrocenyl hydroxymethyl phosphine $FcCH_2P(CH_2OH)_2$ using sodium metabisulfite ($Na_2S_2O_5$)[1]. The product of this reaction was shown to be dependent on the ratio of $FcCH_2P(CH_2OH)_2$ to $Na_2S_2O_5$ (Scheme 5.1) and was unusual in that the reaction of $FcCH_2P(CH_2OH)_2$ with excess $Na_2S_2O_5$ gave an oxidised product, despite $Na_2S_2O_5$ being considered a reducing rather than an oxidising agent.

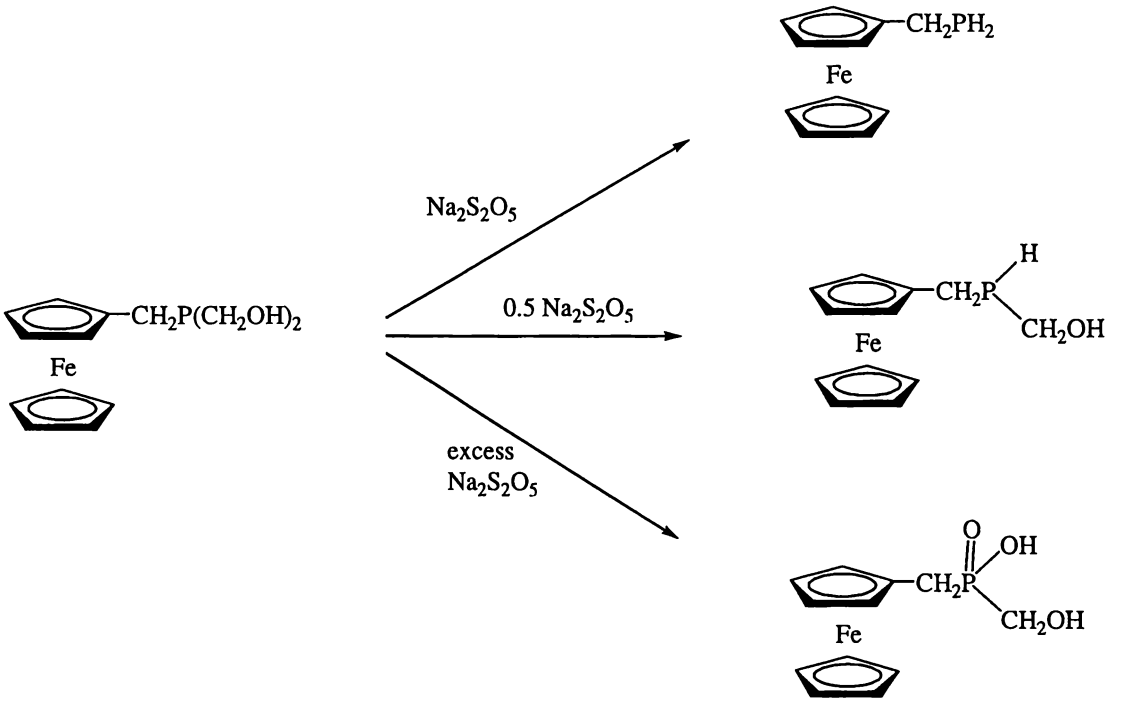

Scheme 5.1: Syntheses Based on the Reaction of $FcCH_2P(CH_2OH)_2$ with $Na_2S_2O_5$.

[1] N. J. Goodwin, W. Henderson, B. K. Nicholson, J. Fawcett and D. R. Russell, *J. Chem. Soc., Dalton Trans.*, 1999, 1793.

The electrochemical behaviour of **15** has also been investigated[2]. The cyclic voltammogram of **15** (Figure 5.1) could be described as complex and is further complicated adsorption of the phosphine onto both platinum and glassy carbon electrodes. Nonetheless features typical of $FcCH_2PR_2$ (R = CH_2OH, Ph, CH_2CH_2CN) species were identified, as well as features unique to this ferrocenyl phosphine.

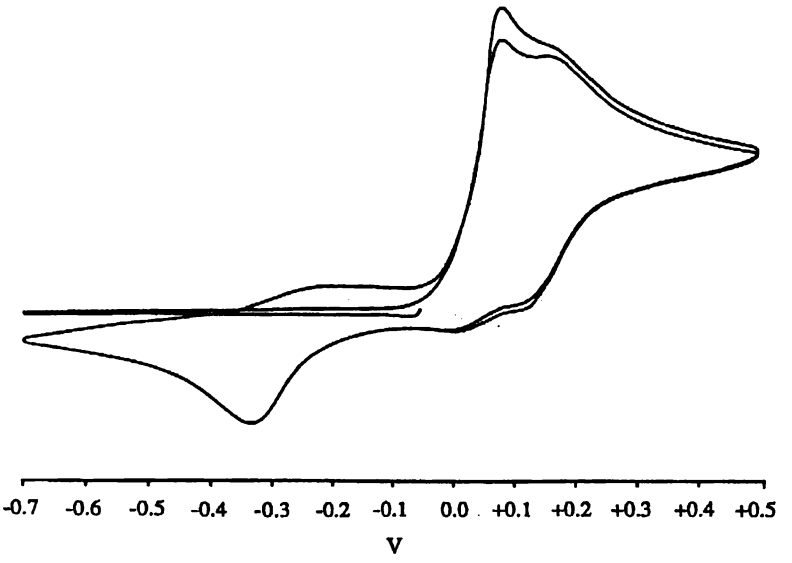

Figure 5.1: Cyclic Voltammogram of $FcCH_2PH_2$ **15***.

The cyclic voltammogram contains two pairs of linked redox processes. The first consists of a cathodic peak at –0.33V coupled to the broad oxidative process at *ca* 0.2V. The second consists of the anodic peaks (at *ca* 0.1V and 0.2V) which are chemically linked and electrochemically reversible. This pattern was found to be typical of $FcCH_2PR_2$ compounds was found to be consistent with the following mechanism:

$$FcCH_2PR_2 \underset{+e}{\overset{-e}{\rightleftharpoons}} [FcCH_2PR_2]^+ \longrightarrow B^+ \underset{+e}{\overset{-e}{\rightleftharpoons}} B^{2+}$$

[2] N. J. Goodwin, Doctoral Thesis, University of Waikato, 1998.

* This Figure is used with permission from N. J. Goodwin, Doctoral Thesis, University of Waikato, 1998.

The first peak is assigned to the oxidation of the ferrocene group to the ferrocinium ion. This then undergoes a bimolecular reaction that transfers charge from the ferrocinium to another part of the molecule. The resulting charged species labelled $\mathbf{B}^+$ contains a regenerated ferrocene centre that undergoes a second oxidation. This second oxidation produces the second peak at 0.3V and the species labelled $\mathbf{B}^{2+}$.

In addition to these ferrocene centred processes, there is an electrochemically irreversible cathodic peak at -0.33V that is coupled to the broad oxidative peak at *ca.* -0.2V. The process generating this redox couple is unknown but seems likely to be centred at the phosphine.

In light of the remarkable stability in air of **15** it was surprising that the chemical oxidation of **15** was not undertaken. The work described in this chapter concerns the chemical oxidation of $FcCH_2PH_2$ using hydrogen peroxide.

5.2: Hydrogen Peroxide Oxidation of $FcCH_2PH_2$ 15

The oxidation of $FcCH_2PH_2$ **15** with excess hydrogen peroxide was initially seen as a simple route to the ferrocenyl phosphonic acid $FcCH_2PO_3H_2$ **3** (see chapter two, Scheme 2.1). The course of this reaction was found to be more complex than simple phosphine oxidation and in hindsight this might have been predicted from the complexities observed in the electrochemistry of **15**.

The reaction of the ferrocenyl primary phosphine **15** with varying mol equivalents of hydrogen peroxide was monitored using $^{31}P\text{-}\{^1H\}$ NMR for several hours. The variable time $^{31}P\text{-}\{^1H\}$ spectrum of the **15**:H_2O_2 (1:1 mol ratio) experiment is given in Figure 5.2.

After five minutes a significant amount of starting material at -131ppm is present, but the spectrum is dominated by the peak at 13.65ppm. In non-decoupled ^{31}P nmr this peak (13.65ppm) splits into a triplet characteristic of a primary phosphine oxide $-P(O)H_2$ group ($^1J_{P\text{-}H}$ 484Hz). Also present at this time is a small peak at ~34ppm which splits into a doublet ($^1J_{P\text{-}H}$ 477Hz) in the $^{31}P\text{-}\{^1H\}$ nmr spectrum. After fifteen minutes a second small peak appears at 42.27ppm. This also splits into a doublet in the non-decoupled spectrum ($^1J_{P\text{-}H}$ 554Hz), indicative of a group containing a single P-H bond. It was likely that one of the small peaks at either 34ppm or 42ppm is due to the ferrocenyl phosphinic acid $FcCH_2P(O)(OH)H$.

After three hours the primary phosphine oxide is still dominant though a small amount of staring material remains. No further change was observed in this reaction after three hours presumably because no further hydrogen peroxide remained.

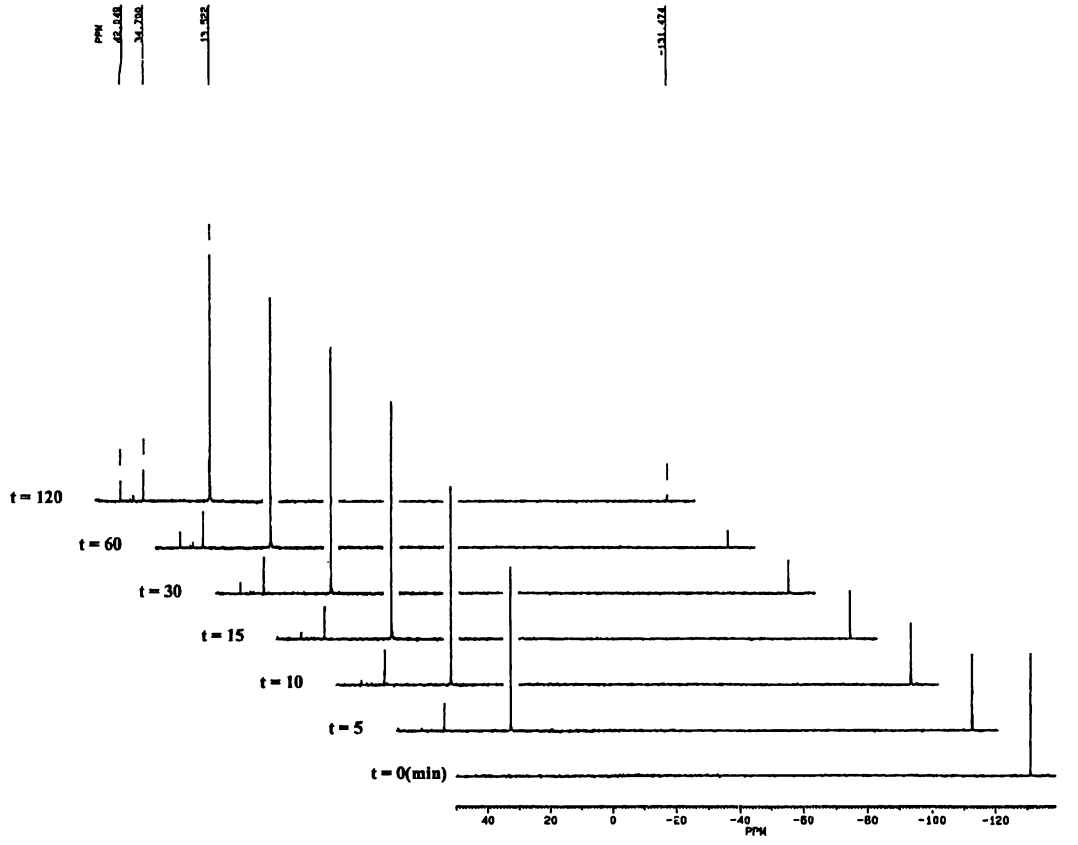

Figure 5.2: Variable Time $^{31}P-\{^{1}H\}$ NMR of the Reaction of $FcCH_2PH_2$ and H_2O_2 in a 1:1 Mol Ratio.

By increasing the ratio of hydrogen peroxide to primary phosphine (2:1, 3:1 and 4:1) the primary phosphine could be completely converted to the primary phosphine oxide within five minutes. Under these conditions further oxidation proceeded only slowly, so that after four hours the dominant phosphorus signal was still that of the phosphine oxide. This peak then slowly diminishes as the peak at 42ppm begins to rise. After twenty-four hours have elapsed, the spectrum is dominated by the peak at 42ppm and very little primary phosphine oxide remains. The peak at 42ppm was initially assigned to the phosphinic acid $FcCH_2P(O)(OH)H$, but subsequent synthesis of this compound proved this to be incorrect. The small peak

at 34ppm which appears after five minutes and remains relatively constant throughout the twenty-four hour experiment is most likely due to the ferrocenyl phosphinic acid. The variable time $^{31}P-\{^{1}H\}$ spectrum of the H_2O_2:**15** = 3:1 experiment is given in Figure 5.3.

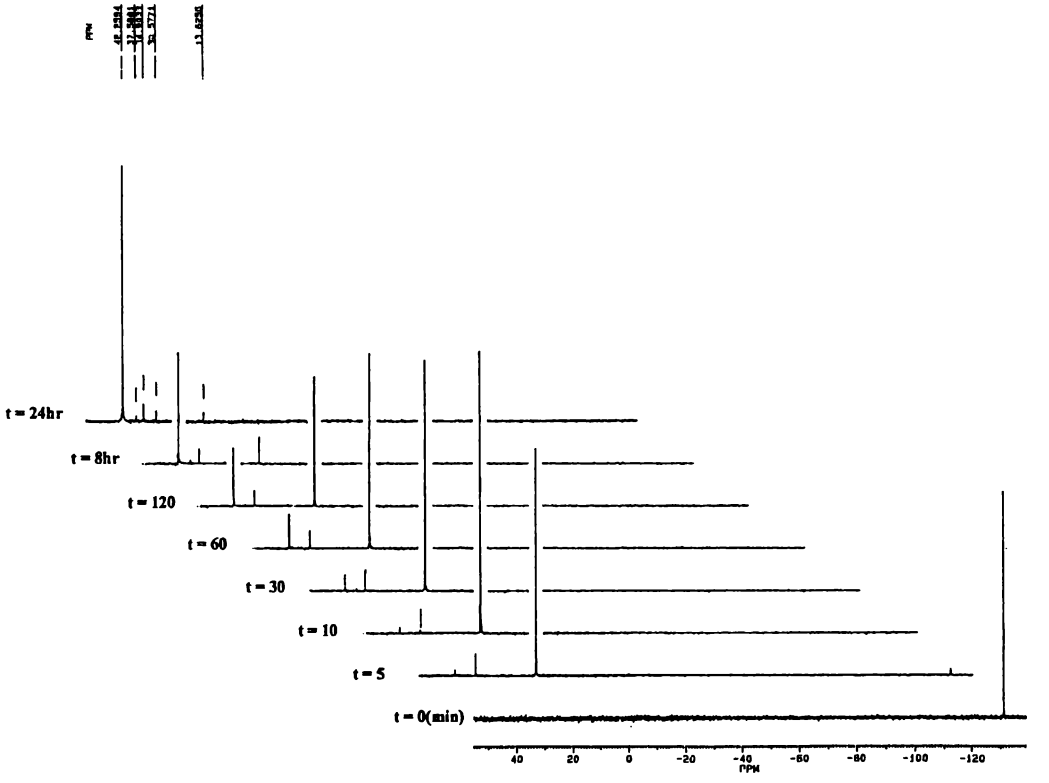

Figure 5.3: Variable Time $^{31}P-\{^{1}H\}$ NMR of the Reaction of $FcCH_2PH_2$ and H_2O_2 in a 1:3 Mol Ratio.

It seems clear that the first oxidation in these experiments is that of the phosphine group to give the primary phosphine oxide $FcCH_2P(O)H_2$. Further oxidation of the phosphorus atom occurs only slowly giving rise to compounds containing a single P-H bond, one of which was identified as the phosphinic acid $FcCH_2P(O)(OH)H$. The major oxidation product, containing one P-H bond at 42ppm remains unassigned. No signal attributable to a phosphonic acid is ever observed.

Increasing the ratio of peroxide to phosphine to 5:1 and 10:1 did not result in any phosphonic acid formation. During the course of these latter experiments, a colour change from yellow to green to yellow was observed over a period of four hours and a brown precipitate fell from solution during the course of the oxidation. This colour change was not observed when the peroxide to phosphine ratio was less

than 5:1. The green colour is characteristic of ferrocenium ion formed by a one electron oxidation of ferrocene. Over a period of several hours the solution slowly becomes yellow again, even in the presence of excess peroxide. This suggests a mechanism by which ferrocene is regenerated and may be analogous to the formation of the species labelled $\mathbf{B}^+$ in the electrochemical oxidation of **15**.

The nature of the precipitate that formed during these reactions remains uncertain. It was found to be insoluble in methanol but dissolved in sodium hydroxide ($0.1 molL^{-1}$), suggesting an acidic nature. The ^{31}P nmr spectrum of the precipitate dissolved in sodium hydroxide contained two phosphorus signals, at 28ppm and 44ppm each split into a doublet ($^1J_{P-H}$ of 509Hz and 458Hz respectively) revealing the presence of a single P-H bond.

5.3: Synthesis of Oxidised Derivatives of $FcCH_2PH_2$ 15

Primary phosphine oxides $R\text{-}P(O)H_2$, phosphinic acids R-P(O)(OH)H and phosphonic acids $R\text{-}PO_3H_2$ are the principal oxidation products of primary phosphines. There exists a large body of literature dealing with phosphinic and phosphonic acids, as these compounds tend to be stable crystalline solids. Much less published material exists concerning the chemistry of primary phosphine oxides, as these are reactive compounds prone to further oxidation and thermally unstable. Primary phosphine oxides were originally prepared by controlled oxidation of primary phosphines with ketones[3]. More recently it has been found that some stable primary phosphines such as 2,4,6-tri-*t*-butylphenyl phosphine can undergo oxidation with hydrogen peroxide and give primary phosphine oxides as the sole product[4].

From the simple oxidation experiments discussed in the previous section, it seemed that the ferrocenyl phosphine oxide $FcCH_2P(O)H_2$ **26** could be prepared in high yield by controlled oxidation of $FcCH_2PH_2$ **15** with hydrogen peroxide (Scheme 5.2).

The reaction of **15** with a three molar excess of hydrogen peroxide was undertaken in thf. After ten minutes the reaction solution was introduced into 10ml of

[3] S. A. Buckler and M. Epstein, *J. Am. Chem. Soc.*, 1960, **82**, 2076.
[4] M. Yoshifuji, K. Shibayama, K. Toyota and N. Inamoto, *Tetrahedron Lett.*, 1983, **24**, 4227.

a two phase water/CH_2Cl_2 system. The layers were separated and the organic solvent removed to give nearly pure $FcCH_2P(O)H_2$ **26** as a yellow powder with a strong odour.

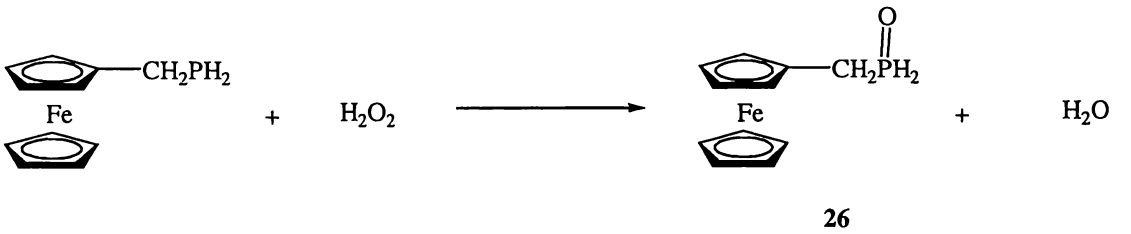

26

Scheme 5.2: Synthesis of $FcCH_2P(O)H_2$ **26**.

Amenable to purification by silica flash column chromatography, **26** proved to be soluble in polar organic solvents and stable in air for long periods. Thermally stable with a defined melting point, the phosphine oxide **26** did undergo slow oxidation in the solution state to give a mixture of the phosphine oxide and phosphinic acid. Characterisation by nmr was routine with the $^{31}P\text{-}\{^1H\}$ spectrum being particularly distinctive (Figure 5.4).

The signal at 9.7ppm is split into a triplet ($^1J_{P\text{-}H}$ 470Hz) of triplets ($^2J_{P\text{-}H}$ 16Hz) by the PH_2 and CH_2 protons respectively. The chemical shift and $^1J_{P\text{-}H}$ values are similar to those observed for other primary phosphine oxides such as 2,4,6-tri-*t*-butylphenylphosphine oxide (-10ppm, $^1J_{P\text{-}H}$ 490Hz)[4] and endo-8-camphanylphosphine oxide (9.2ppm, $^1J_{P\text{-}H}$ 416Hz)[5].

[5] R. A. Berrigan, D. K. Russell, W. Henderson, M. T. Leach, B. K. Nicholson, G. Woodward and C. Harris, *N. J. Chem.*, 2000, **24**, 1.

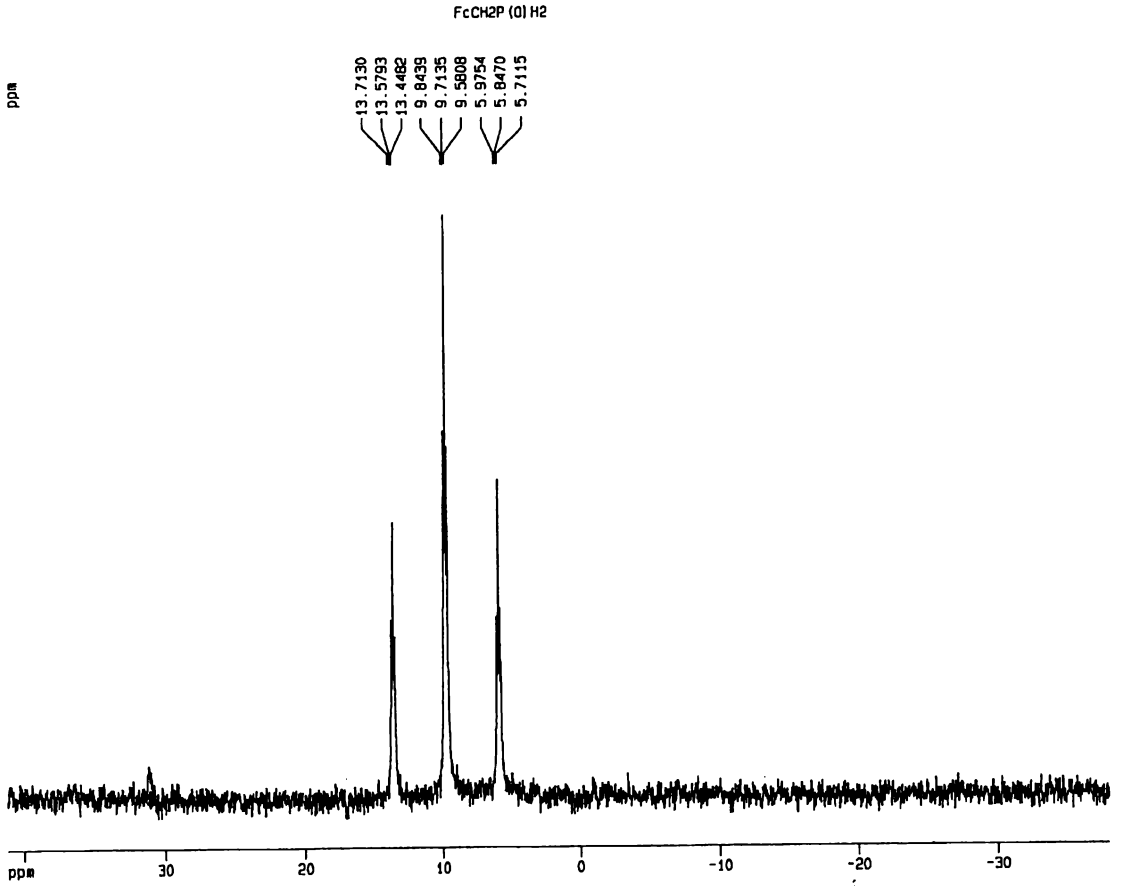

Figure 5.4: Proton Coupled ^{31}P NMR Spectrum of $FcCH_2P(O)H_2$ **26**.

Under positive ion ESMS conditions the $[M+H^+]^+$ (*m/z* 249) ion was observed, but spectra were dominated by a peak at *m/z* 266 assigned to $[M+NH_4^+]^+$. The source of the ammonium ion is acetonitrile that had been previously used as the carrier solvent.

Direct oxidation of the primary phosphine $FcCH_2PH_2$ **15** seemed unlikely to provide a straightforward synthesis of the ferrocenyl phosphinic acid $FcCH_2P(O)(OH)H$ **27**. For this reason the ferrocenyl phosphinic acid $FcCH_2P(O)(OH)H$ **27** was prepared via the ferrocenyl chlorophosphine $FcCH_2PCl_2$. Chlorophosphines are reactive compounds easily prepared from primary phosphines by the action of phosgene[6] and react with water to give phosphinic acids[7]. The ferrocenyl chlorophosphine $FcCH_2PCl_2$ was synthesised by reaction of **15** with

[6] L. Maier, *Helv. Chim. Acta.*, 1963, **46**, 1812.
[7] G. M. Kosolapoff and J. S. Powell, *J. Am. Chem. Soc.*, 1950, **72**, 4291.

triphosgene [bis-(trichloromethyl) carbonate], a solid crystalline compound that provides an easily handled substitute for phosgene[8] (Scheme 5.3). This reaction was followed by ^{31}P nmr and involved a large change in chemical shift from *ca.* -130ppm to 175ppm as the bright yellow chlorophosphine forms (Figure 5.5). Though not fully characterised, $FcCH_2PCl_2$ was found to be remarkably stable in air. Samples left in air slowly became green over a period of several weeks and ^{31}P nmr of these samples revealed the presence of the phosphinic acid.

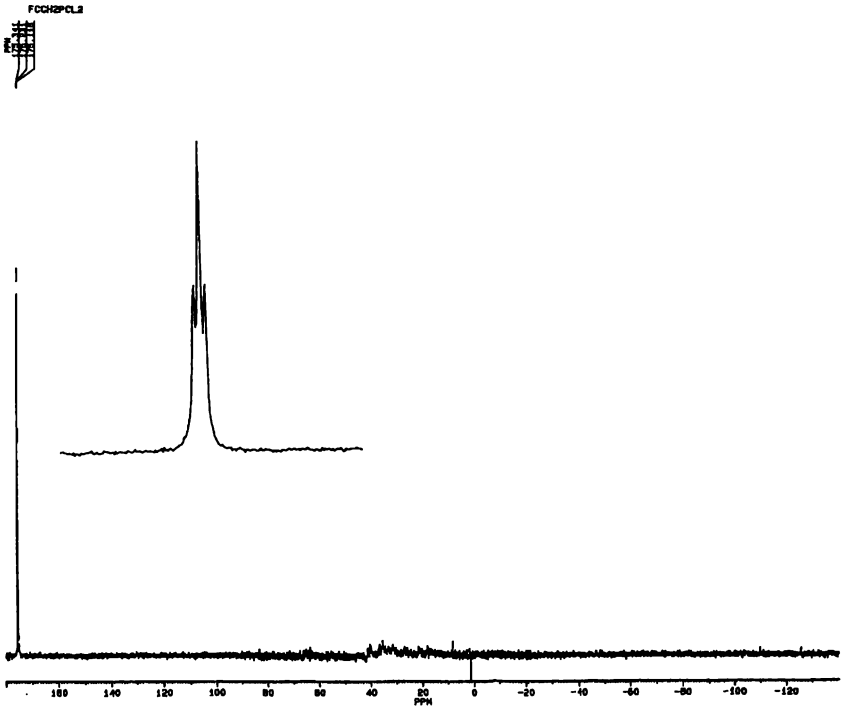

Figure 5.5: Proton Coupled ^{31}P NMR Spectrum of $FcCH_2PCl_2$. Inset: Expansion of the Region 170-180ppm.

Reaction of the ferrocenyl chlorophosphine with water led to the ferrocenyl phosphinic acid $FcCH_2P(O)(OH)H$ **27** (Scheme 5.3).

[8] P. R. M. Muller, *Spec. Chem.*, 1994, **14**, 357.

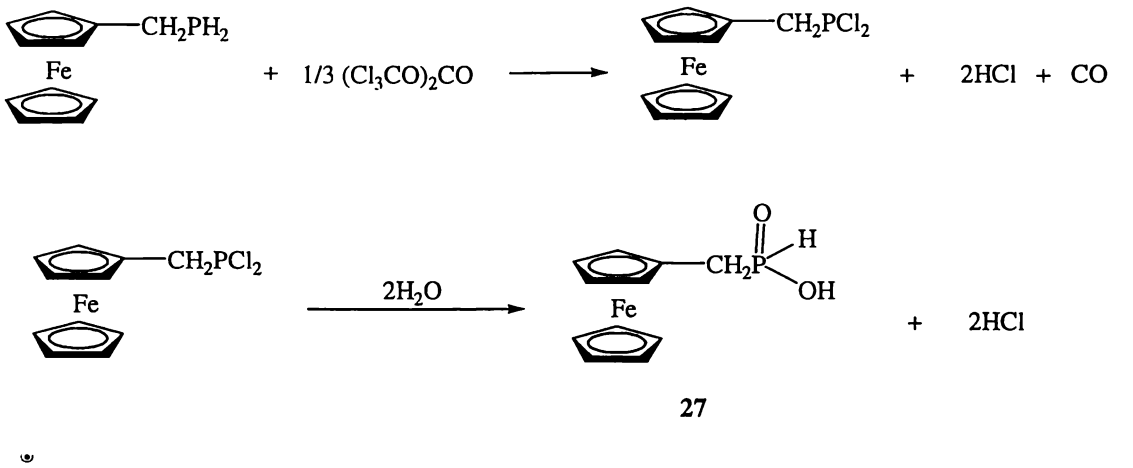

Scheme 5.3: Synthesis of $FcCH_2P(O)(OH)H$ **27**.

The ferrocenyl phosphinic acid **27** is an odourless, air-stable crystalline solid, soluble in polar organic solvents and aqueous base. This compound was routinely characterised by nmr and ESMS. The negative ion ES mass spectrum of **27** was dominated by the $[M\text{-}H^+]^-$ and $[2M\text{-}H^+]^-$ ions at *m/z* 263 and *m/z* 527 respectively. The negative ion ES mass spectrum of **27** at a cone voltage of 60V is given in Figure 5.6.

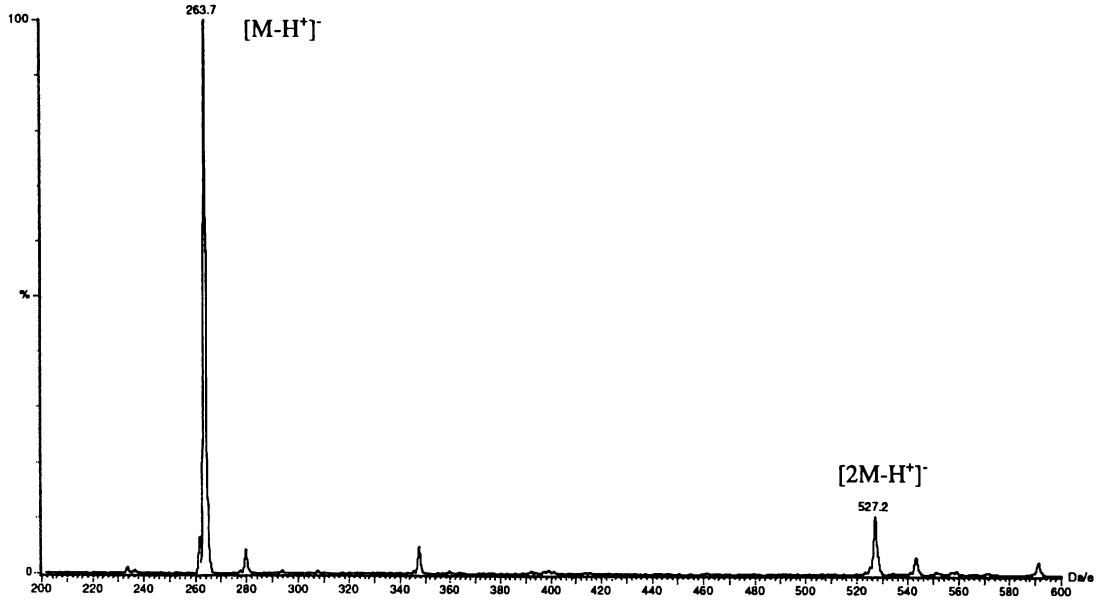

Figure 5.6: The Negative Ion ES Mass Spectrum of $FcCH_2P(O)(OH)H$ **27** at a Cone Voltage of 60V.

5.4: Concluding Remarks

The chemical oxidation of $FcCH_2PH_2$ **15** proceeds smoothly to give the primary phosphine oxide **26** in high yield. Further oxidation results in the formation of a compound possessing a single P-H bond which is not the phosphinic acid $FcCH_2P(O)(OH)H$ **27**. Further oxidation to give the phosphonic acid is complicated by the oxidation of the ferrocene group to the ferricinium ion. The primary phosphine oxide **26** is stable in air and has an odour strongly reminiscent of the parent primary phosphine. The stability of this compound and the intermediate $FcCH_2PCl_2$ in air suggests that stabilisation of air sensitive phosphorus centres by ferrocene may be a general phenomenon. The phosphinic acid **27** is easily prepared from $FcCH_2PCl_2$ by reaction with water.

5.5: Experimental

The ferrocenyl primary phosphine **15** was synthesised using the method described in chapter four. Samples were purified by sublimation prior to use. Triphosgene (Aldrich) was used as supplied. Hydrogen peroxide (Andrew Chemicals 27%w/v) was diluted threefold to a concentration of $3.16 molL^{-1}$ and standardised by titration with a freshly prepared standard solution of aqueous $KMnO_4$. Methanol used as a solvent in oxidation studies was singly distilled and placed under a dinitrogen atmosphere before use.

Electrospray mass spectrometry of **26** was carried out in the positive ion mode. ESMS of **27** was carried out in the negative ion mode. Samples of each compound were introduced to the ES mass spectrometer dissolved in methanol and methanol was used as the carrier solvent.

5.5.1: Oxidation Reactions

A typical oxidation reaction was undertaken as follows:

$FcCH_2PH_2$ **15** (0.0058g, 0.025mmol) was placed in an nmr tube and put under a dinitrogen atmosphere. Methanol (0.4ml) was then added, the tube was capped and the T = 0 ^{31}P-{^{1}H} spectrum acquired. Aqueous H_2O_2 (0.008ml, 0.025mmol, 3.16moll^{-1}) was then added and the time delayed ^{31}P-{^{1}H} spectra were acquired. Each spectrum was acquired by combining sixteen scans over a sweep width of 50000Hz to ensure the full range of phosphorus signals were observed. Samples were referenced with respect to an external reference of 85% orthophosphoric acid and locked and shimmed using a D_2O lock stick. The mole ratios and amounts of phosphine and peroxide used in these experiments are given in Table 5.1.

Table 5.1: Mole Ratios and Quantities Used in $FcCH_2PH_2$ Oxidation Reactions.

Mole Ratio (H_2O_2:Phosphine)	Weight of $FcCH_2PH_2$ (mg)	Volume of H_2O_2* (ml)
1:1	5.8	0.008
2:1	5.0	0.014
3:1	4.8	0.020
4:1	6.1	0.033
5:1	4.8	0.033
10:1	5.1	0.070

C = 3.16molL^{-1}

5.5.2: Syntheses

5.5.2.1: Synthesis of $FcCH_2P(O)H_2$ **26**

Hydrogen peroxide (0.33ml, 3.16molL^{-1}, 1.1mmol) was added to a solution of $FcCH_2PH_2$ **15** (0.08g, 0.36mmol) in thf (2ml). After 10 minutes water (10ml) and CH_2Cl_2 (10ml) was added and the layers separated. The aqueous layer was extracted with a further 10ml of CH_2Cl_2. The combined organic fractions were washed with aqueous sodium hydroxide (10ml, 0.1molL^{-1}) and water (10ml), before being dried ($MgSO_4$) and the solvent removed. The residue, a yellow powder, was further purified by silica flash column chromatography using a CH_2Cl_2 to methanol solvent gradient.

The desired product was eluted with 5% methanol in CH_2Cl_2 and the solvent removed to give 0.049g (66%) of **26** as a crystalline yellow powder.

m.p. 88-90°C.

Elemental Analyses: Found C, 54.35%; H, 5.58%. Calculated For $C_{11}H_{13}FeO_1P$: C, 53.26%; H, 5.28%.

^{31}P-{^1H} NMR ($CDCl_3$): δ 9.92 (*t/t.* $^1J_{P-H}$ 470Hz, $^2J_{H-H}$ 16Hz).

^{13}C-{^1H} NMR ($CDCl_3$): δ 28.82 (*d*, $^1J_{P-C}$ 62Hz, $\underline{C}H_2P$), 68.69 (*s*, C3), 68.93 (*d*, $^3J_{P-C}$ 4Hz, C2), 69.08 (*s*, C4).

^1H NMR ($CDCl_3$): δ 3.14 (2H, *d/t*, $^2J_{P-H}$ 16Hz, $^3J_{H-H}$ 4.5Hz, $C\underline{H}_2P$), 4.16 (9H, *br.s.*, H2,H3,H4), 6.89 (2H, *d/t*, $^1J_{P-H}$ 470Hz, $^3J_{H-H}$ 4.8Hz, $P\underline{H}_2$).

ESMS: (MeOH, c.v. +20V) *m/z* 266 ($[M+NH_4^+]^+$, 100%) 249 ($[M+H^+]^+$, 36%).

5.5.2.2: Synthesis of $FcCH_2P(O)(OH)H$ **27**

A solution of triphosgene (0.144g, 0.48mmol) in CH_2Cl_2 (5ml) was placed under a dinitrogen atmosphere. To this was added a solution of **15** (0.1689g, 0.72mmol) in CH_2Cl_2 (5ml) and the reaction brought to reflux. After 1 hour the ^{31}P nmr showed the reaction to be complete. The solvent was removed to give $FcCH_2PCl_2$ as a bright yellow powder.

^{31}P-{^1H} NMR ($CDCl_3$): δ 175.23 (*t.*, $^2J_{P-H}$ 13.3Hz).

Water (10ml) was added to the dry chlorophosphine and the mixture stirred for eight hours. The solution was then made basic by addition of aqueous sodium hydroxide (5ml, $1molL^{-1}$). The aqueous phase was washed with CH_2Cl_2 (2 × 10ml) before being acidified by the addition of concentrated HCl. The aqueous phase was then extracted with CH_2Cl_2 (2 × 10ml), the combined organic fractions were dried over $MgSO_4$ and the solvent removed to give 0.12g (62%) of **27** as a pale yellow powder.

m.p. 148-152°C dec.

Elemental Analyses: Found C, 50.11%; H, 5.07%. Calculated For $C_{11}H_{13}FeO_2P$: C, 50.04%; H, 4.96%.

^{31}P-{^1H} NMR ($CDCl_3$): δ 35.54 (*d/t.*, $^1J_{P-H}$ 555Hz, $^2J_{P-H}$ 14Hz).

^{13}C-{^1H} NMR ($CDCl_3$): δ 31.81 (*d*, $^1J_{C-P}$ 89Hz, $\underline{C}H_2P$), 68.38 (*s*, C3), 68.98 (*s*, C4), 69.32 (*br. s*, C2), C1 not observed.

^1H NMR ($CDCl_3$): δ 2.88 (2H, *d*, $^2J_{P-H}$ 15Hz, $C\underline{H}_2P$), 4.12-4.22 (9H, *m*, H2/H3/H4), 6.98 (1H, *d*, $^1J_{P-H}$ 552Hz, $P\underline{H}$).

ESMS: (MeOH, c.v. -60V) *m/z* 263 ([M-H^+]$^-$, 100%), 527 ([2M-H^+]$^-$ 9%).

Chapter 6: Synthesis and Characterisation of Ferrocenyl Hydroxymethylphosphines

6.1: Introduction

Hydroxymethylphosphines can be defined as phosphine compounds containing at least one P-CH_2OH group. Tending to be water soluble, these compounds, which can be considered as derivatives of tris-hydroxymethylphosphine ($P(CH_2OH)_3$[1]), possess a wide range of useful chemical properties. An indication of the types of reactions available to hydroxymethylphosphines is given in Scheme 6.1.

Reaction with: Alkyl halides.

$$P(CH_2OH)_3 + RX \longrightarrow [RP(CH_2OH)_3]^+X^-.\ (R= H, Alkyl)^2$$

Activated Olefins[3].

$$P(CH_2OH)_3 + CH_2{=}CHCN \longrightarrow P(CH_2CH_2CN)_3{}^4$$

$$P(CH_2OH)_3 + CH_2{=}CHC(O)OH \longrightarrow P(CH_2CH_2C(O)OH)_3$$

$$P(CH_2OH)_3 + CH_2{=}CHC(O)OR \longrightarrow P(CH_2CH_2C(O)OR)_3$$

$$P(CH_2OH)_3 + CH_2{=}CHC(O)NH_2 \longrightarrow P(CH_2CH_2C(O)NH_2)_3$$

Epoxides.

$$R\text{-}P(CH_2OH)_2 + \underset{\diagup\ \diagdown}{CH_2\text{-}CH_2}\,O \longrightarrow R\text{-}P(CH_2CH_2OH)_2{}^5$$

Isocyanates.

$$R\text{-}P(CH_2OH)_2 + Ph\text{-}N{=}C{=}O \longrightarrow R\text{-}P(CH_2OC(O)\text{-}NH\text{-}Ph)_2{}^6$$

---

[1] M. Reuter and L. Orthner, *Chem. Abs.*, 1960, **54**, 14125a.
[2] (a) R. K. Valetdinov, E. V. Kuznetsov, R. R. Belova, R. K. Mukhaeva, T. I. Malykhina and M. K. Khasanov, *Zh. Obshch. Khim.*, 1967, **37**, 2269. (b) R. K. Valetdinov, E. V. Kuznetsov, M. R. Rakhimova and M. K. Khasanov, *Zh. Obshch. Khim.*, 1967, **37**, 2522.
[3] A. Avery, D. M. Schut, T. J. R. Weakley and D. R. Tyler, *Inorg. Chem.*, 1993, **32**, 233.
[4] S. L. Komissarova, R. K. Valetdinov and E. V. Kuznetsov, *Zh. Obshch. Khim.*, 1971, **41**, 322.
[5] R. K. Valetdinov, S. I. Zaripov and F. Kazan, *Zh. Obshch. Khim.*, 1974, **44**, 1440.
[6] R. K. Valetdinov, S. I. Zaripov, M. K. Khasanov and F. Kazan, *Zh. Obshch. Khim.*, 1973, **43**, 1029.

Amines/Ureas.

$P(CH_2OH)_3 + R_1R_2NC(O)NH_2 \longrightarrow P(CH_2NHC(O)NR_1R_2)_3$[7]

$P(CH_2OH)_3 + R_2NH \longrightarrow P(CH_2NR_2)_3$[8]

Silyl halides.

$P(CH_2OH)_3 + R_3SiCl \longrightarrow P(CH_2OSiR_3)_3$[9]

Scheme 6.1: Some Representative Reactions of Hydroxymethylphosphines.

With such a wide range of synthetic options available it is not surprising that a large number of hydroxymethylphosphines and hydroxymethylphosphine derivatives have precedent in the published literature. A selection of these compounds is given in Figure 6.1.

Hydroxymethylphosphines and hydroxymethylphosphine derivatives have found applications in many different fields of chemistry. They are important in the textile industry for the production of flame retardant materials[10], they have been used to tan leathers[11], style hair[12] and tether enzymes[13] and metal complexes[14] to solid supports. Increasingly they are being used as ligands in co-ordination chemistry, an aspect of hydroxymethylphosphine chemistry that will be discussed in later sections.

---

[7] A. B. Pepperman, D. J. Daigle and S. L. Vail, *J. Org. Chem.*, 1976, **41**, 675.

[8] (a) D. J. Daigle, A. B. Pepperman and W. A. Reeves, *Text. Res. J.*, 1971, **41**, 944. (b) G. Maerkl and G. Y. Jin, *Tetrahedron Lett.*, 1981, **22**, 1105. (c) Y. A. Dorfman, L. V. Levina and L. I. Grekov, *Zh. Obshch. Khim.*, 1994, **64**, 1266. (d) J. G. E. Krauter and M. Beller, *Tetrahedron*, 2000, **56**, 771.

[9] (a) Y. Nagao and H. Sakurai, *Chem. Lett.*, 1976, **4**, 379. (b) V. M. Dyakov, N. M. Kudyakov, M. G. Voronkov, R. K. Valetdinov and V. I. Glukhikh, *Zh. Obshch. Khim.*, 1979, **49**, 800. (c) M. G. Voronkov, N. M. Kudyakov, V. M. Dyakov, V. I. Glukhikh and R. K. Valetdinov, *Dokl. Akad. Nauk.*, 1979, **247**, 609.

[10] (a) A. W. Frank, D. J. Daigle and S. L. Vail, *Text. Res. J.*, 1982, **52**, 678. (b) D. J. Daigle, A. B. Pepperman, G. L. Drake and W. A. Reeves, *Text. Res. J.*, 1972, **42**, 347.

[11] G. R. Collins, C. R. Jones, R. E. Talbot J. Williams and M. Zakikhani, 1998 Patent Application: WO 98-EP6837 19981028.

[12] L. J. Wolfram, *J. Soc. Cosmet. Chem.*, 1969, **20**, 539.

[13] (a) P. R. Oswald, R. A. Evans, W. Henderson, R. M. Daniel and C. J. Fee, *Enzyme Microb. Tech.*, 1998, **23**, 14. (b) F. C. Cochrane, H. H. Petach and W. Henderson, *Enzyme Microb. Tech.*, 1996, **18**, 373. (c) W. Henderson, H. H. Petach and L. S. Bonnington, *Eur. Polym. J.*, 1995, **31**, 981.

[14] (a) T. Shido, T. Okazaki and M. Ichikawa, *J. Catal.*, 1995, **157**, 436. (b) T. Shido, T. Okazaki and M. Ichikawa, *Catal. Lett.*, 1993, **20**, 37.

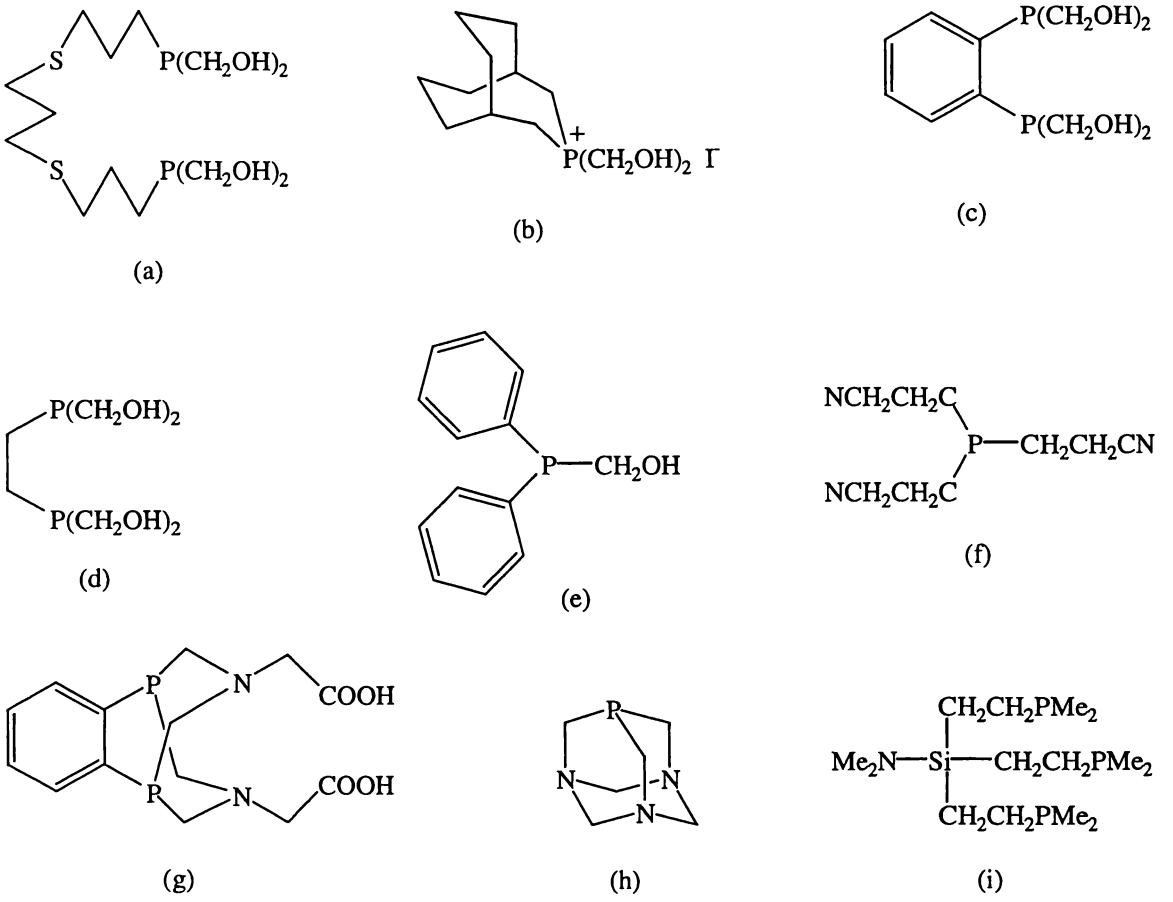

Figure 6.1: Representative Hydroxymethyl Phosphines (a)-(e) and Hydroxymethylphosphine Derivatives (f)-(i). Literature References, (a)[15], (b)[16], (c) and (d)[17], (e)[18], (f)[19], (g)[20], (h)[21], (i)[22].

The first ferrocenyl hydroxymethylphosphine, $FcCH_2P(CH_2OH)_2$ and its derivatives were synthesised in 1996[23] (Scheme 6.2). The ferrocenyl hydroxymethylphosphine was air stable but otherwise reacted as expected.

---

[15] C.J. Smith, N. Li, K. V. Katti, C. Higginbotham and W. A. Volkert, *Nucl. Med. Biol.*, 1997, **24**, 685.
[16] J. Fawcett, P. A. T. Hoye, R. D. W. Kemmit, D. J. Law and D. R. Russell, *J. Chem. Soc., Dalton Trans.*, 1993, 2563.
[17] D. E. Berning, K. V. Katti, C. L. Barnes, W. A. Volkert and A. R. Ketring, *Inorg. Chem.*, 1997, **36**, 2765.
[18] M. Grayson, *J. Am. Chem. Soc.*, 1963, **85**, 19.
[19] M. M. Rauhut, I. Hechenbleikner, H. A. Currier, F. C. Schaefer and V. P. Wystrach, *J. Am. Chem. Soc.*, 1959, **81**, 1103.
[20] D. E. Berning, K. V. Katti, C. L. Charles and W. A. Volkert, *J. Am. Chem. Soc.*, 1999, **121**, 1658.
[21] D. J. Daigle, A. B. Pepperman and S. L. Vail, *J. Heterocycl. Chem.*, 1974, **11**, 407.
[22] J. Grobe and R. Wehmschulte, *Z. Anorg. Allg. Chem.*, 1993, **619**, 563.
[23] N. J. Goodwin, W. Henderson, B. K. Nicholson, J. K. Sarfo, J. R. Fawcett and D. R. Russell, *J. Chem. Soc., Dalton Trans.*, 1997, 4377.

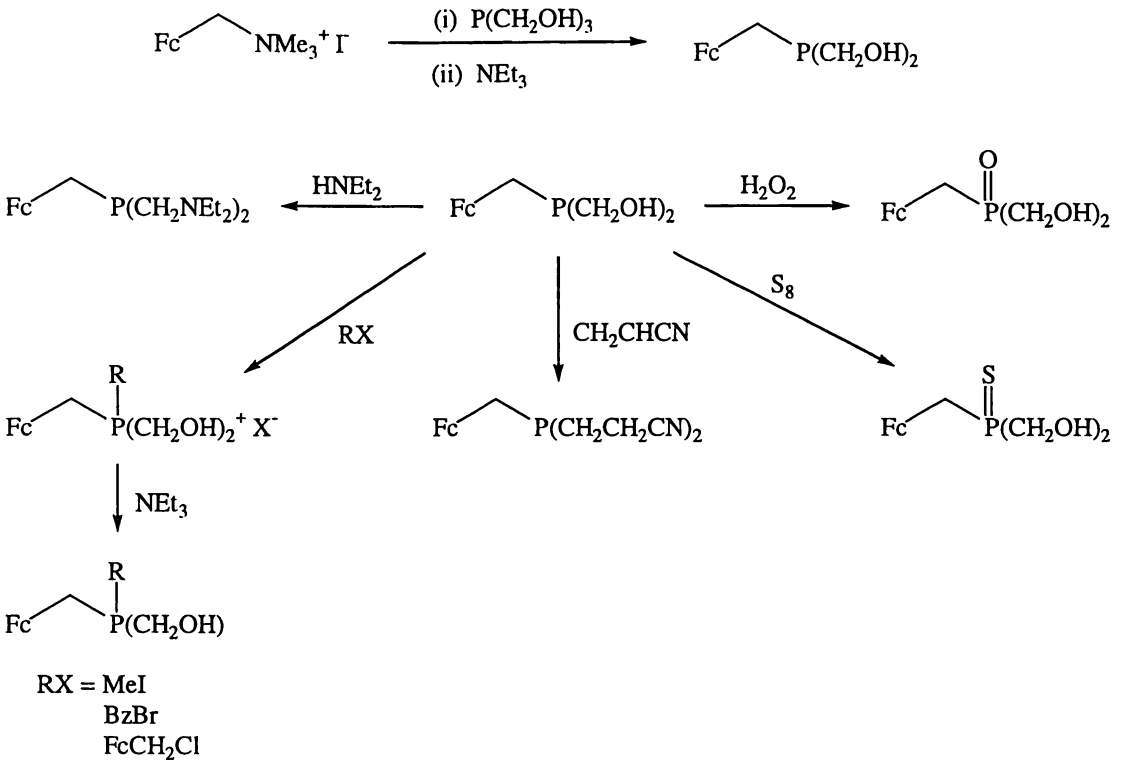

Scheme 6.2: Synthesis and Derivatives of $FcCH_2P(CH_2OH)_2$.

In a separate study, cyclophosphazene ($N_3P_3F_6$) derivatives of the ferrocenyl hydroxymethylphosphine sulfide $FcCH_2P(S)(CH_2OH)_2$ were prepared and their chemistry investigated[24]. The reaction of dilithiated $FcCH_2P(S)(CH_2OH)_2$ with $N_3P_3F_6$ gave exclusively ansa-substituted, endo- and exo-$FcCH_2P(S)(CH_2O)_2[P(F)N]_2(F_2PN)$. These transformed into the spiro-substituted analogue in the presence of fluoride. Alternatively the spiro-substituted compound was accessible via a siloxy ether intermediate, (Scheme 6.3).

[24] K. Muralidharan, N. D. Reddy and A. J. Elias, *Inorg. Chem.*, 2000, **39**, 3988.

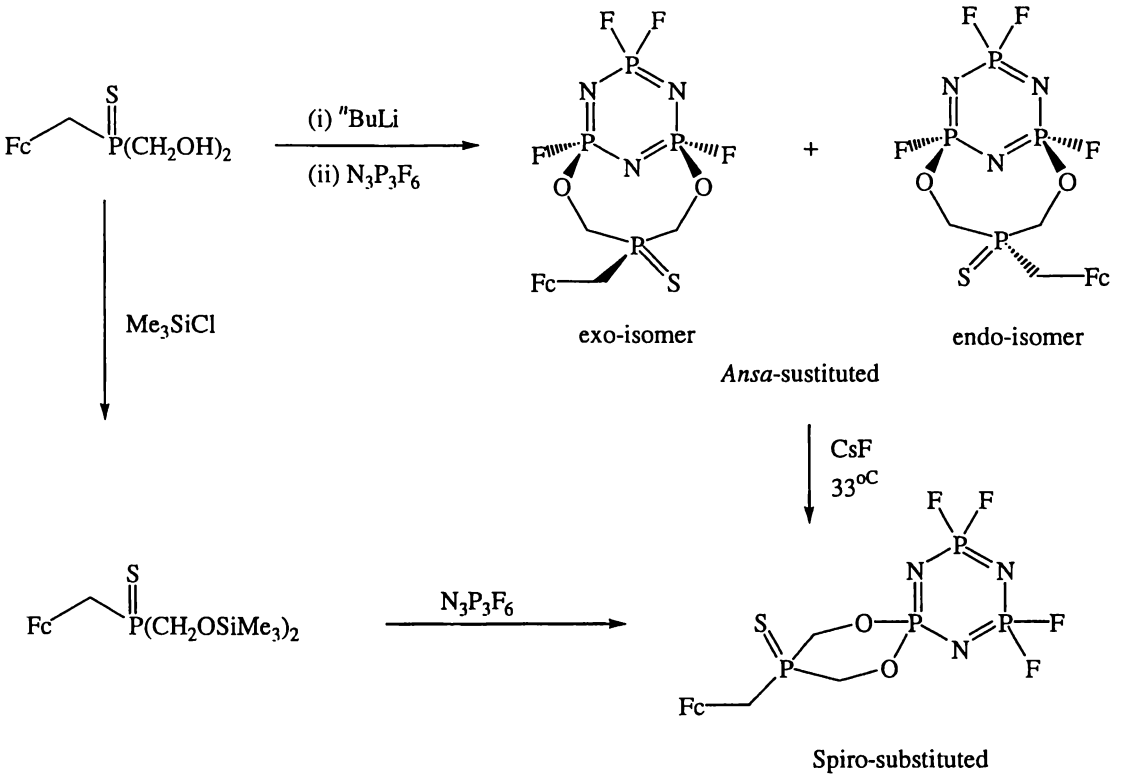

Scheme 6.3: Reactions of $FcCH_2P(S)(CH_2OH)_2$ with $N_3P_3F_6$.

A related chiral (but racemic) ferrocenyl hydroxymethylphosphine $FcCH(CH_3)P(CH_2OH)_2$ has recently been reported. This compound, synthesised using the method outlined in Scheme 6.2 for $FcCH_2P(CH_2OH)_2$, was used as the starting material for a number of derivatives[25] (Scheme 6.4).

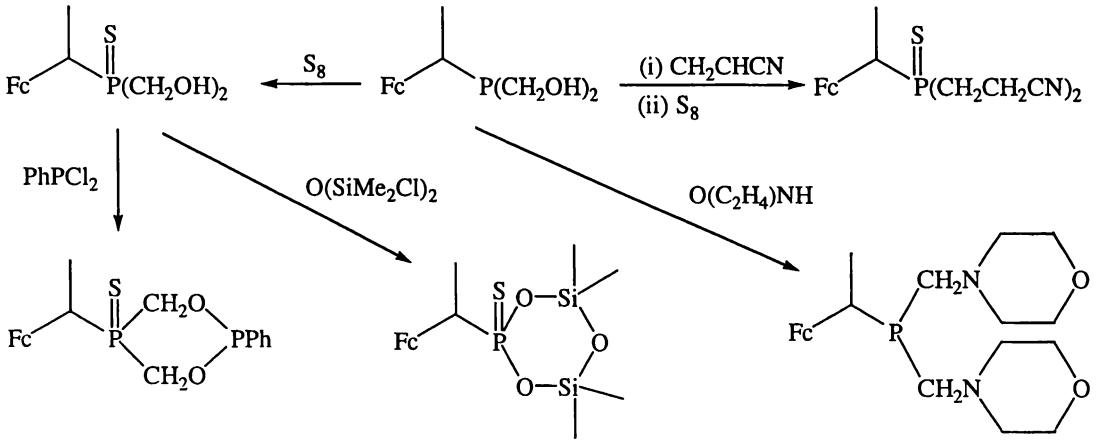

Scheme 6.4: Derivatives of $FcCH(CH_3)P(CH_2OH)_2$.

The primary goal of the work presented in this chapter was to extend the field of ferrocenyl hydroxymethylphosphine chemistry, with especial interest in hydroxymethylphosphine analogues of dppf.

6.2: Synthesis and Characterisation of Novel Ferrocenyl Hydroxymethyl Phosphines

Hydroxymethyl phosphines are easily prepared from primary phosphines by formylation. Formaldehyde[26] and paraformaldehyde[27] react smoothly and reversibly with P-H bonds at standard temperature and pressure to give P-CH_2OH groups in a quantitative yield. (Scheme 6.5). This reaction is subject to catalysis by a number of metal complexes[1,28].

$$R\text{-}PH_2 + 2CH_2O \longrightarrow R\text{-}P(CH_2OH)_2$$

Scheme 6.5: Synthesis of Hydroxymethylphosphines from Primary Phosphines.

A second synthetic approach relies on the chemical manipulation of existing precursors such as $P(CH_2OH)_4^+Cl^-$. This stable phosphonium salt, widely used in the textile industry under the name tetrakis, provides a convenient starting material in the synthesis of many hydroxymethyl phosphines. The course of a typical synthesis from $P(CH_2OH)_4^+Cl^-$ is given in Scheme 6.6.

$$P(CH_2OH)_4^+Cl^- + KOH \longrightarrow P(CH_2OH)_3 + KCl + CH_2O + H_2O$$

$$P(CH_2OH)_3 + R\text{-}X \longrightarrow R\text{-}P(CH_2OH)_3^+X^- \quad (R = \text{Alkyl}, X = \text{Halide})$$

$$R\text{-}P(CH_2OH)_3^+X^- + NEt_3 \longrightarrow R\text{-}P(CH_2OH)_2 + CH_2O + HNEt_3^+X^-$$

Scheme 6.6: Synthesis of Hydroxymethylphosphines from $P(CH_2OH)_4^+Cl^-$.

---

[25] T. V. V. Ramakrishna, A. J. Elias and A. Vij, *J. Organomet. Chem.*, 2000, **602**, 125.
[26] (a) C. J. Smith, V. S. Reddy and K. V. Katti, *Chem. Commun.*, 1996, 2557. (b) C. J. Smith, V. S. Reddy, S. R. Karra, K. V. Katti and L. J. Barbour, *Inorg. Chem.*, 1997, **36**, 1786.
[27] R. Bartsch, S. Hietkamp, S. Morton, H. Peters and O. Stelzer, *Inorg. Chem.*, 1983, **22**, 3624.
[28] (a) L. N. Harrison, P. A. T. Hoye, A. G. Orpen, P. G. Pringle and M. B. Smith, *J. Chem. Soc., Chem. Commun.*, 1989, 1096. (b) P. A. T. Hoye, P. G. Pringle, M. B. Smith and K. Worboys, *J. Chem. Soc., Dalton Trans.*, 1993, 269.

The primary phosphines $FcPH_2$ **16** and 1,1'-Fc'$[PH_2]_2$ **17**, whose preparation was detailed in chapter four, were reacted with excess formaldehyde to give the analogous hydroxymethylphosphines $FcP(CH_2OH)_2$ **28**, and 1,1'-Fc'$[P(CH_2OH)_2]_2$ **29** in high yield, Scheme 6.7. The use of excess formaldehyde led to the initial formation of several products, presumed to be $P[(CH_2O)_nH]_2$ adducts. Exposure of the crude reaction mix to a dynamic vacuum (~1mmHg) over twenty-four hours resulted in the desired hydroxymethyl phosphines as the sole product.

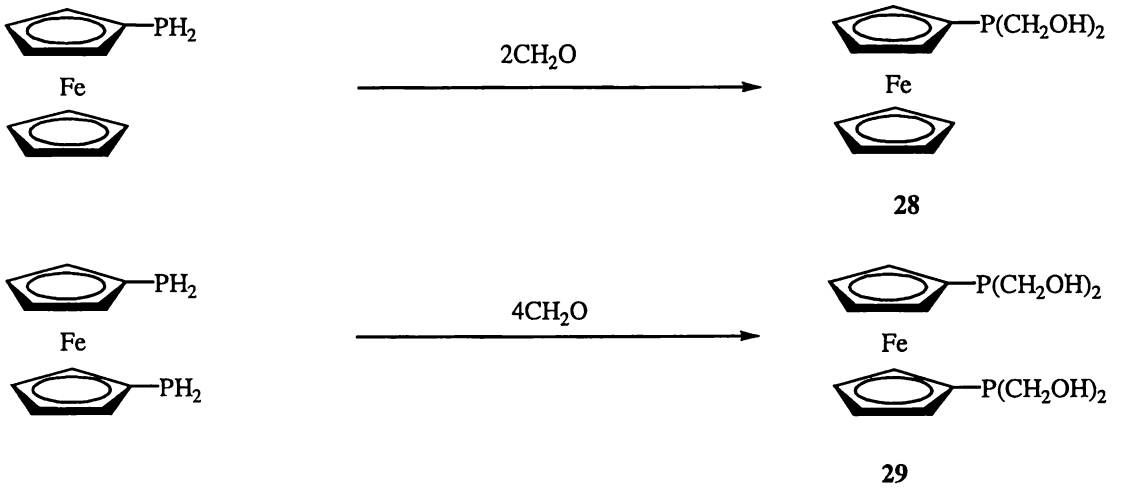

Scheme 6.7: Syntheses of $FcP(CH_2OH)_2$ **28**, and 1,1'-Fc'$[P(CH_2OH)_2]_2$ **29**.

The hydroxymethylphosphine **28** was isolated as a brown crystalline powder that was soluble in polar organic solvents and indefinitely stable in air. This was in marked contrast to the reactivity toward oxygen in air of the parent phosphine $FcPH_2$ **16**.

The hydroxymethylphosphine 1,1'-Fc'$[P(CH_2OH)_2]_2$ proved difficult to obtain in a crystalline form, rather it was isolated as a brown tar. Though **29** was more stable than the analogous primary phosphine 1,1'-Fc'$[PH_2]_2$ **17**, oxidation/decomposition did occur upon exposure to air.

6.2.1: Characterisation of Ferrocenyl Hydroxymethyl Phosphines 28 and 29

The hydroxymethylphosphine $FcP(CH_2OH)_2$ **28** was characterised using the full suite of available techniques (nmr, ESMS, IR, and elemental analyses). The ^{13}C and ^{31}P nmr spectra were routine and assigned by inspection. The ^{1}H nmr spectrum revealed that the hydroxymethyl CH_2 protons were in unique environments with a geminal $^{2}J_{H\text{-}H}$ coupling constant of 13Hz. This was not observed in the ^{1}H nmr spectra of the related compounds $FcCH_2P(CH_2OH)_2$ and $FcCH_2P(S)(CH_2OH)_2$ which suggests that the proximity of the bulky ferrocene group is restricting rotation about the P-CH_2 bond.

The positive ion ES mass spectra of **28** were obtained in the presence of excess silver ions, which simplified the resulting spectra. At low cone voltages the spectra are dominated by peaks at *m/z* 663/665 which are assigned to the $[2M+Ag^+]^+$ ion. Raising the cone voltage leads to the appearance of peaks due to $[M+Ag^+]^+$ (*m/z* 385/387) and $[M]^+$ (*m/z* 278) as shown (Figure 6.2).

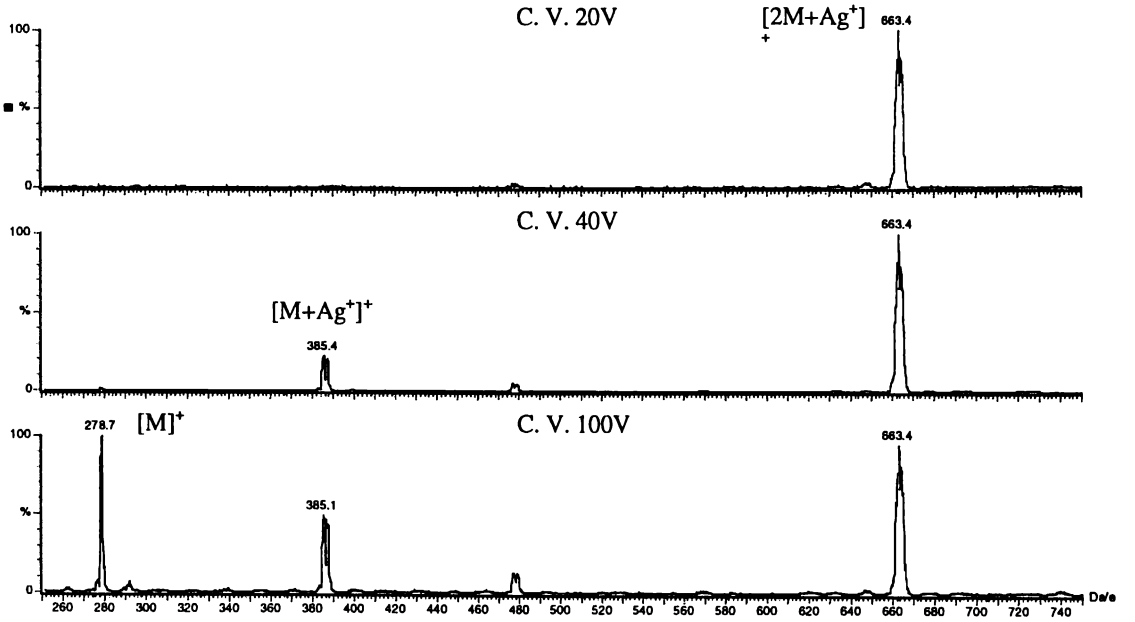

Figure 6.2: Variable Cone Voltage ES Mass Spectra of $FcP(CH_2OH)_2$ **28** in Methanol with Silver Ions Added to Aid Ionisation.

Characterisation of 1,1'-Fc' $[P(CH_2OH)_2]_2$ **29**, was achieved by nmr and ESMS only. The nmr spectra of **29** were routine and assigned by inspection. The positive ion ES mass spectra of **29**, obtained in the presence of silver ions, were dominated by peaks due to the $[2M+Ag^+]^+$ (*m/z* 847/849) and $[M+Ag^+]^+$ (*m/z* 477/479) ions, at low and high cone voltages respectively. The ES mass spectrum of **29** in methanol at a cone voltage of 60V is given in Figure 6.3.

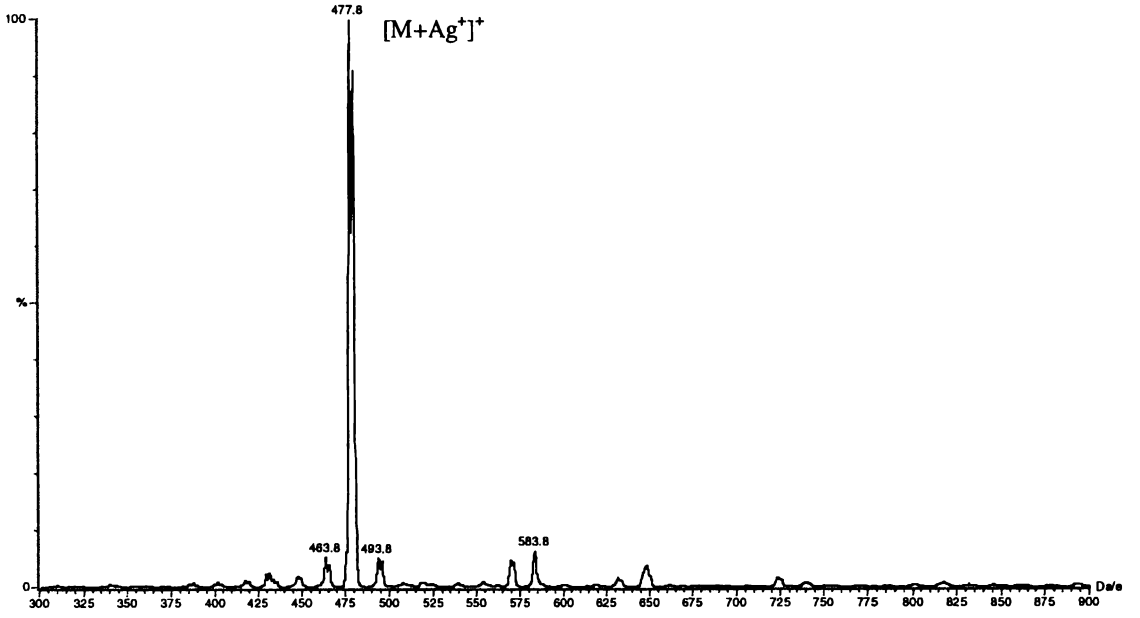

Figure 6.3: The ES Mass Spectrum of 1,1'-Fc'$[P(CH_2OH)_2]_2$ **29** in Methanol at a Cone Voltage of 60V. Silver Ions Added to aid Ionisation.

6.2.2: X-Ray Crystal Structure Determination for Compound $FcP(CH_2OH)_2$ 28

The crystal structure of **28** was of interest for comparison with the structure of $FcCH_2P(CH_2OH)_2$, especially comparison of the hydrogen bonding networks adopted by each compound. Single crystals of **28** suitable for X-ray analysis were grown by diffusion of pentane vapour into a CH_2Cl_2/MeOH (10:1) solution of **28** at -20°C.

The structure was solved from single crystal X-ray diffraction data by direct methods. All hydrogen atoms were found by inspection of the penultimate electron density map and all bond lengths and angles were within accepted ranges. Selected bond lengths and angles are given in Table 6.1, while structure diagrams of **28** are shown in Figure 6.4 and Figure 6.5.

Table 6.1: Selected Bond Lengths (Å) and Angles (°) for $FcP(CH_2OH)_2$ **28**.

Cp Fe-C av.	2.046(2)	C(1)-O(1)	1.425(2)
range	2.035-2.052	C(2)-O(2)	1.423(2)
Cp C-C av.	1.423(3)	O(1)-H(3)	0.6796
range	1.417-1.435	O(2)-H(4)	0.7158
C(11)-P(1)	1.809(2)	H(3)----O(2')	2.0061
P(1)-C(1)	1.849(2)	H(4)----O(1')	1.9526
P(1)-C(2)	1.850(2)		
C(11)-C(15) range	106.88(15)-108.41(17)	C(21)-C(25) range	107.82(18)-108.16(17)
C(12)-C(11)-P(1)	122.22(13)	P(1)-C(1)-O(1)	110.82(13)
C(15)-C(11)-P(1)	130.85(14)	C(1)-O(1)-H(3)	113.11
C(11)-P(1)-C(1)	99.18(8)	C(2)-O(2)-H(4)	106.00
C(11)-P(1)-C(2)	103.07(9)	O(1)-H(3)---O(2')	162.10
P(1)-C(2)-O(2)	115.83(13)	O(2)-H(4)---O(1')	179.16

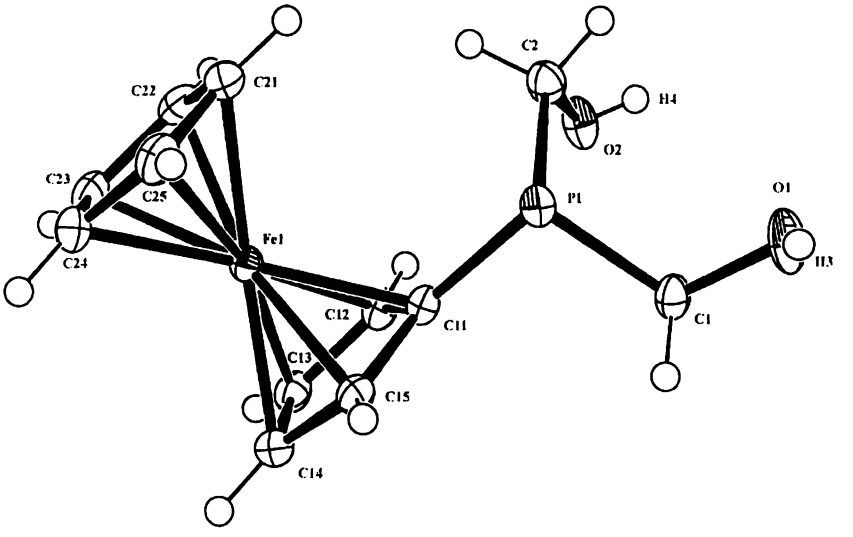

Figure 6.4: Ortep Diagram of $FcP(CH_2OH)_2$ **28** at the 50% probability level.

The hydrogen bonding network of **28** is very similar to that described for $FcCH_2P(CH_2OH)_2$. Each hydroxyl group acts as a hydrogen bond donor and acceptor.

The ferrocenyl hydroxymethylphosphine molecules are arranged into one dimensional chains, cross-linked by hydrogen bonds, running parallel to the *b* axis (Figure 6.5).

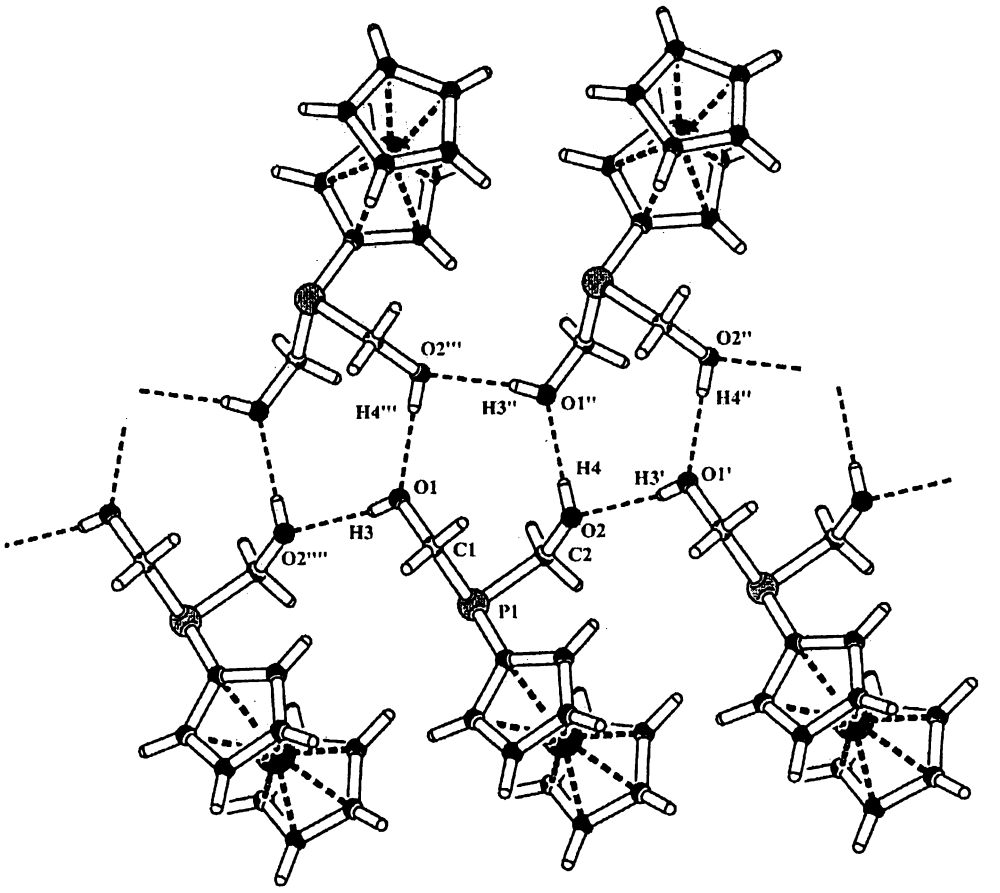

Figure 6.5: Platon Diagram Showing the Hydrogen Bonding in the Structure of $FcP(CH_2OH)_2$ **28**.

There are two distinct hydrogen bonds, H(4)---O(1) (1.95Å) which link two chains together and H(3)---O(2), (2.00Å), which link adjacent molecules in the same chain together. Each molecule is involved in hydrogen bonding interactions with four others. Similar hydrogen bond lengths (1.96Å and 1.94Å) were reported for hydrogen bonds in the structure of $FcCH_2P(CH_2OH)_2$. The two types of bond lead to the formation of ten-membered rings of the type, -O(1)-H(4)-O(2)-H(3)-O(1)-H(4)-O(2)-C(2)-P(1)-C(1)- between three adjacent molecules. The formation of such ten membered rings between three adjacent molecules was observed in the crystal structure of $FcCH_2P(CH_2OH)_2$.

6.2.3: Chalcogenide Derivatives of $FcP(CH_2OH)_2$ 28

Phosphines react readily with chalcogenides, O, S and Se to give the respective phosphine oxides, sulfides and selenides. These derivatives tend to be crystalline air stable compounds, useful in the characterisation of air sensitive phosphines.

The sulfide and oxide of the ferrocenyl hydroxymethylphosphine $FcCH_2P(CH_2OH)_2$ are known compounds (see Scheme 6.2). The oxide was prepared by reacting $FcCH_2P(CH_2OH)_2$ with hydrogen peroxide[23], while the sulfide was synthesised by reaction of the hydroxymethylphosphine with elemental sulfur in refluxing toluene[23,24]. Sulfur in refluxing toluene has also been used to prepare the ferrocenyl hydroxymethylphosphine sulfide $FcCH(CH_3)P(S)(CH_2OH)_2$ (see Scheme 6.3)[25].

The novel ferrocenyl hydroxymethylphosphine oxide $FcP(O)(CH_2OH)_2$ **30**, was prepared from the parent hydroxymethylphosphine by reaction with an equi-molar amount of hydrogen peroxide, (Scheme 6.8). The reaction proceeded smoothly at room temperature and was conveniently monitored by ^{31}P nmr. The oxide **30** is a yellow crystalline solid, stable in air and soluble in methanol, DMSO and water. The melting point of the oxide was not clearly defined. At temperatures above 160°C the crystals appear to evolve gas, before loss of crystallinity at 171-176°C. The gas is most likely formaldehyde, which is known to evolve from hydroxymethyl phosphines upon heating[29].

The syntheses of the analogous sulfide $FcP(S)(CH_2OH)_2$ **31** and selenide $FcP(Se)(CH_2OH)_2$ **32** were accomplished by reaction of the parent hydroxymethylphosphine with the respective element (S_8 or grey selenium) using sonication, (Scheme 6.8). Sonication, or exposure to ultrasound, has become an accepted technique in many areas of synthetic chemistry[30]. Primarily used to increase rates of reaction[31], sonication can also lead to novel or unexpected reactions, such as

---

[29] J. W. Ellis, K. N. Harrison, P. A. T. Hoye, A. G. Orpen, P. G. Pringle and M. B. Smith, *Inorg. Chem.*, 1992, **31**, 3026.

[30] Sonochemistry: The Uses of Ultrasound in Chemistry, T.J. Mason (Ed). The Royal Society of Chemistry, (1990).

[31] (a) S. Takahashi and Y. Shimonishi, *Chem. Lett.*, 1974, **1**, 51. (b) G. J. Price and A. A. Clifton, *Polymer*, 1996, **37**, 3971. (c) F. Chemat, M. Poux and S. A. Galema, *J. Chem. Soc., Perkins Trans. 2*, 1997, **11**, 2371.

the preparation of Grignard reagents in wet ether[32]. Sonication has recently been shown to be useful in the reaction of phosphines with chalcogenides[33].

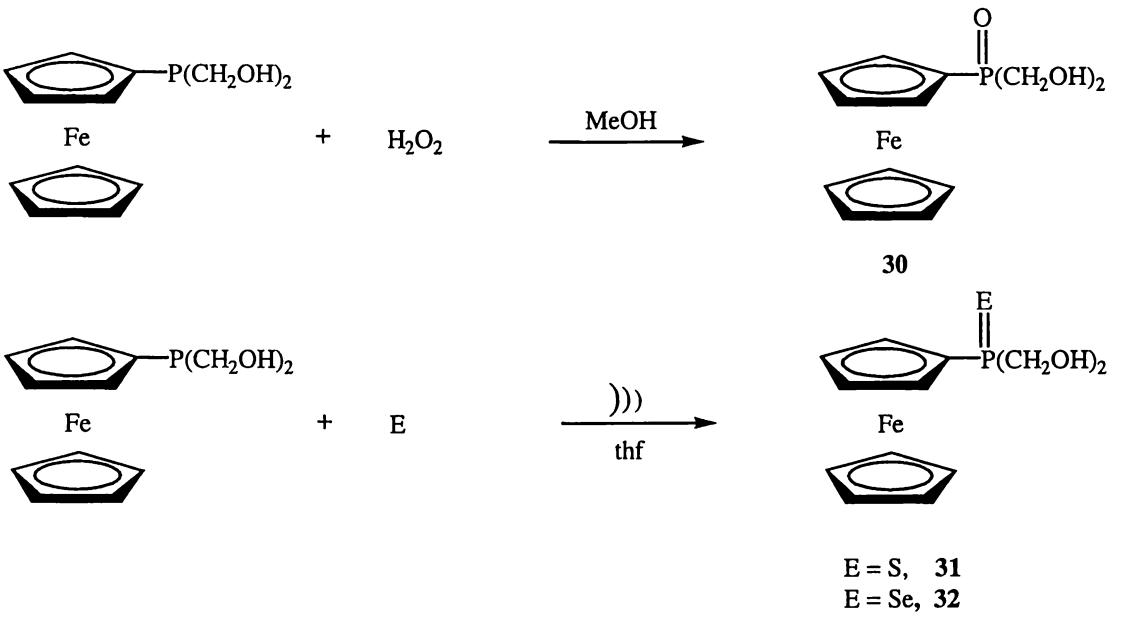

Scheme 6.8: Synthesis of $FcP(E)(CH_2OH)_2$. E = O, S, Se.

In both the sulfidation and selenidation of **28**, the reaction using ultrasound is complete within ten minutes, compared with the five hours reported for the thiolation of analogous $FcCH_2P(CH_2OH)_2$ using S_8 in refluxing toluene.

The sulfide **31** and selenide **32** were crystalline orange compounds with distinctive odours. Both were soluble in polar organic solvents and had clearly defined melting points. All three chalcogenide derivatives of **28** were routinely characterised by nmr, with ^{31}P nmr being particularly useful. The hydroxymethylphosphine starting material has a ^{31}P chemical shift of -25ppm, this moves to between 35 and 50ppm when the phosphorus to chalcogenide bond is formed. In the case of the selenide **32**, the ^{31}P-{^{1}H} spectrum also clearly shows satellite peaks due to I=1/2 ^{77}Se which has a natural abundance of 7%, (Figure 6.6).

[32] D. H. Smith, *J. Chem. Ed.*, 1999, **76**, 142.
[33] N. J. Goodwin, Doctoral Thesis, 1998, University of Waikato.

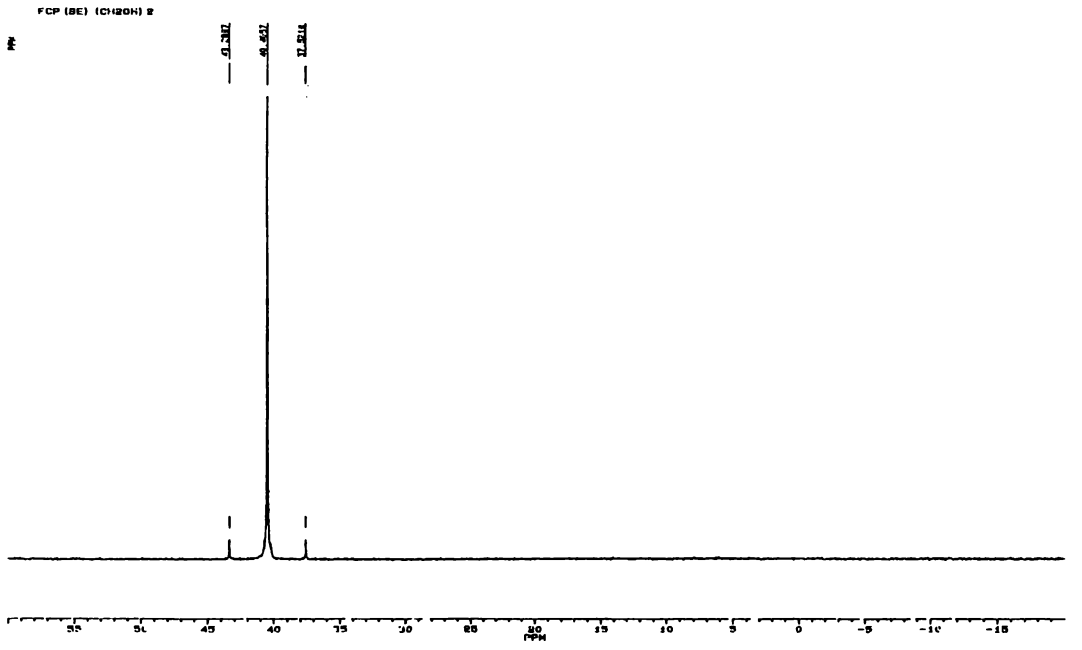

Figure 6.6: The $^{31}P-\{^{1}H\}$ Spectrum of $FcP(Se)(CH_2OH)_2$ **32** showing $^{31}P-^{77}Se$ Satellites ($^{1}J_{P-Se}$ 701Hz).

The ^{1}H nmr spectra of **31** and **32** (dissolved in $CDCl_3$) revealed the non-equivalence of the methylene protons on the CH_2OH groups. These gave an AB coupling pattern characteristic of geminal CH_2 protons with a $^{2}J_{H-H}$ of 13Hz. The ^{1}H nmr spectrum of **31** is given in Figure 6.7.

The chalcogenide atoms provide an excellent site for protonation and the positive ion ES mass spectra of compounds **30-32** are dominated by peaks due to the respective $[M+H^+]^+$ ions. In addition, peaks due to $[2M+H^+]^+$, $[M+Na^+]^+$ and $[2M+Na^+]^+$ were often observed. At higher cone voltages peaks corresponding to loss of CH_2O may be observed. The ES mass spectrum of $FcP(O)(CH_2OH)_2$ **30** at a cone voltage of 40 volts in methanol is given in Figure 6.8.

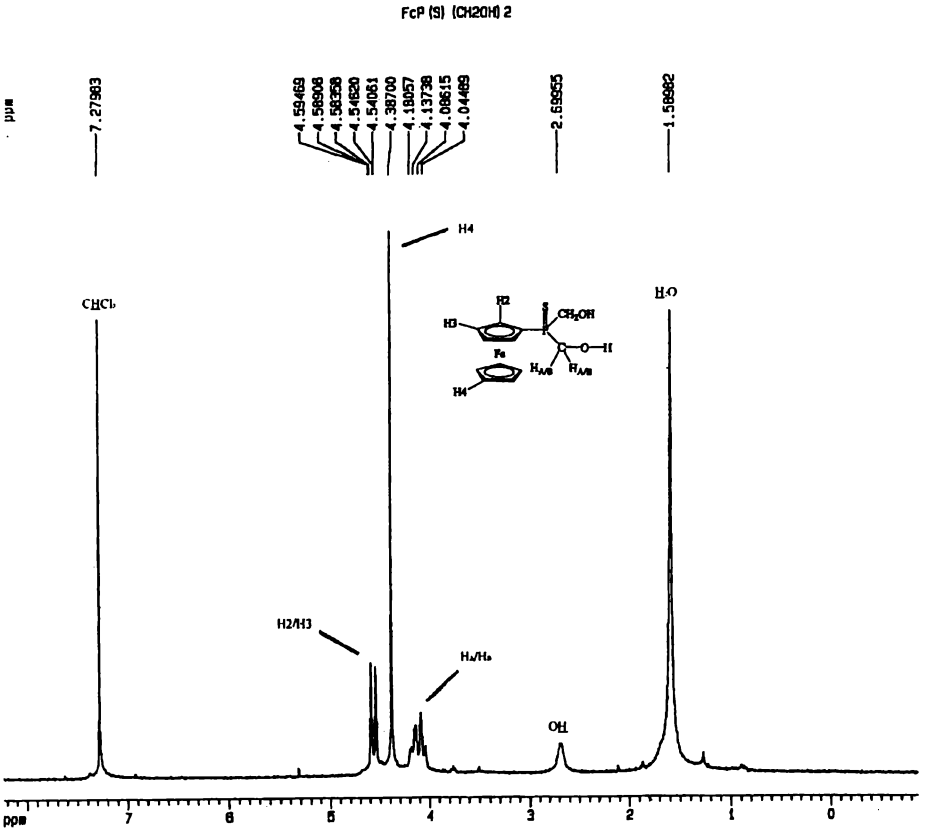

Figure 6.7: The ^{1}H NMR Spectrum of $FcP(S)(CH_2OH)_2$ **31**.

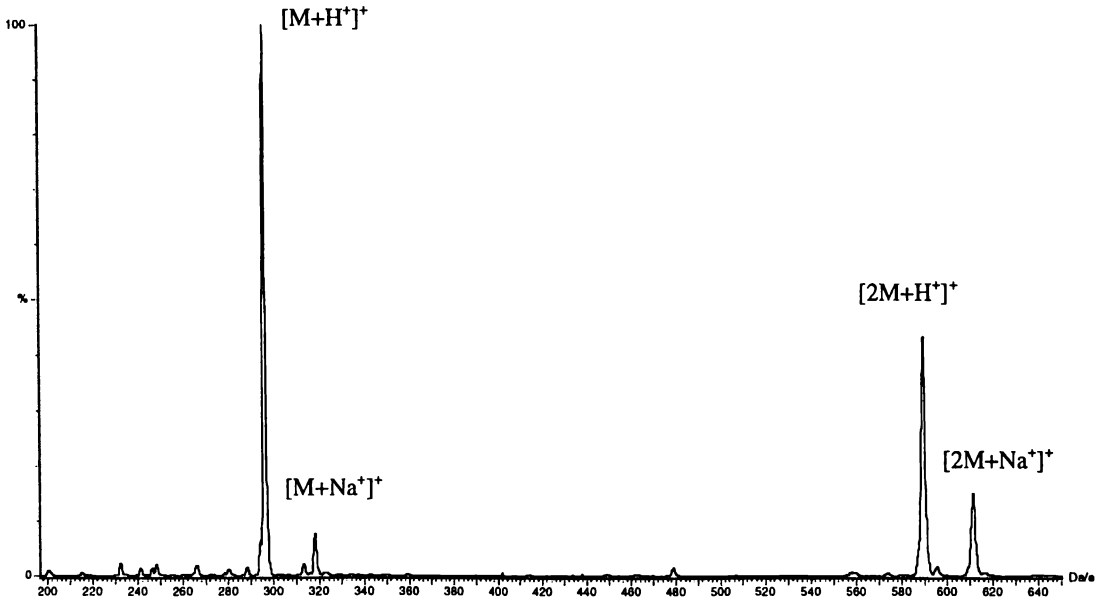

Figure 6.8: The Positive Ion ES Mass Spectrum of $FcP(O)(CH_2OH)_2$ **30** in Methanol at a Cone Voltage of 40V.

The infra-red spectra of **30-32** are dominated by the broad νO-H signal centred at ~3290cm^{-1}. A signal due to the νP=O group could be clearly assigned in the spectrum of **30** (at 1122cm^{-1}). Signals attributable to νP=S and νP=Se were not assigned in the spectra of **31** and **32** respectively. The P=S band is known to be very weak and the P=Se band lies below 400cm^{-1}.[34]

6.2.4: X-Ray Structure Determinations for Compounds 30, 31 and 32

Single crystals of **30** were grown from an Et_2O/CH_2Cl_2/Methanol (10:10:1) solution at -20°C. The structure of **30** was solved routinely from X-ray diffraction data using direct methods. All bond lengths and bond angles are within accepted ranges and selected bond lengths and angles are given in Table 6.2. All hydrogen atoms were found by inspection of the penultimate electron density and included in the final least squares refinement cycle.

Table 6.2: Selected Bond Lengths (Å) and Angles (°) for $FcP(O)(CH_2OH)_2$ **30**.

Cp. Fe-C av.		P(1)-C(2)	1.820(2)
range	2.032-2.061	C(1)-O(1)	1.421(2)
Cp. C-C av.		C(2)-O(2)	1.418(2)
Range	1.418-1.440	O(1)-H(3)	0.7722
C(11)-P(1)	1.781(2)	O(2)-H(4)	0.7785
P(1)-O(3)	1.510(1)	H(3)---O(1')	1.9134
P(1)-C(1)	1.821(2)	H(4)---O(2')	1.9490
C(11)-C(15) range.	107.51-108.65	P(1)-C(1)-O(1)	108.63(10)
C(21)-C(25) range.	107.76-108.25	P(1)-C(2)-O(2)	111.49(11)
C(15)-C(11)-P(1)	123.98(11)	C(1)-O(1)-H(3)	105.80
C(12)-C(11)-P(1)	128.35(11)	C(2)-O(2)-H(4)	107.15
C(11)-P(1)-O(3)	113.56(7)	O(1)-H(3)---O(3')	173.58
C(11)-P(1)-C(1)	107.02(7)	O(2)-H(2)---O(2')	167.86

[34] K. Nakanishi and P. H. Solomon, Infrared Absorbtion Spectroscopy, 1977, Holden Day Ltd.

C(11)-P(1)-C(2)	107.64(7)

The ferrocenyl hydroxymethylphosphine oxide **30** crystallised in the P2(1)/n space group with four molecules in the unit cell. The Cp rings adopt the eclipsed formation typical of mono-substituted ferrocenes. The structure diagram of **30**, with all hydrogen atoms removed except those involved in hydrogen bonding, is displayed in Figure 6.9.

The structure of **30** contains a two dimensional hydrogen bonding network inclined at an angle of *ca.* 30° to the *bc* plane. The hydrogen bonds within this

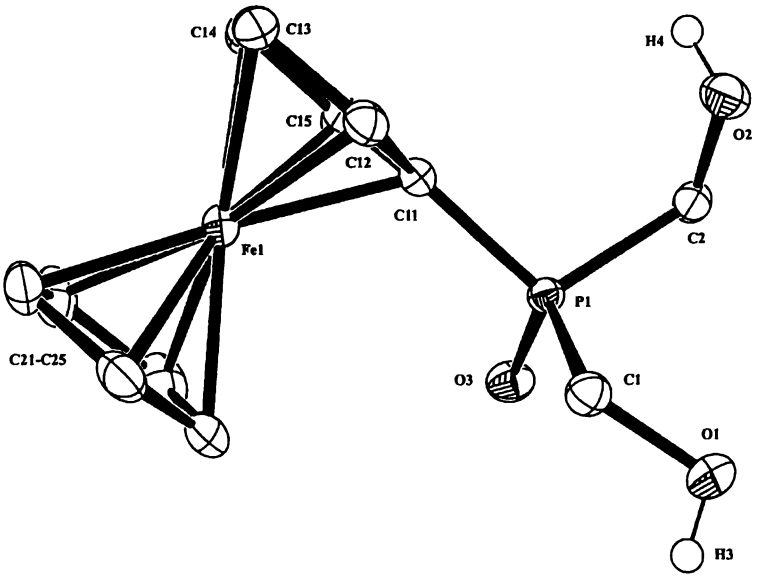

Figure 6.9: Ortep Diagram of $FcP(O)(CH_2OH)_2$ **30** at the 50% Probability Level. All Hydrogen Atoms Omitted Except those Involved in Hydrogen Bonding.

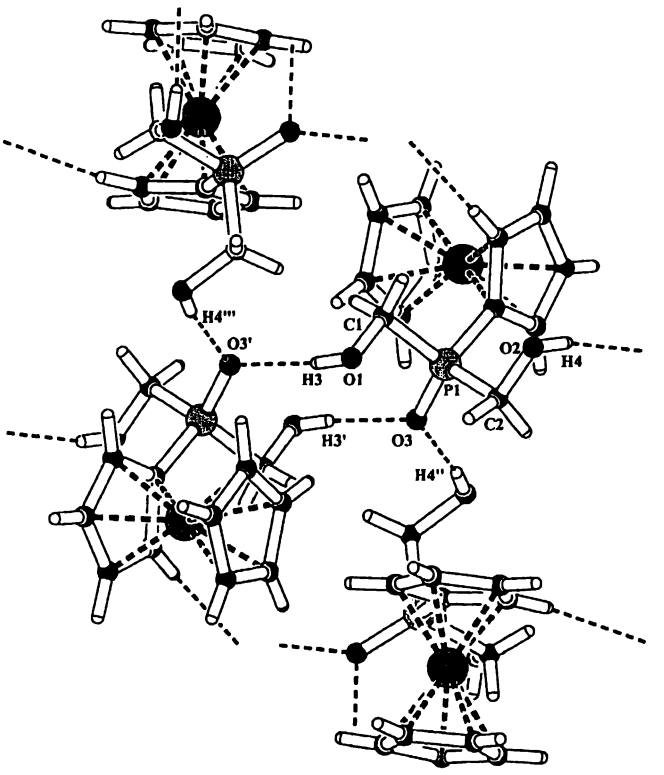

Figure 6.10: Platon Diagram Showing the Hydrogen Bonding in the Structure of $FcP(O)(CH_2OH)_2$ **30**.

network are exclusively between hydroxyl hydrogen atoms and the oxygen atom of the P=O bond. Each molecule of **30** has hydrogen bonding interactions with three adjacent molecules and to one of these, both donor and acceptor hydrogen bonds are formed. As a result two distinct hydrogen bonds are formed, though they are very similar in length and angle about the shared hydrogen, (see Table 6.2). The bonding within this network is shown in Figure 6.10.

Single crystals of $FcP(S)(CH_2OH)_2$ **31** and $FcP(Se)(CH_2OH)_2$ **32** were grown by diffusion of Et_2O vapour into CH_2Cl_2/methanol (10:1) solutions of the respective compounds. Preliminary structural investigations suggested that these two compounds were iso-structural, a phenomenon previously observed in the hydroxymethylphosphine chalcogenide series $(Ph)_2P(E)(CH_2OH)$ (E = O, S and Se)[33]. For this reason full structural analysis of the selenide was not undertaken. The unit cell parameters for both the sulfide and selenide are given in Table 6.3.

Table 6.3: Unit Cell Parameters for $FcP(S)(CH_2OH)_2$ **31** and $FcP(Se)(CH_2OH)_2$ **32**.

Parameter	$FcP(S)(CH_2OH)_2$ **31**	$FcP(Se)(CH_2OH)_2$ **32**
a (Å)	6.1824(1)	6.233(1)
b (Å)	12.3340(2)	12.367(5)
c (Å)	16.5799(1)	16.690(6)
α(°)	90.00	90.00
β(°)	90.101(1)	90.29(2)
γ(°)	90.00	90.00

The structure of $FcP(S)(CH_2OH)_2$ **31** was solved from X-ray diffraction data using direct methods. All hydrogen atoms are in calculated positions except for those involved in hydrogen bonding, which were found by inspection of the penultimate electron density map. The non-substituted cyclopentadienyl ring is significantly disordered and contains the bulk of the residual electron density. All bond lengths and angles fell within accepted ranges except for those on the disordered cyclopentadienyl ring which were smaller than is usual. Selected bond lengths and angles are given in Table 6.3, while structure diagrams of $FcP(S)(CH_2OH)_2$ **31** are given in figures 6.10 and 6.11.

Table 6.4: Selected Bond Lengths (Å) and Angles (°) for $FcP(S)(CH_2OH)_2$ **31**.

Cp Fe-C av.	2.032	P(1)-C(2)	1.835(3)
range	1.995(4)-2.052(3)	P(1)-S(1)	1.955(1)
Cp(1) C-C av.	1.423	C(1)-O(1)	1.415(3)
range	1.412-1.439	C(2)-O(2)	1.421(3)
Cp(2) C-C av.	1.356	O(1)-H(3)	0.9140
range	1.246-1.509	O(2)-O(4)	0.8776
C(11)-P(1)	1.783(3)	H(3)---O(2')	1.8183
P(1)-C(1)	1.835(3)	H(4)---O(1')	1.9396
Cp C(11)-C(15) range	107.3(3)-108.7(3)	Cp C(22)-C25) range	101.9(4)-112.8(6)

C(12)-C(11)-P(1)	127.5(2)	P(1)-C(2)-O(2)	110.63(19)
C(15)-C(11)-P(1)	125.2(2)	C(1)-O(1)-H(3)	108.56
C(11)-P(1)-C(1)	108.01(13)	C(2)-O(2)-H(4)	104.89
C(11)-P(1)-C(2)	102.69(13)	O(1)-H(3)---O(2')	164.72
C(11)-P(1)-S(1)	116.87(10)	O(2)-H(4)-O(1')	153.33
P(1)-C(1)-O(1)	114.26(19)		

The disorder in the non-substituted cyclopentadienyl ring of the ferrocene unit is clearly seen in Figure 6.11.

The hydrogen bonding within this structure (Figure 6.12) is reminiscent of the hydrogen bonding observed in the structure of $FcP(CH_2OH)_2$ **28** (see Figure 6.5). Hydrogen bonds are formed between hydroxyl groups only; the sulfur atom is not involved in any hydrogen bonding. The result is chains consisting of alternating eight and twelve membered rings. This is in marked contrast to hydrogen bonding adopted in the structures of the related ferrocenyl hydroxymethylphosphine sulfides, $FcCH_2P(S)(CH_2OH)_2$ and $FcCH(CH_3)P(S)(CH_2OH)_2$. In each of these compounds both O-H---H bonds and O-H---S bonds are present. The hydrogen bonding in

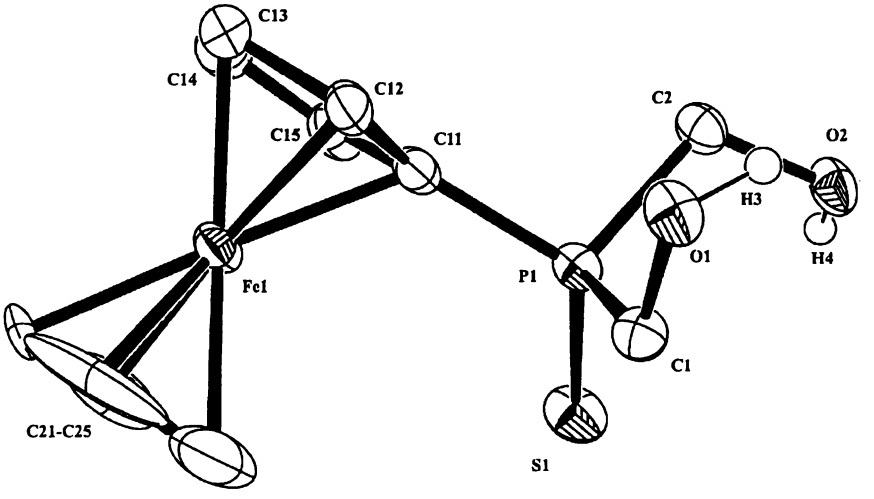

Figure 6.11: Ortep Diagram of $FcP(S)(CH_2OH)_2$ **31** at the 50% Probability Level. All Hydrogen Atoms are Omitted Except those Involved in Hydrogen Bonding.

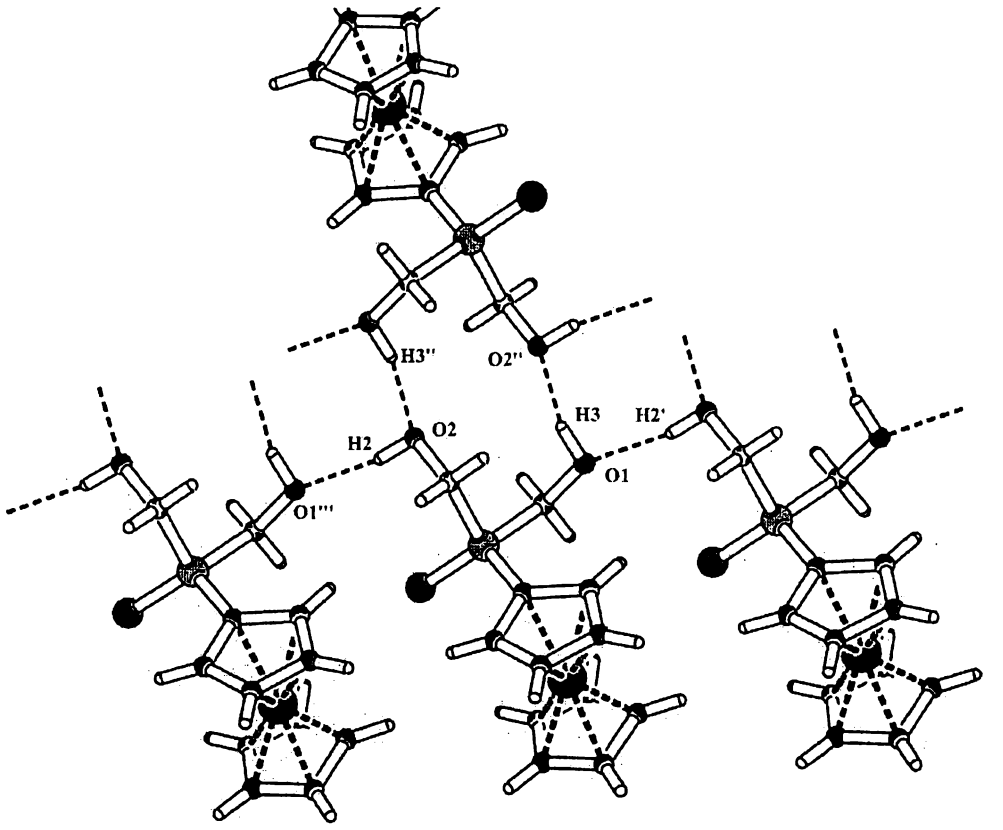

Figure 6.12: Platon Diagram of the Hydrogen Bonding Network in the Structure of $FcP(S)(CH_2OH)_2$ **31**.

$FcCH_2P(S)(CH_2OH)_2$ is composed of short chains of O-H---O bonds terminated at sulfur by O-H---S bonds. Interestingly both compounds also possess bifurcated hydrogen bonds, though in the case of $FcCH_2P(S)(CH_2OH)_2$ it is a O-H hydrogen donating to two oxygen acceptors, while in the case of $FcCH(CH_3)P(S)(CH_2OH)_2$ there are two O-H hydrogens donating to a sulfur atom.

The lack of O-H---S bonds in the structure of **31** is anomalous when compared to those in $FcCH_2P(S)(CH_2OH)_2$ and $FcCH(CH_3)P(S)(CH_2OH)_2$. It may be that removing the CH_2 spacer from between the ferrocene and the phosphorus has increased the effective steric bulk of the ferrocene unit, forcing hydrogen bonding between the more distant hydroxyl groups.

6.2.5: Chalcogenide Derivatives of 1,1'-Fc'[P(CH$_2$OH)$_2$]$_2$ 29

The synthesis of the chalcogenide derivatives of 1,1'-Fc'[P(CH$_2$OH)$_2$]$_2$ **31** was also undertaken. Reaction of **29** with hydrogen peroxide gave the oxide 1,1'-Fc'[P(O)(CH$_2$OH)$_2$]$_2$ **33**, while reaction with sulfur and selenium gave the sulfide 1,1'-Fc'[P(S)(CH$_2$OH)$_2$]$_2$ **34** and selenide 1,1'-Fc'[P(Se)(CH$_2$OH)$_2$]$_2$ **35** respectively (Scheme 6.9).

The synthetic method used in each case was the same as that previously described for the analogous chalcogenide derivatives of FcP(CH$_2$OH)$_2$ **28** and the respective syntheses were again monitored by ^{31}P nmr. The chalcogenides **33-35** are crystalline solids, stable in air but prone to decomposition in solution. All three compounds are soluble in water, methanol and DMSO, while the sulfide and selenide are also soluble in acetone.

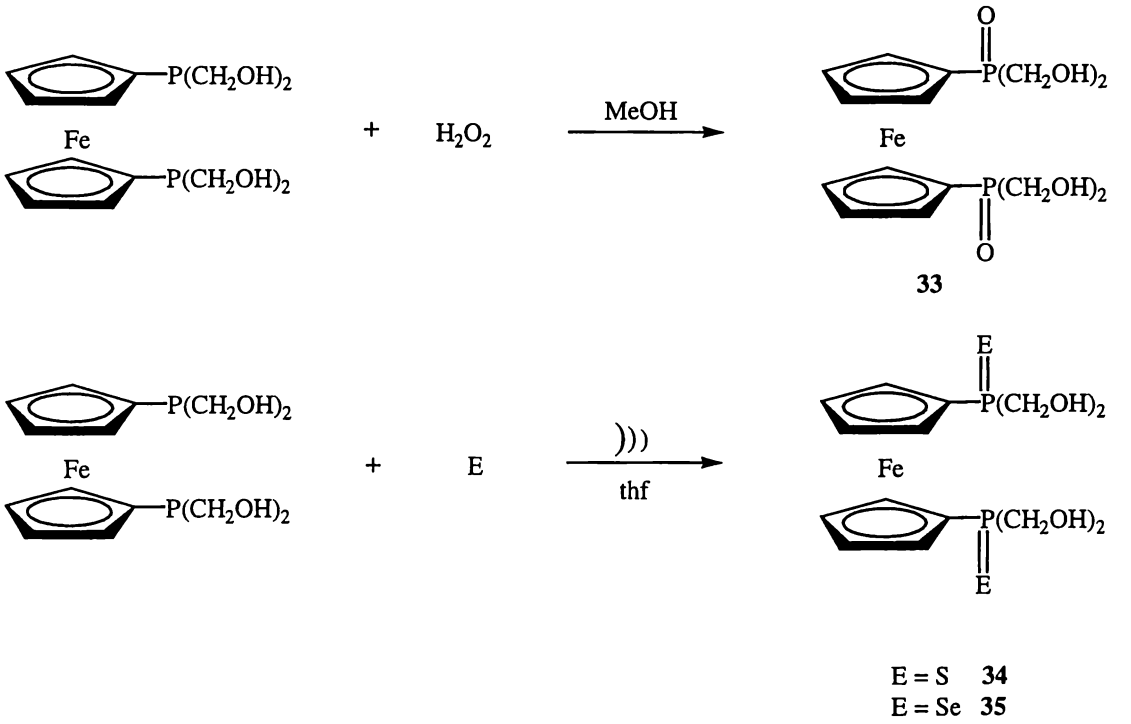

Scheme 6.9: Synthesis of 1,1'-Fc'[P(O)(CH$_2$OH)$_2$]$_2$ **33**, 1,1'-Fc'[P(S)(CH$_2$OH)$_2$]$_2$ **34** and 1,1'-Fc'[P(Se)(CH$_2$OH)$_2$]$_2$ **35**.

As was the case for **28**, **30** and **31**, the ^{1}H nmr spectra of **34** and **35** revealed non-equivalent methylene protons in the -CH$_2$OH groups. The geminal $^2J_{H\text{-}H}$ coupling constants were 13.4Hz and 13.3Hz for **34** and **35** respectively.

Under positive ion ESMS conditions **33-35** proved to be very good at forming $[M+X^+]^+$ adducts with a wide range of cations. For example the spectrum of 1,1'-Fc'$[P(O)(CH_2OH)_2]_2$ **33** in methanol at a cone voltage of 20V was dominated by the peak due to $[M+Na^+]^+$ (*m/z* 425) but also present were peaks assigned to $[M+H^+]^+$ (*m/z* 403), $[M+Li^+]^+$ (*m/z* 409), $[M+K^+]^+$ (*m/z* 441) and $[M+Na^+-CH_2O]^+$ (*m/z* 395). This was without deliberate addition of metal ions.

To simplify the ES mass spectra of the phosphine chalcogenides **33-35** sodium ions were added to the samples as aqueous solutions of NaCl. At low cone voltages, the resulting spectra collapsed to two peaks at $[M+Na^+]^+$ (*m/z* 457)and $[2M+Na^+]^+$ (*m/z* 891), though small peaks due to $[M+Li^+]^+$ and $[M+K^+]^+$ remained. Increasing the cone voltage led to the appearance of peaks assigned to $[M-n(CH_2O)+Na^+]^+$ at *m/z* 427, 397, 367 and 337 for n = 1, 2, 3 and 4 respectively. The ES mass spectra of 1,1'-Fc'$[P(S)(CH_2OH)_2]_2$ **34** at cone voltages of 20V and 60V in methanol with sodium ions added are given in Figure 6.13.

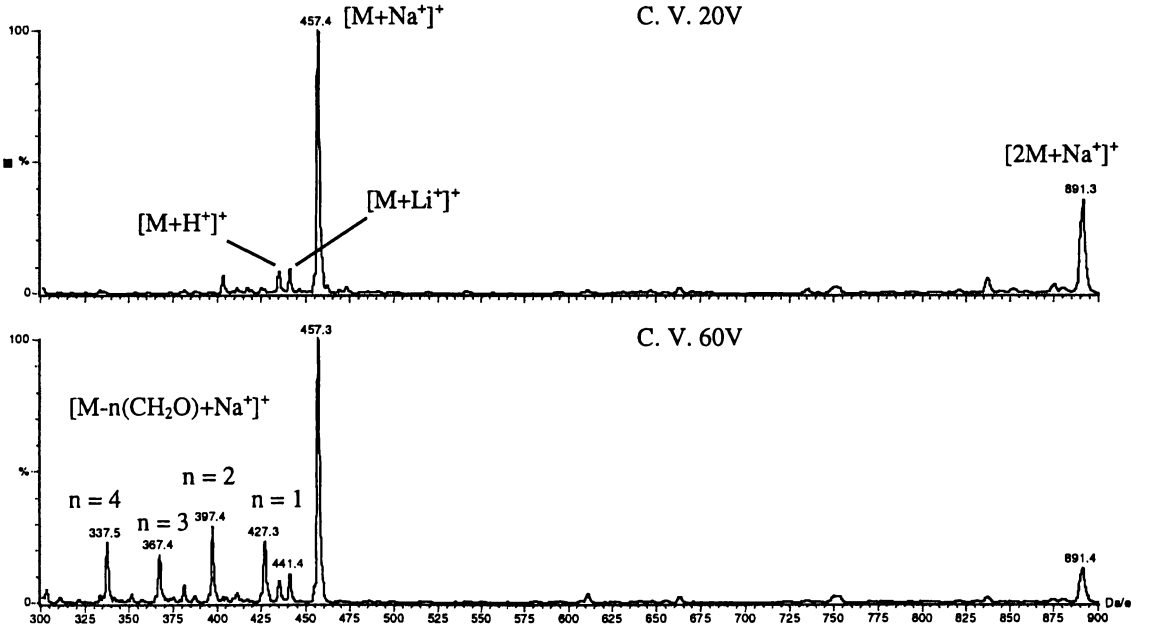

Figure 6.13: The ES Mass Spectra of 1,1'-Fc'$[P(S)(CH_2OH)_2]_2$ **34** in Methanol at Cone Voltages of 20V and 60V with Sodium Ions Added.

6.3: Metal Complexes of Hydroxymethylphosphines

Hydroxymethyl phosphines act as typical phosphine ligands towards metal centres and the use of hydroxymethyl phosphines as ligands in coordination chemistry is a well worn path to water soluble metal complexes. Water solubility is an attractive feature in a catalytic metal complex, as water is a cheap, abundant and environmentally benign solvent. Initial work concentrated on platinum[35], palladium[35a,b], nickel[35b] rhodium[35a] and gold[36] complexes containing tris-hydroxymethyl phosphine $P(CH_2OH)_3$. This chemistry was extended into complexes containing chelating hydroxymethyl phosphines, as these ligands became available and there are now very many examples of metal complexes containing hydroxymethyl phosphines.

Perhaps surprisingly, there are actually few examples of successful catalysis by hydroxymethylphosphine complexes in aqueous systems. Aside from the catalytic synthesis of $P(CH_2OH)_2$ from PH_3 and formaldehyde[1,28], successful systems are rare. The ruthenium complexes $Cp^*Ru(CO)Cl\{P(CH_2OH)_3\}$ and $[Cp^*Ru(CO)\{P(CH_2OH)_3\}]CF_3SO_3$ were shown to be effective catalysts for the selective hydrogenation of sorbic acid in a biphasic water/heptane system[37]. The complexes $[Ir(COD)\{P(CH_2OH)_3\}_3]Cl$ (COD = cyclooctadiene) and $[RhH_2\{P(CH_2OH)_3\}_4]Cl$ have been found to catalyse hydrogenation of cinnamaldehyde and the hydroformylation of 1-pentene respectively[38].

Lastly, the catalytic hydrogenation of carboxylic acids by ruthenium complexes of the type $H_4Ru_4(CO)_8\{P(CH_2OCOR)_3\}_4$ has been reported by Piacenti *et al.*[39]. Though the conversion was low, this report was interesting due to the active involvement of the $P(CH_2OH)_3$ ligand in the catalytic cycle, (the active species in this hydrogenation was found to be the complex $H_4Ru_4(CO)_8\{P(CH_2OH)_3\}_4$ which was formed *in situ* by ester hydrolysis).

---

[35] (a) J. Chatt, G. J. Leigh and R. M. Slade, *J. Chem. Soc., Dalton Trans.*, 1973, 2021. (b) J. W. Ellis, K. N. Harrison, P. A. T. Hoye, A. G. Orpen, P. C. Pringle and M. B. Smith, *Inorg. Chem.*, 1992, **31**, 3026.

[36] (a) S. Komiya, H. Awata, S. Ishimatsu and A. Fukuoka, *Inorg. Chim. Acta.*, 1994, **217**, 201.

[37] B. Dreißen-Holscher and J. Heinen, *J. Organomet. Chem.*, 1998, **570**, 146.

[38] A. Fukuoka, W. Kosugi, F. Morishita, M. Hirano, L. M^{c}Caffrey, W. Henderson and S. Komiya, *Chem. Commun.*, 1999, 489.

[39] A. Salvini, P. Frediani, M. Bianchi, F. Piacenti, L. Pistolesi and L. Rosi, *J. Organomet. Chem.*, 1999, **582**, 218.

A second application of hydroxymethylphosphine complexes is the development of radiopharmaceuticals, complexes of radioactive isotopes used for diagnostic and therapeutic purposes. The introduction of hydroxymethylphosphine ligands into these complexes was pioneered by Katti *et al.* with the synthesis of a 99-Tc complex of $P(CH_2OH)_3$[40]. Hydroxymethylphosphine complexes of 198-Au[41] 188-Re[42] and 105-Rh[43] have since been reported. The recent appearance of these and related compounds in the patent literature[44], is a testament to their efficacy.

6.3.1: Metal Complexes of $FcP(CH_2OH)_2$ 28 and 1,1'-Fc'$[P(CH_2OH)_2]_2$ 29

Gold, ruthenium, platinum and palladium complexes of $FcCH_2P(CH_2OH)_2$ were reported soon after the original synthesis of $FcCH_2P(CH_2OH)_2$ (Figure 6.14)[45].

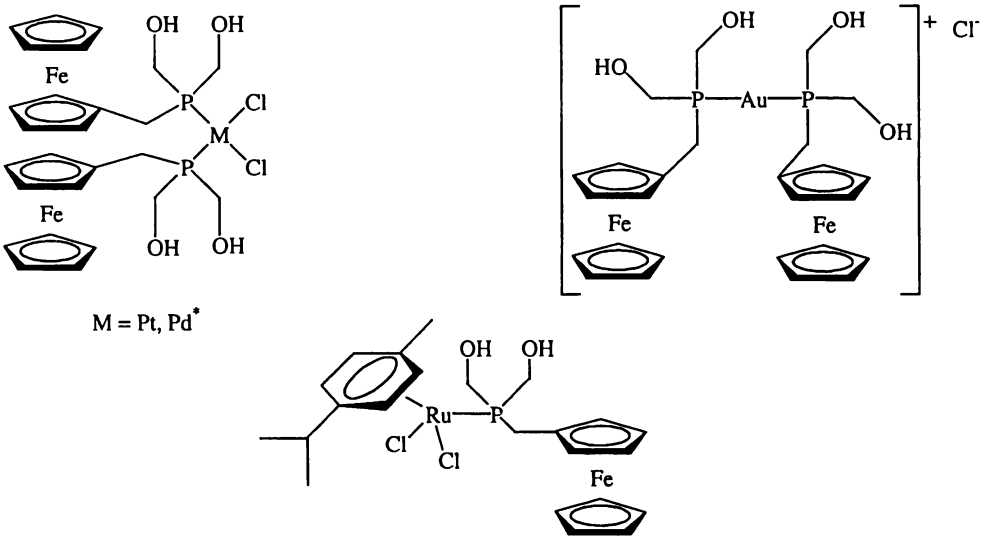

Figure 6.14: Examples of Metal Complexes Containing Ferrocenyl Hydroxymethyl Phosphines, (*Pd Complex may be *cis* or *trans*).

---

[40] D. E. Berning, K. V. Katti, P. R. Singh, C. Higgenbotham, V. S. Reddy and W. A. Volkert, *Nucl. Med. Biol.*, 1996, **23**, 617.

[41] D. E. Berning, K. V. Katti, W. A. Volkert, C. J. Higgenbotham and A. R. Ketring, *Nucl. Med. Biol.*, 1998, **25**, 577.

[42] K. V. Katti, R. Schibli, H. Gali, K. R. Prabhu and W. A. Volkert, Book of Abstr., 217th ACS National meeting March 1999.

[43] C. J. Smith, C. Higgenbotham, K. V. Katti and W. A. Volkert, *Phos. Sulf. Silicon Relat. Chem.*, 1999, **144**, 481.

[44] (a) K. V. Katti, S. R. Karra, D. E. Berning, C. J. Smith, W. A. Volkert and A. R. Ketring, PCT Int. Appl. 1998, WO 98-US4318 19980305. (b) K. V. Katti, D. E. Berning, W. A. Volkert and A. R. Ketring, 1998, PCT Int. Appl. US 97-818078 19970314. (c) S. Liu, PCT int. Appl. WO 98-US10871 19980528.

Since that time no further studies of the coordination chemistry of ferrocenyl hydroxymethyl phosphines have been published. It seemed of interest therefore to prepare and characterise metal complexes of the ferrocenyl hydroxymethyl phosphines **28** and **29**.

Two equivalents of the ferrocenyl hydroxymethylphosphine **28** were reacted with $(COD)PtCl_2$ to give the complex *cis*-$\{FcP(CH_2OH)_2\}_2PtCl_2$ **36** in high yield (Scheme 6.10).

This complex was an air stable orange powder, soluble in polar solvents such as methanol, DMSO and water. The analogous reaction of **28** with $(COD)PdCl_2$ gave a number of products (^{31}P nmr), presumably a mixture of *cis* and *trans* isomers, though several peaks also indicated oxidised phosphorus centres. Purification by recrystallisation was unsuccessful.

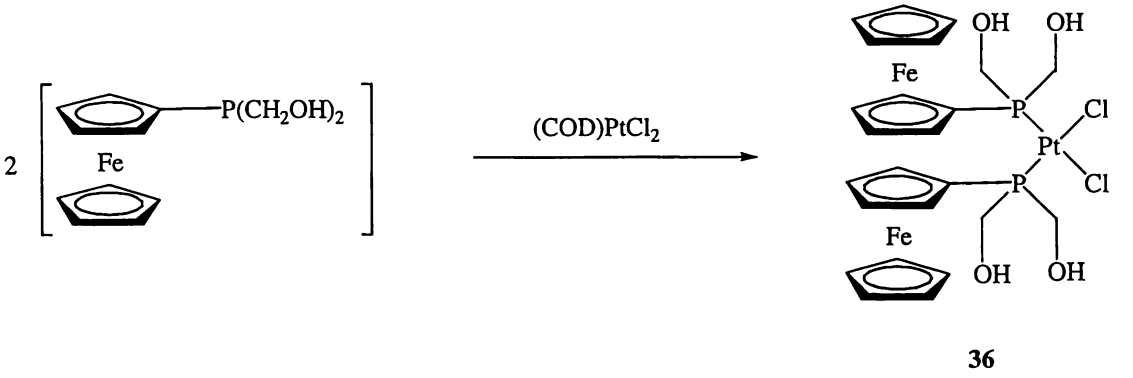

36

Scheme 6.10: Synthesis of *cis*-$\{FcP(CH_2OH)_2\}_2PtCl_2$ **36**.

Characterisation of **36** was achieved by nmr, negative ion ESMS and elemental analyses. ^{31}P nmr was particularly useful due to the large change in chemical shift as the phosphine bound to the platinum centre and concomitant appearance of signals due to ^{31}P-^{197}Pt coupling. The ^{31}P nmr spectrum of **36** is given in Figure 6.15.

[45] N. J. Goodwin and W. Henderson, *Polyhedron*, 1998, **17**, 4071.

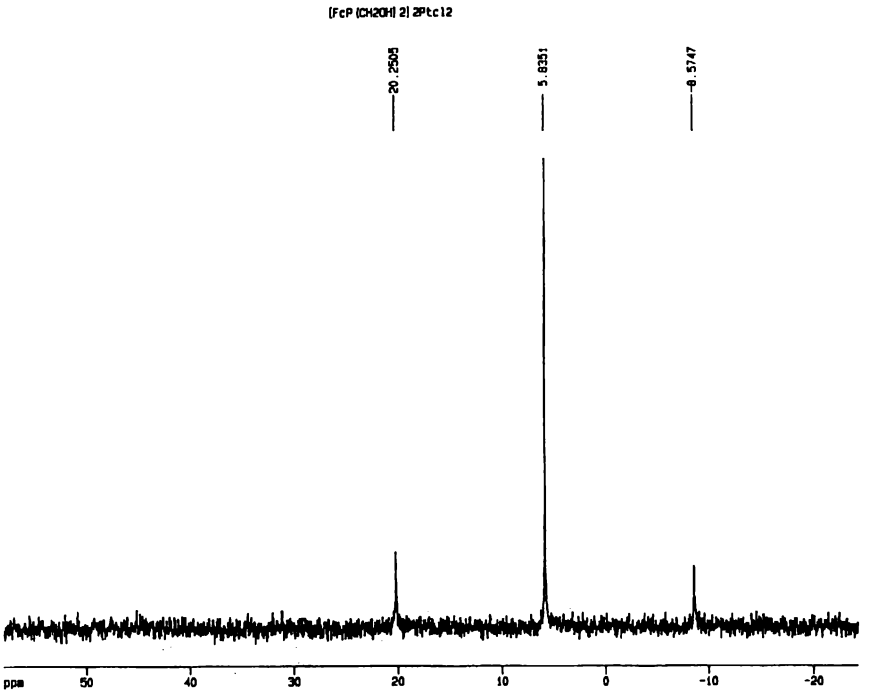

Figure 6.15: The ^{31}P NMR Spectrum of *cis*-$\{FcP(CH_2OH)_2\}_2PtCl_2$ **36** Showing ^{31}P-^{197}Pt Satellites ($^1J_{P\text{-}Pt}$ 3514Hz).

The ESMS behaviour of **36** was of some interest. ES mass spectra of metal halide complexes are usually dominated by the $[M\text{-}Cl^-]^+$ ion[46]. The positive ion spectrum of **36** gave a very weak $[M\text{-}Cl^-]^+$ peak (*m/z* 787). Surprisingly, the negative ion spectrum was dominated by an intense peak at *m/z* 857 (Figure 6.16a). This peak was assigned from its isotope pattern as $[\{FcP(CH_2OH)_2\}_2PtCl_2+Cl^-]^-$ (Figure 6.16b). Presumably the chloride ion is involved in hydrogen bonding with the OH protons

(a)

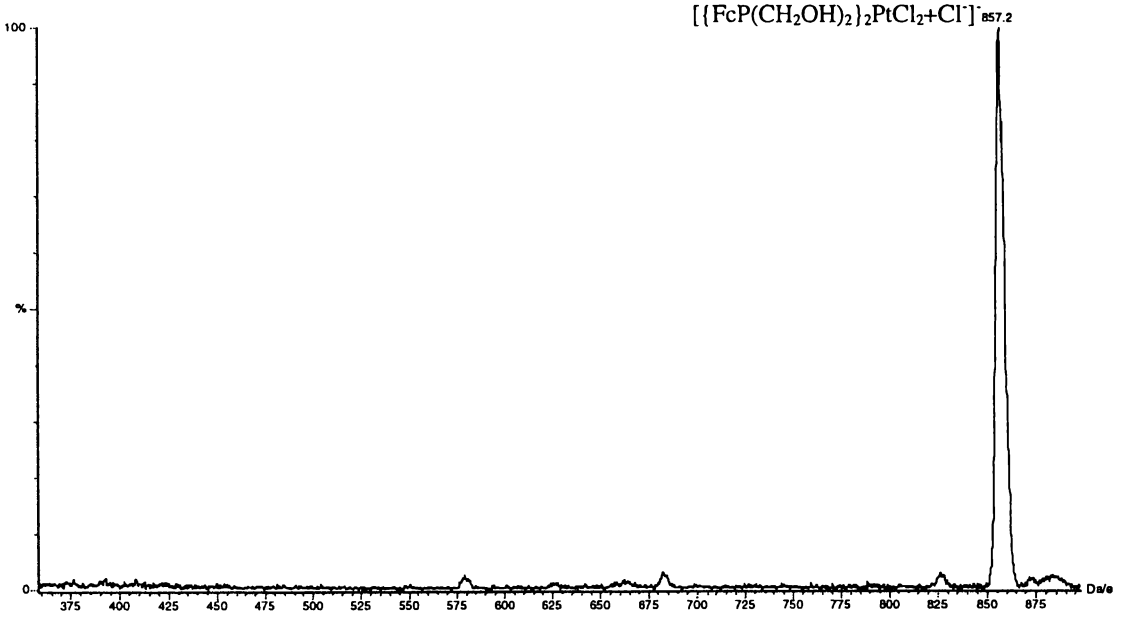

(b)

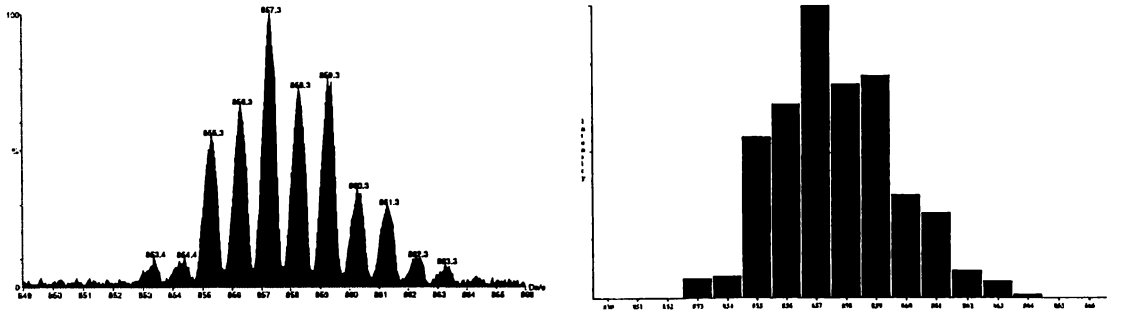

Figure 6.16: (a) The Negative Ion ES Mass Spectrum of **36** in Acetonitrile/Water at a Cone Voltage of 20V. (b) Observed (left) and Calculated (right) Isotope Patterns for $[\{FcP(CH_2OH)_2\}_2PtCl_2+Cl^-]^-$.

The negative ion ES mass spectrum of the crude product from the reaction of **28** with $(COD)PdCl_2$ contained peaks due to $[\{FcP(CH_2OH)_2\}_2PdCl_2+Cl^-]^-$ (*m/z* 767) and $[FcP(CH_2OH)_2PdCl_2+Cl^-]^-$ (*m/z* 491).

The reaction of 1,1'-Fc'$[P(CH_2OH)_2]_2$ **29** with $(COD)PtCl_2$ gave nearly pure 1,1'-Fc'$[P(CH_2OH)_2]_2PtCl_2$ as the principal product. This complex, characterised by ^{31}P nmr and ESMS, was sparingly soluble in water and methanol and soluble in DMSO, though decomposition was observed in DMSO solutions. Under ESMS

[46] W. Henderson and C. Evans, *Inorg. Chim. Acta.*, 1999, **294**, 183.

conditions 1,1'-Fc'$[P(CH_2OH)_2]_2PtCl_2$ displayed the same pattern of behaviour observed for **36**. The negative ion spectrum was dominated by peaks due to $[M+Cl^-]^-$ (*m/z* 671) with a weak peak due to $[2M+Cl^-]^-$ (*m/z* 1236) also being observed (Figure 6.17).

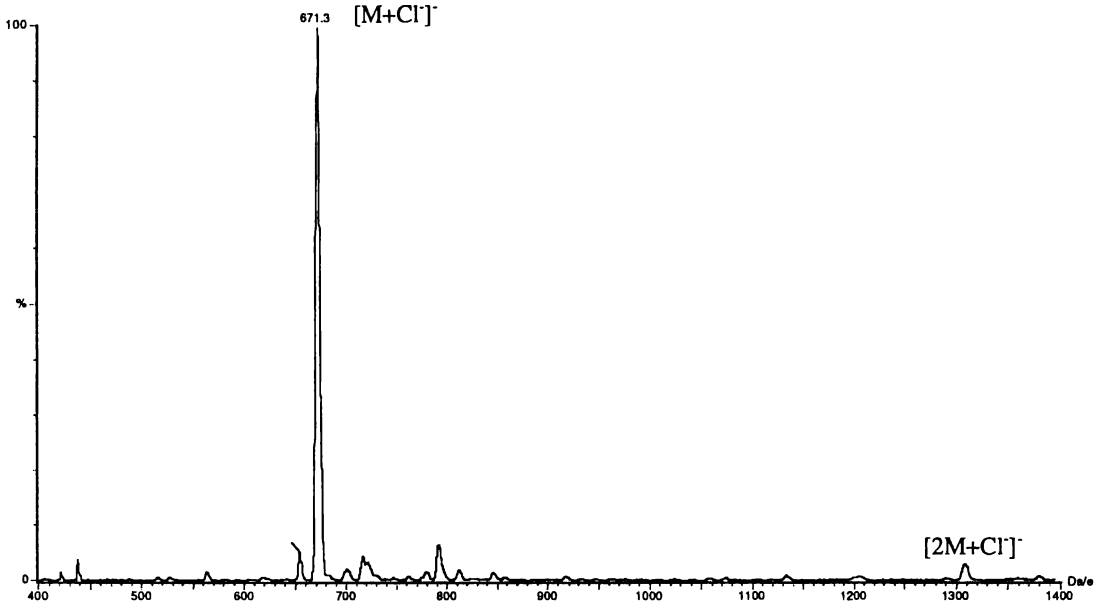

Figure 6.17: The Negative Ion ES Mass Spectrum of Crude 1,1'-Fc'$[P(CH_2OH)_2]_2PtCl_2$ in Methanol at a Cone Voltage of 20V.

The observed and calculated isotope patterns for [1,1'-Fc'$[P(CH_2OH)_2]_2PtCl_2$+Cl^-]$^-$ are given in Figure 6.18.

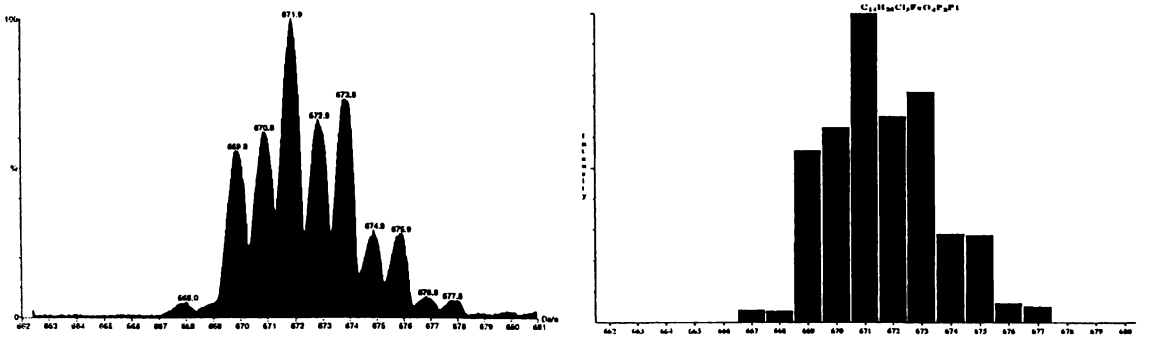

Figure 6.18: Observed (left) and Calculated (right) Isotope Patterns for [1,1'-Fc'$[P(CH_2OH)_2]_2PtCl_2$+Cl^-]$^-$.

The reaction of **29** with $(COD)PdCl_2$ gave $1,1'\text{-}Fc'[P(CH_2OH)_2]_2PdCl_2$ as the major product, identified using ^{31}P nmr and ESMS. The negative ion ES mass spectrum of the crude product is given in Figure 6.19.

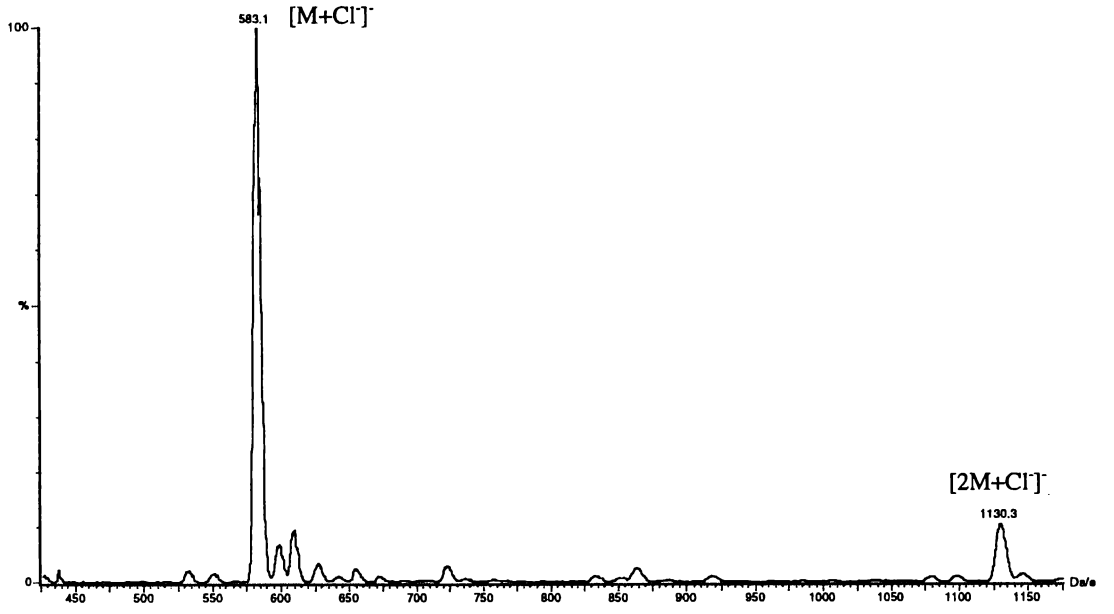

Figure 6.19: Negative Ion ES Mass Spectrum of the Crude Product of the Reaction Between $1,1'\text{-}Fc'[P(CH_2OH)_2]_2$ **29** and $(COD)PdCl_2$ at a Cone Voltage of 20V (M = $1,1'\text{-}Fc'[P(CH_2OH)_2]_2PdCl_2$).

The ferrocenyl hydroxymethylphosphine $1,1\text{-}Fc'[P(CH_2OH)_2]_2$ **29** can be considered a water soluble analogue of dppf and as such, possesses huge potential as a ligand in coordination chemistry. Preliminary results suggest that this compound reacts with metal centres in a fashion typical of other phosphines. The synthesis and characterisation of further metal complexes and investigation into their catalytic abilities (if any) are subjects worthy of further investigation.

6.4: Experimental

General chemical practices are as described in chapter 2 section 2.3, with the following modifications. The starting materials, formaldehyde (40%w/v BDH), selenium (Unilab) and sulfur (BDH) were used as supplied. Hydrogen peroxide

(Andrew Chemicals 27%w/v) was diluted tenfold and standardised by titration with a standard solution of aqueous $KMnO_4$. The platinum complexes, $(COD)PtCl_2$ and $(COD)PdCl_2$ were kindly supplied by Dr. Bill Henderson.

Electrospray mass spectrometry of ferrocenyl hydroxymethyl phosphines **28** and **29** was carried out in the positive ion mode with methanol used as the carrier solvent. Samples were introduced into the ES mass spectrometer as solutions in methanol. Silver ions were added (~0.01 mmol of 0.1 $moll^{-1}$ aqueous $AgNO_3$ per ml of sample solution) to aid ionisation and simplify spectra and the cone voltage was varied to obtain the best results. Ferrocenyl hydroxymethylphosphine chalcogenides were introduced to the ES mass spectrometer as solutions in methanol. Spectra were obtained in the positive ion mode and the cone voltage was varied to obtain best results. Excess sodium ions were added to samples **33-35** using aqueous NaCl ($0.1moll^{-1}$ ~0.01mmol). Ferrocenyl hydroxymethylphosphine platinum and palladium complexes were introduced to the ES mass spectrometer as solutions in methanol with acetonitrile/water used as the carrier solvent. Spectra were obtained in the negative ion mode and cone voltages were varied to optimise spectra quality.

Unambiguous assignment of O<u>H</u> signals in ^1H nmr spectra was achieved by introducing D_2O into the samples. Where observed, the non-equivalent C<u>H</u>$_2$OH protons are assigned as Ha/Hb in the following text. No effort was made to individually assign these protons.

Infra-red spectra for all compounds except **29** were obtained as KBr discs. The infra-red spectrum of **29** was obtained as a neat oil between KBr windows.

Sonication reactions were performed using a NEY ULTRAsonik 104X ultrasound bath. The bath was three quarter filled with water and reaction flasks were placed in zones of maximum cavitation that had been identified using aluminium foil.

6.4.1: Syntheses

6.4.1.1: Synthesis of $FcP(CH_2OH)_2$ **28**

Formaldehyde (0.25ml, 40%w/v, 3.6mmol) was added to a solution of $FcPH_2$ **16** (0.26g, 1.2mmol) in thf (5ml) under dinitrogen. The resulting solution was stirred at room temperature until starting material was no longer observed by ^{31}P nmr (~18

hours). The solvent was then removed and the residue exposed to a dynamic vacuum (~1mmHg) for 72 hours. This resulted in 0.33g (96%) of the desired product as an orange crystalline powder. Crystals suitable for single crystal X-ray analysis were grown by diffusion of pentane vapour into a methanol/CH_2Cl_2 (1:20) solution of **28** at -20°C.

m.p. 100-106°C.

Elemental Analyses: Found C, 51.78%; H, 5.47%. Calculated for $C_{12}H_{15}FeO_2P$: C, 51.83%; H, 5.44%.

^{31}P-{^1H} NMR ($CDCl_3$): δ -24.67 (*br. s.*).

^{13}C-{^1H} NMR ($CDCl_3$): δ 62.90 (*d*, $^1J_{P-C}$ 17Hz, P<u>C</u>H_2OH), 69.08 (s, C4), 70.24 (*d*, $^3J_{P-C}$ 3.8Hz, C3), 73.22 (*d*, $^2J_{P-C}$ 14Hz, C2), C1 not observed.

^1H NMR ($CDCl_3$): δ 2.56 (2H, *br. s.*, PCH_2O<u>H</u>), 4.24 (5H, *s*, H4), 4.30 (2H, *d/d*, $^2J_{H-H}$ 13Hz, $^3J_{H-H}$ 5Hz, Ha/Hb), 4.45 (2H, *br. d*, $^2J_{H-H}$ 13Hz, Ha/Hb), 4.40 (2H, *s*, H3), 4.50 (2H, *s*, H2).

ESMS: (MeOH, c.v. +100V, Ag^+ added) *m/z* 279 ($[M^+]^+$, 100%), 385/387 ($[M+Ag^+]^+$, 49%), 663/665 ($[2M+Ag^+]^+$, 95%).

IR (cm^{-1}): 3261 (br. s), 3096 (m), 2889 (m), 1161 (m), 1106 (m), 1021 (m), 999 (m), 867 (m), 834 (m), 805 (m), 686 (w), 499 (w), 486 (m), 453 (m).

6.4.1.2: Synthesis of 1,1'-Fc'$[P(CH_2OH)_2]_2$ **29**

A solution of 1,1'-Fc'$[PH_2]_2$ **17** (0.24g, 0.97mmol) in thf (5ml) was prepared under a dinitrogen atmosphere. To this was added aqueous formaldehyde (0.41ml, 40%w/v, 5.86mmol) and the reaction stirred at room temperature for 12 hours. At this time the solvent was removed under reduced pressure. The residue was exposed to dynamic vacuum (~1mmHg) for a further twelve hours to give 0.348g (98%) of **29** as a viscous orange brown oil.

^{31}P-{^1H} NMR (d^6-DMSO): δ -30.99 (*br. s.*).

^{13}C-{^{1}H} NMR (d^6-DMSO): δ 61.02 (*d*, $^{1}J_{P-C}$ 6.6Hz, P<u>C</u>H_2OH), 72.45 (*br. s.*, C2), 74.56 (*d*, $^{2}J_{P-C}$ 13Hz, C2), 91.18 (*d*, $^{1}J_{P-C}$ 9Hz, C1).

^{1}H NMR (d^6-DMSO): δ 4.02 (8H, *m*, PC<u>H</u>$_2$OH), 4.34 (4H, *br. s.*, H3), 4.39 (4H, *d*, $^{3}J_{P-H}$ 1.7Hz, H2), 4.89 (3.6H, *br. s.*, PCH_2O<u>H</u>).

ESMS: (MeOH, c.v. +60V, Ag^+ added) *m/z* 477/479 ([M+ Ag^+]$^+$, 100%).

IR (cm^{-1}): 3412 (br. s), 2905 (br. s), 1191 (m), 1159 (m), 1019 (br. m), 871 (m), 831 (m).

6.4.1.3: Synthesis of $FcP(O)(CH_2OH)_2$ **30**

Aqueous hydrogen peroxide (0.05ml, 3.16molL^{-1}, 017mmol) was added to a solution of **28** (0.047g, 0.17mmol) in methanol (2ml). After 15 minutes ^{31}P nmr revealed the reaction to be complete. The solvent was removed under reduced pressure to give 0.048g (97%) of **30** as a yellow powder. Crystals suitable for single crystal X-ray analyses were grown by dissolving **30** in a minimum of methanol/CH_2Cl_2 (1:10) solution, adding petroleum spirits until the solution became cloudy, then cooling to -20°C.

m.p. 159-170°C crystals 'bubble', melting at 171-176 °C

Elemental Analyses: Found C, 49.01%; H, 5.30%. Calculated for $C_{12}H_{15}FeO_3P$: C, 49.01%; H, 5.14%.

^{31}P-{^{1}H} NMR (d^6-DMSO): δ 38.23 (*br. s.*).

^{13}C-{^{1}H} NMR (d^6-DMSO): δ 59.52 (*d*, $^{1}J_{P-C}$ 84Hz, P<u>C</u>H_2OH), 70.88 (*s*, C4), 72.61 (*d*, $^{3}J_{P-C}$ 9.6Hz, C3), 72.75 (*d*, $^{2}J_{P-C}$ 11.4Hz, C2), C1 not observed.

^{1}H NMR (d^6-DMSO): δ 3.97 (4H, *br. s*, PC<u>H</u>$_2$OH), 4.39 (5H, *s*, H4), 4.54 (4H, *br. s*, H2/H3), 5.39 (2H, *br. s*, PCH_2O<u>H</u>).

ESMS: (MeOH, c.v. +20V) *m/z* 295 ([M+H^+]$^+$ 100%).

IR (cm^{-1}): 3289 (br. s), 3096 (m), 2921 (m), 1206 (m), 1185 (m), 1122 (s, νP=O), 1038 (s), 915 (m), 878 (m), 834 (m), 763 (m), 692 (w), 622 (w), 506 (w), 458 (s).

6.4.1.4: Synthesis of $FcP(S)(CH_2OH)_2$ **31**

A solution of **28** (0.043g, 0.15mmol) and sulfur (0.005g, 0.15mmol) in thf (5ml), was sonicated for 30 minutes. The solvent was then removed under reduced pressure to give 0.047g (99%) of **31** as an orange oil that crystallised upon standing.

m.p. 122-126°C.

Elemental Analyses: Found C, 46.33%; H, 4.88%. Calculated for $C_{12}H_{15}FeO_2PS$: C, 46.47%; H, 4.87%.

$^{31}P-\{^1H\}$ NMR ($CDCl_3$): δ 47.64 (*br. s*).

$^{13}C-\{^1H\}$ NMR ($CDCl_3$): δ 61.04 (*d*, $^1J_{P-C}$ 59Hz, $P\underline{C}H_2OH$), 70.03 (*s*, C4), 71.55 (*d*, $^2J_{P-C}$ 12Hz, C2), 72.13 (*d*, $^3J_{P-C}$ 9Hz, C3).

^1H NMR ($CDCl_3$): δ 2.76 (2H, *d/d*, $^3J_{H-H}$ 6Hz, $^3J_{P-H}$ 6Hz, $CH_2O\underline{H}$), 4.05 (2H, *d/d/d*, $^2J_{H-H}$ 13Hz, $^3J_{H-H}$ 4.2Hz, $^2J_{P-H}$ 1.6Hz, Ha/Hb), 4.15 (2H, *d/d/d*, $^2J_{H-H}$ 13Hz, $^3J_{H-H}$ 6.3Hz, $^2J_{P-H}$ 1.6Hz, Ha/Hb), 4.36 (5H, *s*, H4), 4.52 (2H, *d/t*, $^3J_{H-H}$ 3.6Hz, $^4J_{P-H}$ 1.7Hz, H3), 4.56 (2H, *d/t*, $^3J_{H-H}$ 3.5 Hz, $^3J_{P-H}$ 1.7Hz, H2).

ESMS: (MeOH, c.v. +20V) *m/z* 311 ($[M+H^+]^+$, 100%).

IR (cm^{-1}): 3285 (br. s), 3104 (w), 2893 (m), 1416 (m), 1178 (s), 1107 (m), 1039 (s), 881 (w), 831 (m), 766 (m), 712 (m), 618 (m), 485 (m), 465 (m).

6.4.1.5: Synthesis of $FcP(Se)(CH_2OH)_2$ **32**

A solution of **28** (0.1g, 0.4mmol) and selenium (0.3g, 4mmol) in thf (5ml) was sonicated for 30 minutes. At this time the excess selenium was removed by filtration. The solvent was then removed under reduced pressure to give 0.13g (95%) of **32** as an orange oil that crystallised upon standing. Crystals suitable for single crystal X-ray analysis were grown by evaporation to dryness of a methanol/CH_2Cl_2 solution.

m.p. 116-118°C.

Elemental Analyses: Found C, 40.83%; H, 4.49%. Calculated for $C_{12}H_{15}FeO_2PSe$: C, 40.36%; H, 4.23%.

$^{31}P-\{^1H\}$ NMR ($CDCl_3$): δ 39.07 (*br. s.*, *d*, $^1J_{P-Se}$ 701Hz).

^{13}C-{^{1}H} NMR ($CDCl_3$): δ 60.92 (*d*, $^{1}J_{P-C}$ 51Hz P<u>C</u>H_2OH), 70.14 (*s*, C4), 72.16 (*d*, $^{3}J_{P-C}$ 9Hz, C3), 72.28 (*d*, $^{2}J_{P-C}$ 8.5Hz, C2), C1 not observed.

^{1}H NMR ($CDCl_3$): δ 3.1 (2H, *br. s.*, CH_2O<u>H</u>), 4.08 (2H, *d*, $^{2}J_{H-H}$ 12Hz, Ha/Hb), 4.20 (2H, *d*, $^{2}J_{H-H}$ 12Hz, Ha/Hb), 4.36 (5H, *s*, H4), 4.53 (2H, *br. s*, H2), 4.60 (2H, *br. s*, H3).

ESMS: (MeOH, c.v. +20V) *m/z* 358 ([M+H^+]$^+$, 100%).

IR (cm^{-1}): 3297 (br. s), 3105 (w), 2885 (m), 1411 (m), 1175 (s), 1108 (m), 1042 (s), 880 (w), 827 (m), 806 (m), 758 (m), 537 (w), 482 (m).

6.4.1.6: Synthesis of 1,1'-Fc[P(O)$(CH_2OH)_2$]$_2$ **33**

Aqueous hydrogen peroxide (0.22ml of a 3.16molL^{-1} solution, 1.1mmol) was added to a solution of **29** (0.13g, 0.55mmol) in methanol (4ml). The reaction was stirred for 10 minutes, at which time ^{31}P nmr showed the reaction to be complete. The solvent was removed under reduced pressure to give 0.14g (98%) of **33** as a crunchy brown oil.

Elemental Analyses: Found C, 41.85%; H, 5.48%. Calculated for $C_{14}H_{20}FeO_6P_2$: C, 41.81%; H, 5.01%.

^{31}P-{^{1}H} NMR (d^6-DMSO): δ 39.19 (*br.s.*).

^{13}C-{^{1}H} NMR (d^6-DMSO): δ 59.23 (*d*, $^{1}J_{P-C}$ 84Hz, P<u>C</u>H_2OH), 72.25 (*d*, $^{1}J_{P-C}$ 96Hz, C1), 73.90 (*d*, $^{3}J_{P-C}$ 8.5Hz, C3), 74.12 (*d*, $^{2}J_{P-C}$ 10.4Hz, C2).

^{1}H NMR (d^6-DMSO): δ 3.99 (8H, *br. s.*, PC<u>H</u>$_2OH$), 4.71 (8H, *br. s.*, H2/H3), 5.65 (3.7H, *br. s.*, PCH_2O<u>H</u>).

ESMS: (MeOH, c.v. +20V, Na^+ added) *m/z* 305 ([M-4CH_2O+H^+]$^+$ 13%), 335 ([M-3CH_2O+H^+]$^+$ 14%), 365 ([M-2CH_2O+H^+]$^+$ 11%), 395 ([M-CH_2O+H^+]$^+$ 13%), 403 ([M+H^+]$^+$ 6%), 409 ([M+Li^+]$^+$ 6%), 425 ([M+Na^+]$^+$ 100%), 827 ([2M+Na^+]$^+$, 67%).

6.4.1.7: Synthesis of 1,1'-Fc[P(S)$(CH_2OH)_2$]$_2$ **34**

Elemental sulfur (0.02g, 0.63mmol) was added to a solution of **29** (0.06g, 0.15mmol) in methanol (5ml) under a dinitrogen atmosphere. The reaction mixture was exposed to ultrasound for 15 minutes. The solution was filtered to remove excess

sulfur and the solvent removed under reduced pressure to give 0.056g (83%) of **34** as apure (by ^{31}P nmr) orange oil. Diffusion of Et_2O vapour into an acetone solution of the crude product gave 5mg (7%) of crystalline **34**. The low crystalline yield is attributed to decomposition of **34** in concentrated solution.

m.p. 138-143°C.

Elemental Analyses: Found C, 38.84%; H, 4.69%. Calculated for $C_{14}H_{20}FeO_4P_2S_2$: C, 38.72%; H, 4.64%.

^{31}P-{^1H} NMR (d^6-DMSO): δ 43.77(*br.s.*).

^{13}C-{^1H} NMR (d^6-DMSO): δ 62.65 (*d*, $^1J_{P-C}$ 65Hz, P<u>C</u>H_2OH), 73.58 (*d*, $^1J_{P-C}$ 78Hz, C1), 74.80 (*d*, $^3J_{P-C}$ 10Hz, C3), 74.92 (*d*, $^2J_{P-C}$ 9Hz, C2).

^1H NMR (d^6-DMSO): 4.05 (4H, *d/d.*, $^2J_{H-H}$ 13.4Hz, $^3J_{H-H}$ 5.9Hz, Ha/Hb), 4.12 (4H, *d/d*, $^2J_{H-H}$ 13.4Hz, $^3J_{H-H}$ 4.2Hz, Ha/Hb), 4.72 (4H, *m.*, H3), 4.76 (4H, *m.*, H2), 5.69 (4H, *br.m.*, PCH_2O<u>H</u>).

ESMS: (MeOH, c.v. +20V, Na^+ added) *m/z* 435 ($[M+H^+]^+$ 9%), 441 ($[M+Li^+]^+$ 10%), 457 ($[M+Na^+]^+$ 100%), 891 ($[2M+H^+]^+$ 36%).

6.4.1.8: Synthesis of 1,1'-Fc'[P(Se)(CH_2OH)$_2$]$_2$ **35**

An excess of selenium (0.15g, 2mmol) was added to a solution of **29** (0.24g, 0.64mmol) in methanol (5ml). The solution was placed under a dinitrogen atmosphere and sonicated for 5 minutes. The solution was then filtered to remove excess selenium and the solvent removed to give 0.16g (48%) of **35** as an orange brown oil. Evaporation to dryness of a methanol/CH_2Cl_2 solution gave 0.032g (10%) of **35** as bright red crystals.

m.p. 147-149°C.

Elemental Analyses: Found C, 32.54%; H, 4.20%. Calculated For $C_{14}H_{20}FeO_4P_2Se_2$: C, 31.84%; H, 3.82%.

^{31}P-{^1H} NMR (d^6-DMSO): δ 33.18 (*s*, *d*, $^1J_{P-Se}$ 713Hz).

^{13}C-{^1H} NMR (d^6-DMSO): δ 62.64 (*d*, $^1J_{P-C}$ 57Hz, P<u>C</u>H_2OH), 72.14 (*d*, $^1J_{P-C}$ 70Hz, C1), 75.33 (*d*, $^3J_{P-C}$ 6.4Hz, C3), 75.45 (*d*, $^2J_{P-C}$ 7.7Hz, C2).

^{1}H NMR (d^6-DMSO): δ 4.14 (4H, *d/d.*, $^2J_{H-H}$ 13.1Hz, $^3J_{H-H}$ 5.8Hz, Ha/Hb) 4.23 (4H, *d/d*, $^2J_{H-H}$ 13.1Hz, $^3J_{H-H}$ 6.6Hz, Ha/Hb) 4.76 (4H, *br. s.*, H3), 4.82 (4H, *br. s.*, H2), 5.79 (4H, *d/t*, $^3J_{H-H} = {}^3J_{P-H}$ 6Hz $CH_2O\underline{H}$).

ESMS: (MeOH, c.v. +20V, Na^+ added) *m/z* 529 ($[M+H^+]^+$ 29%), 551 ($[M+Na^+]^+$ 100%), 1079 ($[2M+Na^+]^+$ 33%).

IR (cm^{-1}): 3428 (br. s), 3300 (br. s), 3108 (w), 3897 (m), 1184 (s), 1040 (s), 866 (w), 817 (m), 761 (m), 614 (w), 540 (w), 497 (m), 471 (m), 434 (w).

6.4.1.9: Synthesis of $\{FcP(CH_2OH)_2\}_2PtCl_2$ **36**

A solution of $(COD)PtCl_2$ (0.03g, 0.09mmol) in CH_2Cl_2 (5ml) was added to a solution of $FcP(CH_2OH)_2$ (0.05g, 0.18mmol) in CH_2Cl_2 (4ml) at room temperature. The reaction was monitored by ^{31}P nmr and deemed complete after 30 minutes. The volume was reduced to ~1ml and petroleum spirits (5ml) was added. The resulting precipitate was filtered, washed liberally with petroleum spirits (30ml) and dried to give 0.06g (76%) of **36** as an orange powder.

m.p. 208-214°C dec.

Elemental Analyses: Found C, 34.70%; H, 3.70%. Calculated For $C_{24}H_{30}Cl_2Fe_2O_4P_2Pt$: C, 35.06%; H, 3.68%.

^{31}P-{^{1}H} NMR (d^6-DMSO): δ 0.52 (*s*, $^1J_{P-Pt}$ 3514Hz).

^{13}C-{^{1}H} NMR (d^6-DMSO): δ 56.9 (*d*, $^1J_{P-C}$ 53Hz, $P\underline{C}H_2OH$), 70.13 (*s*, C4), 70.73 (*s*, C3), 74.17 (*s*, C2), C1 not observed.

^{1}H NMR (d^6-DMSO): 3.32 (8H, *br. s*, $PC\underline{H}_2OH$), 4.38 (10H, *s*, H4), 4.45 (4H, *s*, H3), 4.61 (4H, *s*, H2), 5.42 (4H, *br. s*, $PCH_2O\underline{H}$).

ESMS: ($MeCN/H_2O$, c.v. -20V) *m/z* 857 ($[\{FcP(CH_2OH)_2\}_2PtCl_2+Cl^-]^-$, 100%).

6.4.1.10: Reaction of $(COD)PdCl_2$ with $FcP(CH_2OH)_2$ **28**

A solution of $(COD)PdCl_2$ (0.023g, 0.08mmol) in CH_2Cl_2 (5ml) was added to a solution of $FcP(CH_2OH)_2$ (0.046g, 0.16mmol) in CH_2Cl_2 (5ml) at room temperature. The reaction solution immediately changed colour from pale orange to deep red. The reaction was stirred in air for 30 minutes before the volume was halved and petroleum

spirits (10ml) was added. The resulting precipitate was filtered, washed liberally with petroleum spirits (30ml) and dried to give 0.035g of a deep red powder. ^{31}P nmr showed a mixture of products.

6.4.1.11: Reaction of 1,1'-Fc'$[P(CH_2OH)_2]_2$ **29** with $(COD)PtCl_2$

To a solution of **29** (0.047g, 0.12mmol) in methanol (5ml) under a dinitrogen atmosphere was added a solution of $(COD)PtCl_2$ (0.048g, 0.12mmol) in CH_2Cl_2 (5ml). As the addition progressed a colour change from orange to red and back to orange was observed. The reaction was stirred for 30 minutes before the volume was halved and Et_2O (20ml) was added. The resulting precipitate was filtered under nitrogen and washed liberally with petroleum spirits before being dried under vacuum. The resulting product was a pale orange powder (0.045g) that was shown to be nearly pure 1,1'-Fc'$[P(CH_2OH)_2]_2PtCl_2$ by ^{31}P-$\{^1H\}$ nmr and ESMS. Purification by recrystallisation was unsuccessful.

^{31}P-$\{^1H\}$ NMR (d^6-DMSO): δ 10.39 (*s*, $^1J_{P\text{-}Pt}$ 3619Hz).
ESMS: (MeOH, c.v. -20V, NaOMe added), *m/z* 671 ($[M+Cl^-]^-$, 100%), 1307 ($[2M+Cl^-]^-$ 4%).

6.4.1.12: Reaction of 1,1'-Fc'$[P(CH_2OH)_2]_2$ **29** with $(COD)PdCl_2$

A solution of $(COD)PdCl_2$ (0.052g, 0.18mmol) in CH_2Cl_2 (5ml) was added to a solution of **29** (0.068g, 0.18mmol) in methanol (5ml) under a dinitrogen atmosphere. An immediate colour change was observed (from orange to dark red) and a small amount of red precipitate formed. The solution was stirred for 30 minutes before the volume was halved and Et_2O (20ml) added. The resulting brick red precipitate was filtered and washed liberally with petroleum spirits before being dried under vacuum. ^{31}P-$\{^1H\}$ and ESMS analysis showed the crude product (0.066g) to be impure 1,1'-Fc'$[P(CH_2OH)_2]_2PdCl_2$. Purification by recrystallisation was unsuccessful.

^{31}P-$\{^1H\}$ NMR (d^6-DMSO): δ 40.10 (*s*)

ESMS: (MeOH, c.v. -10V, NaOMe added), *m/z* 583 ([M+Cl^-]$^-$, 100%), 1131 ([2M+Cl^-]$^-$, 12%).

6.4.2: X-ray Crystal Structure Determinations for $FcP(CH_2OH)_2$ 28, $FcP(O)(CH_2OH)_2$ 30 and $FcP(S)(CH_2OH)_2$ 31

Crystallographic data for **28, 30** and **31** are given in Table 6.10. Single crystals of **28** were obtained as described in section 6.2.2, while single crystals of **30** and **31** were obtained as described in section 6.2.4.

The data sets were collected on a Siemens Smart CCD diffractometer at Auckland University and corrected for absorption using SADABS. All structures were solved using the direct methods option of SHELXL-97 and developed routinely using full matrix least-squares refinement based on F_o^2.

For **28** all non-hydrogen atoms were refined using anisotropic temperature factors and hydrogen atoms were found from peaks of residual electron density in the penultimate electron density map and were refined with isotropic temperature factors. The largest residual electron density peaks in the final density map did not exceed +0.431 or -0.463 eÅ^{-3}.

The structure of **30** was refined with anisotropic temperature factors for all non-hydrogen atoms. All hydrogen atoms were found by inspection of the penultimate electron density map and included in the final refinement cycle with isotropic temperature factors. The largest residual electron density peaks in the final electron density map did not exceed +0.351 or -0.25 eÅ^{-3}

All non-hydrogen atoms in the structure of **31** were refined using anisotropic temperature factors. Hydrogens were placed in calculated positions except for H3 and H4 which were found as peaks of electron density in the penultimate electron density map. The largest residual electron density peaks in the final electron density map were in the plane of the non-substituted cyclopentadienyl ring and did not exceed +1.130 or -0.592 eÅ^{-3}.

Table 6.5: Collected Single Crystal Data and Analysis Parameters for $FcP(CH_2OH)_2$ **28**, $FcP(O)(CH_2OH)_2$ **30** and $FcP(S)(CH_2OH)_2$ **31**.

Parameter	**28**	**30**	**31**
Empirical formula	$C_{12}H_{14}FeO_2P$	$C_{12}H_{14}FeO_3P$	$C_{12}H_{14}FeO_2PS$
Formula weight	278.06	294.06	310.12
Crystal system	Monoclinic	Monoclinic	Monoclinic
a (Å)	12.2386(1)	12.0043(2)	6.1824(1)
b (Å)	6.1101(1)	9.0816(2)	12.3340(2)
c (Å)	16.3344(2)	12.1713(3)	16.5799(1)
α (°)	90	90.00	90
β (°)	110.941(1)	115.953(1)	90.101(1)
γ (°)	90	90.00	90
V (Å^3)	1140.79(3)	1193.08(4)	1264.28(3)
Space group	P2(1)/c	P2(1)/n	P2(1)/n
Z value	4	4	4
D_{calc}	1.619 gcm^{-3}	1.637 gcm^{-3}	1.629 gcm^{-3}
F(000)	576	608	640
λ(Mo Kα) (Å)	0.71	0.71	0.71
μ(Mo Kα) (mm^{-1})	1.44	1.39	1.47
Temperature (K)	150(2)	150(2)	150(2)
2θ range for data collection	$1.8° < \theta < 26.5°$	$2° < \theta < 26.4°$	$2° < \theta < 27°$
Total reflections	10314	6848	7543
Unique reflections	2357 ($R_{int.}$ = 0.0327)	2414 ($R_{int.}$ = 0.0163)	2748 ($R_{int.}$ = 0.0179)
T_{min}	0.789304	0.780287	0.683877
T_{max}	0.972041	0.938976	0.840068
R_1 [I>2σ(I)]	0.0254	0.0209	0.0396
wR_2	0.0659[ϑ]	0.0544[ζ]	0.0975[ϐ]
GOF	1.033	1.036	1.039

[ϑ] $w = [\sigma^2(F_o^2) + (0.0422P^2 + 0.29P]^{-1}$ where $P = (F_o^2 + 2F_c^2)/3$. [ζ] $w = [\sigma^2(F_o^2) + (0.0312P^2 + 0.45P]^{-1}$ where $P = (F_o^2 + 2F_c^2)/3$. [ϐ] $w = [\sigma^2(F_o^2) + (0.0444P^2 + 2.72P]^{-1}$ where $P = (F_o^2 + 2F_c^2)/3$.

Chapter 7: Discussion of Results

7.1: Introduction

The compounds whose synthesis has been chronicled in this thesis were not prepared with specific applications in mind. Rather they were prepared because they are of interest in themselves. Yet once made the questions inevitably arise; What is the significance of these compounds? and what possible uses might these compounds have? This chapter will attempt to provide some answers to these queries as they relate to the three main classes of compounds in this thesis.

7.2: Ferrocenyl Phosphonic Acids

The paucity of ferrocenyl phosphonic acids in the published literature does not reflect the possible usefulness of these compounds. The phosphonic acid group reacts with a wide range of metal ions, leading to the formation of layered materials known as metal phosphonates[1]. A schematic diagram of the structure of zirconium phenylphosphonate[2] is given in Figure 7.1. It can be seen that these materials consist of two distinct regions. An inorganic framework of metal ions and phosphonate groups and an interlamellar region whose chemical environment is dependant on the nature of the phosphonic acid R-group.

The synthesis of metal phosphonates progresses at room temperature under mild conditions, which enables a wide range of functional groups to be introduced into the interlamellar region. Thus the chemical properties of these materials can be altered almost at will. Phosphonic acids bearing an organometallic R-group have previously been used in the preparation of metal phosphonates[3] and further study of such materials incorporating the ferrocenyl phosphonic acids **3**, **4** and **5** would be of some interest.

---

[1] A. Clearfield, *Prog. Inorg. Chem.*, 1998, **47**, 371.
[2] M. D. Poojary, H. L. Hu, F. L. Campbell and A. Clearfield, *Acta. Cryst.*, 1993, **B49**, 996.
[3] R. W. Deemie, M. Rao and D. A. Knight, *J. Organomet. Chem.*, 1999, **585**, 162.

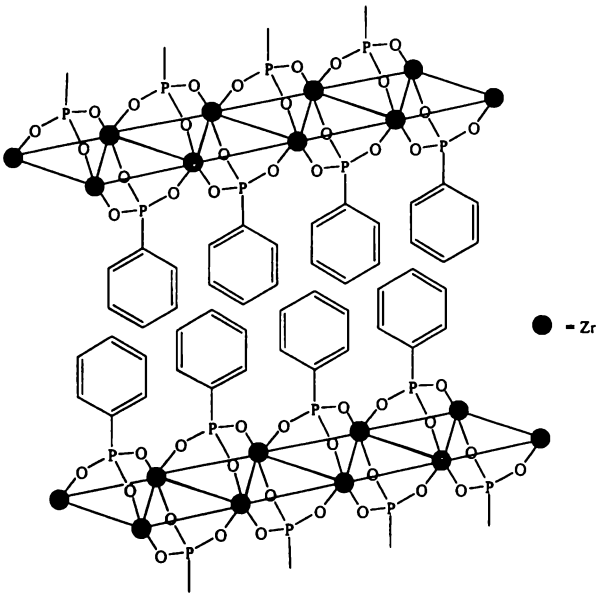

Figure 7.1: A Schematic Representation of Zirconium Phenylphosphonate $Zr(O_3PPh)_2$.

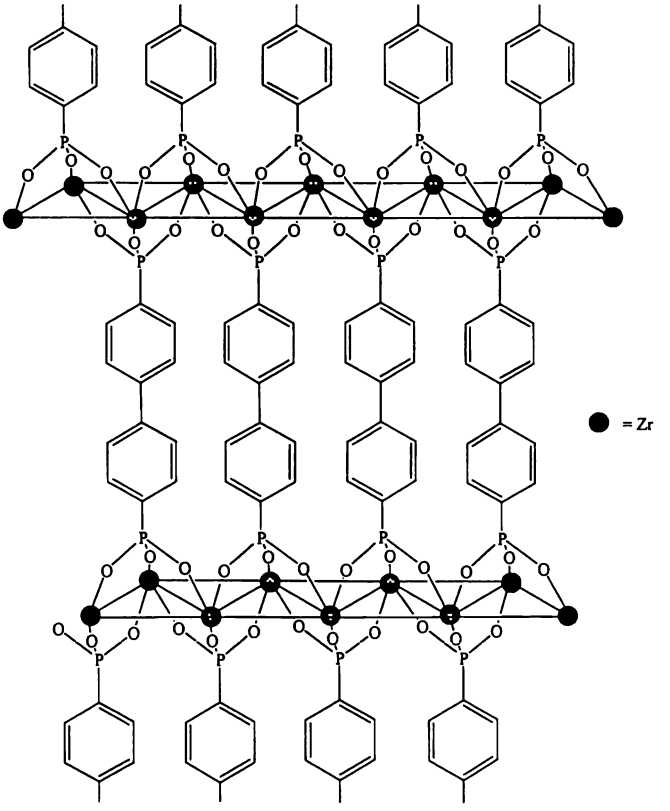

Figure 7.2: A Schematic Representation of $Zr[O_3P(C_6H_4)_2PO_3]$[4]

[4] A. Clearfield, *Chem. Mater.*, 1998, **10**, 2801.

A second structural aspect of layered metal phosphonates occurs when bis-phosphonic acids are used. These compounds form pillars between layers and the resulting materials are known as pillared metal phosphonates[1] (see Figure 7.2). Pillared metal phosphonates are subject to a greater degree of structural control because the distance between successive layers depends on the length of the pillar. The ferrocenyl bis-phosphonic acid **6** and **7** are interesting candidates for the synthesis of pillared redox active metal phosphonates.

Bis-phosphonic acids can also be used to grow metal phosphonate multilayer thin films on suitable substrates[5] (Scheme 7.1).

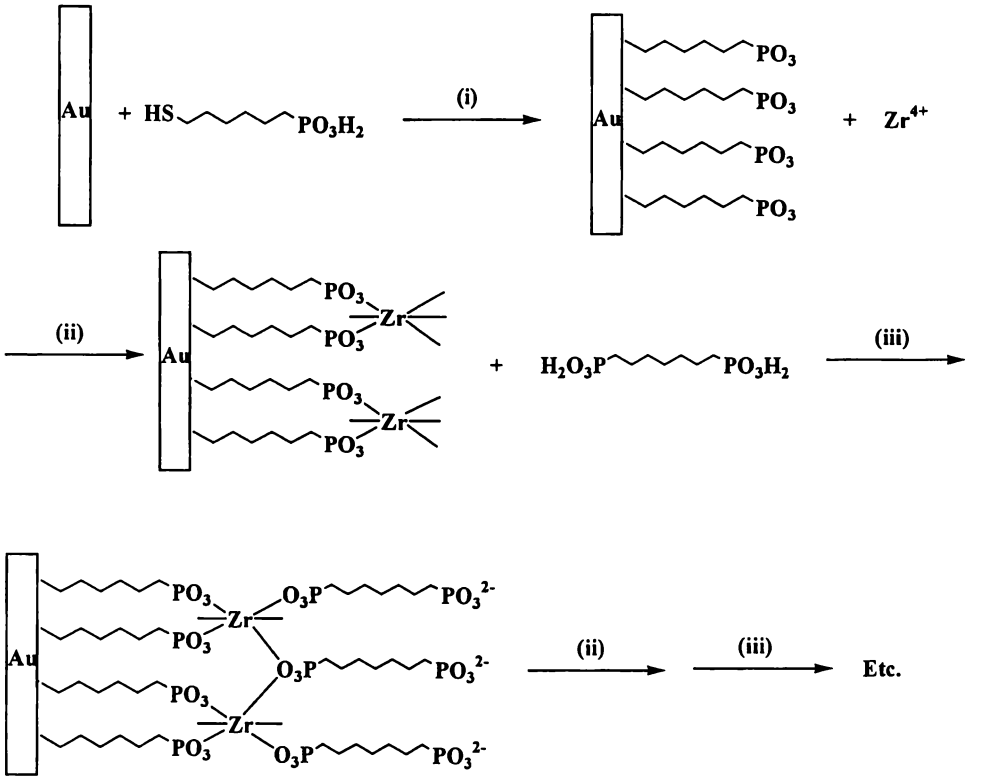

Scheme 7.1: Preparation of Multi-Layer Metal Phosphonate Thin Films on a Gold Surface.

[5] For reviews of this field see: (a) M. E. Thompson, *Chem. Mater.*, 1994, **6**, 1168. (b) H. E. Katz, *Chem. Mater.*, 1994, **6**, 2227. (c) T. E. Mallouk, H. N. Kim, P. J. Olivier and S. W. Keller, in Comprehensive Supramolcular Chemistry, G. Alberti and T. Beins, Eds., Pergamon, NY, 1996, 7, 189.

Synthesis of these thin films is simple and the resulting product is considerably more stable than the analogous Langmuir-Blodgett thin layer films. In addition, the metal ion and bis-phosphonic acid can be altered as successive layers are deposited, this allows for great flexibility in synthesis. Such films have aroused considerable interest as electrode coatings and electroactive materials. The ferrocenyl group has previously been studied as a redox active group on the terminal surface of such multilayer films[6]. The ferrocenyl phosphonic acids prepared in this thesis provide an ideal opportunity to incorporate ferrocenyl groups into such thin films, either on the terminal surface (acids **3**, **4** and **5**) or as an integral part of the multilayers (acids **6** and **7**).

7.3: Primary Ferrocenyl Phosphines

The primary ferrocenyl phosphines described in chapter four are perhaps the most interesting compounds in this thesis. The unique air stability of compounds **15**, **18**, **19** and **20** and of the related primary ferrocenyl arsine **25** is intriguing and worthy of further study. Synthesis of a more complete series of $Mc(CH_2)nPH_2$ (n = 0, 1, 2 etc..., Mc = metallocene,) to determine over what alkyl chain length the stabilisation effect operates. Further work might include the preparation of analogous arsine and stibine compounds as well as the use of different metallocenes (Figure 7.3).

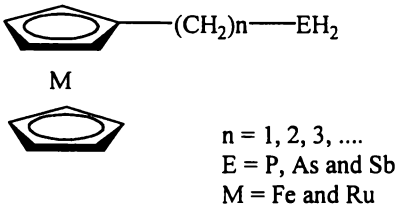

Figure 7.3: Possibilities for Further Synthesis of Primary Metallocene Pnictanes.

The fundamental reason for the stability of these compounds must lie in their electronic structure. For this reason theoretical modelling of the molecular orbital energies, especially the energy of the HOMO of these compounds, would be of

[6] H. –G. Hong and T. E. Mallouk, *Langmuir*, 1991, 7, 2362.

interest. Techniques such as photoelectron spectroscopy would offer valuable insight in this respect.

The stability of the $-CH_2PH_2$ group bound to ferrocene might also enable this group to be used in the design of ferrocenyl ligands intended for catalytic systems. Though the coordination chemistry of the $-PH_2$ group is different from that of the $-PPh_2$ group (due to the weakness of the P-H bond), the introduction of the $-PH_2$ group in place of the more typical PPh_2 group in chiral ligands such as 'JOSIPHOS' or 'TRAPS' would be of interest . Figure 7.4 gives examples of two possible chiral ligands containing the $-PH_2$ group.

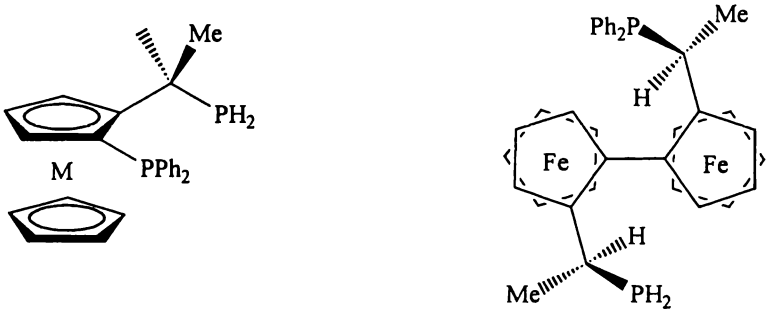

Figure 7.4: Possible Chiral Ferrocenyl Phosphine Ligands Incorporating the $-PH_2$ Group.

7.4: Ferrocenyl Hydroxymethylphosphines

Considering the large amount of study into dppf and related ligands, it is likely that the hydroxymethylphosphine 1,1'-Fc'$[P(CH_2OH)_2]_2$ **29** will prove the most significant compound prepared in this thesis. As a direct analogue of dppf the scope for further work on this compound is extensive.

The preparation and structural characterisation of metal complexes containing **29** as a ligand would be of interest from a purely structural point of view. Would the hydroxymethyl groups form extended hydrogen-bonding networks? Would there be interaction of the hydroxyl oxygen with the metal centre? In addition there are obvious parallels to be investigated in catalysis, with an especial focus on catalysis in aqueous media.

Hydroymethylphosphines react with a wide range of functional groups (see scheme 6.1) so it is possible to envisage a large number of molecular derivatives of **29** that would be interesting ligands in their own right. For example the reaction of **29** with CH_2=CHCN should give 1,1'-Fc'[$P(CH_2CH_2CN)_2$]$_2$ (Scheme 7.2), a molecule whose coordination chemistry should be extensive.

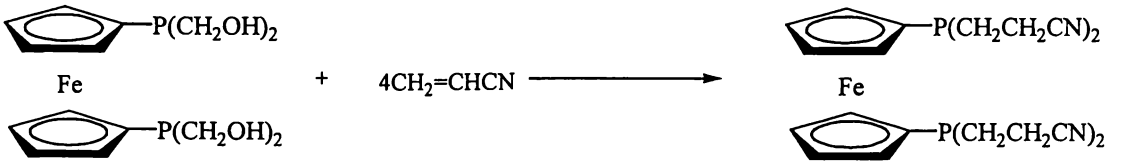

29

Scheme 7.2: Proposed Synthesis of 1,1'-Fc'[$P(CH_2CH_2CN)_2$]$_2$.

Other aspects of ferrocenyl hydroxymethylphosphines chemistry that are worthy of study include their incorporation into polymer systems. Polymers containing the ferrocenyl group have been extensively studied and are the subject of several reviews[7]. The rationale behind such chemistry is the production of polymers with useful properties such as, electrical conductivity, magnetic behaviour or thermal stability. The reaction of the ferrocenyl hydroxymethylphosphine $FcCH_2P(CH_2OH)_2$ with polymers containing free -NH groups (Jeffamine® and chitosan) has been previously studied with promising results[8]. The ferrocenyl hydroxymethylphosphines **28** and **29** should also be amenable to such chemistry.

The preparation of ferrocene coated silicon electrodes has also been undertaken using $FcCH_2P(CH_2OH)_2$ as the ferrocene source[9]. Compounds **28** and **29** would be suitable for analogous studies.

---

[7] (a) R. P. Kingsborough and T. M. Swager, *Prog. Inorg. Chem.*, 1999, **48**, 123. (b) K. E. Gonsalves and X. Chen, *Ferrocenes*, 1995, 497. (c) Ferrocenes, A. Togni and T. Hayashi Eds., VCH Verlagsgesellschaft, Weinheim, Germany, 1995 page 497.

[8] N. J. Goodwin, Doctoral Thesis, University of Waikato, 1998.

[9] R. D. Eagling, J. E. Bateman, N. J. Goodwin, W. Henderson and B. R. Horrocks, *J. Chem. Soc., Dalton Trans.*, 1998, **8**, 1273.

7.5: Conclusion

The synthesis of novel compounds based on ferrocene is a continuing feature in organometallic chemistry. Despite the many years of research and the many thousands of papers, ferrocenyl compounds are still able to throw up surprises for the synthetic chemist. The syntheses of compounds **1-36** involved the application of well-known techniques and well-understood chemistry to a range of ferrocenyl starting materials. The results were almost universally as expected, a tribute to the predictable chemistry of ferrocene. Yet amid compounds **1-36** are those whose properties and potential attest to limits of knowledge regarding ferrocene and its derivatives. Only further investigation will help determine whether the compounds described in this thesis have any place in the wider world of chemistry.

Appendix A

Complete lists of atomic coordinates and bond parameters and tables of thermal parameters and hydrogen atom coordinates for all structures reported in this thesis are listed in the following tables. Tables are listed by order of compound number.

Table A.1: Atomic coordinates and equivalent isotropic displacement parameters for **3**. U(eq) is defined as one third of the trace of the orthogonalized Uij tensor.

atom	x	y	z	U(eq)
Fe(1)	0.0073(1)	0.1090(1)	0.3376(1)	0.021(1)
P(1)	0.2877(1)	0.0400(1)	0.4906(1)	0.017(1)
O(1)	0.3455(1)	-0.0897(1)	0.5197(1)	0.021(1)
O(2)	0.3987(1)	0.1357(1)	0.4631(1)	0.027(1)
O(3)	0.2088(1)	0.1367(1)	0.5316(1)	0.026(1)
C(1)	0.1717(1)	-0.0125(1)	0.4383(1)	0.020(1)
C(11)	0.1334(1)	0.1138(1)	0.4028(1)	0.018(1)
C(12)	0.2054(1)	0.1584(2)	0.3555(1)	0.021(1)
C(13)	0.1382(2)	0.2821(2)	0.3334(1)	0.026(1)
C(14)	0.0249(2)	0.3154(2)	0.3672(1)	0.028(1)
C(15)	0.0221(2)	0.2122(2)	0.4102(1)	0.024(1)
C(21)	-0.0554(2)	0.0618(2)	0.2611(1)	0.034(1)
C(22)	0.0111(2)	-0.0604(2)	0.2846(1)	0.044(1)
C(23)	-0.0620(3)	-0.0991(2)	0.3318(1)	0.054(1)
C(24)	-0.1728(2)	-0.0015(3)	0.3375(1)	0.055(1)
C(25)	-0.1695(2)	0.0981(2)	0.2936(1)	0.042(1)

Table A.2: Bond lengths (Å) for **3**.

Fe(1)-C(23)	2.044(2)	C(11)-C(15)	1.437(2)
Fe(1)-C(24)	2.048(2)	C(11)-C(12)	1.440(2)
Fe(1)-C(22)	2.051(2)	C(12)-C(13)	1.432(2)
Fe(1)-C(11)	2.0524(13)	C(12)-H(12)	0.92(2)
Fe(1)-C(14)	2.052(2)	C(13)-C(14)	1.435(2)
Fe(1)-C(12)	2.0559(14)	C(13)-H(13)	0.97(2)
Fe(1)-C(13)	2.0564(15)	C(14)-C(15)	1.437(2)
Fe(1)-C(21)	2.057(2)	C(14)-H(14)	0.95(2)
Fe(1)-C(15)	2.0576(15)	C(15)-H(15)	0.97(2)
Fe(1)-C(25)	2.064(2)	C(21)-C(25)	1.429(3)
P(1)-O(1)	1.5127(10)	C(21)-C(22)	1.430(3)
P(1)-O(2)	1.5657(11)	C(21)-H(21)	0.92(2)
P(1)-O(3)	1.5668(11)	C(22)-C(23)	1.429(3)

P(1)-C(1)	1.8046(14)	C(22)-H(22)	0.97(2)
O(2)-H(3)	0.78(2)	C(23)-C(24)	1.423(4)
O(3)-H(4)	0.78(2)	C(23)-H(23)	0.97(3)
C(1)-C(11)	1.513(2)	C(24)-C(25)	1.432(3)
C(1)-H(1)	0.96(2)	C(24)-H(24)	0.91(3)
C(1)-H(2)	0.94(2)	C(25)-H(25)	0.98(2)

Table A.3: Bond Angles (°) for **3**.

C(23)-Fe(1)-C(24)	40.69(11)	C(11)-Fe(1)-C(14)	68.98(5)
C(23)-Fe(1)-C(22)	40.84(10)	C(23)-Fe(1)-C(12)	122.79(8)
C(24)-Fe(1)-C(22)	68.58(10)	C(24)-Fe(1)-C(12)	159.17(8)
C(23)-Fe(1)-C(11)	106.19(7)	C(22)-Fe(1)-C(12)	107.06(7)
C(24)-Fe(1)-C(11)	122.47(7)	C(11)-Fe(1)-C(12)	41.03(5)
C(22)-Fe(1)-C(11)	121.29(7)	C(14)-Fe(1)-C(12)	68.56(6)
C(23)-Fe(1)-C(14)	157.89(9)	C(23)-Fe(1)-C(13)	159.43(10)
C(24)-Fe(1)-C(14)	122.45(10)	C(24)-Fe(1)-C(13)	158.62(9)
C(22)-Fe(1)-C(14)	160.13(8)	C(22)-Fe(1)-C(13)	123.24(8)
C(11)-Fe(1)-C(13)	69.13(5)	P(1)-O(3)-H(4)	117.4(15)
C(14)-Fe(1)-C(13)	40.89(6)	C(11)-C(1)-P(1)	112.18(9)
C(12)-Fe(1)-C(13)	40.75(6)	C(11)-C(1)-H(1)	109.8(10)
C(23)-Fe(1)-C(21)	68.55(7)	P(1)-C(1)-H(1)	107.6(11)
C(24)-Fe(1)-C(21)	68.46(8)	C(11)-C(1)-H(2)	110.9(11)
C(22)-Fe(1)-C(21)	40.75(7)	P(1)-C(1)-H(2)	109.0(11)
C(11)-Fe(1)-C(21)	157.81(7)	H(1)-C(1)-H(2)	107.1(15)
C(14)-Fe(1)-C(21)	123.97(6)	C(15)-C(11)-C(12)	107.57(12)
C(12)-Fe(1)-C(21)	122.39(7)	C(15)-C(11)-C(1)	126.97(12)
C(13)-Fe(1)-C(21)	107.81(6)	C(12)-C(11)-C(1)	125.44(12)
C(23)-Fe(1)-C(15)	121.42(8)	C(15)-C(11)-Fe(1)	69.72(8)
C(24)-Fe(1)-C(15)	107.05(8)	C(12)-C(11)-Fe(1)	69.61(8)
C(22)-Fe(1)-C(15)	157.36(7)	C(1)-C(11)-Fe(1)	126.99(9)
C(11)-Fe(1)-C(15)	40.94(5)	C(13)-C(12)-C(11)	108.54(12)
C(14)-Fe(1)-C(15)	40.94(6)	C(13)-C(12)-Fe(1)	69.64(8)
C(12)-Fe(1)-C(15)	68.71(6)	C(11)-C(12)-Fe(1)	69.36(8)
C(13)-Fe(1)-C(15)	68.97(6)	C(13)-C(12)-H(12)	128.0(12)
C(21)-Fe(1)-C(15)	160.25(7)	C(11)-C(12)-H(12)	123.5(12)
C(23)-Fe(1)-C(25)	68.53(9)	Fe(1)-C(12)-H(12)	125.7(12)
C(24)-Fe(1)-C(25)	40.77(8)	C(12)-C(13)-C(14)	107.63(13)
C(22)-Fe(1)-C(25)	68.50(8)	C(12)-C(13)-Fe(1)	69.61(8)
C(11)-Fe(1)-C(25)	159.50(7)	C(14)-C(13)-Fe(1)	69.41(9)
C(14)-Fe(1)-C(25)	108.04(7)	C(12)-C(13)-H(13)	126.1(11)
C(12)-Fe(1)-C(25)	158.45(7)	C(14)-C(13)-H(13)	126.1(11)
C(13)-Fe(1)-C(25)	122.75(7)	Fe(1)-C(13)-H(13)	122.9(11)
C(21)-Fe(1)-C(25)	40.57(8)	C(13)-C(14)-C(15)	108.34(13)
C(15)-Fe(1)-C(25)	123.60(7)	C(13)-C(14)-Fe(1)	69.70(8)
O(1)-P(1)-O(2)	113.28(6)	C(15)-C(14)-Fe(1)	69.72(9)
O(1)-P(1)-O(3)	108.86(6)	C(13)-C(14)-H(14)	126.6(14)
O(2)-P(1)-O(3)	108.26(7)	C(15)-C(14)-H(14)	125.1(14)
O(1)-P(1)-C(1)	112.06(6)	Fe(1)-C(14)-H(14)	124.4(13)
O(2)-P(1)-C(1)	105.95(6)	C(11)-C(15)-C(14)	107.91(13)

O(3)-P(1)-C(1)	108.25(7)	C(11)-C(15)-Fe(1)	69.34(8)
P(1)-O(2)-H(3)	119.1(18)	C(14)-C(15)-Fe(1)	69.34(9)
C(11)-C(15)-H(15)	122.8(12)	C(22)-C(23)-Fe(1)	69.84(10)
C(14)-C(15)-H(15)	129.1(12)	C(24)-C(23)-H(23)	121.6(15)
Fe(1)-C(15)-H(15)	123.1(12)	C(22)-C(23)-H(23)	130.1(15)
C(25)-C(21)-C(22	108.2(2)	Fe(1)-C(23)-H(23)	122.8(14)
C(25)-C(21)-Fe(1)	69.95(9)	C(23)-C(24)-C(25)	108.2(2)
C(22)-C(21)-Fe(1)	69.40(9)	C(23)-C(24)-Fe(1)	69.51(11)
C(25)-C(21)-H(21)	129.1(13)	C(25)-C(24)-Fe(1)	70.20(10)
C(22)-C(21)-H(21)	122.6(14)	C(23)-C(24)-H(24)	122.8(18)
Fe(1)-C(21)-H(21)	123.7(14)	C(25)-C(24)-H(24)	128.9(18)
C(23)-C(22)-C(21)	107.8(2)	Fe(1)-C(24)-H(24)	127.0(17)
C(23)-C(22)-Fe(1)	69.32(11)	C(21)-C(25)-C(24)	107.6(2)
C(21)-C(22)-Fe(1)	69.86(10)	C(21)-C(25)-Fe(1)	69.47(9)
C(23)-C(22)-H(22)	126.5(14)	C(24)-C(25)-Fe(1)	69.03(10)
C(21)-C(22)-H(22)	125.7(14)	C(21)-C(25)-H(25)	127.0(14)
Fe(1)-C(22)-H(22)	124.8(14)	C(24)-C(25)-H(25)	125.2(14)
C(24)-C(23)-C(22)	108.2(2)	Fe(1)-C(25)-H(25)	123.6(14)
C(24)-C(23)-Fe(1)	69.80(11)		

Table A.4: Anisotropic displacement parameters ($Å^2$) for **3**. The anisotropic displacement factor exponent takes the form: $-2\pi^2[h^2a^{*2}U_{11} + ... + 2hka^*b^*U12]$.

atom	U11	U22	U33	U23	U13	U12
Fe(1)	0.022(1)	0.021(1)	0.019(1)	0.000(1)	-0.007(1)	-0.003(1)
P(1)	0.019(1)	0.014(1)	0.018(1)	0.002(1)	-0.004(1)	0.000(1)
O(1)	0.022(1)	0.015(1)	0.025(1)	0.004(1)	-0.005(1)	0.001(1)
O(2)	0.020(1)	0.024(1)	0.038(1)	0.014(1)	-0.006(1)	-0.003(1)
O(3)	0.041(1)	0.016(1)	0.021(1)	0.000(1)	0.001(1)	0.005(1)
C(1)	0.022(1)	0.018(1)	0.019(1)	0.000(1)	-0.004(1)	-0.002(1)
C(11)	0.019(1)	0.019(1)	0.017(1)	-0.002(1)	-0.004(1)	0.000(1)
C(12)	0.020(1)	0.022(1)	0.021(1)	0.000(1)	-0.002(1)	-0.001(1)
C(13)	0.030(1)	0.022(1)	0.024(1)	0.004(1)	-0.008(1)	-0.005(1)
C(14)	0.032(1)	0.021(1)	0.032(1)	-0.004(1)	-0.011(1)	0.006(1)
C(15)	0.024(1)	0.027(1)	0.022(1)	-0.005(1)	-0.002(1)	0.005(1)
C(21)	0.045(1)	0.033(1)	0.023(1)	-0.001(1)	-0.015(1)	-0.007(1)
C(22)	0.060(1)	0.028(1)	0.043(1)	-0.012(1)	-0.026(1)	-0.001(1)
C(23)	0.081(2)	0.034(1)	0.047(1)	0.011(1)	-0.037(1)	-0.030(1)
C(24)	0.044(1)	0.081(2)	0.039(1)	0.006(1)	-0.012(1)	-0.040(1)
C(25)	0.030(1)	0.055(1)	0.040(1)	-0.003(1)	-0.018(1)	-0.007(1)

Table A.5: Hydrogen coordinates and isotropic displacement parameters ($Å^2$) for **3**.

Atom	x	y	z	U(eq)
H(12)	0.2803(21)	0.1113(20)	0.3426(7)	0.035(5)
H(1)	0.2150(18)	-0.0860(20)	0.4175(7)	0.029(5)
H(2)	0.0944(19)	-0.0544(20)	0.4538(7)	0.029(4)
H(14)	-0.0401(23)	0.3901(23)	0.3618(9)	0.044(6)
H(21)	-0.0228(22)	0.1078(23)	0.2312(10)	0.047(6)
H(3)	0.4745(25)	0.1179(25)	0.4679(10)	0.052(7)
H(13)	0.1610(20)	0.3302(21)	0.2999(8)	0.037(5)
H(15)	-0.0446(20)	0.2007(21)	0.4386(8)	0.038(5)
H(25)	-0.2313(24)	0.1800(28)	0.2888(9)	0.059(7)
H(23)	-0.0428(25)	-0.1722(27)	0.3584(10)	0.056(6)
H(4)	0.2031(20)	0.2196(25)	0.5253(8)	0.041(6)
H(22)	0.0925(25)	-0.1062(25)	0.2712(9)	0.056(7)
H(24)	-0.2337(28)	-0.0077(30)	0.3647(10)	0.073(8)

Table A.6: Atomic coordinates and equivalent isotropic displacement parameters for **7**. U(eq) is defined as one third of the trace of the orthogonalized Uij tensor.

atom	x	y	z	U(eq)
Fe(1)	0.0000	0.5000	0.0000	0.025(1)
P(1)	0.4569(1)	0.2086(1)	0.0304(1)	0.023(1)
O(11)	0.3734(2)	0.0966(1)	0.1060(2)	0.036(1)
O(12)	0.5806(2)	0.2867(2)	0.1551(2)	0.036(1)
O(13)	0.5470(2)	0.1537(1)	-0.0809(1)	0.028(1)
C(1)	0.2965(2)	0.3235(2)	-0.0558(2)	0.027(1)
C(11)	0.1929(2)	0.3675(2)	0.0490(2)	0.023(1)
C(12)	0.0455(2)	0.3033(2)	0.0670(2)	0.033(1)
C(13)	-0.0148(3)	0.3768(3)	0.1757(2)	0.045(1)
C(14)	0.0946(3)	0.4857(2)	0.2263(2)	0.043(1)
C(15)	0.2235(2)	0.4803(2)	0.1488(2)	0.031(1)

Table A.7: Bond lengths (Å) for **7**.

Fe(1)-C(11)#1	2.036(2)	O(2)-H(2)	0.74(3)
Fe(1)-C(11)	2.037(2)	O(3)-H(3)	0.66(3)
Fe(1)-C(12)	2.039(2)	C(1)-C(11)	1.499(2)
Fe(1)-C(12)#1	2.039(2)	C(1)-H(1)	0.95(2)
Fe(1)-C(14)#1	2.040(2)	C(1)-H(1A)	0.96(2)
Fe(1)-C(14)	2.040(2)	C(11)-C(15)	1.422(2)
Fe(1)-C(13)	2.041(2)	C(11)-C(12)	1.426(3)
Fe(1)-C(13)#1	2.041(2)	C(12)-C(13)	1.415(3)
Fe(1)-C(15)	2.041(2)	C(12)-H(12)	0.97(3)
Fe(1)-C(15)#1	2.041(2)	C(13)-C(14)	1.413(4)

P(1)-O(1)	1.5027(12)	C(13)-H(13)	0.95(3)
P(1)-O(3)	1.5487(15)	C(14)-C(15)	1.423(3)
P(1)-O(2)	1.5512(14)	C(14)-H(14)	0.87(3)
P(1)-C(1)	1.786(2)	C(15)-H(15)	0.95(2)

Symmetry transformations used to generate equivalent atoms: #1 -x,-y+1,-z

Table A.8: Bond Angles (°) for **7**.

C(11)#1-Fe(1)-C(11)	180.0	O(1)-P(1)-O(3)	108.97(8)
C(11)#1-Fe(1)-C(12)	139.03(7)	O(1)-P(1)-O(2)	113.32(7)
C(11)-Fe(1)-C(12)	40.97(7)	O(3)-P(1)-O(2)	108.36(8)
C(11)#1-Fe(1)-C(12)#1	40.97(7)	O(1)-P(1)-C(1)	111.76(7)
C(11)-Fe(1)-C(12)#1	139.03(7)	O(3)-P(1)-C(1)	108.08(9)
C(12)-Fe(1)-C(12)#1	180.0	O(2)-P(1)-C(1)	106.16(9)
C(11)#1-Fe(1)-C(14)#1	68.71(7)	P(1)-O(2)-H(2)	119.5(22)
C(11)-Fe(1)-C(14)#1	111.29(7)	P(1)-O(3)-H(3)	116.6(24)
C(12)-Fe(1)-C(14)#1	111.76(9)	C(11)-C(1)-P(1)	112.65(12)
C(12)#1-Fe(1)-C(14)#1	68.25(9)	C(11)-C(1)-H(1)	110.2(14)
C(11)#1-Fe(1)-C(14)	111.29(7)	P(1)-C(1)-H(1)	106.1(14)
C(11)-Fe(1)-C(14)	68.71(7)	C(11)-C(1)-H(1A)	109.5(15)
C(12)-Fe(1)-C(14)	68.24(9)	P(1)-C(1)-H(1A)	108.3(15)
C(12)#1-Fe(1)-C(14)	111.75(9)	H(1)-C(1)-H(1A)	109.9(21)
C(14)#1-Fe(1)-C(14)	180.0	C(15)-C(11)-C(12)	107.5(2)
C(11)#1-Fe(1)-C(13)	111.19(7)	C(15)-C(11)-C(1)	126.4(2)
C(11)-Fe(1)-C(13)	68.81(7)	C(12)-C(11)-C(1)	126.2(2)
C(12)-Fe(1)-C(13)	40.60(9)	C(15)-C(11)-Fe(1)	69.78(10)
C(12)#1-Fe(1)-C(13)	139.40(9)	C(12)-C(11)-Fe(1)	69.59(10)
C(14)#1-Fe(1)-C(13)	139.49(10)	C(1)-C(11)-Fe(1)	126.09(11)
C(14)-Fe(1)-C(13)	40.51(10)	C(13)-C(12)-C(11)	108.3(2)
C(11)#1-Fe(1)-C(13)#1	68.81(7)	C(13)-C(12)-Fe(1)	69.78(11)
C(11)-Fe(1)-C(13)#1	111.19(7)	C(11)-C(12)-Fe(1)	69.44(10)
C(12)-Fe(1)-C(13)#1	139.40(9)	C(13)-C(12)-H(12)	128.5(15)
C(12)#1-Fe(1)-C(13)#1	40.60(9)	C(11)-C(12)-H(12)	123.1(15)
C(14)#1-Fe(1)-C(13)#	140.51(10)	Fe(1)-C(12)-H(12)	125.1(14)
C(14)-Fe(1)-C(13)#1	139.49(10)	C(14)-C(13)-C(12)	108.0(2)
C(13)-Fe(1)-C(13)#1	180.0	C(14)-C(13)-Fe(1)	69.71(12)
C(11)#1-Fe(1)-C(15)	139.19(7)	C(12)-C(13)-Fe(1)	69.62(11)
C(11)-Fe(1)-C(15)	40.81(7)	C(14)-C(13)-H(13)	127.0(16)
C(12)-Fe(1)-C(15)	68.50(8)	C(12)-C(13)-H(13)	124.9(17)
C(12)#1-Fe(1)-C(15)	111.50(8)	Fe(1)-C(13)-H(13)	122.7(16)
C(14)#1-Fe(1)-C(15)	139.19(8)	C(13)-C(14)-C(15)	108.3(2)
C(14)-Fe(1)-C(15)	40.81(8)	C(13)-C(14)-Fe(1)	69.78(12)
C(13)-Fe(1)-C(15)	68.52(9)	C(15)-C(14)-Fe(1)	69.66(10)
C(13)#1-Fe(1)-C(15)	111.47(9)	C(13)-C(14)-H(14)	128.5(19)
C(11)#1-Fe(1)-C(15)#	40.81(7)	C(15)-C(14)-H(14)	123.2(19)
C(11)-Fe(1)-C(15)#1	139.19(7)	Fe(1)-C(14)-H(14)	124.9(18)
C(12)-Fe(1)-C(15)#1	111.50(8)	C(11)-C(15)-C(14)	107.9(2)
C(12)#1-Fe(1)-C(15)#1	68.50(8)	C(11)-C(15)-Fe(1)	69.41(10)
C(14)#1-Fe(1)-C(15)#1	40.82(8)	C(14)-C(15)-Fe(1)	69.53(11)

C(14)-Fe(1)-C(15)#1	139.19(8)	C(11)-C(15)-H(15)	122.0(14)
C(13)-Fe(1)-C(15)#1	111.47(9)	C(14)-C(15)-H(15)	130.0(14)
C(13)#1-Fe(1)-C(15)#1	68.53(9)	Fe(1)-C(15)-H(15)	124.4(14)
C(15)-Fe(1)-C(15)#1	180.0		

Symmetry transformations used to generate equivalent atoms: #1 -x,-y+1,-z.

Table A.9: Anisotropic displacement parameters ($Å^2$) for **7**. The anisotropic displacement factor exponent takes the form: $-2\pi^2[h^2a^{*2}U_{11} + ... + 2hka^*b^*U12]$.

atom	U11	U22	U33	U23	U13	U12
Fe(1)	0.024(1)	0.029(1)	0.023(1)	0.005(1)	0.008(1)	0.010(1)
P(1)	0.027(1)	0.025(1)	0.019(1)	0.001(1)	0.009(1)	0.008(1)
O(2)	0.051(1)	0.024(1)	0.042(1)	0.005(1)	0.030(1)	0.010(1)
O(3)	0.030(1)	0.056(1)	0.023(1)	-0.007(1)	0.009(1)	0.001(1)
O(1)	0.037(1)	0.027(1)	0.023(1)	0.002(1)	0.014(1)	0.011(1)
C(1)	0.031(1)	0.027(1)	0.024(1)	0.001(1)	0.007(1)	0.009(1)
C(11)	0.024(1)	0.023(1)	0.023(1)	0.003(1)	0.004(1)	0.009(1)
C(12)	0.031(1)	0.031(1)	0.037(1)	0.013(1)	0.008(1)	0.004(1)
C(13)	0.038(1)	0.062(1)	0.039(1)	0.027(1)	0.020(1)	0.021(1)
C(14)	0.054(1)	0.054(1)	0.022(1)	0.003(1)	0.010(1)	0.032(1)
C(15)	0.032(1)	0.032(1)	0.026(1)	-0.003(1)	0.000(1)	0.010(1)

Table A.10: Hydrogen coordinates and isotropic displacement parameters ($Å^2$) for **7**.

Atom	x	y	z	U(eq)
H(1)	0.2310(29)	0.2769(23)	-0.1390(28)	0.042(6)
H(1A)	0.3463(31)	0.4019(25)	-0.0897(27)	0.051(7)
H(3)	0.5616(33)	0.2916(26)	0.2211(30)	0.044(8)
H(2)	0.3919(36)	0.0238(27)	0.0948(31)	0.052(8)
H(12)	-0.0023(29)	0.2241(28)	0.0094(27)	0.048(7)
H(13)	-0.1163(35)	0.3586(27)	0.2028(30)	0.060(8)
H(14)	0.0877(34)	0.5484(28)	0.2909(31)	0.059(8)
H(15)	0.3148(29)	0.5399(23)	0.1536(25)	0.036(6)

Table A.11: Atomic coordinates and equivalent isotropic displacement parameters for **12**. U(eq) is defined as one third of the trace of the orthogonalized Uij tensor.

atom	x	y	z	U(eq)
Pt(1)	0.1213(1)	0.5376(1)	0.1227(1)	0.017(1)
Fe(1)	0.1352(1)	0.6127(1)	0.3381(1)	0.028(1)

P(1)	0.0771(1)	0.6657(1)	0.1576(1)	0.021(1)
P(2)	0.0873(1)	0.4237(1)	0.1329(1)	0.019(1)
P(3)	0.2143(1)	0.5127(1)	0.0791(1)	0.020(1)
O(1)	0.1420(1)	0.6482(2)	0.1272(1)	0.023(1)
O(2)	0.0403(1)	0.5913(2)	0.1533(1)	0.022(1)
O(3)	0.0413(2)	0.7303(2)	0.1385(1)	0.027(1)
C(1)	0.0931(2)	0.6787(2)	0.2279(2)	0.027(1)
C(11)	0.1233(2)	0.6160(2)	0.2573(2)	0.026(1)
C(12)	0.1908(2)	0.6071(2)	0.2711(2)	0.028(1)
C(13)	0.1973(2)	0.5428(2)	0.3017(2)	0.031(1)
C(14)	0.1342(2)	0.5107(3)	0.3069(2)	0.033(1)
C(15)	0.0891(2)	0.5558(2)	0.2791(2)	0.029(1)
C(21)	0.1053(4)	0.7111(4)	0.3645(3)	0.061(2)
C(22)	0.0654(3)	0.6538(5)	0.3861(3)	0.078(3)
C(23)	0.1066(3)	0.6073(4)	0.4156(3)	0.059(2)
C(24)	0.1689(3)	0.6338(3)	0.4132(2)	0.047(1)
C(25)	0.1693(3)	0.6975(3)	0.3824(2)	0.045(1)
C(31)	0.0189(2)	0.4158(2)	0.1796(2)	0.023(1)
C(32)	0.0222(2)	0.3715(2)	0.2248(2)	0.028(1)
C(33)	-0.0317(2)	0.3657(3)	0.2585(2)	0.035(1)
C(34)	-0.0883(2)	0.4041(3)	0.2472(2)	0.038(1)
C(35)	-0.0918(2)	0.4476(3)	0.2026(2)	0.036(1)
C(36)	-0.0384(2)	0.4538(2)	0.1683(2)	0.028(1)
C(41)	0.0553(2)	0.3805(2)	0.0736(2)	0.022(1)
C(42)	0.0504(2)	0.4199(2)	0.0264(2)	0.024(1)
C(43)	0.0229(2)	0.3888(3)	-0.0186(2)	0.029(1)
C(44)	-0.0002(2)	0.3178(3)	-0.0171(2)	0.030(1)
C(45)	0.0037(2)	0.2791(2)	0.0304(2)	0.031(1)
C(46)	0.0301(2)	0.3098(2)	0.0757(2)	0.026(1)
C(51)	0.1506(2)	0.3681(2)	0.1636(2)	0.023(1)
C(52)	0.1796(2)	0.3996(2)	0.2080(2)	0.027(1)
C(53)	0.2271(2)	0.3629(3)	0.2364(2)	0.034(1)
C(54)	0.2463(2)	0.2948(3)	0.2199(2)	0.040(1)
C(55)	0.2189(2)	0.2633(2)	0.1754(2)	0.035(1)
C(56)	0.1703(2)	0.2994(2)	0.1472(2)	0.026(1)
C(61)	0.2101(2)	0.5493(2)	0.0118(2)	0.023(1)
C(62)	0.1594(2)	0.5951(2)	-0.0036(2)	0.027(1)
C(63)	0.1566(3)	0.6228(3)	-0.0548(2)	0.037(1)
C(64)	0.2054(3)	0.6060(3)	-0.0910(2)	0.038(1)
C(65)	0.2562(3)	0.5605(3)	-0.0767(2)	0.038(1)
C(66)	0.2585(2)	0.5320(2)	-0.0255(2)	0.030(1)
C(71)	0.2453(2)	0.4212(2)	0.0679(2)	0.024(1)
C(72)	0.2150(2)	0.3774(2)	0.0295(2)	0.030(1)
C(73)	0.2380(3)	0.3074(3)	0.0201(2)	0.038(1)
C(74)	0.2914(3)	0.2817(3)	0.0484(2)	0.043(1)
C(75)	0.3221(2)	0.3246(3)	0.0857(2)	0.038(1)
C(76)	0.2992(2)	0.3944(2)	0.0955(2)	0.030(1)
C(81)	0.2823(2)	0.5590(2)	0.1118(2)	0.024(1)
C(82)	0.2884(2)	0.5527(2)	0.1666(2)	0.029(1)
C(83)	0.3420(2)	0.5812(3)	0.1929(2)	0.035(1)

C(84)	0.3899(2)	0.6164(3)	0.1643(2)	0.039(1)
C(85)	0.3840(2)	0.6251(3)	0.1100(2)	0.041(1)
C(86)	0.3298(2)	0.5965(3)	0.0834(2)	0.033(1)
C(91)	0.1044(4)	0.1730(5)	0.3605(4)	0.093(3)
Cl(1)	0.1563(1)	0.1062(1)	0.3826(1)	0.073(1)
Cl(2)	0.0267(1)	0.9558(1)	0.1043(1)	0.098(1)
C(92)	0.0044(4)	0.8774(4)	0.0733(4)	0.094(3)
Cl(3)	0.1366(1)	0.2215(2)	0.3076(1)	0.124(1)
Cl(4)	-0.0785(1)	0.8734(2)	0.0553(2)	0.142(1)

Table A.12: Bond lengths (Å) for **12**.

Pt(1)-O(2)	2.075(3)	C(32)-C(33)	1.392(6)
Pt(1)-O(1)	2.081(3)	C(33)-C(34)	1.384(7)
Pt(1)-P(2)	2.2253(10)	C(34)-C(35)	1.376(8)
Pt(1)-P(3)	2.2378(10)	C(35)-C(36)	1.393(6)
Pt(1)-P(1)	2.6719(10)	C(41)-C(42)	1.390(6)
Fe(1)-C(22)	2.014(6)	C(41)-C(46)	1.400(6)
Fe(1)-C(13)	2.024(5)	C(42)-C(43)	1.384(6)
Fe(1)-C(21)	2.024(6)	C(43)-C(44)	1.390(6)
Fe(1)-C(23)	2.030(6)	C(44)-C(45)	1.391(7)
Fe(1)-C(12)	2.030(5)	C(45)-C(46)	1.376(6)
Fe(1)-C(14)	2.035(5)	C(51)-C(52)	1.387(6)
Fe(1)-C(25)	2.038(5)	C(51)-C(56)	1.392(6)
Fe(1)-C(24)	2.040(5)	C(52)-C(53)	1.380(6)
Fe(1)-C(11)	2.040(5)	C(53)-C(54)	1.377(7)
Fe(1)-C(15)	2.042(5)	C(54)-C(55)	1.375(8)
P(1)-O(3)	1.476(3)	C(55)-C(56)	1.388(7)
P(1)-O(1)	1.563(3)	C(61)-C(62)	1.390(6)
P(1)-O(2)	1.566(3)	C(61)-C(66)	1.396(6)
P(1)-C(1)	1.807(5)	C(62)-C(63)	1.383(7)
P(2)-C(41)	1.809(4)	C(63)-C(64)	1.383(7)
P(2)-C(51)	1.818(4)	C(64)-C(65)	1.379(7)
P(2)-C(31)	1.830(4)	C(65)-C(66)	1.388(7)
P(3)-C(61)	1.819(5)	C(71)-C(76)	1.391(6)
P(3)-C(71)	1.822(4)	C(71)-C(72)	1.400(6)
P(3)-C(81)	1.823(4)	C(72)-C(73)	1.392(6)
C(1)-C(11)	1.502(6)	C(73)-C(74)	1.383(8)
C(11)-C(15)	1.419(7)	C(74)-C(75)	1.375(8)
C(11)-C(12)	1.430(6)	C(75)-C(76)	1.390(6)
C(12)-C(13)	1.418(7)	C(81)-C(86)	1.387(6)
C(13)-C(14)	1.423(7)	C(81)-C(82)	1.386(7)
C(14)-C(15)	1.422(7)	C(82)-C(83)	1.380(7)
C(21)-C(25)	1.405(8)	C(83)-C(84)	1.374(7)
C(21)-C(22)	1.439(11)	C(84)-C(85)	1.378(8)
C(22)-C(23)	1.410(11)	C(85)-C(86)	1.394(7)
C(23)-C(24)	1.364(9)	C(91)-Cl(1)	1.714(8)
C(24)-C(25)	1.403(8)	C(91)-Cl(3)	1.730(8)
C(31)-C(36)	1.393(6)	Cl(2)-C(92)	1.700(8)
C(31)-C(32)	1.396(6)	C(92)-Cl(4)	1.754(8)

Table A.13: Bond Angles (°) for **12**.

O(2)-Pt(1)-O(1)	71.14(11)	C(12)-C(11)-C(1)	127.0(4)
O(2)-Pt(1)-P(2)	99.01(8)	C(15)-C(11)-Fe(1)	69.7(3)
O(1)-Pt(1)-P(2)	168.23(9)	C(12)-C(11)-Fe(1)	69.1(3)
O(2)-Pt(1)-P(3)	162.83(8)	C(1)-C(11)-Fe(1)	124.1(3)
O(1)-Pt(1)-P(3)	93.18(8)	C(13)-C(12)-C(11)	108.4(4)
P(2)-Pt(1)-P(3)	97.31(4)	C(13)-C(12)-Fe(1)	69.3(3)
O(2)-Pt(1)-P(1)	35.82(8)	C(11)-C(12)-Fe(1)	69.8(3)
O(1)-Pt(1)-P(1)	35.74(8)	C(12)-C(13)-C(14)	108.2(4)
P(2)-Pt(1)-P(1)	133.50(4)	C(12)-C(13)-Fe(1)	69.8(3)
P(3)-Pt(1)-P(1)	128.92(4)	C(14)-C(13)-Fe(1)	69.9(3)
C(22)-Fe(1)-C(13)	162.2(3)	C(13)-C(14)-C(15)	107.4(4)
C(22)-Fe(1)-C(21)	41.7(3)	C(13)-C(14)-Fe(1)	69.1(3)
C(13)-Fe(1)-C(21)	155.0(3)	C(15)-C(14)-Fe(1)	69.8(3)
C(22)-Fe(1)-C(23)	40.8(3)	C(11)-C(15)-C(14)	109.0(4)
C(13)-Fe(1)-C(23)	125.5(3)	C(11)-C(15)-Fe(1)	69.6(3)
C(21)-Fe(1)-C(23)	69.2(3)	C(14)-C(15)-Fe(1)	69.3(3)
C(22)-Fe(1)-C(12)	155.4(3)	C(25)-C(21)-C(22)	106.0(6)
C(13)-Fe(1)-C(12)	40.9(2)	C(25)-C(21)-Fe(1)	70.3(3)
C(21)-Fe(1)-C(12)	119.0(3)	C(22)-C(21)-Fe(1)	68.8(4)
C(23)-Fe(1)-C(12)	161.8(3)	C(23)-C(22)-C(21)	107.7(5)
C(22)-Fe(1)-C(14)	124.7(3)	C(23)-C(22)-Fe(1)	70.2(3)
C(13)-Fe(1)-C(14)	41.0(2)	C(21)-C(22)-Fe(1)	69.5(3)
C(21)-Fe(1)-C(14)	161.6(3)	C(24)-C(23)-C(22)	108.4(6)
C(23)-Fe(1)-C(14)	108.6(3)	C(24)-C(23)-Fe(1)	70.8(3)
C(12)-Fe(1)-C(14)	68.9(2)	C(22)-C(23)-Fe(1)	69.0(4)
C(22)-Fe(1)-C(25)	68.2(3)	C(23)-C(24)-C(25)	109.2(6)
C(13)-Fe(1)-C(25)	121.3(2)	C(23)-C(24)-Fe(1)	70.0(3)
C(21)-Fe(1)-C(25)	40.5(2)	C(25)-C(24)-Fe(1)	69.8(3)
C(23)-Fe(1)-C(25)	67.4(3)	C(24)-C(25)-C(21)	108.6(6)
C(12)-Fe(1)-C(25)	107.4(2)	C(24)-C(25)-Fe(1)	69.9(3)
C(14)-Fe(1)-C(25)	156.9(2)	C(21)-C(25)-Fe(1)	69.2(3)
C(22)-Fe(1)-C(24)	67.5(3)	C(36)-C(31)-C(32)	119.9(4)
C(13)-Fe(1)-C(24)	109.0(2)	C(36)-C(31)-P(2)	118.2(3)
C(21)-Fe(1)-C(24)	68.3(2)	C(32)-C(31)-P(2)	121.9(3)
C(23)-Fe(1)-C(24)	39.2(3)	C(33)-C(32)-C(31)	119.9(4)
C(12)-Fe(1)-C(24)	125.8(2)	C(34)-C(33)-C(32)	119.7(5)
C(14)-Fe(1)-C(24)	122.3(2)	C(35)-C(34)-C(33)	120.5(4)
C(25)-Fe(1)-C(24)	40.3(2)	C(34)-C(35)-C(36)	120.5(5)
C(22)-Fe(1)-C(11)	119.8(3)	C(31)-C(36)-C(35)	119.4(5)
C(13)-Fe(1)-C(11)	69.3(2)	C(42)-C(41)-C(46)	119.4(4)
C(21)-Fe(1)-C(11)	105.1(2)	C(42)-C(41)-P(2)	119.7(3)
C(23)-Fe(1)-C(11)	156.4(2)	C(46)-C(41)-P(2)	120.7(3)
C(12)-Fe(1)-C(11)	41.1(2)	C(43)-C(42)-C(41)	120.3(4)
C(14)-Fe(1)-C(11)	69.2(2)	C(42)-C(43)-C(44)	120.4(4)
C(25)-Fe(1)-C(11)	123.9(2)	C(43)-C(44)-C(45)	118.9(4)
C(24)-Fe(1)-C(11)	161.7(2)	C(46)-C(45)-C(44)	121.2(4)
C(22)-Fe(1)-C(15)	107.4(2)	C(45)-C(46)-C(41)	119.6(4)

C(13)-Fe(1)-C(15)	68.7(2)	C(52)-C(51)-C(56)	119.6(4)
C(21)-Fe(1)-C(15)	123.8(2)	C(52)-C(51)-P(2)	114.1(3)
C(23)-Fe(1)-C(15)	122.3(2)	C(56)-C(51)-P(2)	126.3(4)
C(12)-Fe(1)-C(15)	68.4(2)	C(53)-C(52)-C(51)	120.6(4)
C(14)-Fe(1)-C(15)	40.8(2)	C(54)-C(53)-C(52)	119.4(5)
C(25)-Fe(1)-C(15)	160.8(2)	C(55)-C(54)-C(53)	120.8(5)
C(24)-Fe(1)-C(15)	157.1(2)	C(54)-C(55)-C(56)	120.2(4)
C(11)-Fe(1)-C(15)	40.7(2)	C(55)-C(56)-C(51)	119.4(5)
O(3)-P(1)-O(1)	115.3(2)	C(62)-C(61)-C(66)	118.7(4)
O(3)-P(1)-O(2)	116.4(2)	C(62)-C(61)-P(3)	121.1(3)
O(1)-P(1)-O(2)	101.17(15)	C(66)-C(61)-P(3)	120.2(3)
O(3)-P(1)-C(1)	107.4(2)	C(63)-C(62)-C(61)	120.7(4)
O(1)-P(1)-C(1)	110.4(2)	C(62)-C(63)-C(64)	119.8(5)
O(2)-P(1)-C(1)	105.7(2)	C(65)-C(64)-C(63)	120.5(5)
O(3)-P(1)-Pt(1)	140.49(14)	C(64)-C(65)-C(66)	119.6(5)
O(1)-P(1)-Pt(1)	51.05(10)	C(65)-C(66)-C(61)	120.6(4)
O(2)-P(1)-Pt(1)	50.84(10)	C(76)-C(71)-C(72)	119.2(4)
C(1)-P(1)-Pt(1)	112.07(14)	C(76)-C(71)-P(3)	121.7(4)
C(41)-P(2)-C(51)	111.0(2)	C(72)-C(71)-P(3)	119.0(3)
C(41)-P(2)-C(31)	102.4(2)	C(73)-C(72)-C(71)	120.0(5)
C(51)-P(2)-C(31)	103.1(2)	C(74)-C(73)-C(72)	119.8(5)
C(41)-P(2)-Pt(1)	115.62(14)	C(75)-C(74)-C(73)	120.7(4)
C(51)-P(2)-Pt(1)	110.94(14)	C(74)-C(75)-C(76)	119.9(5)
C(31)-P(2)-Pt(1)	112.77(13)	C(71)-C(76)-C(75)	120.4(5)
C(61)-P(3)-C(71)	102.5(2)	C(86)-C(81)-C(82)	119.1(4)
C(61)-P(3)-C(81)	106.2(2)	C(86)-C(81)-P(3)	122.4(4)
C(71)-P(3)-C(81)	103.7(2)	C(82)-C(81)-P(3)	118.4(3)
C(61)-P(3)-Pt(1)	109.65(14)	C(83)-C(82)-C(81)	120.8(4)
C(71)-P(3)-Pt(1)	124.10(14)	C(84)-C(83)-C(82)	119.8(5)
C(81)-P(3)-Pt(1)	109.33(14)	C(83)-C(84)-C(85)	120.5(5)
P(1)-O(1)-Pt(1)	93.21(14)	C(84)-C(85)-C(86)	119.8(5)
P(1)-O(2)-Pt(1)	93.33(13)	C(81)-C(86)-C(85)	120.0(5)
C(11)-C(1)-P(1)	116.8(3)	Cl(1)-C(91)-Cl(3)	112.5(4)
C(15)-C(11)-C(12)	107.0(4)	Cl(2)-C(92)-Cl(4)	114.3(4)
C(15)-C(11)-C(1)	126.0(4)		

Table A.14: Anisotropic displacement parameters ($Å^2$) for **12**. The anisotropic displacement factor exponent takes the form: $-2\pi^2[h^2a^{*2}U_{11} + ... + 2hka^*b^*U12]$.

Atom	U11	U22	U33	U23	U13	U12
Pt(1)	0.017(1)	0.013(1)	0.020(1)	0.000(1)	0.002(1)	0.000(1)
Fe(1)	0.025(1)	0.034(1)	0.025(1)	-0.009(1)	-0.004(1)	0.004(1)
P(1)	0.020(1)	0.017(1)	0.026(1)	-0.002(1)	0.000(1)	0.002(1)
P(2)	0.019(1)	0.014(1)	0.022(1)	0.000(1)	0.001(1)	0.000(1)
P(3)	0.019(1)	0.016(1)	0.024(1)	0.000(1)	0.004(1)	0.002(1)
O(1)	0.023(1)	0.013(1)	0.034(2)	-0.001(1)	0.005(1)	0.000(1)
O(2)	0.017(1)	0.019(1)	0.030(2)	-0.004(1)	0.001(1)	0.002(1)

O(3)	0.031(2)	0.022(2)	0.028(2)	-0.003(1)	-0.002(1)	0.007(1)
C(1)	0.029(2)	0.022(2)	0.030(3)	-0.007(2)	-0.005(2)	0.003(2)
C(11)	0.028(2)	0.026(2)	0.024(3)	-0.008(2)	-0.003(2)	0.004(2)
C(12)	0.027(2)	0.027(2)	0.032(3)	-0.002(2)	0.001(2)	0.004(2)
C(13)	0.032(2)	0.030(2)	0.032(3)	-0.005(2)	-0.002(2)	0.006(2)
C(14)	0.045(3)	0.026(2)	0.028(3)	-0.001(2)	-0.003(2)	0.001(2)
C(15)	0.026(2)	0.031(2)	0.031(3)	-0.008(2)	-0.004(2)	-0.003(2)
C(21)	0.074(4)	0.065(4)	0.044(4)	-0.036(3)	-0.021(3)	0.042(4)
C(22)	0.032(3)	0.137(7)	0.064(5)	-0.069(5)	0.003(3)	0.014(4)
C(23)	0.074(4)	0.074(4)	0.030(4)	-0.019(3)	0.014(3)	-0.010(4)
C(24)	0.063(4)	0.046(3)	0.032(3)	-0.012(3)	-0.017(3)	0.009(3)
C(25)	0.051(3)	0.038(3)	0.046(4)	-0.021(3)	-0.009(2)	0.002(2)
C(31)	0.024(2)	0.018(2)	0.026(3)	-0.004(2)	0.003(2)	-0.003(2)
C(32)	0.030(2)	0.025(2)	0.028(3)	0.000(2)	0.003(2)	-0.004(2)
C(33)	0.041(3)	0.039(3)	0.025(3)	0.003(2)	0.007(2)	-0.010(2)
C(34)	0.031(2)	0.044(3)	0.040(3)	-0.008(2)	0.015(2)	-0.010(2)
C(35)	0.025(2)	0.039(3)	0.044(3)	-0.003(2)	0.006(2)	0.001(2)
C(36)	0.025(2)	0.029(2)	0.031(3)	0.001(2)	0.005(2)	0.001(2)
C(41)	0.020(2)	0.019(2)	0.026(3)	-0.002(2)	0.002(2)	-0.001(2)
C(42)	0.026(2)	0.020(2)	0.027(3)	0.000(2)	0.000(2)	0.003(2)
C(43)	0.030(2)	0.031(2)	0.025(3)	0.004(2)	0.002(2)	0.003(2)
C(44)	0.032(2)	0.034(2)	0.023(3)	-0.008(2)	-0.004(2)	0.000(2)
C(45)	0.038(3)	0.025(2)	0.029(3)	-0.005(2)	-0.001(2)	-0.006(2)
C(46	0.030(2)	0.020(2)	0.028(3)	0.002(2)	0.002(2)	-0.003(2)
C(51)	0.019(2)	0.022(2)	0.028(3)	0.007(2)	0.002(2)	-0.001(2)
C(52)	0.025(2)	0.025(2)	0.032(3)	0.002(2)	-0.001(2)	0.001(2)
C(53)	0.029(2)	0.038(3)	0.036(3)	0.006(2)	-0.006(2)	-0.002(2)
C(54)	0.027(2)	0.036(3)	0.058(4)	0.020(3)	-0.002(2)	0.003(2)
C(55)	0.030(2)	0.019(2)	0.055(4)	0.006(2)	0.005(2)	0.003(2)
C(56)	0.029(2)	0.017(2)	0.033(3)	0.003(2)	0.007(2)	0.000(2)
C(61)	0.024(2)	0.016(2)	0.029(3)	0.002(2)	0.004(2)	-0.004(2)
C(62)	0.028(2)	0.023(2)	0.029(3)	0.002(2)	0.005(2)	0.001(2)
C(63)	0.042(3)	0.033(3)	0.037(3)	0.006(2)	-0.002(2)	0.007(2)
C(64)	0.054(3)	0.033(3)	0.026(3)	0.005(2)	0.005(2)	-0.005(2)
C(65)	0.044(3)	0.036(3)	0.033(3)	-0.003(2)	0.016(2)	0.000(2)
C(66)	0.030(2)	0.027(2)	0.034(3)	-0.001(2)	0.010(2)	0.004(2)
C(71)	0.025(2)	0.016(2)	0.031(3)	0.001(2)	0.009(2)	0.003(2)
C(72)	0.033(2)	0.024(2)	0.032(3)	0.000(2)	0.010(2)	0.000(2)
C(73)	0.051(3)	0.025(2)	0.038(3)	-0.005(2)	0.017(2)	0.002(2)
C(74)	0.057(3)	0.020(2)	0.053(4)	0.004(2)	0.022(3)	0.013(2)
C(75)	0.036(3)	0.029(3)	0.047(3)	0.011(2)	0.010(2)	0.012(2)
C(76)	0.028(2)	0.026(2)	0.035(3)	0.003(2)	0.006(2)	0.002(2)
C(81)	0.021(2)	0.018(2)	0.033(3)	0.001(2)	0.003(2)	0.002(2)
C(82)	0.027(2)	0.027(2)	0.034(3)	0.001(2)	0.001(2)	-0.001(2)
C(83)	0.033(2)	0.036(3)	0.036(3)	0.001(2)	-0.005(2)	0.003(2)
C(84)	0.026(2)	0.040(3)	0.052(4)	-0.008(3)	-0.009(2)	-0.001(2)
C(85)	0.030(3)	0.042(3)	0.050(4)	-0.003(3)	0.007(2)	-0.016(2)
C(86)	0.030(2)	0.036(3)	0.033(3)	0.002(2)	0.003(2)	-0.007(2)
C(91)	0.053(4)	0.121(7)	0.104(7)	0.052(6)	0.029(4)	0.020(5)
Cl(1)	0.046(1)	0.100(1)	0.074(1)	-0.014(1)	-0.001(1)	0.018(1)

Cl(2)	0.087(1)	0.060(1)	0.147(2)	-0.019(1)	-0.027(1)	0.013(1)
C(92)	0.082(5)	0.068(5)	0.131(8)	-0.022(5)	-0.055(5)	0.023(4)
Cl(3)	0.112(2)	0.144(2)	0.115(2)	0.058(2)	0.057(2)	0.024(2)
Cl(4)	0.098(2)	0.119(2)	0.211(3)	-0.071(2)	-0.082(2)	0.051(2)

Table A.15: Hydrogen coordinates and isotropic displacement parameters ($Å^2$) for **12**.

atom	x	y	z	U(eq)
H(1A)	0.1225(2)	0.7212(2)	0.2318(2)	0.032
H(1B)	0.0513(2)	0.6911(2)	0.2456(2)	0.032
H(12)	0.2254(2)	0.6389(2)	0.2613(2)	0.034
H(13)	0.2369(2)	0.5243(2)	0.3162(2)	0.038
H(14)	0.1241(2)	0.4672(3)	0.3255(2)	0.039
H(15)	0.0435(2)	0.5471(2)	0.2757(2)	0.035
H(21)	0.0912(4)	0.7503(4)	0.3427(3)	0.074
H(22)	0.0195(3)	0.6483(5)	0.3814(3)	0.093
H(23)	0.0933(3)	0.5646(4)	0.4340(3)	0.071
H(24)	0.2061(3)	0.6125(3)	0.4297(2)	0.056
H(25)	0.2066(3)	0.7265(3)	0.3749(2)	0.054
H(32)	0.0612(2)	0.3454(2)	0.2325(2)	0.033
H(33)	-0.0297(2)	0.3355(3)	0.2892(2)	0.042
H(34)	-0.1250(2)	0.4004(3)	0.2703(2)	0.046
H(35)	-0.1310(2)	0.4735(3)	0.1951(2)	0.043
H(36)	-0.0410(2)	0.4837(2)	0.1375(2)	0.034
H(42)	0.0661(2)	0.4685(2)	0.0251(2)	0.029
H(43)	0.0198(2)	0.4161(3)	-0.0507(2)	0.034
H(44)	-0.0183(2)	0.2960(3)	-0.0482(2)	0.036
H(45)	-0.0122(2)	0.2307(2)	0.0318(2)	0.037
H(46)	0.0313(2)	0.2832(2)	0.1081(2)	0.031
H(52)	0.1667(2)	0.4469(2)	0.2190(2)	0.033
H(53)	0.2463(2)	0.3843(3)	0.2671(2)	0.041
H(54)	0.2789(2)	0.2693(3)	0.2394(2)	0.048
H(55)	0.2333(2)	0.2168(2)	0.1640(2)	0.042
H(56)	0.1507(2)	0.2772(2)	0.1169(2)	0.032
H(62)	0.1262(2)	0.6074(2)	0.0214(2)	0.032
H(63)	0.1214(3)	0.6534(3)	-0.0650(2)	0.045
H(64)	0.2040(3)	0.6259(3)	-0.1259(2)	0.045
H(65)	0.2894(3)	0.5488(3)	-0.1019(2)	0.045
H(66)	0.2932(2)	0.5005(2)	-0.0157(2)	0.037
H(72)	0.1787(2)	0.3954(2)	0.0099(2)	0.036
H(73)	0.2171(3)	0.2773(3)	-0.0056(2)	0.046
H(74)	0.3070(3)	0.2339(3)	0.0419(2)	0.052
H(75)	0.3589(2)	0.3065(3)	0.1047(2)	0.045
H(76)	0.3206(2)	0.4241(2)	0.1212(2)	0.036
H(82)	0.2553(2)	0.5284(2)	0.1865(2)	0.035
H(83)	0.3457(2)	0.5765(3)	0.2305(2)	0.042
H(84)	0.4274(2)	0.6348(3)	0.1823(2)	0.047

H(85)	0.4167(2)	0.6506(3)	0.0906(2)	0.049
H(86)	0.3255(2)	0.6027(3)	0.0460(2)	0.040
H(91A)	0.0951(4)	0.2068(5)	0.3903(4)	0.112
H(91B)	0.0625(4)	0.1507(5)	0.3494(4)	0.112
H(92C)	0.0142(4)	0.8361(4)	0.0973(4)	0.112
H(92D)	0.0313(4)	0.8715(4)	0.0408(4)	0.112

Table A.16: Atomic coordinates and equivalent isotropic displacement parameters for **13**. U(eq) is defined as one third of the trace of the orthogonalized Uij tensor.

Atom	x	y	z	U(eq)
Pt(1)	0.6624(1)	0.4289(1)	0.2384(1)	0.019(1)
Fe(1)	0.7152(1)	0.7151(1)	0.4793(1)	0.034(1)
P(1)	0.4930(1)	0.5730(1)	0.3210(1)	0.025(1)
P(2)	0.7887(1)	0.4538(1)	0.1331(1)	0.021(1)
P(3)	0.7334(1)	0.2465(1)	0.2625(1)	0.021(1)
O(1)	0.5328(3)	0.4480(2)	0.3366(2)	0.025(1)
O(2)	0.5641(3)	0.5926(2)	0.2302(2)	0.028(1)
O(3)	0.3693(4)	0.6432(3)	0.3120(2)	0.030(1)
C(1)	0.6766(6)	0.5319(4)	0.4280(4)	0.041(2)
C(2)	0.5497(6)	0.5949(4)	0.4149(3)	0.030(2)
C(11)	0.7273(6)	0.5638(4)	0.4931(4)	0.033(2)
C(12)	0.8352(7)	0.5610(5)	0.4834(4)	0.042(2)
C(13)	0.8536(7)	0.5960(5)	0.5588(4)	0.046(2)
C(14)	0.7550(6)	0.6227(5)	0.6143(4)	0.043(2)
C(15)	0.6765(6)	0.6028(5)	0.5747(3)	0.040(2)
C(21)	0.6410(8)	0.8094(6)	0.3513(5)	0.065(3)
C(22)	0.7413(9)	0.8144(7)	0.3608(6)	0.072(3)
C(23)	0.7306(9)	0.8552(6)	0.4401(7)	0.075(3)
C(24)	0.6257(10)	0.8747(5)	0.4810(7)	0.080(3)
C(25)	0.5658(8)	0.8479(5)	0.4256(6)	0.062(2)
C(31)	0.6238(5)	0.2161(4)	0.2347(3)	0.025(2)
C(32)	0.6471(6)	0.1072(4)	0.2467(4)	0.041(2)
C(33)	0.5669(7)	0.0834(5)	0.2222(4)	0.046(2)
C(34)	0.4632(6)	0.1661(5)	0.1854(4)	0.038(2)
C(35)	0.4400(6)	0.2729(5)	0.1735(4)	0.041(2)
C(36)	0.5199(5)	0.2976(4)	0.1987(4)	0.030(2)
C(41)	0.7706(5)	0.1718(4)	0.3862(3)	0.023(1)
C(42)	0.7170(5)	0.2260(4)	0.4569(3)	0.032(2)
C(43)	0.7352(6)	0.1698(5)	0.5530(4)	0.043(2)
C(44)	0.8071(6)	0.0610(5)	0.5772(3)	0.040(2)
C(45)	0.8633(6)	0.0061(4)	0.5080(4)	0.040(2)
C(46)	0.8436(5)	0.0606(4)	0.4126(3)	0.029(2)
C(51)	0.8530(6)	0.1740(4)	0.1917(3)	0.021(2)
C(52)	0.9642(6)	0.1247(4)	0.2218(4)	0.032(2)
C(53)	1.0518(6)	0.0782(5)	0.1623(4)	0.042(2)
C(54)	1.0295(7)	0.0833(5)	0.0707(5)	0.046(2)

C(55)	0.9198(7)	0.1322(5)	0.0404(4)	0.042(2)
C(56)	0.8314(6)	0.1767(4)	0.0993(3)	0.032(2)
C(61)	0.7699(5)	0.4488(4)	0.0136(3)	0.023(1)
C(62)	0.6833(5)	0.4263(4)	-0.0026(3)	0.029(2)
C(63)	0.6662(6)	0.4210(4)	-0.0928(4)	0.035(2)
C(64)	0.7350(6)	0.4388(5)	-0.1665(3)	0.042(2)
C(65)	0.8183(6)	0.4642(5)	-0.1514(3)	0.038(2)
C(66)	0.8354(5)	0.4704(4)	-0.0620(3)	0.030(2)
C(71)	0.7731(5)	0.5914(4)	0.1152(3)	0.025(1)
C(72)	0.6779(5)	0.6798(4)	0.0703(3)	0.033(2)
C(73)	0.6636(6)	0.7853(4)	0.0575(4)	0.045(2)
C(74)	0.7461(7)	0.8017(5)	0.0881(4)	0.048(2)
C(75)	0.8420(7)	0.7150(5)	0.1325(5)	0.051(2)
C(76)	0.8568(6)	0.6093(4)	0.1470(4)	0.036(2)
C(81)	0.9340(5)	0.3669(4)	0.1723(3)	0.023(1)
C(82)	0.9561(6)	0.3409(4)	0.2698(3)	0.026(2)
C(83)	1.0645(6)	0.2793(5)	0.3052(4)	0.035(2)
C(84)	1.1539(6)	0.2425(5)	0.2447(4)	0.042(2)
C(85)	1.1348(6)	0.2672(5)	0.1477(4)	0.038(2)
C(86)	1.0256(6)	0.3282(4)	0.1122(3)	0.031(2)
Cl(1)	0.3503(2)	0.8759(2)	0.0271(1)	0.072(1)
C(91)	0.3712(7)	0.8407(5)	0.1504(5)	0.065(2)
Cl(2)	0.3796(2)	0.9418(2)	0.1885(2)	0.080(1)
C(92)	0.8875(7)	0.3000(5)	0.6470(4)	0.054(2)
Cl(4)	0.9519(2)	0.1896(2)	0.7446(2)	0.098(1)
Cl(3)	0.9430(2)	0.2665(2)	0.5394(1)	0.073(1)

Table A.17: Bond lengths (Å) for **13**.

Pt(1)-O(2)	2.066(3)	C(32)-C(33)	1.377(9)
Pt(1)-O(1)	2.077(3)	C(33)-C(34)	1.386(9)
Pt(1)-P(2)	2.2330(13)	C(34)-C(35)	1.378(8)
Pt(1)-P(3)	2.2656(11)	C(35)-C(36)	1.387(9)
Pt(1)-P(1)	2.6851(14)	C(41)-C(42)	1.390(6)
Fe(1)-C(12)	2.028(6)	C(41)-C(46)	1.396(6)
Fe(1)-C(14)	2.031(5)	C(42)-C(43)	1.405(7)
Fe(1)-C(22)	2.031(6)	C(43)-C(44)	1.368(8)
Fe(1)-C(23)	2.033(6)	C(44)-C(45)	1.383(8)
Fe(1)-C(21)	2.036(7)	C(45)-C(46)	1.391(7)
Fe(1)-C(24)	2.036(7)	C(51)-C(52)	1.384(8)
Fe(1)-C(15)	2.047(5)	C(51)-C(56)	1.405(7)
Fe(1)-C(13)	2.048(7)	C(52)-C(53)	1.385(8)
Fe(1)-C(11)	2.055(5)	C(53)-C(54)	1.385(9)
Fe(1)-C(25)	2.063(7)	C(54)-C(55)	1.367(9)
P(1)-O(3)	1.481(4)	C(55)-C(56)	1.379(9)
P(1)-O(1)	1.571(3)	C(61)-C(66)	1.385(7)
P(1)-O(2)	1.577(3)	C(61)-C(62)	1.399(8)
P(1)-C(2)	1.812(5)	C(62)-C(63)	1.397(6)
P(2)-C(81)	1.812(6)	C(63)-C(64)	1.380(9)
P(2)-C(61)	1.824(4)	C(64)-C(65)	1.379(9)

P(2)-C(71)	1.832(5)	C(65)-C(66)	1.389(7)
P(3)-C(41)	1.827(4)	C(71)-C(72)	1.380(8)
P(3)-C(31)	1.829(6)	C(71)-C(76)	1.412(8)
P(3)-C(51)	1.831(5)	C(72)-C(73)	1.396(7)
C(1)-C(11)	1.505(8)	C(73)-C(74)	1.375(10)
C(1)-C(2)	1.512(9)	C(74)-C(75)	1.375(10)
C(11)-C(12)	1.414(9)	C(75)-C(76)	1.394(7)
C(11)-C(15)	1.420(8)	C(81)-C(86)	1.398(8)
C(12)-C(13)	1.420(8)	C(81)-C(82)	1.405(6)
C(13)-C(14)	1.409(10)	C(82)-C(83)	1.375(8)
C(14)-C(15)	1.427(9)	C(83)-C(84)	1.380(9)
C(21)-C(22)	1.401(11)	C(84)-C(85)	1.392(8)
C(21)-C(25)	1.430(11)	C(85)-C(86)	1.383(9)
C(22)-C(23)	1.403(12)	Cl(1)-C(91)	1.758(7)
C(23)-C(24)	1.387(12)	C(91)-Cl(2)	1.744(7)
C(24)-C(25)	1.436(12)	C(92)-Cl(3)	1.749(7)
C(31)-C(36)	1.380(8)	C(92)-Cl(4)	1.757(7)
C(31)-C(32)	1.406(7)		

Table A.18: Bond Angles (°) for **13**.

O(2)-Pt(1)-O(1)	71.00(12)	C(15)-C(11)-C(1)	126.9(6)
O(2)-Pt(1)-P(2)	94.32(10)	C(12)-C(11)-Fe(1)	68.7(3)
O(1)-Pt(1)-P(2)	164.74(9)	C(15)-C(11)-Fe(1)	69.4(3)
O(2)-Pt(1)-P(3)	166.58(11)	C(1)-C(11)-Fe(1)	126.6(4)
O(1)-Pt(1)-P(3)	96.51(9)	C(11)-C(12)-C(13)	109.5(6)
P(2)-Pt(1)-P(3)	98.45(5)	C(11)-C(12)-Fe(1)	70.8(3)
O(2)-Pt(1)-P(1)	35.87(9)	C(13)-C(12)-Fe(1)	70.4(4)
O(1)-Pt(1)-P(1)	35.72(9)	C(14)-C(13)-C(12)	106.7(6)
P(2)-Pt(1)-P(1)	129.13(4)	C(14)-C(13)-Fe(1)	69.1(4)
P(3)-Pt(1)-P(1)	132.15(4)	C(12)-C(13)-Fe(1)	68.9(4)
C(12)-Fe(1)-C(14)	68.0(3)	C(13)-C(14)-C(15)	109.0(5)
C(12)-Fe(1)-C(22	107.7(4)	C(13)-C(14)-Fe(1)	70.4(3)
C(14)-Fe(1)-C(22)	151.7(3)	C(15)-C(14)-Fe(1)	70.1(3)
C(12)-Fe(1)-C(23)	128.9(4)	C(11)-C(15)-C(14)	107.5(6)
C(14)-Fe(1)-C(23)	119.2(3)	C(11)-C(15)-Fe(1)	70.1(3)
C(22)-Fe(1)-C(23)	40.4(3)	C(14)-C(15)-Fe(1)	68.9(3)
C(12)-Fe(1)-C(21)	117.1(3)	C(22)-C(21)-C(25)	108.7(8)
C(14)-Fe(1)-C(21)	167.3(3)	C(22)-C(21)-Fe(1)	69.7(4)
C(22)-Fe(1)-C(21)	40.3(3)	C(25)-C(21)-Fe(1)	70.6(4)
C(23)-Fe(1)-C(21)	67.7(3)	C(21)-C(22)-C(23)	107.9(9)
C(12)-Fe(1)-C(24)	166.7(4)	C(21)-C(22)-Fe(1)	70.0(4)
C(14)-Fe(1)-C(24)	109.4(3)	C(23)-C(22)-Fe(1)	69.9(4)
C(22)-Fe(1)-C(24)	67.9(4)	C(24)-C(23)-C(22)	109.1(8)
C(23)-Fe(1)-C(24)	39.9(3)	C(24)-C(23)-Fe(1)	70.2(4)
C(21)-Fe(1)-C(24)	68.3(4)	C(22)-C(23)-Fe(1)	69.7(4)
C(12)-Fe(1)-C(15)	68.1(3)	C(23)-C(24)-C(25)	108.5(8)
C(14)-Fe(1)-C(15)	41.0(2)	C(23)-C(24)-Fe(1)	69.9(4)
C(22)-Fe(1)-C(15)	165.7(3)	C(25)-C(24)-Fe(1)	70.5(4)
C(23)-Fe(1)-C(15)	152.6(4)	C(21)-C(25)-C(24)	105.9(8)

C(21)-Fe(1)-C(15)	128.2(3)	C(21)-C(25)-Fe(1)	68.6(4)
C(24)-Fe(1)-C(15)	119.2(4)	C(24)-C(25)-Fe(1)	68.5(4)
C(12)-Fe(1)-C(13)	40.8(2)	C(36)-C(31)-C(32)	119.0(5)
C(14)-Fe(1)-C(13)	40.4(3)	C(36)-C(31)-P(3)	121.5(4)
C(22)-Fe(1)-C(13)	117.8(4)	C(32)-C(31)-P(3)	119.4(5)
C(23)-Fe(1)-C(13)	108.9(3)	C(33)-C(32)-C(31)	120.0(6)
C(21)-Fe(1)-C(13)	150.6(3)	C(32)-C(33)-C(34)	120.4(6)
C(24)-Fe(1)-C(13)	128.9(3)	C(35)-C(34)-C(33)	119.9(6)
C(15)-Fe(1)-C(13)	68.7(3)	C(34)-C(35)-C(36)	120.0(6)
C(12)-Fe(1)-C(11)	40.5(3)	C(31)-C(36)-C(35)	120.7(5)
C(14)-Fe(1)-C(11)	68.4(2)	C(42)-C(41)-C(46)	118.7(4)
C(22)-Fe(1)-C(11)	127.7(3)	C(42)-C(41)-P(3)	118.4(4)
C(23)-Fe(1)-C(11)	166.2(4)	C(46)-C(41)-P(3)	122.7(3)
C(21)-Fe(1)-C(11)	107.3(3)	C(41)-C(42)-C(43)	120.6(5)
C(24)-Fe(1)-C(11)	152.0(4)	C(44)-C(43)-C(42)	119.7(5)
C(15)-Fe(1)-C(11)	40.5(2)	C(43)-C(44)-C(45)	120.6(5)
C(13)-Fe(1)-C(11)	68.7(2)	C(44)-C(45)-C(46)	120.0(5)
C(12)-Fe(1)-C(25)	150.6(3)	C(45)-C(46)-C(41)	120.4(5)
C(14)-Fe(1)-C(25)	129.4(3)	C(52)-C(51)-C(56)	118.5(5)
C(22)-Fe(1)-C(25)	68.4(4)	C(52)-C(51)-P(3)	123.0(4)
C(23)-Fe(1)-C(25)	68.0(3)	C(56)-C(51)-P(3)	118.3(5)
C(21)-Fe(1)-C(25)	40.8(3)	C(51)-C(52)-C(53)	120.5(5)
C(24)-Fe(1)-C(25)	41.0(3)	C(54)-C(53)-C(52)	120.5(7)
C(15)-Fe(1)-C(25)	108.1(3)	C(55)-C(54)-C(53)	119.3(6)
C(13)-Fe(1)-C(25)	167.4(3)	C(54)-C(55)-C(56)	121.1(6)
C(11)-Fe(1)-C(25)	117.4(3)	C(55)-C(56)-C(51)	120.1(6)
O(3)-P(1)-O(1)	115.9(2)	C(66)-C(61)-C(62)	119.1(4)
O(3)-P(1)-O(2)	115.6(2)	C(66)-C(61)-P(2)	122.4(4)
O(1)-P(1)-O(2)	99.7(2)	C(62)-C(61)-P(2)	118.5(4)
O(3)-P(1)-C(2)	110.2(2)	C(63)-C(62)-C(61)	120.5(5)
O(1)-P(1)-C(2)	105.3(2)	C(64)-C(63)-C(62)	119.6(6)
O(3)-P(1)-Pt(1)	140.47(14)	C(65)-C(64)-C(63)	120.0(5)
O(1)-P(1)-Pt(1)	50.52(13)	C(64)-C(65)-C(66)	120.8(5)
O(2)-P(1)-Pt(1)	50.14(12)	C(61)-C(66)-C(65)	119.9(6)
C(2)-P(1)-Pt(1)	109.3(2)	C(72)-C(71)-C(76)	118.9(5)
C(81)-P(2)-C(61)	110.8(2)	C(72)-C(71)-P(2)	119.9(4)
C(81)-P(2)-C(71)	103.7(2)	C(76)-C(71)-P(2)	121.2(4)
C(61)-P(2)-C(71)	102.8(2)	C(71)-C(72)-C(73)	120.7(6)
C(81)-P(2)-Pt(1)	113.69(15)	C(74)-C(73)-C(72)	119.9(6)
C(61)-P(2)-Pt(1)	114.7(2)	C(73)-C(74)-C(75)	120.6(6)
C(71)-P(2)-Pt(1)	110.0(2)	C(74)-C(75)-C(76)	120.2(7)
C(41)-P(3)-C(31)	104.0(2)	C(75)-C(76)-C(71)	119.7(6)
C(41)-P(3)-C(51)	106.1(2)	C(86)-C(81)-C(82)	118.1(6)
C(31)-P(3)-C(51)	102.7(2)	C(86)-C(81)-P(2)	124.7(4)
C(41)-P(3)-Pt(1)	113.82(14)	C(82)-C(81)-P(2)	117.2(4)
C(31)-P(3)-Pt(1)	108.9(2)	C(83)-C(82)-C(81)	121.1(5)
C(51)-P(3)-Pt(1)	119.69(15)	C(82)-C(83)-C(84)	120.0(5)
P(1)-O(1)-Pt(1)	93.8(2)	C(83)-C(84)-C(85)	120.3(7)
P(1)-O(2)-Pt(1)	93.99(14)	C(86)-C(85)-C(84)	119.7(6)
C(11)-C(1)-C(2)	115.9(5)	C(85)-C(86)-C(81)	120.8(5)

C(1)-C(2)-P(1)	115.3(4)	Cl(2)-C(91)-Cl(1)	112.1(3)
C(12)-C(11)-C(15)	107.3(5)	Cl(3)-C(92)-Cl(4)	111.7(4)
C(12)-C(11)-C(1)	125.8(5)		

Table A.19: Anisotropic displacement parameters ($Å^2$)for **13**. The anisotropic displacement factor exponent takes the form: $-2\pi^2[h^2a^{*2}U11 + ... + 2hka^*b^*U12]$.

Atom	U11	U22	U33	U23	U13	U12
Pt(1)	0.019(1)	0.019(1)	0.020(1)	-0.005(1)	0.002(1)	-0.008(1)
Fe(1)	0.038(1)	0.027(1)	0.038(1)	-0.003(1)	-0.004(1)	-0.017(1)
P(1)	0.026(1)	0.023(1)	0.026(1)	-0.007(1)	0.004(1)	-0.011(1)
P(2)	0.022(1)	0.023(1)	0.019(1)	-0.005(1)	0.002(1)	-0.011(1)
P(3)	0.020(1)	0.019(1)	0.022(1)	-0.005(1)	0.000(1)	-0.007(1)
O(1)	0.021(3)	0.024(2)	0.028(2)	-0.008(1)	0.008(2)	-0.010(2)
O(2)	0.034(3)	0.021(2)	0.024(2)	-0.004(1)	0.007(2)	-0.011(2)
O(3)	0.016(4)	0.031(2)	0.040(2)	-0.013(2)	0.003(2)	-0.005(2)
C(1)	0.032(6)	0.032(3)	0.058(3)	-0.020(2)	-0. 010(3)	-0.006(3)
C(2)	0.030(6)	0.026(2)	0.034(2)	-0.011(2)	0.004(2)	-0.012(3)
C(11)	0.033(6)	0.025(2)	0.042(3)	-0.004(2)	-0.006(3)	-0.015(3)
C(12)	0.034(6)	0.037(3)	0.056(3)	-0.014(3)	-0.005(3)	-0.013(3)
C(13)	0.047(7)	0.035(3)	0.057(4)	-0.004 (3)	-0.017(4)	-0.019(3)
C(14)	0.050(7)	0.052(3)	0.037(3)	-0.002(2)	-0.014(3)	-0.032(4)
C(15)	0.046(6)	0.052(3)	0.032(2)	-0.005(2)	0.000(3)	-0.034(4)
C(21)	0.083(9)	0.044(4)	0.058(4)	0.018(3)	-0.024(4)	-0.031(5)
C(22)	0.071(9)	0.074(5)	0.069(5)	0.026(4)	-0.012(5)	-0.052(6)
C(23)	0.079(10)	0.038(4)	0.116(7)	0.013(4)	-0.046(6)	-0.038(5)
C(24)	0.084(10)	0.029(3)	0.113(7)	-0.024(4)	-0.001(6)	-0.010(4)
C(25)	0.048(7)	0.031(3)	0.099(6)	0.001(3)	-0.030(5)	-0.014(4)
C(31)	0.023(5)	0.027(2)	0.028(2)	-0.005(2)	-0.001(2)	-0.014(3)
C(32	0.030(6)	0.028(3)	0.061(3)	0.004(2)	-0.025(3)	-0.012(3)
C(33)	0.048(7)	0.034(3)	0.060(4)	0.005(3)	-0.017(3)	-0.027(4)
C(34)	0.034(6)	0.047(3)	0.045(3)	-0.009(2)	-0.007(3)	-0.027(4)
C(35)	0.022(6)	0.041(3)	0.058(3)	-0.018(3)	-0.010(3)	-0.008(3)
C(36)	0.011(6)	0.029(2)	0.044(3)	-0.012(2)	-0.006(3)	-0.001(3)
C(41)	0.020(5)	0.025(2)	0.023(2)	-0.004(2)	-0.001(2)	-0.011(2)
C(42)	0.034(5)	0.026(2)	0.029(2)	-0.007(2)	0.000(2)	-0.008(3)
C(43)	0.049(6)	0.044(3)	0.027(2)	-0.010(2)	0.003(3)	-0.016(3)
C(44)	0.045(6)	0.042(3)	0.026(2)	-0.001(2)	-0.004(3)	-0.017(3)
C(45)	0.044(6)	0.029(3)	0.037(3)	0.000(2)	-0.009(3)	-0.011(3)
C(46)	0.023(5)	0.022(2)	0.035(2)	-0.008(2)	-0.007(2)	-0.002(2)
C(51)	0.012(5)	0.024(2)	0.028(2)	-0.010(2)	0.005(2)	-0.007(3)
C(52)	0.023(6)	0.030(2)	0.046(3)	-0.015(2)	0.002(3)	-0.011(3)
C(53)	0.023(6)	0.038(3)	0.062(4)	-0.023(3)	0.011(3)	-0.009(3)
C(54)	0.032(7)	0.041(3)	0.064(4)	-0.033(3)	0.029(4)	-0.012(3)
C(55)	0.045(7)	0.042(3)	0.039(3)	-0.023(2)	0.012(3)	-0.015(3)
C(56)	0.030(5)	0.031(2)	0.032(2)	-0.009(2)	-0.002(2)	-0.011(3)
C(61)	0.024(5)	0.023(2)	0.022(2)	-0.005(2)	-0.002(2)	-0.009(2)

C(62)	0.030(5)	0.027(2)	0.023(2)	-0.004(2)	-0.002(2)	-0.009(3)
C(63)	0.036(6)	0.030(2)	0.038(3)	-0.010(2)	-0.011(3)	-0.011(3)
C(64)	0.048(7)	0.043(3)	0.024(2)	-0.012(2)	-0.005(3)	-0.010(3)
C(65)	0.022(6)	0.053(3)	0.023(2)	-0.009(2)	0.003(2)	-0.005(3)
C(66)	0.026(5)	0.036(3)	0.022(2)	-0.003(2)	-0.001(2)	-0.011(3)
C(71)	0.025(5)	0.027(2)	0.023(2)	-0.007(2)	0.007(2)	-0.014(3)
C(72)	0.034(5)	0.026(2)	0.034(2)	-0.002(2)	0.003(2)	-0.014(3)
C(73)	0.051(6)	0.027(3)	0.045(3)	-0.004(2)	0.013(3)	-0.013(3)
C(74)	0.058(7)	0.036(3)	0.062(4)	-0.018(3)	0.015(4)	-0.030(4)
C(75)	0.049(7)	0.048(4)	0.073(4)	-0.024(3)	0.007(4)	-0.032(4)
C(76)	0.031(6)	0.035(3)	0.045(3)	-0.011(2)	-0.001(3)	-0.016(3)
C(81)	0.017(5)	0.031(2)	0.024(2)	-0.008(2)	0.003(2)	-0.012(3)
C(82)	0.015(6)	0.036(3)	0.030(2)	-0.010(2)	-0.002(2)	-0.012(3)
C(83)	0.032(6)	0.046(3)	0.030(2)	-0.007(2)	-0.011(3)	-0.018(3)
C(84)	0.031(6)	0.049(3)	0.048(3)	-0.009(3)	-0.006(3)	-0.020(3)
C(85)	0.020(6)	0.048(3)	0.044(3)	-0.013(3)	0.011(3)	-0.015(3)
C(86)	0.023(6)	0.037(3)	0.029(2)	-0.006(2)	-0.001(3)	-0.010(3)
Cl(1)	0.073(2)	0.079(1)	0.062(1)	-0.017(1)	-0.017(1)	-0.028(1)
C(91)	0.081(8)	0.035(3)	0.055(4)	0.002(3)	0.004(4)	-0.014(4)
Cl(2)	0.061(2)	0.096(2)	0.093(1)	-0.051(1)	-0.002(1)	-0.028(1)
C(92)	0.047(7)	0.047(3)	0.058(4)	-0.013(3)	0.006(3)	-0.015(4)
Cl(4)	0.104(3)	0.076(1)	0.073(1)	-0.001(1)	0.003(1)	-0.017(1)
Cl(3)	0.071(2)	0.065(1)	0.073(1)	-0.026(1)	0.027(1)	-0.025(1)

Table A.20: Hydrogen coordinates and isotropic displacement parameters ($Å^2$) for **13**.

atom	x	y	z	U(eq)
H(1A)	0.6962(6)	0.4554(4)	0.4522(4)	0.049
H(1B)	0.7114(6)	0.5404(4)	0.3662(4)	0.049
H(2A)	0.5286(6)	0.6718(4)	0.4022(3)	0.036
H(2B)	0.5145(6)	0.5757(4)	0.4741(3)	0.036
H(12)	0.8861(7)	0.5396(5)	0.4352(4)	0.051
H(13)	0.9182(7)	0.6004(5)	0.5694(4)	0.056
H(14)	0.7430(6)	0.6490(5)	0.6681(4)	0.052
H(15)	0.6050(6)	0.6135(5)	0.5980(3)	0.048
H(21)	0.6258(8)	0.7851(6)	0.3045(5)	0.079
H(22)	0.8039(9)	0.7942(7)	0.3214(6)	0.086
H(23)	0.7851(9)	0.8672(6)	0.4619(7)	0.090
H(24)	0.5987(10)	0.9008(5)	0.5351(7)	0.096
H(25)	0.4931(8)	0.8543(5)	0.4359(6)	0.074
H(32)	0.7166(6)	0.0513(4)	0.2711(4)	0.049
H(33)	0.5824(7)	0.0113(5)	0.2305(4)	0.055
H(34)	0.4095(6)	0.1496(5)	0.1688(4)	0.046
H(35)	0.3706(6)	0.3286(5)	0.1485(4)	0.049
H(36)	0.5033(5)	0.3698(4)	0.1913(4)	0.036
H(42)	0.6686(5)	0.3001(4)	0.4404(3)	0.038
H(43)	0.6986(6)	0.2064(5)	0.5999(4)	0.051

H(44)	0.8184(6)	0.0236(5)	0.6408(3)	0.048
H(45)	0.9143(6)	-0.0673(4)	0.5252(4)	0.048
H(46)	0.8793(5)	0.0229(4)	0.3662(3)	0.035
H(52)	0.9803(6)	0.1227(4)	0.2825(4)	0.039
H(53)	1.1261(6)	0.0432(5)	0.1839(4)	0.050
H(54)	1.0884(7)	0.0537(5)	0.0303(5)	0.055
H(55)	0.9046(7)	0.1356(5)	-0.0211(4)	0.051
H(56)	0.7572(6)	0.2085(4)	0.0779(3)	0.038
H(62)	0.6368(5)	0.4147(4)	0.0472(3)	0.034
H(63)	0.6088(6)	0.4057(4)	-0.1032(4)	0.042
H(64)	0.7252(6)	0.4337(5)	-0.2264(3)	0.050
H(65)	0.8635(6)	0.4773(5)	-0.2016(3)	0.045
H(66)	0.8908(5)	0.4890(4)	-0.0530(3)	0.036
H(72)	0.6226(5)	0.6689(4)	0.0484(3)	0.039
H(73)	0.5985(6)	0.8444(4)	0.0284(4)	0.054
H(74)	0.7369(7)	0.8720(5)	0.0786(4)	0.058
H(75)	0.8972 (7)	0.7270(5)	0.1530(5)	0.062
H(76)	0.9214(6)	0.5507(4)	0.1774(4)	0.043
H(82)	0.8963(6)	0.3657(4)	0.3110(3)	0.031
H(83)	1.0775(6)	0.2625(5)	0.3700(4)	0.042
H(84)	1.2271(6)	0.2011(5)	0.2687(4)	0.050
H(85)	1.1952(6)	0.2427(5)	0.1070(4)	0.046
H(86)	1.0130(6)	0.3438(4)	0.0475(3)	0.038
H(91A)	0.3092(7)	0.8280(5)	0.1826(5)	0.078
H(91B)	0.4404(7)	0.7736(5)	0.1677(5)	0.078
H(92A)	0.8069(7)	0.3227(5)	0.6479(4)	0.065
H(92B)	0.8987(7)	0.3605(5)	0.6520(4)	0.065

Table A.21: Atomic coordinates and equivalent isotropic displacement parameters for **14**. U(eq) is defined as one third of the trace of the orthogonalized Uij tensor.

Atom	x	y	z	U(eq)
Pt(2)	0.8890(1)	0.4813(1)	0.2401(1)	0.025(1)
Pt(1)	1.7072(1)	1.0093(1)	0.2965(1)	0.024(1)
Fe(1)	1.3086(1)	0.7341(1)	0.2626(1)	0.037(1)
P(2)	1.1038(1)	0.5803(1)	0.3166(1)	0.031(1)
P(1)	1.5249(1)	0.8841(1)	0.2096(1)	0.032(1)
P(22)	0.8413(1)	0.3971(1)	0.1495(1)	0.029(1)
P(21)	0.7132(1)	0.4904(1)	0.2361(1)	0.027(1)
P(12)	1.8978(1)	1.0221(1)	0.3244(1)	0.027(1)
P(11)	1.7153(1)	1.1090(1)	0.3716(1)	0.025(1)
O(21)	0.9785(4)	0.5681(3)	0.3234(2)	0.031(1)
O(22)	1.0690(4)	0.5024(3)	0.2632(2)	0.032(1)
O(23)	1.1929(4)	0.5815(3)	0.3739(2)	0.044(1)
O(11)	1.5246(4)	0.9636(3)	0.2511(2)	0.035(1)
O(12)	1.6630(4)	0.9098(3)	0.2226(2)	0.033(1)
O(13)	1.4587(5)	0.8701(4)	0.1437(2)	0.053(1)

C(31)	1.9073(6)	0.9180(4)	0.3447(3)	0.031(1)
C(32)	1.8050(6)	0.8394(4)	0.3308(3)	0.032(1)
C(33)\	1.8128(7)	0.7602(4)	0.3429(3)	0.040(2)
C(34)	1.9237(8)	0.7575(5)	0.3675(3)	0.046(2)
C(35)	2.0242(7)	0.8340(5)	0.3817(4)	0.046(2)
C(36)	2.0173(6)	0.9141(5)	0.3712(3)	0.039(2)
C(41)	2.0129(5)	1.1057(4)	0.3879(3)	0.031(1)
C(42)	2.0159(6)	1.0907(4)	0.4469(3)	0.034(1)
C(43)	2.1002(6)	1.1532(5)	0.4961(3)	0.040(2)
C(44)	2.1818(7)	1.2312(5)	0.4867(4)	0.046(2)
C(45)	2.1786(6)	1.2474(5)	0.4288(4)	0.047(2)
C(46)	2.0956(6)	1.1841(4)	0.3792(3)	0.038(2)
C(51)	1.9555(5)	1.0406(4)	0.2587(3)	0.034(1)
C(52)	2.0289(7)	1.0000(6)	0.2459(4)	0.051(2)
C(53)	2.0743(9)	1.0175(7)	0.1967(4)	0.065(2)
C(54)	2.0488(9)	1.0767(7)	0.1612(4)	0.066(3)
C(55)	1.9722(10)	1.1146(7)	0.1731(5)	0.070(3)
C(56)	1.9255(9)	1.0959(6)	0.2207(4)	0.057(2)
C(61)	1.8421(5)	1.2158(4)	0.3941(3)	0.029(1)
C(62)	1.8957(6)	1.2604(4)	0.4545(3)	0.038(2)
C(63)	1.9822(7)	1.3468(5)	0.4664(4)	0.048(2)
C(64)	2.0164(6)	1.3896(5)	0.4211(4)	0.049(2)
C(65)	1.9644(6)	1.3454(5)	0.3609(4)	0.042(2)
C(66)	1.8783(6)	1.2597(4)	0.3475(3)	0.035(1)
C(71)	1.5891(5)	1.1436(4)	0.3534(3)	0.028(1)
C(72)	1.6036(6)	1.2319(4)	0.3666(3)	0.037(1)
C(73)	1.5037(7)	1.2535(5)	0.3568(4)	0.046(2)
C(74)	1.3892(6)	1.1880(5)	0.3325(3)	0.042(2)
C(75)	1.3752(6)	1.1004(5)	0.3190(3)	0.044(2)
C(76)	1.4722(6)	1.0773(5)	0.3300(3)	0.041(2)
C(81)	1.6968(5)	1.0605(4)	0.4391(3)	0.028(1)
C(82)	1.7071(6)	0.9789(5)	0.4449(3)	0.036(1)
C(83)	1.6851(7)	0.9379(6)	0.4946(4)	0.050(2)
C(84)	1.6544(7)	0.9790(6)	0.5383(4)	0.050(2)
C(85)	1.6430(6)	1.0587(5)	0.5332(3)	0.045(2)
C(86)	1.6645(6)	1.0999(4)	0.4836(3)	0.036(1)
C(21)	1.1568(5)	0.6827(4)	0.2884(3)	0.034(1)
C(22)	1.1290(6)	0.6940(5)	0.2262(4)	0.044(2)
C(23)	1.1876(8)	0.7858(6)	0.2243(6)	0.065(3)
C(24)	1.2514(8)	0.8318(6)	0.2846(6)	0.070(3)
C(25)	1.2328(7)	0.7687(5)	0.3244(4)	0.051(2)
C(11)	1.4638(6)	0.7830(4)	0.2387(3)	0.034(1)
C(12)	1.3841(7)	0.6975(5)	0.2017(4)	0.047(2)
C(13)	1.3598(8)	0.6340(5)	0.2412(5)	0.056(2)
C(14)	1.4237(7)	0.6783(6)	0.3011(5)	0.056(2)
C(15)	1.4876(6)	0.7706(5)	0.3007(4)	0.043(2)
C(91)	0.6952(5)	0.4980(4)	0.3125(3)	0.030(1)
C(92)	0.7606(6)	0.4698(4)	0.3587(3)	0.035(1)
C(93)	0.7452(7)	0.4747(5)	0.4171(3)	0.043(2)
C(94)	0.6630(7)	0.5066(5)	0.4290(3)	0.047(2)

C(95)	0.5966(7)	0.5332(5)	0.3830(4)	0.044(2)
C(96)	0.6111(6)	0.5291(5)	0.3249(3)	0.039(2)
C(101)	0.5707(5)	0.4023(4)	0.1909(3)	0.031(1)
C(102)	0.5105(6)	0.3338(4)	0.2180(3)	0.037(1)
C(103)	0.4060(7)	0.2625(5)	0.1835(4)	0.047(2)
C(104)	0.3619(7)	0.2600(5)	0.1226(4)	0.047(2)
C(105)	0.4215(6)	0.3276(5)	0.0943(3)	0.040(2)
C(106)	0.5257(6)	0.4000(4)	0.1288(3)	0.035(1)
C(111)	0.7177(6)	0.5941(4)	0.2103(3)	0.031(1)
C(112)	0.6165(6)	0.6106(5)	0.1844(3)	0.036(1)
C(113)	0.6286(7)	0.6915(5)	0.1656(3)	0.044(2)
C(114)	0.7406(8)	0.7574(5)	0.1716(4)	0.047(2)
C(115)	0.8420(7)	0.7426(5)	0.1978(4)	0.043(2)
C(116)	0.8309(6)	0.6619(4)	0.2175(3)	0.036(1)
C(121)	0.7617(6)	0.4320(4)	0.0859(3)	0.034(1)
C(122)	0.6714(7)	0.3716(5)	0.0370(3)	0.044(2)
C(123)	0.6075(8)	0.4025(7)	-0.0099(4)	0.056(2)
C(124)	0.6372(9)	0.4935(7)	-0.0065(4)	0.060(2)
C(125)	0.7278(8)	0.5535(6)	0.0407(4)	0.051(2)
C(126)	0.7917(6)	0.5238(5)	0.0867(3)	0.037(1)
C(131)	0.7599(6)	0.2776(4)	0.1433(3)	0.035(1)
C(132)	0.7031(6)	0.2449(4)	0.1867(3)	0.037(1)
C(133)	0.6388(7)	0.1529(5)	0.1813(4)	0.049(2)
C(134)	0.6331(9)	0.0951(5)	0.1340(4)	0.062(2)
C(135)	0.6901(11)	0.1278(5)	0.0903(5)	0.075(3)
C(136)	0.7547(9)	0.2179(5)	0.0947(4)	0.056(2)
C(141)	0.9800(6)	0.4062(5)	0.1330(3)	0.037(1)
C(142)	1.0454(7)	0.3616(6)	0.1649(4)	0.051(2)
C(143)	1.1532(9)	0.3694(7)	0.1556(5)	0.067(3)
C(144)	1.1975(8)	0.4241(7)	0.1157(5)	0.066(3)
C(145)	1.1359(8)	0.4702(7)	0.0852(5)	0.062(2)
C(146)	1.0230(3)	0.4578(2)	0.0922(2)	0.046(2)
O(1)	2.3109(3)	1.4670(2)	0.3862(2)	0.081(2)
C(1)	2.2816(3)	1.4155(2)	0.3282(2)	0.079(3)
C(2)	1.6599(3)	1.3025(2)	0.5208(2)	0.073(3)
C(3)	2.0411(3)	1.2190(2)	0.0361(2)	0.076(3)
C(4)	0.4694(3)	0.1889(2)	-0.0526(2)	0.091(3)
C(5)	1.4505(3)	0.7023(2)	0.4808(2)	0.094(4)

Table A.22: Bond lengths (Å) for **14**.

Pt(2)-O(22)	2.086(4)	C(65)-C(66)	1.379(10)
Pt(2)-O(21)	2.094(4)	C(71)-C(72)	1.393(9)
Pt(2)-P(22)	2.2416(17)	C(71)-C(76)	1.414(9)
Pt(2)-P(21)	2.2547(15)	C(72)-C(73)	1.400(10)
Pt(2)-P(2)	2.6684(16)	C(73)-C(74)	1.390(11)
Pt(1)-O(12)	2.092(4)	C(74)-C(75)	1.385(11)
Pt(1)-O(11)	2.097(4)	C(75)-C(76)	1.379(10)
Pt(1)-P(12)	2.2545(15)	C(81)-C(86)	1.396(9)
Pt(1)-P(11)	2.2579(16)	C(81)-C(82)	1.403(9)

Pt(1)-P(1)	2.6898(17)	C(82)-C(83)	1.400(10)
Fe(1)-C(21)	2.039(6)	C(83)-C(84)	1.383(13)
Fe(1)-C(22)	2.039(7)	C(84)-C(85)	1.375(12)
Fe(1)-C(13)	2.044(8)	C(85)-C(86)	1.399(10)
Fe(1)-C(15)	2.045(7)	C(21)-C(22)	1.432(11)
Fe(1)-C(14)	2.046(8)	C(21)-C(25)	1.433(10)
Fe(1)-C(12)	2.048(8)	C(22)-C(23)	1.420(11)
Fe(1)-C(11)	2.050(6)	C(23)-C(24)	1.419(16)
Fe(1)-C(23)	2.053(8)	C(24)-C(25)	1.423(14)
Fe(1)-C(25)	2.056(8)	C(11)-C(15)	1.433(10)
Fe(1)-C(24)	2.064(9)	C(11)-C(12)	1.444(10)
P(2)-O(23)	1.505(5)	C(12)-C(13)	1.426(12)
P(2)-O(21)	1.565(4)	C(13)-C(14)	1.408(14)
P(2)-O(22)	1.567(5)	C(14)-C(15)	1.430(11)
P(2)-C(21)	1.795(7)	C(91)-C(92)	1.394(9)
P(1)-O(13)	1.501(5)	C(91)-C(96)	1.411(9)
P(1)-O(11)	1.565(5)	C(92)-C(93)	1.410(10)
P(1)-O(12)	1.576(5)	C(93)-C(94)	1.390(11)
P(1)-C(11)	1.801(7)	C(94)-C(95)	1.383(12)
P(22)-C(121)	1.818(7)	C(95)-C(96)	1.397(11)
P(22)-C(131)	1.824(7)	C(101)-C(102)	1.387(9)
P(22)-C(141)	1.834(7)	C(101)-C(106)	1.399(9)
P(21)-C(111)	1.824(6)	C(102)-C(103)	1.401(10)
P(21)-C(91)	1.832(7)	C(103)-C(104)	1.370(12)
P(21)-C(101)	1.838(6)	C(104)-C(105)	1.392(11)
P(12)-C(51)	1.833(7)	C(105)-C(106)	1.408(9)
P(12)-C(41)	1.832(7)	C(111)-C(112)	1.400(9)
P(12)-C(31)	1.836(7)	C(111)-C(116)	1.410(9)
P(11)-C(61)	1.817(6)	C(112)-C(113)	1.389(10)
P(11)-C(81)	1.821(6)	C(113)-C(114)	1.393(12)
P(11)-C(71)	1.842(6)	C(114)-C(115)	1.388(11)
C(31)-C(32)	1.394(9)	C(115)-C(116)	1.396(9)
C(31)-C(36)	1.398(9)	C(121)-C(122)	1.392(10)
C(32)-C(33)	1.379(9)	C(121)-C(126)	1.407(9)
C(33)-C(34)	1.392(11)	C(122)-C(123)	1.422(11)
C(34)-C(35)	1.362(12)	C(123)-C(124)	1.389(14)
C(35)-C(36)	1.380(10)	C(124)-C(125)	1.371(14)
C(41)-C(46)	1.389(9)	C(125)-C(126)	1.398(10)
C(41)-C(42)	1.395(10)	C(131)-C(132)	1.394(10)
C(42)-C(43)	1.387(10)	C(131)-C(136)	1.410(11)
C(43)-C(44)	1.384(11)	C(132)-C(133)	1.404(10)
C(44)-C(45)	1.373(12)	C(133)-C(134)	1.366(13)
C(45)-C(46)	1.393(10)	C(134)-C(135)	1.401(14)
C(51)-C(56)	1.389(11)	C(135)-C(136)	1.382(12)
C(51)-C(52)	1.395(10)	C(141)-C(146)	1.381(8)
C(52)-C(53)	1.391(12)	C(141)-C(142)	1.403(11)
C(53)-C(54)	1.388(14)	C(142)-C(143)	1.388(12)
C(54)-C(55)	1.392(14)	C(143)-C(144)	1.399(15)
C(55)-C(56)	1.369(12)	C(144)-C(145)	1.379(14)
C(61)-C(62)	1.405(10)	C(145)-C(146)	1.412(9)

C(61)-C(66)	1.410(9)	O(1)-C(1)	1.4215
C(62)-C(63)	1.392(10)	C(2)-C(5)#1	1.355(7)
C(63)-C(64)	1.366(12)	C(5)-C(2)#1	1.355(7)
C(64)-C(65)	1.399(12)		

Symmetry transformations used to generate equivalent atoms: #1 -x+3,-y+2,-z+1

Table A.23: Bond Angles (°) for **14**.

O(22)-Pt(2)-O(21)	70.86(17)	C(42)-C(41)-P(12)	118.7(5)
O(22)-Pt(2)-P(22)	94.77(13)	C(43)-C(42)-C(41)	120.3(6)
O(21)-Pt(2)-P(22)	165.16(12)	C(44)-C(43)-C(42)	119.9(7)
O(22)-Pt(2)-P(21)	164.24(13)	C(45)-C(44)-C(43)	120.3(7)
O(21)-Pt(2)-P(21)	93.73(12)	C(44)-C(45)-C(46)	120.1(7)
P(22)-Pt(2)-P(21)	100.35(6)	C(41)-C(46)-C(45)	120.3(7)
O(22)-Pt(2)-P(2)	35.92(12)	C(56)-C(51)-C(52)	119.2(7)
O(21)-Pt(2)-P(2)	35.89(12)	C(56)-C(51)-P(12)	119.5(5)
P(22)-Pt(2)-P(2)	129.31(5)	C(52)-C(51)-P(12)	121.2(6)
P(21)-Pt(2)-P(2)	128.32(5)	C(53)-C(52)-C(51)	119.9(8)
O(12)-Pt(1)-O(11)	70.62(17)	C(54)-C(53)-C(52)	120.1(8)
O(12)-Pt(1)-P(12	91.33(13)	C(53)-C(54)-C(55)	119.5(8)
O(11)-Pt(1)-P(12)	161.82(13)	C(56)-C(55)-C(54)	120.4(9)
O(12)-Pt(1)-P(11	168.58(12)	C(55)-C(56)-C(51)	120.8(8)
O(11)-Pt(1)-P(11)	98.06(13)	C(62)-C(61)-C(66)	119.0(6)
P(12)-Pt(1)-P(11)	99.91(6)	C(62)-C(61)-P(11)	123.3(5)
O(12)-Pt(1)-P(1)	35.79(12)	C(66)-C(61)-P(11)	117.4(5)
O(11)-Pt(1)-P(1)	35.53(13)	C(63)-C(62)-C(61)	119.0(7)
P(12)-Pt(1)-P(1)	126.30(6)	C(64)-C(63)-C(62)	121.9(7)
P(11)-Pt(1)-P(1)	132.80(5)	C(63)-C(64)-C(65)	119.4(7)
C(22)-Fe(1)-C(21)	41.1(3)	C(66)-C(65)-C(64)	120.1(7)
C(22)-Fe(1)-C(13)	110.0(4)	C(65)-C(66)-C(61)	120.6(7)
C(21)-Fe(1)-C(13)	109.4(3)	C(72)-C(71)-C(76)	118.6(6)
C(22)-Fe(1)-C(15)	178.0(3)	C(72)-C(71)-P(11)	122.4(5)
C(21)-Fe(1)-C(15)	137.3(3)	C(76)-C(71)-P(11)	118.8(5)
C(13)-Fe(1)-C(15)	68.9(4)	C(71)-C(72)-C(73)	120.1(7)
C(22)-Fe(1)-C(14)	137.2(3)	C(74)-C(73)-C(72)	120.9(7)
C(21)-Fe(1)-C(14)	109.3(3)	C(75)-C(74)-C(73)	118.9(6)
C(13)-Fe(1)-C(14)	40.3(4)	C(76)-C(75)-C(74)	121.2(7)
C(15)-Fe(1)-C(14)	40.9(3)	C(75)-C(76)-C(71)	120.3(7)
C(22)-Fe(1)-C(12)	111.4(3)	C(86)-C(81)-C(82)	118.9(6)
C(21)-Fe(1)-C(12)	138.4(3)	C(86)-C(81)-P(11)	121.2(5)
C(13)-Fe(1)-C(12)	40.8(3)	C(82)-C(81)-P(11)	119.8(5)
C(15)-Fe(1)-C(12)	69.0(3)	C(83)-C(82)-C(81)	120.3(7)
C(14)-Fe(1)-C(12)	68.1(4)	C(84)-C(83)-C(82)	119.5(7)
C(22)-Fe(1)-C(23)	40.6(3)	C(85)-C(84)-C(83)	121.0(7)
C(21)-Fe(1)-C(23)	68.6(3)	C(84)-C(85)-C(86)	119.8(7)
C(13)-Fe(1)-C(23)	139.1(5)	C(81)-C(86)-C(85)	120.4(7)
C(15)-Fe(1)-C(23)	141.3(3)	C(22)-C(21)-C(25)	107.6(7)
C(14)-Fe(1)-C(23)	177.7(3)	C(22)-C(21)-P(2)	126.5(5)
C(12)-Fe(1)-C(23)	112.8(4)	C(25)-C(21)-P(2)	125.9(6)

C(22)-Fe(1)-C(11)	140.6(3)	C(22)-C(21)-Fe(1)	69.5(4)
C(21)-Fe(1)-C(11)	177.9(3)	C(25)-C(21)-Fe(1)	70.1(4)
C(13)-Fe(1)-C(11)	69.1(3)	P(2)-C(21)-Fe(1)	126.8(3)
C(15)-Fe(1)-C(11)	41.0(3)	C(23)-C(22)-C(21)	107.9(8)
C(14)-Fe(1)-C(11)	68.6(3)	C(23)-C(22)-Fe(1)	70.2(4)
C(12)-Fe(1)-C(11)	41.3(3)	C(21)-C(22)-Fe(1)	69.4(4)
C(23)-Fe(1)-C(11)	113.5(3)	C(24)-C(23)-C(22)	108.5(8)
C(22)-Fe(1)-C(25)	68.8(3)	C(24)-C(23)-Fe(1)	70.3(5)
C(21)-Fe(1)-C(25)	41.0(3)	C(22)-C(23)-Fe(1)	69.2(4)
C(13)-Fe(1)-C(25)	138.1(3)	C(23)-C(24)-C(25)	108.1(7)
C(15)-Fe(1)-C(25)	110.8(3)	C(23)-C(24)-Fe(1)	69.4(5)
C(14)-Fe(1)-C(25)	110.9(4)	C(25)-C(24)-Fe(1)	69.5(5)
C(12)-Fe(1)-C(25)	178.9(3)	C(24)-C(25)-C(21)	107.9(8)
C(23)-Fe(1)-C(25)	68.2(4)	C(24)-C(25)-Fe(1)	70.1(5)
C(11)-Fe(1)-C(25)	139.3(3)	C(21)-C(25)-Fe(1)	68.9(4)
C(22)-Fe(1)-C(24)	68.3(4)	C(15)-C(11)-C(12)	107.4(6)
C(21)-Fe(1)-C(24)	68.5(3)	C(15)-C(11)-P(1)	127.6(5)
C(13)-Fe(1)-C(24)	177.9(3)	C(12)-C(11)-P(1)	124.9(6)
C(15)-Fe(1)-C(24)	112.7(4)	C(15)-C(11)-Fe(1)	69.4(4)
C(14)-Fe(1)-C(24)	140.1(5)	C(12)-C(11)-Fe(1)	69.3(4)
C(12)-Fe(1)-C(24)	140.7(4)	P(1)-C(11)-Fe(1)	128.6(4)
C(23)-Fe(1)-C(24)	40.4(4)	C(13)-C(12)-C(11)	108.0(8)
C(11)-Fe(1)-C(24)	113.0(3)	C(13)-C(12)-Fe(1)	69.5(5)
C(25)-Fe(1)-C(24)	40.4(4)	C(11)-C(12)-Fe(1)	69.4(4)
O(23)-P(2)-O(21)	114.8(3)	C(14)-C(13)-C(12)	108.0(7)
O(23)-P(2)-O(22)	115.7(3)	C(14)-C(13)-Fe(1)	69.9(5)
O(21)-P(2)-O(22)	101.3(2)	C(12)-C(13)-Fe(1)	69.7(4)
O(23)-P(2)-C(21)	110.9(3)	C(13)-C(14)-C(15)	109.2(7)
O(21)-P(2)-C(21)	105.9(3)	C(13)-C(14)-Fe(1)	69.8(5)
O(22)-P(2)-C(21)	107.3(3)	C(15)-C(14)-Fe(1)	69.5(4)
O(23)-P(2)-Pt(2)	143.0(2)	C(14)-C(15)-C(11)	107.4(7)
O(21)-P(2)-Pt(2)	51.63(16)	C(14)-C(15)-Fe(1)	69.5(4)
O(22)-P(2)-Pt(2)	51.34(16)	C(11)-C(15)-Fe(1)	69.7(4)
C(21)-P(2)-Pt(2)	106.1(2)	C(92)-C(91)-C(96)	118.7(6)
O(13)-P(1)-O(11)	115.4(3)	C(92)-C(91)-P(21)	120.8(5)
O(13)-P(1)-O(12)	114.2(3)	C(96)-C(91)-P(21)	120.4(5)
O(11)-P(1)-O(12)	100.8(2)	C(91)-C(92)-C(93)	120.5(6)
O(13)-P(1)-C(11)	109.0(3)	C(94)-C(93)-C(92)	120.2(7)
O(11)-P(1)-C(11)	109.1(3)	C(95)-C(94)-C(93)	119.5(7)
O(12)-P(1)-C(11)	107.9(3)	C(94)-C(95)-C(96)	121.0(7)
O(13)-P(1)-Pt(1)	140.3(2)	C(95)-C(96)-C(91)	120.1(7)
O(11)-P(1)-Pt(1)	51.09(16)	C(102)-C(101)-C(106)	119.4(6)
O(12)-P(1)-Pt(1)	50.92(16)	C(102)-C(101)-P(21)	119.4(5)
C(11)-P(1)-Pt(1)	110.7(2)	C(106)-C(101)-P(21)	121.1(5)
C(121)-P(22)-C(131)	107.1(3)	C(101)-C(102)-C(103)	120.4(7)
C(121)-P(22)-C(141)	104.9(3)	C(104)-C(103)-C(102)	120.3(7)
C(131)-P(22)-C(141)	103.8(3)	C(103)-C(104)-C(105)	120.3(7)
C(121)-P(22)-Pt(2)	114.9(2)	C(104)-C(105)-C(106)	119.9(7)
C(131)-P(22)-Pt(2)	116.7(2)	C(101)-C(106)-C(105)	119.7(6)
C(141)-P(22)-Pt(2)	108.2(2)	C(112)-C(111)-C(116)	118.3(6)

C(111)-P(21)-C(91)	106.8(3)	C(112)-C(111)-P(21)	124.2(5)
C(111)-P(21)-C(101)	106.8(3)	C(116)-C(111)-P(21)	117.5(5)
C(91)-P(21)-C(101)	103.0(3)	C(113)-C(112)-C(111)	120.2(7)
C(111)-P(21)-Pt(2)	107.8(2)	C(112)-C(113)-C(114)	121.2(7)
C(91)-P(21)-Pt(2)	109.9(2)	C(115)-C(114)-C(113)	119.4(7)
C(101)-P(21)-Pt(2)	121.7(2)	C(114)-C(115)-C(116)	119.9(7)
C(41)-P(12)-C(51)	105.4(3)	C(115)-C(116)-C(111)	121.0(7)
C(41)-P(12)-C(31)	102.3(3)	C(122)-C(121)-C(126)	119.1(6)
C(51)-P(12)-C(31)	105.8(3)	C(122)-C(121)-P(22)	122.6(5)
C(41)-P(12)-Pt(1)	122.5(2)	C(126)-C(121)-P(22)	118.3(5)
C(51)-P(12)-Pt(1)	108.2(2)	C(121)-C(122)-C(123)	120.2(7)
C(31)-P(12)-Pt(1)	111.3(2)	C(124)-C(123)-C(122)	119.1(8)
C(61)-P(11)-C(81)	108.9(3)	C(125)-C(124)-C(123)	121.1(8)
C(61)-P(11)-C(71)	101.8(3)	C(124)-C(125)-C(126)	120.2(8)
C(81)-P(11)-C(71)	101.2(3)	C(125)-C(126)-C(121)	120.3(7)
C(61)-P(11)-Pt(1)	118.3(2)	C(132)-C(131)-C(136)	119.9(6)
C(81)-P(11)-Pt(1)	111.8(2)	C(132)-C(131)-P(22)	120.0(5)
C(71)-P(11)-Pt(1)	113.1(2)	C(136)-C(131)-P(22)	120.1(6)
P(2)-O(21)-Pt(2)	92.5(2)	C(131)-C(132)-C(133)	120.0(7)
P(2)-O(22)-Pt(2)	92.7(2)	C(134)-C(133)-C(132)	120.2(8)
P(1)-O(11)-Pt(1)	93.4(2)	C(133)-C(134)-C(135)	119.9(7)
P(1)-O(12)-Pt(1)	93.3(2)	C(136)-C(135)-C(134)	121.1(8)
C(32)-C(31)-C(36)	118.1(6)	C(135)-C(136)-C(131)	118.9(8)
C(32)-C(31)-P(12)	120.6(5)	C(146)-C(141)-C(142)	120.0(6)
C(36)-C(31)-P(12)	121.2(5)	C(146)-C(141)-P(22)	121.9(5)
C(33)-C(32)-C(31)	120.6(6)	C(142)-C(141)-P(22)	118.1(6)
C(32)-C(33)-C(34)	120.1(7)	C(143)-C(142)-C(141)	120.1(8)
C(35)-C(34)-C(33)	119.8(6)	C(142)-C(143)-C(144)	119.3(8)
C(34)-C(35)-C(36)	120.6(7)	C(145)-C(144)-C(143)	121.3(8)
C(35)-C(36)-C(31)	120.7(7)	C(144)-C(145)-C(146)	118.9(8)
C(46)-C(41)-C(42)	119.1(6)	C(141)-C(146)-C(145)	120.2(6)
C(46)-C(41)-P(12)	122.2(5)		

Table A.24: Anisotropic displacement parameters ($Å^2$) for **14**. The anisotropic displacement factor exponent takes the form: $-2\pi^2[h^2a^{*2}U11 + ... + 2hka^*b^*U12]$.

atom	U11	U22	U33	U23	U13	U12
Pt(2)	0.020(1)	0.019(1)	0.036(1)	0.006(1)	0.011(1)	0.007(1)
Pt(1)	0.019(1)	0.021(1)	0.032(1)	0.005(1)	0.009(1)	0.006(1)
Fe(1)	0.025(1)	0.025(1)	0.062(1)	0.011(1)	0.021(1)	0.006(1)
P(2)	0.021(1)	0.026(1)	0.042(1)	0.005(1)	0.010(1)	0.006(1)
P(1)	0.024(1)	0.030(1)	0.034(1)	0.004(1)	0.008(1)	0.003(1)
P(22)	0.028(1)	0.023(1)	0.039(1)	0.007(1)	0.015(1)	0.010(1)
P(21)	0.022(1)	0.023(1)	0.037(1)	0.006(1)	0.011(1)	0.009(1)
P(12)	0.020(1)	0.024(1)	0.036(1)	0.006(1)	0.010(1)	0.007(1)
P(11)	0.021(1)	0.021(1)	0.033(1)	0.006(1)	0.009(1)	0.007(1)
O(21)	0.023(2)	0.025(2)	0.040(2)	0.003(2)	0.013(2)	0.003(2)

O(22)	0.021(2)	0.026(2)	0.047(3)	0.004(2)	0.013(2)	0.007(2)
O(23)	0.029(2)	0.046(3)	0.051(3)	0.008(2)	0.004(2)	0.012(2)
O(11)	0.022(2)	0.031(2)	0.047(3)	0.002(2)	0.006(2)	0.009(2)
O(12)	0.024(2)	0.032(2)	0.038(2)	0.001(2)	0.012(2)	0.005(2)
O(13)	0.042(3)	0.056(3)	0.041(3)	0.010(2)	0.000(2)	0.004(2)
C(31)	0.028(3)	0.029(3)	0.038(3)	0.005(2)	0.011(3)	0.014(3)
C(32)	0.032(3)	0.025(3)	0.037(3)	0.005(2)	0.009(3)	0.008(2)
C(33)	0.049(4)	0.026(3)	0.039(4)	0.000(3)	0.009(3)	0.012(3)
C(34)	0.066(5)	0.031(4)	0.048(4)	0.006(3)	0.013(4)	0.027(4)
C(35)	0.049(4)	0.048(4)	0.053(4)	0.010(3)	0.015(3)	0.033(4)
C(36)	0.030(3)	0.042(4)	0.050(4)	0.010(3)	0.014(3)	0.016(3)
C(41)	0.020(3)	0.028(3)	0.043(3)	0.001(3)	0.007(2)	0.010(2)
C(42)	0.027(3)	0.030(3)	0.043(4)	0.005(3)	0.009(3)	0.010(3)
C(43)	0.035(3)	0.037(4)	0.043(4)	0.001(3)	0.004(3)	0.015(3)
C(44)	0.037(4)	0.036(4)	0.053(4)	-0.007(3)	-0.001(3)	0.012(3)
C(45)	0.032(3)	0.028(3)	0.069(5)	0.006(3)	0.008(3)	0.003(3)
C(46)	0.029(3)	0.029(3)	0.048(4)	0.005(3)	0.009(3)	0.005(3)
C(51)	0.024(3)	0.035(3)	0.040(3)	0.003(3)	0.015(3)	0.004(2)
C(52)	0.046(4)	0.071(5)	0.051(4)	0.017(4)	0.021(4)	0.034(4)
C(53)	0.064(6)	0.094(7)	0.062(5)	0.021(5)	0.036(5)	0.049(6)
C(54)	0.067(6)	0.081(7)	0.064(6)	0.026(5)	0.044(5)	0.027(5)
C(55)	0.100(8)	0.076(7)	0.073(6)	0.043(5)	0.057(6)	0.053(6)
C(56)	0.072(6)	0.066(5)	0.070(5)	0.034(5)	0.049(5)	0.046(5)
C(61)	0.022(3)	0.021(3)	0.042(3)	0.006(2)	0.009(2)	0.007(2)
C(62)	0.029(3)	0.031(3)	0.046(4)	0.006(3)	0.007(3)	0.005(3)
C(63)	0.037(4)	0.032(4)	0.056(5)	-0.006(3)	0.004(3)	0.001(3)
C(64)	0.031(4)	0.027(3)	0.081(6)	0.012(4)	0.011(4)	0.004(3)
C(65)	0.033(3)	0.035(4)	0.064(5)	0.025(3)	0.020(3)	0.014(3)
C(66)	0.031(3)	0.031(3)	0.046(4)	0.016(3)	0.013(3)	0.013(3)
C(71)	0.027(3)	0.029(3)	0.032(3)	0.008(2)	0.012(2)	0.012(2)
C(72)	0.036(3)	0.030(3)	0.050(4)	0.009(3)	0.014(3)	0.016(3)
C(73)	0.046(4)	0.040(4)	0.065(5)	0.019(3)	0.021(4)	0.028(3)
C(74)	0.036(4)	0.065(5)	0.044(4)	0.022(3)	0.021(3)	0.032(4)
C(75)	0.027(3)	0.050(4)	0.050(4)	0.001(3)	0.010(3)	0.012(3)
C(76)	0.025(3)	0.037(4)	0.057(4)	0.001(3)	0.015(3)	0.007(3)
C(81)	0.018(3)	0.026(3)	0.035(3)	0.006(2)	0.007(2)	0.003(2)
C(82)	0.030(3)	0.034(3)	0.047(4)	0.014(3)	0.013(3)	0.013(3)
C(83)	0.037(4)	0.052(5)	0.071(5)	0.038(4)	0.023(4)	0.019(3)
C(84)	0.039(4)	0.065(5)	0.048(4)	0.030(4)	0.015(3)	0.017(4)
C(85)	0.034(4)	0.054(4)	0.037(4)	0.006(3)	0.013(3)	0.006(3)
C(86)	0.030(3)	0.032(3)	0.040(3)	0.004(3)	0.011(3)	0.007(3)
C(21)	0.020(3)	0.027(3)	0.056(4)	0.007(3)	0.017(3)	0.006(2)
C(22)	0.028(3)	0.042(4)	0.066(5)	0.024(4)	0.017(3)	0.013(3)
C(23)	0.041(4)	0.057(5)	0.125(9)	0.058(6)	0.048(5)	0.028(4)
C(24)	0.044(5)	0.032(4)	0.145(10)	0.018(5)	0.050(6)	0.013(4)
C(25)	0.037(4)	0.026(3)	0.084(6)	-0.006(3)	0.031(4)	0.000(3)
C(11)	0.026(3)	0.030(3)	0.045(4)	0.007(3)	0.014(3)	0.006(2)
C(12)	0.039(4)	0.038(4)	0.064(5)	-0.001(3)	0.025(4)	0.011(3)
C(13)	0.046(4)	0.035(4)	0.101(7)	0.020(4)	0.043(5)	0.017(3)
C(14)	0.041(4)	0.055(5)	0.097(7)	0.045(5)	0.041(5)	0.028(4)

C(15)	0.028(3)	0.053(4)	0.050(4)	0.016(3)	0.017(3)	0.014(3)
C(91)	0.025(3)	0.023(3)	0.037(3)	0.001(2)	0.010(2)	0.004(2)
C(92)	0.026(3)	0.029(3)	0.047(4)	0.009(3)	0.013(3)	0.007(2)
C(93)	0.042(4)	0.040(4)	0.039(4)	0.009(3)	0.011(3)	0.008(3)
C(94)	0.057(5)	0.042(4)	0.041(4)	0.003(3)	0.022(3)	0.015(4)
C(95)	0.044(4)	0.040(4)	0.055(4)	0.005(3)	0.026(3)	0.018(3)
C(96)	0.038(4)	0.033(3)	0.047(4)	0.005(3)	0.013(3)	0.015(3)
C(101)	0.025(3)	0.027(3)	0.038(3)	0.004(2)	0.008(2)	0.010(2)
C(102)	0.033(3)	0.029(3)	0.043(4)	0.008(3)	0.010(3)	0.006(3)
C(103)	0.037(4)	0.037(4)	0.054(4)	0.007(3)	0.012(3)	0.000(3)
C(104)	0.033(4)	0.038(4)	0.058(5)	0.001(3)	0.009(3)	0.004(3)
C(105)	0.032(3)	0.042(4)	0.042(4)	0.001(3)	0.003(3)	0.016(3)
C(106)	0.026(3)	0.034(3)	0.046(4)	0.007(3)	0.012(3)	0.013(3)
C(111)	0.035(3)	0.028(3)	0.035(3)	0.007(2)	0.015(3)	0.015(3)
C(112)	0.037(3)	0.038(4)	0.044(4)	0.010(3)	0.019(3)	0.020(3)
C(113)	0.056(5)	0.049(4)	0.044(4)	0.013(3)	0.019(3)	0.037(4)
C(114)	0.071(5)	0.032(4)	0.055(4)	0.017(3)	0.033(4)	0.028(4)
C(115)	0.050(4)	0.030(3)	0.058(4)	0.014(3)	0.027(4)	0.017(3)
C(116)	0.037(3)	0.025(3)	0.048(4)	0.005(3)	0.017(3)	0.012(3)
C(121)	0.036(3)	0.036(3)	0.038(3)	0.013(3)	0.019(3)	0.019(3)
C(122)	0.046(4)	0.045(4)	0.045(4)	0.009(3)	0.017(3)	0.020(3)
C(123)	0.046(4)	0.084(6)	0.041(4)	0.013(4)	0.011(3)	0.030(4)
C(124)	0.069(6)	0.089(7)	0.054(5)	0.041(5)	0.032(5)	0.053(5)
C(125)	0.055(5)	0.061(5)	0.058(5)	0.031(4)	0.029(4)	0.034(4)
C(126)	0.041(4)	0.035(3)	0.047(4)	0.015(3)	0.023(3)	0.020(3)
C(131)	0.039(3)	0.022(3)	0.045(4)	0.007(3)	0.014(3)	0.012(3)
C(132)	0.038(4)	0.031(3)	0.042(4)	0.009(3)	0.010(3)	0.015(3)
C(133)	0.050(4)	0.037(4)	0.055(5)	0.020(3)	0.013(4)	0.010(3)
C(134)	0.080(6)	0.024(4)	0.070(6)	0.009(4)	0.020(5)	0.010(4)
C(135)	0.110(9)	0.024(4)	0.080(7)	-0.006(4)	0.037(6)	0.013(5)
C(136)	0.076(6)	0.036(4)	0.060(5)	0.007(4)	0.034(5)	0.018(4)
C(141)	0.035(3)	0.035(3)	0.044(4)	0.001(3)	0.016(3)	0.017(3)
C(142)	0.051(5)	0.058(5)	0.061(5)	0.016(4)	0.029(4)	0.033(4)
C(143)	0.063(6)	0.087(7)	0.081(7)	0.019(5)	0.030(5)	0.055(6)
C(144)	0.044(5)	0.088(7)	0.084(7)	0.011(5)	0.034(5)	0.039(5)
C(145)	0.052(5)	0.071(6)	0.079(6)	0.019(5)	0.043(5)	0.026(5)
C(146)	0.040(4)	0.048(4)	0.061(5)	0.013(4)	0.028(4)	0.020(3)
O(1)	0.067(4)	0.088(5)	0.110(6)	0.030(5)	0.028(4)	0.052(4)
C(1)	0.062(6)	0.053(6)	0.131(10)	0.028(6)	0.035(6)	0.028(5)
C(2)	0.079(7)	0.066(6)	0.057(5)	-0.026(4)	-0.007(5)	0.033(5)
C(3)	0.082(7)	0.106(8)	0.037(4)	0.012(5)	0.007(4)	0.040(6)
C(4)	0.165(10)	0.067(6)	0.046(5)	-0.007(4)	0.022(6)	0.059(7)
C(5)	0.070(7)	0.094(9)	0.081(8)	-0.006(6)	0.017(6)	-0.001(6)

Table A.25: Hydrogen coordinates and isotropic displacement parameters ($Å^2$) for **14**.

Atom	x	y	z	U(eq)
H(32)	1.7309	0.8404	0.3131	0.039
H(33)	1.7438	0.7086	0.3347	0.048
H(34)	1.9292	0.7037	0.3741	0.056
H(35)	2.0981	0.8322	0.3987	0.055
H(36)	2.0865	0.9659	0.3819	0.047
H(42)	1.9610	1.0384	0.4534	0.041
H(43)	2.1020	1.1429	0.5354	0.048
H(44)	2.2390	1.2728	0.5197	0.056
H(45)	2.2320	1.3007	0.4227	0.056
H(46)	2.0955	1.1944	0.3400	0.045
H(52)	2.0475	0.9613	0.2703	0.061
H(53)	2.1219	0.9895	0.1877	0.077
H(54)	2.0825	1.0910	0.1296	0.079
H(55)	1.9527	1.1528	0.1486	0.084
H(56)	1.8731	1.1205	0.2277	0.069
H(62)	1.8737	1.2325	0.4861	0.046
H(63)	2.0178	1.3764	0.5064	0.058
H(64)	2.0738	1.4477	0.4302	0.059
H(65)	1.9880	1.3737	0.3298	0.050
H(66)	1.8437	1.2308	0.3074	0.042
H(72)	1.6798	1.2766	0.3819	0.045
H(73)	1.5140	1.3124	0.3666	0.055
H(74)	1.3232	1.2028	0.3255	0.051
H(75)	1.2990	1.0563	0.3021	0.053
H(76)	1.4606	1.0177	0.3220	0.049
H(82)	1.7286	0.9519	0.4156	0.044
H(83)	1.6910	0.8835	0.4981	0.060
H(84)	1.6413	0.9523	0.5716	0.060
H(85)	1.6210	1.0850	0.5626	0.054
H(86)	1.6571	1.1540	0.4803	0.043
H(22)	1.0811	0.6491	0.1929	0.053
H(23)	1.1846	0.8114	0.1895	0.078
H(24)	1.2974	0.8927	0.2961	0.084
H(25)	1.2643	0.7810	0.3665	0.061
H(12)	1.3539	0.6860	0.1596	0.057
H(13)	1.3103	0.5738	0.2293	0.067
H(14)	1.4244	0.6518	0.3356	0.067
H(15)	1.5357	0.8145	0.3345	0.052
H(92)	0.8147	0.4475	0.3509	0.042
H(93)	0.7900	0.4567	0.4479	0.051
H(94)	0.6528	0.5099	0.4675	0.056
H(95)	0.5414	0.5542	0.3909	0.053
H(96)	0.5654	0.5469	0.2944	0.047
H(102)	0.5397	0.3351	0.2593	0.045
H(103)	0.3665	0.2167	0.2020	0.057

H(104)	0.2918	0.2130	0.1000	0.056
H(105)	0.3925	0.3249	0.0528	0.048
H(106)	0.5646	0.4461	0.1103	0.042
H(112)	0.5409	0.5672	0.1796	0.043
H(113)	0.5607	0.7019	0.1488	0.053
H(114)	0.7474	0.8108	0.1580	0.056
H(115)	0.9172	0.7864	0.2024	0.052
H(116)	0.8991	0.6527	0.2356	0.043
H(122	0.6528	0.3108	0.0351	0.053
H(123)	0.5466	0.3623	-0.0424	0.067
H(124)	0.5949	0.5140	-0.0368	0.072
H(125)	0.7468	0.6142	0.0420	0.062
H(126)	0.8543	0.5648	0.1181	0.045
H(132)	0.7079	0.2840	0.2193	0.044
H(133)	0.6000	0.1313	0.2100	0.059
H(134)	0.5913	0.0341	0.1308	0.074
H(135)	0.6844	0.0881	0.0577	0.089
H(136)	0.7942	0.2389	0.0661	0.067
H(142)	1.0164	0.3269	0.1923	0.061
H(143)	1.1956	0.3385	0.1757	0.081
H(144)	1.2699	0.4295	0.1095	0.079
H(145)	1.1682	0.5088	0.0605	0.075
H(146)	0.9775	0.4844	0.0694	0.055
H(1)	2.2705	1.4967	0.3844	0.121
H(1A)	2.3012	1.4546	0.2997	0.118
H(1B)	2.1978	1.3787	0.3149	0.118
H(1C)	2.3260	1.3786	0.3307	0.118

Table A.26: Atomic coordinates and equivalent isotropic displacement parameters for **25**. U(eq) is defined as one third of the trace of the orthogonalized Uij tensor.

atom	x	y	z	U(eq)
Fe(1)	0.1721(1)	0.4997(1)	0.3863(1)	0.022
As(1)	0.5214(1)	0.7885(1)	0.3437(1)	0.092
C(1)	0.3309(4)	0.7994(7)	0.4045(5)	0.052
C(2)	0.4167(4)	0.6814(9)	0.4190(7)	0.066
C(11)	0.2483(3)	0.7136(6)	0.4565(4)	0.042
C(12)	0.2442(3)	0.5849(6)	0.5550(4)	0.042
C(13)	0.1484(3)	0.5576(5)	0.5695(3)	0.034
C(14)	0.0949(3)	0.6691(5)	0.4806(4)	0.035
C(15)	0.1560(3)	0.7644(5)	0.4126(4)	0.040
C(21)	0.2187(3)	0.4175(6)	0.2205(4)	0.049
C(22)	0.2420(3)	0.2955(7)	0.3169(5)	0.056
C(23)	0.1581(4)	0.2352(5)	0.3589(4)	0.057
C(24)	0.0842(3)	0.3229(6)	0.2864(4)	0.048
C(25)	0.1226(4)	0.4356(6)	0.2004(4)	0.046
C(111)	0.3642(4)	0.6975(6)	0.4809(4)	0.039

C(112)	0.3860(4)	0.7739(6)	0.3419(4)	0.049

Table A.27: Bond lengths (Å) for **25**.

Fe(1)-C(22)	2.032(4)	C(11)-C(111)	1.660(7)
Fe(1)-C(23)	2.033(4)	C(12)-C(13)	1.423(6)
Fe(1)-C(12)	2.036(4)	C(13)-C(14)	1.411(6)
Fe(1)-C(24)	2.037(4)	C(14)-C(15)	1.404(6)
Fe(1)-C(14)	2.038(4)	C(21)-C(25)	1.379(7)
Fe(1)-C(21)	2.041(4)	C(21)-C(22)	1.379(7)
Fe(1)-C(13)	2.042(3)	C(22)-C(23)	1.414(8)
Fe(1)-C(11)	2.042(4)	C(23)-C(24)	1.393(7)
Fe(1)-C(15)	2.045(4)	C(24)-C(25)	1.407(7)
Fe(1)-C(25)	2.045(4)	C(111)-C(112)	1.6363
As(1)-C(112)	1.950(5)	C(1)-C(11)	1.518(7)
As(1)-C(2)	1.966(6)	C(2)-C(111)	1.066(8)
C(1)-C(112	1.111(8)	C(2)-C(112)	1.117(8)
C(1)-C(111)	1.170(7)	C(11)-C(15)	1.403(7)
C(1)-C(2)	1.517(9)	C(11)-C(12)	1.428(6)

Table A.28: Bond Angles (°) for **25**.

C(22)-Fe(1)-C(23)	40.7(2)	C(112)-C(2)-C(1)	46.9(4)
C(22)-Fe(1)-C(12)	109.45(18)	C(111)-C(2)-As(1)	147.0(6)
C(23)-Fe(1)-C(12)	117.78(19)	C(13)-C(12)-C(11)	72.6(4)
C(22)-Fe(1)-C(24)	67.51(19)	C(13)-C(12)-Fe(1)	111.9(4)
C(23)-Fe(1)-C(24)	40.0(2)	C(11)-C(12)-Fe(1)	107.4(4)
C(12)-Fe(1)-C(24)	150.2(2)	C(14)-C(13)-C(12)	121.2(4)
C(22)-Fe(1)-C(14)	168.9(2)	C(14)-C(13)-Fe(1)	131.4(4)
C(23)-Fe(1)-C(14)	129.8(2)	C(12)-C(13)-Fe(1)	164.1(4)
C(12)-Fe(1)-C(14)	68.11(16)	C(15)-C(14)-C(13)	88.5(4)
C(24)-Fe(1)-C(14)	108.82(17)	C(15)-C(14)-Fe(1)	42.9(3)
C(22)-Fe(1)-C(21)	39.6(2)	C(13)-C(14)-Fe(1)	70.0(2)
C(23)-Fe(1)-C(21)	67.40(19)	C(11)-C(15)-C(14)	69.3(2)
C(12)-Fe(1)-C(21)	130.54(19)	C(112)-C(2)-As(1)	128.3(3)
C(24)-Fe(1)-C(21)	67.18(17)	C(1)-C(2)-As(1)	118.6(3)
C(14)-Fe(1)-C(21)	150.07(19)	C(15)-C(11)-C(12)	108.0(4)
C(22)-Fe(1)-C(13)	130.7(2)	C(15)-C(11)-C(1)	69.8(2)
C(23)-Fe(1)-C(13)	108.64(17)	C(12)-C(11)-C(1)	69.7(2)
C(12)-Fe(1)-C(13)	40.84(17)	C(15)-C(11)-C(111)	107.2(4)
C(24)-Fe(1)-C(13)	117.15(17)	C(12)-C(11)-C(111)	69.6(2)
C(14)-Fe(1)-C(13)	40.48(16)	C(1)-C(11)-C(111)	69.3(2)
C(21)-Fe(1)-C(13)	168.8(2)	C(15)-C(11)-Fe(1)	108.6 (4)
C(22)-Fe(1)-C(11)	117.9(2)	C(12)-C(11)-Fe(1)	70.1(2)
C(23)-Fe(1)-C(11)	151.0(2)	C(1)-C(11)-Fe(1)	69.9(2)
C(12)-Fe(1)-C(11)	41.00(19)	C(111)-C(11)-Fe(1)	108.8(4)
C(24)-Fe(1)-C(11)	167.7(2)	C(11)-C(15)-Fe(1)	69.8(2)
C(14)-Fe(1)-C(11)	68.00(17)	C(14)-C(15)-Fe(1)	69.6(2)
C(21)-Fe(1)-C(11)	109.22(17)	C(25)-C(21)-C(22)	108.7(4)
C(13)-Fe(1)-C(11)	68.76(16)	C(25)-C(21)-Fe(1)	70.4(2)

C(22)-Fe(1)-C(15)	150.1(2)	C(22)-C(21)-Fe(1)	69.9(2)
C(23)-Fe(1)-C(15)	167.8(2)	C(21)-C(22)-C(23)	108.1(4)
C(12)-Fe(1)-C(15)	67.99(18)	C(21)-C(22)-Fe(1)	70.6(3)
C(24)-Fe(1)-C(15)	129.9(2)	C(23)-C(22)-Fe(1)	69.7(3)
C(14)-Fe(1)-C(15)	40.23(17)	C(24)-C(23)-C(22)	107.3(4)
C(21)-Fe(1)-C(15)	118.06(18)	C(24)-C(23)-Fe(1)	70.1(2)
C(13)-Fe(1)-C(15)	68.06(16)	C(22)-C(23)-Fe(1)	69.6(3)
C(11)-Fe(1)-C(15)	40.14(19)	C(23)-C(24)-C(25)	107.7(4)
C(22)-Fe(1)-C(25)	66.72(19)	C(23)-C(24)-Fe(1)	69.8(2)
C(23)-Fe(1)-C(25)	67.34(18)	C(25)-C(24)-Fe(1)	70.1(2)
C(12)-Fe(1)-C(25)	168.1(2)	C(21)-C(25)-C(24)	108.2(4)
C(24)-Fe(1)-C(25)	40.32(19)	C(21)-C(25)-Fe(1)	70.1(2)
C(14)-Fe(1)-C(25)	117.89(17)	C(24)-C(25)-Fe(1)	69.5(2)
C(21)-Fe(1)-C(25)	39.4(2)	C(2)-C(111)-C(1)	85.3(6)
C(13)-Fe(1)-C(25)	150.17(19)	C(2)-C(111)-C(112)	42.6(4)
C(11)-Fe(1)-C(25)	129.54(19)	C(1)-C(111)-C(112)	42.7(4)
C(15)-Fe(1)-C(25)	109.28(17)	C(2)-C(111)-C(11)	133.9(5)
C(112)-As(1)-C(2)	33.1(2)	C(1)-C(111)-C(11)	62.1(4)
C(112)-C(1)-C(111)	91.6(5)	C(112)-C(111)-C(11)	98.2(2)
C(112)-C(1)-C(2)	47.2(4)	C(1)-C(112)-C(2)	85.9(5)
C(111)-C(1)-C(2)	44.4(4)	C(1)-C(112)-C(111)	45.6(4)
C(112)-C(1)-C(11)	142.3(5)	C(2)-C(112)-C(111)	40.3(4)
C(111)-C(1)-C(11)	75.0(4)	C(1)-C(112)-As(1)	140.8(4)
C(2)-C(1)-C(11)	112.2(5)	C(2)-C(112)-As(1)	74.2(4)
C(111)-C(2)-C(112)	97.1(6)	C(111)-C(112)-As(1)	108.62(13)
C(111)-C(2)-C(1)	50.2(4)		

Table A.29: Anisotropic displacement parameters ($Å^2$) for **25**. The anisotropic displacement factor exponent takes the form: $-2\pi^2[h^2a^{*2}U11 + ... + 2hka^*b^*U12]$.

a	U11	U22	U33	U23	U13	U12
Fe(1)	0.029	0.018	0.019	-0.001	0.005	0.000
As(1)	0.050	0.110	0.122	0.015	0.032	-0.023
C(1)	0.053	0.042	0.057	0.001	-0.004	-0.014
C(2)	0.050	0.064	0.085	0.008	0.015	-0.009
C(11)	0.054	0.038	0.037	-0.016	0.016	-0.019
C(12)	0.045	0.045	0.032	-0.017	-0.011	0.010
C(13)	0.056	0.027	0.020	-0.004	0.012	-0.004
C(14)	0.041	0.034	0.030	-0.011	0.006	0.007
C(15)	0.070	0.020	0.030	-0.003	0.008	0.000
C(21)	0.066	0.045	0.043	-0.020	0.031	-0.019
C(22)	0.052	0.053	0.059	-0.031	-0.008	0.024
C(23)	0.128	0.018	0.026	-0.005	0.013	-0.011
C(24)	0.044	0.055	0.047	-0.034	0.016	-0.018
C(25)	0.079	0.033	0.023	-0.007	-0.007	0.013

Table A.30: Hydrogen coordinates and isotropic displacement parameters ($Å^2$) for **25**.

atom	x	y	z	U(eq)
H(1A)	0.380(4)	0.773(7)	0.335(5)	0.062
H(1B)	0.352(4)	0.916(7)	0.451(5)	0.062
H(2A)	0.408(4)	0.574(9)	0.381(6)	0.079
H(2B)	0.378(4)	0.687(8)	0.493(6)	0.079
H(12)	0.2952	0.5288	0.6015	0.051
H(13)	0.1254	0.4806	0.6269	0.040
H(14)	0.0299	0.6779	0.4690	0.042
H(15)	0.1382	0.8475	0.3488	0.048
H(21)	0.2609	0.4776	0.1763	0.059
H(22)	0.3022	0.2593	0.3488	0.067
H(23)	0.1532	0.1524	0. 4231	0.069
H(24)	0.0209	0.3095	0.2936	0.057
H(25)	0.0890	0.5094	0.1403	0.056

Table A.31: Atomic coordinates and equivalent isotropic displacement parameters for **28**. U(eq) is defined as one third of the trace of the orthogonalized Uij tensor.

Atom	x	y	z	U(eq)
Fe(1)	8287(1)	7691(1)	431(1)	15(1)
P(1)	6520(1)	4733(1)	1215(1)	17(1)
O(1)	5833(2)	2537(2)	2387(1)	28(1)
O(2)	5823(1)	8343(2)	1945(1)	24(1)
C(1)	6795(2)	3786(3)	2347(1)	20(1)
C(2)	5536(2)	7067(3)	1168(1)	21(1)
C(11)	7909(2)	6045(3)	1385(1)	17(1)
C(12)	8314(2)	8218(3)	1676(1)	20(1)
C(13)	9454(2)	8458(3)	1654(1)	22(1)
C(14)	9776(2)	6461(3)	1357(1)	22(1)
C(15)	8830(2)	4973(3)	1189(1)	19(1)
C(21)	6747(2)	8022(3)	-614(1)	23(1)
C(22)	7272(2)	10098(3)	-346(1)	23(1)
C(23)	8390(2)	10069(3)	-421(1)	22(1)
C(24)	8562(2)	7975(3)	-729(1)	23(1)
C(25)	7548(2)	6704(3)	-849(1)	24(1)

Table A.32: Bond lengths (Å) for **28**.

Fe(1)-C(15)	2.0356(18)	O(1)-C(1)	1.425(2)
Fe(1)-C(11)	2.0417(17)	O(2)-C(2)	1.423(2)
Fe(1)-C(23)	2.0464(18)	C(11)-C(15)	1.435(2)
Fe(1)-C(24)	2.0466(18)	C(11)-C(12)	1.437(3)
Fe(1)-C(22)	2.0467(18)	C(12)-C(13)	1.417(3)

Fe(1)-C(12)	2.0479(17)	C(13)-C(14)	1.419(3)
Fe(1)-C(25)	2.0493(18)	C(14)-C(15)	1.420(3)
Fe(1)-C(14)	2.0500(18)	C(21)-C(22)	1.418(3)
Fe(1)-C(21)	2.0510(19)	C(21)-C(25)	1.423(3)
Fe(1)-C(13)	2.0517(18)	C(22)-C(23)	1.417(3)
P(1)-C(11)	1.8094(18)	C(23)-C(24)	1.418(3)
P(1)-C(1)	1.8496(18)	C(24)-C(25)	1.417(3)
P(1)-C(2)	1.8501(19)		

Table A.33: Bond Angles (°) for **28**.

C(15)-Fe(1)-C(11)	41.22(7)	C(25)-Fe(1)-C(13)	163.76(8)
C(15)-Fe(1)-C(23)	155.03(8)	C(14)-Fe(1)-C(13)	40.49(8)
C(11)-Fe(1)-C(23)	162.63(8)	C(21)-Fe(1)-C(13)	154.23(8)
C(15)-Fe(1)-C(24)	120.41(8)	C(11)-P(1)-C(1)	99.18(8)
C(11)-Fe(1)-C(24)	154.86(8)	C(11)-P(1)-C(2)	103.07(9)
C(23)-Fe(1)-C(24)	40.54(8)	C(1)-P(1)-C(2)	99.58(9)
C(15)-Fe(1)-C(22)	163.15(8)	O(1)-C(1)-P(1)	110.82(13)
C(11)-Fe(1)-C(22)	125.05(7)	O(2)-C(2)-P(1)	115.83(13)
C(23)-Fe(1)-C(22)	40.50(8)	C(15)-C(11)-C(12)	106.88(15)
C(24)-Fe(1)-C(22)	68.22(8)	C(15)-C(11)-P(1)	122.22(13)
C(15)-Fe(1)-C(12)	68.80(7)	C(12)-C(11)-P(1)	130.85(14)
C(11)-Fe(1)-C(12)	41.14(7)	C(15)-C(11)-Fe(1)	69.16(9)
C(23)-Fe(1)-C(12)	125.50(8)	C(12)-C(11)-Fe(1)	69.66(9)
C(24)-Fe(1)-C(12)	163.06(8)	P(1)-C(11)-Fe(1)	123.93(9)
C(22)-Fe(1)-C(12)	107.09(8)	C(13)-C(12)-C(11)	108.26(16)
C(15)-Fe(1)-C(25)	108.01(8)	C(13)-C(12)-Fe(1)	69.93(10)
C(11)-Fe(1)-C(25)	119.70(7)	C(11)-C(12)-Fe(1)	69.20(9)
C(23)-Fe(1)-C(25)	68.14(8)	C(12)-C(13)-C(14)	108.41(17)
C(24)-Fe(1)-C(25)	40.48(8)	C(12)-C(13)-Fe(1)	69.64(10)
C(22)-Fe(1)-C(25)	68.29(8)	C(14)-C(13)-Fe(1)	69.69(10)
C(12)-Fe(1)-C(25)	154.65(8)	C(13)-C(14)-C(15)	108.06(17)
C(15)-Fe(1)-C(14)	40.66(7)	C(13)-C(14)-Fe(1)	69.82(10)
C(11)-Fe(1)-C(14)	68.93(7)	C(15)-C(14)-Fe(1)	69.12(10)
C(23)-Fe(1)-C(14)	120.48(8)	C(14)-C(15)-C(11)	108.39(16)
C(24)-Fe(1)-C(14)	108.51(8)	C(14)-C(15)-Fe(1)	70.21(10)
C(22)-Fe(1)-C(14)	154.59(8)	C(11)-C(15)-Fe(1)	69.61(10)
C(12)-Fe(1)-C(14)	68.31(8)	C(22)-C(21)-C(25)	108.04(17)
C(25)-Fe(1)-C(14)	126.63(8)	C(22)-C(21)-Fe(1)	69.59(10)
C(15)-Fe(1)-C(21)	126.13(8)	C(25)-C(21)-Fe(1)	69.63(11)
C(11)-Fe(1)-C(21)	106.99(7)	C(23)-C(22)-C(21)	107.91(17)
C(23)-Fe(1)-C(21)	68.03(8)	C(23)-C(22)-Fe(1)	69.74(10)
C(24)-Fe(1)-C(21)	68.11(8)	C(21)-C(22)-Fe(1)	69.91(11)
C(22)-Fe(1)-C(21)	40.50(8)	C(22)-C(23)-C(24)	108.16(17)
C(12)-Fe(1)-C(21)	119.66(8)	C(22)-C(23)-Fe(1)	69.76(10)
C(25)-Fe(1)-C(21)	40.60(8)	C(24)-C(23)-Fe(1)	69.74(11)
C(14)-Fe(1)-C(21)	163.78(8)	C(25)-C(24)-C(23)	108.07(18)
C(15)-Fe(1)-C(13)	68.41(7)	C(25)-C(24)-Fe(1)	69.86(10)
C(11)-Fe(1)-C(13)	68.80(7)	C(23)-C(24)-Fe(1)	69.72(10)
C(23)-Fe(1)-C(13)	108.00(8)	C(24)-C(25)-C(21)	107.82(18)

C(24)-Fe(1)-C(13)	126.47(8)	C(24)-C(25)-Fe(1)	69.66(11)
C(22)-Fe(1)-C(13)	119.78(8)	C(21)-C(25)-Fe(1)	69.76(11)
C(12)-Fe(1)-C(13)	40.44(7)		

Table A.34: Anisotropic displacement parameters ($Å^2$) for **28**. The anisotropic displacement factor exponent takes the form: $-2\pi^2[h^2a^{*2}U_{11} + ... + 2hka^*b^*U12]$.

atom	U11	U22	U33	U23	U13	U12
Fe(1)	17(1)	14(1)	15(1)	0(1)	6(1)	0(1)
P(1)	20(1)	14(1)	18(1)	-2(1)	9(1)	-1(1)
O(1)	40(1)	15(1)	41(1)	-5(1)	30(1)	-7(1)
O(2)	31(1)	16(1)	34(1)	-4(1)	22(1)	-2(1)
C(1)	25(1)	16(1)	23(1)	2(1)	12(1)	-1(1)
C(2)	21(1)	21(1)	24(1)	1(1)	11(1)	2(1)
C(11)	21(1)	15(1)	16(1)	2(1)	8(1)	0(1)
C(12)	26(1)	17(1)	17(1)	-1(1)	9(1)	-1(1)
C(13)	23(1)	22(1)	17(1)	1(1)	4(1)	-5(1)
C(14)	18(1)	24(1)	22(1)	5(1)	6(1)	2(1)
C(15)	21(1)	16(1)	21(1)	4(1)	8(1)	2(1)
C(21)	18(1)	32(1)	17(1)	4(1)	4(1)	-1(1)
C(22)	27(1)	22(1)	19(1)	6(1)	6(1)	6(1)
C(23)	27(1)	20(1)	18(1)	5(1)	6(1)	-3(1)
C(24)	25(1)	29(1)	18(1)	2(1)	12(1)	1(1)
C(25)	31(1)	22(1)	17(1)	-3(1)	8(1)	-3(1)

Table A.35: Hydrogen coordinates and isotropic displacement parameters ($Å^2$) for **28**.

atom	x	y	z	U(eq)
H(1)	6891(18)	4970(40)	2749(14)	24(5)
H(1A)	7470(20)	3030(40)	2538(14)	23(5)
H(2)	5530(20)	8010(40)	682(16)	35(6)
H(2A)	4780(20)	6500(40)	1028(13)	25(5)
H(3)	5770(20)	1560(50)	2178(17)	39(8)
H(4)	5380(20)	8110(40)	2124(16)	28(7)
H(12)	7898(19)	9240(40)	1838(14)	26(6)
H(13)	9908(19)	9670(40)	1802(13)	23(5)
H(14)	10494(19)	6230(30)	1301(12)	18(5)
H(15)	8832(19)	3470(40)	977(13)	26(5)
H(21)	5990(20)	7630(40)	-637(17)	35(7)
H(22)	6940(20)	11280(40)	-106(15)	37(6)
H(23)	8940(20)	11180(40)	-272(15)	33(6)
H(24)	9230(20)	7490(40)	-809(16)	31(7)
H(25)	7420(20)	5330(40)	-1027(15)	32(6)

Table A.36: Atomic coordinates and equivalent isotropic displacement parameters for **30**. U(eq) is defined as one third of the trace of the orthogonalized Uij tensor.

Atom	x	y	z	U(eq)
Fe(1)	5484(1)	2007(1)	2064(1)	16(1)
P(1)	3858(1)	2782(1)	3655(1)	14(1)
C(11)	4206(1)	1572(2)	2695(1)	16(1)
C(12)	5116(1)	413(2)	3047(1)	19(1)
C(13)	5077(2)	-209(2)	1956(2)	24(1)
C(14)	4167(1)	548(2)	939(2)	24(1)
C(15)	3627(1)	1651(2)	1385(1)	21(1)
O(1)	4800(1)	3401(1)	6013(1)	26(1)
O(2)	2677(1)	501(1)	4083(1)	25(1)
O(3)	3599(1)	4345(1)	3186(1)	21(1)
C(1)	5140(1)	2658(2)	5177(1)	19(1)
C(2)	2528(1)	2027(2)	3809(1)	20(1)
C(21)	6491(2)	3795(2)	2992(2)	29(1)
C(22)	7297(2)	2631(2)	3032(2)	26(1)
C(23)	7050(2)	2280(2)	1805(2)	25(1)
C(24)	6094(2)	3222(2)	1013(2)	31(1)
C(25)	5746(2)	4161(2)	1750(2)	33(1)

Table A.37: Bond Lengths (Å) for **30**.

Fe(1)-C(11)	2.0324(14)	P(1)-C(1)	1.8213(15)
Fe(1)-C(15)	2.0360(15)	C(11)-C(15)	1.436(2)
Fe(1)-C(25)	2.0433(17)	C(11)-C(12)	1.440(2)
Fe(1)-C(21)	2.0439(17)	C(12)-C(13)	1.425(2)
Fe(1)-C(12)	2.0462(15)	C(13)-C(14)	1.419(2)
Fe(1)-C(22)	2.0489(16)	C(14)-C(15)	1.423(2)
Fe(1)-C(23)	2.0523(16)	O(1)-C(1)	1.4212(19)
Fe(1)-C(24)	2.0529(17)	O(2)-C(2)	1.4185(19)
Fe(1)-C(14)	2.0582(16)	C(21)-C(25)	1.419(3)
Fe(1)-C(13)	2.0617(16)	C(21)-C(22)	1.419(3)
P(1)-O(3)	1.5106(11)	C(22)-C(23)	1.425(2)
P(1)-C(11)	1.7816(15)	C(23)-C(24)	1.418(3)
P(1)-C(2)	1.8205(16)	C(24)-C(25)	1.426(3)

Table A.38: Bond Angles (°) for **30**.

C(11)-Fe(1)-C(15)	41.35(6)	C(12)-Fe(1)-C(13)	40.59(6)
C(11)-Fe(1)-C(25)	117.40(7)	C(22)-Fe(1)-C(13)	117.98(7)
C(15)-Fe(1)-C(25)	107.86(7)	C(23)-Fe(1)-C(13)	108.41(7)
C(11)-Fe(1)-C(21)	107.90(6)	C(24)-Fe(1)-C(13)	128.65(7)
C(15)-Fe(1)-C(21)	128.93(7)	C(14)-Fe(1)-C(13)	40.30(7)
C(25)-Fe(1)-C(21)	40.63(8)	O(3)-P(1)-C(11)	113.56(7)
C(11)-Fe(1)-C(12	41.35(6)	O(3)-P(1)-C(2)	110.37(7)

C(15)-Fe(1)-C(12)	69.31(6)	C(2)-P(1)-C(1)	105.11(7)
C(25)-Fe(1)-C(12)	151.29(7)	C(15)-C(11)-C(12)	107.62(13)
C(21)-Fe(1)-C(12)	117.76(7)	C(15)-C(11)-P(1)	123.98(11)
C(11)-Fe(1)-C(22)	128.61(6)	C(12)-C(11)-P(1)	128.35(11)
C(15)-Fe(1)-C(22)	167.41(7)	C(15)-C(11)-Fe(1)	69.46(8)
C(25)-Fe(1)-C(22)	68.37(8)	C(12)-C(11)-Fe(1)	69.84(8)
C(21)-Fe(1)-C(22)	40.57(7)	P(1)-C(11)-Fe(1)	124.08(8)
C(12)-Fe(1)-C(22)	107.85(7)	C(13)-C(12)-C(11)	107.51(13)
C(11)-Fe(1)-C(23)	167.17(6)	C(13)-C(12)-Fe(1)	70.29(9)
C(15)-Fe(1)-C(23)	150.48(7)	C(11)-C(12)-Fe(1)	68.81(8)
C(25)-Fe(1)-C(23)	68.24(7)	C(14)-C(13)-C(12)	108.65(14)
C(21)-Fe(1)-C(23)	68.23(7)	C(14)-C(13)-Fe(1)	69.72(9)
C(12)-Fe(1)-C(23)	128.49(7)	C(12)-C(13)-Fe(1)	69.12(9)
C(22)-Fe(1)-C(23)	40.67(7)	C(13)-C(14)-C(15)	108.28(14)
C(11)-Fe(1)-C(24)	150.98(7)	C(13)-C(14)-Fe(1)	69.98(9)
C(15)-Fe(1)-C(24)	117.26(7)	C(15)-C(14)-Fe(1)	68.82(9)
C(25)-Fe(1)-C(24)	40.76(7)	C(14)-C(15)-C(11)	107.93(14)
C(21)-Fe(1)-C(24)	68.37(8)	C(14)-C(15)-Fe(1)	70.50(9)
C(12)-Fe(1)-C(24)	166.55(7)	C(11)-C(15)-Fe(1)	69.19(8)
C(22)-Fe(1)-C(24)	68.33(7)	O(1)-C(1)-P(1)	108.63(10)
C(23)-Fe(1)-C(24)	40.40(7)	O(2)-C(2)-P(1)	111.49(11)
C(11)-Fe(1)-C(14)	68.84(6)	C(25)-C(21)-C(22)	108.23(15)
C(15)-Fe(1)-C(14)	40.68(6)	C(25)-C(21)-Fe(1	69.67(10)
C(25)-Fe(1)-C(14)	128.90(8)	C(22)-C(21)-Fe(1)	69.90(9)
C(21)-Fe(1)-C(14)	167.27(7)	C(21)-C(22)-C(23)	107.76(16)
C(12)-Fe(1)-C(14)	68.51(6)	C(21)-C(22)-Fe(1)	69.53(9)
C(22)-Fe(1)-C(14)	150.89(7)	C(23)-C(22)-Fe(1)	69.80(9)
C(23)-Fe(1)-C(14)	117.64(7)	C(24)-C(23)-C(22)	108.25(15)
C(24)-Fe(1)-C(14)	108.13(7)	C(24)-C(23)-Fe(1)	69.82(10)
C(11)-Fe(1)-C(13)	68.71(6)	C(22)-C(23)-Fe(1)	69.53(9)
C(15)-Fe(1)-C(13)	68.41(7)	C(23)-C(24)-C(25)	107.76(16)
C(25)-Fe(1)-C(13)	166.91(7)	C(23)-C(24)-Fe(1)	69.78(9)
C(21)-Fe(1)-C(13	151.28(7)	C(25)-C(24)-Fe(1)	69.26(10)
C(11)-P(1)-C(2)	107.64(7)	C(21)-C(25)-C(24)	108.00(16)
O(3)-P(1)-C(1)	112.65(7)	C(21)-C(25)-Fe(1)	69.71(9)
C(11)-P(1)-C(1)	107.02(7)	C(24)-C(25)-Fe(1)	69.98(10)

Symmetry transformations used to generate equivalent atoms

Table A.39: Anisotropic displacement parameters ($Å^2$) for **30**. The anisotropic displacement factor exponent takes the form: $-2\pi^2[h^2a^{*2}U_{11} + ... + 2hka^*b^*U12]$.

atom	U11	U22	U33	U23	U13	U12
Fe(1)	16(1)	16(1)	17(1)	2(1)	8(1)	1(1)
P(1)	14(1)	14(1)	13(1)	-1(1)	6(1)	-1(1)
C(11)	16(1)	16(1)	19(1)	-2(1)	9(1)	-2(1)
C(12)	22(1)	15(1)	23(1)	2(1)	12(1)	-1(1)

C(13)	26(1)	17(1)	33(1)	-5(1)	18(1)	-2(1)
C(14)	21(1)	30(1)	22(1)	-9(1)	11(1)	-4(1)
C(15)	15(1)	26(1)	19(1)	-3(1)	7(1)	0(1)
O(1)	29(1)	29(1)	20(1)	-9(1)	11(1)	-7(1)
O(2)	31(1)	24(1)	18(1)	0(1)	8(1)	-9(1)
O(3)	24(1)	15(1)	21(1)	1(1)	8(1)	2(1)
C(1)	18(1)	20(1)	16(1)	0(1)	6(1)	-1(1)
C(2)	19(1)	24(1)	19(1)	-5(1)	10(1)	-3(1)
C(21)	32(1)	23(1)	41(1)	-8(1)	25(1)	-12(1)
C(22)	20(1)	29(1)	30(1)	-1(1)	12(1)	-7(1)
C(23)	24(1)	26(1)	34(1)	-1(1)	20(1)	-2(1)
C(24)	37(1)	33(1)	31(1)	10(1)	23(1)	0(1)
C(25)	38(1)	20(1)	51(1)	11(1)	29(1)	3(1)

Table A.40: Hydrogen coordinates and isotropic displacement parameters ($Å^2$) for **30**.

Atom	x	y	z	U(eq)
H(1)	5820(18)	3090(20)	5134(17)	4(5)
H(1A)	5340(16)	1670(20)	5404(16)	22(4)
H(2)	1780(20)	2270(20)	3087(19)	33(5)
H(2A)	2490(20)	2520(20)	4499(19)	36(5)
H(3)	5220(20)	4090(30)	6220(20)	42(7)
H(4)	2390(19)	80(20)	3460(20)	33(6)
H(12)	5659(16)	120(20)	3846(17)	22(4)
H(13)	5605(19)	-1000(20)	1927(17)	34(5)
H(14)	3966(18)	360(20)	108(19)	34(5)
H(15)	3027(18)	2340(20)	921(17)	24(5)
H(21)	6429(19)	4260(20)	3702(19)	39(6)
H(22)	7840(20)	2110(20)	3723(19)	32(5)
H(23)	7459(19)	1590(20)	1600(18)	32(5)
H(24)	5727(19)	3180(20)	190(20)	35(6)
H(25)	5070(20)	4820(20)	1430(20)	41(6)

Table A.41: Atomic coordinates and equivalent isotropic displacement parameters for **31**. U(eq) is defined as one third of the trace of the orthogonalized Uij tensor.

Atom	x	y	z	U(eq)
Fe(1)	2108(1)	6200(1)	1382(1)	25(1)
P(1)	-142(1)	6178(1)	3275(1)	20(1)
S(1)	-2215(1)	7354(1)	3106(1)	33(1)
O(1)	3546(3)	5772(2)	4142(1)	26(1)
O(2)	-2216(3)	5435(2)	4586(1)	28(1)
C(1)	2183(4)	6624(2)	3879(2)	24(1)
C(2)	-1294(4)	5052(2)	3856(2)	24(1)

C(11)	865(4)	5518(2)	2396(2)	23(1)
C(12)	3026(5)	5128(2)	2257(2)	26(1)
C(13)	3049(6)	4613(3)	1494(2)	36(1)
C(14)	953(6)	4670(3)	1158(2)	40(1)
C(15)	-409(5)	5224(3)	1705(2)	33(1)
C(21)	3130(12)	7728(3)	1593(3)	69(2)
C(22)	1293(11)	7805(4)	1287(4)	79(2)
C(23)	1169(9)	7366(4)	597(3)	67(2)
C(24)	3149(15)	6925(3)	376(3)	109(3)
C(25)	4541(7)	7191(4)	1098(5)	103(3)

Table A.42: Bond lengths (Å) for **31**.

Fe(1)-C(25)	1.995(4)	P(1)-S(1)	1.955(1)
Fe(1)-C(24)	2.000(4)	O(1)-C(1)	1.415(3)
Fe(1)-C(21)	2.018(4)	O(2)-C(2)	1.421(3)
Fe(1)-C(23)	2.024(4)	C(11)-C(15)	1.436(4)
Fe(1)-C(11)	2.032(3)	C(11)-C(12)	1.439(4)
Fe(1)-C(15)	2.039(3)	C(12)-C(13)	1.416(4)
Fe(1)-C(12)	2.042(3)	C(13)-C(14)	1.412(5)
Fe(1)-C(22)	2.049(5)	C(14)-C(15)	1.415(5)
Fe(1)-C(13)	2.051(3)	C(21)-C(22)	1.246(8)
Fe(1)-C(14)	2.052(3)	C(21)-C(25)	1.369(9)
P(1)-C(11)	1.783(3)	C(22)-C(23)	1.267(8)
P(1)-C(2)	1.835(3)	C(23)-C(24)	1.390(9)
P(1)-C(1)	1.835(3)	C(24)-C(25)	1.509(9)

Table A.43: Bond Angles (°) for **31**.

C(25)-Fe(1)-C(24)	44.4(3)	C(22)-Fe(1)-C(14)	142.1(2)
C(25)-Fe(1)-C(21)	39.9(3)	C(13)-Fe(1)-C(14)	40.27(15)
C(24)-Fe(1)-C(21)	68.0(2)	C(11)-P(1)-C(2)	102.69(13)
C(25)-Fe(1)-C(23)	68.17(19)	C(11)-P(1)-C(1)	108.01(13)
C(24)-Fe(1)-C(23)	40.4(3)	C(2)-P(1)-C(1)	104.16(13)
C(21)-Fe(1)-C(23)	62.4(2)	C(11)-P(1)-S(1)	116.87(10)
C(25)-Fe(1)-C(11)	137.4(3)	C(2)-P(1)-S(1)	112.43(9)
C(24)-Fe(1)-C(11)	176.2(3)	C(1)-P(1)-S(1)	111.60(10)
C(21)-Fe(1)-C(11)	111.26(16)	O(1)-C(1)-P(1)	114.26(19)
C(23)-Fe(1)-C(11)	135.9(2)	O(2)-C(2)-P(1)	110.63(19)
C(25)-Fe(1)-C(15)	178.0(3)	C(15)-C(11)-C(12)	107.3(3)
C(24)-Fe(1)-C(15)	136.8(3)	C(15)-C(11)-P(1)	125.2(2)
C(21)-Fe(1)-C(15)	138.1(2)	C(12)-C(11)-P(1)	127.5(2)
C(23)-Fe(1)-C(15)	111.71(17)	C(15)-C(11)-Fe(1)	69.64(16)
C(11)-Fe(1)-C(15)	41.30(11)	C(12)-C(11)-Fe(1)	69.71(15)
C(25)-Fe(1)-C(12)	110.84(18)	P(1)-C(11)-Fe(1)	128.33(15)
C(24)-Fe(1)-C(12)	142.4(3)	C(13)-C(12)-C(11)	107.7(3)
C(21)-Fe(1)-C(12)	113.28(17)	C(13)-C(12)-Fe(1)	70.09(17)
C(23)-Fe(1)-C(12)	174.7(2)	C(11)-C(12)-Fe(1)	68.93(15)
C(11)-Fe(1)-C(12)	41.36(11)	C(14)-C(13)-C(12)	108.7(3)
C(15)-Fe(1)-C(12)	69.09(12)	C(14)-C(13)-Fe(1)	69.91(19)

C(25)-Fe(1)-C(22)	64.9(2)	C(12)-C(13)-Fe(1)	69.43(17)
C(24)-Fe(1)-C(22)	65.4(2)	C(13)-C(14)-C(15)	108.5(3)
C(21)-Fe(1)-C(22)	35.7(2)	C(13)-C(14)-Fe(1)	69.82(18)
C(23)-Fe(1)-C(22)	36.2(2)	C(15)-C(14)-Fe(1)	69.30(18)
C(11)-Fe(1)-C(22)	111.75(18)	C(14)-C(15)-C(11)	107.9(3)
C(15)-Fe(1)-C(22)	113.7(2)	C(14)-C(15)-Fe(1)	70.24(18)
C(12)-Fe(1)-C(22)	138.4(2)	C(11)-C(15)-Fe(1)	69.05(16)
C(25)-Fe(1)-C(13)	113.12(18)	C(22)-C(21)-C(25)	112.0(5)
C(24)-Fe(1)-C(13)	114.26(19)	C(22)-C(21)-Fe(1)	73.5(3)
C(21)-Fe(1)-C(13)	141.9(2)	C(25)-C(21)-Fe(1)	69.2(3)
C(23)-Fe(1)-C(13)	144.9(2)	C(21)-C(22)-C(23)	112.8(6)
C(11)-Fe(1)-C(13)	68.73(12)	C(21)-C(22)-Fe(1)	70.8(3)
C(15)-Fe(1)-C(13)	68.24(14)	C(23)-C(22)-Fe(1)	70.8(3)
C(12)-Fe(1)-C(13)	40.48(12)	C(22)-C(23)-C(24)	110.7(5)
C(22)-Fe(1)-C(13)	177.6(2)	C(22)-C(23)-Fe(1)	73.0(3)
C(25)-Fe(1)-C(14)	141.5(3)	C(24)-C(23)-Fe(1)	68.9(3)
C(24)-Fe(1)-C(14)	111.86(18)	C(23)-C(24)-C(25)	101.9(4)
C(21)-Fe(1)-C(14)	177.8(2)	C(23)-C(24)-Fe(1)	70.7(2)
C(23)-Fe(1)-C(14)	115.95(18)	C(25)-C(24)-Fe(1)	67.6(2)
C(11)-Fe(1)-C(14)	68.72(12)	C(21)-C(25)-C(24)	102.5(4)
C(15)-Fe(1)-C(14)	40.46(14)	C(21)-C(25)-Fe(1)	70.9(3)
C(12)-Fe(1)-C(14)	68.28(13)	C(24)-C(25)-Fe(1)	68.0(2)

Symmetry transformations used to generate equivalent atoms

Table A.44: Anisotropic displacement parameters ($Å^2$) for **31**. The anisotropic displacement factor exponent takes the form: $-2\pi^2[h^2a^{*2}U_{11} + ... + 2hka^*b^*U12]$.

atom	U^{11}	U^{22}	U^{33}	U^{23}	U^{13}	U^{12}
Fe(1)	33(1)	22(1)	19(1)	5(1)	-3(1)	-6(1)
P(1)	17(1)	21(1)	24(1)	4(1)	1(1)	1(1)
S(1)	24(1)	31(1)	43(1)	9(1)	1(1)	9(1)
O(1)	19(1)	33(1)	26(1)	8(1)	0(1)	3(1)
O(2)	24(1)	34(1)	26(1)	9(1)	7(1)	9(1)
C(1)	22(1)	24(1)	26(1)	1(1)	0(1)	1(1)
C(2)	21(1)	24(1)	28(1)	5(1)	3(1)	-1(1)
C(11)	27(1)	21(1)	23(1)	5(1)	0(1)	-3(1)
C(12)	31(2)	24(1)	23(1)	6(1)	6(1)	5(1)
C(13)	54(2)	25(2)	30(2)	2(1)	13(1)	3(1)
C(14)	66(2)	27(2)	28(2)	-3(1)	1(2)	-16(2)
C(15)	38(2)	30(2)	30(2)	6(1)	-6(1)	-11(1)
C(21)	128(5)	31(2)	46(2)	13(2)	-11(3)	-27(3)
C(22)	106(5)	33(2)	98(4)	24(3)	41(4)	8(3)
C(23)	74(3)	53(3)	72(3)	40(3)	-30(3)	-21(2)
C(24)	244(9)	29(2)	54(3)	-3(2)	99(4)	-32(3)
C(25)	24(2)	57(3)	229(8)	95(4)	3(3)	-9(2)

Table A.45: Hydrogen coordinates and isotropic displacement parameters ($Å^2$) for **31**.

atom	x	y	z	U(eq)
H(1A)	0.3032	0.7129	0.3562	0.029
H(1B)	0.1654	0.7011	0.4348	0.029
H(2A)	-0.2397	0.4692	0.3537	0.029
H(2B)	-0.0169	0.4528	0.3976	0.029
H(12)	0.4197	0.5202	0.2606	0.032
H(13)	0.4246	0.4290	0.1255	0.043
H(14)	0.0537	0.4390	0.0660	0.048
H(15)	-0.1871	0.5372	0.1630	0.039
H(21)	0.3498	0.8002	0.2097	0.082
H(22)	0.0136	0.8148	0.1538	0.095
H(23)	-0.0076	0.7343	0.0282	0.080
H(24)	0.3521	0.6560	-0.0095	0.131
H(25)	0.5992	0.7031	0.1185	0.124
H(3)	0.2855	0.5399	0.4542	0.044(11)
H(4)	-0.3420	0.5758	0.4440	0.047(11)

Appendix B

Gas chromatograms for compounds **15**, **18**, **19**, **20** and **25** are given below. Where more than on peak is observed, that belonging to the compound in question is marked with an asterisk.

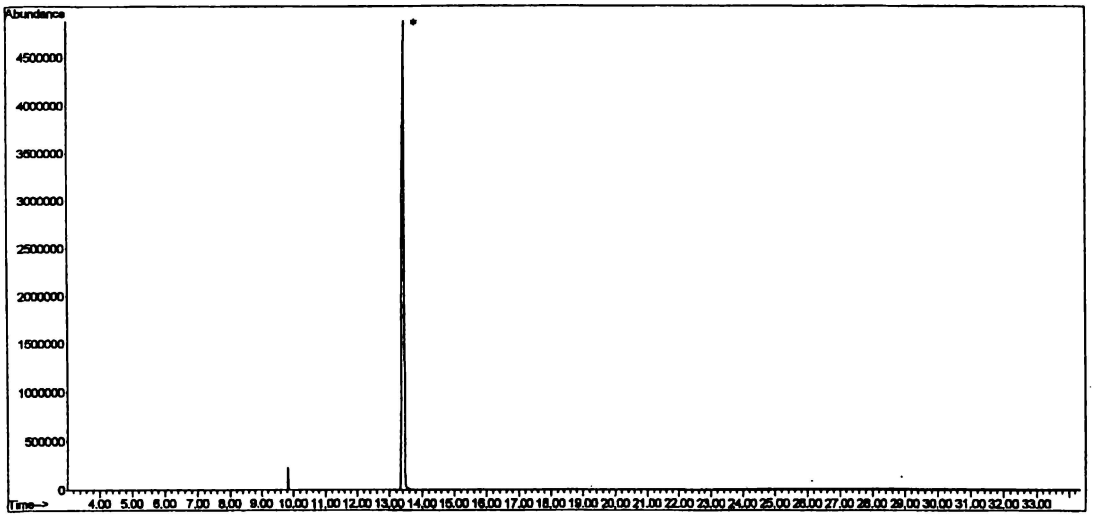

Figure B1: Gas Chromatogram of **15**.

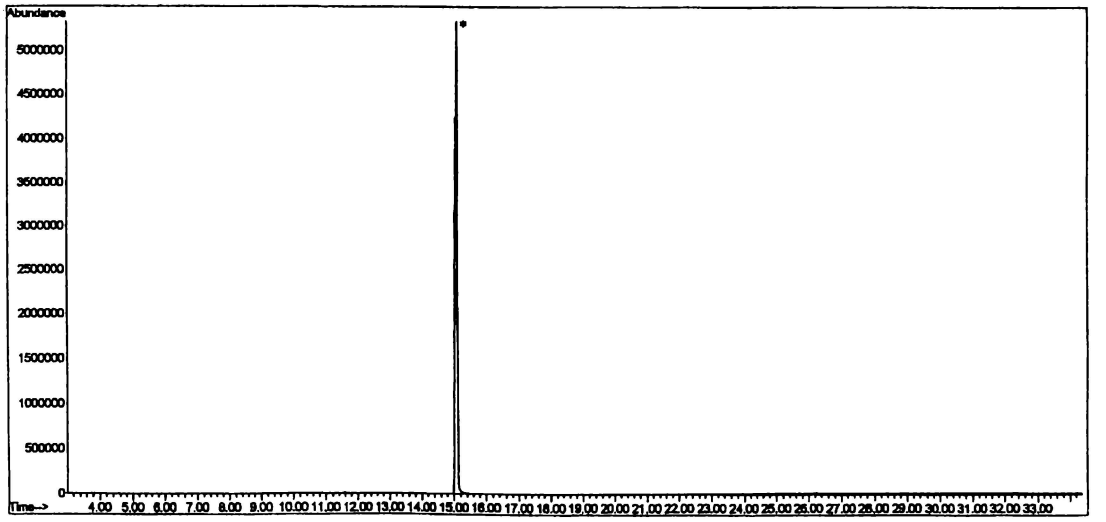

Figure B2: Gas Chromatogram of **18**.

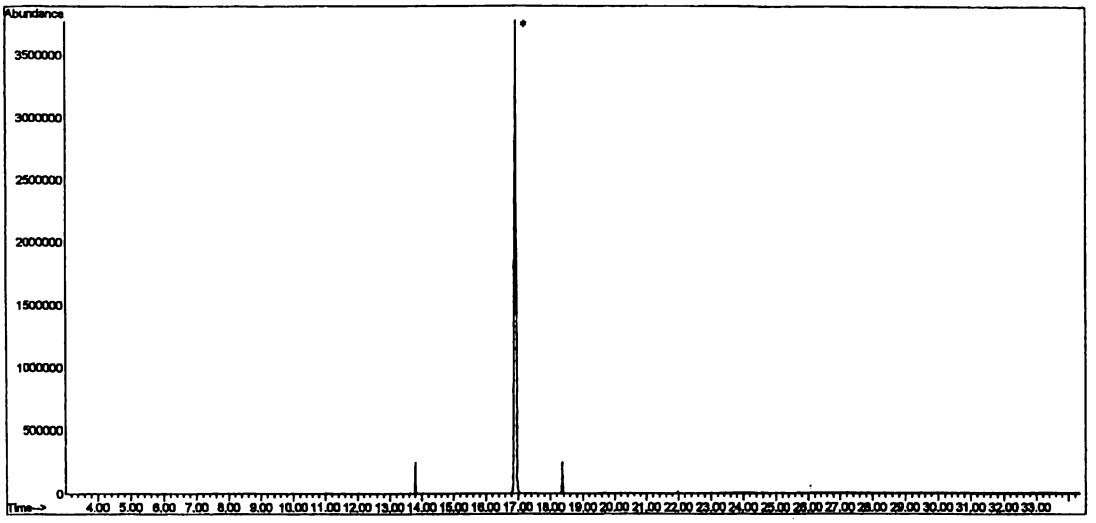

Figure B3: Gas Chromatogram of **19**.

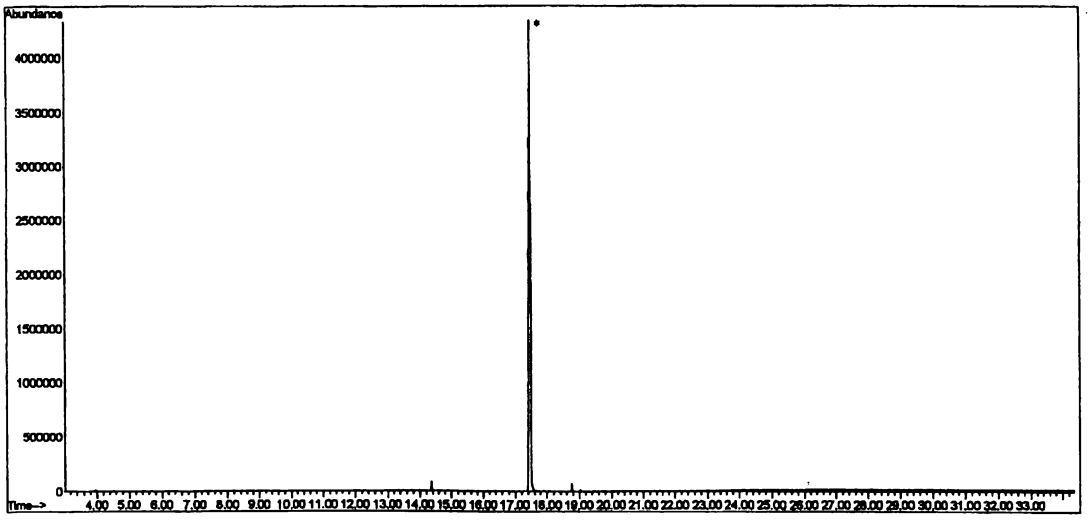

Figure B4: Gas Chromatogram of **20**.

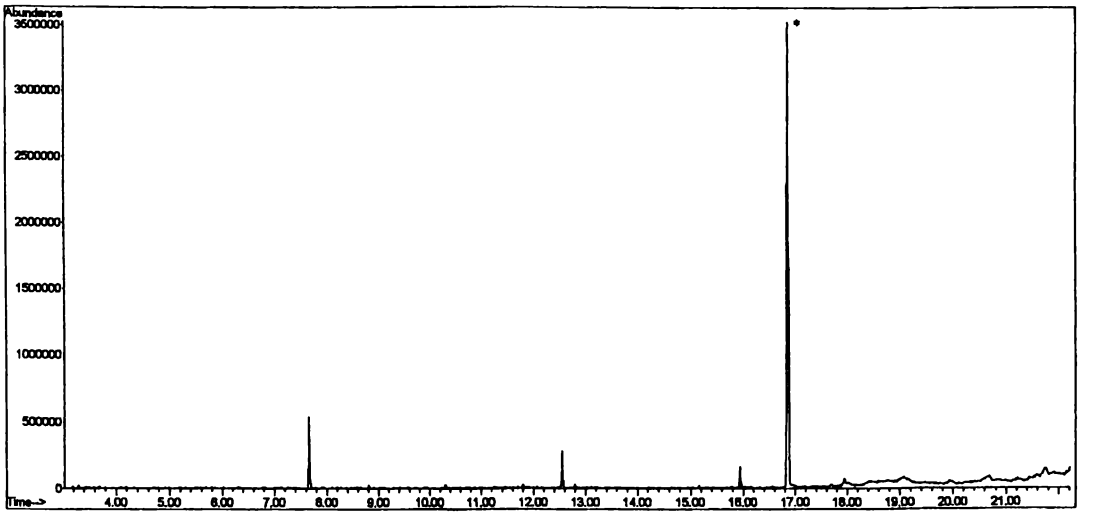

Figure B5: Gas Chromatogram of **25**.

Gas chromatograms for 1,1'-Fc'$(CH_2OH)_2$ and 1,2-Fc'$(CH_2OH)_2$ are given below. Both of these compounds were prone to thermal decomposition in the GC. The peak due to the parent diol is marked with an asterisk.

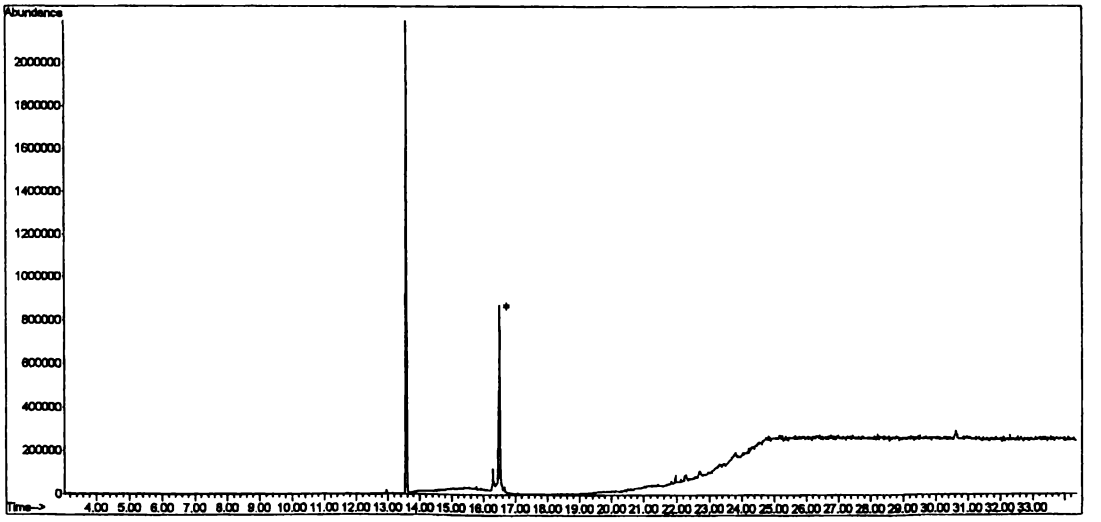

Figure B6: Gas Chromatogram of 1,1'-Fc'$(CH_2OH)_2$.

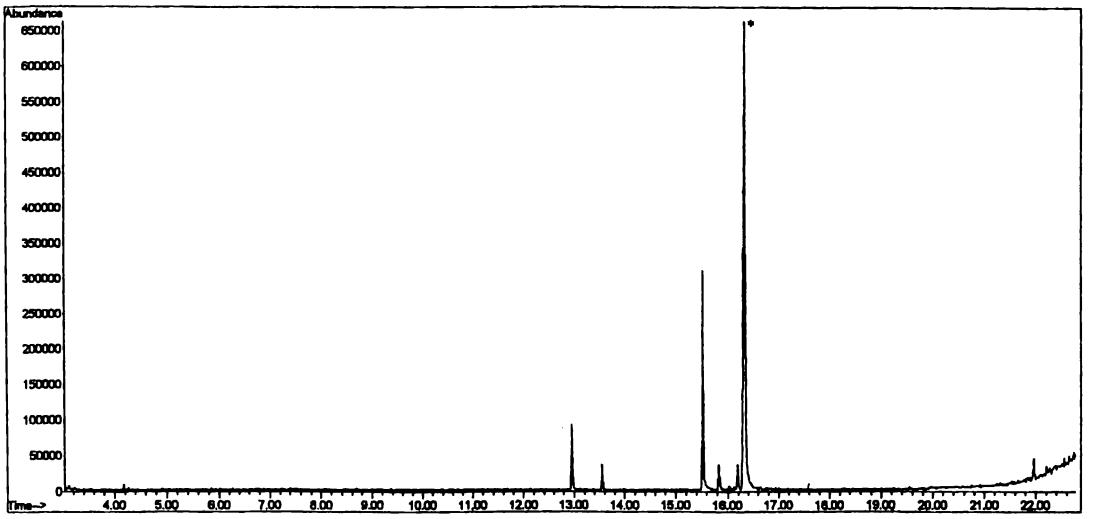

Figure B7: Gas Chromatogram of 1,2-Fc'$(CH_2OH)_2$.

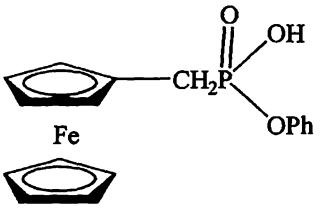

1

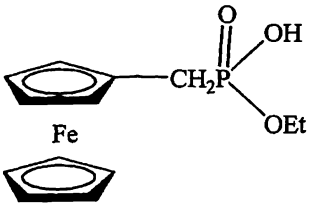

2

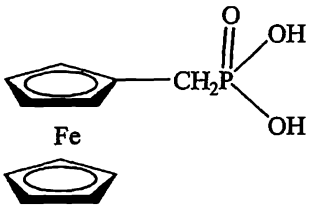

3

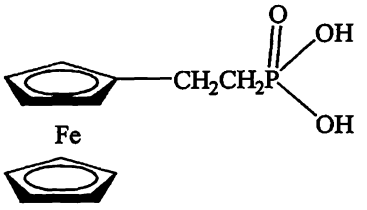

4

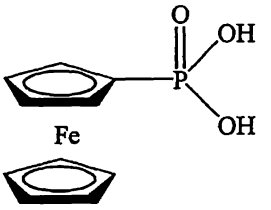

5

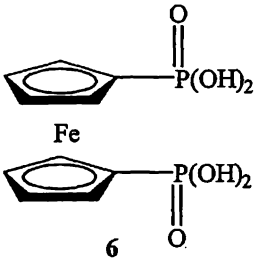

6

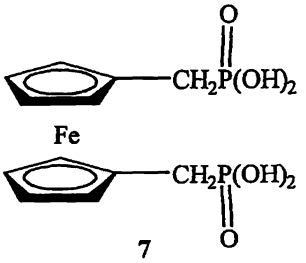

7

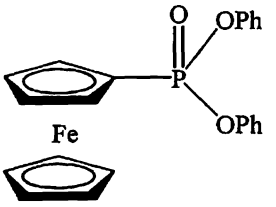

8

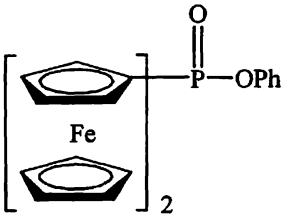

8a

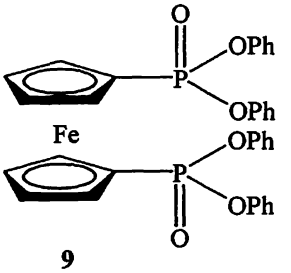

9

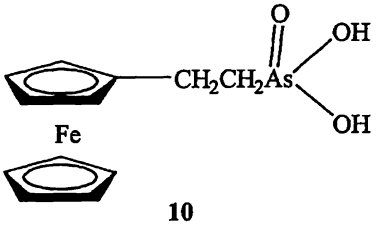

10

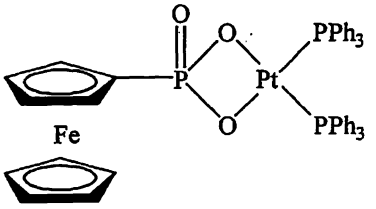

11

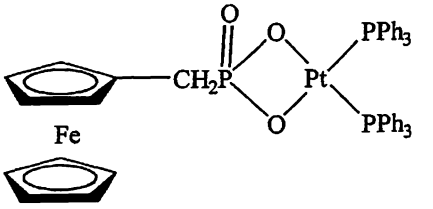

12

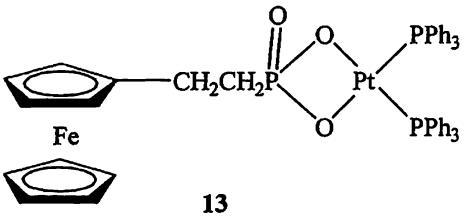

13

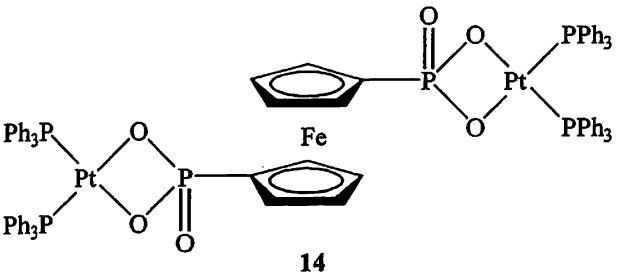

14

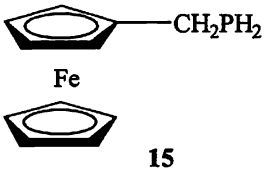

15

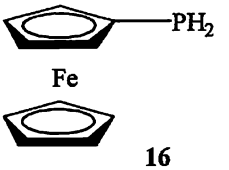

16

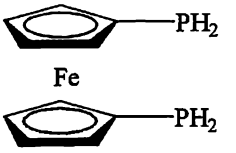

17

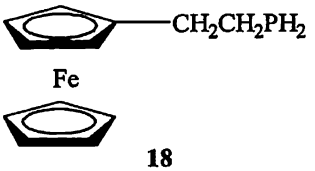

18

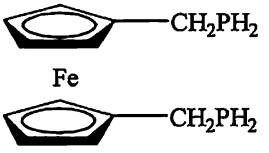

19

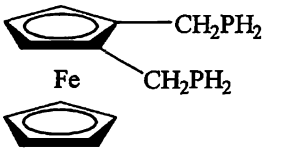

20

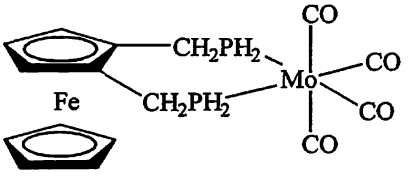

21

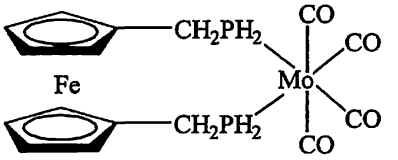

22

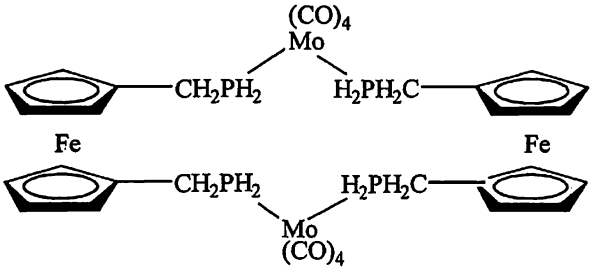

22a

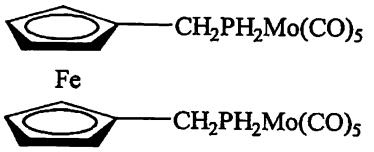

23

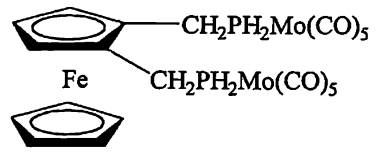

24

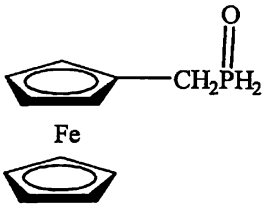

26

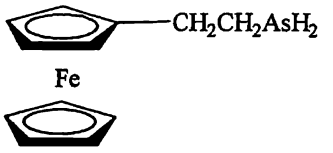

25

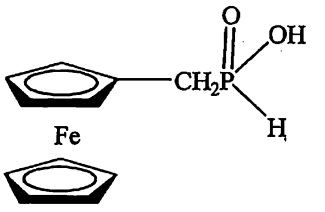

27

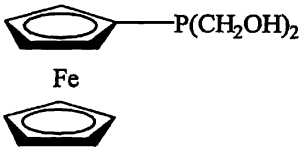

28

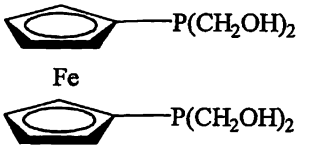

29

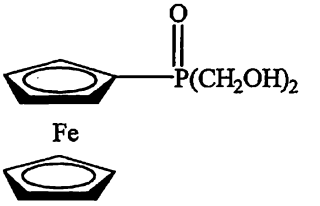

30

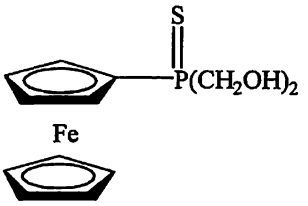

31

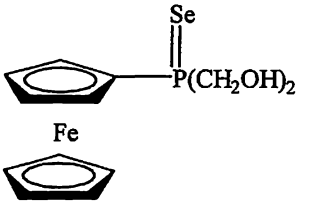

32

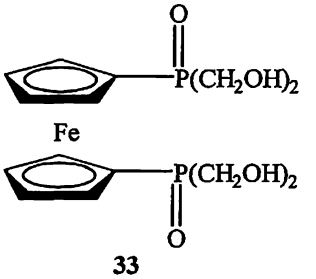

33

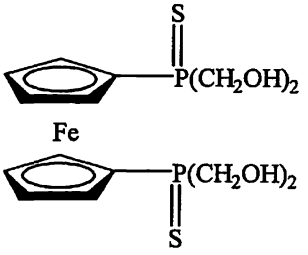

34

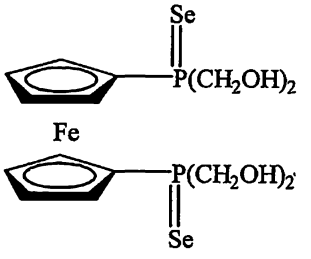

35

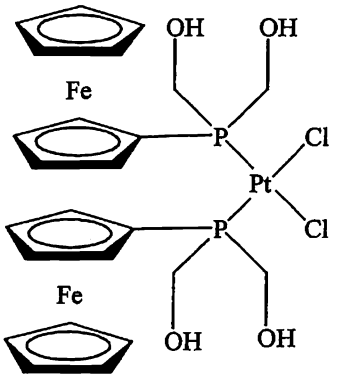

36